



University
of Glasgow

Sutthiwarotamakun, Rungrut (2011) *Peripheral autoimmunity induces central neuro-inflammation and hippocampal neurogenesis impairment in a murine model of collagen induced Rheumatoid Arthritis.*
PhD thesis.

<http://theses.gla.ac.uk/3027/>

Copyright and moral rights for this thesis are retained by the author

A copy can be downloaded for personal non-commercial research or study, without prior permission or charge

This thesis cannot be reproduced or quoted extensively from without first obtaining permission in writing from the Author

The content must not be changed in any way or sold commercially in any format or medium without the formal permission of the Author

When referring to this work, full bibliographic details including the author, title, awarding institution and date of the thesis must be given

**‘Peripheral autoimmunity induces central
neuro-inflammation and hippocampal
neurogenesis impairment in a murine model
of collagen induced Rheumatoid Arthritis’**

Rungrut Sutthiwarotamakun
BSc in.Pharmacy, MRes in Biomedical Sciences



This thesis is submitted to the University of
Glasgow for the degree of Doctor of Philosophy

Division of Immunology, Infection and
Inflammation
Faculty of Medicine
University of Glasgow

November 2011

Abstract

Background: Psychiatric disorders are common in patients with autoimmune diseases such as rheumatoid arthritis. These disorders are poorly understood and are an important co-morbidity. They may occur as a consequence of the effects of the autoimmune inflammation on the central nervous system. Peripheral inflammation inducing central cytokine production in the CNS has been documented in acute inflammatory models such as after systemic LPS challenge, and cytokine administration has been shown to induce cognitive impairment and mood disorders. These disorders may be due to the central action of cytokines on neurogenesis and reduced hippocampal neurogenesis has been implicated in depression and cognitive decline. Peripheral inflammation and some specific cytokines have been reported to inhibit hippocampal neurogenesis, resulting in cognition impairment and depressive-like behaviour in animal models.

Hypothesis: Based on this evidence, we hypothesized that peripheral inflammation associated with arthritis can induce central production of inflammatory mediators in the brain contributing to reduction in hippocampal neurogenesis thereby offering a mechanism and potential therapeutic targets for RA-associated psychiatric disorders.

Aims and Methods: The aim of this project is 1) to investigate whether peripheral immune/inflammatory responses during arthritis can induce changes in inflammatory mediators in brains of collagen induced arthritis (CIA) mice, using this as a model for an adaptive immune response contributing to neurological disease development similar to the human disease. We used Luminex bead-based screening assays to determine a wide range of inflammatory mediator proteins in single small volume samples obtained from mouse brain tissues. In the same tissues, the transcription levels of genes encoding these inflammatory mediators were also quantified using real-time PCR and quantified as absolute copy numbers. 2) To investigate whether peripheral immune/inflammatory responses during arthritis can induce changes in hippocampal neurogenesis in brains of collagen induced arthritis (CIA) mice, we also measure changes in hippocampal neurogenesis in CII immunized mice using the immunohistochemistry of neuronal marker doublecortin (DCX). In order to confirm that changes in both inflammatory mediators and hippocampal

neurogenesis were due to peripheral inflammation, CII immunized mice were given peripheral anti TNF- α etanercept treatment. Inflammatory mediator profiles and hippocampal neurogenesis in brains of etanercept-treated CII immunized mice were compared to PBS -treated CII immunized mice and naive control mice.

Results: Systemic etanercept treatment attenuated arthritis in CII immunized mice. IL-1 β , IL-5, CXCL1 and FGF2 protein were increased in the serum of CII immunized mice. In addition, we found up-regulation of protein and gene concentrations of IL-1 β , IL-1- α , TNF- α , IL-6, IFN- γ , IL-2, IL-12, IL-4, IL-5, CXCL1, CXCL0 and CCL2, VEGF and FGF2 in brains of CII immunized mice compared to those in naive control mice. The reduction in number of DCX-positive neurons in the dentate gyrus of CII immunized mice compared to those in naive control mice, suggesting the impairment in hippocampus neurogenesis in CII immunized mice. In addition, reduction of inflammatory mediators, including IL-1 β , TNF- α , IL-12, CXCL1, and increases of IL-6, IL-2 and VEGF and FGF2 protein concentrations were observed in brains of etanercept-treated CII immunized mice compared to those in untreated CII immunized mice. In addition, the impairment in hippocampal neurogenesis was reversed by peripheral etanercept treatment in CII immunized mice. In conclusion, the data of this thesis shows that peripheral inflammation during arthritis potentially induces production of inflammatory mediators in brains of CII immunized mice. Up-regulation of these inflammatory mediators in the brain may be associated with the impairment in hippocampal neurogenesis of CII immunized mice. In addition, peripheral etanercept treatment seems to have protective effect against peripheral-induced brain inflammation and the impairment in hippocampal neurogenesis in CII immunized mice.

In summary, we demonstrated that peripheral inflammation resulting from arthritis may induce brain inflammation and contribute to the impairment of hippocampal neurogenesis. Systemic etanercept treatment not only attenuated joint inflammation, but also reduced brain inflammation and reversed the impairment in hippocampal neurogenesis resulting from peripheral inflammation in CII immunized mice.

Conclusion and prospect: These data provide an important new insight into a potential mechanism underlying psychiatric disorders in chronic inflammatory disease. We suggest that when considering management of chronic disorders, the potential physiological effects on the brain should also be considered. This may be difficult to quantify for example when assessing reduced hippocampal neurogenesis. Therefore we propose some experimental studies that could follow from this thesis might include a search for a systemic biomarker such as BDNF that might provide information of CNS changes, perhaps by a comparative transcriptional analysis of normal and inflamed brain. The experimental model in our study did not include a cognitive or memory end-point as an index of brain function, and this aspect could also be included in future experiments to complete the link from systemic inflammation to psychological changes. We also noted that there may be neurological changes that occur in immunized mice that do not yet show signs of arthritis, and if so perhaps depression may occasionally reflect a pre-clinical chronic condition.

However, we feel we have provided sufficient evidence that there is a strong link between systemic inflammation with physiological changes in the brain that might suggest that therapeutic choices for RA could reduce inflammation as well as attenuate depression associated with arthritis.

Table of Contents

ABSTRACT	2
TABLE OF CONTENTS	5
LIST OF TABLES	10
LIST OF FIGURES	11
LIST OF FIGURES	11
ACKNOWLEDGEMENT	15
AUTHOR'S DECLARATION	17
ABBREVIATIONS	18
CHAPTER 1	27
INTRODUCTION	27
1.1 Immune system	28
1.1.1 Overview of immune system.....	28
1.1.2 Cytokines.....	30
1.1.3 Chemokines.....	32
1.2 Rheumatoid Arthritis	34
1.2.1 Aetiology of RA.....	34
1.2.2 Pathogenesis of RA	36
1.2.3 Roles of cytokines in RA	37
1.2.4 Collagen induced arthritis: murine model of RA	43
1.2.5 Rheumatoid arthritis as a systemic inflammatory disease and its association with neurological diseases	45
1.3 Immunology of the central nervous system.....	47
1.3.1 Astrocytes.....	47
1.3.2 Microglia.....	48
1.3.3 Innate immunity in the central nervous system (CNS)	51
1.3.4 Adaptive immunity in the CNS	51
1.3.5 The role of inflammatory mediators in the CNS	54
1.4 Inflammation in the CNS.....	57
1.5 Immune signals from the peripheral circulation induce brain inflammation.....	58
1.6 Barriers of the central nervous system	59
1.6.1 Blood Brain Barrier (BBB)	59
1.7 Communication between the immune system and the central nervous system (CNS)	70
1.8 Depression.....	74

1.9 Hippocampal neurogenesis	75
1.9.1 The role of neurogenesis in hippocampal function	76
1.9.2 Hippocampal neurogenesis and depression	77
1.10 Cytokines, peripheral inflammation and depression	80
1.10.1 Depression and rheumatoid arthritis.....	80
1.10.2 Immune activation in depression patients	82
1.10.3 The cytokine hypothesis of depression	84
1.10.4 Possible mechanism underlying cytokine-induced depression	85
1.10.5 Cytokine-mediated inflammation and decreased hippocampal neurogenesis in depression.....	86
1.10.6 Role of peripheral inflammation in hippocampal neurogenesis.....	87
1.11 Aims and hypothesis.....	92
CHAPTER 2	94
MATERIALS AND METHODS	94
2.1 General reagents & buffers	95
2.1.1 Materials and reagents	95
2.2 Buffers and culture media	95
2.3 In vitro procedures	96
2.3.1 Animal welfare	96
2.3.2 Mice	96
2.3.3 Induction of collagen-induced arthritis in DBA1 mice.....	96
2.4 Collection of serum from mice and processing of brain tissue for gene and protein analysis	101
2.5 cDNA synthesis by reverse transcription (RT)-PCR.....	102
2.6 Real-time PCR using SYBR Green I dye	103
2.6.1 Primer design and optimization.....	104
2.6.2 Optimizing primers for SYBR Green real-time PCR	106
2.6.3 Agarose gel electrophoresis	107
2.6.4 Generation of a DNA standard for real-time polymerase chain reaction	108
2.6.5 Plasmid verification and quantification	109
2.6.6 Real-time PCR assay	110
2.6.7 Normalization of cDNA samples	112
2.7 Cytokine and chemokine protein expression analysis.....	114
2.7.1 Protein extraction from brain tissue	114
2.7.2 Normalization of a relative total protein concentration using BCA protein assay	115
2.7.3 Measurement of multiple cytokines using a suspension bead array assay and a Luminex platform.....	116
2.7.4 Enzyme immuno-assay (ELISA) protocol	119
2.8 Free-floating section staining for doublecortin (DCX).....	123
2.8.1 Tissue processing	123
2.8.2 Cryostat cutting and free-floating section process	123
2.8.3 Immunohistochemistry.....	125
2.8.4 Quantifying doublecortin [DCX]-positive cells.....	128
2.9 Statistical analysis	129
CHAPTER 3	131

INCREASED CONCENTRATION OF INFLAMMATORY MEDIATORS IN THE BRAIN ASSOCIATED WITH COLLAGEN-INDUCED EXPERIMENTAL ARTHRITIS.	131
3.1 Introduction and aims.....	132
3.2 Results.....	134
3.2.1 Induction of arthritis in DBA1 mice.....	134
3.2.2 Changes in inflammatory mediator protein concentration in serum of CII immunized mice (both arthritic mice and non-arthritic mice)	137
3.2.3 Changes in inflammatory mediator protein concentrations in brains of CII immunized mice (both arthritic mice and non-arthritic mice)	139
1000 X AMOUNT OF IL-13 PROTEIN IN 50 ML (PG)	139
AMOUNT OF TOTAL BRAIN PROTEIN IN 50 ML (MG)	139
3.2.4 Cytokine gene expression profiles in the brains of CII immunized mice (both arthritic mice and non-arthritic mice).....	148
3.2.5 Comparisons of gene and protein expression of inflammatory mediators in arthritic and non-arthritic mouse brains	154
3.2.6 Correlations between chemokine mRNA and protein concentration in arthritic and non-arthritic mouse brains	157
3.2.7 Correlations between inflammatory mediator protein concentration and mRNA expression levels and arthritis scores.....	158
3.3 Result chapter 3; Summary of findings.	161
3.4 Discussion.....	163
3.4.1 Elevations of inflammatory mediator mRNA and protein concentration in CII immunized mouse brains.....	163
CHAPTER 4	175
TIME-COURSE CHANGES IN INFLAMMATORY MEDIATOR CONCENTRATIONS IN THE BRAIN AND SERUM DURING COLLAGEN II-INDUCED EXPERIMENTAL ARTHRITIS	175
4.1 Introduction and aims.....	176
4.2 Results.....	179
4.2.1 Induction of arthritis in DBA1 mice.....	179
4.2.2 Time course analysis of serum inflammatory mediator protein concentration in CII immunized mice.....	185
4.2.3 Time-course analysis of inflammatory mediator protein concentrations in the brains of CII immunized mice by Luminex cytokine 20-Plex.....	190
4.2.4 Time-course analysis of inflammatory mediator protein concentrations in the brain homogenates of CII immunized mice validated by ELISA assays	195
4.2.5 Cytokine gene expression profiles in CIA mouse brains by Real-time PCR	205
4.2.6 Comparison between time course changes in inflammatory mediator protein and mRNA levels in brain of CII immunized mice	212
4.2.7 Summary; longitudinal changes in mRNA and protein concentrations in brain of CII immunized mice.....	216
4.3 Result chapter 4: Summary of major findings.....	218
4.4 Discussion.....	221
4.4.1 Longitudinal changes in peripheral inflammatory mediators in CII immunized mice.	222
4.4.2 Association between peripheral inflammation and increased concentrations of brain inflammatory mediators: possible evidence that peripheral inflammatory cytokine signals induce neuro-inflammation.	225

4.4.3	The potential interplay between inflammatory mediators in brains of CII immunized mice: Possible evidence for ongoing immune activation and inflammatory processes.	230
-------	--	-----

CHAPTER 5 238

EFFECTS OF TUMOUR NECROSIS FACTOR (TNF) BLOCKADE USING RECOMBINANT HUMAN SOLUBLE TNF-RECEPTOR (ETANERCEPT) ON INFLAMMATORY MEDIATOR PROFILES IN BRAINS OF ARTHRITIC MODEL MICE 238

5.1	Introduction	239
5.2	Results	241
5.2.1	Effect of etanercept on development of collagen induced arthritis (CIA).	241
5.2.2	Effect of etanercept on serum inflammatory mediator protein concentrations in CII immunized mice on day 14, day 32 and day 35 by Luminex cytokine 20-plex assay	249
5.2.3	Changes in inflammatory mediator protein concentrations in the brains of etanercept-treated and untreated CII immunized mice on day 14, day 32 and day 35	250
5.2.4	Changes in inflammatory mediator gene expression in the brains of etanercept treated and PBS treated CII immunized mice on day 14, day 32 and day 35 by real-time PCR	261
5.3	Summary; Effects of etanercept on inflammatory mediator mRNA and protein profiles in brains of CII immunized mice	265
5.4	Result chapter 5: Summary of major findings.....	268
5.5	Discussion	269
5.5.1	Effect of etanercept on the amelioration of joint disease in CII immunized mice	269
5.5.2	Effects of peripheral etanercept treatment on inflammatory mediators in brains of CII immunized mice; possible evidence of peripheral inflammatory signal inducing neuro-inflammation	271
5.5.3	Effects of peripheral etanercept treatment on pro-inflammatory cytokines in brains of CII immunized mice	273
5.5.4	Effects of peripheral etanercept treatment on TNF- α in brains of CII immunized mice	273
5.5.5	Effects of peripheral etanercept treatment on IL-1 β in brains of CII immunized mice	274
5.5.6	Effects of peripheral etanercept treatment on Th1 cytokines in brains of CII immunized mice	275
5.5.7	Effects of peripheral etanercept treatment on Th2 cytokines in brains of CII immunized mice	276
5.5.8	Effects of peripheral etanercept treatment on chemokines in brains of CII immunized mice.....	278
5.5.9	Effects of peripheral etanercept treatment on growth factors in brains of CII immunized mice	278

CHAPTER 6 281

EFFECT OF PERIPHERAL INFLAMMATION AND ETANERCEPT ON HIPPOCAMPAL NEUROGENESIS IN ARTHRITIS MODEL MICE..... 281

6.1	Introduction	282
6.2	Immunohistochemistry of Doublecortin (DCX) in mouse hippocampus	285
6.2.1	Optimization of Doublecortin Immuno-histochemistry	285
6.3	Induction of arthritis in DBA1 mice	292
6.3.1	CIA experimental procedure.....	292
6.3.2	Clinical response.....	294

6.4	Changes in number of DCX-positive neurons in the dentate gyrus in CII immunized mice.....	295
6.4.1	Changes in number of DCX-positive neurons in the dentate gyrus in arthritic mice ..	295
6.4.2	Changes in number of DCX-positive neurons in the dentate gyrus in non-arthritic mice ..	298
6.4.3	Comparison of changes in number of DCX-positive neurons in the dentate gyrus between naïve control, arthritic and non-arthritic mice ..	300
6.5	Effect of etanercept on hippocampal neurogenesis in CII immunized mice	301
6.5.1	Administration of etanercept and induction of arthritis in DBA1 mice; CIA experimental procedure.....	302
6.5.2	Effect of etanercept on the development of collagen induced arthritis (CIA)	304
6.5.3	Changes in hippocampal neurogenesis in CII immunized mice before the onset of arthritis on day 14.....	310
6.5.4	Effect of etanercept on hippocampal neurogenesis during period of clinical manifestation of arthritis	313
6.5.5	Longitudinal changes of hippocampal neurogenesis in PBS-treated CII immunized mice.	331
6.5.6	Longitudinal changes of hippocampal neurogenesis in antigen-naïve control mice.	333
6.6	Result chapter 6: Summary of major findings.....	334
6.7	Discussion.....	337
6.7.1	The role of Doublecortin (DCX) in neuronal maturation in the adult hippocampus ...	337
6.7.2	Reduction in hippocampal neurogenesis in CII immunized mice.	339
6.7.3	Effect of etanercept on impairment of hippocampal neurogenesis in CII immunized mice.....	343
6.7.4	Severity of arthritis was not associated changes in hippocampal neurogenesis in arthritic mice, and the reduction in hippocampal neurogenesis in non-arthritic mice	347
CHAPTER 7	350
GENERAL DISCUSSION AND CONCLUSION	350
7 GENERAL DISCUSSION AND CONCLUSION.....		351
7.1 Suggestions for future studies		362
7.1.1	Hypothesis; there is migration of immune cells from the periphery into the brain of CII immunized mice.	362
7.1.2	Hypothesis; there is local production of inflammatory mediators by astrocytes and microglia in the brain of CII immunized mice.	363
7.1.3	Hypothesis; difference inflammatory mediators play different role in hippocampal neurogenesis.....	363
7.1.4	Hypothesis; the reduction in the number of neurons in the hippocampus of CII immunized mice could be the result of neurodegeneration.	364
7.1.5	Hypothesis; Peripheral inflammation has effects on neurotransmitter and neurotropic factors in brains of CII immunized mice, that are associated with the pathological mechanism of depression.	365
8 REFERENCES.....		367
9 APPENDICES		414

List of Tables

TABLE 2.1 CLINICAL SCORES OF C57BL/6 MICE WITH CIA.	99
TABLE 2.2 PRIMER SEQUENCES USED FOR THE AMPLIFICATION OF BRAIN TISSUE CDNA.	106
TABLE 2.3 CONTROL TISSUE USED TO TEST SPECIFICITY OF PRIMERS.	107
TABLE 2.4 LIST OF COMPONENTS IN THE MASTERMIX USED FOR REAL-TIME PCR ASSAY.	111
TABLE 2.5 CONDITIONS FOR REAL-TIME PCR PROTOCOL	111
TABLE 2.6 AN EXAMPLE OF NORMALISATION USING A HOUSEKEEPING GENE TO DETERMINE LEVELS OF GENE "X".	114
TABLE 2.7 CYTOKINE ANALYSIS BY ELISA.....	120
TABLE 2.8 CYTOKINE, CHEMOKINES AND GROWTH FACTOR ANALYSIS BY ELISA.	121
TABLE 3.1 VALUES OF PROTEIN CONCENTRATIONS OF INFLAMMATORY MEDIATORS DETECTED BY A LUMINEX ASSAY IN BRAIN TISSUE HOMOGENATE SAMPLES OF NAÏVE CONTROL MICE AND CII IMMUNIZED MICE.	141
TABLE 3.2 SUMMARY OF INFLAMMATORY MEDIATOR PROTEIN PROFILES IN BRAINS OF CII IMMUNIZED MICE.	147
TABLE 3.3 SUMMARY OF INFLAMMATORY MEDIATOR GENE EXPRESSION PROFILES IN BRAINS OF CII IMMUNIZED MICE.	154
TABLE 3.4 A SUMMARY OF INFLAMMATORY MEDIATOR GENE MRNA EXPRESSION AND PROTEIN PROFILES IN ARTHRITIC MOUSE BRAINS AND NON-ARTHRITIC MOUSE BRAINS.	156
TABLE 4.1 NUMBERS OF ARTHRITIC MICE, MEAN ARTHRITIS SCORES, AND MEAN SWELLING SCORES OF CII IMMUNIZED MICE IN EACH TIME POINT GROUPS.	185
TABLE 4.2 LONGITUDINAL CHANGES IN CONCENTRATIONS BRAIN INFLAMMATORY MEDIATOR PROFILES IN BRAINS OF CII IMMUNIZED MICE RELATIVE TO THOSE OF THOSE IN CONTROL MICE.	217
TABLE 5.1 NUMBERS OF ARTHRITIC MICE, MEAN ARTHRITIS SCORES, AND MEAN SWELLING SCORES OF CIA MICE IN ETANERCEPT-TREATED AND PBS-TREATED GROUPS.	249
TABLE 5.2 EFFECTS OF ETANERCEPT ON INFLAMMATORY MEDIATOR PROTEIN AND MRNA PROFILES IN BRAINS OF ETANERCEPT-TREATED CII IMMUNIZED MICE RELATIVE TO THOSE OF PBS-TREATED CII IMMUNIZED MICE.	266
TABLE 6.1 NUMBERS OF ARTHRITIC MICE, MEAN ARTHRITIS SCORES, AND MEAN SWELLING SCORES OF CIA MICE IN ETANERCEPT-TREATED AND PBS-TREATED GROUPS.....	310
TABLE 6.2 INDIVIDUAL ARTHRITIS SCORE, INDIVIDUAL PAW SWELLING SCORES AND NUMBER OF DCX-POSITIVE NEURONS OF ARTHRITIC MICE IN ETANERCEPT-TREATED AND PBS-TREATED GROUPS	318
TABLE 6.3 INDIVIDUAL ARTHRITIS SCORE, INDIVIDUAL PAW SWELLING SCORES AND NUMBER OF DCX-POSITIVE NEURONS OF NON-ARTHRITIC MICE IN ETANERCEPT-TREATED AND PBS-TREATED CII IMMUNIZED GROUPS ON DAY 32.....	319
TABLE 6.4 INDIVIDUAL ARTHRITIS SCORE, INDIVIDUAL SWELLING SCORES AND NUMBER OF DCX-POSITIVE NEURONS OF CII IMMUNIZED MICE IN ETANERCEPT-TREATED AND PBS-TREATED GROUPS ON DAY 35	328

List of Figures

FIGURE 1.1 STRUCTURE OF THE BBB AND TIGHT JUNCTION.	61
FIGURE 1.2 THE COMMUNICATION BETWEEN THE BRAIN AND THE PERIPHERAL IMMUNE SYSTEM..	73
FIGURE 1.3. HIPPOCAMPAL NEUROGENESIS AND NEURONAL CIRCUIT.....	76
FIGURE 2.1 SUMMARY OF THE CIA EXPERIMENTAL PROCEDURE.	98
FIGURE 2.2 A CORONAL RAT BRAIN ATLAS DIAGRAM (PAXINOS AND WATSON, 1998).	124
FIGURE 2.3 CORONAL BRAIN SECTIONS AT THE LEVEL OF HIPPOCAMPUS.	125
FIGURE 2.4 STEPS INVOLVED IN TISSUE PROCESSING, CRYOSTAT CUTTING AND DCX STAINING. .	127
FIGURE 2.5 THE ORDER OF DCX-STAINED BRAIN SECTIONS OF ONE MOUSE BRAIN ONTO SLIDES. .	129
FIGURE 3.1 THE EXPERIMENTAL PROCEDURE OF COLLAGEN II-INDUCED EXPERIMENTAL ARTHRITIS (CIA) MODEL.	135
FIGURE 3.2 DEVELOPMENT AND SEVERITY OF ARTHRITIS DISEASE IN CII IMMUNIZED MICE OVER 42 DAYS OF EXPERIMENTAL ARTHRITIS COURSE.	136
FIGURE 3.3 PAW HISTOLOGY OF AN ARTHRITIC MOUSE.	137
FIGURE 3.4 SERUM INFLAMMATORY MEDIATOR PROFILES IN CII IMMUNIZED MICE.	138
FIGURE 3.5 CHANGES IN PRO-INFLAMMATORY CYTOKINE CONCENTRATION IN BRAINS OF CII IMMUNIZED MICE.	142
FIGURE 3.6 CHANGES IN A TH1 CYTOKINE LEVEL IN BRAINS OF CII IMMUNIZED MICE.	143
FIGURE 3.7 CHANGES IN TH2 CYTOKINE CONCENTRATION IN BRAINS OF CII IMMUNIZED MICE. ...	144
FIGURE 3.8 CHANGES IN CHEMOKINE CONCENTRATION IN BRAIN OF CII IMMUNIZED MICE.	145
FIGURE 3.9 CHANGES IN A GROWTH FACTOR LEVEL IN BRAIN OF CII IMMUNIZED MICE.	146
FIGURE 3.10 CHANGES IN TH1 CYTOKINE MRNA LEVELS IN BRAINS OF CII IMMUNIZED MICE.	150
FIGURE 3.11 CHANGES IN CHEMOKINE MRNA EXPRESSION LEVELS IN BRAINS OF CII IMMUNIZED MICE.	152
FIGURE 3.12 CHANGES IN GROWTH FACTOR MRNA LEVELS IN BRAINS OF CII IMMUNIZED MICE. ..	152
FIGURE 3.13 CORRELATIONS OF MRNA AND PROTEIN CONCENTRATION FOR CXCL1 AND CXCL10 IN ARTHRITIC AND NON-ARTHRITIC MOUSE BRAINS.	158
FIGURE 3.14 CORRELATIONS OF INFLAMMATORY MEDIATOR PROTEIN CONCENTRATION AND ARTHRITIS SCORE IN ARTHRITIC MICE.....	159
FIGURE 3.15 CORRELATIONS OF INFLAMMATORY MEDIATOR GENE EXPRESSION LEVELS AND ARTHRITIS SCORE IN ARTHRITIC MICE.....	160
FIGURE 4.1 CIA EXPERIMENTAL PROCEDURE FOR TIME COURSE EXPERIMENT.	181
FIGURE 4.2 DEVELOPMENT AND SEVERITY OF ARTHRITIS DISEASE OF EACH GROUP OF CII IMMUNIZED MICE AT EACH TIME POINT.	183
FIGURE 4.3 INDIVIDUAL CLINICAL SCORES AND THICKNESS OF THE PAWS OF INDIVIDUAL CII IMMUNIZED MICE IN EACH GROUP.	184
FIGURE 4.4 TIME-COURSE OF A SERUM PRO-INFLAMMATORY CYTOKINE IN CII IMMUNIZED MICE. .	186
FIGURE 4.5 TIME-COURSE OF A SERUM TH2 CYTOKINE IN CII IMMUNIZED MICE.	188
FIGURE 4.6 TIME-COURSE OF A SERUM CHEMOKINE IN CII IMMUNIZED MICE.	189
FIGURE 4.7 TIME-COURSE OF A SERUM GROWTH FACTOR IN CII IMMUNIZED MICE.....	190
FIGURE 4.8 TIME-COURSE OF A TH1 CYTOKINE PROTEIN CONCENTRATIONS IN BRAINS OF CII IMMUNIZED MICE BY A LUMINEX ASSAY.	192
FIGURE 4.9 TIME-COURSE OF A CHEMOKINE PROTEIN CONCENTRATIONS IN BRAINS OF CII IMMUNIZED MICE BY A LUMINEX ASSAY.	193
FIGURE 4.10 TIME-COURSE OF A GROWTH FACTOR (FGF2) PROTEIN CONCENTRATIONS IN BRAINS OF CII IMMUNIZED MICE BY A LUMINEX ASSAY.	194
FIGURE 4.11 TIME-COURSE OF A GROWTH FACTOR (VEGF) PROTEIN CONCENTRATIONS IN BRAINS OF CII IMMUNIZED MICE BY A LUMINEX ASSAY.	195
FIGURE 4.12 TIME-COURSE OF A PRO-INFLAMMATORY CYTOKINES (TNF- α) PROTEIN CONCENTRATIONS IN BRAINS OF CII IMMUNIZED MICE BY AN ELISA ASSAY.	196
FIGURE 4.13 TIME-COURSE OF A PRO-INFLAMMATORY CYTOKINES (IL-1 β) PROTEIN CONCENTRATIONS IN BRAINS OF CII IMMUNIZED MICE BY AN ELISA ASSAY.	197
FIGURE 4.14 TIME-COURSE OF A TH1 CYTOKINES (IL-12) PROTEIN CONCENTRATIONS IN BRAINS OF CII IMMUNIZED MICE BY AN ELISA ASSAY.....	199

FIGURE 4.15 TIME-COURSE OF A TH2 CYTOKINE (IL-4) PROTEIN CONCENTRATIONS IN BRAINS OF CII IMMUNIZED MICE BY AN ELISA ASSAY.	200
FIGURE 4.16 TIME-COURSE OF A TH2 CYTOKINE (IL-10) PROTEIN CONCENTRATIONS IN BRAINS OF CII IMMUNIZED MICE BY AN ELISA ASSAY.	201
FIGURE 4.17 TIME-COURSE OF A CHEMOKINE (CCL2) PROTEIN CONCENTRATIONS IN BRAINS OF CII IMMUNIZED MICE BY AN ELISA ASSAY.	202
FIGURE 4.18 DIFFERENCES IN INFLAMMATORY MEDIATOR PROTEIN CONCENTRATIONS IN BRAINS OF ARTHRITIC MICE AND NON-ARTHRITIC MICE.	204
FIGURE 4.19 DIFFERENCES IN VEGF AND CXCL1 PROTEIN CONCENTRATIONS IN BRAINS OF ARTHRITIC MICE AND NON-ARTHRITIC MICE.	204
FIGURE 4.20 TIME-COURSE OF A TH1 (IL-12) MRNA EXPRESSION LEVELS IN BRAINS OF CII IMMUNIZED MICE BY REAL-TIME PCR.	206
FIGURE 4.21 TIME-COURSE OF A CHEMOKINE (CXCL1) MRNA LEVELS IN BRAINS OF CII IMMUNIZED MICE BY REAL-TIME PCR.	207
FIGURE 4.22 TIME-COURSE OF A CHEMOKINE (CXCL10) MRNA CONCENTRATIONS IN BRAINS OF CII IMMUNIZED MICE BY REAL-TIME PCR.	208
FIGURE 4.23 TIME-COURSE OF A GROWTH FACTOR (FGF2) MRNA LEVELS IN BRAINS OF CII IMMUNIZED MICE BY REAL-TIME PCR.	209
FIGURE 4.24 TIME-COURSE OF A GROWTH FACTOR (VEGF) MRNA LEVELS IN BRAINS OF CII IMMUNIZED MICE BY REAL-TIME PCR.	210
FIGURE 4.25 DIFFERENCES IN INFLAMMATORY MEDIATOR MRNA LEVELS IN BRAINS OF ARTHRITIC MICE AND NON-ARTHRITIC MICE.	211
FIGURE 4.26 DIFFERENCES IN CXCL1 MRNA LEVELS IN BRAINS OF ARTHRITIC MICE AND NON-ARTHRITIC MICE.	211
FIGURE 4.27 LONGITUDINAL CHANGES OF A TH1 (IL-12) CYTOKINE PROTEIN CONCENTRATIONS AND MRNA EXPRESSION LEVELS IN BRAINS OF CII IMMUNIZED MICE.	213
FIGURE 4.28 LONGITUDINAL CHANGES OF A CHEMOKINE (CXCL1) PROTEIN CONCENTRATIONS AND MRNA EXPRESSION LEVELS IN BRAINS OF CII IMMUNIZED MICE.	214
FIGURE 4.29 LONGITUDINAL CHANGES OF A GROWTH FACTOR (FGF2) PROTEIN CONCENTRATIONS AND MRNA EXPRESSION LEVELS IN BRAINS OF CII IMMUNIZED MICE.	215
FIGURE 4.30 LONGITUDINAL CHANGES OF A GROWTH FACTOR (VEGF) PROTEIN CONCENTRATIONS AND MRNA EXPRESSION LEVELS IN BRAINS OF CII IMMUNIZED MICE.	216
FIGURE 4.31 POTENTIAL MECHANISMS OF IMMUNE ACTIVATION INDUCED BY PERIPHERAL INFLAMMATORY CYTOKINE SIGNALS OCCURRING IN BRAINS OF CII IMMUNIZED MICE.	236
FIGURE 5.1 ADMINISTRATION OF ETANERCEPT DURING THE CIA EXPERIMENTAL PROCEDURE.	243
FIGURE 5.2 EFFECT OF ETANERCEPT ON SEVERITY OF ARTHRITIS IN CII IMMUNIZED MICE ON DAY 32 (GROUPS 1-3).	245
FIGURE 5.3 EFFECT OF ETANERCEPT ON SEVERITY OF ARTHRITIS IN CII IMMUNIZED MICE ON DAY 35 (GROUPS 4 AND 5).	246
FIGURE 5.4 EFFECT OF ETANERCEPT ON SEVERITY OF ARTHRITIS IN ALL CII IMMUNIZED MICE IN GROUP 2, 3, 4 AND 5.	248
FIGURE 5.5 EFFECTS OF ETANERCEPT ON BRAIN PRO-INFLAMMATORY CYTOKINE PROTEIN PROFILES IN CII IMMUNIZED MICE ON DAYS 14, 32 AND 35.	253
FIGURE 5.6 EFFECTS OF ETANERCEPT ON BRAIN TH1 CYTOKINE PROTEIN PROFILES IN CII IMMUNIZED MICE ON DAY 32 AND DAY 35.	255
FIGURE 5.7 EFFECTS OF ETANERCEPT ON BRAIN TH2 CYTOKINE PROTEIN PROFILES IN CII IMMUNIZED MICE ON DAY 32 AND DAY 35.	258
FIGURE 5.8 EFFECTS OF ETANERCEPT ON BRAIN CHEMOKINE (CXCL1) PROTEIN PROFILES IN CII IMMUNIZED MICE ON DAY 32 AND DAY 35.	259
FIGURE 5.9 EFFECTS OF ETANERCEPT ON BRAIN GROWTH FACTOR PROTEIN PROFILES IN CII IMMUNIZED MICE ON DAY 32 AND DAY 35.	260
FIGURE 5.10 EFFECTS OF ETANERCEPT ON A BRAIN PRO-INFLAMMATORY CYTOKINE GENE EXPRESSION PROFILES IN CII IMMUNIZED MICE ON DAY 32 AND DAY 35.	262
FIGURE 5.11 EFFECTS OF ETANERCEPT ON A BRAIN CHEMOKINE GENE EXPRESSION PROFILES IN CII IMMUNIZED MICE ON DAY 32 AND DAY 35.	264
FIGURE 5.12 EFFECTS OF ETANERCEPT ON A BRAIN GROWTH FACTOR GENE EXPRESSION PROFILES IN CII IMMUNIZED MICE ON DAY 32 AND DAY 35.	265
FIGURE 6.1 IMMUNOFLUORESCENT STAINING OF DCX.	286

FIGURE 6.2 IMMUNOFLUORESCENT STAINING OF DCX, NEUN AND PI.....	288
FIGURE 6.3 AN OVERLAY IMAGE OF TRIPLE IMMUNOFLUORESCENT STAINING OF DCX, NEUN AND PI IN THE DENTATE GYRUS OF A DBA1 MOUSE.....	289
FIGURE 6.4 AVIDIN-BIOTIN-PEROXIDASE IMMUNO-HISTOCHEMISTRY OF DCX	290
FIGURE 6.5 AVIDIN-BIOTIN-PEROXIDASE IMMUNO-HISTOCHEMISTRY OF DCX IN THE DENTATE GYRUS OF A DBA 1 MOUSE	291
FIGURE 6.6 HIGH MAGNIFICATION OF A REPRESENTATIVE IMAGE OF DCX IMMUNO-HISTOCHEMISTRY IN THE DENTATE GYRUS OF A DBA1 MOUSE.....	291
FIGURE 6.7 THE EXPERIMENTAL PROCEDURE OF COLLAGEN II-INDUCED EXPERIMENTAL ARTHRITIS MODEL FOR HIPPOCAMPAL NEUROGENESIS ANALYSIS	293
FIGURE 6.8 DEVELOPMENT AND SEVERITY OF ARTHRITIS DISEASE IN CII IMMUNIZED MICE OVER 42 DAYS OF EXPERIMENTAL ARTHRITIS COURSE	294
FIGURE 6.9 CHANGES IN HIPPOCAMPAL NEUROGENESIS IN ARTHRITIC MICE ON DAY 42.....	296
FIGURE 6.10 CHANGES IN HIPPOCAMPAL NEUROGENESIS IN ARTHRITIC MICE ON DAY 42	297
FIGURE 6.11 CHANGES IN NUMBER OF DCX-POSITIVE CELLS IN DENTATE GYRUS OF ARTHRITIC MICE ON DAY 42	297
FIGURE 6.12 CHANGES IN HIPPOCAMPAL NEUROGENESIS IN NON-ARTHRITIC MICE ON DAY 42....	299
FIGURE 6.13 CHANGE IN NUMBER OF DCX-POSITIVE CELLS IN DENTATE GYRUS OF NON-ARTHRITIC MICE ON DAY 42	300
FIGURE 6.14CHANGES IN NUMBER OF DCX-POSITIVE CELLS IN DENTATE GYRUS OF ARTHRITIC AND NON-ARTHRITIC MICE ON DAY 42	301
FIGURE 6.15 ADMINISTRATION OF ETANERCEPT AND CIA EXPERIMENTAL PROCEDURE FOR HIPPOCAMPAL NEUROGENESIS ANALYSIS	303
FIGURE 6.16 EFFECT OF ETANERCEPT ON SEVERITY OF ARTHRITIS IN CII IMMUNIZED MICE ON DAY 32	305
FIGURE 6.17 EFFECT OF ETANERCEPT ON SEVERITY OF ARTHRITIS IN CII IMMUNIZED MICE ON DAY 35	307
FIGURE 6.18 EFFECT OF ETANERCEPT ON SEVERITY OF ARTHRITIS IN ALL CII IMMUNIZED MICE IN GROUP 2, 3, 4 AND 5	309
FIGURE 6.19 DCX IMMUNO-HISTOCHEMISTRY IN THE DENTATE GYRUS OF CONTROL UNTREATED MICE AND CII IMMUNIZED MICE ON DAY 14	312
FIGURE 6.20 CHANGES IN NUMBER OF DCX-POSITIVE CELLS IN DENTATE GYRUS OF CII IMMUNIZED MICE ON DAY 14	313
FIGURE 6.21 ANALYSIS PLAN TO COMPARE DCX STAINING PATTERN IN BRAINS OF PBS-TREATED, ETANERCEPT-TREATED CII IMMUNIZED MICE AND NAÏVE CONTROL MICE ON DAY 32	315
FIGURE 6.22 DCX IMMUNO-HISTOCHEMISTRY IN THE DENTATE GYRUS OF ONE NAÏVE CONTROL, ONE PBS-TREATED AND ONE ETANERCEPT-TREATED CII IMMUNIZED MOUSE IN SET A.....	316
FIGURE 6.23 DCX IMMUNO-HISTOCHEMISTRY IN THE DENTATE GYRUS OF ONE NAÏVE CONTROL, ONE PBS-TREATED ARTHRITIC AND ONE ETANERCEPT-TREATED ARTHRITIC MOUSE IN SET B	317
FIGURE 6.24 DCX IMMUNO-HISTOCHEMISTRY IN THE DENTATE GYRUS OF ONE CONTROL, ONE PBS- TREATED AND ONE ETANERCEPT-TREATED CII IMMUNIZED MOUSE IN SET C (NEITHER DEVELOPED ARTHRITIS)	319
FIGURE 6.25 NUMBER OF DCX-POSITIVE CELLS IN DENTATE GYRUS OF PBS-TREATED AND ETANERCEPT-TREATED CII IMMUNIZED MICE ON DAY 32.....	321
FIGURE 6.26 ANALYSIS PLAN TO COMPARE DCX STAINING PATTERN IN BRAINS OF PBS-TREATED, ETANERCEPT-TREATED CII IMMUNIZED MICE AND NAÏVE CONTROL MICE ON DAY 35	322
FIGURE 6.27 DCX IMMUNO-HISTOCHEMISTRY IN THE DENTATE GYRUS OF ONE NAÏVE CONTROL, ONE PBS-TREATED ARTHRITIC AND ONE ETANERCEPT NON-ARTHRITIC MOUSE IN SET D	323
FIGURE 6.28 DCX IMMUNO-HISTOCHEMISTRY IN THE DENTATE GYRUS OF ONE NAÏVE CONTROL, ONE PBS-TREATED ARTHRITIC AND ONE ETANERCEPT-TREATED NON-ARTHRITIC MOUSE IN SET E.....	324
FIGURE 6.29 DCX IMMUNO-HISTOCHEMISTRY IN THE DENTATE GYRUS OF ONE NAÏVE CONTROL, ONE PBS-TREATED ARTHRITIC AND ONE ETANERCEPT ARTHRITIC MICE IN SET F	325
FIGURE 6.30 DCX IMMUNO-HISTOCHEMISTRY IN THE DENTATE GYRUS OF ONE NAÏVE CONTROL, ONE PBS-TREATED NON-ARTHRITIC AND ONE ETANERCEPT NON-ARTHRITIC MOUSE IN SET G	326

FIGURE 6.31 DCX IMMUNO-HISTOCHEMISTRY IN THE DENTATE GYRUS OF ONE NAÏVE CONTROL, ONE PBS-TREATED NON-ARTHRITIC AND ONE ETANERCEPT NON-ARTHRITIC MOUSE IN SET H	327
FIGURE 6.32 NUMBER OF DCX-POSITIVE CELLS IN THE DENTATE GYRUS OF PBS-TREATED AND ETANERCEPT-TREATED CII IMMUNIZED MICE ON DAY 35, COMPARED WITH ANTIGEN-NAÏVE CONTROL MICE	330
FIGURE 6.33 CORRELATION OF THE NUMBER OF DCX-POSITIVE CELLS AND RA SCORE	331
FIGURE 6.34 TIME-COURSE OF THE NUMBER OF DCX-POSITIVE NEURONS IN THE DENTATE GYRUS OF CII IMMUNIZED MICE	332
FIGURE 6.35 LONGITUDINAL CHANGES OF DCX-POSITIVE NEURONS IN DENTATE GYRUS OF CII IMMUNIZED MICE SACRIFICED ON THE DAY 14, 32 AND 35	333
FIGURE 6.36 LONGITUDINAL CHANGES OF DCX-POSITIVE NEURONS IN DENTATE GYRUS OF CONTROL MICE SACRIFICED ON THE DAY 14, 32 AND 35	334
FIGURE 7.1 SUMMARY OF THE MAJOR FINDINGS FROM THIS THESIS ENTITLED; ‘PERIPHERAL AUTOIMMUNITY INDUCES CENTRAL NEURO-INFLAMMATION AND HIPPOCAMPAL NEUROGENESIS IMPAIRMENT IN A MURINE MODEL OF COLLAGEN INDUCED RHEUMATOID ARTHRITIS’.	353

Acknowledgement

I would like to thank my supervisors; Professor Iain McInnes, Dr. Jonathan Cavanagh and Professor Gerard Graham for offering me the opportunity to undertake this challenging project, and for the patient guidance, encouragement and advice they have provided throughout.

I am particularly grateful to Prof. McInnes who provided the financial support for my studies. Dr. Jonathan Cavanagh my clinical supervisor configured this 'Bench to Bedside' project for me. He integrated his clinical observations into this neuro-immunology project and provided valuable advice for my PhD project from his psychiatrist prospective. I would like to thank Prof. Graham for his excellent scientific supervision, critical comments and advice on how to structure a good thesis.

I have become deeply indebted to Dr. Charles McSharry who stood by me and helped me throughout this project. Dr. Charles has been very supportive especially with proof-reading. His care and support helped me overcome the inevitable difficulties towards the end of my PhD.

I would like to give a special thanks to Professor Andrew Todd from the spinal cord research group who helped me develop the immuno-histochemistry technique for doublecortin for the analysis of hippocampal neurogenesis. I would also like to thank Dr. Bernard Leung who helped me conduct an important experiment on the effect of etanercept on brain inflammation and hippocampal neurogenesis. I would like to thank Mr. James Reilly for his assistance in the preparation of paw tissue preparation and histology. He has also shown special interest in my work and helps me for brain tissue preparation and hippocampal neurogenesis images.

I would like to thank two of my best friends Dr. Clive McKimmie and Dr. Helen Baldwin. Clive is a proper neuro-immunologist and shared his enthusiasm and knowledge of neuroimmunology with me. He not only became a close colleague who provided help and advice, he was also my best friend and looked after me when things were difficult.

Dr. Helen Baldwin was my classmate in the Mres course when I was in Newcastle University in 2004 and she was the one who helped me through the difficulties as an overseas student during my first year in the UK. She was like a heroine who always showed up when I was having a hard time. Meeting Helen again here in Glasgow seemed to be a miracle. Helen very kindly helped me with my thesis with her great scientific knowledge, her constructive feedback for my thesis and her most useful advice.

I am particularly thankful to Mr. Peter Togneri who provided me the great supports throughout the writing up my result chapters. He made my writing up time became more enjoyable.

I would like to thank Dr. Sameer Jauhar who helped and supported me in so many ways. Also, I am extremely grateful to Sameer's parents Dr. Pramod Jauhar and Mrs. Pamela Jauhar, who have kindly looked after me as their own daughter during my stay in Glasgow.

Lastly, I would like to give a special thanks to my family back home in Thailand. My mom, my dad and my brother have worked so hard to support me here. I have kept strong until the end of my PhD program because of my mom. I really hope one day I will have an opportunity to return all the sacrifices she has done for me. This thesis is the best thing I can do for our family and I hope you are proud of me, mom.

Author's declaration

I hereby declare that the work presented in this thesis is original and is all my own work and effort. My work analysing hippocampal neurogenesis was in collaboration with Prof. Andrew Todd. Dr Bernard Leung helped me practically with some experiments giving etanercept to CIA mice.

This thesis in whole or in part has not been submitted anywhere for any award. Where reagents, materials or practical support has been provided by others, due acknowledgement has been made.

Rungrut Sutthiwarotamakun

November 2011

Abbreviations

¹H-MRSI	Proton magnetic resonance spectroscopy
ACH	Acetylcholine
ACPA	anticitrullinated protein antibodies
ACTH	Adrenocorticotropic hormone
AD	Alzheimer's disease
ADAMTS	A disintegrin and metalloproteinase with thrombospondin motifs
Ag	Antigen
AIA	Adjuvant induced arthritis
AJs	Adherent junctions
AKA	Anti-keratin antibodies
AMPA	alpha-amino-3-hydroxy-5-methylisoxazole-4-propionic acid
AMT	Absorptive mediated transport
ANS	Autonomic nervous system
AP	Area prostroma
APCs	Antigen presenting cells
APF	Anti-perinuclear factor
AVP	Arginine-vasopressin
AZT	Azidothymidine

BBB	Blood brain barrier
BCR	B cell receptor
BDI	Beck Depression Inventory
BDNF	Brain derived neurotrophic factor
CFA	Complete Freund's Adjuvant
ChREAE	Chronic relapsing experimental autoimmune encephalomyelitis
CIA	Collagen-induced arthritis
CII	Collagen type-II
CIITA	Class II trans-activator
CLN	Cervical lymph nodes
CNS	Central nervous system
CRH	Corticotrophin-releasing hormone
CRP	C-reactive protein
CSF	Cerebrospinal fluid
CVOs	Circumventricular organs
DAB	3,3-diaminobenzidine
DARC	Duffy antigen receptor for chemokines
DCX	Doublecortin
DG	Dentate gyrus

ds	double-strand
E	Epinephrine
EAE	Experimental autoimmune encephalomyelitis
EBV	Epstein-Barr virus
ECM	Extracellular matrix
ECs	Endothelial cells
ECT	Electroconvulsive therapy
ELISA	Enzyme-linked immunosorbent assay
EPDS	Edinburgh Postnatal Depression Scale
FGF2	Fibroblast growth factor 2
FGFR	Fibroblast growth factor receptor
GBS	Group B Streptococci
GCRs	Glucocorticoid receptors
GFAP	Glial fibrillary acidic protein
GLC	Granular cell layer
GPCRs	G-protein couple receptors
GWA	Genome-wide association
HBMECs	Human brain microvessel endothelial cells
HPA	Hypothalamo-pituitary-adrenal

HRP	Horse radish peroxidase,
ICAM-1	Intercellular adhesion molecule-1
IDO	Indoleamine 2,3-dioxygenase
IFA	Incomplete Freund's adjuvant
IFN-β	Interferon-beta
IFNR	Interferon receptor
IFN-α	Interferon-alpha
IFN-γ	Interferon gamma
Ig	Immunoglobulin
IL	Interleukin
IL-10	Interleukin-10
IL-12	Interleukin-12
IL-13	Interleukin-13
IL-17	Interleukin-17
IL-1α	Interleukin-1alpha
IL-1β	Interleukin-1beta
IL-2	Interleukin-2
IL-22	Interleukin - 22
IL-4	Interleukin-4

IL-5	Interleukin-5
IL-6	Interleukin-6
IL-8	Interleukin-8
ISF	Interstitial fluid
JAMs	Junctional adhesion molecules
KA	Kynurenic acid
LB	Lysogeny broth
LDL	Low density lipoprotein
L-KYN	Kynurenine
LPS	Lipopolysaccharide
LTD	Long term depression
LTP	Long term potentiation
L-TRP	L-tryptophan
LTB	Lymphotoxin- β
MAdCAM	Mucosal addressin cell adhesion molecule
MADRs	Montgomery-Åsberg Depression Rating Scale
MAF	Macrophage angiogenic factor
MBP	Myelin basic protein
M-CSF	Macrophage colony-stimulating factor

MHC	Major histocompatibility complex
ML	Molecular layer
MMP	Matrix metalloproteinases
MOG	Myelin oligodendrocyte glycoprotein
MR	Mannose receptor
MRS	MR spectroscopic
MS	Multiple sclerosis
Mt	Mycobacterium tuberculosis
NAA	N-acetylaspartate
NE	Norepinephrine
NK cells	Natural killer cells.
NKT-cells	Natural killer T cells
NMDA	<i>N</i> -methyl-D-aspartate
NO	Nitric oxide
NODs	Nucleotide-binding oligomerization domains
NPCs	Neuronal progenitor cells
NRIs	Noradrenaline reuptake inhibitors
OCPs	Osteoclast precursors
OPG	Osteoprotegerin

OVLT	Organum vasculosum of the lamina terminalis
PAMPs	Pathogen-associated molecular patterns
PB	Phosphate buffer
PBS	Phosphate buffered saline
PCR	Polymerase chain reaction
PECAM-1	Platelet-endothelial cell adhesion molecule
PI	Propidium iodide
PLP	Proteolipid apoprotein
PRRs	Pattern recognized receptors
PSGL-1	P-selectin glycoprotein ligand-1
PVN	Paraventricular nucleus
QUIN	Quinolinic acid
RA	Rheumatoid arthritis
RANKL	Produce receptor activator of nuclear factor- κ B ligand
RPE	R-Phycoerythrin
RT-PCR	Reverse-transcriptase polymerase chain reaction
SAS	Subarachnoid space
sEPSC	excitatory postsynaptic currents
SERT	Serotonin transporter

SFO	Subfornical organ
SGZ	Subgranular zone
sIPSC	Inhibitory postsynaptic currents
SPECT	Single photon emission computed tomography
SRs	Scavenger receptors
SSRI	Serotonin re-uptake inhibitors
SVZ	Sub-ventricular zone
Tc	Cytotoxic T
TCRs	T-cell receptors
TEA	Tris-acetate-EDTA buffer
TGF-β	Transforming growth factor beta
Th	Helper T cells
Th1	Type 1 helper T cells
Th17	Type 17 helper T cells
Th2	Type 2 helper T cells
TID	TNF-induced demyelination
TJs	Tight junctions
TLRs	Toll-like receptors
TMB	3,3',5,5'-tetramethylbenzidine

TMEV	Theiler's murine encephalomyelitis virus
TNBS	2,4,6-trinitrobenzene sulfonic acid
TNFR I	Tumor necrosis factor receptor I
TNFR II	Tumor necrosis factor receptor II
TNFRs	Tumor necrosis factor receptors
TNF-α	Tumor necrosis factor-alpha
TNF-β	Tumor necrosis factor beta
TUNEL	Terminal deoxynucleotidyl transferase dUTP nick end labeling
VCAM-1	Vascular cell adhesion molecule-1
VE	Vascular endothelial
VEGF	Vascular endothelial growth factor
VEGFR1	Vascular endothelial growth factor receptor 1
VEGFR2	Vascular endothelial growth factor receptor 2
ZO-1	Zonular occludins-1

Chapter 1

Introduction

1.1 Immune system

1.1.1 Overview of immune system

The immune system is a complex network of cells and molecules that has a fundamental role in homeostasis and in defending against infection and cancer. The immune system can be functionally divided into two categories, namely innate immunity and adaptive immunity, which usually work together to eliminate pathogens (Delves and Roitt, 2000a). Innate immunity is the first line of nonspecific immune defence, which involves phagocytic cells, including macrophages, neutrophils, basophils, mast cells, eosinophils, and natural killer (NK) cells. These cells bind to invading microorganisms using pattern recognized receptors (PRRs), which recognize a large number of molecules that share a common structural motif or pattern (Medzhitov, 2007). There are two main families of PRRs, which are the toll-like receptors (TLRs) and the nucleotide-binding oligomerization domains (NODs) (Martinon and Tschopp, 2005). The ligands of PRRs on phagocytes are pathogen-associated molecular patterns (PAMPs), which are usually conserved microbial structures with repeat sugar or amino-acid motifs that do not occur on mammalian cells. Constituents of bacterial walls, including lipopolysaccharide (LPS), peptidoglycan, lipoteichoic acids and cell-wall lipoproteins are common bacterial PAMPs (Medzhitov, 2007). Phagocytes internalize and destroy pathogens by the process including phagocytosis followed by fusion of the phagosome with a lysosome containing proteolytic enzyme resulting in microbial lysis. The molecular components of innate immunity include complement, acute-phase proteins and cytokines including interferon (Medzhitov and Janeway, 2000).

Adaptive immunity, by contrast, is a highly specific response that can recognise any antigenic epitopes on a particular pathogen. The adaptive immune response involves antigen recognition by lymphocytes, which are T cells and B cells. The main subsets of T cells function either as effector or cytotoxic T (Tc) cells that directly attack the pathogens, or as helper T (Th) cells that enhance immune response. B cells function mainly to produce antibodies that are stimulated by, are conditioned by and can bind to antigens. When antibodies bind to a pathogen, the antibody can cause the activation of the complement system and

assist phagocytosis by innate cells to internalize the pathogen and destroy this by enzyme lysis. Both T cells and B cells originate from pluripotent stem cells in the fetal liver and in the bone marrow. The bone marrow-resident stem cells develop to be B cells, while those that travel to the thymus develop into T cells (Delves and Roitt, 2000b).

The activation and the proliferation of antigen-specific T and B cells (clonal expansion) occur in the secondary lymphoid tissues such as lymph nodes, spleen, and mucosa-associated lymphoid tissue. B cells migrate to germinal centre, where B cells hyper-mutate the variable region of their immunoglobulin genes and undergo class switching, leading to the production of diversity of specific antibodies. Each B cell has a unique antigen receptor, called the B cell receptor (BCR), which is activated by its specific antigen in the context of an antigen-presenting cell. This leads to a differentiation and maturation of B cells into plasma cells that secrete specific antibodies with the same specificity as their antigen receptor (Kuppers, 2005) .

The clonal expansion of T cells occurs in the peri-arteriolar lymphoid sheaths of the lymph node (Delves and Roitt, 2000b). The professional antigen presenting cells (APCs), including dendritic cells, B cells and macrophages present antigen to naïve T cells in the context of the major histocompatibility complex (MHC) (Carter, 2000). B cells present antigens to T cells via their membrane-bound antibodies, while dendritic cells and macrophages pinocytose antigens and process them internally by combining antigen fragments into an assembling major histo-compatibility complex (MHC) and present to T cells in that context. These APC cells, particularly dendritic cells, express co-stimulatory molecules such as CD28 (the B7 ligand), CD154 (the CD40 ligand), and CD2 (the CD58 ligand). These co-stimulatory molecules that bind to the appropriate ligands expressed on T cells generate signals that are essential for T cell activation (Delves and Roitt, 2000b). T cells express T-cell receptors (TCRs) that recognize specific antigen. T cell antigen recognition, in the context of the MHC presentation, results in clonal proliferation of T cells expressing the same TCR that target the specific antigen. T cells expressing the CD4 molecule recognize antigens presented by MHC class II, and usually act as helper T cells. CD4 T cells can be divided in 2 major types (Mosmann and Sad, 1996). Type 1 (Th1) helper T cells function to enhance bactericidal activity of phagocytic cells such as

macrophages by producing cytokines such as interleukin-2, interferon gamma (IFN γ). Type 2 (Th2) helper T cells function to help B cell differentiation and the production of antibodies by releasing growth and differentiation cytokines such as interleukin-4 (IL-4), interleukin-5 (IL-5), interleukin-6 (IL-6), and interleukin-10 (IL-10). There are further subdivisions of T helper cell subsets characterised largely by the function of the characteristic cytokine they produce, for example Th-17 cells produce interleukin-17 (IL-17) that promotes autoimmunity. T cells expressing CD8 molecule recognize antigens presented by MHC class I, and usually function as cytotoxic killer T cells. CD8⁺ cytotoxic T (Tc)-cells that recognize and directly bind and destroy cells that are infected with viruses, and CD3/56/16⁺ NKT-cells that recognise conserved microbial and cancer-related glycolipid structures presented in the context of CD1 (Delves and Roitt, 2000b).

Antigen presentation to naïve lymphocytes during the primary immune response also generates memory T and B cells, which are characterized by the expression of CD45RO on their cell surface. After a subsequent encounter with the same antigen, the secondary immune response initiated by memory lymphocytes is more rapid than the primary immune response. In addition, the secondary immune response is quantitatively and qualitatively more sophisticated than the primary immune response. For example, memory lymphocytes enhance proliferation of specific T cells in larger numbers, and B cells to produced higher concentrations and producing higher affinity antibodies during the secondary immune response compared to those in the primary immune response (Parkin and Cohen, 2001).

1.1.2 Cytokines

Cytokines are a group of small peptides that are responsible for the communication between cells of the immune system. Cytokines are secreted by all cell types, especially lymphocytes and monocytes/macrophages, for example in response to pathogens (Marshall, 1992), and are recognised by cells that have cell membrane receptors for that cytokine in order to respond. Cytokines are structurally varied, but may share several characteristics. For example, the same cytokine may be generated from various cell types, and have differing effects on several different cell types. Individual cytokines seldom function in

isolation. They tend to work in networks and can function synergistically or antagonistically, which regulate positively and negatively other cytokine production or function. Most cytokines function locally in the tissue where they were produced, either affecting the function of the cell type that produced it (autocrine action), or binds to its receptor in nearby cells and affects their function (paracrine action). In addition, each set of immune cells synthesise a particular group of cytokines, depending on the type of cell and whether, and how, it has been stimulated (Tayal and Kalra, 2008). Pro-inflammatory cytokines, including interleukin 1beta (IL-1 β), interleukin 6 (IL-6), tumour necrosis factor - alpha (TNF- α), are produced from mononuclear cells such as macrophages in response to infection, inflammation and tissue damage (Haddad, 2002). TNF- α is one of the most potent cytokines because it up-regulates other cytokines, such as IL-1, IL-6, and some chemokines which can direct the cellular and behavioural signs of infection and inflammation, including fever and increasing the serum acute phase protein concentrations. TNF- α also stimulates the cell surface expression of the major histocompatibility antigens.

The TNF- α receptor consists of two cell surface receptor proteins (p55, p75). This receptor complex can be shed from the cells surface and in this soluble form can bind TNF- α and prevent its inflammatory function. This observation has been developed for translational purposes, and the use of a recombinant form of the soluble tumour necrosis factor receptor as a TNF- α antagonist is now an effective therapeutic for autoimmune disease such as rheumatoid arthritis (O'Shea et al., 2002).

Cytokines produced from lymphocytes are sometimes called lymphokines. They are non-immunoglobulin polypeptide substance produced by T cells and natural killer cells that regulate the functions of other cells. Lymphokines, including IL-2, interferon-gamma (IFN- γ), interleukin-12 (IL-12) and tumor necrosis factor beta (TNF- β) are produced from Th1 cells (Tayal and Kalra, 2008). IFN- α is produced by phagocytes (monocyte and granulocyte), while IFN- β is produced mainly by stromal cells fibroblasts and epithelial cells. IFNs are produced in response to viral infection and function to inhibit viral replication and destroy cancer cells. IFNs, particularly interferon-alpha (IFN- α), are used widely as immunotherapy for cancers, hepatitis B and C (Jaeckel et al., 2001).

Th2 cells produce IL-4, IL-5, IL-6, IL-10, and IL-13, and the production of these Th2 cytokines is inhibited by Th1 cytokines such as IL-12 and IFN- γ . IL-4 and IL-10 promote humoral immunity by stimulating the growth and activation of mast cells and eosinophils, and the differentiation of B cells into antibody-secreting B cells. In addition, IL-4 and IL-10 are considered to be major anti-inflammatory cytokines since they inhibit macrophage activation, T-cell proliferation and the production of pro-inflammatory cytokines (Opal and DePalo, 2000).

1.1.3 Chemokines

Chemokines are a large family of structurally homologous cytokines that regulate trafficking of various types of leukocytes from the blood to tissue by recognition of a concentration gradient. They are small (8-10 kDa) secreted proteins that are divided into four groups, namely XC, CC, CXC and CX3C, based on the number and location of the two N-terminal cysteine residues (Fernandez and Lolis, 2002). There are approximately 50 chemokines recently identified and all of them can regulate leukocyte migration. Leukocytes are the major source of CC and CXC chemokines, but these are also produced by various cell types, such as endothelial cells, epithelial cells, and fibroblasts. Various CC chemokines are also produced by antigen activated T cells, acting as a connection between adaptive immunity and recruitment of inflammatory leukocytes (Slettenaar and Wilson, 2006). Chemokine production is mainly induced by pro-inflammatory cytokines IL-1, IL-2, TNF- α , γ -interferon and the bacterial product LPS, while TGF- β , IL-4, IL-10 can inhibit chemokine production (Rottman, 1999a). Chemokines are divided functionally into two major categories; housekeeping chemokines and inflammatory chemokines. Housekeeping chemokines, including CCL25, CCL17, CCL 27, CCL19, CCL21 and CXCL12, are homeostatic and constitutively produced and secreted. They regulate the trafficking of lymphocytes and dendritic cells to the lymphoid tissues (Graham, 2009). They also function to co-localize B and T cells with antigen on the surface of antigen presenting cells in the lymphatic system (Fernandez and Lolis, 2002). Inflammatory chemokines, including CCL1, CCL2, CCL3, CCL4, CCL5 and CXCL1, CXCL2, CXCL3, CXCL4, CXCL5, CXCL6, CXCL7, CXCL8, CXCL9, CXCL10 and CXCL11, are produced by various cells in response to inflammatory stimuli and induce the migration of leukocytes to these sites of inflammation. In the

inflammatory process, CXCL1, CXCL2, CXCL3, CXCL4, CXCL5, CXCL6, CXCL7, CXCL8 regulates neutrophil trafficking and CXCL9, CXCL10, CXCL11 regulate activated T-cell trafficking (Graham, 2009). The CC chemokines function mainly on monocytes, macrophages, lymphocytes, and eosinophils (Adams and Lloyd, 1997). Chemokines function by interacting with chemokine receptors containing seven-transmembrane α -helical domains, which belongs to the family of G-protein couple receptors (GPCRs). These consist of single polypeptide chains with three extracellular and three intracellular loops, an acidic amino-terminal domain involved in ligand binding, and a serine/threonine-rich intracellular carboxy terminal domain (Mantovani et al., 2006). The amino acid sequence DRYLAIV in the second intracellular loop domain is the unique structure characteristic of chemokine receptors (Rottman, 1999b). Ten signalling receptors for the CC chemokines (CCR1, CCR2, CCR3, CCR4, CCR5, CCR6, CCR7, CCR8, CCR9, CCR10), seven CXCR chemokine receptors (CXCR1, CXCR2, CXCR3, CXCR4, CXCR5, CXCR6, CXCR7) and single receptor for XC and CX3C families are identified so far (Graham, 2009). Multiple chemokine ligands can bind to the same receptor. For instance, CCR1 is able to bind ten ligands with high affinity, while CCR3 has fifteen specific ligands (Rottman, 1999b). There is another group of chemokine receptors called silent chemokine receptors, which do not induce signal transduction due to alterations in the canonical DRYLAIV motif found in the second intracellular loop of the signalling chemokine receptor. The group of silent receptors are Duffy antigen receptor for chemokines (DARC), D6 (or CCBP2), CCX-CKR (or CCRL1) regulate inflammatory and immune response by various mechanisms, including acting as decoy receptors and as scavenger receptors (Graham, 2009); (Heinzel et al., 2007). For example, the D6 receptor has a role in the resolution of inflammation by binding chemokines that are expressed only in response to inflammatory stimuli (Mantovani et al., 2006).

1.2 Rheumatoid Arthritis

Rheumatoid Arthritis (RA) is a systemic chronic inflammatory disease characterized by joint pain, stiffness, and swelling. There are associated remodelling changes including pannus formation and destruction of cartilage, bone and associated soft tissue (Klareskog et al., 2009). These pathological features eventually lead to disability. The annual incidence of RA has been reported to be around 20 to 50 cases per 100,000 of the population. Women are affected up to three times as often as men (Tobon et al., 2010). The immunopathogenesis of RA is complex and appears to involve primarily auto-immune mechanisms. IgM, IgA and IgG subclasses 1-4 anti-citrullinated protein antibodies (ACPA), anti-keratin antibodies (AKA), anti-perinuclear factor (APF) and anti-RA33 antibodies are elevated in the serum of RA patients, and their titres have also been associated with severity of the disease. These rheumatoid factors and auto-antibodies can also be used to predict the development of RA in early arthritis (Lin and Li, 2010); (Agrawal et al., 2007); (Nell et al., 2005). The major component of the RA pannus is hypertrophic synovial membrane, which consists of hyperproliferation of Type A synoviocytes (macrophage-like synovial cells) and Type B synoviocytes (fibroblasts-like synoviocytes) along with immune cells that infiltrate the synovial membrane. T cells can constitute up to 50 % of cells in RA synovial and most of these are CD4⁺ CD45RO⁺ memory T cells. Only 5% or fewer are B lymphocytes or plasma cells. Rheumatoid factors, ACPA and anti-collagen antibody are also found in synovial tissue (Bartok and Firestein, 2010). RA is considered as a non-organ-specific autoimmune disease. This is because subcutaneous nodules, vasculitis, pulmonary fibrosis are common complication of RA (Williams, 2006).

1.2.1 *Aetiology of RA*

The aetiology of RA remains undefined. Both genetic factors and environmental factors contribute to the cause of the disease.

A major risk factor that links genetic susceptibility and RA is the association of the disease with an antigenic epitope in the HLA-DR β -chain that is shared with microbial antigens. This shared epitope is a highly conserved amino acid sequence (QKRAA) at residues 67, 70, 71, 72 and 74, which have been associated

with severe RA. It is located in the third hypervariable region of DR4, DR14 and DR1 β -chains that are expressed on macrophages, B cells and antigen presenting cells. The 65 kD heat shock protein from *Mycobacterium tuberculosis* and 40kd-*Escherichia coli* dnaJ, and Epstein-Barr virus (EBV) gp110 also contain the shared epitope (QKRAA) on DR β 1*0401 (Albert and Inman, 1999); (Toussirot and Roudier, 2008). The RA-associated HLA alleles are members of HLA-DRB1*0404 group (e.g. *0401, *0404, *0405, *0408, HLA-DRB1*0101, HLA-DRB1*0102, HLA-DRB1*1402 and HLA-DRB1*1001 (Holoshitz, 2010).

Several genetic polymorphisms associated with RA have been identified by genome-wide association (GWA) studies. Several population studies have demonstrated an association between a missense SNP in the PTPN22 gene, which encodes a phosphatase involved in intracellular T cell signalling, with an increased risk and rate of progression of RA (Lie et al., 2007, Begovich et al., 2004). In addition, other genetic polymorphisms of various cytokine and cytokine-receptor genes, such as those encoding TNF, IL-1, IL-10 and IL-18, have been studied intensively in RA. For example, a -857C/T SNP at the TNFA promoter has been associated with RA and with better responses to etanercept (recombinant human soluble TNF receptor) therapy (Kang et al., 2005).

A strong association between cigarette smoking and the presence of HLA-DRB1*0404 or other HLA alleles comprising the shared epitope has been reported for the ACPA-positive group of RA patients. One epidemiological study demonstrated that the relative risk of developing RA was increased 20-fold in the ACPA-positive group of RA patients who had two alleles for the shared epitope and had ever smoked cigarettes (Klareskog et al., 2006). It is possible that smoking can induce citrullination in certain proteins in the lungs. These citrullinated proteins activate the immune response by binding specifically to HLA-DR molecules comprising the shared epitope on antigen-presenting cells, which eventually result in the production of ACPA. These antibodies to citrullinated protein can contribute to the development of RA in the joint (Klareskog et al., 2009).

A twin study in heritability demonstrated that the genetic contribution to RA accounted for 50-60% of the variation in liability to disease, suggesting that

environmental factors, such as smoking, are also major contributors to RA (MacGregor et al., 2000). In addition, several viral and bacterial infections, including the Epstein-Barr virus (EBV), parvovirus and lentiviruses, and bacteria including *Mycoplasma*, *Mycobacteria* and *Yersinia* species, can be risk factors for the development of RA. Other environmental factors including breast feeding, oral contraceptives use, or regular alcohol consumption may be protective against the development of RA (Liao et al., 2009).

1.2.2 Pathogenesis of RA

The activation of T lymphocytes, particularly the CD4⁺ helper Th1 subset, is part of the initiation of the destructive immune response in RA (McInnes and Schett, 2007). These cells infiltrate the synovial membrane and are activated by antigen presenting cells (e.g. dendritic cells and B cells). Along with antigen presented in the context of MHC, additional co-stimulation, such as CD28-B7 receptor family (CD80/86), is necessary for T cell activation. Activated Th1 cells produce cytokines including IL-2, IFN γ and TNF- α . These Th1 cytokines stimulate monocytes, macrophages, and synovial fibroblasts to produce IL-1, IL-6 and TNF- α and to secrete matrix metalloproteinases (MMPs). Activated Th1 cells also stimulate B cells, via CD40 ligand mediated co-stimulation, to produce rheumatoid factor and auto-antibodies. Immune complexes, formed by auto-antibodies, induces macrophage to produce TNF- α by complement activation (Klareskog et al., 2009). These activated macrophages, lymphocytes and fibroblasts can also stimulate angiogenesis by activating synovial cells to produce angiogenic factors, such as macrophage angiogenic factor (MAF), vascular endothelial growth factor (VEGF), prostaglandins E1 and E2, IL-8 and angiopoietin-1 (Szekanecz et al., 2009). Endothelial cells in the synovium are activated and adhesion molecules such as intercellular adhesion molecule-1 (ICAM-1), vascular cell adhesion molecule-1 (VCAM-1), P-selectin, and E-selectin, are upregulated to promote the recruitment of immune cells into the joint. Activated Th1 cells and synoviocytes also produce receptor activator of nuclear factor- κ B ligand (RANKL) and macrophage colony-stimulating factor (M-CSF). These two cytokines promote the differentiation of osteoclast precursors (OCPs) into mature osteoclasts that have bone-resorbing activity. RANKL expression is also regulated by TNF- α , IL-1 β , IL-6 and IL-17. The activity of RANKL is inhibited by osteoprotegerin (OPG), a soluble decoy receptor that belongs to the TNF-

receptor superfamily. TNF- α and IL-1 β also induce chondrocytes and fibroblasts to produce a disintegrin and metalloproteinase with thrombospondin motifs (ADAMTS) and MMPs, which degrade proteoglycan and collagen in the cartilage (McInnes and Schett, 2007).

1.2.3 Roles of cytokines in RA

1.2.3.1 Roles of pro-inflammatory cytokines in RA

Cytokines play major roles at each stage of the pathogenesis of RA by regulating autoimmunity, chronic inflammatory synovitis and the destruction of joint tissue. Several cytokines, including granulocyte macrophage colony-stimulating factor (GM-CSF), IL-1, IL-6, IL-2, IL-12, IL-15, IL-13, IL-17, IL-18, IFN γ , TNF α , and TGF- β interact in a complex network contributing to RA pathogenesis (McInnes and Schett, 2007). TNF- α , IL-1 and IL-6 are considered as principle cytokines that regulates each stage of the pathogenesis of RA. Antibodies against these cytokines, especially TNF- α and their receptor antagonists are major therapeutic targets for RA drug development (Seymour et al., 2001). TNF- α (Cope et al., 1992), IL-1 (Wood et al., 1983) and IL-6 (Waage et al., 1989) and their receptors are highly expressed in the inflamed synovial membrane tissue in RA patients and synovial macrophages are the major source of these pro-inflammatory cytokines (Brennan and McInnes, 2008). TNF- α is a pro-inflammatory cytokine that is highly expressed on macrophages and T cells. TNF- α acts by binding to TNF receptors, namely TNFR1 (p55) and TNFR2 (p75) (H. E. Seymour 2001). There are also soluble forms of TNFR that function to modulate inflammatory response by inhibiting TNF- α activity. These soluble forms of TNFRs, including p75 have been developed to be efficient therapy for arthritis such as etanercept or anti-TNF- α ; Infliximab (Seymour et al., 2001). TNF- α initiates the immune response by inducing the production of other pro-inflammatory cytokines, including IL-1 β , IL-6, IL-23 and GM-CSF from antigen presenting cells. IL-1 β also has been implicated in pathological mechanism of RA (Abramson and Amin, 2002), although so far to date it has not been well developed as powerful treatment for RA (Brennan and McInnes, 2008). There are 2 distinct IL-1 receptors, namely type I and type II (Sims et al., 1988). Type I IL-1R is expressed predominately on T cells and fibroblasts, while Type II IL-1R is expressed on activated T cells, B cells, monocytes and neutrophils (McMahan et al., 1991). IL-1 β and TNF- α have

synergistic effects on the process of inflammatory joint destruction of RA. However, TNF- α seems to play the main role in synovial inflammation, while IL-1 β seems to regulate mainly bone erosion and cartilage damage (Zwerina et al., 2007). IL-6 is produced by fibroblasts, activated T cells, activated monocytes or macrophages and endothelial cells (Van Snick, 1990). IL-6 signals via IL-6 receptor, which is a complex of receptor subunits and two signal-transducing gp130 subunits (Jones et al., 2006). IL-6 can regulate the humoral immune response by activating B-cell maturation and the production of auto-antibodies (Dayer and Choy, 2010). In addition, IL-6 also enhances the acute phase response during inflammation by stimulating production of the full range of acute phase proteins in hepatocytes (Dayer and Choy, 2010). In addition, IL-6 also contributes to other inflammatory pathways of RA including osteoclast activation, pannus formation, and mediating chronic synovitis (Dayer and Choy, 2010). IL-1 β , TNF- α and IL-6 share many similar activities and have synergic effects on several pathological pathways of RA, including the ability to enhance cytokine production, proliferation of T cells and B cells, and MMP production by synovial cells and chondrocytes. They also enhance the leukocyte recruitment process by activating the production of chemokines, including CCL5, CCL2, CCL8, and CCL12, together with adhesion molecules such as E-selectin and VCAM-1 on endothelium (Brennan and McInnes, 2008).

1.2.3.2 Roles of T cell derived cytokines in RA

Cytokines of T helper subsets play crucial roles in the regulation of the adaptive immune responses and the immuno-pathology of rheumatoid arthritis. CD4⁺T cells are divided on the basis of cytokine secretion patterns and effector functions into 2 distinct CD4⁺T cells subset, namely Th1 and Th2 cells. Th1 (IL-2, IFN- γ and IL-12) cytokines mediate macrophage-dependent inflammation and delayed-type hypersensitivity reactions (Schulze-Koops and Kalden, 2001), whereas Th2 (IL-4, IL-5, IL-10, IL-13) cytokines play important roles in antibody-mediated allergic reactions and macrophage deactivation (Kozanidou et al., 2005); (Xu et al., 2008).

1.2.3.2.1 Role of Th1 cell cytokines in RA

The chronically inflamed RA synovial membrane is characterized by an accumulation of infiltrating CD4⁺T cells, which are predominately of the Th1 phenotype (Dolhain et al., 1996). These Th1 cells and effector cytokines, including IL-2, IL-12 and IFN- γ produced by these Th1 cells are thought to play a pathogenic role in the immunopathology of RA. IL-2, IL-12 and IFN- γ were found to be highly expressed in synovial fluid, synovial tissue and peripheral blood of RA patients (Berner et al., 2000); (Canete et al., 2000); (Morita et al., 1998). IL-2, IL-12 and IFN- γ are considered as important regulatory cytokines for different stages of the pathogenesis of RA. IFN- γ produced mainly by activated T-cells and NK cells is considered to be a major effector Th1 cytokine (Farrar and Schreiber, 1993). IFN- γ and its IFN- γ receptor are known to function as a pro-inflammatory cytokine complex in RA (Tsuda et al., 2009). IFN- γ activates macrophages (Nathan et al., 1983), enhancing the ability of antigen presentation via up-regulation of MHC class II expression in various cell types (Jahn et al., 1987). In addition, IFN- γ also promotes the production of IgG2a in mouse and IgG1 in human, which are involved in antibody-dependent cell cytotoxicity (Schulze-Koops and Kalden, 2001); (Finkelman et al., 1988).

IL-2 acts via the IL-2 receptor (CD25, IL-2R) and has a major role in clonal expansion of antigen-primed T cells (Schroeter and Jander, 2005). However, IL-2 has also been reported to activate apoptosis of antigen activated T cells in IL-2 deficient mice. This suggests that IL-2 also functions as a regulator of immune homeostasis following antigen clearance (Refaeli et al., 1998). The actual role of IL-2 in arthritis has not been well elucidated. Studies in experimental arthritis demonstrated that IL-2 could have both direct pro-inflammatory effects and indirect anti-inflammatory effects mediated by IFN- γ on the severity of arthritis disease (Thornton et al., 2000).

IL-12 is a 70-kd disulfide-linked heterodimeric cytokine comprising p40 and p35 chains that produced mainly by macrophage-lineage cells and dendritic cells (Malfait et al., 1998). IL-12 binds with IL-12 receptors consisting of 2 subunits designed IL-12B1 and IL-12B2 (Presky et al., 1996). IL-12 has a vital role in cell mediated immunity by inducing differentiation of T cell precursors into the Th1 phenotype (Malfait et al., 1998). In addition, IL-12 also stimulates the

proliferation of activated T and NK cells and the production of IFN- γ by both T and NK cells (O'Garra and Arai, 2000). However, the role of IL-12 in the pathological mechanism of RA is still unclear. The administration of IL-12 to the CIA mouse model of RA has been reported to dramatically attenuate the severity of arthritis disease (Malfait et al., 1998). In contrast, the induction of collagen-induced arthritis (CIA) in IL-12 deficient mice has been reported to increase the severity of arthritis, suggesting that IL-12 paradoxically mediates protection from autoimmune inflammation (Murphy et al., 2003).

1.2.3.2.2 Role of Th2 cell cytokines in RA

Th2 cell cytokines, including IL-4, IL-5, IL-10 and IL-13 play a crucial role in the humoral immune response; including stimulating maturation of B lymphocytes into plasma cells, stimulating immunoglobulin class switching from IgM to IgE and IgG1 (in mouse) or IgG4 (in man) isotypes, promoting allergic immune responses and eosinophil activation (Schulze-Koops and Kalden, 2001); (Kurowska-Stolarska et al., 2008); (Punnonen et al., 1993); (Pope et al., 2001).

IL-4 and IL-10 have been reported to play protective roles in autoimmune disease (Schulze-Koops and Kalden, 2001). Increases in IL-10 concentrations in the peripheral blood and serum have been reported in RA patients compared with healthy controls. IL-4 mRNA and IL-4 producing T cells were detectable at low levels in the synovial fluid of RA patients. The major cellular sources of IL-10 are T cells, B cells, and monocytes/macrophages, whereas IL-4 is mainly produced by Th2 cells. In RA, IL-10 can be produced by cells in the synovial membrane. IL-10 functions via the IL-10 receptor which is composed of at least two subunits that are members of the interferon receptor (IFNR) family (Moore et al., 2001). IL-4 acts through the IL-4 receptor, which is a receptor complex consisting of IL-4R α chain and γ chain (Nelms et al., 1999). IL-4 and IL-10 have been shown to prevent autoimmunity by inhibiting Th1 proliferation, synovial inflammation and tissue destruction in RA (Schulze-Koops and Kalden, 2001). IL-4 and IL-10 can down-regulate the production of IL-1 and TNF- α by peripheral blood monocytes and by synovial tissue from RA patients (Briolay et al., 1992); (de Waal Malefyt et al., 1991). Importantly, IL-4 and IL-10 also function to down-regulate the production of Th1 cytokines IFN- γ and IL-2, and to suppress their cell-mediated immune response (Romagnani, 1994). The combination of IL-4 and

IL-10 has been shown to reduce severity of arthritis and protect cartilage degradation in experimental arthritis (Joosten et al., 1997). An imbalance of Th1/Th2 cytokine has been proposed to play an important role in the pathogenesis of rheumatoid arthritis (Canete et al., 2000). Therefore IL-4 and IL-10 seem to be potential therapeutic agents for RA.

IL-5 and/or IL-13 play an important role in allergic asthma and helminthic infection (Kurowska-Stolarska et al., 2008); (Artis et al., 1999). IL-5 is produced mainly by Th2 cells and mast cells (Gregory et al., 2003), while IL-13 is produced by T cells, mast cells, basophils, dendritic cells, and keratinocytes (Schmid-Grendelmeier et al., 2002). IL-13 acts via the IL-13R α 1 and IL-13R α 2 (Mentink-Kane and Wynn, 2004), while IL-5 function is via the IL-5 receptor consisting of IL-5 α and IL-5 β subunits. Both IL-13 and IL-5 function mainly to regulate eosinophil trafficking and activation (Pope et al., 2001); (Ogata et al., 1998). Little is known about their role in the immuno-pathogenesis of RA. Both clinical and experimental arthritis studies showed that IL-5 and IL-13 may play a crucial role during the development of arthritis. Increases in IL-13 and IL-5 protein levels have been reported in synovial fluid of RA patients and up-regulation of serum IL-5 has been reported in experimental arthritis during the early stages and onset of disease (Hitchon et al., 2004); (Schaefer et al., 1999). Both IL-13 and IL-5 have been reported to exacerbate the severity of arthritis by promoting IgE and IgG antibody isotype switching by B cells in CIA mice (Xu et al., 2008).

1.2.3.3 Roles of chemokines in RA

Chemokines and their receptors play crucial roles in RA pathogenesis mainly via the recruitment of leukocytes to the inflamed joint (Iwamoto et al., 2008). Recent studies also suggest that chemokines also play important roles in the destruction of bone and cartilage and fibroblast proliferation.

CXCL1 (Lisignoli et al., 1999); (Bischoff et al., 2005), CXCL8 (Kraan et al., 2001), CXCL5 (Koch et al., 1995), CXCL9, CXCL10 (Kuan et al., 2010), CCL2 (Szekanecz et al., 2003), CCL5 (Yang et al., 2009) and CCL3 (Katschke et al., 2001) are elevated in the synovial fluid and in serum of RA patients. Synovial macrophages, T cells, synoviocytes and chondrocytes produce various chemokines stimulated mainly by IL-1 β , TNF- α and IFN- γ , and bacterial

lipopolysaccharide (LPS) (Iwamoto et al., 2008). CXCL1 functions as a potent neutrophil chemo-attractant by binding both CXCR1 and CXCR2 receptors (Luttichau, 2010). CXCL1 has been reported in osteoblasts and in synovial fluid from rheumatoid arthritis patients (Lisignoli et al., 1999); (Bischoff et al., 2005). CXCL1 has also been reported to regulate angiogenesis during the inflammatory process (Barcelos et al., 2004). This group of C-X-C chemokines can bind to the same receptor CXCR2 (Charo and Ransohoff, 2006), and blocking the CXCR2 receptor has been reported to inhibit the development of experimental arthritis (Barsante et al., 2008); (Lusitani et al., 2003). CCL2, CCL5 and CCL3 are potent chemokines that function predominantly by recruiting and activating monocytes, Th2 cells, B cells, NK cells, basophils, eosinophils and memory T lymphocytes. CCL2 and CCL5 can stimulate chondrocytes to produce MMP, increase proteoglycan release and inhibit proteoglycan synthesis by chondrocytes (Borzi et al., 2000). CXCL9 and CXCL10 function as potent T-lymphocyte chemotactic factors by binding into the receptor CXCR3, preferentially on the Th1-lymphocyte subset. In addition, CXCL10 induced RANKL expression in CD4+ T cells, which promote bone resorption by inducing osteoclast formation and survival (Lee et al., 2009). Fibroblast-like synoviocyte proliferation is also induced by CXCL10 and CXCL9 and CCL13, leading to synovial hyperplasia (Garcia-Vicuna et al., 2004).

1.2.3.4 The role of growth factors in RA

Joint destruction in RA is mediated mainly by pannus formation (McGonagle, 2010). Changes in the synovium during the formation of pannus are characterized by neovascularisation, inflammatory cell infiltration and synovial hyperplasia (Brenchley, 2001). The initiation of the pannus formation process, including angiogenesis and synovial hyperplasia in RA, is mainly regulated by angiogenic growth factor such as fibroblast growth factor 2 (FGF2) and vascular endothelial growth factor (VEGF) (Roccaro et al., 2005). Fibroblast growth factor 2 is a wide-spectrum mitogenic, angiogenic, and neurotrophic factor that binds to FGF receptors (FGFR) and regulates various biological processes, including embryogenesis, wound healing, angiogenesis, and maintenance of neuronal networks (Manfe et al., 2010). In RA, mast cells and vascular cells are the major sources of FGF2 (Qu et al., 1995). FGF2 functions mainly in mediating cartilage and bone destruction and synovial hyperplasia in RA (Qu et al., 1995). FGF2 also

has a role in angiogenesis and recruitment of immune cells into the inflamed site (Malemud, 2007). Another growth factor that is also found highly expressed in synovial tissue of RA patients is VEGF (Nagashima et al., 1995). VEGF is a potent angiogenic factor that functions via tyrosine kinase receptors, VEGFR1 (also known as Flt-1) and VEGFR2 (also known as KDR/flk-1) (Malemud, 2007). The major cellular sources of VEGF in RA are macrophages, fibroblasts surrounding microvessels, vascular smooth muscle cells and synovial lining cells (Nagashima et al., 1995). VEGF not only has a crucial role in neovascularisation in pannus formation, but also stimulates endothelial progenitor cells and regulates the recruitment of leukocytes (Kim et al., 2001, Lyden et al., 2001); (Asahara et al., 1999). In addition, VEGF in the inflamed synovium may stimulate and promote cartilage degradation via the production of MMPs (Martel-Pelletier et al., 2001). Both FGF2 and VEGF have been shown to have detrimental effects on the severity of arthritis in the experimental arthritis mouse model (Yamashita et al., 2002); (Afuwape et al., 2003).

1.2.4 Collagen induced arthritis: murine model of RA

Collagen induced arthritis (CIA) is an important experimental rodent model of RA, which is extensively used to study pathogenesis, to generate hypotheses and to develop potential treatments for this autoimmune disease (Kannan et al., 2005).

Immunological changes associated with RA include an increase in the numbers of collagen type-II (CII) specific T cells and increased concentrations of anti-CII antibodies in the synovial fluid and serum of RA patients during the early phase of disease in RA (Kim et al., 2004); (Kim et al., 1999); (Ohnishi et al., 2003); (Mullazehi et al., 2007). This clinical evidence suggests that collagen type II is one of the major autoantigens that has a crucial role in the initiation of the destructive immune response in RA. Since collagen type II is a component of articular cartilage, immunization with CII of heterologous species may induce joint destruction (Cho et al., 2007). This concept of CIA pathogenesis was first applied in the rat model (Trentham et al., 1977), and subsequently in susceptible strains of mice (Courtenay et al., 1980). The genetically susceptible mouse strains are DBA/1, B10.Q and B10.RIII, which have H2q or H2r haplotypes on the MHC locus (Brand et al., 1996). The C57BL/6 (H-2b) mouse strain has also

been demonstrated to be susceptible to CIA induction (Campbell et al., 2000);(Inglis et al., 2008). In addition, male mice are more susceptible to CIA than females (Nandakumar et al., 2003). Collagen type II from various species, including bovine, porcine, chicken and human have demonstrated their ability to induce arthritis in rodent models (Myers et al., 1995).

After immunization with type II heterologous collagen in complete Freund's adjuvant, mice usually develop asymmetrical polyarthritis at around 3 weeks (Inglis et al., 2008). Similar to human RA, pathological features of arthritis in CIA mice include synovial inflammatory cell infiltration, cartilage and bone erosion and synovial hyperplasia (Asquith et al., 2009b). The proliferation of CII-specific CD4⁺ T cells is observed in the local lymph nodes during 3-5 weeks after the first immunization (Lee et al., 2006).The joint inflammation in CIA mice lasts for 2-3 weeks after the onset of disease, followed then by a recovery phase (Inglis et al., 2008).

1.2.4.1 Immunopathogenesis of Collagen induced arthritis

Similar to human RA, the pathological mechanisms in the CIA model involve both cell-mediated and humoral immune responses (Brand et al., 2003). Both T and B lymphocytes play crucial roles in the development of the disease (Holmdahl et al., 2002). The presence of collagen type-II specific T cells in the arthritic joints suggests that T cells may directly regulate the immuno-pathogenesis in the CIA model (Holmdahl et al., 1988). The initiation of a cell mediated immune response in the CIA model is presumably driven by Th1 cells via the production of IFN γ , lymphotoxin- β , (LT β) and TNF- α (McInnes and Schett, 2007). The disease progression and the inflammation phases may be mediated by humoral factors including antibodies and complement (Schulze-Koops and Kalden, 2001). Mauri et al., 1996 described the relationship between Th1 and Th2 cytokines in CIA models by measuring cytokine levels of cultured draining lymph node cells isolated from CIA mice during the induction and the progression phases of inflammatory joint disease. IFN- γ was detected in the lymph node cell culture during the induction phase of the disease, and stimulation with collagen type II caused a 10-fold increase in IFN- γ production. In addition, the IFN- γ levels were further elevated throughout the progression phase of disease. In contrast, the concentration of Th2 cytokines such as IL-4 and IL-10 were dominant during the

recovery phase of the disease. These data confirm that Th1 lymphocyte cytokines may be the important regulators for the onset and the development of arthritis (Mauri et al., 1996). B lymphocytes and plasma cells are responsible for the production of anti-collagen antibody. This antibody binds to cartilage and activates antibody and complement-mediated immune destruction (Holmdahl et al., 2002). IgG2 is the dominant subclass of anti-collagen antibody in the CIA model, and the concentrations of IgG2a and IgG2b antibody were markedly increased during the highest severity phase of the disease (Brand et al., 2003); (Brand et al., 1996).

1.2.5 Rheumatoid arthritis as a systemic inflammatory disease and its association with neurological diseases

Rheumatoid arthritis is a systemic autoimmune disease in which the peripheral inflammation (beyond arthritis) is reflected by the presence of extra-articular diseases such as systemic vasculitis (blood vessel inflammation), subcutaneous nodules and pulmonary nodules and fibrosis in approximately 30% of RA patients (Young and Koduri, 2007). A recent study demonstrated that the distribution of pro-inflammatory CD4⁺ T cells lacking the costimulatory molecule CD28 (CD4⁺CD28^{null} T cells) in the peripheral blood of RA patients has been associated with these extra-articular manifestations (Fasth et al., 2007). For example, RA patients with persistent expansion of CD4⁺CD28^{null} T cells developed atherosclerotic disease more significantly than RA patients without this expansion. In addition, anti-TNF- α treatment in RA was shown to attenuate these atherosclerotic changes, demonstrating a contribution of this cell subset in atherosclerosis development in RA (Gerli et al., 2004). Therefore, it is suggested that the activation of peripheral adaptive immune responses during arthritis not only affects joints, but also contributes to the inflammation in other organs such as the skin, lung, cardiovascular system and peripheral nerves (Turesson and Matteson, 2004).

Accumulating evidence suggests that the brain is also affected by peripheral inflammation during arthritis. Psychiatric disorders such as depression and anxiety are common in RA, suggesting that peripheral inflammation during arthritis may cause alterations in the brain neurobiology. However, the mechanism underlying psychological disorders in RA is still unclear. A preliminary

study using a single photon emission computed tomography (SPECT) scan of 6 RA patients showed a reduction in serotonin transporter (SERT) density, along with improvements in physical and mental functions after receiving anti-TNF- α treatment, suggesting that circulating cytokines generated during autoimmune activation in RA may cause changes in the serotonin system that induce the development of depression (Cavanagh et al., 2010). Neuroimaging studies showed several CNS lesions in the brains of RA patients, which resolved after steroid treatment, suggesting that CNS inflammatory demyelination is also inducible by systemic inflammation during arthritis (Tsai et al., 2008); (Tajima et al., 2004). This CNS inflammatory demyelination is also the major clinical feature of multiple sclerosis (MS) (Zuvich et al., 2009). MS is generally considered to be a CNS autoimmune disease directed against CNS myelin proteins, including myelin basic protein (MBP), myelin oligodendrocyte glycoprotein (MOG) and proteolipid apoprotein (PLP) (Zozulya and Wiendl, 2008). However, the precise pathological mechanism of MS is unknown. The immunopathogenesis of MS has been investigated intensively by using animal models of MS, including experimental autoimmune encephalomyelitis (EAE), which shares some of the clinical and neuropathological features of MS (Sriram and Steiner, 2005). Both clinical studies in MS patients and animal studies in the EAE model suggest that Th1 and Th17 CD4⁺ cells, and trafficking of these cells from the periphery into the brain play an important role in the initiation of episodes of demyelination in the relapsing-remitting phase of MS (Weiner, 2008); (Pender et al., 2000); (Greer et al., 2008); (Das et al., 1997); (Kebir et al., 2007); (Stromnes et al., 2008); (Klein, 2004). Interestingly, rheumatoid arthritis is a systemic autoimmune disease that shares similar pathological mechanisms with MS. The aetiology of both autoimmune diseases is influenced by genes in the HLA region, particularly the class II genes. In addition, CD4⁺ T cells are thought to play a crucial role in both MS and RA pathogenesis. Therefore, it is possible that lesions of CNS inflammatory demyelination reported in brains of RA patients may be the result of circulating CD4⁺ T cells stimulated by the auto-immune inflammatory process and migrate into the brains during arthritis. These peripherally activated CD4⁺ T cells may include some that recognise and become activated by myelin proteins in the CNS or in secondary lymph nodes, and then exacerbate inflammatory demyelination process in the brains. However, to date, activation of the adaptive immune

response in the brain associated with peripheral joint inflammation of RA has not been well elucidated.

1.3 Immunology of the central nervous system

The central nervous system (CNS) is an important organ and needs to be protected from pathogens. Physiological mechanisms of immune defence in the CNS are still unclear (Carson, 2002). In the past, the CNS was viewed as ‘an immune privileged site’, characterized by the presence of an intact blood-brain barrier (BBB) (Carson, 2002). The BBB serves as a physical barrier preventing the influx of immune cells and inflammatory mediators into the CNS during inflammation (Abbott et al., 2010). Over the last 20 years, the CNS has been considered an ‘immune-privileged’ organ (Carson et al., 2006) however, more recent evidence suggests that the CNS is both immune competent and actively interactive with the peripheral immune system (Dantzer et al., 2008). In addition, immune cells such as macrophages and dendritic cells are present at the choroid plexus and meninges of the brain (Dantzer et al., 2008). Importantly, brain parenchymal cells such as microglia and astrocytes can initiate inflammatory processes by producing inflammatory mediators (cytokines and chemokines) (Whitney et al., 2009).

1.3.1 Astrocytes

The astrocyte is a non-neuronal cell type in the central nervous system (CNS), characterized as being a star shaped cell with numerous extended branches surrounding nearby neurons and blood vessels (Nair et al., 2008), (Wang and Bordey, 2008). Astrocytes are the most abundant subtype of glial cells in the CNS, comprising approximately 90% of CNS-resident cells in human brain (Nair et al., 2008). Unlike microglia that are derived from cells of the immune system, astrocytes are derived from the same lineage as neurons and oligodendrocytes (Bolton and Eroglu, 2009) That could be the reason why astrocytes also have neuronal function as well as regulation of immune response. Astrocytes are multifunctional cells and are involved in various essential CNS functions, including synaptic homeostasis and transmission, regulation of CNS blood flow, and supply of energy metabolites (Blackburn et al., 2009). In addition, astrocytes can also respond to inflammatory conditions such as infection,

trauma, ischemia and neurodegenerative disease by a process called reactive astrogliosis (Sofroniew, 2009).

1.3.2 Microglia

Microglia are central nervous system (CNS) macrophage-like cells, comprising 5-20% of the total glial cell population (Graeber and Streit, 2010). Microglia in the normal brain are characterized by small cell bodies with a number of fine, branched processes, which is often called ramified microglia (Graeber and Streit, 2010). In response to virus or bacterial infections or CNS injury, activated ramified microglia exhibit morphological changes, including shortening of cellular processes and enlargement of their cell bodies. This phenotype is called amoeboid microglia (Town et al., 2005). The origin of the microglia lineage is still undefined. Microglia share a large number of cell surface markers with mononuclear phagocytes, including CD11b (Mac-1, β 2 integrin), CD11c (LeuM5), CD45 (leukocyte common antigen), CD64 (Fc γ receptor 1), CD68 (macrophage antigen), complement type 3 receptor (CR3), B7-2 (CD86), and major histocompatibility complex (MHC) class I and II antigens, and Toll-like receptors (Yang et al., 2010). Based on these similarities in cell surface markers, it is implied that microglia may be derived from the same lineage as peripheral macrophages (Yang et al., 2010).

1.3.2.1 Astrocytes and microglia as immune cells in the CNS

1.3.2.1.1 Role of astrocytes and microglia in CNS innate immunity

Both microglia and astrocytes play important roles in innate and adaptive immune responses in the brain (Yang et al., 2010). Astrocytes and microglia also play a potential role in mediating innate immunity by expressing various pattern recognition receptors (PRRs), especially TLRs in response to viral and bacterial infections (Farina et al., 2007). TLR2, TLR3, TLR4, TLR5 and TLR9 have been reported to be expressed in human and mouse astrocytes (Farina et al., 2007). Primary cultured mouse microglia express TLR1, TLR2, TLR3, TLR4, TLR5, TLR6, TLR7, TLR8 and TLR9 (Olson and Miller, 2004). Human microglia express TLR1, TLR2, TLR3, TLR4, TLR5, TLR6, TLR7 and TLR8 (Bsibsi et al., 2002). Interestingly, TLR expression by microglia is predominantly in the circumventricular organs (CVOs) and meninges; areas which can directly access

the blood circulation (Chakravarty and Herkenham, 2005), suggesting that microglia prevent the entry of pathogens into the CNS by recognising pathogens that are present in the periphery. Astrocytes and microglia seem to have different important roles in response to viral and bacterial infections. A study in cultured fetal human astrocytes showed that TLR3 is constitutively expressed under normal physiological conditions. Another *in vitro* study using cultured adult human astrocytes showed that TLR2, TLR3, TLR4 gene expression could be detectable under normal physiological conditions (McKimmie et al., 2005). However, stimulation with various cytokines, including TNF- α , IL-1 β , IFN- γ , IL-12, IL-4, IL-6, also strongly induced TLR3 gene expression, but had no effect on TLR4 gene expression and down-regulated TLR2 gene expression (Bsibsi et al., 2006). TLR3 is implicated in host anti-viral response by recognizing double-strand (ds) viral nucleic acid. This, in turn, activates immune cells such as peripheral blood monocytes to express anti-viral cytokines including IFN- α , TNF- α and IL-1 β (Pan et al., 2011). This evidence suggested that astrocytes may play a crucial protective role during CNS viral infection. In contrast, microglia predominately express TLR2 and TLR4, which are implicated in the protection against bacterial infections. Both TLR2 and TLR4 recognizing bacterial cell wall component have been associated with the pathology of neuro-degeneration (Carpentier et al., 2008);(Takeuchi et al., 1999); *in vitro* studies have demonstrated that microglia respond to Group B Streptococcus (GBS) infection by expressing TLR-2, which then induces neuronal apoptosis in bacterial meningitis (Lehnardt et al., 2006). LPS-induced-TLR4 expression in microglia *in vitro* can cause dramatic neuronal loss and oligodendrocyte death (Lehnardt et al., 2002); (Lehnardt et al., 2003). Other components of innate immunity, including complement receptors, mannose receptor (MR) and scavenger receptors (SRs), have also been reported to be expressed on astrocytes and microglia (Farina et al., 2007); (Barnum, 1999).

1.3.2.1.2 *Role of astrocytes and microglia in CNS adaptive immunity*

Astrocytes and microglia can also function as non-professional antigen presenting cells (APCs); presenting antigen in the context of MHC molecules, and can contribute to adaptive immunity (Yang et al., 2010); (Constantinescu et al., 2005). Under normal physiological conditions, resting microglia and astrocytes

express very low levels of MHC class I and class II molecules (O'Keefe et al., 2002); (Kreutzberg, 1996); (Massa, 1993). In normal human spinal cords, only 14% of the microglia population express MHC class II (Stoll et al., 2006). However, in various CNS diseases, including infection, injury, neurodegenerative disease and CNS autoimmune disease, the MHC is up-regulated on microglia and astrocytes (Yang et al., 2010); (Soos et al., 1998). IFN- γ is a potent inducer of MHC of both microglia and astrocytes (Wong et al., 1984); (Yang et al., 2004). The ability of astrocytes and microglia to present myelin basic protein (MBP) to CD4⁺T cells in the context of MHC requires an MHC class II transactivator called CIITA, which can be also induced by IFN- γ (O'Keefe et al., 1999); (Badie et al., 2002); (Soos et al., 1998). Astrocytes and microglia also require additional co-stimulatory molecules such as the CD28-B7 receptor family CD80 (B7-1)/CD86 (B7-2) in order to activate CD4⁺ and CD8⁺ T cells (Sedgwick et al., 1991); (Nikcevich et al., 1997), (Tan et al., 1998); (Issazadeh et al., 1998).

In addition to direct activation of T cells by antigen presentation, astrocytes and microglia also enhance T-cell activation by the production of a variety of cytokines. Astrocytes are cellular sources of interleukin IL-1, IL-6, IL-10, interferon (IFN)- α , IFN- β , tumour necrosis factor (TNF)- α , transforming, growth factor (TGF)- β ; and colony-stimulating factors, GM-CSF, M-CSF (Dong and Benveniste, 2001) in the CNS. Microglia produce a variety of cytokines, including IL- α , IL-1 β (Giulian et al., 1986), IL-5 (Sawada et al., 1993), IL-6 (Sawada et al., 1992), TNF- α (Sawada et al., 1989), and TGF β (Constam et al., 1992), IL-12 (Xu and Drew, 2007), IL-13 (Shin et al., 2004), IL-16 (Liebrich et al., 2007), IL-17 (Kawanokuchi et al., 2008), and IL-23 (Sonobe et al., 2008). These cytokines can activate the differentiation of Th1, Th2 and Th17 lymphocytes (O'Garra and Arai, 2000); (Miljkovic et al., 2007). Astrocytes play a role in the activation and expansion of both Th1 and Th17 T cells via the production of IL-12 and IL-23 (Constantinescu et al., 2005). Co-cultures of astrocytes, which produced IL-23p19 and common IL-12/IL-23p40, and myelin basic protein-stimulated T-cells were demonstrated to up-regulate the production of Th1 and Th17 cytokines such as IL-17 and IFN- γ (Miljkovic et al., 2007). Astrocytes also play a role in T cell recruitment into the CNS via chemokine production (Kim et al., 2011).

1.3.3 *Innate immunity in the central nervous system (CNS)*

Innate immune responses to CNS viral and bacterial infection, inadvertently leads to collateral neuronal damage and neurological dysfunction (Nguyen et al., 2002). Resident microglia and astrocytes mediate host immune response against viral/bacterial infection by expressing innate immune receptors such as toll-like receptors (TLRs) that recognize pathogen related molecular patterns on pathogens. Activation of these toll-like receptors (TLRs) results in the production of cytokines to help protect the CNS against pathogens (Pan et al., 2011). However, the cytokines produced during this innate immune activation can also have detrimental effects on neurons. CNS bacterial infections such as Group B Streptococci (GBS) can activate TLR2 expressed on microglia to produce nitric oxide (NO) that is protective against the organism by its cytotoxicity, but also causes neuronal injury (Lehnardt et al., 2006). Neuronal apoptosis in HIV-1 associated dementia is thought to be induced by cytokines including TNF- α , IL-1 β , IL-6 produced by activated microglia/astrocytes (Kaul, 2009); (Sheng et al., 2000). In addition, activation of the immune response in the CNS has been implicated in the neurodegeneration of some neurological diseases, including Alzheimer's disease (AD) and Parkinson's disease (Whitney et al., 2009). Accumulation of extracellular fibrils of amyloid- β and intracellular neurofibrillary tangles in the neuron causes the formation of senile plaques, and eventually leads to neurodegeneration in Alzheimer's disease (Weiner and Frenkel, 2006). Amyloid- β peptides can also initiate innate immunity in the CNS (Weiner and Frenkel, 2006) by directly activating astrocytes and microglia to produce various cytokines and chemokines, including TNF- γ , IL-1 β , IL-6 IFN- γ , CCL2, CXCL10, which can damage neurons (Akama and Van Eldik, 2000); (Zaheer et al., 2008). These observations may suggest that CNS innate immunity can play crucial roles in host defence against microbial/viral pathogens and pathologic amyloid-beta particles. Paradoxically, it also can cause neurotoxicity and damage neurons.

1.3.4 *Adaptive immunity in the CNS*

Medawar 1948 was one of the first to suggest that the inability of initiating lymphocyte responses within the CNS was due to the absence of major components of the adaptive immune system (Medawar, 1948). These include

professional APCs such as dendritic cells (DCs), adaptive immune cells such as T lymphocytes and B lymphocytes, constitutive MHC class I and II expression on CNS parenchymal cells, and lymphatic vessels in the brain parenchyma (Engelhardt, 2006). The CNS is also protected by the BBB, which prevents the influx of immune cells and inflammatory mediators into the CNS during inflammation (Abbott et al., 2010). Although low numbers of T cells are found in the CSF of healthy individuals, they seem to be involved in immune-surveillance of the CNS in the absence of inflammation (Engelhardt, 2006). Under this normal physiological condition, CNS-resident cells such as astrocytes and microglia express low levels of MHC class II and T-cell costimulation/adhesion molecules, which is restrictive for T-cell activation in the CNS (O'Keefe et al., 2002); (Kreutzberg, 1996); (Massa, 1993). It is still unclear how T cells recognize target antigens and initiate adaptive immune response within the CNS.

It has been hypothesized that the antigen presentation by APCs can occur outside the CNS in the nearby lymph nodes such as in cervical lymph nodes (CLN) (Goverman, 2009). CNS myelin auto-antigens such as proteolipid protein (PLP) and myelin basic protein (MBP) that are synthesised by oligodendrocytes can drain from the brain tissue into the lymphatic systems through the perivascular space between the brain tissue and BBB (Ichimura et al., 1991). The perivascular space is connected to the brain- cerebrospinal fluid (CSF) barrier called the subarachnoid space (SAS), which is eventually linked to cervical lymph nodes via the lymphatics of the nasal mucosa (Koh et al., 2005). Evidence for this includes the observation that neuronal antigens and proteins, including MBP, PLP, NF-L (Neurofilament triplet L) and MAP-2 (Microtubule-Associated Protein) were detected in CLN of MS patients and EAE mice, and these have been associated with neuronal damage (Fabriek et al., 2005); (van Zwam et al., 2009). Langerhans' cells and lymph node dendritic cells in CLN can present CNS antigens such as MBP and PLP in the context of MHC class II (Cumberbatch et al., 1991), resulting in CD4⁺ T cell and CD8⁺ T cell activation (Goverman, 2009). It has been demonstrated that activated T lymphocytes migrate back from the CLN into the brain via the route of lymphatics of the nasal mucosa (Goldmann et al., 2006). The localization of type IV collagen auto-antibody was observed in the CLN after the injection of type IV collagen into the CSF (Walter et al., 2006). Several studies showed that the CLN could be the initial peripheral activation site for

autoimmune-mediated CNS demyelinating diseases (Goverman, 2009). The onset of clinical symptoms of EAE correlated with increased activation of PLP specific CD4⁺ T cells in the CLNs (Zhang et al., 2008). Surgical removal of the cervical lymph nodes reduced the severity and delayed the onset of EAE (Furtado et al., 2008).

In addition to the regional nodes, several recent studies also suggest that T cells can be activated by recognizing target antigens directly in the CNS and not necessarily in the cervical lymph nodes or other peripheral lymphoid organs. A study by Greter *et al* showed that adoptive transfer of pre-activated myelin oligodendrocyte/glycoprotein (MOG)-specific T cells into splenectomized mice with a complete absence of lymph nodes and Peyer's patches resulted in the same development of EAE as seen in wild type mice (Greter et al., 2005). This study suggests that antigen presentation by APCs in the secondary lymphoid tissues is not necessary for the activation of T cells before their migration into the CNS and the development of disease (Greter et al., 2005). This is supported by another study by McMahon *et al* showing that activation of dye-labeled naive proteolipid protein (PLP)₁₃₉₋₁₅₁-specific T cells occurred directly in the brain and not in the cervical lymph nodes or other peripheral lymphoid organs (McMahon et al., 2005).

Dendritic cells (DC) have been demonstrated to play crucial roles in the distribution of CNS antigens and to present antigens to T lymphocytes and B lymphocytes at the peripheral and CNS levels (Zozulya et al., 2010). Both myeloid DCs and plasmacytoid DCs have been found in the CSF of healthy donors (Pashenkov et al., 2001). In addition, MHC class II⁺ DCs are also present in the perivascular space, meninges and the choroid plexus of the non-inflamed normal brain (McMenamin et al., 2003). DCs located at the CNS have been shown to play a role in transporting CNS antigens from the CNS to the CLN (de Vos et al., 2002). Karman *et al* has demonstrated the migration of DCs from the brain to CLNs after the injection of DCs into the mouse brain parenchyma. After immunization with OVA, the number of increased OVA-specific CD8⁺ T cells in the CLNs correlated with increased injected OVA-loaded DC numbers. The injection of increasing numbers of OVA-load DCs also led to a dose-dependent increase in the number of OVA-specific CD8⁺ T cells in brain, suggesting that DCs also play a role in the homing of antigen (Ag)-specific T cells into brain (Karman

et al., 2004). In a murine EAE model, intracerebral microinjection of activated DCs increased the onset and clinical course of EAE, along with T-cell infiltration (Zozulya et al., 2009). Myeloid DCs originating from the bone marrow were shown to accumulate in the brain during the course of EAE, where they preferentially activated Th17 lymphocytes; producing IL-17 which is the key mediator for EAE immune responses (Bailey et al., 2007). Brain DCs also showed preference to migrate to B-cell follicles rather than T-cell areas in lymph nodes (Hatterer et al., 2006). Intra-CSF injection of mouse dendritic cells to EAE mice also resulted in increased serum MOG-specific-antibody (Hatterer et al., 2008). These data suggest that mDCs play an important role in B lymphocyte activation and in the antibody response in autoimmunity. DCs have been demonstrated to play crucial roles in T cells activation in the non-lymphoreticular environment of the CNS. A study in splenectomized mice lacking lymph nodes and Peyer's patches showed that CNS-infiltrating CD11c⁺ dendritic cells were essential for the disease development of EAE (Greter et al., 2005). An *ex vivo* study also showed that CD11c⁺ dendritic cells were the most effective at activating the proliferation of (PLP)₁₃₉₋₁₅₁-specific T cells in the CNS compared to CD11c⁻ microglia and CD11c⁻ macrophages (McMahon et al., 2005).

CNS antigen presentation can occur at the BBB level. The cerebrovascular endothelium of BBB constitutively expresses MHC class II and the co-stimulatory molecule CD86 (B7-2) (McCarron et al., 1991); (Omari and Dorovini-Zis, 2003). Upon stimulation by inflammatory cytokines such as TNF- α and IFN- γ , cerebrovascular endothelium can also express MHC class I, CD80 (B7-1) and the class II trans-activator (CIITA) (Tennakoon et al., 2001); (Seino et al., 1995); (Girvin et al., 2002). Recognition of CNS cognate antigens presented by cerebral endothelial cells has been demonstrated to be essential for CD4⁺ T lymphocyte and CD8⁺ T lymphocyte migration into the brain (Galea et al., 2007); (Manes and Pober, 2008).

1.3.5 *The role of inflammatory mediators in the CNS*

Neuro-inflammation has been long considered only to have a destructive role in the CNS, however accumulating evidence recently suggests that neuro-inflammation also has a neuroprotective function (Minghetti L 1999); (Nordvall G, et al. 2000); (Stoll G, 2002). Interestingly, several studies suggest that the

balance between maintenance of homeostasis of the CNS and induction of neurodegeneration may be dependent on the initiation of specific types of immune response (Byram et al., 2004); (Polazzi and Contestabile, 2002); (Hofstetter et al., 2003). Inflammatory mediators such as cytokines and chemokines are now recognised to have both neuroprotective and neurotoxic aspects. Cytokines and chemokines produced from neurons have been reported to function as neuromodulators, which may be essential for the maintenance of normal CNS function including neuro-regeneration (Carson et al., 2006).

1.3.5.1 The role of cytokines in the CNS

Cytokines not only function to regulate the immune response in the CNS, they can also function as neuro-modulators. Pro-inflammatory cytokines, including IL-1 β , IL-6 and TNF- α can enhance excitatory synaptic transmission via alpha-amino-3-hydroxy-5-methylisoxazole-4-propionic acid (AMPA)- and *N*-methyl-D-aspartate (NMDA)-synaptic activation and suppress inhibitory synaptic transmission via GABA- and glycine synaptic inhibition (Kawasaki et al., 2008).

IL-1 β and TNF- α can cause neurodegeneration via excito-neurotoxicity. Excito-neurotoxicity is the mechanism of neuronal cell death caused by prolonged exposure to glutamate, leading to the excitatory signal via NMDA receptor activation. This causes excessive influx of Ca₂⁺ into the neuron, which is neurotoxic and induces neuronal damage (Fan and Raymond, 2007). TNF- α induces glutamate release from microglia and the production of glutaminase, the enzyme that generates glutamate from glutamine, and together these eventually result in increased neuronal cell death (Takeuchi et al., 2006). IL-1 β induces excito-neurotoxicity by activating tyrosine phosphorylation of NMDA receptors, resulting in increased intracellular Ca₂⁺ and loss of cultured hippocampal neurons (Viviani et al., 2006). In contrast, IL-6 showed a neuro-protective role against NMDA-induced death of cerebellar granule neurons (Wang et al., 2009a). This evidence suggests that pro-inflammatory cytokines can be either neuroprotective or neurotoxic via the modulation of neurotransmission.

TGF- β has a major role in neuroprotection (Qian et al., 2008) and is considered to be a therapeutic target of neurodegenerative diseases such as Alzheimer's disease. TGF- β 1 and TGF- β 2 demonstrated neuroprotective activities against

several neurotoxic stimuli, including excitotoxicity (Boche et al., 2003), and neuronal apoptosis (Zhu et al., 2002a). TGF- β has been reported to be neuronal protective against A β -neurotoxicity, which may be the cause of Alzheimer's disease (Caraci et al., 2008); (Uribe-San Martin et al., 2009). These findings suggest that TGF- β has a protective role in the pathogenesis of Alzheimer's disease.

1.3.5.2 The role of chemokines in the CNS

Chemokines and their receptors are expressed within the cytoplasm of neurons in several selective brain regions, including the cerebral cortex, nucleus accumbens, striatum, amygdala, thalamus, hypothalamus, hippocampus, substantia nigra, mammillary bodies, raphe nuclei, neocortex, basal nuclei, brain stem and cerebellum (Westmoreland et al., 2002); (Banisadr et al., 2002). Accumulating evidence suggests that chemokines might function as neuromodulators. Similar to neurohormones, neuropeptides and neurotrophins, chemokines and their receptors such as CCL21, CXCR4, and CXCR5 are packaged to the large vesicle and transported into the dendritic processes and axons (de Jong et al., 2008); (Westmoreland et al., 2002). Injured neurons were shown to release CCL21 into the synaptic cleft and to activate microglia. This may provide a communication between neuron-microglia that might be the pathway to activate microglia that are located distant from the primary lesion (de Jong et al., 2005). Chemokines such as CXCL12 might be involved in neuronal communication such as during cholinergic and dopaminergic neurotransmission. It has been reported that CCR2 co-localized with neurotransmitters on cholinergic neurons, dopaminergic neurons and vasopressinergic neurons (Banisadr et al., 2003). In addition, CCL2 treated neurons isolated from hippocampus, hypothalamus and cortex showed increased Ca_2^+ influx into the cells, suggesting that CCR2 may regulate the release of neurotransmitters (Banisadr et al., 2005). Interestingly, recent findings showed that CXCL12/CXCR4 and CX3CL1/CX3CR1 co-localized with serotonergic neurons. Both CX3CL1 and CXCL12 enhanced the amplitude of inhibitory postsynaptic currents (sIPSC) via GABA synaptic activation in serotonergic neurons. In addition, CXCL12 could also induce glutamate-mediated membrane depolarization and increase the amplitude of excitatory postsynaptic currents (sEPSC) via glutamate synaptic activation. These data suggest the modulation effects of chemokines on 5-HT

neurotransmission that may lead to this being a therapeutic strategy of chemokines for depression (Heinisch and Kirby, 2009); (Heinisch and Kirby, 2010).

CXCL12/CXCR4 is also involved in neuronal death during HIV-1-associated dementia. HIV-1 glycoprotein gp120 induces neuronal death by binding to CXCR4 (Kaul and Lipton, 1999); (Bachis and Mocchetti, 2004); (Choi et al., 2007). Other chemokines are involved in neuronal survival and exhibit their neuroprotective effects. CXCL1 and CXCL8 prevent cerebellar granule neurons from apoptotic death induced by low K^+ (Limatola et al., 2000); (Limatola et al., 2002). CX3CL1/CX3CR1 showed neuroprotection against excitotoxicity in hippocampal neurons (Lauro et al., 2008). CXCL1 protected hippocampal neurons from apoptosis induced by β -amyloid peptide (Watson and Fan, 2005). This evidence suggests that chemokines not only have an inflammatory function by regulating the recruitment of monocytes and leukocytes into the CNS, they also act as neuromodulators to regulate neural transmission and support survival and development of neurons.

1.4 Inflammation in the CNS

Inflammation not only has a crucial role in host defence responses, but also contributes to hypersensitivity diseases and in several central nervous system (CNS) disorders such as Alzheimer's and Parkinson diseases (Whitney et al., 2009). However, inflammation in the brain is different from that in peripheral tissues in several aspects, including mechanism of initiation and degree of sensitivity (Whitney et al., 2009). The migration of peripheral T-cell and antibodies into the CNS is restricted by BBB (Banks, 2010). An inflammatory process in the CNS seems to be initiated mainly by the activation of resident microglia and astrocytes in response to cellular damage or exposure to pathogens (Whitney et al., 2009). Activated microglia and astrocytes release anti- and pro-inflammatory cytokines including IFN- γ , TNF- α , IL-1 β , IL-6, IL-4 and IL-10 (Whitney et al., 2009). These inflammatory mediators can disrupt the BBB, which may or may not be associated directly with more recruitment of monocytes and lymphocytes to cross through the BBB into the site of inflammation (Hickey, 1999); (Lossinsky and Shivers, 2004). However, up-regulation of pro-inflammatory cytokines such as IFN- γ , TNF- α , IL-1 β , IL-6 can

activate BBB endothelial cells to produce chemokines and adhesion molecules that facilitate the infiltration of monocytes and lymphocytes from the peripheral circulation into the brain (Engelhardt, 2006). These recruited monocytes and lymphocytes become activated and produce more inflammatory mediators in the CNS, which can contribute to neuronal damage and changes in neurobiology in the CNS. However, inflammatory processes in the CNS may also contribute to neuroprotection essential in maintaining homeostasis in the CNS (Whitney et al., 2009) .

1.5 Immune signals from the peripheral circulation induce brain inflammation

Peripheral inflammation-induced neuroinflammation has been well documented. Acute brain inflammation induced by viral/bacterial encephalitis causes transient increases in cytokine production and microglia activation in the CNS. Several studies in models of hypoxia-ischemia and LPS/virus induced acute CNS inflammation demonstrated that the CNS usually responds to acute inflammation by up-regulating inflammatory mediators in transient kinetic patterns (Barichello et al., 2010); (Bluthe et al., 1999); (Sakata et al., 1991); (Quan et al., 1994); (Barichello et al., 2009). For example, experimental intra-cerebroventricular LPS injection demonstrated that IL-1 β , TNF- α , IL-6, MCP-1 reached their peak levels (4-7 fold increases compare to the control) at 6 hours after the challenge (Rankine et al., 2006), before a sharp reduction in cytokine levels back to the base line. Increases in cytokine production and microglia activation in the CNS have also been reported in chronic inflammatory disease such as the experimental models of arthritis. Microglia activation, along with increases in IL-1 β , TNF- α and IL-6 were observed in spinal cord of adjuvant induced arthritis (Bao et al., 2001). A similar observation has been reported in CIA rats. Longitudinal changes in IL-1 β , TNF- α and IL-6 gene expression were observed in brains of CIA rats (del Rey et al., 2008). In addition, inducing a gut inflammation model of colitis using 2,4,6-trinitrobenzene sulfonic acid (TNBS) resulted in the activation of microglia and the production of TNF- α in rat brains. Interestingly, increases in the TNF- α protein level and the number of activated microglia in hippocampal dentate gyrus (DG) have been associated with brain excitability and seizure susceptibility (Riazi et al., 2008). A study by Terrando et al., showed that peripheral inflammation caused by peripheral surgical trauma could induce

increases in IL-1 β , which was inhibited by peripheral treatment of anti-TNF- α (Terrando et al., 2010). However, the mechanism by which the inflammatory signal from the periphery induces brain inflammation is not well understood. Multiple mechanisms are implicated in peripheral inflammation-induced neuroinflammation, including blood brain barrier (BBB) breakdown and recruitment of immune cell from the periphery. However, changes in permeability of BBB and up-regulation of inflammatory mediators and adhesion molecule facilitating the immune trafficking to the CNS are primarily induced by peripheral/central inflammation.

1.6 Barriers of the central nervous system

There are three main barriers between blood and brain: (i) The blood brain barrier; which is the barrier between the lumen of cerebral blood vessels and brain tissue. (ii) The blood - cerebro spinal fluid barrier located between choroid plexus blood vessels and the CSF, which provides a non restrictive barrier: (iii) arachnoid barriers which form the middle layer of the meninges, covering the whole brain (Correale and Villa, 2009).

1.6.1 Blood Brain Barrier (BBB)

1.6.1.1 Structure of the blood brain barrier

The BBB consists of the endothelial cells that form the walls of brain and spinal cord capillaries. These endothelial cells (ECs) are connected strongly to each other by tight junctions (TJs) and adherent junctions (AJs) (Correale and Villa, 2009).

The TJs function to restrict transport of macromolecules and hydrophilic molecules between blood and the brain interstitial fluid (ISF). The tight junction complex comprises integral membrane proteins occludin, claudins 3, 5 and 12, and junctional adhesion molecules (JAMs). Occludin and claudins consist of four transmembrane domains with two extracellular loops, which associate and bind to each other across the intracellular cleft. The end terminal cytoplasmic domain of occludin regulates trans-epithelial migration of neutrophils and also function to maintain TJs aggregation and barrier function. Claudins function to regulate size-selective diffusion of hydrophilic molecules. JAMs are members of

the immunoglobulin (Ig) superfamily, which play a role in leukocyte trafficking. JAMs have a single transmembrane domain and the extracellular portion consists of immunoglobulin-like loops formed by disulfide bonds. Carboxi-terminal cytoplasmic tails of occludin, claudins and JAMs are linked to cytoplasmic adaptor proteins such as zonular occludins-1 (ZO-1), ZO-2, ZO-3, which are connected to the actin/myosin cytoskeletal system within cells (Abbott et al., 2010).

Adherent junctions (AJs) consist of membrane proteins such as vascular endothelial (VE)-cadherin (also known as adherin 5, type 2 or CD144) and platelet-endothelial cell adhesion molecule (PECAM-1), which are linked to actin skeleton proteins via adaptor molecules called catenins. AJs are essential for the formation of tight junctions, since they provide support for BBB structure and attachment between cells (Abbott et al., 2010).

CNS capillaries are surrounded by, and associated with, several cell types; including pericytes, astrocytes, microglia and neuronal processes, which form a functional unit called the neuronal vascular unit. The interaction between neuronal vascular unit and CNS capillaries results in the bi-directional regulation of blood flow, microvascular permeability, cell matrix interactions, neurotransmitter turnover, angiogenesis and neurogenesis (Zlokovic, 2008). Pericytes are vascular cells that extend their long cytoplasmic processes encircling the endothelial capillaries. Pericytes highly express the contractile protein α -smooth muscle actin, which regulates blood flow via endothelial cell contraction and relaxation (Zlokovic, 2008). Both endothelial cells and pericytes are enclosed and contribute to the local basement membrane, which consists of different extracellular matrix (ECM) structural proteins such as collagen and laminin (Correale and Villa, 2009). The local basement membrane is surrounded by the endfoot processes from astrocytes, which function mainly in the induction and maintenance of BBB properties (Abbott et al., 2006). The structure of the BBB and a tight junction is shown in Figure 1.1.

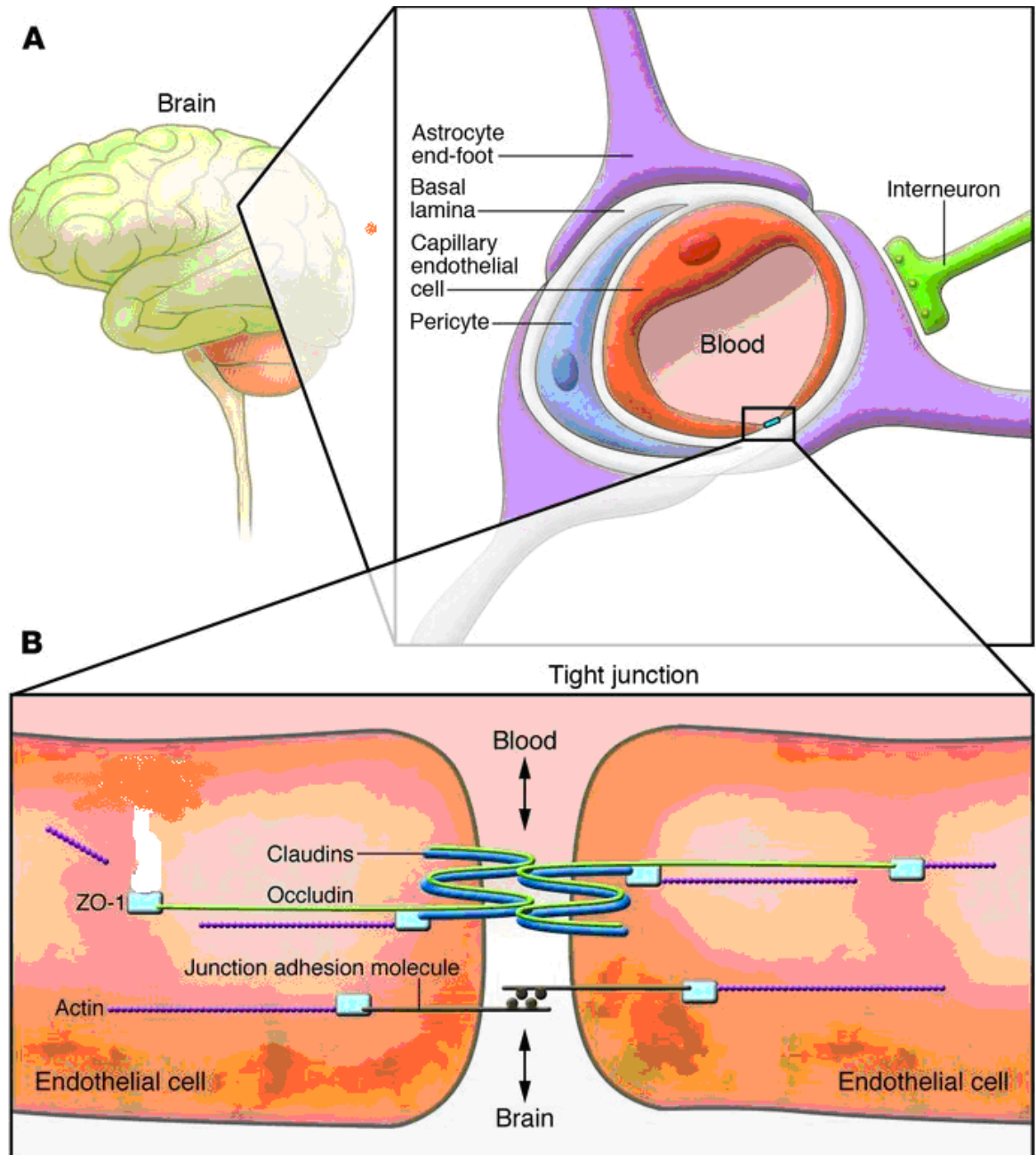


Figure 1.1 Structure of the BBB and tight junction.

(A) The structure of BBB mainly consists of capillary endothelial cells surrounded by the neuronal vascular unit (pericytes, astrocytes and neuronal processes). (B) The tight junction complex comprises integral membrane proteins (claudins, occludin, and junction adhesion molecule) on adjacent endothelial cells. The image were taken from (Chou and Messing, 2008) by kind permission of The Journal of Clinical Investigation.

1.6.1.2 1.6.1.2. Transport across the blood brain barrier

Under normal physiological conditions, tight junctions between endothelial cells only allow the entry of water, ethanol and small gas molecule such as O_2 and CO_2 via the paracellular route. Most of the molecules are transported across the endothelial wall transcellularly into the brain. Small lipid-soluble and non-polar molecules including drugs such as barbiturates, diazepam, phenobarbital and phenytoin can diffuse passively through the lipid membrane to reach their

neuronal targets in the brain. However, the transcellular bidirectional transportation of water soluble compounds and macromolecules requires a variety of BBB transport systems (Abbott et al., 2006). Many essential polar nutrients such as glucose and amino acids are transported by carrier-mediated transport, which depends on concentration gradients in the direction from blood to brain (Abbott et al., 2010). Active efflux transport requires the energy from ATP to lipid-soluble compounds out of the brain. This active transport system also has neuroprotective and detoxifying functions by reducing influx of many drugs, including azidothymidine (AZT), and enhancing their efflux from the brain (Abbott et al., 2006). Large proteins including neuroactive peptides, cytokines, chemokines, transferrin, low density lipoprotein (LDL), IgG, insulin and insulin growth factor enter the brain by specific receptor-mediated transcytosis. This involves binding of circulating proteins to their specific receptors expressed on the endothelial cells. The protein-receptor complex is internalised into an endocytic vesicle, which travels across the cytoplasm to be released at the opposite side of the cell (Jones and Shusta, 2007). Cationic proteins such as albumin and other plasma proteins are transported into the brain by absorptive mediated transport (AMT). This involves the interaction between an excess positive charge on the molecule and negative charge on the BBB surface, which induces endocytosis and subsequent transcytosis (Herve et al., 2008).

1.6.1.3 Blood brain barrier disruption in neuro-inflammation

Studies of models of CNS autoimmunity and virus induced neuro-inflammation have shown evidence of enhanced BBB dysfunction, associated with the development of a CNS inflammation. Increased BBB permeability can involve the entry and clearance of various viruses including West Nile virus (Wang et al., 2004), rabies virus (Phares et al., 2006), and adenovirus type 1 (Gralinski et al., 2009). In addition, retroviral-infected lymphocytes have been associated with BBB dysfunction and changes in BBB structure (Afonso et al., 2007). The blood brain barrier permeability in EAE mice showed a positive correlation with the disease severity (Fabis et al., 2007).

1.6.1.4 Peripheral inflammation-induced blood brain barrier disruption

BBB disruption can also be induced from the periphery, and one good example is the case of systemic infection associated with sepsis (Sharshar et al., 2005). In experimental models of this, peripheral inflammatory stimulation by LPS causes microglia activation and increased concentrations of serum cytokines (Stolp et al., 2009), leading to a transient increase in BBB permeability in the white matter tissue of neonatal rats (Stolp et al., 2005a, Stolp et al., 2005b); (Stolp et al., 2007). Subcutaneous administration of complete Freund's adjuvant (CFA) enhanced BBB permeability to [¹⁴C] sucrose and down-regulated tight junctional protein expression (Huber et al., 2001). Increased permeability of the blood-brain barrier was also observed in murine experiments of induced surgical pain stress (Oztas et al., 2004) and systemic thermal injury (Berger et al., 2007). Interestingly, BBB breakdown in several non-CNS chronic inflammatory diseases, such as intestinal inflammation (colitis) (Natah et al., 2005), obesity (Hafezi-Moghadam et al., 2007) and diabetes (Hawkins et al., 2007) are thought to be due to the effect of circulating inflammatory mediators.

1.6.1.5 Mechanisms of inflammation-induced blood–brain barrier dysfunction

Circulating cytokines for example TNF- α (Tsao et al., 2001) and IL-1 β (Blamire et al., 2000) can induce BBB disruption and interfere with BBB function by several mechanisms. The effect of TNF- α on BBB permeability was demonstrated to be associated with microglial activation (Nishioku et al., 2010a). TNF- α and IL-1 β have been reported to modulate the active transport system across BBB via the regulation of P-glycoprotein expression (Yu et al., 2007); (Bauer et al., 2007); (von Wedel-Parlow et al., 2009). IL-1 β has been shown to regulate BBB permeability via the hypoxia-angiogenesis pathway (Argaw et al., 2006). Systemic administration of IL-1 β results in the damage of BBB structure, including loss of the tight junctional protein, claudin-5 and basal lamina protein, collagen-IV (McColl et al., 2008). Adhesion molecules induced by cytokines also have a crucial role in BBB disruption. Blocking P-selectin and integrin alpha-v beta-3 resulted in the reduction of BBB leakage (Jin et al., 2010); (Shimamura et al., 2006). Chemokines such as CCL2 are also involved in changes in BBB permeability. Blocking CCL2/CCR2 in a mouse model of stroke caused a

reduction in BBB permeability, along with re-syntheses of tight junctional proteins such as occludin, zonula occludin-1 and 2, and claudin-5 (Dimitrijevic et al., 2006). Cytokines produced from neutrophils and T lymphocytes were also demonstrated to enhance BBB disruption (Joice et al., 2009). IL-17 and IL-22 released from Th17 cells were also shown to damage BBB via disruption of tight junctions (Kebir et al., 2007).

1.6.1.6 Possible transport mechanisms for peripheral cytokines into the brain

Circulating cytokines may enter the brain across a damaged BBB. However, there is no promising evidence demonstrating a direct association between concentrations of brain cytokines and BBB breakdown. This also suggests that the transportation of cytokine across BBB may be a complex mechanism that is still unresolved. It is likely that because of their biological importance that circulating cytokines can enter the brain by various well-controlled mechanisms. However, this has still to be established but some experimental results are shown below.

1.6.1.6.1 Entry of cytokines into the brain at circumventricular sites

Circumventricular organs (CVOs) are exceptional areas in the brain that are not covered by the BBB. They function to monitor changes in peripheral biochemical substances such as hormones and facilitate the secretion of neuroendocrine hormones into the blood (Johnson and Gross, 1993). Although CVOs are permeable to macromolecules, a study using ^{125}I -IL-1 β showed that CVOs were only responsible for less than 5% of total brain uptake of IL-1 β (Plotkin et al., 1996). A recent study in an EAE model demonstrated intensive staining of MHC class II $^+$ /CD45 $^+$ leukocytes, ICAM-1 and VCAM-1 at the CVOs, suggesting that CVOs are also the route for leukocyte infiltration into the CNS (Schulz and Engelhardt, 2005). Since CVOs are areas without a BBB, it is possible that these are the first areas of brains that perceive inflammatory cytokine signals from the peripheral circulation. Several studies using *in situ* hybridization showed that TNF- α and IL-1 β gene expression was induced rapidly during the first 2 hours after LPS administration in brain regions such as the circumventricular organs (CVOs) and the choroid plexus (Quan et al., 1998); (Breder et al., 1994). These data suggest

that peripheral immune signals can be passed transiently into the brain at the level of the choroid plexus and circumventricular organs (CVOs) (Price et al., 2008).

1.6.1.6.2 Direct entry of cytokines to the CNS across the BBB

Cytokines are transported into the CNS by various transport mechanisms. TNF- α , IL-1 α , IL-1 β , IL-2 and IL-6 have been reported to be transported into the CNS by a saturable transport system (Gutierrez et al., 1993); (Banks et al., 1994a, Banks et al., 1991); (Banks et al., 2004, Banks et al., 1994b). Recent findings show that chronic morphine exposure and withdrawal can enhance a saturable transport of IL-2 into the CNS (Lynch and Banks, 2008). A saturable efflux system has also been proposed as a mechanism to limit the accumulation of cytokines in the brain in order to limit neurotoxicity (Banks et al., 2004). In addition, the saturable efflux system could mediate transportation of cytokine such as IL-2 used as cytokine therapy for patients with cancer (Banks et al., 2004). It has been reported that patients with leptomeningeal metastases who were given intraventricular IL-2 injection showed transient up-regulation of IL-2 and other cytokines such as IL-1 β , TNF- α and IL-6 in the CSF (List et al., 1992). High concentrations of IL-2 in the periphery of these patients after the cytokine therapy may cause a saturable efflux of IL-2 into the brain. It is still unclear how saturable efflux systems could explain the transportation mechanism of cytokines during peripheral inflammation. This is because the up-regulation of peripheral cytokines between the example of peripheral inflammatory diseases and the example of cytokine therapy is different in terms of concentrations of cytokines in the periphery. Concentration of cytokines in the periphery could be increased during systemic inflammatory diseases, but whether it is higher than the concentration of the same cytokines in the brain that would cause a saturable efflux of cytokines from the periphery into the brain is still unclear. A few studies suggest that the transport of TNF- α across the BBB requires p55 and p75 TNF receptors. TNFR p55/p75(-/-) double knockout mice were unable to uptake ^{125}I -TNF- α into the brain and the spinal cord (Pan and Kastin, 2002). This concept was supported by the observation in wild type mice that the up-regulation of p55 and p75 TNF receptor gene expression in injured spinal cord corresponded to increased ^{125}I -TNF- α uptake (Pan et al., 2003). A recent finding

demonstrated that p55 and p75 receptor-mediated TNF- α transport across BBB may involve endocytosis. Microvessel endothelial cells of rat brains showed the ability to endocytose ^{125}I -TNF- α in a time-dependent manner. In addition, confocal imaging also exhibited the co-localization of p55 and p75 TNF receptors and caveolin-1; the endocytic membrane vesicle, in TNF- α treated RBE4 cells (Pan et al., 2007). An *in vitro* study using a blood-brain barrier model generated by co-culture of porcine brain microvascular endothelial cells with astrocytes demonstrated that the penetration of IL-1 β occurred in a temperature-dependent manner that appeared to depend on the IL-1 receptor (Skinner et al., 2009).

1.6.1.6.3 Activation of cytokine production in the CNS by stimulating peripheral afferent nerves

The up-regulation of cytokines in the CNS can be regulated by the afferent vagus nerve (Thayer and Sternberg, 2009). Removing the abdominal site of the afferent vagus nerve (vagotomy) results in reduced expression of IL-1 β mRNA in rodent brains after peripheral administration of either LPS (Laye et al., 1995) or IL-1 β (Hansen et al., 1998). Interestingly, activating the afferent vagus nerve by electrical stimulation resulted in increased IL-1 β gene expression in the rat brain (Hosoi et al., 2000).

1.6.1.6.4 Peripheral inflammation induces local production of cytokines by microglia

Peripheral inflammation can activate CNS immune cell such as resident microglia to produce local cytokines by unknown mechanisms. Activated microglia isolated from aged mice after intraperitoneal injection of LPS showed up-regulation of IL-1 β , IL-10, TLR2 and MHC class II mRNA (Henry et al., 2009). In addition, the activation of microglia and the production of TNF- α in rat brains have been reported in a model of gut inflammation (Riazi et al., 2008). Chemokines released from CNS activated microglia can also attract leukocyte recruitment into the CNS, leading to the production of cytokines by peripheral leukocytes. Elevated CXCL2 levels, increased numbers CCR2 $^{+}$ monocytes, and microglial activation were observed in the brains of mice with liver inflammation (D'Mello et al., 2009). It is still unclear how circulating cytokines enter the brain and

activate microglia in the brain parenchyma. One possibility is that circulating cytokines may activate microglia and astrocytes located at the CVOs such as in the subfornical organ (SFO), the organum vasculosum of the lamina terminalis (OVLT) and the area prostroma (AP) (McKinley et al., 2003). The important evidence suggesting that microglia at the CVOs are more sensitive to inflammatory cytokine signals from the periphery and may be activated quicker than microglia in other part of brain parenchyma is that the increased TLR expression by microglia is predominantly in the CVOs and meninges (Chakravarty and Herkenham, 2005). Transient increases in TLR4 and TLR2 gene expression were observed in choroid plexus subgroups of CVOs such as the organum vasculosum of the lamina terminalis (OVLT), and subfornical organ (SFO) in rat brains after systemic injection of LPS or gram-negative bacterial cell wall components (Laflamme and Rivest, 2001); (Laflamme et al., 2001). This was followed by rapid transcription of inflammatory mediators such as TNF- α and CCL2 within these areas (Laflamme et al., 2003). This suggests that microglia located at CVOs may play an important role as the first line of defence against the entry of pathogens into the CNS by recognising pathogens that are present in the periphery.

1.6.1.7 Immune cell trafficking into the CNS

Under CNS inflammatory conditions, the expression of adhesion molecules and chemokines is induced on BBB endothelium, and these promote adhesion and help attract circulating leukocytes to enter into the inflamed CNS (Banks, 2010). BBB disruption induced by CNS inflammatory conditions may facilitate greater immune cells recruitment from the periphery. However, it is still controversial whether BBB breakdown is directly associated with an increase in immune cells recruitment from the periphery. Several studies reported that BBB disruption is a neutrophil-mediated process, which is associated with leukocyte recruitment. A study by Bolton et al. reported the loss of BBB integrity including the proteins occludin and zonula occludens-1 from cerebral vascular endothelium during neutrophil-induced BBB disruption (Bolton et al., 1998). This suggests that neutrophils may activate a signalling cascade leading to the loss of BBB integrity and BBB disruption. In contrast, several studies also suggest that the loss of BBB integrity is not simply to facilitate more leukocyte recruitment from the

periphery into the brain (Carson et al., 2006). It has been reported that perivascular cells are continuously replaced by peripheral macrophages in the healthy CNS. This suggests that there may be homeostatic trafficking of monocytes from the periphery into the basement membrane at the surface of the BBB (Bechmann et al., 2001). This also means BBB integrity is designed to permit selective leukocyte trafficking into the CNS. In addition, to date there is no evidence demonstrating a direct correlation between the severity of BBB breakdown and the amount of leukocyte recruitment during CNS inflammation. One possibility is that the BBB is still able to restrict T-lymphocyte migration into the CNS during BBB disruption by selectively expressing adhesion molecules on the brain microvascular endothelial cells. For example, vascular cell adhesion molecule (VCAM), but not the mucosal addressin cell adhesion molecule (MAdCAM), has been shown to be highly expressed on the endothelial cells of the lesions from MS patients (Allavena et al., 2010). Therefore, only T-lymphocytes that express specific receptors for these adhesion molecules can enter into the inflamed CNS (Engelhardt et al., 1998). T-cells from inflamed mouse brains expressed a high level of $\alpha 4\beta 1$ integrin, the receptor for VCAM-1, but a low level of $\alpha 4\beta 7$ integrin; the receptor for MAdCAM (Engelhardt et al., 1994).

Immune cell trafficking into the CNS is a multiple step process. The initial step involves a weak interaction between leukocytes and endothelium and the leukocyte rolling along the microvascular wall (Banks, 2010). This step is mediated mainly by E- or P- selectins, which bind to P-selectin glycoprotein ligand-1 (PSGL-1) (Alon and Ley, 2008). Peripheral $CD4^+$ T cells in CSF of MS patients expressed higher PSGL-1 and transmigrated through BBB endothelium at a faster pace compared with those of healthy controls, suggesting an essential role of PSGL-1 in the $CD4^+$ T cell entry into the inflamed CNS, and also suggesting an essential role of P-selectin-PSGL-1 binding in the early phase of leukocyte entry into the CNS (Bahbouhi et al., 2009). Rolling leukocytes are exposed to chemokines, leading to further reduced rolling speed, and eventual tethering to endothelial cells by $\alpha 4\beta 1$ integrin-VCAM-1 binding (Engelhardt, 2006). Additionally or alternatively, T cells may be captured by the endothelium without rolling, via $\alpha 4\beta 1$ integrin-VCAM-1 binding (Banks, 2010). The $\alpha 4\beta 1$ integrin has an essential role in EAE development; T cells isolated from integrin $\beta 1$ deficient mice showed the inability to adhere firmly to endothelium

(Bauer et al., 2009). Natalizumab, the anti- $\alpha 4$ integrin antibody, inhibited $\alpha 4$ integrin-mediated firm adhesion, but not the initial contact, of human T cells with the endothelium during EAE (Coisne et al., 2009). These findings demonstrated that the $\alpha 4\beta 1$ integrin functions mainly in firm adhesion rather than the initial contact of T cell to the BBB. Integrin activation is mediated by the signalling from G protein coupled chemokine receptors (Constantin, 2008). The binding of chemokines expressed by endothelium and chemokine receptors on the surface of leukocytes causes integrin conformational changes, resulting in the firm adhesion of leukocytes with the endothelium (Alon and Dustin, 2007).

The production of several chemokines is up-regulated by endothelial cells upon the activation of cytokines during CNS inflammation. CXCL12 gradients stimulated VCAM/ICAM-mediated T-lymphocyte-endothelium adhesion, and promoted the migration of CD4⁺ T cells and CD8⁺T cells through human brain microvessel endothelial cells (HBMECs) (Liu and Dorovini-Zis, 2009). *In situ* hybridization and immuno-histochemistry showed that CCL19 and CCL21 were predominately expressed in the brain and spinal cord tissue of EAE mice (Alt et al., 2002). These chemokines also activated the firm adhesion of CCR7⁺ T cells to the endothelium of inflamed CNS in binding assays on frozen sections of EAE brains (Columba-Cabezas et al., 2003). Long term genetic over-expression of IL-1 β in the hippocampus of the mouse brain resulted in BBB leakage, up-regulation of CCL2, CXCL1, CXCL2 and a dramatic infiltration of neutrophils into the hippocampus. Interestingly, knocking out the CXCR2 gene in these mice with CNS over-expression of IL-1 β exhibited a significant reduction in neutrophil infiltration, but failed to prevent BBB leakage (Shaftel et al., 2007). The infiltration of CD45⁺ T cells into the sub-ventricular zone (SvZ); a preferential site of inflammatory lesions in EAE, has been associated with the constitutive expression and the up-regulation of CXCL10 in SvZ during EAE development (Muzio et al., 2010).

The firm adhesion of leukocytes with endothelial cells leads to the diapedesis of leukocytes across the BBB. The mechanism underlying the penetration of leukocytes through the tight junction is still undefined. Some *in vitro* studies suggested that it may involve the transient down-regulation of tight junctional elements such as claudin-1/3 and occludin-1 (Xu et al., 2005). The occludin loss

in monocyte diapedesis has been associated with the activity of matrix metalloproteinase enzymes (Reijerkerk et al., 2006).

1.7 Communication between the immune system and the central nervous system (CNS)

The communication between peripheral and the CNS immune systems is bi-directional. The brain perceives the peripheral inflammatory signal and can coordinate responses via the autonomic nervous system (ANS) and hypothalamo-pituitary-adrenal (HPA) systems (Maier, 2003). The activation of both the autonomic nervous system (ANS) and HPA system is considered to be the negative feedback from the brain to regulate the levels of immune response in the periphery (Kin and Sanders, 2006) (Figure 1.2).

CNS modulates stress and the immune response via the sympathetic nervous system (SNS) and the parasympathetic nervous system (PNS). Nerves of the autonomic nervous system originate from the spinal cord, and both sympathetic catecholamine fibres and parasympathetic cholinergic fibres distribute and innervate various effector organs and immune organs, including thymus, bone marrow, lymph nodes and spleen (Nance and Sanders, 2007). Activation of the SNS during stress and peripheral inflammation results in the release of catecholamines, including norepinephrine (NE; noradrenalin) and epinephrine (E; adrenalin), from nerve terminals and from the adrenals (Tjurmina et al., 1999). NE and E bind to two types of receptors: alpha (α) and beta (β) adrenoceptors (AR). Most adaptive and innate immune cells such as CD8⁺ and CD4⁺ T cells, and NK cells express predominately β 2AR (Nance and Sanders, 2007), whereas monocytes and macrophages express α 1AR (Kavelaars, 2002). The sympathetic system has a crucial role in regulation of the immune response; particularly immuno-suppression. Deletion of the mouse peripheral sympathetic nervous system has been shown to increase the proliferation of CD8⁺ T cells in response to viral infection (Grebe et al., 2009). Enhancing NE level using the noradrenaline reuptake inhibitors (NRIs) desipramine and atomoxetine, has been shown to inhibit the expression of the chemokines, CXCL10 and CCL5, and adhesion molecules VCAM-1 and ICAM-1 in the cortex and hippocampus in mice with LPS-induced systemic inflammation, suggesting a role for NE in preventing leukocyte recruitment into the brain (O'Sullivan et al., 2010). The

parasympathetic nervous system (PNS) has recently been renamed the cholinergic anti-inflammatory pathway. Activation of the parasympathetic vagus nerve results in release of acetylcholine (ACH), which binds with nicotinic acetylcholine receptors and inhibits cytokine production in immune cells (Tracey, 2002). Stimulation of the nicotinic acetylcholine receptor $\alpha 7$ subunit has been shown to inhibit TNF- α production in macrophages, suggesting that the PNS is an essential regulator of inflammation (Parrish et al., 2008); (Wang et al., 2003).

The CNS also responds to stressors by activating the hypothalamo-pituitary-adrenal (HPA) axis in order to maintain homeostasis (Kern et al., 2008). Stress initiates the HPA processes by activating the paraventricular nucleus (PVN) of the hypothalamus to release corticotrophin-releasing hormone (CRH) and arginine-vasopressin (AVP). CRH and AVP then stimulate the anterior pituitary gland to release adrenocorticotrophic hormone (ACTH) into the circulation. Circulating ACTH stimulates glucocorticoid-producing cortex cells in the adrenal glands to release corticosteroid hormones including cortisol (in human) or corticosterone (in rodents) (Lanfumeijer et al., 2008). These corticosteroids function as anti-inflammatory hormones and their levels are normally up-regulated during inflammation and infection (Hadid et al., 1999). It has also been reported that increased HPA activity, which is characterized by increased serum cortisol and ACTH levels, has been associated with degrees of anxiety and social stress (Takahashi et al., 2005). Corticosteroids bind with two types of intracellular steroid receptors, the mineralocorticoid (MR) or type I receptor, and the glucocorticoid receptor (GCR) or type II receptor. These receptors are constitutively expressed in the limbic brain areas, thus they are believed to be involved in development of various mood and anxiety disorders (e.g. depression and social phobia) (Lanfumeijer et al., 2008). Both receptor types are expressed in various immune cells (monocytes and lymphocytes), and play a role in immune regulation (Miller et al., 1994). GCRs have been shown to be inducible during adaptive and innate immune responses (Spies et al., 2007); (Bartholome et al., 2004). GCR is a cytoplasmic nuclear factor receptor that forms a complex with cortisol and then translocates to the nucleus. This complex is a transcription factor and binds to sites on DNA leading to regulation of gene transcription of proteins involved in immune function (e.g. suppressing the transcription of pro-

inflammatory cytokines) (Lekander et al., 2009). Activation of the HPA by cytokines has been reported to induce somatic signs and symptoms such as fever. It has been hypothesized that cortisol released after HPA axis activation creates energy by supporting the breakdown of glycogen and the conversion of amino acids, leading to an increase in the core body temperature (Maier, 2003). An increase in core temperature is involved in host defence against infection and in inflammation by inhibiting the rapid proliferation of bacteria and assembly of outer coat proteins of viruses. In addition, host immune functions including T-cell activation and complement activation are much more efficient at fever temperatures (Watkins and Maier, 1999). Fever is one of the major symptoms of sickness behaviour, which is characterized by fever, fatigue, loss of appetite (anorexia), loss of interest in social and sexual interaction, reduced reactivity to reward (anhedonia), decline in mood and cognitive function. Sickness behaviour is common in peripheral inflammation/infection such as during sepsis and autoimmune disease (Dantzer et al., 2008). However, whether activation of HPA by cytokines underlies sickness behaviour in peripheral inflammatory conditions is still controversial. IL-1 β antagonism has been reported to inhibit sickness responses such as fever, increased HPA activity and reduced food and water intake (Milligan et al., 1998). In contrast, IL-6 has been reported to induce HPA activation and fever, but not sickness behaviour (Lenczowski et al., 1997).

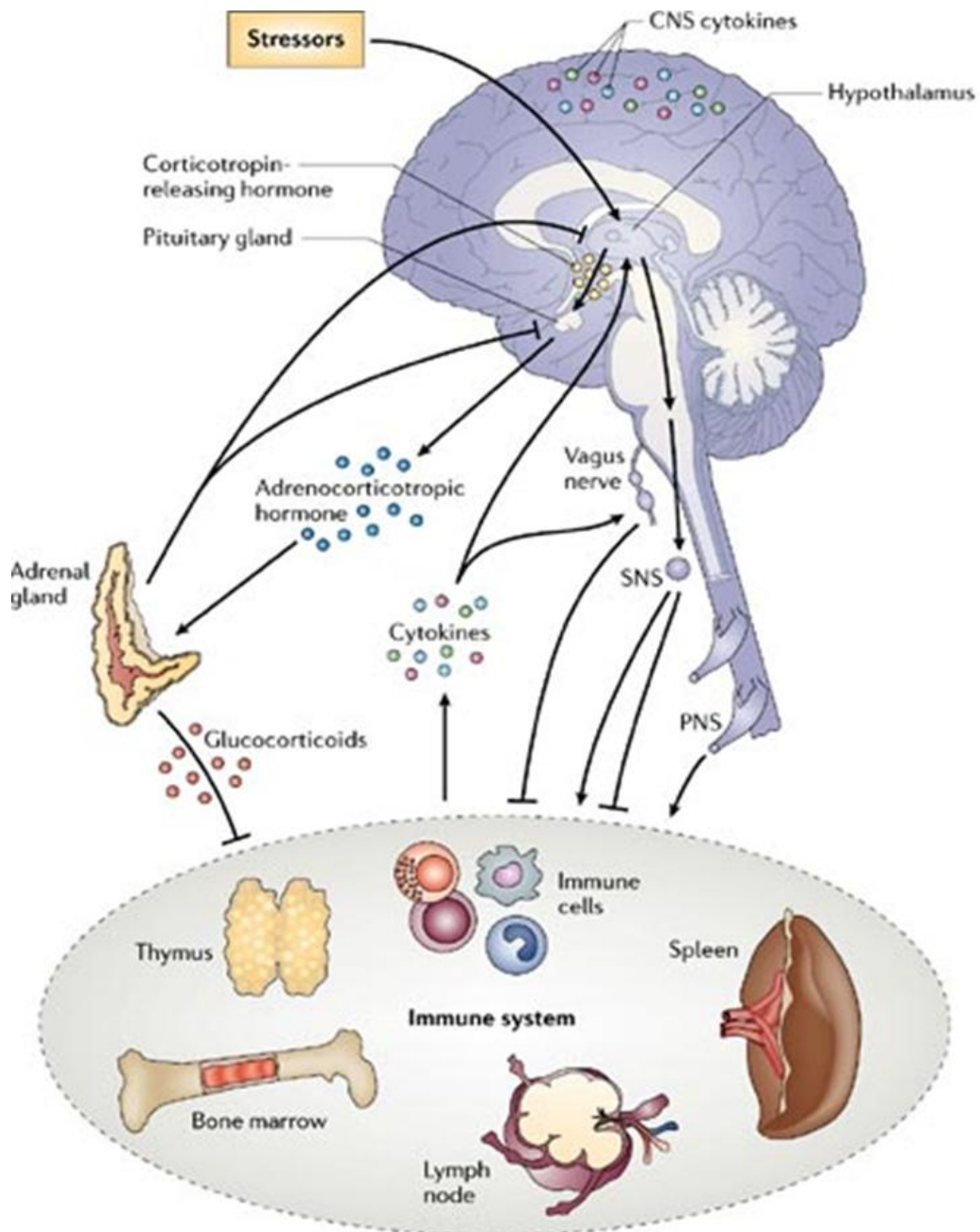


Figure 1.2 The communication between the brain and the peripheral immune system. The brain can regulate peripheral inflammation via the automatic nervous and neuroendocrine systems. The autonomic pathway of the nervous system is further divided into the sympathetic and parasympathetic nervous systems. The sympathetic system activates the immune response via the neurotransmitter norepinephrine, while the parasympathetic nervous system inhibits the immune response via the neurotransmitter acetylcholine. Peripheral inflammation and cytokines activate the hypothalamus to release corticotropin-releasing hormone, which in turn activate the pituitary gland to release adrenocorticotropic hormone. This hormone, in turn, activates the adrenal gland to produce glucocorticoids which suppress inflammation. The image were taken from (Sternberg, 2006) by kind permission of Nature Reviews Immunology.

1.8 Depression

Depression is characterized by a combination of behavioural, emotional, psychomotor and cognitive symptoms, including significant weight loss, insomnia or hypersomnia, reduced appetite, fatigue, extreme feelings of guilt or worthlessness, concentration difficulties and suicidal thoughts (Gotlib and Joormann, 2010). Depression is a common psychiatric disorder that affects up to 25% of women and 12% of men (Gelenberg, 2010). Depression is often a comorbid condition with other mental and physical illnesses; most frequently with anxiety disorders (Castaneda et al., 2008).

Major depressive disorder (MDD) affects some 6% of the population during their lifetime. Major depressive disorder is a heterogeneous disorder with complex aetiology. Many mechanisms have been investigated including, sociological, psychological and biological. There are no clear, unequivocal mechanisms specific to depression and the majority of cases may be a combination of aetiologies. Abnormalities of the monoamine neurotransmitter system have been proposed to be the main pathological mechanism of depression. Based on this monoamine hypothesis, low levels of one or more of the monoamine neurotransmitters, which are serotonin, noradrenalin and dopamine, can induce depression (Singh, 1970). Among these, serotonin is considered to play a major role in the pathological mechanism of depression. It has been demonstrated that depression is caused by abnormalities of the serotonin transporter (SERT) at several levels, including the expression of the SERT gene in different functional polymorphisms (5-HTTLPR), the re-uptake activity of SERT and the level of SERT expressed in the brain. Therefore SERT is considered to be an important therapeutic target site for anti-depressants (Belmaker and Agam, 2008). Several effective anti-depressants that are designed to modulate the serotonergic system, including selective serotonin re-uptake inhibitors (SSRI) and 5-HT₂ receptor antagonists and 5-HT_{1A} receptor partial agonists, are reported to be efficient treatments for depression (Williams et al., 2000a). Recently, there are a number of new psychological theories about the aetiology of depression. The 'neurotrophin hypothesis of depression' is based on accumulating evidence suggesting an association between the cytokine brain derived neurotrophic factor (BDNF) and the psychological and cognitive aspects of depression (Martinowich et al., 2007). Serum BDNF concentrations are lower

in depressed patients, and increase in response to anti-depressant treatment (Matrisciano et al., 2009). Although clinical evidence for this theory exists, the direct *in vivo* evidence showing that reduced endogenous gene expression of BDNF can lead to depression/ depression-like behaviour is still controversial (Sakata et al., 2010); (Chourbaji et al., 2004). It has been suggested that the absence of BDNF in the brain does not cause depression- or anxiety-like behaviour, but rather inhibition of an improved behavioural response to anti-depressants (Saarelainen et al., 2003); (Chen et al., 2006).

Clinical evidence suggests that the neuroendocrine system has a crucial role in regulating psychological conditions (Heiser et al., 2008). HPA axis activation and dysregulation are common in depression and stress-related psychological disorders. Approximately 43% of depression patients exhibit increased concentrations of cortisol and corticotropin-releasing hormone (CRH), and a poor ability to reduce cortisol release as measured by an impaired feedback response to exogenous dexamethasone. Activation of the HPA axis in depression patients can also be attenuated by long-term anti-depressants (Varghese and Brown, 2001). Adult brain neurogenesis is a novel theory of depression that has generated enormous interest over the past decade and will be discussed in the next section.

1.9 Hippocampal neurogenesis

The hippocampus is the major brain region that has a crucial role in encoding episodic memories, especially spatial memory and working memory, which are often considered as parts of cognition (Burgess et al., 2002). Within the hippocampus, the dentate gyrus (DG) generates new neurons throughout life; this is known as neurogenesis (Deng et al., 2010). Neuronal progenitor cells (NPCs) in the subgranular zone (SGZ) of the dentate gyrus differentiate into granular neurons. These cells develop electrical properties and integrate into functional circuits by extending their axonal projections along mossy fibre pathways to the CA3 area of the hippocampus. Neuronal circuits in the hippocampus have been implicated in cognitive memory and learning, involving the processing of new information (Bruehl-Jungerman et al., 2007). The memory formation depends on changes in synaptic long term potentiation (LTP) and long term depression (LTD) (Howland and Wang, 2008). Bliss et al., in 1973 first

demonstrated that LTP was inducible by stimulating dentate gyrus granule cells, which transmit the nerve signals to the CA3 region via the mossy fibre pathway (Bliss and Gardner-Medwin, 1973). CA3 pyramidal neurons then transmit excitatory synaptic signals to the CA 1 region; which has been implicated in memory storage and consolidation, via glutamate release and NMDA/AMPA receptor activation (Kullmann and Lamsa, 2007). Hippocampal neurogenesis and neuronal circuit s shown in Figure 1.3.

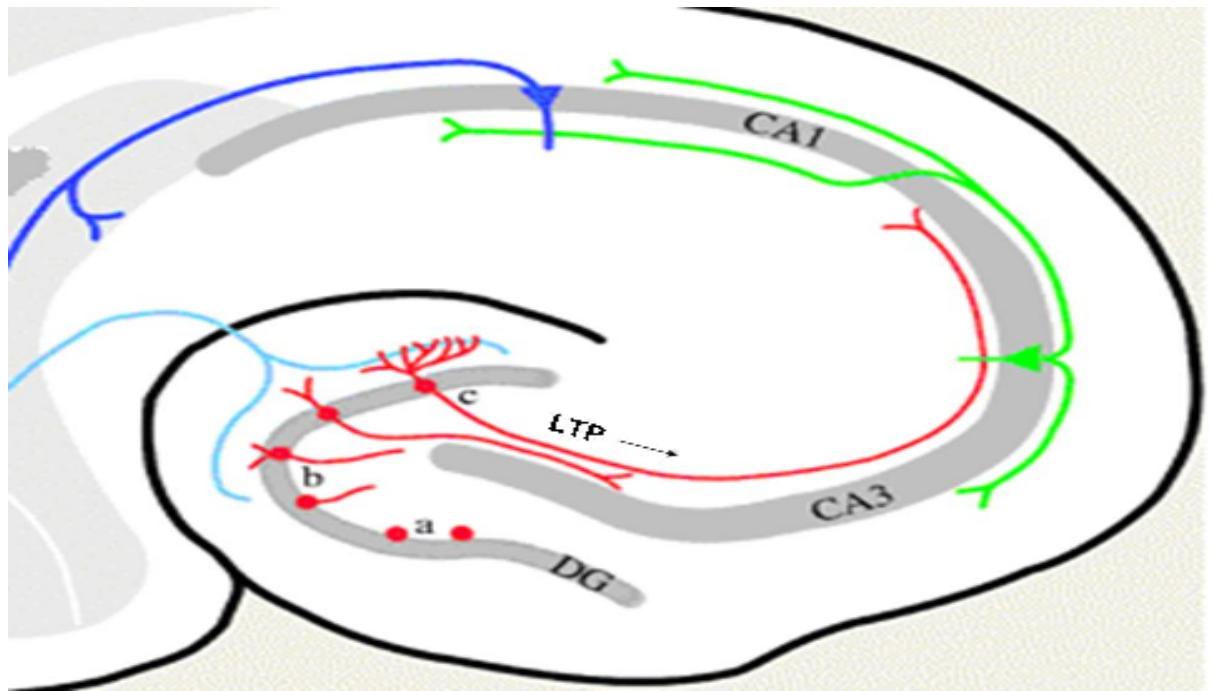


Figure 1.3. Hippocampal neurogenesis and neuronal circuit. Neuronal progenitor cells (NPCs) differentiate into granular neurons and integrate into the circuit by extending their axonal projections along mossy fibre pathways to the CA3 area of the hippocampus (red). These mossy fibre pathways function to transmit neuronal signals in the form of synaptic long term potentiation (LTP). Neurons at CA3 then transmit excitatory synaptic signals to the CA 1 region (green). The image were taken from (Amrein and Lipp, 2009) by kind permission of *Biology Letters*.

1.9.1 The role of neurogenesis in hippocampal function

How neurogenesis contributes to hippocampal function is largely unknown. Accumulating evidence suggests that hippocampal neurogenesis has a crucial role in hippocampal-dependent learning and memory (Deng et al., 2010). Therefore, deficits in adult hippocampal neurogenesis may underlie the cognitive deficits developed in depression (Sahay and Hen, 2007). Biogenic rtTA-Bax mice with genetic deletion of neurogenesis show an impairment in performance on hippocampal-dependent learning and memory tasks, including

water maze and contextual fear conditioning (Dupret et al., 2008). Farioli-Vecchioli and colleague demonstrated that changes in differentiation timing of neurons in the adult dentate gyrus also resulted in spatial learning and memory deficiency, along with a reduction in long-term potentiation of synaptic plasticity (Farioli-Vecchioli et al., 2008); (Farioli-Vecchioli et al., 2009). These findings suggested that these immature DG neurons are highly active and able to transmit synaptic plasticity and encode the memory at a specific stage of their differentiation.

Computational models of DG newly born neuron function also suggested that neurogenesis also has a crucial role not only in encoding memory, but also in the consolidation of memory. Without neurogenesis, a sparse subset of mature DG neurons encode the initial memory via a synaptic transmission to a limited set of pyramidal cells in CA3, leading to a unique pattern of activated CA3 cell networks for the initial memory. The later memory is encoded by another subset of mature DG neurons, resulting in another unique pattern of activated CA3 cell networks for the later memory. The patterns of both activated CA3 cell networks for the initial and the later memories thus do not overlap. On the other hand, with neurogenesis, both initial and later memories are encoded equally by immature DG neurons. This leads to two overlapping patterns of activated CA3 cell networks, suggesting that the initial memory is consolidated and protected from encoding the later memory. However, these immature DG neurons will mature and die in a short period of time (~ 3 weeks to ~ 2 months) (Zhao et al., 2006). Therefore, the memory of a new event that occurs at a much later time is encoded by a different set of immature DG neurons, which are no longer able to encode the initial memory. This leads to two independent patterns of activated CA3 cell networks. This finding suggested that hippocampal neurogenesis may be responsible for encoding and consolidating memories of events that occur closer in time. However, the retrieval of long-term memory in human may be hippocampal-independent or regulated by other brain regions (Aimone et al., 2006).

1.9.2 Hippocampal neurogenesis and depression

The ‘hippocampal neurogenesis hypothesis of depression’ is based on accumulating evidence showing a reduction of hippocampal neurogenesis in the

model of stress-related mood disorders. Animal experiments showed that stress or chronic treatment with corticosterone caused reduced hippocampal neurogenesis, along with a decreased hippocampal volume (Brummelte and Galea, 2010); (Czeh et al., 2001). Other important evidence supporting this hypothesis is that anti-depressants increase hippocampal neurogenesis in both animals and humans. Anti-depressants such as fluoxetine, agomelatine, imipramine and electroconvulsive therapy (ECT) have been reported to increase neurogenesis in various species, including rodents, nonhuman primates and humans, and reverse reduced neurogenesis that is induced by stress and cerebral ischemia (Perera et al., 2007); (Malberg et al., 2000); (Banasr et al., 2006); (Schiavon et al., 2010). A neurogenesis study of frozen hippocampus isolated from depression patients showed a reduction in neurons expressing neural progenitor (NPCs) markers compared to those of healthy control subjects. Interestingly, the number of neural progenitor (NPCs) cells in the hippocampus of depression patients who received long-term SSRIs- and tricyclic antidepressants (TCAs)-treatment was higher than those of untreated depression patients (Boldrini et al., 2009). Importantly, hippocampal neurogenesis is considered to be a potential therapeutic target site of the action of anti-depressant drugs because hippocampal neurogenesis was shown to be essential for behavioural effects of anti-depressants in mice. Serotonin 1A receptor deficient mice treated with fluoxetine or imipramine treatment showed higher level of appetite, measured by a depressive-like behaviour test called the suppressed feeding test, compared to untreated serotonin 1A receptor deficient mice. However, after ablation of neurogenesis by x-irradiation, serotonin 1A receptor deficient mice that received antidepressants showed no difference in the level of appetite compared to those without the treatment (Santarelli et al., 2003). However, it is still unclear whether impairment in hippocampal neurogenesis is an aetiological factor for depression. Reductions in hippocampal volume have been reported in depressed patients (von Gunten and Ron, 2004); (Frodl et al., 2006). It has been hypothesized that the decrease in neurogenesis in the SGZ of the dentate gyrus may also be the main contributor to decreased hippocampal volume. However, there is no direct evidence showing that changes in adult hippocampal neurogenesis account for the reduction in hippocampal volume in patients with depression. Decreased numbers of progenitor cells were observed in the hippocampus of depression patients. Immuno-histochemical

staining showed a reduction in the number of neurons expressing the progenitor cell marker, MCM2, in frozen hippocampus tissues isolated from 10 depression patients, compared to those from 10 sex- and age-matched healthy control subjects (Lucassen et al., 2010). However, methods and devices for imaging of neurogenesis in live human brains are still not fully developed. Therefore, the indirect approach is to use proton magnetic resonance spectroscopy (^1H -MRSI) to identify changes in neuro-metabolites that reflect neuronal dysfunction, glial reaction and energy metabolism. N-acetylaspartate (NAA) is one of the neuronal markers that is commonly used in proton MR spectroscopic (MRS) imaging. This is because NAA is a metabolite of aspartate, which is the main amino acid consumed by CNS neurons (Maletic-Savatic et al., 2008). Patients with mild cognitive deficiency also showed a reduced NAA in the hippocampus (Wang et al., 2009b). However, it has been reported that inhibition of hippocampal neurogenesis using X-irradiation does not cause a reduction of hippocampal volume (Santarelli et al., 2003). Pathohistological studies of post-mortem tissue suggested that increased apoptosis of mature neurons or glial cells are the cause of the reduction in hippocampal volume (Czeh and Lucassen, 2007); (Sahay et al., 2007). Preclinical studies showed that changes in the hippocampal neurogenesis volume resulted from changes in morphology of neurons such as reduced dendritic complexity, but not from ablation of hippocampal neurogenesis (Santarelli et al., 2003); (McEwen, 2005). In addition, it is still controversial whether the impairment in hippocampal neurogenesis is directly associated with depression-like or anxiety-like behaviour. Transgenic mice with a neurogenesis deficiency exhibited an increase in anxiety-related behaviour (Revest et al., 2009). In contrast, a study by Saxe *et al* reported that the inhibition of hippocampal neurogenesis does not influence anxiety-related behaviour tested by open field, light-dark choice test, and elevated plus-maze tests (Saxe et al., 2006). Moreover, an increase in hippocampal neurogenesis by anti-depressants does not always correlate with an improvement in depression-like or anxiety-like behaviour in animals. A study in BALB/cj mice showed that chronic fluoxetine treatment improved depressive behaviour without inducing changes in hippocampal neurogenesis (Huang et al., 2008). This finding is supported by another study by Bessa 2009 showing that the effect of anti-depressants on depression-like behaviour depended on neuronal remodelling, but not hippocampal neurogenesis (Bessa et al., 2009). In contrast, hippocampal

neurogenesis has been reported to be the essential target site for the effects of anti-depressants on depression-like or anxiety-like behaviour in animals (Santarelli et al., 2003). This evidence suggests that anti-depressants may have both neurogenesis-dependent and -independent effects on depression-like or anxiety-like behaviour (David et al., 2009). The evidence in support of and in conflict with the 'hippocampal neurogenesis hypothesis of depression' suggests that the role of hippocampal neurogenesis in the aetiology of depression need to be further investigated.

1.10 Cytokines, peripheral inflammation and depression

Recent attempts have been made to classify this disorder and one approach has been to explore the co-morbid depression seen in many medical illnesses. There is increasing evidence of association between inflammation and major depressive disorder (MDD) and this comes primarily from 3 clinical observations.

- i) Inflammatory medical illnesses - both CNS and peripheral - are associated with greater rates of major depression.
- ii) MDD even in the absence of medical illness is associated with raised inflammatory markers.
- iii) Patients treated with cytokines for various illnesses are at risk of developing major depressive illness.

Sub-typing depression may help uncover the role of biological mechanisms that may be specific to these subtypes. Depression with a prominent inflammatory component may be one such subtype. The uncovering of different biological mechanisms relating to depressive subtypes may also aid the development and targeting of new treatment strategies.

1.10.1 Depression and rheumatoid arthritis

Depression is associated with several chronic inflammatory diseases such as RA, MS, psoriasis as well as diabetes (Engum et al., 2005), obesity (Atlantis et al., 2009), and cardiovascular disease (Pitt and Deldin, 2010). In RA, the prevalence

of depression is 14%-46% (Katz and Yelin, 1993); (Dickens et al., 2002). A recent clinical study of 82 RA patients showed that the prevalence of depression was 41.5% and the degree of depression was positively associated with the duration of RA disease (Isik et al., 2007). Depression was shown to increase the risk of mortality in RA; a study of 1290 RA patients showed that those who had suffered from persistent or recurrent depression over the first 4 year period of disease had higher mortality rates compared to those without depression during an 18-year observation period (Ang et al., 2005). Higher rates and specific patterns of suicide have also been reported in RA patients with depression. 11% of hospital outpatients with rheumatoid arthritis (13 of 123) experienced suicidal thoughts (ideation) (Treharne et al., 2000). In a study of 19 suicide victims who had hospital-treated RA, 52.6% were female. In addition, 90% of these female RA patients had suffered from co-morbid depression and had chosen a violent suicide method, compared to male RA patients who committed suicide (Timonen et al., 2003). The cause of depression in RA is unclear. Similar to other painful conditions, depression associated with RA is often considered to be a simple consequence of the experience of chronic pain. This concept was supported in a large-scale study of 22131 RA patients, using a questionnaire of the Symptom Intensity Scale, showing that pain and fatigue were the strongest predictors of self-reported depression (Wolfe and Michaud, 2009). However, a relation between pain and depression in RA is still unclear because a study by Mindham *et al* indicated that pain and disability in RA are not potent factors that can contribute to depression (Mindham et al., 1981), and a clinical study of 218 RA patients showed that depression in RA patients is not only associated with pain, but correlated with the concentration of the acute phase response inflammation marker C-reactive protein (CRP) level in the blood (Kojima et al., 2009). This suggests the hypothesis that 'peripheral inflammation may participate in depression in RA'.

Several reports also suggest that sleep disorders are associated with chronic inflammatory diseases such as rheumatoid arthritis (RA), asthma and systemic lupus erythematosus (SLE) (Janson et al., 1996, Gudbjornsson and Hetta, 2001, Bourguignon et al., 2003, Keefer et al., 2006). However, it is still unclear whether sleep abnormalities in patients with these chronic inflammatory diseases are the result of pain, stress or depression that is associated with these

chronic inflammatory diseases. It is also possible that sleep disturbance itself could be a result of disease-related immune changes, which increased risk of depression in patients with these chronic inflammatory diseases. Vice versa, sleep deprivation has been reported to alter immune system functions by increasing the activity of natural killer (NK) cells and monocytes (Dinges et al., 1994). Prolong periods of wakefulness can also result in an increase in serum IL-6 and TNF soluble receptor concentrations (Shearer et al., 2001). The activation of immune responses caused by sleep deprivation may have a negative impact on the availability of tryptophan to the brain and hence reducing synthesis of serotonin (5-HT), which could be a possible underlying pathological mechanism of depression (Fernstrom et al., 1990). A study by Song et al., demonstrated an inverse relationship between the low availability of plasma tryptophan and high serum IL-1RA, IL-6 and IL-8 concentrations in patients with primary sleep disorders associated with major depression (Song et al., 1998). This study suggests that sleep disruption plays a detrimental role in immune-inflammation that possibly causes or contributes to depression. Therefore, it seems logical to consider sleep disturbances as one of the factors that negatively influences chronic inflammatory diseases and that it possibly plays a role in depression in the context of chronic inflammatory diseases.

1.10.2 Immune activation in depression patients

Important evidence supporting the ‘inflammation-induced depression in RA’ hypothesis includes the increased concentrations of cytokines, immune cells and inflammatory marker such as CRP in the blood of depression patients.

Alterations in the serum concentrations of various cytokines, including TNF- α , IL-1 β , IL-6, IL-4, IL-10, IL-8, IL-4, IFN- γ , GM-CSF and IL-12, in depression patients have been reported. However, some of these cytokine changes have not been consistent in different studies, depending on the particular cytokine and the measurement technique used. For example, a study of serum cytokine concentrations in 49 depression patients using a human 22-plex multi-cytokine detection (Luminex) system showed increased concentrations of 15 cytokines/chemokines including IL-10 and GM-CSF (Simon et al., 2008). In contrast, a study in 12 depressive patients using an Enzyme-linked immunosorbent assay (ELISA) method showed lower than normal serum IL-10

concentrations (Dhabhar et al., 2009). Serum levels of GM-CSF within normal levels, measured by using a Bio-Plex human cytokine kit, was observed in 122 depression patients (Lehto et al., 2010a). A recent meta-analysis of 24 studies looking at serum cytokine concentrations in major depression demonstrated that IL-6 and TNF- α were 2 cytokines that were consistently found to be higher than normal (Dowlati et al., 2010). An increased serum TNF- α concentration has been associated with suicidal tendency in depression patients (Eller et al., 2009) and the concentrations of both soluble TNF- α receptors, sTNFR-1 and sTNFR2 were also increased in the serum of depression patients (Grassi-Oliveira et al., 2009). IL-6 and TNF- α were also up-regulated in the CSF of depression patients (Palhagen et al., 2010). A positive correlation between CSF TNF- α and IL-6 with the depression score; measured by Postpartum Blues Scale and Edinburgh Postnatal Depression Scale (EPDS), was observed in depressive women during delivery and during the postpartum period (Boufidou et al., 2009). Suicide attempters showed higher than normal IL-6 concentration in the CSF, and this correlated with Montgomery-Åsberg Depression Rating Scale (MADRS) (Lindqvist et al., 2009). These data suggest that TNF- α and IL-6 may have a major role in the immuno-pathology of depression. Interestingly, chemokines have recently been shown to have a role in depression. Serum concentrations of MCP-1, MIP-1B and IL-8 were reduced in patients with major depression, suggesting that chemokines may play a protective role in the pathology of depression (Lehto et al., 2010b).

Several studies have demonstrated that cell-mediated immune activation may be a key component in the pathogenesis of depression (Maes, 2010). Several studies demonstrated an imbalance of Th1 and Th2 cytokines in depression patients. The Th1/Th2 ratio, as indicated by the serum IFN- γ /IL-4 concentration ratio was increased in depressive patients, but this ratio returned to the normal baseline after anti-depressant treatment (Myint et al., 2005); (Kim et al., 2008). The serum IL-1 β /IL-10 ratio was also increased in patients with acute melancholic depression (Huang and Lee, 2007). A recent study of 27 patients with major depression showed a 3-fold increase in the Th1/Th2 cell ratio as shown by the concentration ratio of serum IL-2/IL-10. In addition, in depression patients a reduction in CD4⁺CD25⁺ regulatory T cells in peripheral blood, along with a reduced 5-HT1a receptor expression on these regulatory T cells were

observed. A shift in the Th1/Th2 ratio in depression suggests that activation of the inflammatory response may play a role in immuno-pathological mechanism of depression. The association between reduced CD4⁺CD25⁺ regulatory T cells and a decrease in 5HT receptor also suggests that the immune dysregulation during depression may affect the serotonergic system, which eventually contributes to the development of depression (Li et al., 2010).

1.10.3 *The cytokine hypothesis of depression*

The 'cytokine hypothesis of depression' states that peripheral inflammation can cause changes in cytokine expression profiles in the brain, leading to various neurological outcomes such as alterations in the neurotransmitter and neuroendocrine systems. These eventually may result in somatic and psychological symptoms such as sickness behaviour, depression and cognitive dysfunction (Schiepers et al., 2005). This hypothesis is based on the evidence showing that cytokine therapy can induce neuro-psychiatric symptoms in patients with cancer or chronic hepatitis C. Cytokines such as IFN- α and IL-2 can be used as immunotherapy for the treatment of chronic hepatitis C and cancer (Bonaccorso et al., 2001); (El-Zayadi, 2009); (Pasquini et al., 2008). Approximately 30% of patients who received IFN- α therapy develop sickness-like symptoms, anxiety and major depression, which are the major side effects of immunotherapy (Quarantini et al., 2007). The sickness-like symptoms, including lack of sleep, loss of appetite, weight loss and fatigue usually occurred during the first 2-4 weeks of the therapy and can be early indicators for depression which usually developed 1-3 months after the treatment (Robaey et al., 2007); (Franzen et al., 2010). IFN- α therapy also has an effect on other neuro-psychological functions such as locomotor activities. Chronic hepatitis C patients who receive IFN- α exhibited slower response times in the rapid visual information processing task. This locomotor impairment has also been associated with increased depressive symptoms and fatigue (Majer et al., 2008). IFN- α induced impairment of locomotor activity and depressive behaviour have also been observed in a non-human primate model, using rhesus monkeys and in a mouse model (Felger et al., 2007). In addition, changes in behavioural symptoms have also been associated with alterations in neurotransmitter levels such as 5-

HT and dopamine in the CNS of these models (Felger et al., 2007); (Litteljohn et al., 2010).

1.10.4 Possible mechanism underlying cytokine-induced depression

Possible mechanisms underlying cytokine-induced depression are still unclear. The central effects of pro-inflammatory cytokines on the neurotransmitter system, neuroendocrine, neurotropic factor and hippocampal neurogenesis may contribute to the development of depression.

Peripheral inflammation and cytokines can modulate neurotransmitter systems such as serotonin (5-HT), dopamine (DA), and noradrenaline (NA) via the regulation of neurotransmitter biosynthesis and their transporter activities. (MohanKumar et al., 1999). A study by Zhu *et al* demonstrated that interleukin-1 β and tumor necrosis factor- α stimulated the transport activity of the serotonin transporter in serotonergic neurons of mouse midbrain and striatum, in a dose- and time-dependent manner (Zhu et al., 2006). The effect of pro-inflammatory cytokines on tryptophan metabolism, particularly the indoleamine 2,3-dioxygenase (IDO) pathway, has recently been considered to be one potential mechanism underlying inflammation-induced depression. The IDO pathway seems to be the most important link between inflammation and serotonin metabolism. IDO degrades L-tryptophan (L-TRP), an amino acid precursor of serotonin (5HT), via the kynurenine pathway during immune activation (Kwidzinski and Bechmann, 2007). L-tryptophan is catabolized into L-kynurenine (L-KYN), which is metabolised further to quinolinic acid (QUIN) and kynurenic acid (KA) (Kwidzinski and Bechmann, 2007). The expression of IDO is induced mainly by IFN- γ and TNF- α in several immune cells, including macrophages (Thomas et al., 2001), dendritic cells (Jurgens et al., 2009, Dai and Gupta, 1990), and fibroblast (Dai and Gupta, 1990). IFN- γ induction of IDO was also found in astrocytes (Suh et al., 2007) and microglia (Yadav et al., 2007). IDO also has a crucial role in immuno-suppression by inhibiting the proliferation of CD4⁺ T cells and CD8⁺ T cells (Forouzandeh et al., 2008) and of regulatory T cells (Munn and Mellor, 2007). Both clinical and experimental studies have demonstrated that depressive-like behaviour induced by systemic inflammation or cytokines could be mediated by IDO activation. Systemic LPS injection-induced IDO activation,

along with increased IL-6 and TNF- α production by microglia in the cortex and hippocampus of the mouse brain, caused depressive-like behaviour in mice (O'Connor et al., 2009); (Connor et al., 2008). A decrease in peripheral tryptophan, and the positive correlation between CSF QUIN, CSF cytokine and depressive symptoms were observed in depressive patients during hepatitis C treatment with IFN- α (Raison et al., 2010). This evidence suggests that peripheral inflammation may induce the expression of IDO enzyme as a negative feedback to suppress inflammation. However, IDO enzyme causes the reduction of precursor of 5HT, leading to depression during inflammation. In addition, peripheral inflammation and chronic inflammatory diseases induce the HPA axis to release CRH and glucocorticoids that in turn affect the neurobiology of cognition and mood (Pace et al., 2007). The central action of cytokines may also account for the reduction of the neurotropic factors such as BDNF. Several experimental studies showed that a reduction of BDNF in the hippocampus caused by cytokines, has been reported to cause an impairment in cognition. Peripheral inflammation in mice caused a reduction of hippocampal BDNF and also showed an impairment in hippocampal-dependent memory (Bilbo et al., 2008). A potential mechanism underlying cytokine-induced depression can be suggested; this is that cytokines can mediate decreased neurogenesis, thereby causing depression.

1.10.5 Cytokine-mediated inflammation and decreased hippocampal neurogenesis in depression

Hippocampal dysfunction due to a reduction in neurogenesis has been demonstrated to be a major contributor to the cognitive impairment aspect of depression. Adaptive and innate immune responses, immune cells and inflammatory mediators resulting from peripheral inflammation have their roles in the regulation of neurogenesis. It has been hypothesised that 'impairment of hippocampal neurogenesis by immune activation may be an underlying mechanism of the depression that develops during systemic inflammation'. This hypothesis is based on several recent studies showing that alterations in hippocampal neurogenesis by cytokines, immune cells and immune activation can contribute to behavioural changes in animal models. Socially isolated mice over-expressing interleukin-1 receptor antagonist in the hippocampus showed an improvement in memory impairment and a recovery from suppressed

neurogenesis (Ben Menachem-Zidon et al., 2008). Learning experience-induced-neurogenesis has been associated with the recruitment of CNS-specific T cells and the activation of microglia (Ziv et al., 2006). In contrast, autoimmune-prone cytokine B-cell-activating factor (BAFF) transgenic mice; a model of systemic lupus erythematosus, rheumatoid arthritis and Sjögren's syndrome, showed decreased hippocampal neurogenesis and LTP, along with increased anxiety behaviour (Crupi et al., 2010). These findings suggest different roles for T cells and B cells in the regulation of neurogenesis, which can contribute to different aspects (cognition and mood) of depression. Based on this evidence, hippocampal neurogenesis can be considered as an important link between inflammation and depression.

1.10.6 Role of peripheral inflammation in hippocampal neurogenesis

Accumulating evidence suggests that inflammatory processes, both local and systemic, can reduce the proliferation and survival of new neurons. Ekdahl *et al* found that administering LPS locally into brains gave rise to microglial activation in the hippocampus which resulted in strongly impaired neurogenesis (Ekdahl et al., 2003). Monje ML *et al* also demonstrated the effect of systemic inflammation on adult hippocampal neurogenesis. Inducing peripheral inflammation using i.p. injection of LPS in female rats, leads to the inhibition of neurogenesis in the adult dentate gyrus. Interestingly, the reduced neurogenesis can be reversed by indomethacin, a cyclooxygenase COX1/COX2 inhibitor. This result also indicated that the decrease of neurogenesis caused by chronic inflammation was associated with a progressive decline in learning and memory (Monje ML et al., 2003).

1.10.6.1 Role of cytokines in hippocampal neurogenesis

There are various possible mechanisms underlying peripheral inflammation suppression of hippocampal neurogenesis. This may be due to the direct effect of pro-inflammatory cytokines produced during the inflammatory process on morphological development in the hippocampus. IL-1 β is an important regulator of brain cytokine networks that contribute to the inflammatory process of various neurodegenerative diseases (Allan et al., 2005). Peripheral LPS administration resulted in increased IL-1 β concentrations in the rodent

hippocampus (Csolle and Sperlagh, 2010). In addition, the hippocampus itself is the brain area with the most intense expression of IL-1 β and its receptor (Allan et al., 2005). *In vivo* cell cycle and proliferation analysis using bromodeoxyuridine (BrdU) demonstrated that after 1 week of IFN- α administration in rats, a reduced number of BrdU labelled proliferating cells was observed in the dentate gyrus. Interestingly, following the injection of IFN- α , an increased concentration of IL-1 β was also observed in the hippocampus. Moreover, with co-administration of IL-1 β receptor antagonist, the IFN- α -induced suppression of the neurogenesis in the adult dentate gyrus was completely blocked. This suggests that the IFN- α inhibits neuronal proliferation in the dentate gyrus via IL-1 β signalling (Kaneko N et al., 2006).

1.10.6.2 Role of chemokines in hippocampal neurogenesis

Chemokines, particularly the CXCL12/CXCR4 ligand and receptor, have crucial roles in hippocampal neurogenesis; particularly in the regulation of the survival and maturation of neuronal progenitor cells. CXCR4 has a direct role in the regulation of the migration of granule cells. CXCR4 gene-deficient mice showed a dramatic decrease in the distribution of dividing precursor cells from the ventricular zone to the dentate gyrus (Bagri et al., 2002). CXCL12 also enhanced human neuronal progenitor cell proliferation (Wu et al., 2009). Smaller and morphologically immature cells of the hippocampal dentate gyrus were observed in CXCR4 gene-deficient mice (Lu et al., 2002). CXCL12, which functions as a chemo-attractant for leukocytes, also shows a chemo-attractive activity for embryonic cerebellar neurons in the meninges (Zhu et al., 2002b). CXCL12 also has an effect on the maturation and differentiation of hippocampal neurons by regulating axonal patterning at an early stage of neuronal development. Hippocampal neurons treated with CXCL12 showed specific morphology with shorter axons and more axonal branches compared to normal hippocampal neurons (Pujol et al., 2005). CXCL12 also showed an effect on axon outgrowth into other types of neurons and acts as a chemotactic molecule that influences axonal guidance in cultured retinal ganglion cells (Chalasani et al., 2003). Increased axonal elongation was observed in cerebellar granule neurons treated with CXCL12 in a dose-dependent manner (Arakawa et al., 2003).

1.10.6.3 Role of innate immunity in hippocampal neurogenesis

Recent findings showed that innate immunity is also involved in hippocampal neurogenesis; mainly via TLRs. TLR2 gene-deficient mice showed a reduction in hippocampal neurogenesis. In contrast, TLR4 deficient mice exhibited increased proliferation and neuronal differentiation (Rolls et al., 2007); (Keene et al., 2009). Activating TLR3 suppressed neural progenitor cell proliferation *in vivo*, while hippocampal neural progenitor cells in TLR2 deficient mice showed greater maturation compared to controls (Lathia et al., 2008).

1.10.6.4 Role of adaptive immunity in hippocampal neurogenesis

The role of the adaptive immune response in hippocampal neurogenesis is still controversial. A study by Ziv et al., suggested that T cells supported hippocampal neurogenesis (Ziv et al., 2006). This observation is confirmed by a study showing an increase in hippocampal neurogenesis in arthritis model mice (AIA model). The author of that study suggested that the increase in hippocampal neurogenesis was regulated by T cells (Wolf et al., 2009a). In contrast, a study by Wang *et al* showed that activated T cells inhibited neurogenesis (Wang et al., 2010). In addition, B cells also showed to reduced hippocampal neurogenesis (Crupi et al., 2010). It seems therefore that lymphocytes can contribute to neurogenesis but that little is known about the mechanisms.

1.10.6.5 Potential indirect regulation of hippocampal neurogenesis associated with inflammation

As well as the direct effect of cytokines, immune cells and immune activation, hippocampal neurogenesis could be regulated by indirect pathways associated with inflammation such as from the neuroendocrine system or neurotrophic factors. Peripheral inflammation and chronic inflammatory diseases induce the HPA axis to release CRH and glucocorticoids that in turn affect the neurobiology of cognition and mood (Rohleder et al., 2010). Animal experiments showed that stress and chronic treatment with corticosterone caused reduced hippocampal neurogenesis, along with a decreased hippocampal volume (Brummelte and Galea, 2010); (Czeh et al., 2001). Chronic administration of corticosterone was shown to inhibit hippocampal neurogenesis and reduce hippocampal volume,

along with increased anxiety (light dark box test) and depression (forced swim test) -like behaviour, suggesting that corticosterone not only induces depression via the serotonergic system, but also via neurogenesis (Murray et al., 2008). Chronic stress and glucocorticoid treatment may suppress hippocampal neurogenesis by inhibiting BDNF production in the hippocampus (Smith et al., 1995). A swim stress test was shown to inhibit BDNF mRNA expression and TrkB signalling in the mouse hippocampus (Shi et al., 2010). However, there is no direct evidence showing that peripheral inflammation-induced CRH/glucocorticoids suppress hippocampal neurogenesis. However, a recent study of human hippocampal progenitor cells showed that the anti-depressant sertraline increased hippocampal neurogenesis via the glucocorticoid receptor (Anacker et al., 2011). This finding revealed a new concept of glucocorticoids action on hippocampal neurogenesis, suggesting that glucocorticoids may not only suppress neurogenesis, but can also support hippocampal neurogenesis. This finding could be significant in the case of glucocorticoid resistance in patients with chronic inflammatory disease. Glucocorticoid resistance is common in patients with RA and asthma (Barnes and Adcock, 2009), and it is characterized mainly by glucocorticoid receptor dysfunction of lymphocytes (Rohleder et al., 2010). Glucocorticoid resistance exaggerates inflammation and hyperactivity of corticotropin releasing hormone and sympathetic nervous system pathways, which may have detrimental effect on hippocampal neurogenesis (Pace et al., 2007). It is possible that the anti-depressant may also have an effect to activate the glucocorticoid receptor at the peripheral level and reduce HPA activation. This may result in enhanced hippocampal neurogenesis. However, it would be interesting to test this hypothesis.

BDNF has also been shown to modulate proliferation, survival, differentiation and dendritic development of hippocampal progenitors. Ablation of BDNF expression in the hippocampus with gene-deleted mice resulted in decreased hippocampal neurogenesis (Choi et al., 2009). Interestingly, ablation of BDNF in the hippocampus resulted in a reduction in neurogenesis, along with increased behaviour associated with depression, suggesting a role for BDNF-induced neurogenesis in the psychological aspect of depression (Taliaz et al., 2010). Although the association of BDNF and depression has been demonstrated by several clinical and experimental studies, the role of BDNF in inflammation-

induced-depression via neurogenesis has not been well documented. Several animal studies suggested that induction of peripheral inflammation, using LPS or IL-1 β can induce a reduction of BDNF protein and mRNA in various regions in the brain (Guan and Fang, 2006), particularly in the synaptosome of pyramidal cells in CA1, CA3 and dentate gyrus in the hippocampus (Lapchak et al., 1993); (Schnydrig et al., 2007). Paradoxically, preventing learning experience by isolating mice socially caused reduced hippocampal BDNF, which was reversed by IL-1 β antagonist (Barrientos et al., 2003). IL-1 β -induced memory deficits may be mediated via BDNF mRNA reduction in the hippocampus. The role of BDNF in hippocampal neurogenesis associated with depressive-like behaviour requires further investigation.

Based on experimental evidence, the peripheral inflammation-induced changes in hippocampal neurogenesis seems to be one of the putative mechanisms underlying inflammation-induced depression. However, there is no clinical evidence in humans emerging to support this hypothesis. The 'hippocampal neurogenesis hypothesis of depression' was originally based on observations showing that anti-depressants could increase hippocampal neurogenesis. However, so far there is no direct evidence of anti-depressants modulating immune response and inducing changes in hippocampal neurogenesis. Although several clinical studies have shown that anti-depressant therapy might help to reduce interferon-induced psychiatric or depressive symptoms (Raison et al., 2007). One mechanism underlying the protective effect against cytokine therapy-induced depression is that many anti-depressants have anti-inflammatory effects that can modulate cell-mediated immune responses (Capuron et al., 2002). Anti-depressants can also have direct effects on microglia. Anti-depressants such as fluvoxamine, reboxetine, imipramine and risperidone were shown to reduce IL-6 production by IFN- γ -activated microglia in vitro (Hashioka et al., 2007). However, there is no direct evidence showing that anti-depressants can reverse impairment of hippocampal neurogenesis via the suppression of inflammation. Therefore, further investigation for peripheral inflammation-induced changes in hippocampal neurogenesis in depression is required.

1.11 Aims and hypothesis

To summarise the main points of the Introduction linking depression with immunity: Clinical depression has been associated with chronic inflammatory diseases. This appears to be an important clinical co-morbidity and the mechanisms are poorly understood. The active involvement of the immune response was implicated when cytokine therapy itself was shown to induce depression in cancer and hepatitis C patients. In experimental models, systemic LPS challenge can induce an innate systemic inflammatory response as well as an immune response in the CNS. The involvement of cytokines in this process was shown by systemic administration of cytokines (TNF- α , IFN- γ) which caused a reduction in hippocampal neurogenesis in the brain. An impairment in hippocampal neurogenesis has been implicated in depression, cognitive decline and depressive-like behaviour in humans and in animal models. However, there are very few studies that have investigated the effects of peripheral inflammation on hippocampal neurogenesis in chronic inflammatory disease models. An investigation of this may lead to better understanding of depression in chronic inflammatory diseases, leading to an evidence based approach to treatment.

Therefore, the **hypothesis** of this project is that:

‘Peripheral inflammation and cytokines associated with Rheumatoid Arthritis affect central production of inflammatory mediators in the brain which in turn impair hippocampal neurogenesis. This may lead to cognitive decline and mood disorders often seen in arthritis patients.’

In order to test this hypothesis, the **aims** of this project are:

Preamble: Rheumatoid Arthritis is one of the most studied chronic inflammatory diseases associated with psychiatric disorders. The major aim of this project is to investigate evidence of brain inflammation and changes in hippocampal neurogenesis in collagen induced arthritis (CIA), a well-established murine model of RA.

Several experimental approaches have been conducted using this CIA model in order to address this general question, with the following specific aims:

1. To investigate changes in central production of inflammatory mediators in the brain, which may be associated with peripheral joint inflammation in arthritis. We determined changes in protein concentrations and mRNA expression levels of inflammatory mediators in brains of CII immunized mice compared with control mice.
2. To investigate the association between peripheral inflammation and central production of inflammatory mediators. We determined longitudinal changes in serum of inflammatory mediators along with longitudinal changes in protein and mRNA concentrations of inflammatory mediators in brains CII immunized mice. An extended aim of this experiment included providing additional information of brain immune activation and the interplay between inflammatory mediators in the brain of CII immunized mice throughout the development of disease and clinical signs of arthritis.
3. To investigate the effect of systemic (peripheral) treatment using the recombinant humanised soluble TNF receptor drug etanercept to mediate TNF-blockade on central production of inflammatory mediators in brains of CII immunized mice during the period of clinical signs of arthritis. We aim to determine changes in inflammatory mediators in the brains of etanercept-treated compared with PBS-treated CII immunized mice and each of these with antigen-naïve healthy control mice. An extended aim is to confirm that changes in inflammatory mediator profiles in brains of CII immunized mice were due to peripheral inflammation during arthritis.
4. To investigate a possible mechanism of associated depression by studying the effect of peripheral inflammation on hippocampal neurogenesis. We aim to analyze changes in hippocampal neurogenesis in CII immunized mice by determining changes in the number of DCX-positive neurons as a marker of neurogenesis. To confirm that any changes in hippocampal neurogenesis were a result of peripheral inflammation, we aim to investigate the effects of etanercept on changes in hippocampal neurogenesis in CII immunized mice.

Chapter 2

Materials and methods

2.1 General reagents & buffers

2.1.1 *Materials and reagents*

General Chemicals: All chemicals were purchased from Sigma-Aldrich (Poole, Dorset, UK) or Fisher Scientific (Loughborough, Leicestershire, UK), unless otherwise indicated.

Plastics: Plastics used for quantitative PCR assays and nuclease free centrifuge tubes were purchased from Applied Biosystems (Warrington, UK), Fisher Scientific (Leicestershire, UK). ELISA plates were purchased from Thermo Labsystems (Cheshire, UK)

Gelatin-coated slides: Gelatin-coated slides were prepared by dipping glass slides (VWR International, Ltd, Leighton Buzzard, UK) in a solution consisting of 5 g Type I Gelatin (Sigma, Poole, Dorset, UK) and 0.5 g chrome alum (Sigma, Poole, Dorset, UK) in 1 litre of water. After leaving to air dry, slides were stored at 4°C until required.

2.2 Buffers and culture media

0.2 M Phosphate buffer, pH 7.4: 0.2 M phosphate buffer (PB) was prepared by mixing 1120 ml Solution A (37.44g NaH_2PO_4 in 1200 ml dH_2O) and 2880 ml Solution B (37.44g Na_2HPO_4 in 1200 ml dH_2O), and then adjusting the pH to 7.4. PB buffer was diluted to 0.1 M with dH_2O before use.

0.3 M Phosphate buffered saline [PBS]: double strength PBS was prepared by mixing 200 ml 0.2 M PB buffer with 72g NaCl and 1800 ml dH_2O .

Phosphate buffered saline: PBS was purchased from Invitrogen (Paisley, UK).

Tris-acetate-EDTA (TAE) buffer: 50x stock solution of TAE was prepared by dissolving 242g of Tris base in 750 ml dH_2O . The solution was then mixed further with 57.1 ml glacial acetic acid and 100 ml 0.5 M EDTA (pH8). The final volume was then made up to 1000 ml with dH_2O . This stock buffer was then diluted 1:50 with dH_2O before use.

ELISA wash buffer: wash buffer consisted of PBS and 0.05% Tween 20.

4% paraformaldehyde in 50 mM phosphate buffer: 100 ml of 37-40% formaldehyde, 6.5g Na₂HPO₄ and 4g NaH₂PO₄ were mixed in 900ml distilled water.

2.3 In vitro procedures

2.3.1 *Animal welfare*

All animals were maintained in the pathogen-free facilities of the Joint Research Facility (JRF), and the Clinical Research Facility (CRF) at the Biological Services of the University of Glasgow. All procedures were conducted under project licences approved by the United Kingdom Home Office and in accordance with the Animal (Scientific procedures) Act 1986.

2.3.2 *Mice*

Male DBA/1 mice: Male mice weighing 20g were purchased from Harlan Laboratories Inc. (Bicester, Oxon, UK) at approximately 8 weeks of age and were kept in quarantine for one week before experimental procedures.

All mice were culled according to a licenced schedule 1 method.

2.3.3 *Induction of collagen-induced arthritis in DBA1 mice*

Preparation of collagen in Freund's complete adjuvant:

CIA (collagen-induced arthritis) is a commonly used experimental animal model of arthritis since it shares several similarities in pathology and/or pathogenesis to that of RA disease in humans. This concept of CIA pathogenesis was first applied in the rat model (Trentham et al., 1977), and subsequently in susceptible strains of mice (Courtenay et al., 1980). In our study, we chose to induce arthritis using collagen in DBA/1 mice (H-2q) since it is considered to be the most susceptible and most widely used strain (Inglis et al., 2008). To induce arthritis, male 8-week-old DBA/1 mice (Harlan, Bicester, Oxon, UK) weighing 20 g were immunized with Type II bovine collagen (MD Biosciences, St.Paul, MN,

USA). Briefly, this involved preparation of 2 mg/ml type II bovine collagen dissolved in 0.05 M glacial acetic acid overnight at 4°C. To make a final concentration of 1 mg/ml, the collagen was emulsified with an equal volume of 4 mg/ml Complete Freund's Adjuvant (CFA) (MD Biosciences, St.Paul, MN, USA). The collagen /CFA emulsion was prepared on ice using a hand-held homogenizer freshly on the day of immunization (day 0).

The stability of the emulsion was tested by adding one drop of the emulsion into a beaker of water. If the emulsion is stable, the drop will remain intact. If the emulsion spreads onto the water surface, then the emulsion is not stable, and the preparation should be re-emulsified.

Experimental arthritis model:

Mice were sensitised on day 0 and challenged on day 21. From day 17 onward, mice were examined every 2 days for signs of arthritis. In detail, on day 0, the area at the base of the tail of each mouse was shaved with clippers and the skin was sterilized with 70% ethanol. The emulsion of collagen/CFA was transferred to a 1ml plastic syringe fitted with a gauge 26 needle. Each mouse was injected intradermally with a sensitisation dose of 50 µl of collagen/CFA emulsion at approximately 1-2 cm from the tail base. A whitish bolus beneath the dermis should be visible. 50ul ul of the collagen/CFA emulsion was administered at both side of the tail base so that each mouse received a total of 100 µg of collagen. Mice were monitored daily for any signs of local ulceration. The second collagen challenge immunization was conducted on day 21. This consisted of 200 µg of bovine collagen in 200 µl of PBS injected intra-peritoneally into each mouse Figure 2.1.

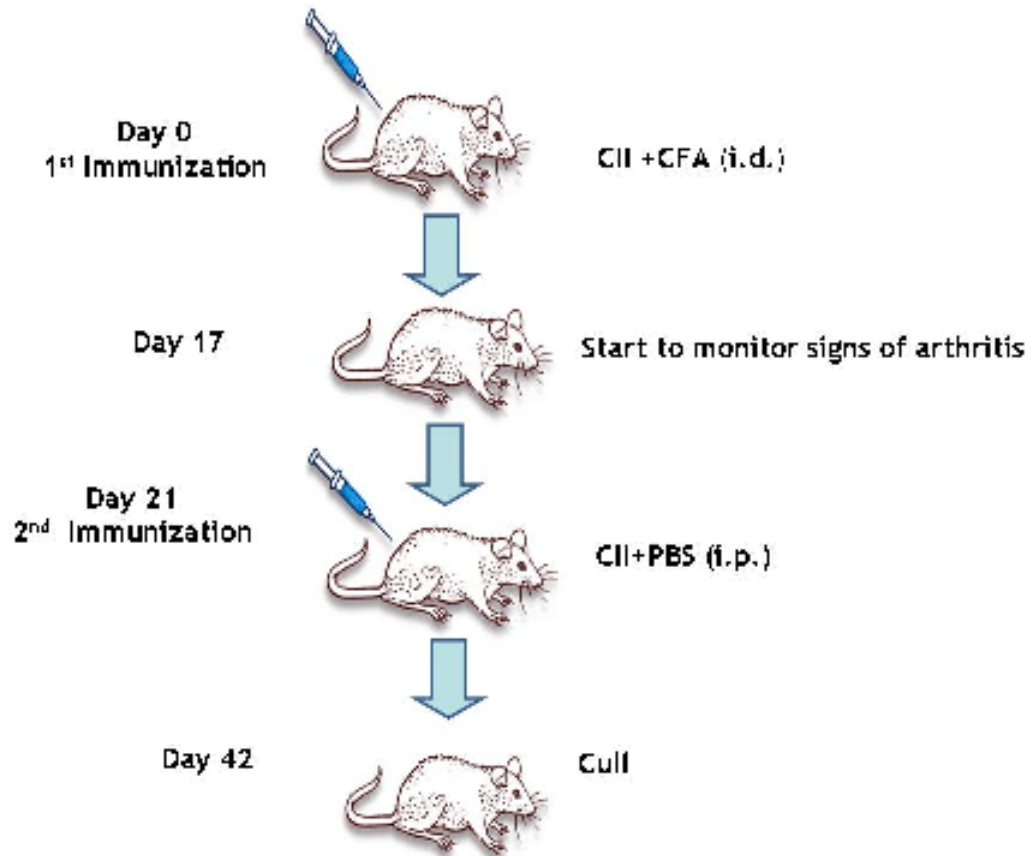


Figure 2.1 Summary of the CIA experimental procedure

The total experimental duration was 6 weeks. The animals were immunized (sensitised) with type II collagen (CII) + CFA at the beginning of the experiment and boosted (challenged) with type II collagen (CII) + PBS 3 weeks later. The signs of arthritis were monitored from day 17 after immunization onwards. Details in the text above.

Evaluation of arthritis

CII immunized mice usually developed signs of arthritis around day 19 after immunization, but these were monitored from day 16 after immunization onwards. Two clinical evaluations were used to measure the severity of joint inflammation in arthritic mice; clinical arthritic score and paw thickness measurement. The arthritis severity in all CIA experiments was verified independently by expertises including Dr. Darren Asquith, Mr. Maurice Dixon and Dr. Bernard Leng.

A. Clinical arthritic score; Paw inflammation of arthritic mice was monitored using a subjective scoring method. Individual paws were assigned a score based on the criteria shown in Table 2.1. The scores of each paw were summed, giving a maximum severity score of 16. The mean arthritis index is the sum of the score of all mice divided by the number of mice in each group.

Severity score	Appearances	Description
Score 0; Normal		No inflammation
Score 1; inflamed digits		Definite redness and swelling limited to individual digits ("sausage digits").
Score 2; Erythema		Moderate redness and swelling of ankle and wrist with swelling of one or more digits.
Score 3; Erythema plus swelling		Severe swelling and erythema extending over whole paw/joint including digits.
Score 4; ankylosis plus loss of function		Maximally inflamed paw or ankylosed paw. If the paw is ankylosed, the mouse cannot grip the wire top of the cage using front paws or walk up a cage lid held at a 45 degree angle.

Table 2.1 Clinical scores of C57BL/6 mice with CIA
 Images were taken from (Inglis et al., 2008) and (Rosloniec et al., 2010) by kind permission of the Editor of *Nature Protocols* and *Current Protocols*. The scores of each mouse were summed, giving a maximum severity score of 16.

B. Paw thickness measurements; Paw thickness measurements were used as an objective measure of arthritic swelling to confirm the subjective clinical arthritic score. Mice were held by the scruff of the neck and paw thickness was measured with a dial calliper (Kroeplin, Munich, Germany). Mean paw thickness index is the sum of the paw thickness of all mice divided by the number of mice.

2.3.3.1 Preparation of paws for H&E histological analysis

2.3.3.1.1 Paw tissue processing

Mouse paws were dissected just above the ankles and the skin and the toes were removed for better penetration of fixation buffer into the tissue. The joints were transfer to a universal container with 7 ml of 4% paraformaldehyde in 50 mM phosphate buffer. After fixation for 72hr, joints were then decalcified using a 5 - 10% solution of nitric acid in distilled water for 2-3 weeks with a daily change of solution. After decalcification, mouse decalcified joint tissues were transferred to 70% ethanol and embedded in paraffin. Paraffin-embedded tissues were cut to 6 µm using a microtome (Bright Instrument Co Ltd, Huntingdon, UK) which produced a continuous paraffin wax ribbon of sections. To separate individual sections, the ribbon of sections was floated onto a flotation water bath set at 40°C and each section were separated using a scalpel blade and transferred onto a charge slide (Superfrost plus, VWR International, Ltd, Leighton Buzzard, UK). Slides were air dried on a hotplate (Raymond A Lamb Hotplate, Thermo Labsystems, Cheshire, UK) at 55°C for 30 minutes. The slides were then stored at 4°C until required.

2.3.3.1.2 Haematoxylin and Eosin immunohistochemistry

Haematoxylin and Eosin (H&E) immunohistochemistry is a standard histological method. Haematoxylin is a blue basic dye binding to negatively charged DNA or RNA, which is commonly used for nuclear staining. Eosin is a pink acid dye that binds to positively charged cell elements such as mitochondria or other cytoplasmic elements.

The slides were put into an oven (GenLab, Cheshire, UK) at 60°C for 2-3 min to melt the wax and were re-hydrated following these re-hydration steps;

Dewax in Xylene	-	3 minutes x 2
100% Alcohol (Ethanol)	-	3 minutes x 2
90% Alcohol	-	3 minutes x 2
70% Alcohol	-	3 minutes x 2
Running Water	-	3 minutes

Sections were dipped in Harris Haematoxylin (Sigma, Poole, Dorset, UK) for 2 minutes and in running water for 3 minutes to remove excess stain. Slides were then counter stained with 1% Eosin (Sigma, Poole, Dorset, UK) for 2 minutes and excess stain was washed off in running water. Finally, sections were dehydrated following these dehydration steps;

70% Alcohol	-	30 seconds
90% Alcohol	-	1 minute
100% Alcohol	-	3 minute x 2
Xylene	-	3 minutes x 2

Sections were mounted in DPX (VWR, UK) and a cover slip (VWR, UK) using a Pasteur pipette. After drying overnight, all the sections were examined by microscopy.

2.4 Collection of serum from mice and processing of brain tissue for gene and protein analysis

Mice were terminally anesthetized with a halothane:oxygen mixture. Once anaesthetised, the thoracic cavity was opened and the blood collected by cardiac puncture. The blood was allowed to coagulate for 1hour at room temperature, and the serum was separated from blood by centrifugation (3,000 rpm for 30 minutes). The serum was collected and stored at -80° C for later analysis.

The brain was removed and dissected bilaterally across the midline. The right hemispheres were snap frozen immediately in liquid nitrogen and stored at -80 °C. The left hemisphere of each brain was homogenised and the soluble component was separated by centrifugation (3,000 rpm for 30 minutes) and stored at -80°C for subsequent protein analysis. The right hemisphere of each brain was processed for RNA extraction and gene expression analysis as detailed below.

2.5 cDNA synthesis by reverse transcription (RT)-PCR

Reverse transcription and polymerase chain reaction (RT-PCR) is a two-step protocol. Firstly converting extracted RNA to stable cloned (c)DNA using reverse transcriptase enzymes. Secondly the PCR creates an equivalent number of the more stable cDNA molecules which are then analysed by Real-time PCR (Gallo, 1972).

In detail, cDNA was synthesized from typically 1.5 µg of total extracted RNA using a commercial Superscript II[®] reverse transcriptase kit (Invitrogen, Paisley, UK) as per manufacturer's instruction. The following components were set up in a 1.5 nuclease-free microcentrifuge tube:

Component	Volume per reaction
500 µg/ml Oligo(dT) ₁₂₋₁₈	1 µl
1.5 µg of total RNA	X µl
10 mM dNTP mix	1 µl
DEPC* water	Up to 10 µl

* This is water treated with 0.1% v/v diethylpyrocarbonate (DEPC) for at least 1 hour at 37°C to inactivate ribonucleases, and then autoclaved to inactivate traces of DEPC.

To denature the RNA, the mixture was heated at 65°C for 5 minutes in the heating block of a polymerase chain reaction (PCR) machine (Eppendorf® Mastercycler Gradient PCR, Hamburg, Germany) and quick chilled on ice for 1 minute. A reverse-transcriptase (RT) master mix was prepared to contain the following components (supplied in the kit) per reaction;

Component	Volume per reaction
5X First-Stand Buffer	4 μ l
0.1 M DTT	2 μ l
50 mM MgCl ₂	2 μ l
40 units/ μ l RNase OUTTM (RNase inhibitor)	1 μ l

9 μ l of master mix was added to each denatured RNA sample and incubated for 2 minutes at 42 °C. 1 μ l of 200 units of Superscript II was added and incubated for 50 minutes at 42 °C followed by a 15-minute inactivation step at 70 °C. cDNA was then diluted 1: 5 with DEPC water and stored at -20°C until use in real-time PCR analysis of required target gene.

2.6 Real-time PCR using SYBR Green I dye

Real-time RT-PCR is widely used to determine biologically relevant changes in mRNA transcription levels in cells and tissue (Nolan et al., 2006). Instead of mRNA levels being directly measured, real-time PCR measures complementary DNA (cDNA) because this is more stable molecule than mRNA (Nolan et al., 2006). Real-time PCR employs fluorescent reporter dyes to bind with the cDNA amplification products of the PCR reaction (Nolan et al., 2006). Therefore, the fluorescence signal increases as the dye binds to the increasing amount of cDNA in the reaction tube. In real-time PCR, we determine the number of PCR cycles at which the increased fluorescent signal (and therefore cDNA) first crosses a pre-determined threshold background fluorescence. The point at which the fluorescent signal first rises above the baseline signal is called the threshold cycle (Ct). Therefore, the greater the copy number of initial target genes at the beginning of the assay, the fewer threshold cycles are required for the

fluorescence to reach the threshold level of detection (Nolan et al., 2006). There are several approaches to monitor PCR products, including dyes that bind to the double-stranded DNA (i.e. SYBR[®] Green) or sequence specific probes (i.e. Molecular Beacons or TaqMan[®] Probes). Both detection approaches are potentially rapid and sensitive (Nolan et al., 2006). However, their principles of detection and optimisation are different, resulting in different advantages and disadvantages. In our study, we used the simple, inexpensive SYBR-Green system to detect the PCR product as it accumulates during Real-time PCR cycles.

2.6.1 *Primer design and optimization*

Real-time PCR reaction consists of multiple cycles of denaturation, annealing and extension steps. This requires a pair of the specific oligonucleotide primers that bind to the cDNA template as a start point of real-time PCR reaction. Optimal design of the PCR primers is an important initial step for accuracy and specific quantification of the real-time PCR assay. There are several considerations when designing real-time PCR primers for the SYBR-Green I system. The annealing temperature is restricted to 58-60°C, which corresponds to the optimal working conditions for the Taq DNA polymerase enzyme and the length of the PCR product is set between 80 and 150 bp. In addition, Forward & reverse primers should have similar T_m s (ideally within 0.5°C of each other but no more than 1°C apart) for the greater PCR product yield. Finally, to avoid primer dimers, the primers should have low or no self complementarity (Ponchel et al., 2003). All primers used in this project were designed using Primer3 software (available online @: http://www.broad.mit.edu/cgi-bin/primer/primer3_www.cgi/).

Primer specification:

- between 18 and 20 base-pairs (bp) in length
- between 45 and 55% GC content (50% optimal)
- melting temperatures (T_m s) between 59.5°C and 61°C
- Max self complementarity: 3
- Max 3'self complementarity: 1
- product size between 100-140 base-pairs (bp) in length
- BLAST analysis (<http://www.ncbi.nlm.nih.gov/BLAST/>) was used to ensure that primer sets amplify the genes of interest with high specificity.

The primers used are listed in Table 2.2.

Genes	Forward	Reverse
mouse IL-1 β	5'-GTGTAATGAAAGACGGCACA-3'	5'-AGAAACAGTCCAGCCCATAC-3'
mouse IL-1 α	5'-GATGTCCAACCTTCACCTTCA -3'	5'-ACAACTTCTGCCTGACGA -3'
mouse IL-2	5'-CTGAGCAGGATGGAGAATTACAG-3'	5'-CGCAGAGGTCCAAGTTCATC-3'
mouse IL-4	5'- CGGCATTTTGAACGAGGT-3'	5'- TTGGAAGCCCTACAGACGAG-3'
mouse IL-5	5'- GCTTCCTGCTCCTATCTAACTTCA-3'	5'- TCAACCTTCTCTCTCCCCAAG-3'
mouse IL-6	5'-TTCCATCCAGTTGCCTTCTT-3'	5'-ATTTCCACGATTTCCCAGAG-3'
mouse IL-10	5'- CAACATACTGCTAACCGACTCCT-3'	5'- TGGGGCATCACTTCTACCA-3'
mouse IL-12	5'- ATGTGGAATGGCGTCTCTGT-3'	5'- AGTTCAATGGGCAGGGTCT-3'
mouse IL-13	5'-AGGGAGGAGGGTTGAGGA-3'	5'-TTTCTGTAGGGATGGGATGG-3'
mouse CCL1	5'-ATGGGCTCCTCCTGTCCT-3'	5'-TCTCTGGTGCTGGGATGG-3'
mouse CXCL1	5'-AACCGAAGTCATAGCCACACTC-3'	5'-TGGGGACACCTTTTAGCATC-3'
mouse CCL2	5'-CTCACCTGCTGCTACTCATTCA-3'	5'-CCATTCCTTCTTGGGGTCA-3'
mouse CXCL2	5'-AAGTTTGCCTTGACCCTGAA-3'	5'-TCTCTTTGGTTCTTCCGTTG-3'
mouse CCL3	5'-CAGCCAGGTGTCATTTTCCT-3'	5'-CAGGCATTCAGTTCAGGTC-3'
mouse CXCL10	5'-GCTCAAGTGGCTGGGATG-3'	5'-GAGGACAAGGAGGGTGTGG-3'

mouse IFN-g	5'-ATTGCGGGGTTGTATCTGG-3'	5'-TCCTCCCATCAGGAGCAC-3'
Genes	Forward	Reverse
mouse TNF- α	5'-CCCTTTACTCTGACCCCTTT-3'	5'-AACCTGACCACTCTCCCTTT-3'
mouse FGF2	5'-CGTCAAACACTACAACCTCCAAGCA-3'	5'-CAGCAGCCGTCCATCTTC-3'
mouse VEGF	5'-CCTCGTCTCCTCTCCTTACCC-3'	5'-CACTCACACACACAGCCAAGT-3'
mouse GAPDH	5'-AACCTGACCACTCTCCCTTT-3'	5'-TATTATGGGGGTCTGGGATG-3'

Table 2.2 Primer sequences used for the amplification of brain tissue cDNA
 All primers were purchased at Vhbio (www.vhbio.com) and diluted at the appropriate dilution (Vhbio, Gateshead, UK).

2.6.2 Optimizing primers for SYBR Green real-time PCR

The optimization of the primer concentration is essential for sensitivity, specificity, reproducibility of the real-time PCR assay. Each set of primers work efficiently under different concentration conditions. Inappropriate primer concentrations in the real-time PCR assay results in non-specific primer binding and the creation of primer-dimers. For optimization, a primer titration was performed from 50 to 12.5 μ M final concentration using conventional PCR. cDNA synthesized from a tissue or cell line known to express the gene(s) of interest was used as the template for testing the specificity of the primer. The mRNA from various cell types and tissue expressing genes of interest was used to generate cDNA control templates for optimizing primers as listed on Table 2.3.

Mouse cDNA template sources	Mouse Primers
macrophages	IL-1 β , IL-1 α , IL-10, IL-12, TNF- α , GAPDH
LPS-stimulated macrophages	IL-6, CCL1, CXCL1, CCL2, CXCL2, CCL3, CXCL10
Th1 cells	IL-2, IFN-g, IL-12
Th2 cells	IL-4, IL-5, IL-13, IL-10
NIH3T3 fibroblast	FGF2, VEGF

Table 2.3 Control tissue used to test specificity of primers

Conventional PCRs for the validation of the specificity of the designed primers against target genes were performed in 50 μ l reactions with the addition of 1.5 mM MgCl₂ and employing ReddyMix™ PCR Master Mix (Abgene, Epsom, UK). Reactions were performed using the PCR machine (Eppendorf® Mastercycler Gradient, Hamburg, Germany) under the following conditions: One cycle at 94°C for 10 min, and 35 cycles of 94°C for 20s, 59°C or 60°C or 61°C for 20s, and 72°C for 20s, one cycle of 72°C for 10 min. The PCR product were analysed by running in 2% agarose gels containing ethidium bromide (Sigma, Poole, Dorset, UK) and visualizing for a single specific band and the absence of primer dimer products.

2.6.3 Agarose gel electrophoresis

PCR products were visualised in 2% w/v agarose gels. Agarose gels were prepared by heating 3 g agarose (Invitrogen, Paisley, UK) in 150 ml Tris-acetate-EDTA (TAE buffer) in a microwave at full power for approximately 5 minutes until the agarose was completely dissolved. Approximately 5 μ l ethidium bromide (Sigma, Poole, Dorset, UK) were added and mixed by swirling the flask. The melted agarose was then poured into a gel tray, the ends of which were sealed with two layers of tape. A well-comb was placed into the melted agarose to

form wells large enough to accommodate at least 25 μl . When the gel solidified, the comb and the tapes were removed and the gel was placed into an electrophoresis chamber containing TAE buffer. 25 μl of the PCR products were load into each well of the agarose gel next to a well containing a size-marker 1 Kbp DNA ladder (Invitrogen, Paisley, UK). The gel electrophoresis was run at 100V for 40 minutes. DNA bands were visualized under UV light in a lightbox (Gel logic 200 imaging system, NY, US) and images recorded using Kodak camera and software.

2.6.4 *Generation of a DNA standard for real-time polymerase chain reaction*

A known real-time PCR standard is required as a positive control as well as a reference for measuring the absolute copy number of a transcript in an unknown test sample. DNA plasmids containing cloned target sequences are used as standards in quantitative PCR. These constructions of DNA plasmids were generated by cloning DNA fragments that contain genes of interest into a commercial TOPO vector (Invitrogen, Paisley, UK) using the manufacturer's instructions. Briefly, PCR products generated using the QPCR primers were isolated and purified from the agarose gel by the QIAquick PCR Purification Kit according to manufacturer's instructions (Qiagen, West Sussex, UK). 4 μl PCR product, 1 μl salt solution (Invitrogen, Paisley, UK), and 1 μl PCR4 TOPO vector were mixed together. 3 μl of the mixture was added to a preparation of competent bacteria containing TOPO vector. Following incubation on ice for 30 minutes, the bacterial preparation was subjected to heat shock at 42°C for 30 seconds, and then 2 minutes on ice. 300 μl of supermedium (Invitrogen, Paisley, UK) was added into the mixture of bacteria with TOPO vector before 15 minutes incubation in a shaking incubator (Innova 4400, New Brunswick, Cambridge, UK) for 40 min. 200 μl of the mixture of bacteria with TOPO vector was plated by spreading onto a selective growth medium in a petri dish; i.e. LB agar containing 50 μg Ampicillin (Sigma, Poole, Dorset, UK) under aseptic conditions, and incubated overnight at 37°C. Next day, a single typical colony containing TOPO vector was picked and inoculated into 5 mL of LB broth and incubated for 16 hours at 37°C in a shaking incubator. Cells were harvested by centrifugation at

1200 rpm for 4 minutes. Plasmids was isolated and purified by Qiaprep Spin Mini-Prep Kit according to manufacturer's instructions (Qiagen, West Sussex, UK).

2.6.5 Plasmid verification and quantification

The existence of the genes of interest in the resulting DNA fragments can be verified by checking the length of the DNA fragments obtained after digestion with specific restriction enzymes. The digestion scheme was as follows:

10 μl aqueous solution containing DNA plasmid, 7.5 μl DEPC water, 0.5 μl EcoRI enzyme (Invitrogen, Paisley, UK) and 2 μl 10 X buffer H (Invitrogen, Paisley, UK) were mixed together and incubated in a 37°C water bath for 1 hour. Agarose gel electrophoresis was used to confirm the length of the DNA fragments separated from cut vectors.

The concentration of plasmids was measured by UV spectrophotometry (Eppendorf® BioPhotometer, Hamburg, Germany) at 260 nm wavelength in $\mu\text{g}/\text{ml}$. Plasmid copy numbers were then calculated using the following formulae, with IL-1 β used as an example:

The PCR® 4-TOPO® vector containing a DNA fragment of the IL-1 β gene was 4,500 bp in size and had a concentration of 2.059×10^{-8} g per μl .

Copies of molecule per mole = 6.023×10^{23} (Avogadro's constant)

Average molecular weight for double stranded nucleotide = 660 Daltons

Molecular weight of double stranded DNA = 660 Daltons * PCR product length

$$= 660 * 4500 \text{ bp}$$

$$= 2,970,000 \text{ Daltons}$$

Copies DNA per μl = $(6.023 \times 10^{23} * \text{mass per } \mu\text{l}) / \text{Molecular weight DNA}$

$$= (6.023 \times 10^{23} * 2.059 \times 10^{-8}) / 2,970,000 \text{ Daltons}$$

= 4,175,541,077 copies per μl

2.6.6 Real-time PCR assay

Absolute quantification was used to measure the amount of transcription of the gene of interest by real-time PCR assay. The absolute quantification uses a standard curve to calculate the absolute number of transcripts in unknown samples. The standard curve for the required target gene was generated from a 10-fold serial dilution of DNA plasmids containing cloned target sequences as the template described in 2.5.5. The template was diluted in DEPC water to generate the dynamic range between 10^8 and 10^2 copies in a volume of 500 μl . The amount of cDNA (and thereby the amount of tissue mRNA) is measured by an index called the cycle threshold (CT). This is the number of denaturing and re-annealing cycles required for the fluorescent signal to exceed the background or 'threshold' level; ie more mRNA will require fewer cycles for the fluorescent signal to exceed background levels. The values in each dilution were measured in triplicate using a real-time QPCR with the primer sets to generate the standard curves for the gene of interest. This range of the template concentration resulted in a Ct of between 20 and 32 since a 10-fold difference in concentration corresponds to 3.3 cycles. Standard curves were run at least once for every primer pair in order to check the efficiency of the real-time PCR assay. A graph is made of the standard curve by plotting the Ct values on the y axis and the log of the number of copies on the x axis. The slope of the line of this plot will give the efficiency of the reaction according to the equation $E=10^{-(1/\text{slope})-1}$. A reaction of 100% efficiency represents a slope of -3.33 (Nolan et al., 2006).

All amplification reactions of samples or standards were performed in triplicate. Each reaction consists of components listed in Table 2.4;

Component	Stock concentration	Volume to add for single 20 μ l reaction
DEPC water		8 μ l
Power SYBR Green PCR Master Mix	X2	10 μ l
Primers; Forward primer Reverse primer	50 μ M, 25 μ M, 12.5 μ M	0.5 μ l 0.5 μ l
Sample/standard	1:5 diluted sample cDNA synthesis or the template concentration containing 10 ⁸ and 10 ² copies	2 μ l

Table 2.4 List of components in the mastermix used for real-time PCR assay
A working batch of mixture consisted of water, Power SYBR Green PCR Master Mix (Applied Biosystems, Warrington, UK) and primers (VHBio, Gatehead, UK) was made sufficient for all real-time PCR reactions. To prepare a master-mix in triplicate for each sample, 6 μ l of cDNA or standard was added in a “mixing” well of a nuclease-free 24-well plate (Thermo Labsystems, Cheshire, UK), along with 54.5 μ l mixture. Approximately, 19.8 μ l of this master-mix was added to each well of a 96-well optical reaction plate (MicroAmp, Applied Biosystems, Warrington, UK). The plate was sealed by an adhesive sealing film and gently centrifuged to ensure that the components settle to the bottom of the wells. The plate assay was run on a real-time PCR instrument (ABI PRISM 7900HT Sequence Detection System, Applied Biosystems, Warrington, UK] using the protocol in Table 2.5.

Denaturation			10 seconds at 95°C
40 cycles	Annealing	15 seconds at 95°C	
	Extension	1 min at 60°C.	

Table 2.5 Conditions for real-time PCR protocol

A melting curve analysis was performed with a temperature gradient of 0.1°C/s from 70 to 95°C following each PCR run to identify the specific amplified product and distinguish them from primer dimers and other small amplification artifacts. The principle of melting curve analysis is that the two strands of double-stranded DNA separate or “melt” apart at the specific temperature, depending on both its size and the energy required to disrupt the different hydrogen bonds of its nucleotide composition. This temperature is called the melting temperature (T_m). During the melt curve analysis, each sample was heated gradually from the user defined temperature below the T_m of the products to a temperature above their melting point. Within this temperature gradient, fluorescent dye released by the double-stranded DNA product at the T_m is detected by the real-time machine and the accurate T_m data reported for every single amplified product. The melting peak of a single amplified product appears as a single sharp peak at the T_m , whereas peaks of small primer dimers appear at lower temperatures (Nolan et al., 2006).

2.6.7 Normalization of cDNA samples

Although real-time RT-PCR is considered to be an efficient and sensitive approach to determine biologically relevant changes in gene expression levels, technical as well as biological variation can cause variability of the data. Various errors resulting from inter-sample variability in RNA degradation during storage, variation introduced during RNA isolation and variation during cDNA synthesis, can cause unavoidable variation in the amount of the final cDNA product (Huggett et al., 2005). One common approach to minimize these errors is to normalize the cDNA sample using housekeeping genes as internal comparative standards. Housekeeping genes are typically constitutive genes that are expressed at a relatively stable level. Since these housekeeping genes are essential for cell metabolism, but not cell differentiation, it is therefore commonly assumed that the transcription of the housekeeping gene is unaffected by experimental conditions (Suzuki et al., 2000). There are several housekeeping genes that have been used as reference genes for real-time PCR assays. In our study, a housekeeping gene GAPDH (glyceraldehyde-3-phosphate dehydrogenase) was used as the reference gene for normalization. GAPDH is one of the most commonly used housekeeping genes that has been reported to be

appropriate for certain experimental situations (Andersen et al., 2004). The gene expression level of each sample was normalized against a ratio of its GAPDH content in relation to the 75th percentile of GAPDH levels of all samples assayed (an example of the normalisation process is shown in Table 2.6). The 75th percentile of GAPDH gene copy number is calculated from GAPDH levels of all samples assayed and used as a reference to avoid a false calculation resulting from the percentage of gene level expression below the standard curve. This is because real-time PCR also reports an intensity value although the gene is below the standard range. These intensity values are considered as background assay 'noise' and are less reliable, and therefore more likely to fall into the lower percentile ranking on the array. The difference of each sample calculated from the 75th percentile is reliable and the change of gene X levels in the sample is on the assumption that the ratio of GAPDH is consistent. Any sample having a GAPDH content/75th percentile varying by more than a factor of 2 from the 75th percentile was discarded from the analysis due to an assumption of compound errors during sample processing.

A	B	C	D	E
Sample Name	Level of gene x copies	Level of GAPDH copies	Ratio to 75th Percentile (column C/71.25)	Normalised level of gene X (column B/D)
Sample 1	200	800	0.889	225
Sample 2	1000	4000	4.444	225
Sample 3	240	900	1.000	240
Sample 4	200	200	0.222	900
Sample 5	160	800	0.889	180
	75th percentile	900		

Table 2.6 An example of normalisation using a housekeeping gene to determine levels of gene “X”

Before normalization, sample 2 in column B has a higher value of gene X (1000 copies) than sample 4 (200 copies). After normalization, the results show that the level of gene X in sample 2 was similar to the other samples. This was due to the high level of cDNA in this sample. The opposite situation is seen in the pre-normalised levels of gene X in sample 4 which appears low, although the actual level is much higher, indicating that there was actually only a small amount of cDNA in this sample.

2.7 Cytokine and chemokine protein expression analysis

2.7.1 Protein extraction from brain tissue

The snap-frozen brain tissues were thawed, weighed, transferred to tubes on ice containing approximately 3.4 ml of T-PER (Fisher Scientific UK Ltd., Loughborough, UK), and Halt™ Protease inhibitor cocktail (Fisher Scientific Ltd., Loughborough, UK) at a proportion of 1:100 of T-PER stock reagent. The brain

tissues were homogenized, incubated at room temperature for 10 minutes and centrifuged at $10,000 \times g$ for 10 minutes at 4°C . Supernatants were transferred to clean microcentrifuge tubes, frozen at -80°C and thawed on ice. These protein preparations were further analysed for cytokine and chemokine protein levels by Luminex and ELISA.

2.7.2 Normalization of a relative total protein concentration using BCA protein assay

2.7.2.1 Protein assay

Total protein concentrations in the brain tissue homogenates were determined using a BCA protein assay kit (Pierce Biotechnology, Cheshire, UK) according to the manufacturer's instruction. Briefly, the homogenate supernatant samples were diluted 1:10 with PBS and quantified in triplicate. BSA was diluted in PBS to give concentrations suitable for a standard curve (20-2,000 $\mu\text{g}/\text{ml}$). 25 μl of each standard and unknown sample replicate was added into a microplate well (Thermo Labsystems, Cheshire, UK). Working Reagent (WR) was prepared by mixing 50 parts of BCA reagent A and 1 part of BCA reagent B supplied in the kit, followed by adding 200 μl of the WR to each well and mixing thoroughly on a plate shaker for 30 seconds. The plate was covered with an adhesive plastic plate-cover and incubated at 37°C for 30 minutes. After cooling the plate at room temperature, the optical density was measured at 560 nm on a plate reader (Dynex Technologies Ltd., Worthing, UK). The test sample protein concentrations were generated by interpolation of their optical density to the optical density curve of the known protein standards.

2.7.2.2 Normalization of protein samples

An example of the calculation used to quantify the concentration of one cytokine normalised for the total protein in one brain extract is given below:

The mean OD value of triplicate measurements of a protein extract of brain tissue from a wild type mouse (WT 1) is 0.464, which corresponded to a protein concentration of 708.7 $\mu\text{g}/\text{ml}$.

However, this is the concentration of a sample at 1:10 dilution, therefore the concentration of the neat sample is $10 \times 708.7 \mu\text{g/ml} = 7087 \mu\text{g/ml}$.

50 μl of each sample is used for one multiple cytokine Luminex assay.

1,000 μl (1 ml) contains 7087.03 μg total proteins

50 μl contains $\frac{50 \times 7087.03}{1,000} = 354.35$ μg total protein

1,000

According to the Luminex result, for example, the mean protein concentration of triplicate measurements of, for example, IL-13 is 55.03 $\mu\text{g/ml}$

1,000 μl contains 55.03 μg IL-13 protein

50 μl contains $\frac{50 \times 55.03}{1,000} = 2.75$ μg IL-13 protein

1,000

Based on these calculations, a 50 μl solution of WT 1 mice brain proteins contains 354.35 μg total proteins and 2.75 μg for IL-13.

354.35 μg total protein contains 2.75 μg IL-13

1,000 μg total protein contains $\frac{1,000 \times 2.75}{354.35} = 7.765$ μg IL-13/mg total brain protein

In summary, 1 mg total brain proteins of the WT1 sample contains 7.765 μg IL-13.

2.7.3 Measurement of multiple cytokines using a suspension bead array assay and a Luminex platform

Quantifying the concentrations of many cytokines and chemokines in a small volume of biological fluid is now possible using a multiplex system. Multiple cytokines (TNF α , IFN γ , IL-1 α , IL-1 β , IL-2, IL-4, IL-5, IL-6, IL-10, IL-12 [p40], IL-12

[p40/ p70], IL-13, IL-17), chemokines (IL-8, IP-10, KC, MCP-1, MIG, MIP-1 α , MIP-1 β , MIP-3 β , RANTES), and growth factors (FGF basic, GM-CSF, PDGF-BB, VEGF) were quantified in the soluble extracts from brain tissue and in mouse serum using a mouse 20-plex Luminex kit (Invitrogen, Paisley, UK) on a Bio-Plex system (Bio-Rad Laboratories Ltd. Hemel Hempstead, UK), according to the user manual. The steps are detailed as follows:

2.7.3.1 Plate preparation for Luminex assay

A 96-well filter bottom microplate was used for the luminex assay. 15 ml working solution concentrate x 20 was diluted with 285ml of deionized or distilled water. This diluted working solution was used to pre-wet the filter bottom of the plate (100 μ l/well) and the content in the wells was removed by a vacuum pump.

2.7.3.2 Preparation of beads

The principal of the Luminex assay is based on a bead-based suspension array using capture antibodies against an analyte immobilized onto a microsphere (bead). Captured analytes (including standards of known analyte concentration, control specimens and unknown test samples) are detected mostly using the flow cytometry principle. 2.5 μ l of capture bead stock solution was resuspended by sonication for 2-3 minutes and then diluted in 2ml of working solution. 200 μ l of diluted capture beads were pipetted into each well. The fluid containing these capture beads was removed through the filter base of the plate using a vacuum pump, and the plate was similarly washed twice with working solution. The plate was dried by blotting the filter onto paper towel. 50 μ l incubation buffer was added to each well. This was immediately followed by pipetting 50 μ l assay diluent to sample wells, but not in the standard wells.

2.7.3.3 Preparation of standard curve

The standard curve was generated by using serial dilutions of the kit lyophilized standards reconstituted in assay diluent: T-PER reagent (1:1). This was chosen because T-PER reagent was used as the diluent for brain tissue homogenates. For serum analysis, the standards were diluted in assay diluent buffer provide in the kit. A mixture of 50% assay diluent plus 50% T-PER reagent was also used as the

blank in this assay. 1 ml of mixture of 50% assay diluent plus 50% T-PER reagent was added into the bottle containing the lyophilised kit cytokine standard and left for 10 minutes to reconstitute. A series of 1:3 serial dilution standard samples was generated by diluting 150 µl top standard from the standard stock solution into the first of a series of eppendorf tubes containing 300 mixture of 50% assay diluent plus 50% T-PER reagent and serially diluted 1 in 3. 100 µl of standard and blank was added into standard wells containing diluted antibody-coated bead complexes and incubation buffer.

2.7.3.4 Assay procedure and analysis

50 µl of sample was added into sample wells containing diluted antibody-coated bead complexes, assay diluent and incubation buffer. The assay plate was covered with tinfoil (to minimise light quenching of the fluorochrome) and incubated at room temperature for 2 hours on a plate-shaker to agitate the beads. At this first incubation, the test analytes will bind to the capture antibodies on the beads. The fluid content in the wells are removed by a vacuum pump, followed by 2 washes with working buffer (100 µl/well) and the filter-bottom of the plate was dried using paper towel. Analyte-specific biotinylated detector antibodies were diluted in biotin diluent (1:10), 100 µl of detection antibody was added to each well and incubated for 1 hour at room temperature on the plate-shaker. During this second incubation, the analyte-specific biotinylated detector antibodies recognize their target cytokines that are bound to the appropriate beads. The excess fluid contents in the wells were removed by a vacuum pump, followed by 3 wash with working buffer (100 µl/well). Streptavidin conjugated to the fluorescent protein, R-Phycoerythrin (Streptavidin-RPE) was diluted (1:10) in Streptavidin-RPE diluent and add into each well (100 µl/well). The plate was then incubated for 30 minutes at room temperature on the plate-shaker. During this final incubation, the Streptavidin-RPE binds to the bionylated detector antibodies linked with immune complex on the beads, forming a four-member solid phase sandwich. The excess fluid content in the wells was removed by a vacuum pump, followed by 3 wash with working buffer (100 µl/well) to remove unbound Streptavidine-RPE. The plate was dried by blotting on paper towel and incubated overnight with working solution (100 µl/well) at 4°C. Next day, the beads were analysed with the Luminex 100 analyzer instrument (Luminex Corp., Austin, TX). The

concentrations of one or more analytes were determined by monitoring the spectral properties of the beads and the amount of associated R-Phycoerythrin (RPE) fluorescence. The fluorescence was proportional to the concentration of the analyte and quantified with reference to the fluorescence of the known concentration of the standard curve.

2.7.4 Enzyme immuno-assay (ELISA) protocol

Individual concentrations of IL-1 α , IL-1 β , IL-2, IL-4, IL-5, IL-6, IL-10, IL-12 [p40/p70], IL-13, IL-17, IP-10, KC, MCP-1, VEGF and TNF α were measured using enzyme linked immuno-assay (ELISA) in protein preparations from brain tissue. The concentrations of antibodies and buffers used for the analysis of each cytokine are shown in Table 2.7 and Table 2.8.

Cytokines	Coating buffer	Blocking buffer & Antibody diluents	Concentration of capture antibody	Concentration of detection antibody	Streptavidin HRP dilution	Substrate Solution	Standard curve range
mouse TNF- α Cat # 559603 BD Bioscience	0.1 M Sodium Carbonate, pH 9.5	PBS with 10% FBS, pH 7	1:250 (50 μ l/well)	1:250 (50 μ l/well)	1:250 (50 μ l/well)	TMB	2 ng/ml-4 pg/ml
mouse IL-1 β eBioscience	ELISA/ELISPOT coating buffer	5x Assay Diluent	1:250 (50 μ l/well)	1:250 (50 μ l/well)	1:250 (50 μ l/well)	TMB	4 ng/ml-4 pg/ml
mouse IL-2 Peprotech	PBS	0.05% Tween - 20, 0.1% BSA in PBS	1 μ g/ml (100 μ l/well)	0.25 μ g/ml (100 μ l/well)	1:2000 (100 μ l/well)	ABTS	8 ng/ml-4 pg/ml
mouse IL-4 Peprotech	PBS	0.05% Tween - 20, 0.1% BSA in PBS	1 μ g/ml (100 μ l/well)	1 μ g/ml (100 μ l/well)	1:2000 (100 μ l/well)	ABTS	4 ng/ml-4 pg/ml
mouse IL-5 eBioscience	ELISA/ELISPOT coating buffer	5x Assay Diluent	1:250 (50 μ l/well)	1:250 (50 μ l/well)	1:250 (50 μ l/well)	TMB	2 ng/ml-2 pg/ml
mouse IL-6 Peprotech	PBS	0.05% Tween - 20, 0.1% BSA in PBS	2 μ g/ml (100 μ l/well)	0.5 μ g/ml (100 μ l/well)	1:2000 (100 μ l/well)	ABTS	6 ng/ml-4 pg/ml
mouse IL-12 Peprotech	PBS	0.05% Tween - 20, 0.1% BSA in PBS	1 μ g/ml (100 μ l/well)	0.25 μ g/ml (100 μ l/well)	1:2000 (100 μ l/well)	ABTS	5 ng/ml-300 pg/ml

Table 2.7 Cytokine analysis by ELISA.

Mouse cytokines, chemokines and growth factors were analysed using capture and detection antibody listed above. The capture antibody was diluted in appropriate coating buffer and the detection antibody was diluted in the diluent supplied by the manufacturer. The final concentration of each antibody, the volume added to each well, and standard ranges are shown.

Cytokines	Coating buffer	Blocking buffer & Antibody diluents	Concentration of capture antibody	Concentration of detection antibody	Streptavidin HRP dilution	Substrate Solution	Standard curve range
mouse IL-13 eBioscience	ELISA/ELISPOT coating buffer	5x Assay Diluent	1:250 (50 µl/well)	1:250 (50 µl/well)	1:250 (50 µl/well)	TMB	2 ng/ml-4 pg/ml
mouse CCL2 eBioscience	ELISA/ELISPOT coating buffer	5x Assay Diluent	1:250 (50 µl/well)	1:250 (50 µl/well)	1:250 (50 µl/well)	TMB	4 ng/ml-4 pg/ml
mouse VEGF Peprotech	PBS	0.05% Tween - 20, 0.1% BSA in PBS	1 µg/ml (100 µl/well)	0.5 µg/ml (100 µl/well)	1:2000 (100 µl/well)	ABTS	4 ng/ml-4 pg/ml

Table 2.8 Cytokine, chemokines and growth factor analysis by ELISA.

A mouse cytokine (IL-13), a chemokine (CCL2) and a growth factor (VEGF) were analysed using capture and detection antibody listed above. The capture antibody was diluted in appropriate coating buffer and the detection antibody was diluted in the diluent supplied by the manufacturer. The final concentration of each antibody, the volume added to each well, and standard ranges are shown.

The ELISA procedure involved briefly, 96-well microtitre plates (Thermo Labsystems, Cheshire, UK) were coated with capture antibody diluted in coating buffer at appropriate concentrations according to the manufacture's instructions. The plates were covered with an adhesive plastic cover and incubated overnight at 4°C. The coating buffer containing capture antibody was removed the next day and the plates were washed 3 times by repeatedly filling and emptying the wells with 200 µl wash buffer, and soaking the wells for 5 minutes in between each wash. Washing was by flicking empty the plate over a sink. The remaining drops were removed by patting the plate upside down on a paper towel. To block the remaining protein-binding sites in the coated wells, 200 µl blocking buffer was added into each well and the plates were incubated at 37°C for 1 hour. Following 3 further washes as above, 50 µl of protein sample were added to each well in duplicate or triplicate in different experiments. For quantitative data, the optical density of the unknown test samples was compared against the optical density of a standard curve consisting of serial dilutions of a known quantity of the cytokine to be assayed. Standards in duplicate, and blank wells with no cytokine were run with each plate to ensure accuracy. The plates were covered with adhesive plastic covers and then incubated on the shaking machine for 2 hours at room temperature. The samples were removed and the plates were washed 5 times, followed by adding 50 µl of diluted detection antibody in blocking buffer and incubation at room temperature for 1 hour. The detecting antibody was an antibody that specifically recognised the cytokine to be measured and that was conjugated to an enzyme that would allow subsequent detection. In this case, the plates were washed and streptavidin-horse radish peroxidase (HRP), diluted 1:1000 with diluent, was added to each well, followed by incubation on a plate-shaker for 1 hour at room temperature. After this, and following 3 washes, the activity of the bound enzyme was detected by a colour change by adding 100 µl of colourless substrate solutions including TMB (3,3',5,5'-tetramethylbenzidine) or ABTS (2,2'-azino-di-[3-ethyl-benzothiazoline-6 sulfonic acid] di-ammonium salt), which changed colour after enzyme activity.. The optimum optical density was read at 630 nm for TMB and 410 nm for ABTS on a microplate spectrophotometer (Dyner Technologies Ltd., Worthing, UK). A standard curve was prepared from the optical densities produced from the serial dilutions of known standard, with

concentration on the x axis (log scale) vs absorbance on the Y axis (linear). The concentration of the sample was interpolated from this standard curve.

2.8 Free-floating section staining for doublecortin (DCX)

The immature neuronal marker doublecortin (DCX) is commonly used to quantify change in hippocampal neurogenesis. DCX is a highly hydrophilic microtubule-associated protein that is specifically expressed in migrating neuronal precursors in the dentate gyrus in the hippocampus (Couillard-Despres et al., 2005). The doublecortin (DCX) antibody is hydrophilic which restricts penetration into the hydrophobic brain tissue, therefore, immunohistochemistry of DCX is best achieved by free-floating Immunohistochemistry, in which thick frozen-cut sections were incubated floating free in plastic wells containing diluted DCX antibody solution. Increasing the penetration of antibody into the tissue is a major advantage of the free-floating Immunohistochemistry since free-floating tissue in antibody solution allows tissue to be exposed to the antibody from both (back and front) sides. High salt solution (0.3 M PBS) was used as diluent and washing solutions, and these reduced non-specific staining by decreasing charge-induced non-specific binding (Pastor-Soler et al., 2010).

2.8.1 Tissue processing

Mice were terminally anesthetized with halothane:oxygen. The brains were removed, and immersion-fixed in 4% paraformaldehyde in 50 mM phosphate buffer for 48 h. Brains were then cryoprotected by immersion in a 30% (W/V) sucrose; PBS solution at 4°C until the brains sink (usually 24 hours). Brains were stored in liquid nitrogen until required.

2.8.2 Cryostat cutting and free-floating section process

The middle segment of a mouse brain, which contains the hippocampus, was dissected, mounted in OCT embedding compound (Tissue-Tek® O.C.T™ Sakura Finetek, Zoeterwoude, Natherlands) and frozen in the cryostat (Thermo Electron Corporation, Thermo Labsystems, Cheshire, UK) set at -20°C. The brain was cut into sequential 60 µm coronal sections. Each 60 µm brain section, containing hippocampus as illustrated between plates 24 and 48 of the histology mouse

brain atlas of Paxinos and Watson *et al.*, 1998 (Paxinos and Watson, 1998) (Figure 2.2, Figure 2.3), was lifted out from the blade serially with a paintbrush to minimize folding or wrinkling. Each section was transferred serially into wells containing 0.1 M PB buffer, and immuno-histochemistry of doublecortin was performed in that 24 well plate on an orbital shaker. 200 μ l of all washing buffer and antibody solutions was transferred to each well and removed from the well in each step using a Pasteur pipette.

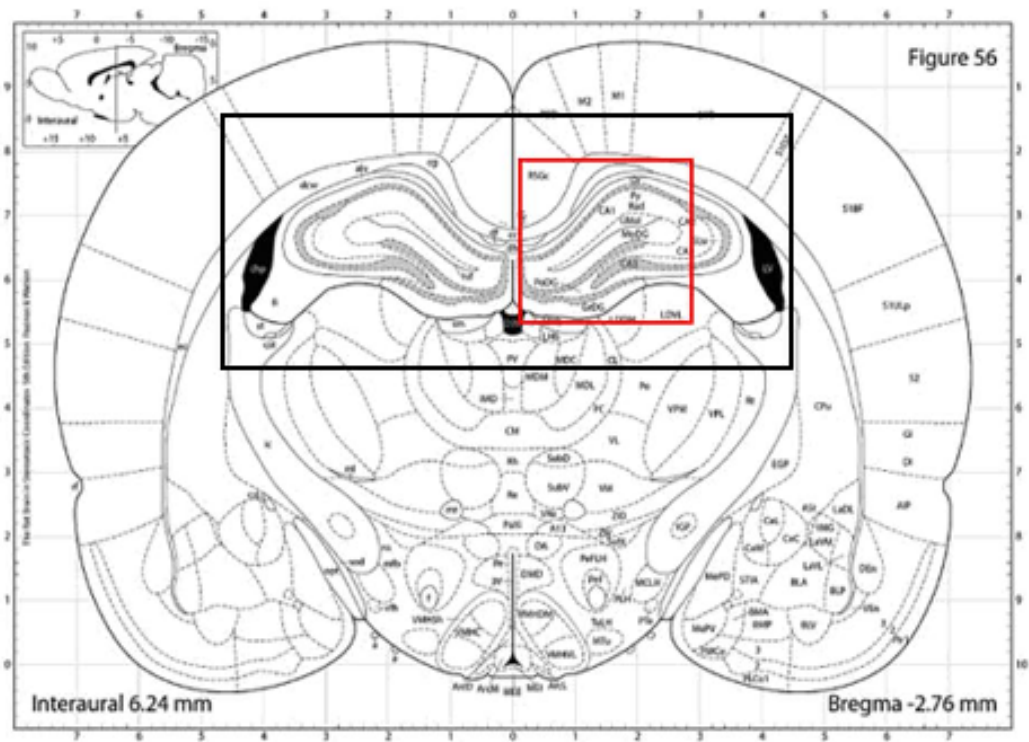


Figure 2.2 A coronal rat brain atlas diagram (Paxinos and Watson, 1998). A black box shows the hippocampal region characterized by butterfly-shaped area. Dentate Gyrus (DG) is a part of hippocampus (a smaller red box), which is the specific area of DCX immunohistochemistry.

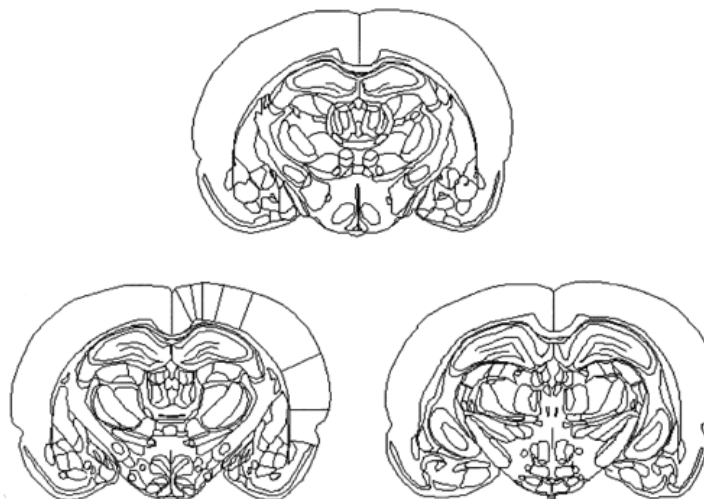


Figure 2.3 Coronal brain sections at the level of hippocampus. Diagrammatic illustrations displaying levels of coronal brain sections that were taken, which are based on a standard mouse brain stereotaxic atlas (Paxinos and Watson, 1998). Images were taken from (O'Neill and Clemens, 2001) by a kind permission of the Editor of *Current Protocols in Neuroscience*.

2.8.3 Immunohistochemistry

Free-floating sections were immersed in 50% ethanol for 30 min before immunostaining to enhance antibody penetration. The sections then were washed 3 times with 0.1 M PB buffer for 5 minutes each. To block endogenous peroxidase, sections were incubated with 0.3% H₂O₂ (Sigma, Poole, Dorset, UK) in 0.1 PB for 30 min.

2.8.3.1 Chromogenic immunostaining of doublecortin (DCX)

For chromogenic immuno-staining, sections were washed in 0.3 M PBS for 3 times 5 minutes each, and then incubated overnight at 4°C with rabbit α -doublecortin polyclonal antibody, 1:500 (ab18723, Abcam, Cambridge, UK) in a solution containing 0.3 M PBS, 0.3% Triton-X 100. Sections were then washed extensively 3 times for 5 minutes each, with 0.3 M PBS and further incubated with goat anti-rabbit IgG conjugated with biotin (Vector Laboratories, Peterborough, UK) at 1:200 dilution in 0.3 M PBS, 0.3% Triton-X 100 for 1 hour at room temperature. To form the avidin-biotin-peroxidase complex, the sections were subsequently incubated in 200 μ l 0.2 M PB buffer containing Avidin DH and biotinylated horseradish peroxidase H from VECTASTAIN® ABC kits (Vector Laboratories, Burlingame, CA, USA) for 30 minutes at room temperature. This was followed by 2 washes with 0.3 M PBS and 1 wash with 0.1 M PB buffer. The peroxidase activity was quantified by using a diaminobenzidine substrate (DAB kit, Vector

laboratories, Peterborough, UK), prepared in H₂O according to the manufacturer's instructions, before briefly rinsing 3 times with 0.1 M PB buffer. Sections were placed on gelatin-coated slides using a wet paintbrush in a 4 serial section sequences per slides according to the columns in a 24 well plate. Sections were dried overnight in a glass chamber soaked with 4% paraformaldehyde in 50 mM phosphate buffer. The sections were alcohol dehydrated and cleared with xylene following these steps:

H ₂ O	5 minutes
70% Ethanol	5 minutes
90% Ethanol	5 minutes
100% Ethanol	5 minutes
100% Ethanol	5 minutes
100% Ethanol	5 minutes
70% Ethanol	5 minutes
Xylene	5 minutes
Xylene	5 minutes

One drop of DPX mounting media (VWR International Ltd., Lutterworth, UK) was transferred over the tissue sections using a Pasteur pipette and a cover slip (VWR International Ltd., Lutterworth, UK) gently placed over tissue section. The DCX was allowed to dry before visualising with a Zeiss Axiostar plus microscope (Carl Zeiss, Germany) with a x40 objective.

2.8.3.2 Fluorescence immunostaining of doublecortin (DCX)

For fluorescence immunodetection, sections were washed extensively and incubated with the mixture of species-specific primary antibodies consisting of goat polyclonal α -doublecortin antibody 1:500 (DCX C-18, Santa Cruz

Laboratories, Santa Cruz, CA, USA), mouse α -NeuN, 1:500 (Chemocon, Temecula, CA, USA) and Cy-5 dk-mouse, 1:100 (Strattech Scientific, Luton, UK). Sections were then incubated with a cocktail of fluorochrome-conjugated species-specific secondary antibodies comprising of donkey anti-goat IgG conjugated with Alexa 488, 1:500 (Molecular Probes, Eugene, OR, USA) and antimouse IgG conjugated with Rhodamine Red-X, 1: 1000 (Strattech Scientific, Luton, UK) for 2 hours at room temperature. Sections were then stained with propidium iodide (Sigma, Poole, UK; 1% in PBS) in the presence of RNase (Sigma; 10 mg/ml) to reveal cell nuclei. Sections were placed on glass slides and mounted in glycerol-based anti-fade medium (Vectashield; Vector Laboratories, Peterborough, UK) and examined with a Bio-Red MRC 1024 Confocal laser scanning microscope (Hemel Hempstead, UK) equipped with a krypton argon laser, through a x60 oil immersion objective lens.

The process of DCX immunohistochemistry is shown in Figure 2.4.

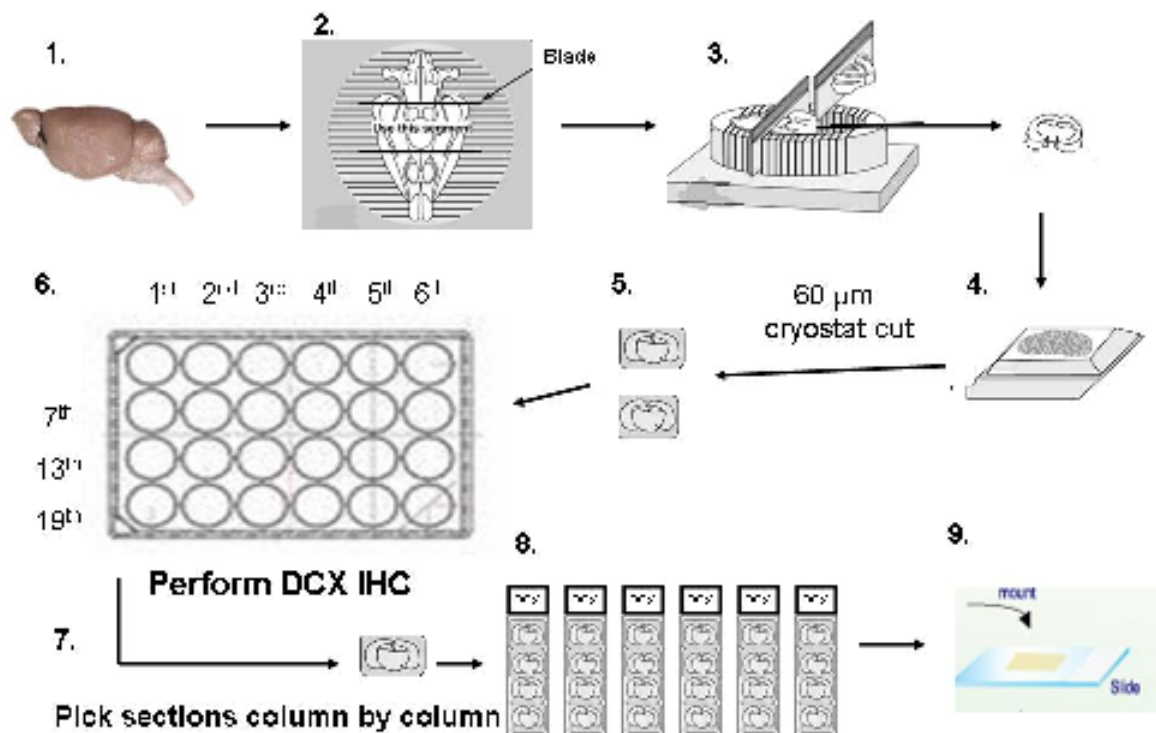


Figure 2.4 Steps involved in tissue processing, cryostat cutting and DCX staining. (1) Fixation and Cryoprotection of brain tissue. (Kim et al.) & (3) Remove the middle segment (which contains the hippocampus). (4) Embed this segment in OCT embedding matrix and freeze it in -20°C in the cryostat machine, cryostat cut sections into 60 µm. (5) Collect and transfer sections serially in 0.2 M PB buffer in a 24-well tissue culture plate. (6) Perform DCX immuno-histochemistry in the 24-well tissue culture plate. (7) Pick sections

one by one with a wet paintbrush and transfer to gelatine-coated slides serially corresponding to each of the 24-well plate columns. Mount slides with DPX mounting media. Images were taken from (O'Neill and Clemens, 2001) by a kind permission of the Editor of *Current Protocols in Neuroscience*.

2.8.4 Quantifying doublecortin [DCX]-positive cells

Simple cell counting is a rapid method to quantify neuron numbers in the hippocampus in several publications (Couillard-Despres et al., 2005). The numbers of DCX-positive cells in our study were counted by a similar counting method in a double-blind fashion. The slide labels were masked and DCX-positive cells in the dentate gyrus were counted by a blind observer. Each brain, DCX stained brain sections were placed in a horizontal serial fashion on gelatine coated-slides. DCX-positive cells were counted on every sixth (60 μm) coronal section through the dentate gyrus by using a Zeiss Axiostar plus (Carl Zeiss, Germany) with a x40 objective lens. This means the 6th, 12th, 18th and 24th sections were selected. The numbers of DCX-positive cells in the dentate gyrus were counted in both hemispheres (Figure 2.5). The sum of these counts was multiplied by six to generate estimates of absolute numbers.

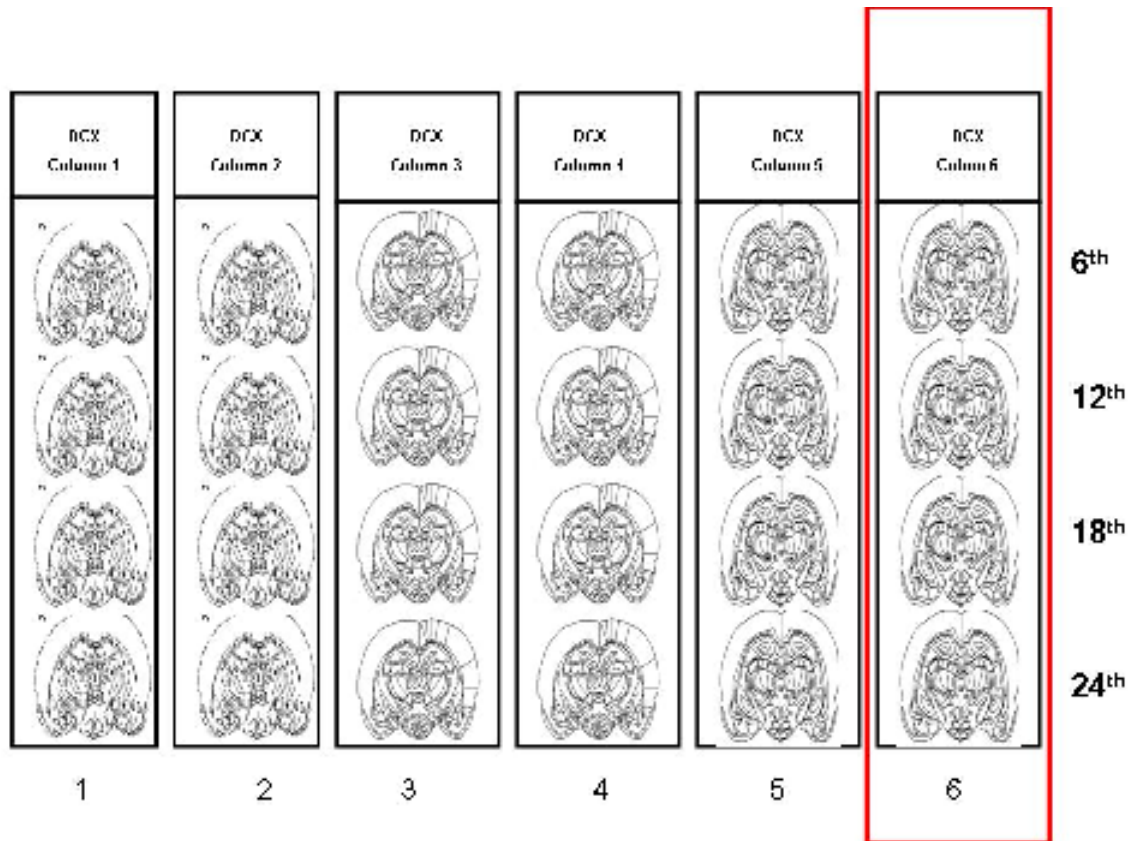


Figure 2.5 The order of DCX-stained brain sections of one mouse brain onto slides. Twenty-four DCX-stained brain sections were placed in a horizontal serial fashion on 6 gelatin-coated slides (from left to right). This order corresponded to the serial order in the 24-well tissue culture plate. 6th, 12th, 18th and 24th sections located at the 6th slide (red box) were used to quantify the number of DCX-positive neuron in the dentate gyrus.

2.9 Statistical analysis

Inflammatory mediator levels below the detection limits of Luminex, ELISA or real-time PCR assays were allocated the value of the detection limit for statistical analysis rather than zero, in order to use the information that the level was low.

Continuous variables were summarised as mean and standard deviation if normally distributed, or median and inter-quartile range if they had a skewed distribution. The distribution of the continuous variable data was inspected by Bartlett's test to confirm the normal distribution. The appropriate parametric test used to compares three or more unmatched groups is the one-way ANOVA. Therefore, this was used as the multiple comparison test for comparing inflammatory mediator concentrations and protein/gene expression levels between 3 groups of mice (arthritic, non-arthritic and naïve control groups). Bonferroni test was used as a post-hoc test for a multiple-comparison correction.

The Student's *t*-test was occasionally used to compare inflammatory mediator concentrations and protein/gene expression levels between 2 experimental groups (arthritic and non-arthritic groups).

In our longitudinal studies, we compared inflammatory mediator concentrations in brains of CII immunized and naïve control mice across time points and between these 2 groups of mice at each time point. Two-way ANOVA is the most suitable test for these longitudinal studies because it determines how a response is affected by two different factors (different groups of mice and different time points). Therefore, two-way Analysis of Variance (ANOVA) with Bonferroni multiple comparison tests were used to evaluate longitudinal inflammatory mediator production, with overall significance for factors of CII immunized/naïve control mice and time. In addition, Two-way Analysis of Variance (ANOVA) with Bonferroni multiple comparison tests were also used to confirm any significant difference in arthritis score, paw thickness and arthritis incidence between CII immunized/naïve control mice. Pearson's correlation coefficient was used for correlation analysis. Calculations for statistical analysis were performed with Prism software version 4 (Graphpad Software, San Diego, CA, US). $P < 0.05$ (*), $P < 0.01$ (**) and $P < 0.001$ (***) were considered as statistically significant.

Chapter 3

**Increased concentration of inflammatory mediators
in the brain associated with collagen-induced
experimental arthritis.**

3.1 Introduction and aims

Rheumatoid arthritis is a systemic autoimmune disease in which, in addition to joint disease, the peripheral inflammation is reflected by the presence of extra-articular organ manifestations such as systemic vasculitis (blood vessel inflammation), subcutaneous nodules and pulmonary fibrosis in approximately 30% of RA patients (Young and Koduri, 2007). Accumulating evidence suggests that the brain may also be affected by peripheral inflammation during arthritis. For example, neuroimaging studies showed several CNS lesions in the brains of RA patients, which resolved after steroid treatment, suggesting that CNS inflammatory demyelination may also be inducible by systemic inflammation during arthritis (Tsai et al., 2008); (Tajima et al., 2004). Psychiatric disorders such as depression and anxiety are also common in RA, and this observation may be a potential novel area of clinical research based on the hypothesis that these may be due to peripheral inflammation during arthritis causing alterations in brain neurobiology. To date, there are few studies investigating the potential mechanisms underlying psychological disorders in RA. One preliminary study using a single photon emission computed tomography (SPECT) scan of 6 RA patients showed a reduction in serotonin transporter (SERT) density, along with improvement in physical and mental functions after receiving anti-TNF- α treatment, suggesting that circulating cytokines generated during autoimmune activation in RA may cause changes in the serotonin system that induced the development of depression (Cavanagh et al., 2010). A hypothesis based on this clinical observation is supported by studies in animal model of RA; a study using a transient model of RA by Bao *et al.*, showed that both mRNA and protein concentration of IL-1 β , IL-6 and TNF- α were elevated in the spinal cord of AIA rats (Bao et al., 2001). Similar observations were reported in a chronic model of RA; brains of CIA rats showed up-regulation of the expression of various cytokine genes, including TNF- α , IL-1 β and IL-6 (del Rey et al., 2008). In addition, a transient increase in hippocampal neurogenesis has been reported in the brains of AIA rats, suggesting that neuroinflammation induced by peripheral inflammation may contribute to neurobiological changes during the course of arthritis (Wolf et al., 2009b).

Based on this evidence, we hypothesised that the systemic immune response activated during arthritis can induce brain inflammation and neurobiological

changes, which may help explain the mechanism underlying psychological disorders associated with RA. Therefore, the aim of this chapter is to investigate changes in a wide range of inflammatory mediator proteins in the brain of CIA mouse model of arthritis using Luminex bead-based screening assays. We also determine changes in concentration of mRNA encoding these inflammatory mediators using real-time PCR and quantified as absolute copy numbers.

3.2 Results

3.2.1 *Induction of arthritis in DBA1 mice*

The aim of this experiment is to investigate whether peripheral immune/inflammatory responses occurring during arthritis can change the protein and gene expression profiles of inflammatory mediators (cytokines, chemokines, growth factors) in the brains.

Experimental procedure: 19 DBA1 mice were immunized by intradermal injection of type II collagen in complete Freund's adjuvant on day 0. On day 21, mice were given an i.p. booster injection of type II collagen dissolved in PBS. 7 sex- and age-matched DBA1 mice were used as the naïve control and were not immunized or boosted with type II collagen. The signs of arthritis in CII immunized mice were monitored from day 16 after immunization onwards and arthritis severity in this experiment were verified independently by Dr. Darren Asquith. Groups of both CII immunized and control mice were sacrificed on day 42 and serum was collected for the determination of peripheral inflammatory mediator proteins by a luminex multi-parameter assay. The brain of each mouse was isolated and snapped frozen in liquid nitrogen and stored at -80°C . Half of each brain was processed for protein extraction and inflammatory mediator protein analysis by luminex; the other half was processed for RNA extraction and inflammatory mediator gene expression determined by real-time PCR. The experimental procedure of collagen II-induced experimental arthritis (CIA) model is summarized in Figure 3.1.

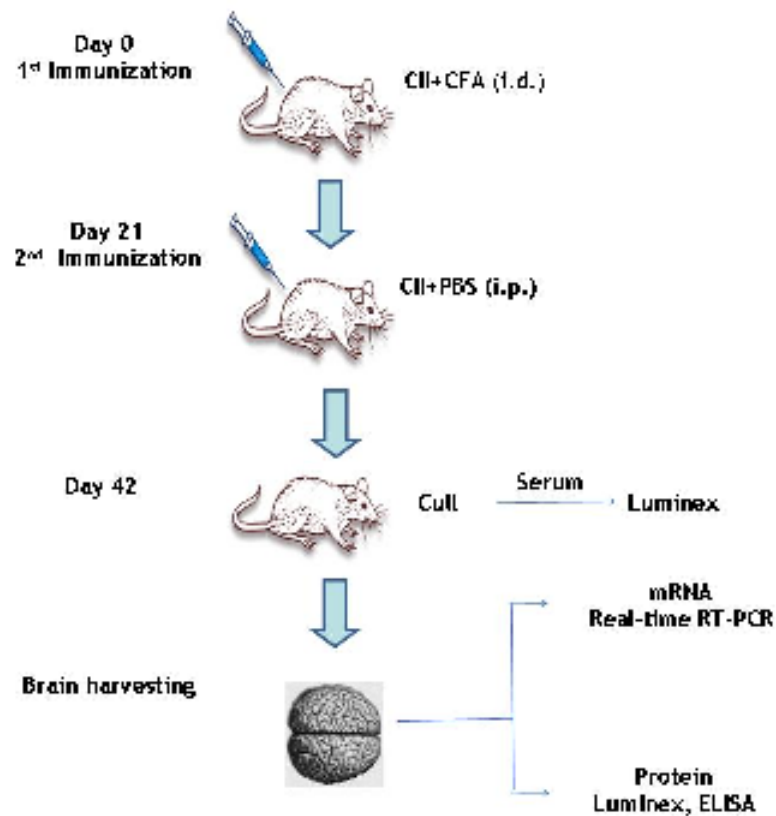


Figure 3.1 The experimental procedure of collagen II-induced experimental arthritis (CIA) model

DBA1 mice at 6-8 weeks of age were separated into two groups: i) 7 control mice; ii) 19 immunized mice. Mice were immunized with 100 μ g type II bovine collagen + complete Freund's adjuvant (CFA) at day 0 and then challenged on day 21 with 200 μ g type II collagen. A group of 7 naïve DBA1 mice which were not immunized and not treated with type II collagen was used as a control group. Serum and brains from control and CII-immunized mice were harvested at Day 42. Each mouse brain was dissected into left and right hemispheres. One half was processed for mRNA extraction and measurements of inflammatory mediator transcripts by real-time PCR. Protein was extracted from the other half brain after homogenisation of the tissue and used to determine inflammatory mediator protein concentration a Luminex assay.

Clinical response: Some of the CII-immunized mice started to show clinical signs of arthritis from day 19 onwards and there were 12 out of the 19 CII immunized mice that developed arthritis (63% incidence) on day 42 (Figure 3.2A). 7 of the 19 mice did not develop arthritis although they had an identical immunization and challenge, and these were therefore considered as potentially different and formed a separate 'immunised but non-arthritis' study group.

CII immunized mice showed a significant increase in paw thickness compared to those in naïve control mice ($P < 0.0001$). The mean paw thickness and the mean arthritis score for the whole group of CII-immunized mice ($n=19$) on day 42 were 1.9 ± 0.1 mm and 4.5 ± 1.2 respectively (Figure 3.2B), (Figure 3.2C). Haematoxylin and eosin staining of a hind paw tissue section of an

arthritic mouse (this mouse had a clinical score of 12 on day 42) showed cartilage and bone damage/erosion and synovial hyperplasia in the joint (Figure 3.3)

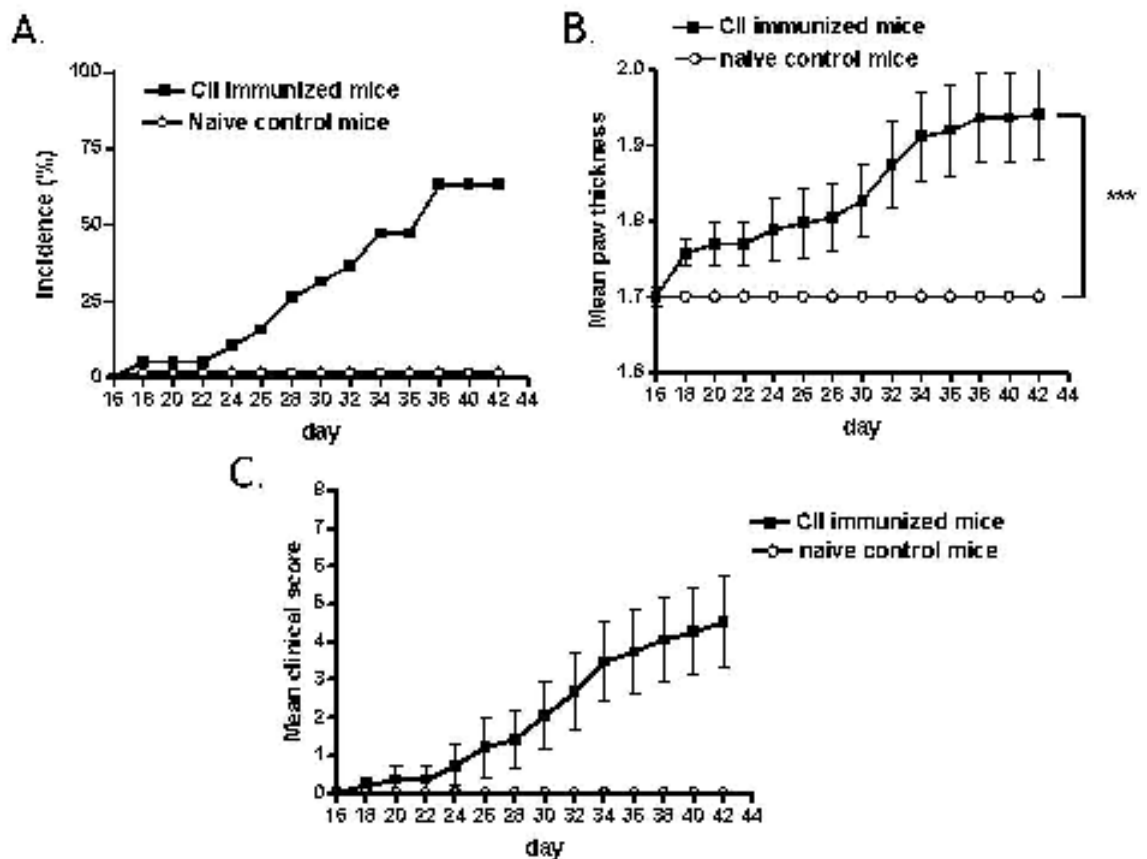


Figure 3.2 development and severity of arthritis disease in CII immunized mice over 42 days of experimental arthritis course

The signs of arthritis in CII immunized mice were monitored from day 16 after immunization onwards. (A) shows the percent incidence of arthritis in CII immunized mice, which was calculated from the number of CII immunized mice with arthritis divided by the total number of CII immunized mice used. The signs of arthritis were observed in CII immunized mice from day 18 onwards and there were 12 out of total 19 CII immunized mice developed arthritis on day 42. Mean clinical arthritic score and mean paw thickness were used as clinical evaluations to measure the severity of joint inflammation in arthritic mice. (B) shows the mean paw thickness of CII immunized mice which was calculated from the sum of the paw thickness of all mice divided by the number of mice. (C) shows the mean clinical score of CII immunized mice which was calculated from the sum of the clinical scores of all mice divided by the number of mice. Mean paw thickness, mean clinical score and %incidence in 19 CII immunised mice (filled squares) were compared with those values of 7 naive control mice (open circles). Data represent as mean \pm SEM. (n=19 CII immunised mice). Statistical analysis of data was performed using two-way ANOVA for multiple comparison, compared with a group of control naive mice; *P<0.05, ** P<0.01, *** P<0.001.

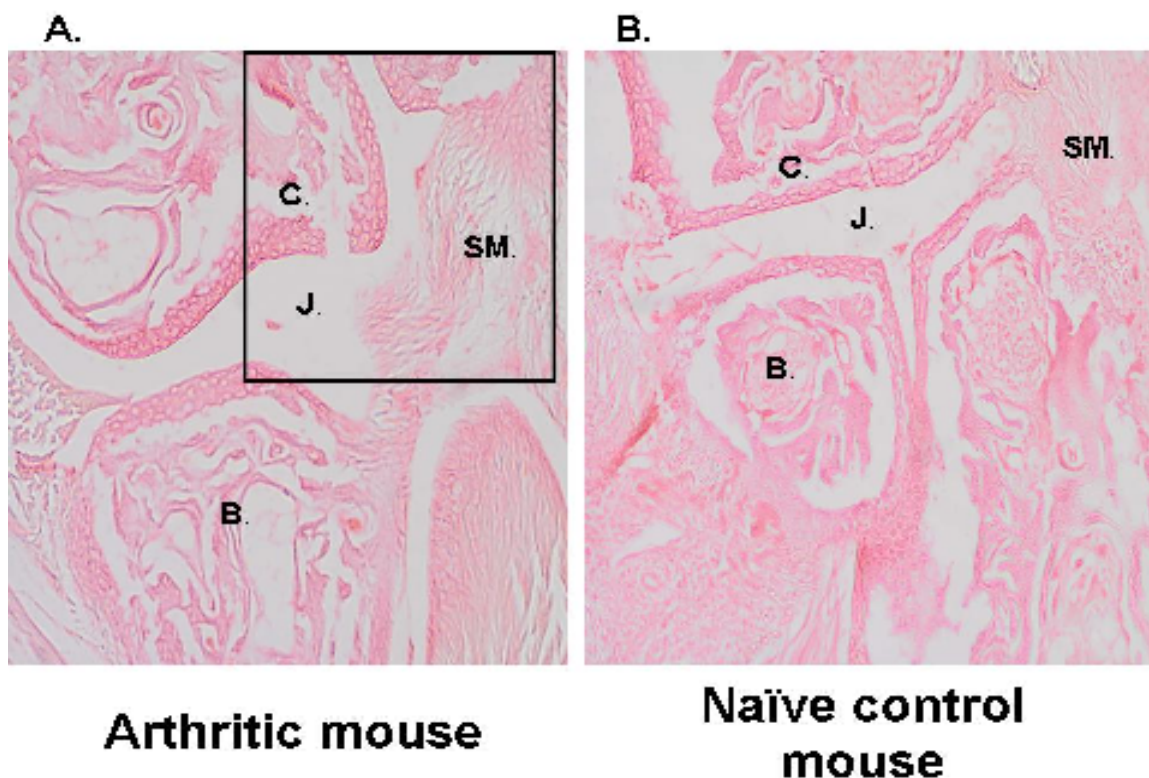


Figure 3.3 Paw histology of an arthritic mouse
 (A) a representative histological image (10 x magnification) of a section of an arthritic mouse paw (this arthritic mouse had a clinical score of 12 on day 42). A smaller box section shows the area of joint inflammation in this arthritic mouse. Cartilage and bone damage/erosion, cartilage loss and synovial hyperplasia were observed in an inflamed hind paw of this arthritic mouse compared to a representative histological image (10 x magnification) of a section of a naïve mouse paw (B). Abbreviations; B = Bone, C = Cartilage, J = Joint space, SM = synovial membrane.

3.2.2 Changes in inflammatory mediator protein concentration in serum of CII immunized mice (both arthritic mice and non-arthritic mice)

To investigate systemic inflammatory signals in the periphery of CII immunized mice, inflammatory mediator proteins in serum collected from naïve control mice and CII immunized mice on day 42 were determined using a Luminex cytokine 20-Plex assay. Serum concentrations of CXCL1 and FGF protein were within the assay detection limits (CXCL1 35 - 3023 pg/ml; and FGF2 27 - 3552 pg/ml). Concentrations of the other serum inflammatory mediators (TNF- α , IFN- γ , IL-1 α , IL-1 β , IL-4, IL-5, IL-6, IL-10, IL-12 [p40], IL-12[p40/p70], IL-13, IL-17), chemokines (CXCL10, CCL2, CXCL9, CCL3, CCL4, CCL19, CCL5), and growth factors (GM-CSF, PDGF-BB, VEGF) in brain tissue of mice of all experimental groups were lower than the detection limit of the Luminex assay.

One-way ANOVA analysis demonstrated that there were significant differences in serum concentration of CXCL1 among the three groups of mice ($P < 0.0001$). Post hoc analysis with Bonferroni correction demonstrated significant increases in serum concentration of CXCL1 in CII immunized mice (both arthritic and non-arthritic) compared to those in naïve control mice. The mean values of serum CXCL1 (arthritic versus naïve control) was 51.1 ± 2.6 pg/ml versus 33.6 ± 1.5 pg/ml ($P < 0.001$). The serum concentration of CXCL1 was also elevated in CII immunized mice that did not develop arthritis compared to those in the naïve controls. The mean values of serum CXCL1 (non-arthritic versus naïve control) was 54.8 ± 6.8 pg/ml versus 33.6 ± 1.5 pg/ml ($P < 0.001$). There was no significant difference in serum CXCL1 concentration between arthritic and non arthritic mice (Figure 3.4A). These results are consistent with a study in CIA model by Kurowska *et al.*, showing an elevation of serum CXCL1 detected using a Luminex assay in CII immunized mice compared to the controls. FGF2 was another inflammatory mediator detected in serum of mice from all the experimental groups. However, one-way ANOVA analysis showed that there was no significant difference in serum FGF2 concentration between naïve control mice and CII immunized mice ($P = 0.4093$) (Figure 3.4B)

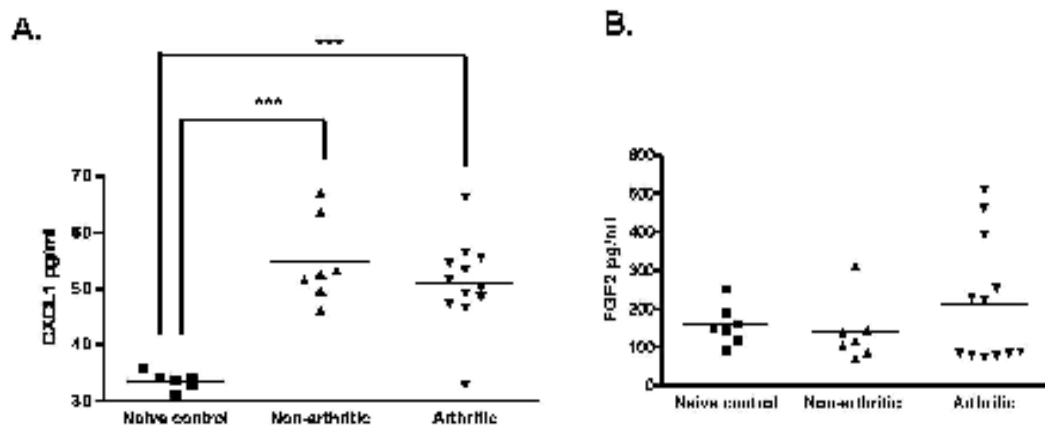


Figure 3.4 Serum inflammatory mediator profiles in CII immunized mice
 Concentrations of inflammatory mediator protein concentration (pg/ml) determined by Luminex-based multiplex cytokine assay in serum of naïve control mice (n=7 naïve control mice) and CII immunized mice (n=19 CII immunized mice). The group of CII immunized mice consisted of 7 non-arthritic mice and 12 arthritic mice. Mice from all experimental groups were sacrificed and serum samples were collected on day 42. Only CXCL1 and FGF2 protein concentration were detectable at the detection limit. Data are presented as the mean values. (* $P < 05$; ** $P < 01$; *** $P < 001$ by one-way ANOVA analysis)

3.2.3 *Changes in inflammatory mediator protein concentrations in brains of CII immunized mice (both arthritic mice and non-arthritic mice)*

To investigate changes in inflammatory mediator profiles in brains of CII immunized mice that did (arthritic mice) or did not (non-arthritic mice) develop arthritis compared to naïve control mice, Luminex cytokine 20-Plex assay was used to measure the protein concentration of various inflammatory mediators including proinflammatory cytokines (IL-6, IL-1 β , TNF- α and IL-1 α), Th1 cytokines (IL-2, IL-12 and IFN- γ), Th2 cytokines (IL-4, IL-5, IL-10, IL-13), chemokines (CXCL1, CXCL10, CCL2, CCL3) and growth factors (FGF2, VEGF) in half brain tissue homogenate samples from mice of all experimental groups. Each sample was measured in triplicate. Values were reported as pg/ml. These values were extrapolated from the standard curves of known concentrations of a single mixed inflammatory mediator standard. Examples of the standard curves for each inflammatory mediators generated in the Luminex assay used in the experiment are shown in Appendix 1A and Appendix 1B. The standard curves of this Luminex assay demonstrated the dynamic range and sensitivity desired for the assay. In addition, these standard curves were to show that the Luminex assay was run in an acceptable performance manner.

Values of inflammatory mediator concentrations in each brain tissue homogenate sample (pg/ml) were then normalized with the total protein concentration of brain tissue ($\mu\text{g/ml}$) of that sample, and presented as pg/mg total brain protein. To calculate the amount of inflammatory mediator protein level as pg/mg total brain protein, amounts of inflammatory mediator proteins and of total brain protein in 50 μl of each sample were firstly calculated. For example, the protein concentration of IL-13 in sample A measured by Luminex was 55.03 pg/ml, therefore 50 μl of sample A contains 2.8 pg IL-13. The protein concentration of sample A measured by BCA protein assay was 7087.03 $\mu\text{g/ml}$, therefore 50 μl of sample A was 354.35 μg total brain tissue. Finally, amount of IL-13 protein in 1 mg total brain protein (pg/mg total brain tissue) was calculated using the following equation

$$\frac{1000 \times \text{Amount of IL-13 protein in } 50 \mu\text{l (pg)}}{\text{Amount of total brain protein in } 50 \mu\text{l (mg)}}$$

Therefore, 1 mg total brain proteins of sample A contained 7.765 pg of IL-13.

Values of protein concentrations of IL-1 α , IL-2, IL-4, IL-5, IL-6, IL-10, IL-13, CXCL1, CXCL10 and FGF2 obtained from the Luminex assay in brain tissue homogenate samples of mice from all experimental groups were all within the detection limits of the assay. Table 2.1 shows the dynamic range for each inflammatory mediator generated in the Luminex assay, and the mean values of protein concentrations (pg/ml) of these inflammatory mediators in brain tissue homogenate samples of both naïve control mice and CII immunized mice before normalization. This is to show that the actual values of these inflammatory mediator protein concentration in brain tissue homogenate samples of mice from all experimental groups were within the detection limit of the assay, although the amount of some brain inflammatory mediators protein in these mice seemed lower than the detection limit of the Luminex assay after the normalization by total brain protein (pg/mg total brain protein).

Inflammatory mediators	Dynamic range of detection limits (pg/ml)	mean concentrations of brain inflammatory mediator proteins in 50 μ l brain tissue homogeneous (pg/ml)	
		Naïve control mice	CII immunized mice
IL-1 α	20.9 - 14733.5	13.8 \pm 4.0	36.4 \pm 14.1
IL-2	17.6 - 13999.8	47.2 \pm 23.1	107.3 \pm 44.3
IL-4	12.7 - 13452	10.1 \pm 1.6	23.5 \pm 11.7
IL-5	6.4 - 10204.5	18.9 \pm 2.4	31.4 \pm 9.6
IL-6	8.3 - 9161.9	7.8 \pm 2.1	15.1 \pm 6.9
IL-10	46.2 - 40630.0	200.9 \pm 60.0	454.4 \pm 294.1
IL-13	25.3 - 20070.0	22.2 \pm 6.9	46.5 \pm 25.3
CXCL1	33.4 - 14796.0	85.4 \pm 9.7	168.5 \pm 58.0
CXCL10	33.5 - 38592.1	76.1 \pm 8.2	154.1 \pm 55.6
FGF2	34.8 - 11084.3	522.8 \pm 47.0	927.7 \pm 296.4

Table 3.1 Values of protein concentrations of inflammatory mediators detected by a Luminex assay in brain tissue homogenate samples of naïve control mice and CII immunized mice

Dynamic range of detection limits of the Luminex assay were generated by standard curve of known quantities of mouse recombinant inflammatory mediators. Protein concentrations of IL-1 α , IL-2, IL-4, IL-5, IL-6, IL-10, IL-13, CXCL1, CXCL10 and FGF2 obtained from the Luminex assay in 50 μ l brain tissue homogenate samples of mice from all experimental groups were obtained from the Luminex assay as pg/ml. Values of protein concentrations of these inflammatory mediators were eventually normalized by total brain protein as presented as pg/mg total brain protein. The mean value of total protein concentration of brain tissue in 50 μ l of brain tissue homogenate samples of naïve control and CII immunized mice were 4694 \pm 473 μ g/ml and 4795 \pm 683 μ g/ml. Protein concentrations of mean concentrations of brain inflammatory mediator proteins were presented by (pg/ml) \pm SD.

3.2.3.1 Pro-inflammatory cytokine profiles in the brains of CII immunized mice (both arthritic mice and non-arthritic mice)

Pro-inflammatory cytokines, including IL-1 β , IL-1 α , IL-6 and TNF- α , are produced by mononuclear cells such as macrophages and are involved in the initiation of the immune response. The amounts of these proinflammatory cytokines were determined in the brains of naïve control mice, arthritic mice and CII immunized mice with no arthritis, but only IL-1 α and IL-6 were detectable. One-way ANOVA analysis showed that there was no significant difference in brain IL-1 α and IL-6 protein concentration between naïve control non arthritic mice and arthritic mice ($P = 0.0543$ and $P = 0.8445$ respectively) (Figure 3.5A, Figure 3.5B).

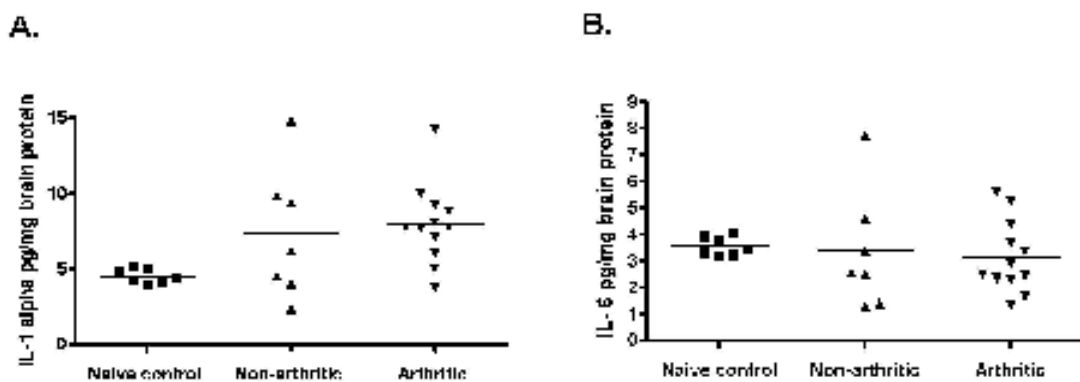


Figure 3.5 Changes in pro-inflammatory cytokine concentration in brains of CII immunized mice

The dots represent protein concentration of IL-1 α and IL-6 (pg/mg total brain protein) determined by Luminex-based multiplex cytokine assay in brain tissue homogenate of naïve control mice (n=7 naïve control mice), non-arthritic mice (n=7 non-arthritic mice), and, arthritic mice (n=12 arthritic mice). All mice were sacrificed and brains were collected on day 42. Data are presented as the mean values. (* $P < 05$; ** $P < 01$; *** $P < 001$ by one-way ANOVA analysis). Bars represent the mean values.

3.2.3.2 Th-1 cytokines profile in the brains of CII immunized mice (both arthritic mice and non-arthritic mice)

Th-1 cytokines, including IL-12, IL-2 and IFN- γ , were determined in the brain of naïve control mice and CII immunized mice with and without arthritis. IL-2 was the only cytokine in this category that was up-regulated in arthritic mouse brains compared to those in the naïve control group. One-way ANOVA analysis demonstrated that there was a significant difference in protein concentration of IL-2 among the three groups of mice ($P = 0.0343$). Post hoc analysis with Bonferroni correction demonstrated the significant difference in protein concentration of IL-2 between arthritic mice and naïve control mice. The mean value of IL-2 (arthritic versus naïve control) was 24.4 ± 10.2 pg/mg total brain

protein versus 11.6 ± 2.2 pg/mg total protein ($P < 0.05$). There was no significant difference in brain IL-2 protein concentration between naïve control mice and non-arthritic mice (Figure 3.6). There were no significant differences in brain IL-2 concentrations between arthritic and non-arthritic mice.

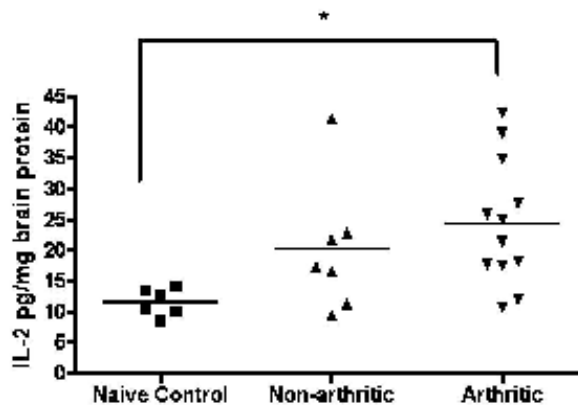


Figure 3.6 Changes in a Th1 cytokine level in brains of CII immunized mice
The dots represent protein concentration of IL-2 (pg/mg total brain protein) determined by Luminex-based multiplex cytokine assay in brain tissue homogenate of naïve control mice ($n=7$ naïve control mice), non-arthritic mice ($n=7$ non-arthritic mice), and, arthritic mice ($n=12$ arthritic mice). All mice were sacrificed and brains were collected on day 42. Data are presented as the mean values. (* $P < 05$; ** $P < 01$; *** $P < 001$ by one-way ANOVA analysis). Bars represent the mean values. Bars represent the mean values.

3.2.3.3 Th-2 cytokine profiles in the brains of CII immunized mice (both arthritic mice and non-arthritic mice)

Th-2 cytokines, including IL-4, IL-5, IL-10 and IL-13 were determined in the brains of naïve control mice and CII immunized mice with and without arthritis. One-way ANOVA analysis showed that there was no significant difference in brain IL-4 protein concentration between naïve control mice and CII immunized mice ($P = 0.6696$) (Figure 3.7A). One-way ANOVA analysis demonstrated that there were significant differences in protein concentration of IL-5 and IL-13 among the three groups of mice ($P = 0.0199$ and $P = 0.0355$ respectively) (Figure 3.7B and Figure 3.7D). Post hoc analysis with Bonferroni correction demonstrated significant increases in concentration of IL-5 and IL-13 in brains of arthritic mice compared to those in naïve control mice. The mean values of IL-5 (arthritic versus naïve control) were 6.8 ± 2.0 pg/mg total protein versus 4.10 ± 0.69 pg/mg total protein ($P < 0.05$). The mean value of IL-13 (arthritic versus naïve control) was 10.0 ± 3.6 pg/mg total protein versus 5.4 ± 0.6 pg/mg total protein ($P < 0.05$). There was no significant difference in brain IL-5, IL-10, and IL-13

protein concentration between naïve control mice and non-arthritic mice (Figure 3.7B and Figure 3.7D). There were no significant differences in brain IL-5 and IL-13 concentrations between arthritic and non-arthritic mice. One-way ANOVA analysis suggested that there was no significant difference in brain IL-10 protein concentration between naïve control mice and CII immunized mice ($P = 0.1196$) (Figure 3.7C).

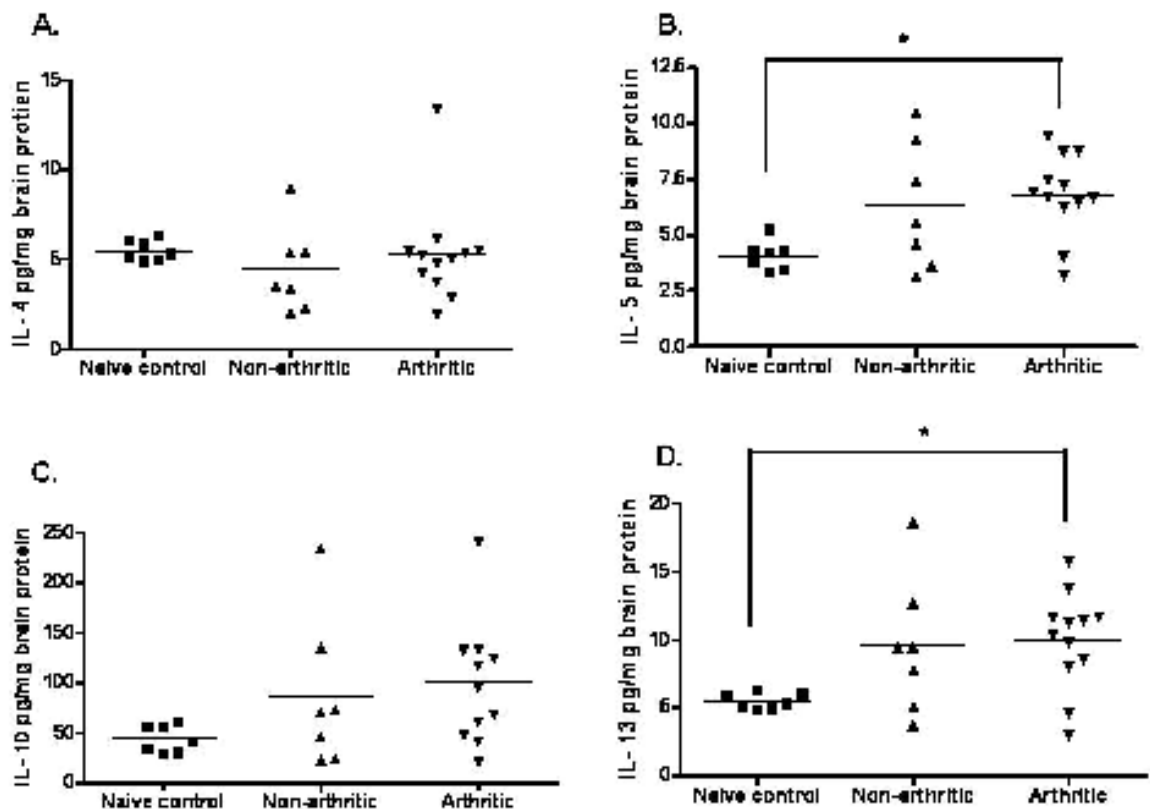


Figure 3.7 Changes in Th2 cytokine concentration in brains of CII immunized mice
The dots represent protein concentration of IL-4, IL-5, IL-10, IL-13 (pg/mg total brain protein) determined by Luminex-based multiplex cytokine assay in brain tissue homogenate of naïve control mice (n=7 naïve control mice), non-arthritic mice (n=7 non-arthritic mice), and, arthritic mice (n=12 arthritic mice). All mice were sacrificed and brains were collected on day 42. Data are presented as the mean. (* $P < 05$; ** $P < 01$; *** $P < 001$ by one-way ANOVA analysis) Bars represent the mean values.

3.2.3.4 Chemokine profiles in the brains of CII immunized mice (both arthritic mice and non-arthritic mice)

Chemokines produced by activated immune cells, including CXCL1, CXCL10, CCL-2 and CCL3, were determined in the brains of naïve control mice and CII immunized mice with and without arthritis. One-way ANOVA demonstrated that there were significant differences in protein concentration of CXCL1 and CXCL10 among the three groups of mice ($P = 0.0012$ and $P = 0.0037$ respectively) (Figure

3.8A and Figure 3.8B). Post hoc analysis with Bonferroni correction demonstrated that brain protein concentrations of CXCL1 and CXCL10 in CII immunized mice were significant higher than those in naïve control mice. The mean values of CXCL1 and CXCL10 (arthritic versus naïve control) were 37.4 ± 12.7 pg/mg total protein versus 14.1 ± 1.5 pg/mg total protein ($P < 0.01$), and 35.6 ± 11.1 pg/mg total protein versus 16.5 ± 2.4 pg/mg total protein ($P < 0.01$) respectively. There was no significant difference in the brain CXCL-10 protein level between naïve control mice and non-arthritic mice. However, there was a significant increase in CXCL1 protein level in CII immunized mice without arthritis compared to those in the naïve control group. The mean value of CXCL1 (non-arthritic versus naïve control) was 33.6 ± 14.8 pg/mg total protein versus 14.1 ± 1.5 pg/mg total protein ($P < 0.05$) (Figure 3.8A and Figure 3.8B). There were no significant differences in brain CXCL1 and CXCL10 concentrations between arthritic and non-arthritic mice.

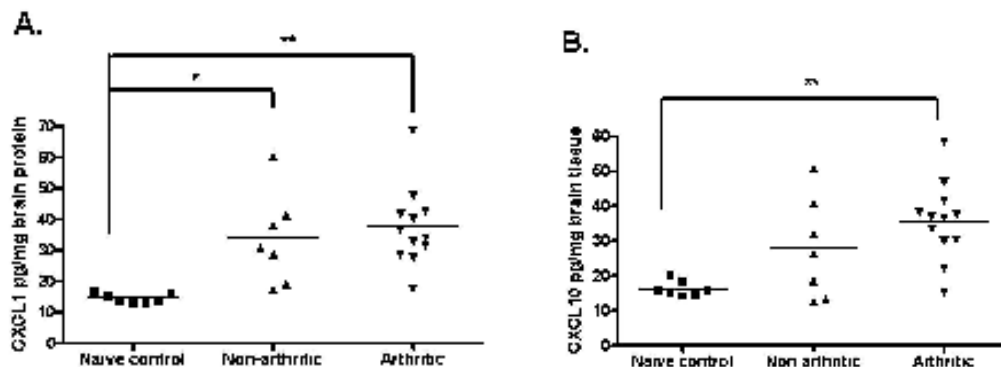


Figure 3.8 Changes in chemokine concentration in brain of CII immunized mice
The dots represent protein concentration of CXCL1 (A) and CXCL10 (B) (pg/mg total brain protein) determined by Luminex-based multiplex cytokine assay in brain tissue homogenate of naïve control mice (n=7 naïve control mice), non-arthritic mice (n=7 non-arthritic mice), and, arthritic mice (n=12 arthritic mice). All mice were sacrificed and brains were collected on day 42. Data are presented as the mean values. (* $P < 0.05$; ** $P < 0.01$; *** $P < 0.001$ by one-way ANOVA analysis). Bars represent the mean values.

3.2.3.5 Growth factor profiles in the brain of CII immunized mice (both arthritic mice and non-arthritic mice)

Growth factors such as FGF2 and VEGF were quantified in the brains of naïve control mice and CII immunized mice with and without arthritis. FGF2 which is produced abundantly by CNS resident cells was detected in high concentration in brains from all groups of mice. One-way ANOVA demonstrated that there were significant differences in serum concentration of FGF2 among the three groups of mice ($P = 0.0136$). Post hoc analysis with Bonferroni correction demonstrated

that the protein level of FGF2 in arthritic mouse brains was significantly higher than those in the naïve control group. The mean value of FGF2 (arthritic versus naïve control) was 204.0 ± 58.5 pg/mg total protein versus 109.9 ± 19.1 pg/mg total protein ($P < 0.05$). There was no significant difference in brain FGF2 protein level between naïve control mice and non-arthritic mice (Figure 3.9). There were no significant differences in brain FGF concentrations between arthritic and non-arthritic mice.

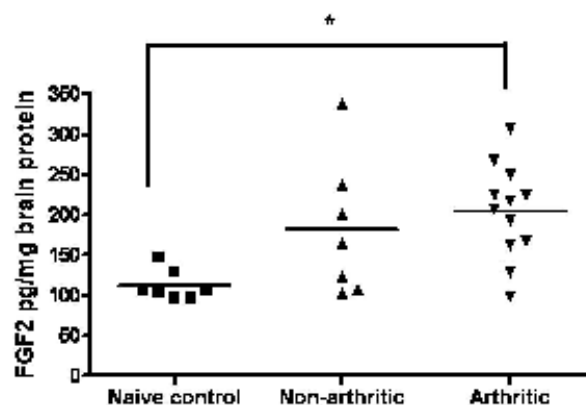


Figure 3.9 Changes in a growth factor level in brain of CII immunized mice
The dots represent protein concentration of FGF2 (pg/mg total brain protein) determined by Luminex-based multiplex cytokine assay in brain tissue homogenate of naïve control mice (n=7 naïve control mice), non-arthritic mice (n=7 non-arthritic mice), and, arthritic mice (n=12 arthritic mice). All mice were sacrificed and brains were collected on day 42. Data are presented as the mean values. (* $P < 0.05$; ** $P < 0.01$; *** $P < 0.001$ by one-way ANOVA analysis) Bars represent the mean values.

In summary: numerous inflammatory mediator protein, including IL-1 α , IL-2, IL-4, IL-5, IL-6, IL-10, IL-13, CXCL1, CXCL10 and FGF2 were detected by the Luminex assay in brain tissue homogeneous of mice from all experimental groups. Significant increases in protein concentration of IL-2, IL-5, IL-13, CXCL1, CXCL10 and FGF2 were observed in brain tissue of CII immunized mice that develop arthritis compared to those in the naïve control mice. The inflammatory mediator protein concentration seemed to increase in non-arthritic mouse brains, although one-way ANOVA analysis showed that the concentrations were not significantly different compared to those in naïve control mice. Only CXCL1 protein concentration was significantly elevated in non-arthritic mouse brains.

Table 3.2 shows a summary of these data as mean \pm SD of fold changes of inflammatory mediator protein profiles in brains of CII immunized mice (both arthritic and non-arthritic) in comparison to those in brains of naïve control

mice. Data were categorized into 5 groups (pro-inflammatory cytokines, Th1 cytokines, Th2 cytokines, chemokines and growth factors). Our data showed that inflammatory mediator protein concentration in brains of CII immunized mice significantly increased from 1.7 - to 2.6 - fold compared with those in naïve control. Among these inflammatory mediators, the greatest mean fold change was observed in the group of chemokines (CXCL1 and CXCL10). The highest mean fold change of 2.6 was observed for CXCL1 protein concentration in brains of arthritic mice. Interestingly, the second highest fold change was still CXCL1 (2.4-folds), however, observed in brains of non-arthritic mice. The lowest mean fold change of 1.7 folds was observed in IL-5 in arthritic mouse brains.

Inflammatory mediator protein concentration	Arthritic		Non-arthritic	
	Fold changes of Protein concentration	<i>P</i> value	Fold changes of Protein concentration	<i>P</i> value
Pro-inflammatory cytokines				
IL-1 α	1.8 \pm 0.8	NS	1.7 \pm 1.3	NS
Th1 cytokines				
IL-2	2.1 \pm 4.6	< 0.05*	1.7 \pm 4.8	NS
Th2 cytokines				
IL-5	1.7 \pm 2.6	< 0.05*	1.5 \pm 4.1	NS
IL-10	2.0 \pm 4.5	NS	1.9 \pm 5.7	NS
IL-13	1.9 \pm 6.5	< 0.05*	1.8 \pm 9.1	NS
Chemokines				
CXCL1	2.6 \pm 8.7	< 0.01**	2.4 \pm 10	< 0.05*
CXCL10	2.2 \pm 4.7	< 0.01**	1.7 \pm 6.1	NS
Growth factors				
FGF2	1.9 \pm 3.5	< 0.05*	1.7 \pm 4.4	NS

Table 3.2 summary of inflammatory mediator protein profiles in brains of CII immunized mice

Data summary was presented as mean \pm SD of fold changes of inflammatory mediator protein profiles in brains of CII immunized mice (both arthritic and non-arthritic) in comparison to those in brains of naïve control mice. One-way ANOVA analysis (**P* < 005; ***P* < 002; ****P* < 001) was used to demonstrate significant increase in inflammatory mediator protein concentration in arthritic and non-arthritic mouse brain compared to those in control mouse brains. NS = not statistically significant.

3.2.4 Cytokine gene expression profiles in the brains of CII immunized mice (both arthritic mice and non-arthritic mice)

Significant increases in various inflammatory mediator protein concentration including IL-1 α , IL-2, IL-5, IL-10, IL-13, CXCL1, and CXCL10 were detected by the Luminex assay in brains of CII immunized mice, especially in brains of arthritic mice, compared to those in naïve control mice. However, we could not define the cellular source of these inflammatory mediator proteins in the brains of arthritic mice. It is possible that they were either produced from peripheral immune cells and transported into the brains, or produced from local immune cells such as astrocytes and microglia. To investigate this, we therefore investigated the mRNA expression levels of these brain inflammatory mediators at the transcription level, which can be another indicator of neuro-inflammation during the process of peripheral joint inflammation. Changes in mRNA expression level of these inflammatory mediators in brains of CII immunized mice may suggest local production by astrocytes, microglia or by peripheral immune cells trafficking into the brain. Real-time PCR was employed to determine mRNA expression levels of the same 20 inflammatory mediators as measured by Luminex (above); including proinflammatory cytokines (IL-6, IL-1 β , TNF- α and IL-1 α), Th1 cytokines (IL-2, IL-12 and IFN- γ), Th2 cytokines (IL-4, IL-5, IL-10, IL-13), chemokines (CXCL1, CXCL10, CCL2, CCL3), growth factors (FGF2, VEGF) using RNA extracted from the other half of the brain tissue.

The expression level of mRNA of these inflammatory mediators in brains tissue of mice from all experimental groups were quantified as cycle threshold (Ct) values by real-time PCR assays. These Ct values were then calculated as absolute copy number of target genes using standard curves generated from amplification of 10-fold serial dilutions of known quantities of a plasmid containing the target sequences. The absolute mRNA copy numbers of inflammatory mediators were normalized to GAPDH expression as described in the Materials and Methods chapter and reported as arbitrary units. mRNA expression levels of IFN- γ , CXCL1, CXCL10, VEGF and FGF in brains of mice from all experimental groups were detectable within detection limits of the assay. This was demonstrated by the transcription values of these brain samples being within the linear dynamic range of the standard curve (Appendix 2). Specificity of the real-time PCR assay was determined by melting curve analysis as described in the Materials and

Methods section. Examples of melting curve analysis of each inflammatory mediator are shown in Appendix 3.

3.2.4.1 Pro-inflammatory cytokine mRNA profiles in the brains of CII immunized mice (both arthritic mice and non-arthritic mice)

The gene expressions of pro-inflammatory cytokines including IL-6, IL-1 β , TNF- α and IL-1 α were determined in brains of mice from all experimental groups. However, the expression levels of these pro-inflammatory cytokines in all brain samples were lower than the detection limit. Despite an increase in IL-1 α protein concentration in arthritic mouse brains, there was no equivalent increase in IL-1 α mRNA expression levels detected in brains of these arthritic mouse brains. These may suggest that the timing of induction and half-life of mRNA had finished while the protein was maintained, and/or there may be active transportation of IL-1 α protein from the periphery into the brains of arthritic mice.

3.2.4.2 Th-1 cytokines mRNA profiles in the brains of CII immunized mice (both arthritic mice and non-arthritic mice)

Gene expression of Th-1 cytokines, including IL-12, IL-2 and IFN- γ , were determined in the brain of control mice and mice with and without arthritis. One-way ANOVA followed by Bonferroni's post-hoc comparison tests showed that the expression of IFN- γ was up-regulated significantly in CII immunized mouse (both arthritic and non-arthritic mice) brains compared to those of control mice ($P = 0.0131$). The mean value of IFN- γ (arthritic versus naïve control) was 305 ± 132 versus 138 ± 43 ($P < 0.05$). There were no significant differences in brain IFN- γ gene expression concentration between arthritic and non-arthritic mice. There were also no significant differences in brain IFN- γ gene expression concentration between arthritic and non-arthritic mice (Figure 3.10). Despite up-regulation in IFN- γ mRNA expression levels in both arthritic and non-arthritic mouse brains, there was no significant IFN- γ protein level detected in brains of these CII immunized mouse brains. This may be difficult to interpret. It may suggest that the local mRNA translation of IFN- γ in brains of CII immunized mice was still ongoing, or that any newly synthesised IFN- γ was metabolised, or indeed that there was epigenetic or post-transcriptional modifications that prevented synthesis of IFN- γ .

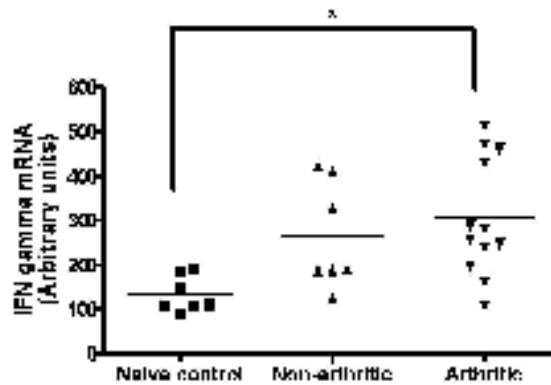


Figure 3.10 Changes in Th1 cytokine mRNA levels in brains of CII immunized mice
The dots represent mRNA expression levels of IFN- γ determined by real-time PCR in half brain tissue homogenate of naïve control mice (n=7 naïve control mice), non-arthritic mice (n=7 non-arthritic mice), and, arthritic mice (n=12 arthritic mice). The levels of mRNA were normalized to GAPDH expression and shown as arbitrary units. All mice were sacrificed and brains were collected on day 42. Data are presented as the mean values. (*P < 05 ; **P < 01; ***P < 001 by one-way ANOVA analysis) Bars represent the mean values.

3.2.4.3 Th-2 cytokines mRNA profiles in the brains of CII immunized mice (both arthritic mice and non-arthritic mice)

The mRNA of Th-2 cytokines, including IL-4, IL-5, IL-10 and IL-13 gene expression were determined in the brains of naïve control mice and CII immunized mice with and without arthritis. However, there was no transcription of these Th2 cytokines detected in the brain of mice from all experimental groups. Interestingly, Th2 cytokines including IL-5, IL-10 and IL-13 protein concentration were increased significantly in arthritic mouse brains compared to those in naïve control mice, while there was no significant mRNA expression levels detected in the same brains of these arthritic mice. These observations may suggest that the timing of induction and half-life of mRNA had finished while the protein was maintained, and/or transportation of these Th2 cytokine proteins from the periphery into the brains of arthritic mice.

3.2.4.4 Chemokine mRNA profiles in the brains of CII immunized mice (both arthritic mice and non-arthritic mice)

Expression levels of mRNA for CXCL1, CXCL10, CCL2 and CCL3 were determined in the brains of mice from all experimental groups. One-way ANOVA demonstrated that there were significant differences in protein concentration of CXCL1 and CXCL10 among the three groups of mice ($P = 0.0009$ and $P = 0.0002$ respectively) (Figure 3.11A and Figure 3.11B). Post hoc analysis with Bonferroni

correction demonstrated that CXCL1 and CXCL10 were increased significantly in brains of both arthritic and non-arthritic mice compared to those in naïve control mice. The mean values of CXCL1 (arthritic versus naïve control) was 3160 ± 828 versus 1212 ± 162 ($P < 0.001$). Similar to the protein profile, mRNA level of CXCL1 was also increased in non-arthritic mouse brains. The mean values of CXCL1 (non-arthritic versus naïve control) was 2818 ± 991 versus 1212 ± 162 ($P < 0.05$). There were no significant differences in brain CXCL1 gene expression levels between CIA and non-CIA mice (Figure 3.11A). The data suggest that there was local production of CXCL1 in the brains of CII immunized mice by CNS immune cells and peripheral immune cells trafficking into the brains. The possibility that there was also a transportation of CXCL1 protein into the brain of CII immunized mice was supported by the data showing the same CXCL1 protein profiles in serum of these CII immunized mice. Increases in serum CXCL1 protein concentration were observed in CII immunized mice as well as an increase in mRNA and protein concentration in their brains.

CXCL10 was another chemokine that was increased in the brains of CII immunized mice. The mean values of CXCL10 (arthritic versus naïve control) was 442 ± 150 versus 163 ± 35 ($P < 0.001$). The up-regulations of CXCL10 gene expression was also observed in brains of non-arthritic mice compared to those in naïve control mice. There were no significant differences in brain CXCL10 gene expression concentration between naïve control mice and non-arthritic mice. CXCL10 gene expression in arthritic mouse brains was significant higher than those in non-arthritic mouse brains. The mean values of CXCL10 (arthritic versus non-arthritic) was 442 ± 150 versus 283 ± 120 ($P < 0.05$) (Figure 3.11B). The significant higher level of CXCL10 in arthritic mice compared to those in non-arthritic mice suggests that the production of CXCL10 in the brain may be associated with peripheral joint inflammation in arthritic mice.

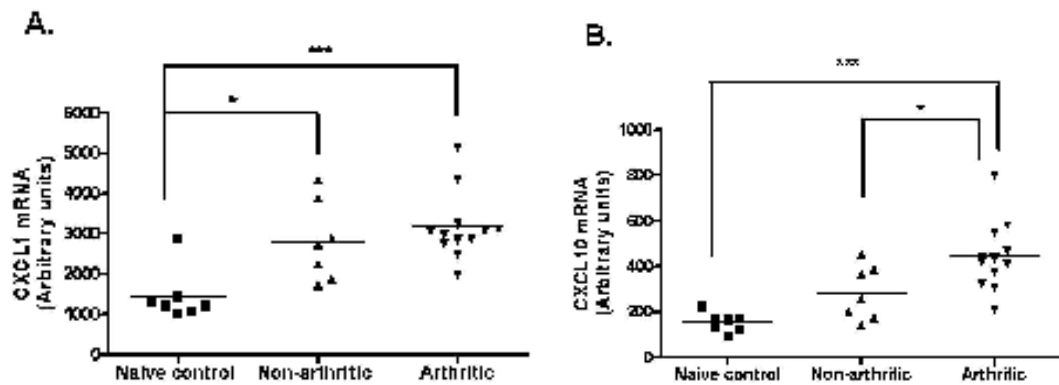


Figure 3.11 Changes in chemokine mRNA expression levels in brains of CII immunized mice. The dots represent mRNA levels of CXCL1 (A) and CXCL10 (B) determined by real-time PCR in half brain tissue homogenate of naïve control mice (n=7 naïve control mice), non-arthritic mice (n=7 non-arthritic mice), and, arthritic mice (n=12 arthritic mice). The levels of mRNA were normalized to GAPDH expression and shown as arbitrary units. All mice were sacrificed and brains were collected on day 42. Data are presented as the mean values. (* $P < 0.05$; ** $P < 0.01$; *** $P < 0.001$ by one-way ANOVA analysis) Bars represent the mean values.

3.2.4.5 Growth factor mRNA profiles in the brains of CIA mice

Growth factors such as FGF2 and VEGF were detectable in the brains of control mice and mice with and without arthritis. One-way ANOVA analysis showed that there was no significant difference in the gene expression level of FGF2, although the FGF2 protein concentration in arthritic mice was increased compared to the naïve control mice ($P = 0.4803$) (Figure 3.12A). The data suggest that there may be the transportation of FGF2 into the CNS in the arthritic mice during the course of the disease. One-way ANOVA analysis showed that there was no significant difference in brain VEGF between naïve control mice and CII immunized mice ($P = 0.0674$) (Figure 3.12B).

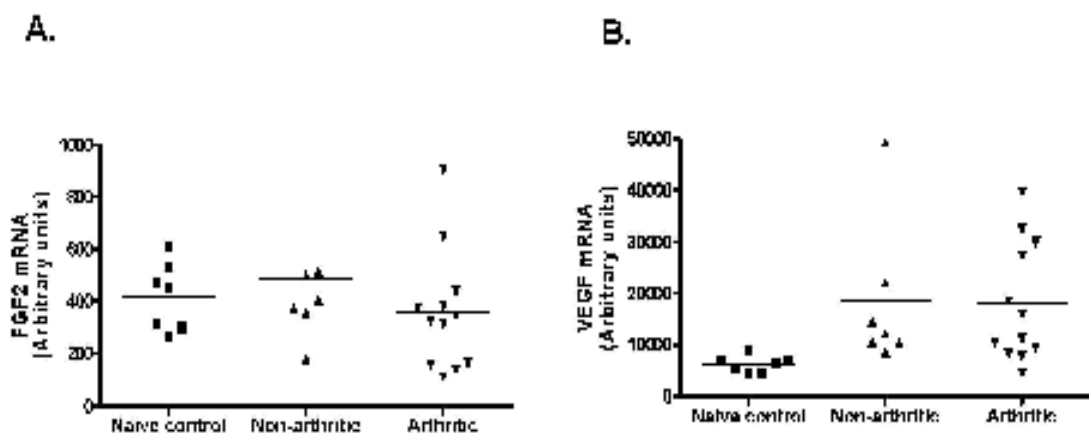


Figure 3.12 Changes in growth factor mRNA levels in brains of CII immunized mice. The dots represent mRNA levels of FGF2 (A) and VEGF (B) determined by real-time PCR in half brain tissue homogenate of naïve control mice (n=7 naïve control mice), non-arthritic mice (n=7 non-arthritic mice), and, arthritic mice (n=12 arthritic mice). The levels of mRNA were normalized to GAPDH expression and shown as arbitrary units. All mice were

sacrificed and brains were collected on day 42. Data are presented as the mean values. (*P < 05 ; **P < 01; ***P < 001 by one-way ANOVA analysis) Bars represent the mean values.

In summary: Real-time PCR detected increases in the Th1 cytokine (IFN- γ), chemokines (CXCL1 and CXCL10) and growth factors (FGF2 and VEGF) in brain tissue of mice from all experimental groups. Expression levels of IFN- γ , CXCL1, CXCL10 and VEGF were significantly increased in the brains of CII immunized mice (both arthritic and non-arthritic) compared to those in naïve control mice. Table 3.3 shows a summary of these data as mean \pm SD of fold changes of inflammatory mediator gene expression in brains of CII immunized mice (both arthritic and non-arthritic) in comparison to those in brains of naïve control mice. Data were categorized into 3 groups (a Th1 cytokine, chemokines and a growth factor). Our data showed that inflammatory mediator mRNA expression levels in brains of CII immunized mice were significantly increased from 1.7 - to 3.0 - fold compared with those in naïve control. Among these inflammatory mediators, the greatest mean fold increase was for the growth factor VEGF mRNA expression levels in brains of non-arthritic (3-fold) and arthritic (2.9-fold) mice. This also suggest that there was a similar degree of elevation of VEGF mRNA expression levels in brains of immunised and challenged mice irrespective of whether they developed frank arthritis. This observation was also seen for CXCL1 mRNA and protein concentration which were similar in both arthritic and non arthritic mouse brains, and both were higher than control mice. This suggests that there may be a biological association between gene expression and protein level in brains of CII immunized mice.

Inflammatory mediators genes	Arthritic		Non-arthritic	
	Fold changes of mRNA concentration	<i>P</i> value	Fold changes of mRNA concentration	<i>P</i> value
Th1 cytokines				
IFN- γ	2.2 \pm 3.0	< 0.05*	1.9 \pm 2.8	NS
Chemokines				
CXCL1	2.6 \pm 5.1	< 0.001***	2.3 \pm 6.1	< 0.05*
CXCL10	2.7 \pm 4.3	< 0.001***	1.7 \pm 3.4	NS
Growth factors				
VEGF	2.9 \pm 7.3	NS	3.0 \pm 9.0	NS
FGF2	1.8 \pm 0.9	NS	1.2 \pm 2.2	NS

Table 3.3 Summary of inflammatory mediator gene expression profiles in brains of CII immunized mice

Data was presented as mean \pm SD of fold changes of inflammatory mediator mRNA profiles in brains of CII immunized mice (both arthritic and non-arthritic) in comparison to those in brains of naïve control mice. One-way ANOVA analysis (**P* < 05 ; ***P* < 01; ****P* < 001) was used to demonstrate significant increase in inflammatory mediator mRNA expression levels in arthritic and non-arthritic mouse brain compared to those in control mouse brains. NS = not statistically significant.

3.2.5 Comparisons of gene and protein expression of inflammatory mediators in arthritic and non-arthritic mouse brains

In summary, our data demonstrated different profiles of inflammatory mediator gene and protein expression in arthritic mouse (arthritic mouse) brains and non-arthritic mouse brain (Table 3.4). Most of the inflammatory mediator proteins detectable by Luminex including IL-1 α , IL-2, IL-5, IL-10, IL-13, CXCL10, and FGF2 were increased significantly in arthritic mouse brains, while CXCL1 was the only inflammatory mediator that up-regulated significantly in both CIA and non-CIA mouse brains. By contrast, increases in inflammatory mediator mRNA, including IFN- γ , CXCL1, CXCL10, VEGF, were observed in both arthritic and non-arthritic mouse brains.

IL-2 protein was the only Th1 cytokine up-regulated in brains of arthritic mice compared to those in naïve control mice, while IFN- γ mRNA concentration were increased in brains of both arthritic and non-arthritic mice compared to those in

naïve control mice. There was no Th2 cytokine (IL-5, IL-10, IL-13) mRNA detectable in either arthritic and non-arthritic mouse brains, while protein concentration of these Th2 cytokines were significantly increased in brains of arthritic mice compared to those in naïve control mice. Interestingly, similar protein concentration and gene expression profiles of CXCL1 were observed in both arthritic and non-arthritic mouse brains. Similarly, CXCL10 gene and protein expressions were increased in both arthritic mouse brains. Differences between CXCL10 mRNA concentration of arthritic and non-arthritic mouse brains were also observed. In the category of growth factor, FGF2 protein was increased only in arthritic mouse brains, while elevations of VEGF mRNA were observed in both arthritic and non-arthritic mice.

Inflammatory Mediators	Protein and mRNA expression levels in brains of CII-immunized compared with naïve control mice.			
	Protein		mRNA	
	Arthritic	Non-arthritic	Arthritic	Non-arthritic
Pro-inflammatory cytokines				
IL-1 α	NS	NS	undetectable	undetectable
Th1 cytokines				
IL-2	< 0.05*	NS	undetectable	undetectable
IFN- γ	undetectable	undetectable	< 0.01**	NS
Th2 cytokines				
IL-5	< 0.05*	NS	undetectable	undetectable
IL-10	NS	NS	undetectable	undetectable
IL-13	< 0.05*	NS	undetectable	undetectable
Chemokines				
CXCL1	< 0.01**	0.05*	< 0.001***	< 0.05*
CXCL10	< 0.01**	NS	< 0.001***	NS
Growth factor				
FGF2	< 0.05*	NS	NS	NS
VEGF	NS	NS	NS	NS

Table 3.4 A summary of inflammatory mediator gene mRNA expression and protein profiles in arthritic mouse brains and non-arthritic mouse brains

Differences between inflammatory mediator concentration in immunized mouse brains (Arthritic/Non-arthritic mouse brains) and control groups were analyzed by Student's t-test (*P < 05 ; **P < 01; ***P < 001). NS = not statistically significant.

3.2.6 Correlations between chemokine mRNA and protein concentration in arthritic and non-arthritic mouse brains

Inflammatory mediator gene expression concentration measured by real-time PCR have been shown to correspond with protein concentration in several studies (Young et al., 2008); (Stemme et al., 2001). A study by Mehra *et al.*, suggest that the positive relationship between protein and mRNA concentration may reflect the post-transcription, post-translation and protein synthesis process within the tissue. Our data showed similar patterns of gene and protein profiles of CXCL1 and CXCL10 (Mehra et al., 2003). Particularly, both CXCL1 mRNA and protein concentration were increased in brains of both arthritic and non-arthritic mice. The relationship between protein and mRNA expression concentration of CXCL1 and CXCL10 within the same samples was examined using the Pearson's correlation coefficient analysis. However, there was no statistically significant correlation between their protein and mRNA expression within the same samples across all experimental groups (Figure 3.13A, Figure 3.13B, Figure 3.13C). The data suggest that CXCL1 and CXCL10 in brains of these CII immunized mice may not be produced locally in the brain. However, it is also possible that there were productions of CXCL1 and CXCL10 in the brain as well as transportation of these chemokines from the periphery.

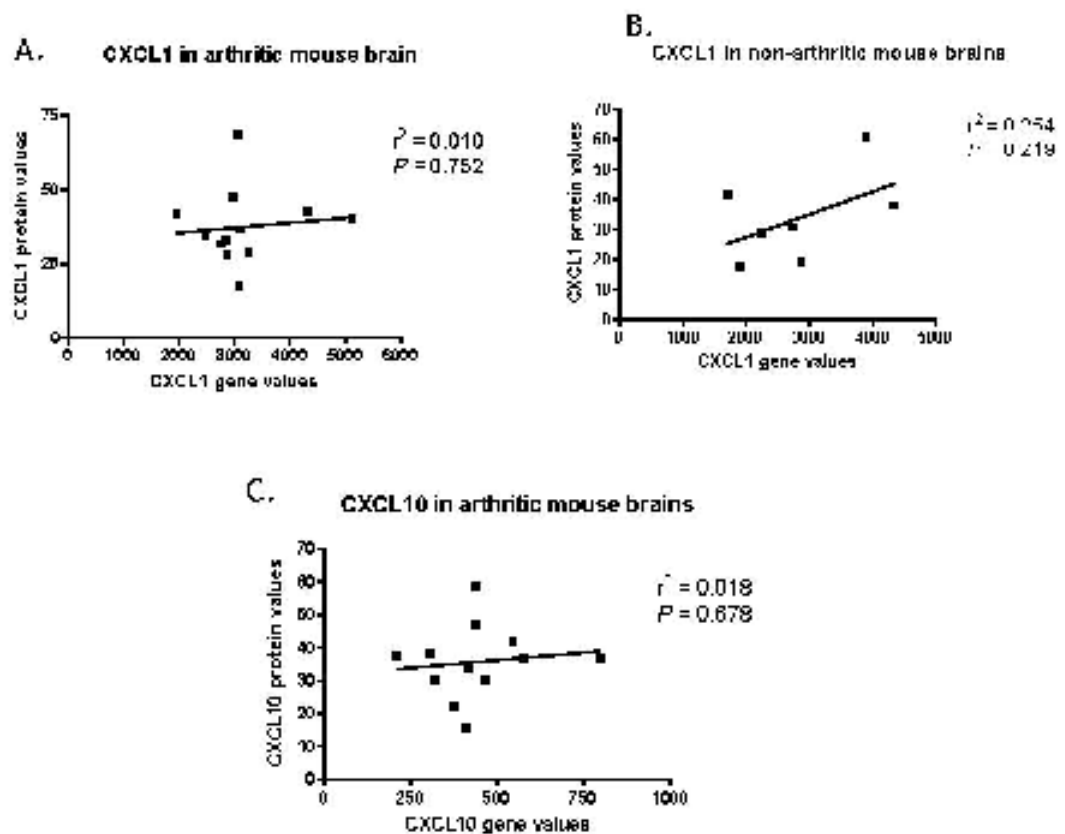


Figure 3.13 Correlations of mRNA and protein concentration for CXCL1 and CXCL10 in 12 arthritic and 7 non-arthritic mouse brains
 Dot plots show relationships between CXCL1 and CXCL10 mRNA (arbitrary units) and protein level (pg/ug total brain protein) within the samples from 12 arthritic and 7 non-arthritic group analysed by Pearson's correlation coefficient analysis. (A) shows the correlation between CXCL1 mRNA value and CXCL1 protein value for arthritic mouse brains ($r^2 = 0.010$, $P = 0.752$). (B) shows the correlation between CXCL1 mRNA value and CXCL1 protein value for non-arthritic mouse brains ($r^2 = 0.254$, $P = 0.249$). (C) shows the correlation between CXCL1 mRNA value and CXCL10 protein value for arthritic mouse brains ($r^2 = 0.01795$, $P = 0.678$).

3.2.7 *Correlations between inflammatory mediator protein concentration and mRNA expression levels and arthritis scores*

To determine whether the disease severity of the experimental arthritis was associated with up-regulation of brain inflammatory mediators in arthritic mice, brain inflammatory mediator protein and mRNA and the arthritis score of each arthritic mouse was compared using the Pearson's correlation coefficient analysis. None of the brain inflammatory mediator protein or mRNA levels correlated with arthritis scores in arthritic mice (Figure 3.14A-Figure 3.14D, Figure 3.15A-Figure 3.15H). It appeared that the mediator measurement at a single time point was not a good measure of clinical expression of this chronic disease.

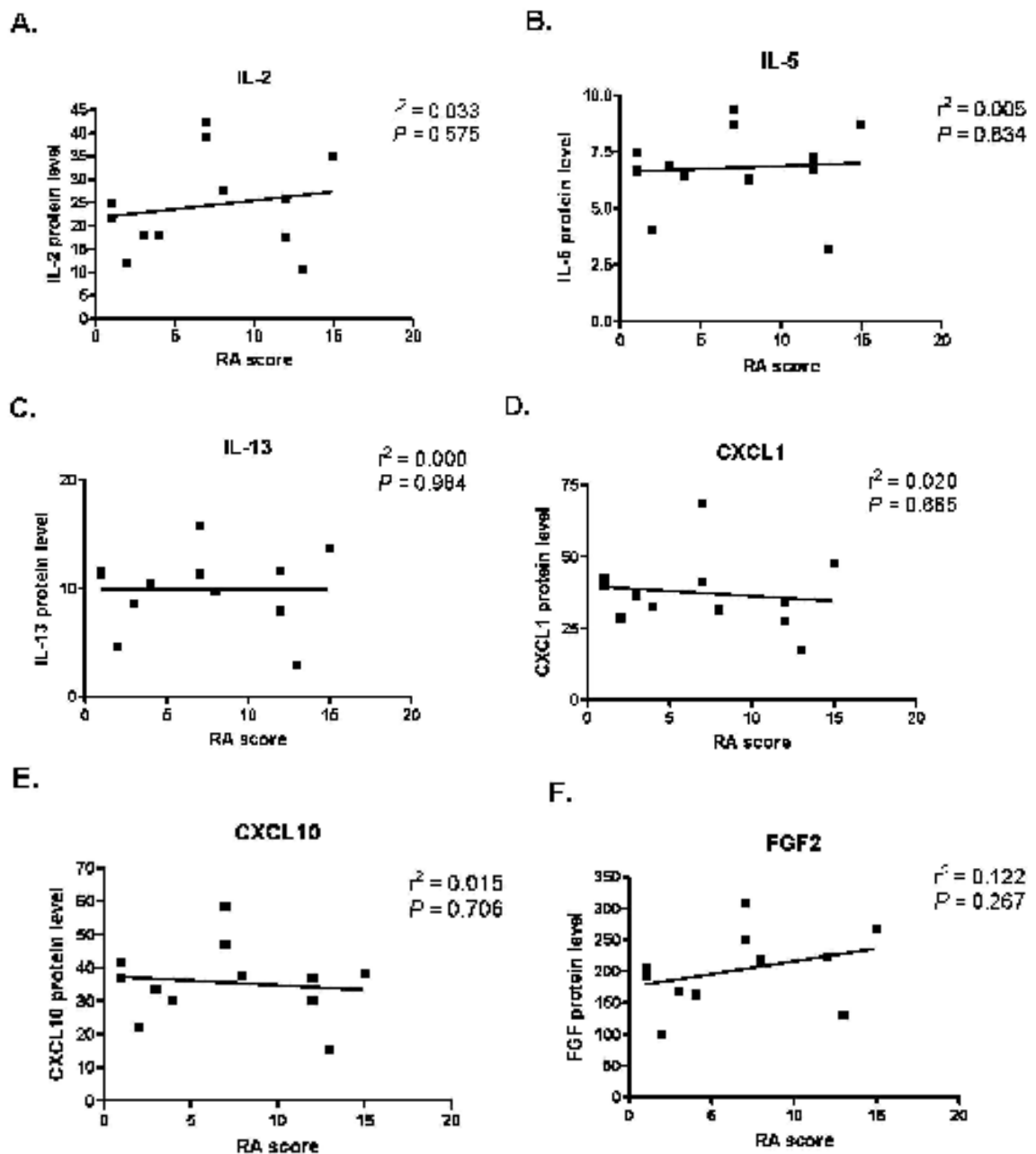


Figure 3.14 Correlations of inflammatory mediator protein concentration and arthritis score in 12 arthritic mice

Dot plots show relationships between brain inflammatory protein concentration (pg/μg total brain protein) and arthritis score within the samples from arthritic group (n = 12 arthritic mice) analysed by Pearson's correlation coefficient analysis. (A) shows the correlation between brain IL-2 protein value and arthritis scores in CIA mice ($r^2 = 0.033$, $P = 0.575$). (B) shows the correlation between brain IL-5 protein value and arthritis scores in arthritic mice ($r^2 = 0.005$, $P = 0.834$). (C) shows the correlation between brain IL-13 protein value and arthritis scores in arthritic mice ($r^2 = 0.000$, $P = 0.984$). (D) shows the correlation between brain CXCL1 protein value and arthritis scores in arthritic mice ($r^2 = 0.020$, $P = 0.665$). (E) shows the correlation between brain CXCL10 protein value and arthritis scores in arthritic mice ($r^2 = 0.015$, $P = 0.706$). (F) shows the correlation between brain FGF protein value and arthritis scores in arthritic mice ($r^2 = 0.122$, $P = 0.267$).

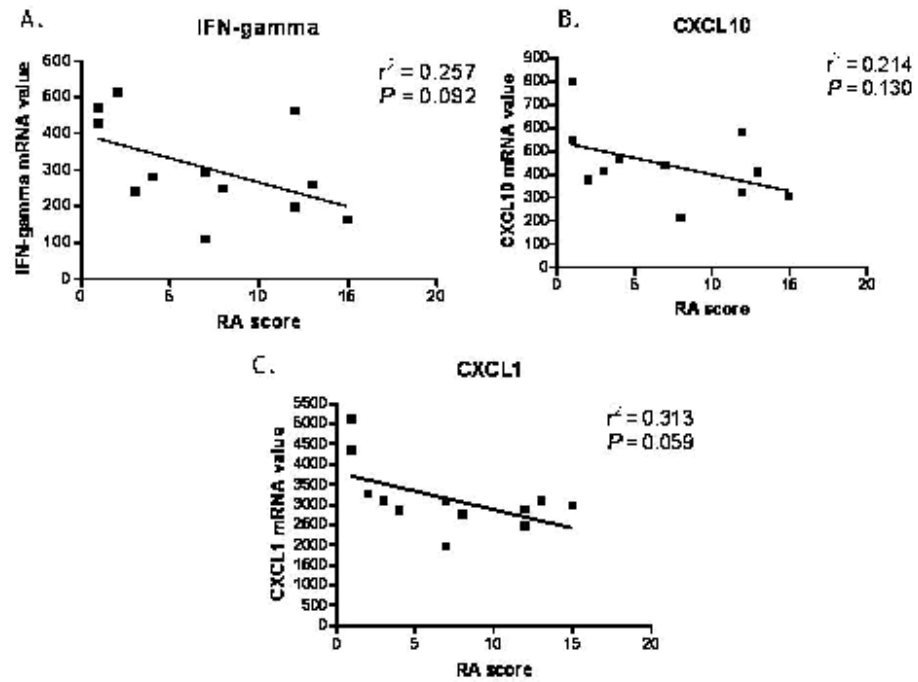


Figure 3.15 Correlations of inflammatory mediator gene expression levels and arthritis score in arthritic mice

Dot plots show relationships between brain inflammatory mediator mRNA (number of copies/GAPDH copies) and arthritis score within the samples from arthritic group ($n = 12$ arthritic mice) analysed by Pearson's correlation coefficient analysis. (A) shows the correlation between brain IFN- γ mRNA value and arthritis scores in arthritic mice ($r^2 = 0.257$, $P = 0.092$). (B) shows the correlation between brain CXCL10 mRNA value and arthritis scores in arthritic mice ($r^2 = 0.214$, $P = 0.130$). (C) shows the correlation between brain CXCL1 mRNA value and arthritis scores in arthritic mice ($r^2 = 0.313$, $P = 0.059$).

3.3 Result chapter 3; Summary of findings.

The aim of this chapter was to investigate the evidence for and the potential process of peripheral inflammation-induced-brain inflammation in an autoimmune disease model of RA. A Luminex bead-based assay and real-time PCR assays were used to explore changes in inflammatory mediator protein concentration and expression levels respectively in brains of CII immunized mice that may be involved in the process of immune or inflammatory response activation in the brain during arthritis. We found;

1. Increased concentrations of IL-2, IL-5, IL-13, CXCL1, CXCL10 and FGF2 protein in brains of CII immunized mice with arthritis compared to naïve control mice.
2. Increased concentration of serum CXCL1 protein in both arthritic and non-arthritic mice compared to naïve control mice.
3. CXCL1 was the only inflammatory mediator that was increased in brains of non-arthritic mice compared to naïve control mice.
4. Increased IFN- γ , CXCL1 and CXCL10 mRNA expression levels were observed in brains of both arthritic and non-arthritic mice compared to naïve control mice.
5. The patterns of serum CXCL1 protein concentration, brain CXCL1 mRNA expression levels and brain CXCL1 protein concentration of mice of all experimental groups were related.
6. There was a significant increase in CXCL10 mRNA expression level in arthritic compared with non-arthritic mouse brains.
7. The degrees of fold-increase compared to control mice of CXCL1 mRNA and protein concentration were similar in both arthritic and non-arthritic mouse brains.
8. There was no significant correlation between CXCL1 and CXCL10 gene and protein expression levels of both arthritic and non-arthritic brains.

9. There was no significant correlation between the brain inflammatory mediator mRNA and protein levels and the arthritis scores.

3.4 Discussion

For clarity, I will set out the discussion in logical sections interpreting the results in sequence. I will summarise and draw conclusions from these at the end.

3.4.1 *Elevations of inflammatory mediator mRNA and protein concentration in CII immunized mouse brains.*

In this chapter we have shown elevations of IL-1 α , IL-2, IL-5, IL-10, IL-13, CXCL1, CXCL10 and FGF2 protein and mRNA expression levels in brains of CII immunized mice, particularly in those CII immunized mice that developed arthritis. We also found increases in serum CXCL1 protein in these CII immunized mice. Compared with control healthy mice, our data suggest that peripheral inflammatory signal may be associated with the activation of an immune or inflammatory response in the brain during arthritis.

3.4.1.1 **Increased pro-inflammatory cytokine protein concentration in arthritic mouse brains**

Among the pro-inflammatory cytokines (IL-1 β , IL-1 α , IL-6 and TNF- α) investigated in brain tissue of both CII immunized and naïve control mice. The brain IL-1 α protein levels in arthritic mice seemed to be higher than those of naïve control mice on day 42. However, one-way ANOVA suggested that there was no significant difference in brain IL-1 α protein among all 3 groups (naïve control, non-arthritic and arthritic groups). This may reflect small sample numbers. Therefore, it is worthwhile to repeat these experiments using the larger numbers of animals.

IL-1 α is a potent pro-inflammatory cytokine produced by glial cells, macrophages and synovial fibroblasts. IL-1 α was found highly expressed in the inflamed synovia of RA patients (Brennan et al., 1989). The activities of IL-1 α also play a pathogenic role in rheumatoid arthritis, particularly in cartilage destruction (RA) (Dayer and Fenner, 1992). Transgenic mice over-expressing IL-1 α showed chronic synovitis and cartilage destruction, as a result of stimulation of matrix protein degrading enzymes; matrix metalloproteinase (MMP)-3 and MMP-13 produced by chondrocytes (Niki et al., 2004); (Rowan et al., 2003). Under physiological conditions, IL-1 (both IL-1 α and IL-1 β) is almost undetectable in the CNS.

However, after injury (e.g. stroke, haemorrhage, trauma), IL-1 family cytokines are produced by microglia, the resident brain immune cells (Luheshi et al., 2009). In experimental models, peripheral immune challenge results in increased production of IL-1 both peripherally and centrally (Higgins and Olschowka, 1991); (Quan et al., 1994); (Maness et al., 1998). Our data showed an increase of IL-1 α protein concentration in the brain of CII immunized mice that developed arthritis, but not non-arthritic mice and suggests that the local increase may be associated with the peripheral joint inflammation. The increase of IL-1 α protein concentration in brains of arthritic mice may also indicate an inflammatory process in brains of these mice during the course of arthritis disease. Our data also showed that there was no gene expression of IL-1 α detectable in brains of these arthritic mice despite significant amount of IL-1 α detectable in the same brains. This suggests that there may be the transportation of IL-1 α protein from the periphery to the brain. However, we found no serum IL-1 α in these arthritic mice therefore other possibilities are that IL-1 α may enter the brain via migration of peripheral immune cells into the brain during the course of the arthritis, or that IL-1 α is involved at another time-point. The question of how and when IL-1 α is localized and/or transported from the periphery into the brain is unresolved, especially since there was no significant serum IL-1 α detectable at that time point in these arthritic mice. This is an important and complex topic that needs further investigation. Useful experiments might include time-point experiments as outlined in results chapter 4.

3.4.1.2 Elevations of a Th1 cytokine protein and gene expression concentration in CII immunized mouse brains

RA is thought to be a Th1-cell driven disease, and Th1 (IL-2, IFN- γ and IL-12) cytokines may be part of the initiation of the destructive immune response in RA (McInnes and Schett, 2007). We found significant elevation of Th1 cytokine concentration in brains of arthritic mice. IL-2 protein concentration and IFN- γ were increased in CII immunized mice compared to those in the naïve control mice. It is possible that there is an association between the increases of these Th1 cytokines in the brains and the inflamed joints of these arthritic mice.

In systemic immune responses, IL-2 is produced by activated CD4⁺ T-cells and this augments the secretion of IFN- γ . IL-2 acts via the IL-2 receptor (CD25,

IL-2R) and functions in clonal expansion of antigen-primed T-cells (Schroeter and Jander, 2005). Increases in IL-2 protein concentration were detected in both synovial fluid and peripheral blood of RA patients (Berner et al., 2000). Importantly, it has been reported that IL-2 was also highly expressed in paws of arthritic mice (Thornton et al., 1999). We found increases in IL-2 protein concentration and it is possible that circulating IL-2 produced by inflamed joints and associated lymphoid organs migrate into the brains of these CII immunized mice. IL-2 can also be producible by microglia locally in the CNS (Sredni-Kenigsbuch, 2002). However, IL-2 gene expression was undetectable in brains of these arthritic mice, suggesting that IL-2 protein in arthritic mouse brains may be transported mainly from the periphery. However, we found no IL-2 protein level in serum these arthritic mice, suggesting that IL-2 protein may possibly enter the brain via trafficking of peripheral Th1 cells into the brain. The issue of when and how IL-2 enters the brain during the course of arthritis still remains unclear and needs further investigation.

IFN- γ is an important regulator that has been implicated in the pathology of RA and also found highly expressed in both synovial fluid and peripheral blood of RA patients (Canete et al., 2000). IFN- γ is produced by activated T cells and NK cells (Farrar and Schreiber, 1993). IFN- γ is usually undetectable in the CNS except in the context of inflammation, when immune cells cross the blood-brain barrier and enter the CNS (Millward et al., 2007). During the CNS inflammatory process, IFN- γ is produced by microglia and functions to amplifies the adaptive immune response in the CNS by activating astrocytes and microglia to express MHC class I and class II (Yang et al., 2004); (Wong et al., 1984). IFN- γ also plays an important role in leukocyte migration into the CNS via activation of chemokine production by astrocytes and microglia (Sredni-Kenigsbuch, 2002). Our data showed elevations of IFN- γ gene expression concentration in brain of CII immunized mice, suggesting that there may be the production of IFN- γ locally in the brain. The increased level of IFN- γ mRNA concentration in brains of these CII immunized mice may also indicate the CNS inflammatory process and immune cell migration into the brains of these CII immunized mice. However, the mechanism of how IFN- γ gene expression was induced and the cellular source of IFN- γ in the brain of these CII immunized mice are still unclear. This may be associated with the elevations of IL-2 protein that also function to enhance the

expression of IFN- γ in Th1 cells (Schroeter and Jander, 2005). This question can be addressed by using immunohistochemistry of both IL-2 protein and markers for Th1 or/and microglia to investigate the co-localization of IL-2 with these immune cells in brain sections of CII immunized mice.

3.4.1.3 Elevations of a Th2 cytokine protein and gene expression concentration in arthritic mouse brains

Th2 cytokines such as IL-4, IL-5 and IL-13 play crucial roles in humoral immunity such as regulating B lymphocytes to mature to plasma cells and to stimulating immunoglobulin class switching from IgM to IgE and IgG1 (in mouse) or IgG4 (in man) isotypes (Schulze-Koops and Kalden, 2001). Anti-inflammatory cytokines produced by Th2 such as IL-4 and IL-10 also function to inhibit Th1 proliferation, prevent autoimmunity, synovial inflammation and tissue destruction in RA (Schulze-Koops and Kalden, 2001). Both clinical and animal studies demonstrated that Th2 cytokines were expressed in a low level in synovial fluid of RA patients and in draining lymph node cells during the onset, and the highest severity phase of the disease (Kusaba et al., 1998); (Mauri et al., 1996). Our data showed the up-regulation of IL-5, IL-13 and IL-10 protein concentration, but not gene expression, in arthritic mouse brains compared to those in the control mouse brains.

IL-5 and/or IL-13 play an important role in allergic asthma and helminthic infection (Kurowska-Stolarska et al., 2008). IL-5 is produced mainly by Th2 cells and mast cells (Gregory et al., 2003), while IL-13 is produced by T cells, mast cells, basophils, dendritic cells, and keratinocytes (Schmid-Grendelmeier et al., 2002). However, little is known about the role of IL-5 and IL-13 in pathogenesis and immune responses of RA. IL-5 and IL-13 expression has been reported in synovial tissues of RA patients. A study by Xu *et al.*, in CIA model suggest that IL-5 and IL-13 exacerbate the severity of arthritis disease by promoting the production of specific IgG and IgE synthesis by B cells and antibody isotype switching in CIA. These antibodies then could bind to Fc receptors on mast cells and subsequently activate mast cell degranulation or/and form immune complex with antigen (Xu et al., 2008). Although IL-5 and IL-13 could also be produced by microglia and astrocytes in the brain (Sawada et al., 1993); (Shin et al., 2004), we found no gene expression of either IL-5 or IL-13 in brains of arthritic mice.

This suggests that there was no local production of these Th2 cytokine in the brain. In addition, elevations of both IL-5 and IL-13 were observed only in CII immunized mice with arthritis, suggesting that IL-5 and IL-13 may be transported from the periphery to the brain during the course of RA. However, the issue of whether IL-13 and IL-5 are transported to the brain by themselves or via the peripheral Th2 trafficking into the brain need further investigations.

The brain IL-10 protein levels in arthritic mice seemed to be higher than those of naïve control mice on day 42. However, one-way ANOVA suggested that there was no significant difference in brain IL-10 protein among all 3 groups (naïve control, non-arthritic and arthritic groups). This may reflect a small sample number. Therefore, it is worthwhile to repeat these experiments using the larger numbers of animals.

IL-10 predominantly an anti-inflammatory cytokine that is produced by monocytes, T cells, B cells, DCs, epithelial cells (McInnes and Schett, 2007). IL-10 could inhibit the production of Th1 cytokine such as IFN- γ (Rizzo et al., 1998). CIA mice receiving neutralizing anti-IL-10 antibodies demonstrated a delay of the onset and an increase in the severity of arthritis (Kasama et al., 1995). In the CNS, IL-10 is produced by microglia and astrocytes and also plays a potent anti-inflammatory and neuroprotective role in several CNS diseases (Schroeter and Jander, 2005). Increases in IL-10 protein concentration were observed in brains of arthritic mice, but no gene expression detectable. This suggests that there may be a transportation of IL-10 from the periphery into the brain of these arthritic mice. It has been reported that the protein concentration of IL-10 were elevated in the lymph nodes of CII immunized mice transiently 3 day after immunization and the low concentration of IL-10 protein were detectable throughout the time of clinical manifestation (Mauri et al., 1996). We could not detect serum IL-10 in the arthritic mice and we determined the brain IL-10 protein level in these mice at only one time point (day 42 after immunization). It is also possible that the transportation and the accumulation of IL-10 protein may occur at the earlier time point throughout 42 day of experimental period. Therefore, conducting time point experiment to investigate overtime changes of brain inflammatory mediators in brains of CII immunized mice would be useful to test this hypothesis.

3.4.1.4 Elevations of a chemokine protein and gene expression concentration in CII immunized mouse brains

Chemokines are a group of inflammatory mediator that function to regulate recruitment of leukocytes and angiogenesis in the inflammatory process (Koch, 2005). In RA, synovial fibroblasts produce chemokine, which function to attract leukocytes into the synovial tissue (Koch, 2005). In our study, we found elevations of CXCL1 and CXCL10 protein and gene concentration in brains of CII immunized mice (both arthritic and non-arthritic mice). Our data may indicate the recruitment of immune cells into the brain of CII immunized mice.

CXCL1 functions as a potent neutrophil chemo-attractant by binding both CXCR1 and CXCR2 receptors (Luttichau, 2010). CXCL1 have been reported in osteoblasts and synovial fluid from rheumatoid arthritis patients (Lisignoli et al., 1999), (Bischoff et al., 2005). An administration of CXCL1 antibody has shown to delay the onset and reduce in the disease severity of CIA mice (Kasama et al., 1995). We found the up-regulation of CXCL1 protein in serum of CII immunized mice. Our data are consistent with a study by Kurowska-Stolarska *et al* showing the increase concentration of serum CXCL1 in CIA mice (data are in press PNAS). Interestingly, the serum CXCL1 protein profiles of these CII immunized mice were similar to brain CXCL1 protein profiles for both arthritic and non-arthritic mice. These data suggest that there may be transportation of CXCL1 from the periphery into the brain of these CII immunized mice. We also found up-regulation CXCL1 gene expression in these CII immunized mice, suggesting that there was also the local production of CXCL1 in the brain of these CII immunized mice. Interestingly, degrees of fold elevations of brain CXCL1 mRNA and protein concentration were quite similar for both arthritic and non-arthritic mice. This seems pretty convincing evidence suggest that both brain CXCL1 protein and gene could be generated locally within the CNS and by the same cellular source. However, we found no significant correlation between mRNA and protein concentration of brain CXCL1 in CII immunized mice. Therefore we cannot conclude from our data set about the location and the cellular source of the CXCL1 production in brains of these CII immunized mice. Microglia and astrocytes are the major source of CXCL1 in the brain and it has been demonstrated that the induction of peripheral inflammation by LPS could induce microglia activation and the production of CXCL1 in the brain (Brown et al.,

2010). CXCL1 was transiently expressed at circumventricular organs (CVOs), which are exceptional areas in the brain that are not covered by BBB, after the peripheral LPS induction (Reyes et al., 2003). On the other hand CXCL1 can be produced inside the brain during the neuroinflammatory process such as encephalomyelitis (Rubio and Sanz-Rodriguez, 2007) or injury via IL-1 β signalling, leading to the infiltration of neutrophils into the brain (McColl et al., 2007). The elevations of CXCL1 may indicate leukocyte infiltration into the brains of CII immunized mice. However, the location, cellular source of brain CXCL1 and the relationship between peripheral CXCL and brain CXCL1 need further investigation.

CXCL10 functions as a potent T-lymphocyte recruiter by binding into the receptor CXCR3, preferentially on the Th1-lymphocyte subset. In RA, CXCL10 induced CCL5 expression in CD4⁺ T cells, which promote bone resorption by inducing osteoclast formation and survival (Lee et al., 2009). The up-regulation of CXCL10 has been reported in serum and inflamed joints of CIA mice sacrificed on day 42 (Kwak et al., 2008). CXCL10 has also been implicated in pathogenesis of neuroinflammatory diseases. CXCL10 and its receptor, CXCR3, are highly expressed by the CNS and by CNS infiltrating lymphocytes, respectively, only in patients with ongoing CNS inflammation such as viral encephalitis and multiple sclerosis (Klein, 2004). The pathological mechanism of these neuroinflammatory diseases involves the infiltration of leukocytes into the CNS and CXCL10 has been reported to regulate peripheral Th1 infiltration into the CNS during these neuroinflammatory diseases (Klein, 2004). Therefore, the elevations of both CXCL10 gene and protein concentration in brains of CII immunized mice could be an important indicator of the presence of neuro-inflammation that may/may not associated with the peripheral joint inflammation. Interestingly, elevations of CXCL10 protein were only observed in brains of CII mice with arthritis and there were differences in CXCL10 mRNA concentration between arthritic and non-arthritic mice. These observations in our study may suggest that the elevations of brain CXCL10 in arthritic mice may be associated with Th1 infiltration from the peripheral inflammatory joints into the brains. This hypothesis is supported by a study in CIA model showing that non-arthritic mice showed a significant deficiency in T cell responses and significantly lower concentration of anti-CII Abs after the secondary challenge compared to mice that developed arthritis

(Pan et al., 2004). Another interesting observation is that there were increases in CXCL10 mRNA concentration in non-arthritic mouse, but no CXCL10 detectable in the same mouse brains. This suggests that there was a local production of CXCL10 in the brain of non-arthritic mice. It has been reported that the induction of CXCL10 gene expression in the brain depends on IFN- γ (Carter et al., 2007). Therefore, it is possible that elevations of CXCL10 mRNA concentration may be associated with elevations of IFN- γ mRNA concentration observed in non-arthritic mouse brain. It is also possible that the pathway of brain CXCL10 production in non-arthritic mice is different from those in arthritic mice. This is because the peripheral administration of CFA can also cause microglia activation and cytokine production in the CNS (Raghavendra et al., 2004). Therefore, CII immunized mice received CFA that did not develop arthritis could also induce the production of brain cytokines/chemokines without migration of immune cells and cytokines/chemokines from inflamed joint to the brain.

3.4.1.5 Elevations of a growth factor protein and gene expression concentration in CII immunized mouse brains

We also found elevations of FGF2 protein concentration in brains of arthritic mice and elevations of VEGF mRNA concentration in both arthritic and non-arthritic mice. The elevations of these angiogenic factors may indicate changes in BBB properties that occurred during the systemic joint inflammatory process.

Fibroblast growth factor 2 is a wide-spectrum mitogenic, angiogenic, and neurotrophic factor that bind to FGFR (FGF receptors and regulates various biological processes, including embryogenesis, wound healing, angiogenesis, and maintenance of neuronal networks (Manfe et al., 2010). In RA, FGF2 is produced mainly by endothelial cells and fibroblast; predominantly at the sites of chronic inflammation (Malemud, 2007). Elevation of FGF2 was observed in the synovial tissue of patients with RA (Thomas et al., 2000), and this worsened the joint inflammation in CIA rats (Yamashita et al., 2002). FGF2 play a crucial role in the final step of osteoclastic bone resorption in rheumatoid arthritis joint destruction that is preceded by recruitment and differentiation of osteoclasts by other factors (Chikazu et al., 2000). FGF2 also play a role in angiogenesis and recruitment of the immune cell into the inflamed site (Malemud, 2007). An *in*

vivo study showed that FGF2 synergistically enhanced the recruitment of monocytes, T cells and PMNs in response to a variety of inflammatory mediators, including IFN- γ , TNF- α and CCL-2. FGF2 also enhanced leukocyte recruitment to sites of inflammation by inducing endothelial adhesion molecule expression such as ICAM-1 and integrins (Zittermann and Issekutz, 2006). We found elevations of FGF2 protein in brains of arthritic mice, but no FGF2 gene expression detectable in the same brain, suggesting that there may be the contribution of FGF2 from the peripheral inflamed joint into the brain. However, we could not detect FGF2 protein concentration in these arthritic mice but the concentrations were not different from those in naïve control mice. Therefore, we cannot conclude from our experiment about the location and cellular source of FGF2 in the brains of these arthritic mice. One reason is that we only investigated the expression of the protein concentration at one time point on day 42, it is possible the contribution of FGF2 from the periphery into the brains of arthritic mice may occur at the earlier time point. Therefore, it is important to investigate changes of these brain inflammatory mediators in other time point throughout experimental time period.

The brain VEGF protein levels in arthritic mice seemed to be higher than those of naïve control mice on day 42. However, one-way ANOVA suggested that there was no significant difference in brain VEGF protein among all 3 groups (naïve control, non-arthritic and arthritic groups). This may reflect a small sample number. Therefore, it is worthwhile to repeat these experiments using the larger numbers of animals.

VEGF and its receptor VEGFr play a crucial role in angiogenesis process in RA because the pannus formation in RA requires neovascularisation that regulate mainly by VEGF. VEGF was highly expressed by RA synovium (Nagashima et al., 1995) and also thought to play an important role in the chronic edema and swelling in arthritis joint (Malemud, 2007). We found elevations of VEGF mRNA in both arthritic and non-arthritic mice, but there was no VEGF protein detectable in brains of these CII immunized mice. This suggests that they may be the local production in the brains. However, the mechanism of how VEGF mRNA expression was induced in the brains of these CII immunized mice is still unclear. One possibility is that FGF2 also has an autocrine effect on angiogenesis by inducing vascular endothelial growth factor (VEGF) in endothelial cells (Seghezzi

et al., 1998). Therefore, the increased VEGF gene expression in arthritic mouse brains could be associated with the up-regulation of FGF protein level. We could not address the question of why VEGF mRNA concentrations were increased in non-arthritic mouse brain. One possible explanation is that VEGF is also an angiogenic factor that enhance BBB permeability, and BBB disruption is observed in several models of neuroinflammation such as EAE and viral encephalomyelitis models (Kirk and Karlik, 2003); (Sasaki et al., 2010). The up-regulations of VEGF mRNA concentration in CII immunized mouse brains could be an indicator of BBB breakdown in this model. The BBB breakdown in the brain is often followed by the infiltration of leukocyte into the brain. The administration of VEGF into mouse brains result in breakdown of the blood-brain barrier, leukocyte recruitment into the brain (Croll et al., 2004b). Therefore, the up-regulation of VEGF mRNA concentration in brains of non-immunized mice may be associated with the increases in CXCL1 and CXCL10 that may function to regulate peripheral leukocyte recruitment into the brain.

In this study, we demonstrated increases of various inflammatory mediators, including IL-1 α , IL-2, IFN- γ , IL-5, IL-10, IL-13, CXCL1, CXCL10 and FGF2 in brains of CII immunized mice. However, we could not detect some inflammatory such as IL-1 cytokines, including IL-1 β , TNF- α and IL-6, that have been reported to be increase in the CNS of mouse models of RA (Bao et al., 2001); (del Rey et al., 2008). A study by Boa *et al.*, reported elevations of both protein and mRNA concentration of these pro-inflammatory cytokines (IL-1 β , TNF- α and IL-6) in spinal cord of AIA mice (Adjuvant-induced arthritis model) (Bao et al., 2001). Differences in the procedure for inducing arthritis and immunopathogenesis may account for contradictory results from the literature. Adjuvant induced arthritis (AIA) is an arthritis model, induced by a single intradermal injection of complete Freund's adjuvant (CFA) consisting of heat-killed *Mycobacterium tuberculosis* (Mt) and incomplete Freund's adjuvant (IFA) (Hossain et al., 2001). Polyarthritis rapidly develops around 10 days after immunization using adjuvant and the whole course of the disease lasts for 21 days (Bendele, 2001). In addition, the AIA model is Th1-cell and neutrophil dependent, and complement-independent. There is no evidence demonstrating that B-cells play a role in the pathogenesis of AIA. By contrast, the immune response of CIA involves both CII-specific T-cells and B-cells, which produce antibodies to type II collagen. The differences in the

immunopathological mechanism of both arthritic models may cause different peripheral inflammatory mediator profiles, which may result in different brain inflammatory mediator expression patterns. For example, TNF- α , IFN- γ , IL-1, IL-6, and IL-17A are dominant in the periphery of AIA model, while several pro- and anti-inflammatory cytokines, including TNF- α and IL-1 β , IL-6, IL-12, IL-1Ra, IL-10 and TGF- β , are highly expressed in the periphery of mice with CIA (Hegen et al., 2008). In addition, time course studies of inflammatory mediator expressions in peripheral tissue (paws and lymph nodes) of CIA mouse model reveal increases of different cytokines/chemokines expressions at different time points (Thornton et al., 1999);(Rioja et al., 2004);(Mauri et al., 1996). A study by Mauri *et al.*, show increases of IL-10, IFN- γ and TNF- α in the culture lymph node of CIA mice between day 3 - day 6 after immunization (Mauri et al., 1996). Another study by Rioja *et al* showed transient increases of IL-1 β and IL-6 mRNA and protein concentration in paws of arthritic mice during the first 4 days after immunization, while the prolonged expression of TNF- α mRNA and protein concentration throughout 15 days after immunization (Rioja et al., 2004). Another study by Thornton et al., demonstrated different cytokine expression patterns in paws of CIA mice. Transient increases in IL-2, IL-6 and TNF- α mRNA were observed during the early disease stage (day 21-day 28 after immunization), while CXCL2 and IL-1 β mRNA concentration were increased later during day 35 after immunization (Rioja et al., 2004). These evidence suggest the possibility that the contribution of inflammatory mediators from inflamed joint to the brain could be manifested at anytime throughout the experimental course. In this chapter, we only determined brain inflammatory mediator concentration in brain of CII immunized on the final day of the experimental course on day 42. Therefore, we hypothesized that some cytokines, particularly pro-inflammatory cytokines IL-1 β , TNF- α , IL-6 that we could not detect in CII-immunized mouse brain at this time point, may be up-regulated at earlier time point. This hypothesis is supported by a recent data showing the transient elevations of IL-1 β mRNA concentration during first 10 days after immunization and elevations of IL-6 mRNA concentration during early stage of arthritis disease in CIA rat brains (day 20 - day 30 after immunization) (del Rey et al., 2008). In addition, experimental evidence showing the elevations of cytokine/chemokine expression in paws of CIA mice during the early time point of CIA experimental course (Rioja et al., 2004) and (Thornton et al., 1999) can also explain our

observation of disassociation between arthritic scores and brain inflammatory mediator concentration in arthritic mice in our study. It is possible that peripheral joint inflammation may involve production of brain inflammatory mediators at earlier time point in the CIA experimental course, but the elevations of these inflammatory mediator concentration observed in these arthritic mice at late time point of the CIA experimental course (day 42) may be generated from local cellular sources in the brain. Therefore, time course experiment of inflammatory mediator expressions in brains of CII-immunized mice is essential for further investigations of brain-immune system-joint communication.

In summary: this chapter we demonstrated elevations of various inflammatory mediators, including IL-1 α , IL-2, IFN- γ , IL-5, IL-10, IL-13, CXCL1, CXCL10, FGF2 in brains of CII immunized mice, which may indicate the immune activation and inflammatory process in the brains of CII immunized mice. However, our data raised several questions; (i) how these inflammatory mediators access from the periphery into the brain, (ii) when these inflammatory mediators access from the periphery into the brain, (iii) what cellular sources of these inflammatory mediators in the brain, (iv) how peripheral joint inflammation signals CNS immune cells to produce these inflammatory mediators in the brain. In an attempt to address these questions, in the next chapter, we conducted time course experiment of inflammatory mediator expressions in brains of CII-immunized mice. This was to investigate the association between arthritis disease development and overtime changes in inflammatory mediator concentration in brains of CII-immunized mice, which may indicate brain-immune system-joint communication in this model.

Chapter 4

Time-course changes in inflammatory mediator concentrations in the brain and serum during collagen II-induced experimental arthritis

4.1 Introduction and aims

In the previous results chapter (Chapter 3), we showed increased concentrations of inflammatory mediator mRNA and protein, including IL- α , IL-2, IL-5, IL-10, IL-13, CXCL1, CXCL10, FGF2 and VEGF in brains of mice immunized with collagen II in Freund's adjuvant; particularly in those mice that subsequently developed arthritis. However, we could not demonstrate a clear association between the increased concentrations of these brain inflammatory mediators and peripheral joint inflammation as indicated by the lack of association between the arthritis scores and the concentrations of the inflammatory mediators in the brains. In addition, we could not detect some cytokines such as IL-1 β , TNF- α and IL-6, that have been reported to be elevated in the CNS of arthritic mice (Bao et al., 2001). One reason for that may have been because we only determined brain inflammatory mediator expression mice at only one time point on day 42; which was the final day of the experimental course of the collagen induced arthritis (CIA) model. Therefore, the aim of this chapter was to determine the changes in brain inflammatory mediators at other time points during the development of experimental arthritis to investigate potential pathological pathways of how peripheral joint inflammation might signal to the brain to increase synthesis of inflammatory mediators.

Background: Collagen induced arthritis (CIA) in mice is considered to be a disease model of chronic inflammatory arthritis (Luross and Williams, 2001). In this model longitudinal changes in cytokine concentrations are found in peripheral tissues including the joints and lymph nodes following initial sensitisation with collagen (Rioja et al., 2004). Several studies investigated a cytokine expression cascade in the progression of RA by measuring cytokine expression in the peripheral tissues at different time points throughout the CIA experimental course (Thornton et al., 1999); (Rioja et al., 2004); (Mauri et al., 1996). These studies often divided the CIA experimental course into several phases such as the acute phase (onset phase) and the chronic phase (Geng et al., 2008); (Mauri et al., 1996), and investigated longitudinal changes in cytokine patterns at different phases of the course of experimental disease. The acute phase (onset phase) occurs after immunization and is characterized by rapid disease progression (Mauri et al., 1996). The chronic phase of the disease course is characterized by erosion of cartilage but the disease progression becomes

slower than during the acute (onset) phase (Geng et al., 2008). Studies suggest that different cytokine expression patterns that occur during these different phases are associated with differences in pathological stages of arthritis. A study by Thornton *et al.*, showed that elevation of IL-2, IL-1 β and CXCL2 mRNA in the paws may be associated with more leukocyte and neutrophil infiltration into the paw during the onset of disease. In contrast, TGF- β may be associated with increased fibrosis and the number of fibroblast/macrophage type cells in the paw during the chronic stage (Thornton et al., 1999). In addition, accumulating evidence also showed the contribution of different cytokines in different peripheral tissues at different phases of disease. For example, Th1 cytokines such as IL-12 and IFN- γ are predominately expressed in lymph nodes and the spleen and in the peritoneal cavity during the acute phase (onset phase). In contrast, IFN- γ is expressed for a limited period around the time of disease onset in the joint, but prolonged expression of IL-1, IL-10, TNF- α , TGF- β and IL-6 are detected in the joint during the chronic phase (Okamoto et al., 2000); (Stasiuk et al., 1996); (Mussener et al., 1997). If there is a contribution of inflammatory mediators from the peripheral inflamed tissues (joints and lymph nodes) into the brain in the CIA model, then the longitudinal changes in brain inflammatory mediators should correspond or be associated with longitudinal changes in peripheral inflammatory mediators throughout CIA experimental course. This hypothesis is supported by a study by del Rey *et al* showing that the longitudinal change in brain IL- β mRNA concentrations corresponded to the longitudinal change in IL- β protein in lymph nodes in CIA rats (del Rey et al., 2008) .

Based on this evidence, we hypothesized that there may be longitudinal changes in brain inflammatory mediators associated with peripheral inflammatory mediator changes throughout the progression of disease in CII immunized arthritis mice. The aims of this chapter are:-

- (i) To determine changes in inflammatory mediators in brains of CII immunized mice at different time points.
- (ii) To determine changes in peripheral inflammatory mediators at different time points by measuring inflammatory mediator protein concentrations in the serum of CII immunized mice.

The data obtained from this time-course experiment may provide the additional evidence of how peripheral joint inflammation signals to the brain to produce local inflammatory mediators. In addition, the results from this experiment may also provide interesting insights into up- and down-regulation of the brain cytokine network, which may reflect the biological interplay and the local cellular sources of brain inflammatory mediators over the course of arthritis disease.

4.2 Results

4.2.1 Induction of arthritis in DBA1 mice

In the type-II collagen-induced arthritis model, the disease progression always develops from the acute phase into the chronic phase (Ohmachi et al., 2002). Several studies suggest that the CIA experimental course can be divided into several phases; (i) disease onset period, where CII immunized mice started to develop disease; (ii) acute phase period, where arthritis disease severity and disease progression increase rapidly, (iii) chronic or transition to chronic phase, where arthritis disease severity and disease progression increases slower than the last period but the paw swelling and the cartilage erosion are still manifest (Geng et al., 2008). A report by Ferraccioli *et al.*, divided the CIA experimental period into 2 phases after the secondary immunization (or boosting). The early disease was defined as occurring on days 12-15 after day 21 (corresponding to the first clinical signs of joint swelling). The late disease phase was defined as days 23-25 after boosting (corresponding to the maximum clinical signs of joint swelling) (Ferraccioli et al., 2010). Based on mean arthritis score, mean paw thickness and %incidence of arthritis in CII immunized mice of the previous chapter (Chapter 3; section 3.2.1), all of the CII immunized mice started to show signs of arthritis during day 22-day 28, therefore we considered this period as a disease onset period. Arthritis disease severity and disease progression in the CII immunized mice increased dramatically during day 28-day 35, we therefore considered this period as early disease phase. We considered that last stage of CIA experimental course (day 35-day 42 after immunization) as a late disease phase since most of CII immunized mice developed paw swelling slower than the last period and paw swelling in some of the mice stopped or decreased.

Several studies have reported the increases in inflammatory mediators, including IL-2, IL-6, TNF- α , CXCL1 and IL-10 in peripheral tissue such as paws and lymph nodes of CIA animals at both early and late stages of the experimental course of CIA (day 22- to day 42) (Thornton et al., 1999);(Rioja et al., 2004);(Mauri et al., 1996). These suggest the possibility that the contribution of inflammatory mediators from peripheral inflamed tissues (paws and lymph node) to the brain could be manifested at anytime during the stage of disease progression. We hypothesized that some cytokines, particularly pro-inflammatory cytokines IL-

1β , $\text{TNF-}\alpha$, IL-6 that we could not detect in CII immunized mice on day 42, may be detectable in earlier time points throughout the stage of disease progression (day 22 -day 42). This hypothesis is supported by a study showing up regulation of IL- 1α , IL-6 and $\text{TNF-}\alpha$ in CNS tissue of arthritis rats on day 21 (Bao et al., 2001). Based on this evidence and hypothesis, we measured the expression of inflammatory mediators in brains of CII immunized mice in 4 appropriate time points after immunization; throughout both early and late stages of disease progression. We started on day 22 after immunization because day 22 is considered to be the time point of the RA disease onset in this experimental arthritis model.

In this chapter, we randomly divided CII immunized mice into 4 groups (n=6 each), which were culled on days 22, 28, 35 and 42 respectively. 24 DBA1 mice were immunized by intradermal injection of type II collagen in Freund's complete adjuvant on day 0, and rechallenged by intraperitoneal injection of collagen II in PBS on day 21 and then culled at different time points (days 22, 28, 35, 42) throughout the disease course. The signs of arthritis in CII immunized mice were monitored from day 16 after immunization onwards and arthritis severity in this experiment were verified independently by Mr. Maurice Dixon. 4 groups (6 mice per group) of sex- and age-matched untreated non-immunized DBA1 mice were used as antigen-naïve control groups, which were also culled on days 22, 28, 35, 42. Serum and brains of all experimental groups of mice were harvested and snap-frozen in liquid nitrogen and stored at -80°C . Half of each brain was processed for protein extraction and inflammatory mediator protein analysis by luminex; the other half was processed for RNA extraction and the inflammatory mediator gene expression was determined by real-time PCR (Figure 4.1).

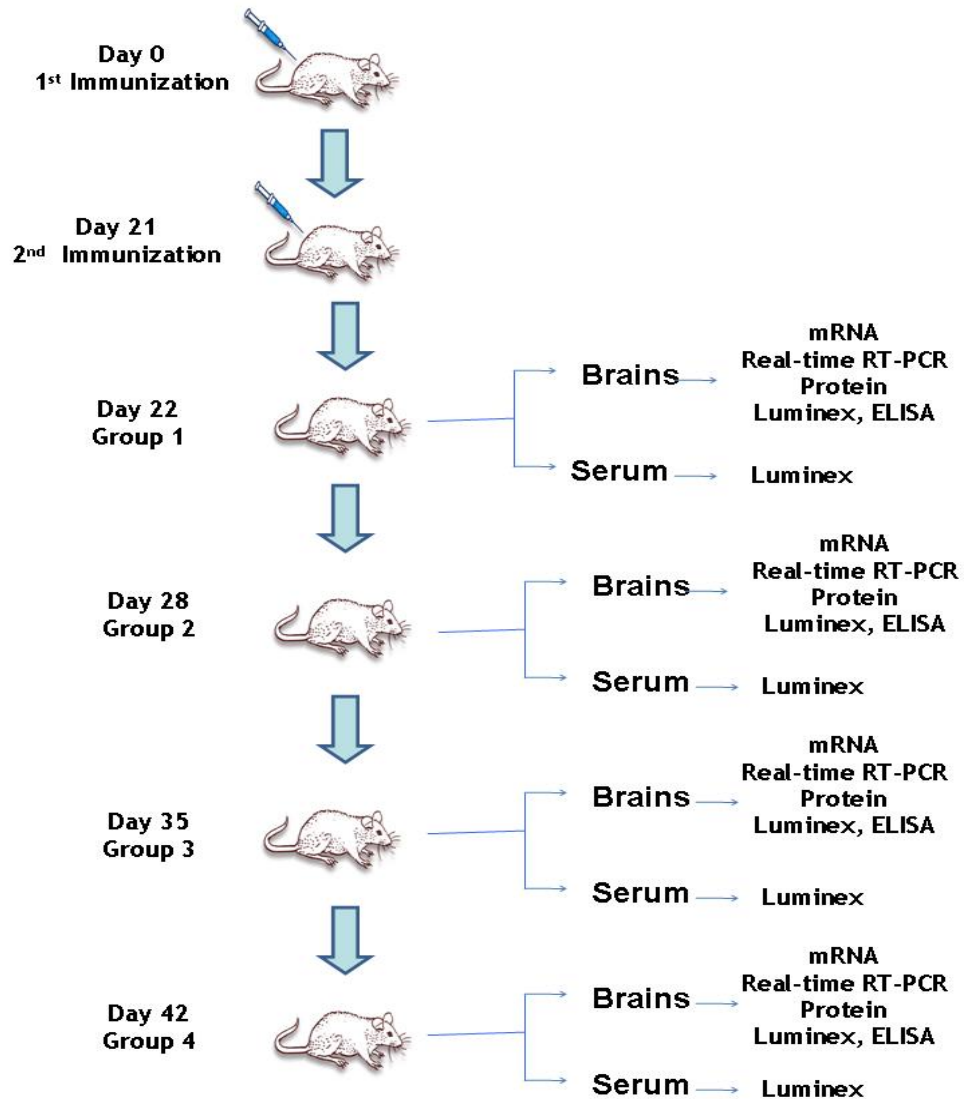


Figure 4.1 CIA experimental procedure for time course experiment
 24 DBA1 mice at 6-8 weeks of age were immunized with 100 μ g type II bovine collagen + complete Freund's adjuvant (CFA) at day 0 and then challenged on day 21 with 200 μ g type II collagen. Mice were randomly divided into 4 groups (6 mice/group), which were culled on different days (days 22, 28, 35, 42) as indicated. Another 4 groups of untreated normal mice culled on the same days indicated were used as controls. Brain and serum from mice of all experimental groups were collected and processed for inflammatory mediator measurements using Luminex, ELISA and real-time PCR.

4.2.1.1 Development and severity of arthritis disease of each group of CII immunized mice at each time point.

All 6 CII immunized mice in Group 1 were culled on day 22 after immunization, there was no mice in that group developed arthritis.

On day 28 after immunization, another 6 CII immunized mice in Group 2 were culled. There were 2 CII immunized mice in that group with arthritis (33.33% incidence) at the day of cull. The onset of arthritis disease of CII immunized mice in Group 2 occurred between days 26 and 28 after immunization. The mean

clinical score and the mean paw thickness of CII in Group 2 calculated on the cull day were 1.67 ± 0.7 and 1.84 ± 0.05 mm, respectively. CII immunized mice in this group also showed a significant increase in paw thickness compared to those in naïve control mice ($P=0.0022$) (Figure 4.2A, Figure 4.2B, Figure 4.2C).

CII immunized mice in Group 3 ($n=6$) were culled on day 35 after immunization. At that time point, there were 3 CII immunized in Group 3 developed arthritis (50% incidence). Arthritic mice in this group started to show signs of arthritis between day 22 and day 28 after immunization. The mean clinical score and the mean paw thickness of CII in Group 3 calculated on the cull day were 3.17 ± 1.87 and 1.95 ± 0.14 mm, respectively. A significant increase in paw thickness was observed in CII immunized mice in this group compare to those in naïve control mice ($p=0.0032$) (Figure 4.2A, Figure 4.2B, Figure 4.2C).

At the final time point on day 42, 6 CII immunized mice in Group 4 were harvested. 3 CII immunized in this group developed arthritis and the clinical signs of arthritis were observed in these arthritic mice between day 20 and day 28 (50% incidence) after immunization. The mean arthritis score and the mean paw thickness of CII in Group 4 calculated on the cull day were 3.33 ± 1.63 and 2.04 ± 0.09 mm, respectively. Overall mean paw thickness of CII immunized mice of Group 4 was significantly higher than those in naïve control mice ($P<0.0001$) (Figure 4.2A, Figure 4.2B, Figure 4.2C).

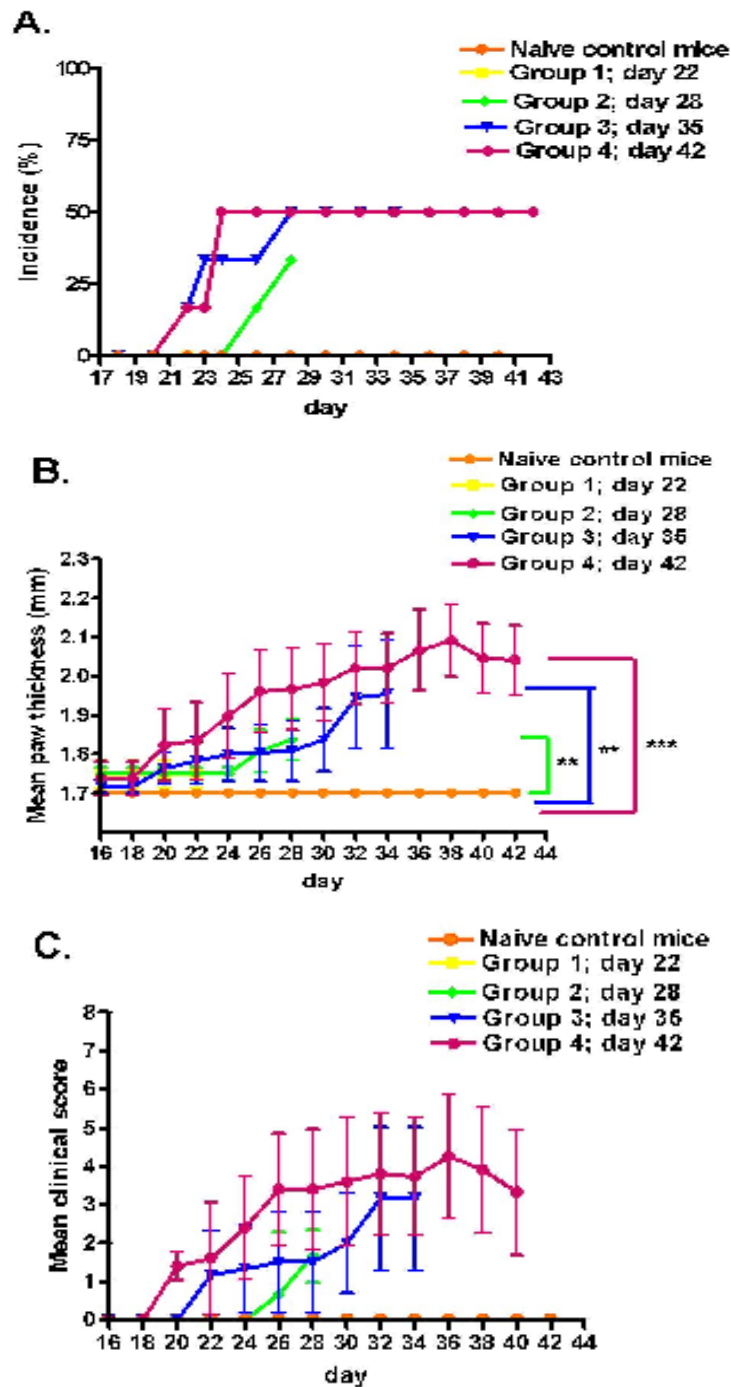


Figure 4.2 Development and severity of arthritis disease of each group of CII immunized mice at each time point

24 CII immunized mice were divided into 4 groups (6 mice/group), which were culled on different days (days 22, 28, 35, 42 after immunization) throughout CIA experimental course. (A) shows incidence of arthritis of each group of CII immunized mice at each time point, which was calculated from number of CII immunized mice with arthritis/total number of CII immunized mice used and present as percentage. The signs of arthritis in CII immunized mice were monitor from day 16 after immunization onwards. The first group of CII immunized mice (Group 1) were culled on day 22 after immunization. There was no CII immunized mice in that group developed arthritis (yellow line). CII immunized mice in Group 2 started to show signs of arthritis from day 26 after immunization onwards and all the CII immunized mice in Group 2 were culled on day 28 (green line). CII immunized mice in Group 3, which were culled on day 35 after immunization, started to show signs of arthritis from day 22 onwards and on the day of cull there were 3 CII mice in that group developed arthritis (blue line). At the terminal day of CIA experimental course (day 42), another 6 CII immunized mice were culled and there were 3 CII immunized mice developed arthritis on the day of cull. These arthritic mice in Group 4 started to develop arthritis from day 20 after immunization

onwards. (B) shows mean paw thickness of CII immunized mice which was calculated from the sum of the paw thickness of all mice divided by the number of mice in each time point group. (C) shows mean clinical of CII immunized mice which was calculated from the sum of the clinical scores of all mice divided by the number of mice in each time point group. Both mean clinical score and mean paw thickness of each time point were calculated on the day of cull. Mean paw thickness, mean clinical score and %incidence in CII immunised mice (n= 6 CII immunised mice /group) were compared with those values of naïve control mice (n = 6/group) at each time point. Data represent as mean \pm SEM. (n=6 CII immunised mice /group). Statistical analysis of data was performed using two-way ANOVA for multiple comparison, compared with a group of control naïve mice; *P<0.05, ** P<0.01, *** P<0.001.

Individual clinical scores and thickness of the paws of individual CII immunized mice in each group calculated on the cull day are show in Figure 4.3. The numbers of arthritic mice, mean arthritis scores, and mean swelling scores in each group are shown in Table 4.1.

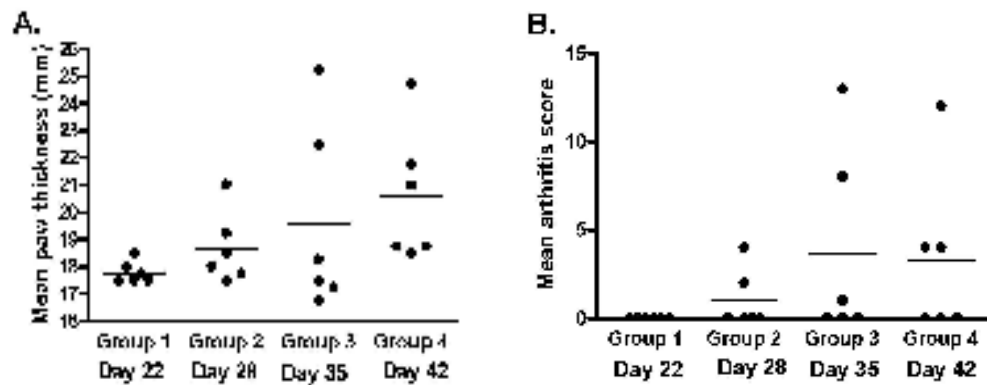


Figure 4.3 Individual clinical scores and thickness of the paws of individual CII immunized mice in each group

(A) the dots represent mean paw thickness for each mouse calculated by sum of thickness of all four paws divided by 4. (B) the dots represent a cumulative arthritis score for all paws of each mouse, with a maximum score of 16 per mouse. Each group of CII immunized mice (n=6 CII immunised mice/group) were culled of different time points as indicated (Group 1; day 22, Group 2; day 28, Group 3; day 35 and Group 4; day 42) and both individual clinical scores and individual paw thickness were calculated on the day of cull. Bars represent the mean values. (*P < 05; **P < 01; ***P < 001 by one-way ANOVA analysis)

Group	Day of cull	Number of arthritic mice (6 mice/group)	Mean arthritic scores	Maximum arthritic scores	Mean paw diameter (mm)
1	Day 22	0/6	0	0	1.7
2	Day 28	2/6	1	4	1.84
3	Day 35	3/6	3.17	10	1.95
4	Day 42	3/6	3.33	12	2.04

Table 4.1 Numbers of arthritic mice, mean arthritis scores, and mean swelling scores of CII immunized mice in each time point groups

Mice immunized with type II collagen were divided into 4 groups (group 1, 2, 3 and 4) which were culled on days as indicated. Numbers of immunized mice developed arthritis from each time point group were counted on the cull day. Mean arthritis scores (total arthritis score/number of mice in the group), maximum arthritis score and mean swelling of immunized mice from each time point group were calculated on the cull day.

4.2.2 Time course analysis of serum inflammatory mediator protein concentration in CII immunized mice.

To investigate changes in peripheral inflammatory mediators over the time course of arthritis, a Luminex cytokine 20-Plex assay was used to determine the protein concentration of several cytokines and chemokines in serum collected from control mice and CIA mice on days 22, 28, 35 and 42. Longitudinal changes in serum IL-1 β , IL-5, CCL2 and FGF2 were observed in CII immunized mice.

4.2.2.1 Changes in serum pro-inflammatory cytokine protein concentrations in CII immunized mice

The pro-inflammatory cytokines TNF- α , IL-1 β and IL-6 were measured in serum of CII immunized and naïve control mice. Protein IL-1 β was the only cytokine in this category that showed a change in CII immunized mouse serum compared to those in the naïve control group. Two-way ANOVA analysis followed by Bonferroni posttests demonstrated that IL-1 β in serum was significantly higher in CII immunized mice compared to those in naïve control mice on day 22 and 28 after the immunization ($P < 0.0001$). The mean value of serum IL-1 β (CII immunized versus naïve control) on day 22 and day 28 was 237.3 ± 21.3 pg/ml versus 176.6 ± 0.9 pg/ml ($P < 0.0001$), and 254.9 ± 64.5 pg/ μ g total protein

versus 176.5 ± 1.3 pg/ml ($P = 0.0139$) respectively. This was followed by a significant decline in serum IL-1 β protein concentrations to the base-line concentration from day 28 to day 42 (Figure 4.4A). One-way ANOVA demonstrated that there were significant differences in serum IL-1 β concentrations among the four groups of mice culled on day 22, 28, 35 and 42 ($P = 0.0027$). Post hoc analysis with Bonferroni correction demonstrated that concentrations of serum IL-1 β in CII immunized mice on day 22 and day 28 were significantly higher than serum IL-1 β concentrations on day 35 and day 42. The mean value of serum IL-1 β of CII immunized mice (day 22 versus day 42) was 237.3 ± 21.3 pg/ml versus 178.5 ± 1.3 pg/ml ($P < 0.01$). The mean value of serum IL-1 β of CII immunized mice (day 28 versus day 35) was 254.9 ± 64.5 pg/ml versus 189.9 ± 21.7 pg/ml ($P < 0.05$), while the mean value of IL-1 β of CII immunized mice (day 28 versus day 42) was 254.9 ± 64.5 pg/ml versus 178.55 ± 1.3 pg/ml ($P < 0.05$) ((Figure 4.4B). These data suggest that serum IL-1 β protein concentration peaked during 22 to 28 days after immunization, and then decreased to the base line concentration from day 28 to day 42.

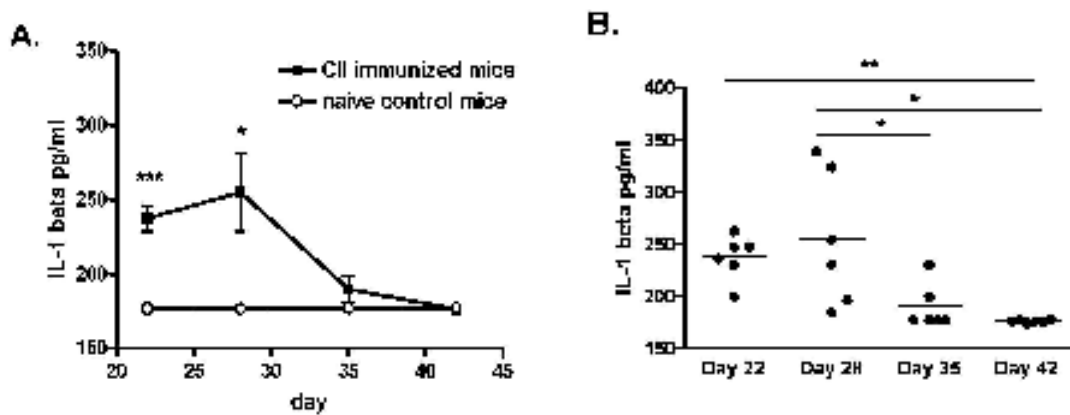


Figure 4.4 Time-course of a serum pro-inflammatory cytokine in CII immunized mice (A) Mice immunized with type II collagen (filled squares) were culled on day 22, 28, 35, 42 and serum samples from CII immunized mice of all time points were collected for peripheral inflammatory mediator measurement using a Luminex assay. Serum samples collected from naive control mice (open circle) culled on the days indicated were used as controls. IL-1 β protein concentrations in serum are expressed as pg/ml. Data represent means \pm SEM ($n =$ CII immunised mice/group). Statistical analysis of data was performed using two-way ANOVA, compared with naïve control mice: * $P < 0.05$, ** $P < 0.01$, *** $P < 0.001$. (B) shows longitudinal changes of serum IL-1 β concentrations in a group of CII immunized mice culled on the days indicated. Bars represent mean values: (* $P < 0.05$; ** $P < 0.01$; *** $P < 0.001$ by one-way ANOVA analysis).

4.2.2.2 Changes in serum Th1 cytokine protein concentrations in CII immunized mice

IFN- γ , IL-2 and IL-12 were Th1 cytokines that were selected for analysis in the serum of CII immunized and control mice. However, there were no Th1 cytokines detectable in serum of any mice from all the experimental groups.

4.2.2.3 Changes in serum Th2 cytokine protein concentrations in CIA mice

Th-2 cytokines, including IL-4, IL-5, IL-10 and IL-13 were selected for analysis in the serum of naïve control mice and CII immunized mice. IL-5 was the only one of these Th2 cytokine that was detectable in the serum of CII immunized mice. Two-way ANOVA analysis followed by Bonferroni posttests demonstrated that IL-5 in serum was significantly higher in CII immunized mice compared to those in naïve control mice on day 22 and 28 after the immunization ($P = 0.037$). The mean values of serum IL-5 (CII immunized versus naïve control) on day 22 and day 28 were 209.8 ± 39.1 pg/ml versus 160.8 ± 2.0 pg/ml ($P = 0.012$), and 195.2 ± 29.2 pg/ml versus 161.2 ± 1.6 pg/ml ($P = 0.0171$) respectively (Figure 4.5A). The serum IL-5 concentration of CII immunized mice thereafter decreased continuously during day 28 to day 42. One-way ANOVA followed by Bonferroni's post-hoc comparison tests demonstrated that there were significant differences in serum IL-5 concentrations among the four groups of mice culled on day 22, 28, 35 and 42 ($P = 0.0067$). The serum IL-5 concentrations of CII immunized mice on day 22 were significantly higher than those on day 35 (209.8 ± 39.1 pg/ml versus 164.2 ± 14.4 pg/ml; $P < 0.05$), and on day 42 (209.8 ± 39.1 pg/ml versus 159.6 ± 2.5 pg/ml; $P < 0.05$). There were no significant differences between serum IL-5 concentrations of CII immunized mice on day 28 and those on day 35 and day 42 (Figure 4.5B). These data suggest that serum IL-5 protein concentrations peaked during 22 days after immunization, and then decreased to the baseline concentration from day 28 to day 42.

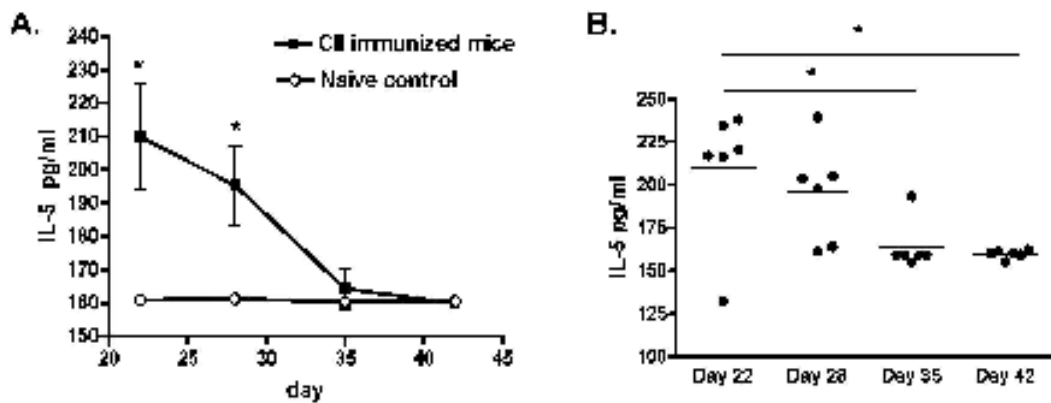


Figure 4.5 Time-course of a serum Th2 cytokine in CII immunized mice

(A) Mice immunized with type II collagen (filled squares) were culled on day 22, 28, 35, 42 and serum samples from CII immunized mice of all time points were collected for peripheral inflammatory mediator measurement using a Luminex assay. Serum samples collected from naïve control mice (open circle) culled on the days indicated were used as controls. IL-5 protein concentrations in serum are expressed as pg/ml. Data represent means \pm SEM ($n = 6$ CII immunised mice/group). Statistical analysis of data was performed using two-way ANOVA, compared with naïve control mice: * $P < 0.05$. (B) shows longitudinal changes of serum IL-5 concentrations in a group of CII immunized mice culled on the days indicated. Bars represent mean values: (* $P < 0.05$; ** $P < 0.01$; *** $P < 0.001$ by one-way ANOVA analysis)

4.2.2.4 Changes in serum chemokine protein concentrations in CII immunized mice

Among the chemokines analysed (CXCL1, CXCL10, CCL2 and CCL3), only the serum concentration of CCL2 in CII immunized mice increased significantly at day 22 and day 28 compared to those of the naïve controls. Two-way ANOVA analysis followed by Bonferroni posttests demonstrated that CCL2 in serum was significantly higher in CII immunized mice compared to those in naïve control mice on day 22 and day 28 after the immunization ($P = 0.001$). The mean value of serum CCL2 (CII immunized versus naïve control) on day 22 and day 28 were 175.5 ± 18.5 pg/ml versus 139.0 ± 1.0 pg/ml ($P = 0.0007$), and 174.8 ± 22.4 pg/ml versus 137.9 ± 1.7 pg/ml ($P = 0.0025$) respectively (Figure 4.6A). One-way ANOVA followed by Bonferroni's post-hoc comparison tests demonstrated that there were significant differences in serum CCL2 concentrations among the four groups of mice culled on day 22, 28, 35 and 42 ($P = 0.0007$). There was a decrease in serum CCL2 concentration of CII immunized mice after day 28. The serum concentration of CCL2 in CII immunized mice on day 35 and day 42 were significantly lower than those on day 22. The mean value of serum CCL2 of CII immunized mice (day 22 versus day 35) was 175.5 ± 18.5 pg/ml versus 146.3 ± 11.4 pg/ml ($P < 0.05$), while the mean value of serum CCL2 of CII immunized mice (day 22 versus day 42) was 175.5 ± 18.5 pg/ml versus 139.7 ± 1.4 pg/ml ($P < 0.01$). A significant reduction of serum CCL2 was also observed in CII

immunized mice on day 35 and day 42 compared to those on day 28. The mean value of serum CCL2 of CII immunized mice (day 28 versus day 35) was 174.8 ± 22.4 pg/ml versus 146.3 ± 11.4 pg/ml ($P < 0.05$), while the mean value of serum CCL2 of CII immunized mice (day 28 versus day 42) was 174.8 ± 22.4 pg/ml versus 139.7 ± 1.4 pg/ml ($P < 0.01$) (Figure 4.6B).

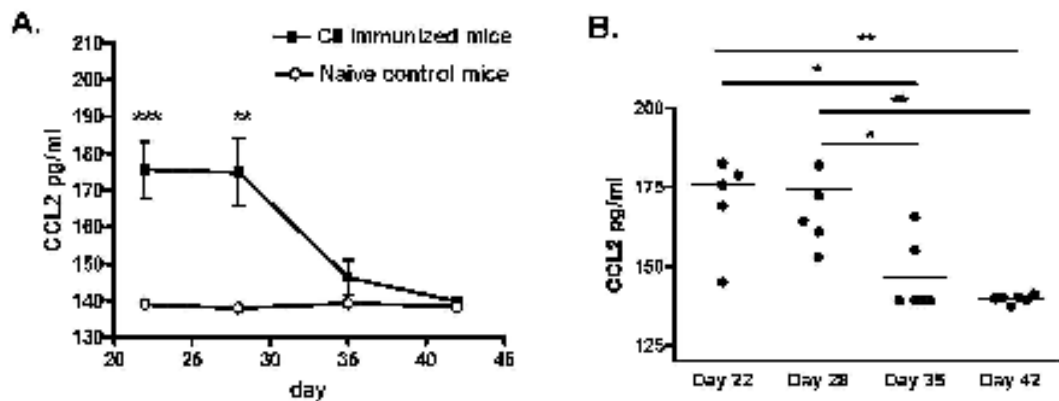


Figure 4.6 Time-course of a serum chemokine in CII immunized mice

(A) Mice immunized with type II collagen (filled squares) were culled on day 22, 28, 35, 42 and serum samples from CII immunized mice of all time points were collected for peripheral inflammatory mediator measurement using a Luminex assay. Serum samples collected from naïve control mice (open circle) culled on the days indicated were used as controls. CCL2 protein concentrations in serum are expressed as pg/ml. Data represent means \pm SEM ($n = 6$ CII immunised mice/group). Statistical analysis of data was performed using two-way ANOVA, compared with naïve control mice: ** $P < 0.01$, *** $P < 0.001$. (B) shows longitudinal changes of serum CCL2 concentrations in a group of CII immunized mice culled on the days indicated. Bars represent mean values: (* $P < 0.05$; ** $P < 0.01$; *** $P < 0.001$ by one-way ANOVA analysis).

4.2.2.5 Changes in serum growth protein concentrations in CII immunized mice

Growth factor concentrations including fibroblast growth factor (FGF2) and vascular endothelial growth factor (VEGF) were determined in the serum of naïve control mice and CII immunized mice. Two-way ANOVA analysis followed by Bonferroni posttests demonstrated that FGF2 in serum was significantly higher in CII immunized mice compared to those in naïve control mice on day 22 and 28 after the immunization ($P < 0.0001$). Significantly higher concentrations of serum FGF2 protein were observed on day 22 and day 28 compared to those of the naïve controls. The mean value of serum FGF2 (CII immunized versus naïve control) on day 22 and day 28 were 3243.8 ± 644.4 pg/ml versus 719.4 ± 0.7 pg/ml ($P < 0.0001$), and 2482.0 ± 1283.2 pg/ml versus 719.7 ± 1.0 pg/ml ($P = 0.0072$) respectively (Figure 4.7A). One-way ANOVA demonstrated that there were significant differences in serum FGF2 concentrations among the four groups

of mice culled on day 22, 28, 35 and 42 ($P < 0.0001$). Post hoc analysis with Bonferroni correction demonstrated that concentrations of serum FGF2 protein of CII immunized mice dropped significantly between days 28 to 42. The mean value of serum FGF2 of CII immunized mice (day 22 versus day 35) was 3243.8 ± 644.4 pg/ml versus 803.3 ± 135.7 pg/ml ($P < 0.001$), while the mean value of serum FGF2 of immunized mice (day 22 versus day 42) was 3243.8 ± 644.4 pg/ml versus 719.7 ± 1.2 pg/ml ($P < 0.001$). Serum FGF2 concentration of CII immunized mice on day 35 and day 42 were also significant lower than those of immunized mice on day 28. The mean value of serum FGF2 of CII immunized mice (day 28 versus day 35) was 2482.0 ± 1283.2 pg/ml versus 803.3 ± 135.7 pg/ml ($P < 0.01$), while the mean value of serum FGF2 of immunized mice (day 28 versus day 42) was 2482.0 ± 1283.2 pg/ml versus 719.7 ± 1.2 pg/ml ($P < 0.01$) (Figure 4.7B).

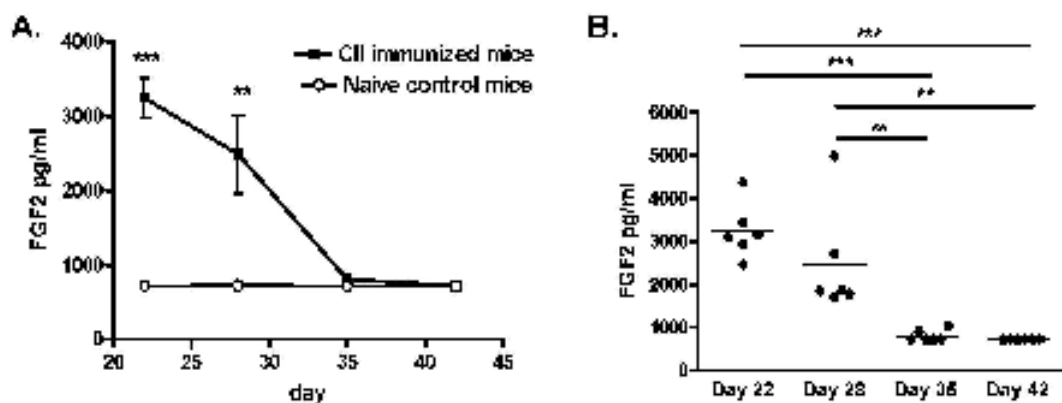


Figure 4.7 Time-course of a serum growth factor in CII immunized mice (A) Mice immunized with type II collagen (filled squares) were culled on day 22, 28, 35, 42 and serum samples from CII immunized mice of all time points were collected for peripheral inflammatory mediator measurement using a Luminex assay. Serum samples collected from naïve control mice (open circle) culled on the days indicated were used as controls. FGF2 protein concentrations in serum are expressed as pg/ml. Data represent means \pm SEM ($n = 6$ CII immunised mice/group). Statistical analysis of data was performed using two-way ANOVA, compared with naïve control mice: ** $P < 0.01$, *** $P < 0.001$. (B) shows longitudinal changes of serum FGF2 concentrations in a group of CII immunized mice culled on the days indicated. Bars represent mean values: (* $P < 0.05$; ** $P < 0.01$; *** $P < 0.001$ by one-way ANOVA analysis).

4.2.3 Time-course analysis of inflammatory mediator protein concentrations in the brains of CII immunized mice by Luminex cytokine 20-Plex

We performed a time-course study on the protein concentrations of various inflammatory mediators including the pro-inflammatory cytokines (IL-6, IL-1 β , TNF- α and IL-1 α), Th1 cytokines (IL-2, IL-12 and IFN- γ), Th2 cytokines (IL-4, IL-

5, IL-10 and IL-13), chemokines (CXCL1, CXCL10, CCL2 and CCL3) and growth factors (FGF and VEGF) in half brain tissue homogenate samples of CIA and control mice from all experimental groups using a Luminex cytokine 20-Plex assay. We found longitudinal changes in protein concentrations of IL-2, CXCL1, VEGF and FGF2 in the brains of CII immunized mice.

4.2.3.1 Time-course analysis of pro-inflammatory cytokine protein concentrations in the brains of CII immunized mice by Luminex cytokine 20-Plex assay

The protein concentrations of pro-inflammatory cytokines including IL-6, IL-1 β , TNF- α and IL-1 α were assayed in brain homogenates of mice from all experimental groups. However, the concentrations of these pro-inflammatory cytokines in all brain samples were lower than the assay detection limit.

4.2.3.2 Time-course analysis of Th-1 cytokine protein concentrations in the brains of CII immunized mice by Luminex cytokine 20-Plex

The protein concentration of Th-1 cytokines, including IL-12, IL-2 and IFN- γ , were assayed in the brain tissue of CII immunized mice and control mice culled on days 22, 28, 35 and 42. Two-way ANOVA analysis followed by Bonferroni posttests demonstrated that IL-2 protein concentrations in brain tissue were significantly higher in CII immunized versus naïve control mice on day 35 ($P = 0.0016$). The mean value of brain IL-2 (CII immunized versus naïve control) on day 35 was 2.6 ± 0.9 pg/mg total brain protein versus 1.7 ± 0.4 pg/mg total brain protein ($P = 0.0357$) (Figure 4.8A). The brain IL-2 concentrations of CII immunized mice increased significantly from day 28 to day 35. One-way ANOVA analysis showed that there was also no significant difference in brain IL-2 protein concentrations in different groups of CII immunized mice culled on day 22, day 28, day 35 and day 42 (Figure 4.8B).

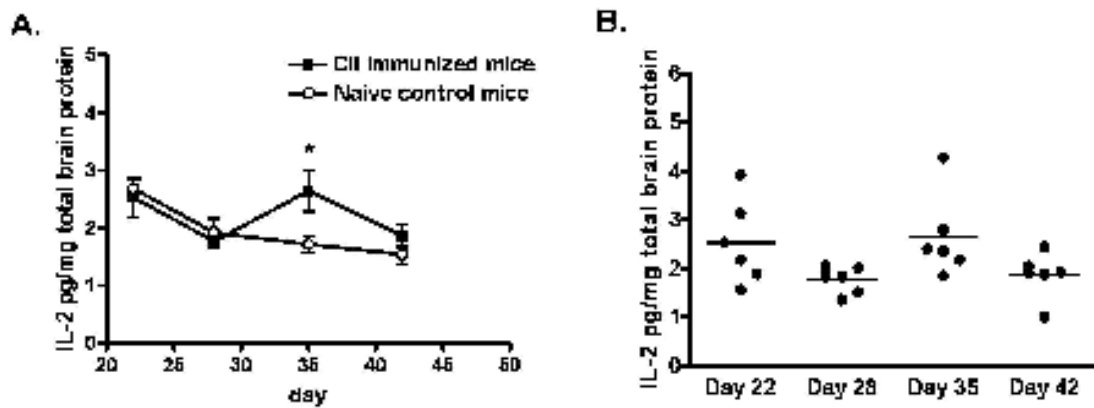


Figure 4.8 Time-course of a Th1 cytokine protein concentrations in brains of CII immunized mice by a Luminex assay

(A) Mice immunized with type II collagen (filled squares) were culled on days 22, 28, 35, 42 and brains from CII immunized mice at all time points were harvested. Brain samples collected from naïve control mice (open circle) culled on the days indicated were used as controls. IL-2 protein concentrations in brain tissue homogenate of mice from all experimental groups were determined using a Luminex assay. IL-2 concentrations in brain tissue, normalized against total brain protein, are expressed as pg/mg total brain protein. Data represent means \pm SEM. ($n = 6$ CII immunised mice/group). Statistical analysis of data was performed using two-way ANOVA compared with naïve control mice: * $P < 0.05$. (B) shows longitudinal changes of brain IL-2 in CII immunized mice culled on the days indicated. Bars represent mean values: (* $P < 05$; ** $P < 01$; *** $P < 001$ by one-way ANOVA analysis).

4.2.3.3 Time-course analysis of Th-2 cytokine protein concentrations in the brains of CII immunized mice by Luminex cytokine 20-Plex

The protein concentrations of Th2 cytokines including IL-4, IL-5, IL-10 and IL-13 were assayed in brains of mice from all experimental groups. However, the concentrations of these Th2 cytokines in all brain samples were lower than the assay detection limits.

4.2.3.4 Time-course analysis of chemokine protein concentrations in the brains of CII mice by Luminex cytokine 20-Plex

Among the chemokines quantified in mouse brains (CXCL1, CXCL10, CCL2 and CCL3), CXCL1 was the only chemokine that was detectable in mouse brain tissue within the detection limits of the assay. Two-way ANOVA analysis followed by Bonferroni posttests demonstrated that there was no significant difference between brain CXCL1 protein concentrations in CII immunized mice and naïve control mice across all time points (Figure 4.9A). One-way ANOVA analysis followed by Bonferroni posttests demonstrated that there was also no significant difference in brain CXCL1 protein concentrations in different groups of CII immunized mice culled on day 22, day 28, day 35 and day 42 (Figure 4.9B).

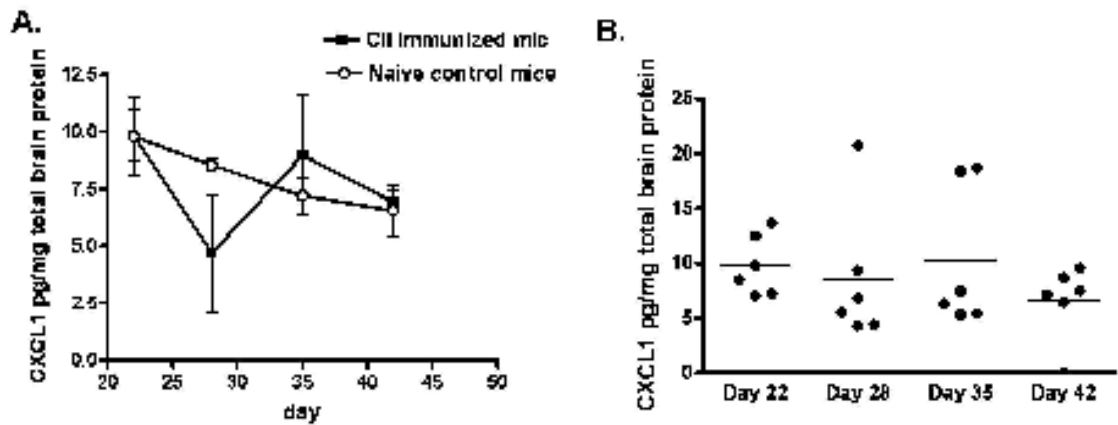


Figure 4.9 Time-course of a chemokine protein concentrations in brains of CII immunized mice by a Luminex assay

(A) Mice immunized with type II collagen (filled squares) were culled on days 22, 28, 35, 42 and brain from CII immunized mice at all time points were harvested. Brain samples collected from naïve control mice (open circle) culled on the days indicated were used as controls. CXCL1 protein concentrations in brain tissue homogenate of mice from all experimental groups were determined using a Luminex assay. CXCL1 concentrations in brain tissue, normalized against total brain protein, are expressed as pg/mg total brain protein. Data represent means \pm SEM. ($n = 6$ CII immunised mice/group). Statistical analysis of data was performed using two-way ANOVA compared with naïve control mice: * $P < 0.05$, ** $P < 0.01$, *** $P < 0.001$. (B) shows longitudinal changes of brain CXCL1 in CII immunized mice culled on the days indicated. Bars represent mean values: (* $P < 0.05$; ** $P < 0.01$; *** $P < 0.001$ by one-way ANOVA analysis).

4.2.3.5 Time-course analysis of growth factor protein concentrations in the brains of CII immunized mice by Luminex cytokine 20-Plex assay

The protein concentration concentrations of VEGF and FGF2 were detectable within the detection limits of the assay. Two-way ANOVA analysis followed by Bonferroni posttests demonstrated that FGF2 protein concentrations in brain tissue were significantly higher in CII immunized versus naïve control mice on day 42 ($P < 0.001$). The mean value of brain FGF2 (CII immunized versus naïve control) on day 42 was 242.3 ± 46.4 pg/mg total brain protein versus 183.3 ± 40.2 pg/mg total brain protein ($P = 0.0402$) (Figure 4.10A). There was a continuous downward trend in brain FGF protein concentrations of CII immunized mice. One-way ANOVA demonstrated that there were significant differences in FGF2 protein concentrations among the four groups of mice on day 22, 28, 35 and 42 ($P = 0.0006$). Post hoc analysis with Bonferroni correction demonstrated that concentrations of brain FGF2 of CII immunized mice on day 22 were significantly higher than those of immunized mice culled on day 28, day 35 and day 42. The mean value of brain FGF2 of immunized mice (day 22 versus day 28) was 502.4 ± 133.5 pg/mg total brain protein versus 345.5 ± 72.6 pg/mg total brain protein ($P < 0.05$). The mean value of brain FGF2 of CII immunized mice (day 22 versus day 35) was 502.4 ± 133.5 pg/mg total brain protein versus

324.9 ± 83.0 pg/mg total brain protein ($P < 0.05$), while the mean value of brain FGF2 of CII immunized mice (day 22 versus day 42) was 502.4 ± 133.5 pg/mg total brain protein versus 242.3 ± 46.4 pg/mg total brain protein ($P < 0.01$) (Figure 4.10B).

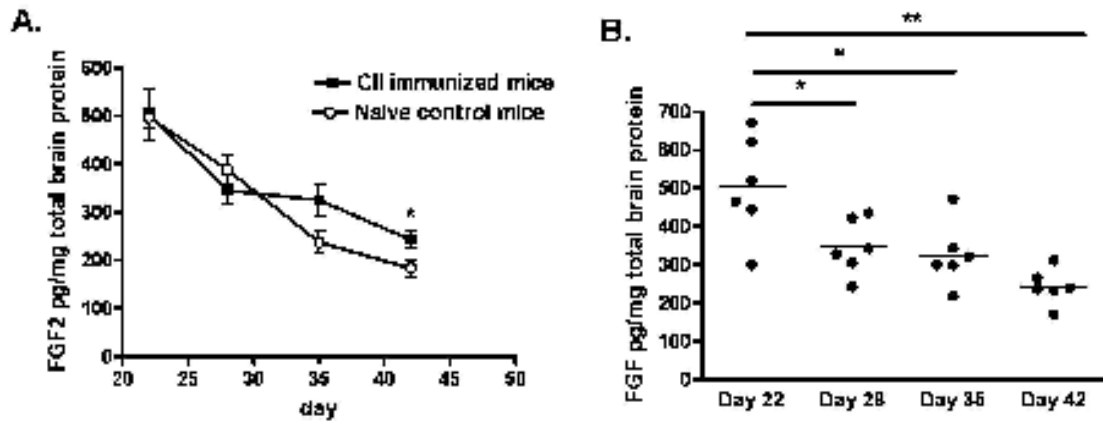


Figure 4.10 Time-course of a growth factor (FGF2) protein concentrations in brains of CII immunized mice by a Luminex assay
(A) Mice immunized with type II collagen (filled squares) were culled on days 22, 28, 35, 42 and brain from CII immunized mice at all time points were harvested. Brain samples collected from naïve control mice (open circle) culled on the days indicated were used as controls. FGF2 protein concentrations in brain tissue homogenate of mice from all experimental groups were determined using a Luminex assay. FGF2 concentrations in brain tissue, normalized against total brain protein, are expressed as pg/mg total brain protein. Data represent means ± SEM. ($n = 6$ CII immunised mice/group). Statistical analysis of data was performed using two-way ANOVA compared with naïve control mice: * $P < 0.05$, ** $P < 0.01$, *** $P < 0.001$. **(B)** shows longitudinal changes of brain FGF2 in CII immunized mice culled on the days indicated. Bars represent mean values: (* $P < 0.05$; ** $P < 0.01$; *** $P < 0.001$ by one-way ANOVA analysis).

Two-way ANOVA analysis followed by Bonferroni posttests demonstrated that a significant difference in brain VEGF protein concentration was observed in immunized mice and control mice on day 42 ($P = 0.0015$). The mean value of brain VEGF protein concentration (CII immunized versus naïve control) on day 42 was 9.3 ± 1.7 pg/mg total brain protein versus 7.0 ± 1.2 pg/mg total brain protein ($P = 0.0219$) (Figure 4.11A). One-way ANOVA demonstrated that there was also no significant difference in brain VEGF protein concentrations in different groups of CII immunized mice culled on day 22, day 28, day 35 and day 42 (Figure 4.11B).

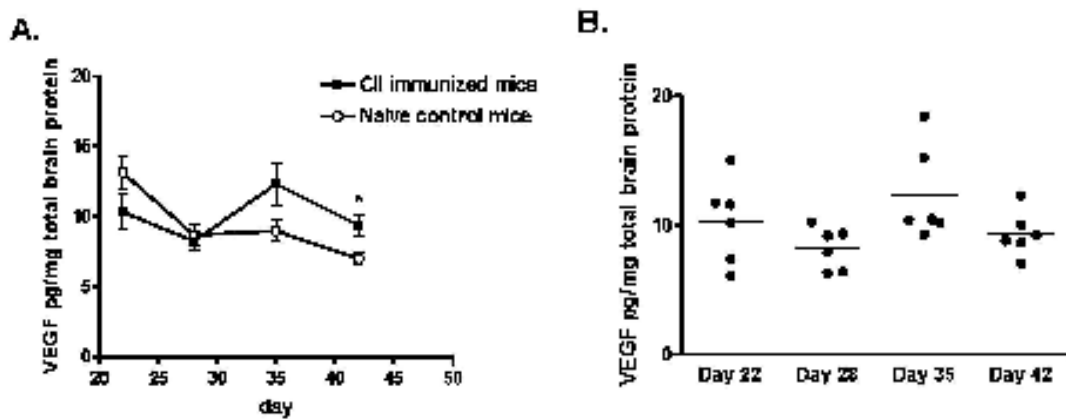


Figure 4.11 Time-course of a growth factor (VEGF) protein concentrations in brains of CII immunized mice by a Luminex assay

(A) Mice immunized with type II collagen (filled squares) were culled on days 22, 28, 35, 42 and brain from CII immunized mice at all time points were harvested. Brain samples collected from naïve control mice (open circle) culled on the days indicated were used as controls. VEGF protein concentrations in brain tissue homogenate of mice from all experimental groups were determined using a Luminex assay. VEGF concentrations in brain tissue, normalized against total brain protein, are expressed as pg/mg total brain protein. Data represent means \pm SEM. ($n = 6$ CII immunised mice/group). Statistical analysis of data was performed using two-way ANOVA compared with naïve control mice: * $P < 0.05$. (B) shows longitudinal changes of brain VEGF in CII immunized mice culled on the days indicated. Bars represent mean values: (* $P < 0.05$; ** $P < 0.01$; *** $P < 0.001$ by one-way ANOVA analysis).

4.2.4 Time-course analysis of inflammatory mediator protein concentrations in the brain homogenates of CII immunized mice validated by ELISA assays

In this chapter, we used a Luminex assay to determine longitudinal changes in protein concentrations in brains of CII immunized mice. We only found significant changes of IL-2, VEGF and FGF2 protein concentrations in brains of CII immunized mice compared to those in naïve control mice. In contrast, data from previous chapter showed a broader range of inflammatory mediator proteins that were up-regulated in the brains of CII immunized mice. In this chapter, we could not detect various inflammatory mediators such as IL-1 α , IL-4, IL-5, IL-6, IL-10, IL-13 and CXCL10 that were detectable by the same Luminex assay in the brains of CII immunized mice in the last chapter. We therefore repeated the analysis using potentially more sensitive ELISA assays as an alternative to determine longitudinal changes in these inflammatory mediators in brains of CII immunized mice. TNF- α , IL-1 β , IL-4, IL-5, IL-6, IL-10, IL-12, and IL-13, CCL2, VEGF ELISA kits were used to measure changes in inflammatory mediators that were undetectable by Luminex in brains of mice from all experimental groups. Longitudinal changes in TNF- α , IL-1 β , IL-4, IL-10, IL-12 and CCL2 protein concentrations were observed in brains of CII immunized mice.

4.2.4.1 Time-course analysis of pro-inflammatory cytokine protein concentrations in the brains of CII immunized mice by ELISA assays

Pro-inflammatory cytokines, including IL-1 β , IL-6 and TNF- α , were determined in brains of mice from all experimental groups using commercial ELISA kits. IL-1 β and TNF- α protein concentrations in half brain tissue homogenate samples of mice from all experimental groups were detectable within the assay limits of detection.

Two-way ANOVA analysis followed by Bonferroni posttests demonstrated that TNF- α protein concentrations in brains were significantly higher in immunized versus control mice on days 35 and 42 ($P = 0.001$). The mean value of brain TNF- α (CII immunized versus naïve control) on day 35 was 44.1 ± 7.6 pg/mg total brain protein versus 29.1 ± 3.7 pg/mg total brain protein ($P = 0.0113$), while the mean value of TNF- α (CII immunized versus naïve control) on day 42 was 47.1 ± 12.4 pg/mg total brain protein versus 29.1 ± 1.8 pg/mg total brain protein ($P = 0.0075$) (Figure 4.12A). One-way ANOVA analysis showed that there was also no significant difference in brain TNF- α protein concentrations in different groups of CII immunized mice culled on day 22, day 28, day 35 and day 42. (Figure 4.12B).

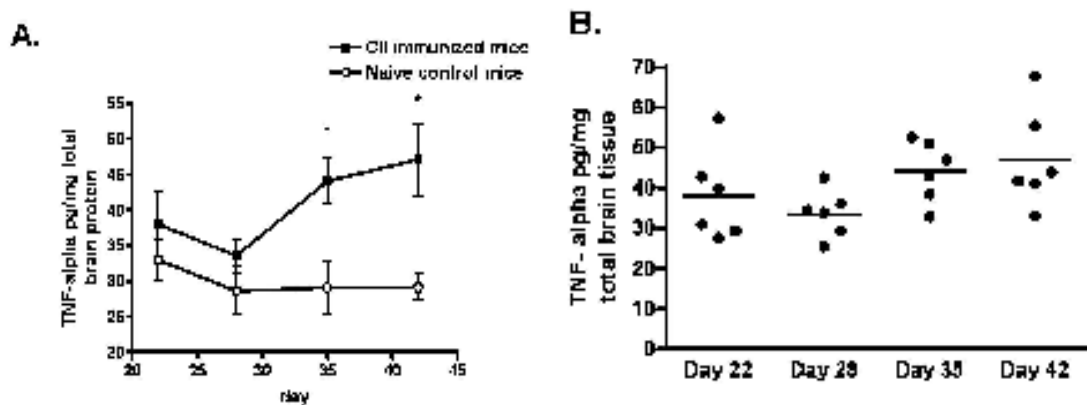


Figure 4.12 Time-course of a pro-inflammatory cytokines (TNF- α) protein concentrations in brains of CII immunized mice by an ELISA assay

(A) Mice immunized with type II collagen (filled squares) were culled on days 22, 28, 35, 42 and brain from CII immunized mice at all time points were harvested. Brain samples collected from naïve control mice (open circle) culled on the days indicated were used as controls. TNF- α protein concentrations in brain tissue homogenate of mice from all experimental groups were determined using an ELISA assay. TNF- α concentrations in brain tissue, normalized against total brain protein, are expressed as pg/mg total brain protein. Data represent means \pm SEM. ($n = 6$ CII immunised mice/group). Statistical analysis of data was performed using two-way ANOVA compared with naïve control mice: * $P < 0.05$, ** $P < 0.01$, *** $P < 0.001$. (B) shows longitudinal changes of brain TNF- α in CII immunized mice culled on

the days indicated. Bars represent mean values: (* $P < 0.05$; ** $P < 0.01$; *** $P < 0.001$ by one-way ANOVA analysis).

Two-way ANOVA analysis followed by Bonferroni posttests demonstrated that brain IL-1 β protein concentrations in CII immunized mice were significantly increased compared to those in naïve control mice on day 22 ($P = 0.0011$). The mean value of brain IL-1 β (CII immunized versus naïve control) on day 22 was 341.7 ± 68.5 pg/mg total brain protein versus 226.9 ± 60.1 pg/mg total brain protein ($P = 0.0235$) (Figure 4.13A). One-way ANOVA demonstrated that there were significant differences in IL-1 β protein concentrations among the four groups of mice culled on day 22, 28, 35 and 42 ($P = 0.0069$). The concentration of IL-1 β protein in brain of CII immunized mice seemed to peak on day 22. IL-1 β protein concentrations in brains of CII immunized mice on day 22 were also significantly higher than those in brains of CII immunized mice on day 35 and day 42. The mean value of brain IL-1 β of CII immunized mice (day 22 versus day 35) was 341.7 ± 68.5 pg/mg total brain protein versus 225.6 ± 72.4 pg/mg total brain protein ($P < 0.05$), while the mean value of brain IL-1 β of CII immunized mice (day 22 versus day 42) was 341.7 ± 68.5 pg/mg total brain protein total brain protein versus 190.8 ± 19.1 pg/mg total brain protein ($P < 0.01$) (Figure 4.13B).

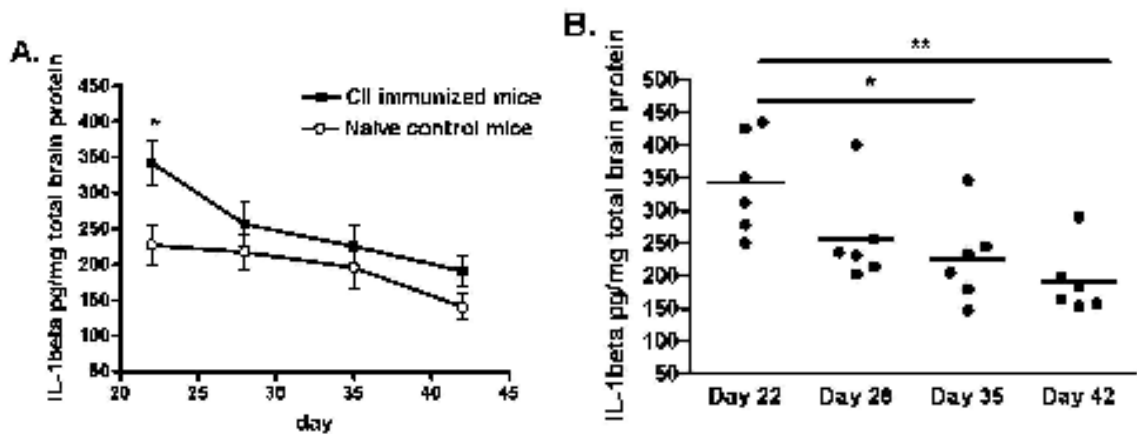


Figure 4.13 Time-course of a pro-inflammatory cytokines (IL-1 β) protein concentrations in brains of CII immunized mice by an ELISA assay (A) Mice immunized with type II collagen (filled squares) were culled on days 22, 28, 35, 42 and brain from CII immunized mice at all time points were harvested. Brain samples collected from naïve control mice (open circle) culled on the days indicated were used as controls. IL-1 β protein concentrations in brain tissue homogenate of mice from all experimental groups were determined using an ELISA assay. IL-1 β concentrations in brain tissue, normalized against total brain protein, are expressed as pg/mg total brain protein. Data represent means \pm SEM. ($n = 6$ CII immunised mice/group). Statistical analysis of data was performed using two-way ANOVA compared with naïve control mice: * $P < 0.05$, ** $P < 0.01$, *** $P < 0.001$. (B) shows longitudinal changes of brain IL-1 β in CII immunized mice culled on the days indicated. Bars represent mean values: (* $P < 0.05$; ** $P < 0.01$; *** $P < 0.001$ by one-way ANOVA analysis).

4.2.4.2 Time-course analysis of Th-1 cytokine protein concentrations in the brains of CII immunized mice by ELISA assays

IL-12 was the only Th1 cytokine detectable using an ELISA assay in brain tissue of mice from all experimental groups. Two-way ANOVA analysis followed by Bonferroni posttests demonstrated that brain IL-12 concentrations were significantly elevated in CII immunized mice versus naïve control mice on days 22, 28, 35 and 42 ($P < 0.0001$). The mean value of brain IL-12 (CII immunized versus naïve control) on day 22 was 1514.7 ± 714.3 pg/mg total brain protein versus 251.7 ± 26.4 pg/mg total brain protein ($P = 0.0018$). The mean value of brain IL-12 (CII immunized versus naïve control) on day 28 was 1011.9 ± 273.0 pg/mg total brain protein versus 257.2 ± 32.1 pg/mg total brain protein ($P = 0.0009$). The mean value of brain IL-12 (CII immunized versus naïve control) on day 35 was 949.6 ± 398.4 pg/mg total brain protein versus 442.0 ± 86.3 pg/mg total brain protein ($P = 0.02$). The mean value of brain IL-12 (CII immunized versus naïve control) on day 42 were 615.6 ± 86.2 pg/mg total brain protein versus 241.1 ± 74.5 pg/mg total brain protein ($P < 0.0001$) (Figure 4.14A). A downward trend in the brain IL-12 protein concentrations was observed in CII immunized mice over the period of 21 days after immunization. One-way ANOVA demonstrated that there was a significant difference in IL-12 protein concentrations among the four groups of mice culled on day 22, 28, 35 and 42 ($P = 0.0110$). Post hoc analysis with Bonferroni correction demonstrated that the brain IL-12 protein concentrations in CII immunized mice on day 42 were significantly lower than those of CII immunized mice on day 22. The mean value of brain IL-12 of CII immunized mice (day 22 versus day 42) was 1514.7 ± 714.3 pg/mg total brain protein versus 615.6 ± 86.2 pg/mg total brain protein ($P < 0.01$) (Figure 4.14B).

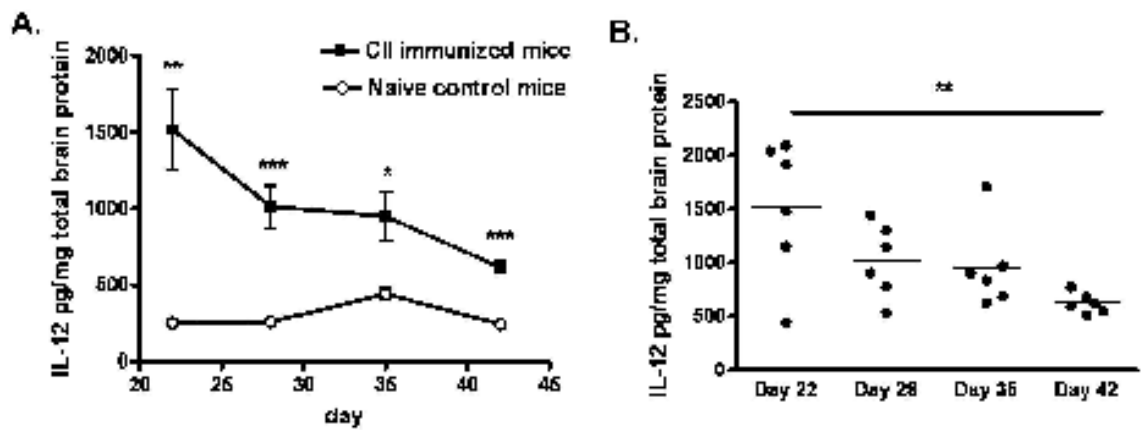


Figure 4.14 Time-course of a Th1 cytokines (IL-12) protein concentrations in brains of CII immunized mice by an ELISA assay

(A) Mice immunized with type II collagen (filled squares) were culled on days 22, 28, 35, 42 and brain from CII immunized mice at all time points were harvested. Brain samples collected from naïve control mice (open circle) culled on the days indicated were used as controls. IL-12 protein concentrations in brain tissue homogenate of mice from all experimental groups were determined using an ELISA assay. IL-12 concentrations in brain tissue, normalized against total brain protein, are expressed as pg/mg total brain protein. Data represent means \pm SEM. ($n = 6$ CII immunised mice/group). Statistical analysis of data was performed using two-way ANOVA compared with naïve control mice: * $P < 0.05$, ** $P < 0.01$, *** $P < 0.001$. (B) shows longitudinal changes of brain IL-12 in CII immunized mice culled on the days indicated. Bars represent mean values: (* $P < 0.05$; ** $P < 0.01$; *** $P < 0.001$ by one-way ANOVA analysis).

4.2.4.3 Time-course analysis of Th-2 cytokine protein concentrations in the brains of CII immunized mice measured by ELISA assays

IL-4 and IL-10 protein concentrations were detectable by ELISA in brain tissue of mice from all experimental groups.

Two-way ANOVA analysis followed by Bonferroni posttests demonstrated that brain IL-4 protein concentrations were up-regulated significantly in CII immunized mice compared to those in naïve control mice on day 22 and day 28 ($P = 0.0002$). The mean value of brain IL-4 (CII immunized versus naïve control) on day 22 was 1011.3 ± 267.1 pg/mg total brain protein versus 473.0 ± 54.1 pg/mg total brain protein ($P = 0.0015$), while the mean value of brain IL-4 (CII immunized versus naïve control) on day 28 was 815.2 ± 188.4 pg/mg total brain protein versus 473.5 ± 38.6 pg/mg total brain protein ($P = 0.0037$) (Figure 4.15A). The brain IL-4 protein concentrations in brain of CII immunized mice peaked during day 22 and day 28 after immunization. One-way ANOVA demonstrated that there were significant differences in IL-4 protein concentrations among the four groups of mice culled on day 22, 28, 35 and 42 ($P = 0.0002$). Post hoc analysis with Bonferroni correction demonstrated that brain IL-4 protein concentrations in CII immunized mice on day 22 were significantly

higher than those in CII immunized mice on day 35 and day 42. The mean value of brain IL-4 of CII immunized mice (day 22 versus day 35) was 1011.3 ± 267.1 pg/mg total brain protein versus 483.4 ± 246.4 pg/mg total brain protein ($P < 0.01$), while the mean value of brain IL-4 of CII immunized mice (day 22 versus day 42) was 1011.3 ± 267.1 pg/mg total brain protein versus 424.5 ± 145.2 pg/mg total brain protein ($P < 0.001$). CII immunized mice on day 35 and day 42 showed significant lower concentrations of brain IL-4 protein compared to those in CII immunized mice on day 28. The mean value of brain IL-4 of CII immunized mice (day 28 versus day 42) was 815.2 ± 188.4 pg/mg total brain protein versus 424.5 ± 145.2 pg/mg total brain protein ($P < 0.05$) (Figure 4.15B).

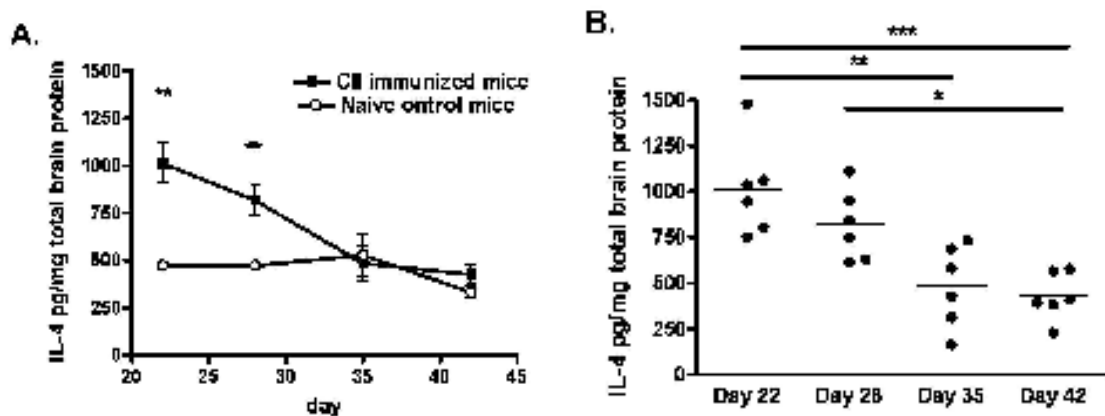


Figure 4.15 Time-course of a Th2 cytokine (IL-4) protein concentrations in brains of CII immunized mice by an ELISA assay

(A) Mice immunized with type II collagen (filled squares) were culled on days 22, 28, 35, 42 and brain from CII immunized mice at all time points were harvested. Brain samples collected from naïve control mice (open circle) culled on the days indicated were used as controls. IL-4 protein concentrations in brain tissue homogenate of mice from all experimental groups were determined using an ELISA assay. IL-4 concentrations in brain tissue, normalized against total brain protein, are expressed as pg/mg total brain protein. Data represent means \pm SEM. ($n = 6$ CII immunised mice/group). Statistical analysis of data was performed using two-way ANOVA compared with naïve control mice: * $P < 0.05$, ** $P < 0.01$, *** $P < 0.001$. (B) shows longitudinal changes of brain IL-4 in CII immunized mice culled on the days indicated. Bars represent mean values: (* $P < 0.05$; ** $P < 0.01$; *** $P < 0.001$ by one-way ANOVA analysis).

Two-way ANOVA analysis followed by Bonferroni posttests demonstrated that significant increases in IL-10 protein concentrations were observed in brains of CII immunized mice compared to naïve control mice on days 22, 28, 35, 42 ($P < 0.0001$). The mean value of brain IL-10 (CII immunized versus naïve control) on day 22 was 1175.6 ± 134.0 pg/mg total brain protein versus 381.1 ± 54.3 pg/mg total brain protein ($P < 0.0001$), while the mean value of brain IL-10 (CII immunized versus naïve control) on day 28 was 787.0 ± 94.6 pg/mg total brain protein versus 396.2 ± 38.4 pg/mg total brain protein ($P < 0.0001$). The mean

value of brain IL-10 (CII immunized versus naïve control) on day 35 was 1030.9 ± 221.2 pg/mg total brain protein versus 488.1 ± 80.9 pg/mg total brain protein ($P = 0.0003$), while the mean value of brain IL-10 (CII immunized versus naïve control) on day 42 was 932.6 ± 121.7 pg/mg total brain protein versus 429.1 ± 34.3 pg/mg total brain protein ($P = 0.0003$) (Figure 4.16A). The brain IL-10 protein concentration in CII immunized mice fluctuated throughout the 21 days after immunization. A significant drop in brain IL-10 protein concentration was observed during day 22 to day 28, followed by a significant increase brain IL-10 protein concentration from day 28 to day 42. One-way ANOVA demonstrated that there was a significant difference in IL-10 protein concentrations among the four groups of mice culled on day 22, 28, 35 and 42 ($P = 0.0052$). Post hoc analysis with Bonferroni correction demonstrated a significant down-regulation in brain IL-10 protein concentration in CII immunized mice on day 28 compared to those in CII immunized mice on day 22. The mean value of brain IL-10 of CII immunized mice (day 22 versus day 28) was 1175.6 ± 140.0 pg/mg total brain protein versus 787.00 ± 94.59 pg/mg total brain protein ($P < 0.01$). (Figure 4.16B)

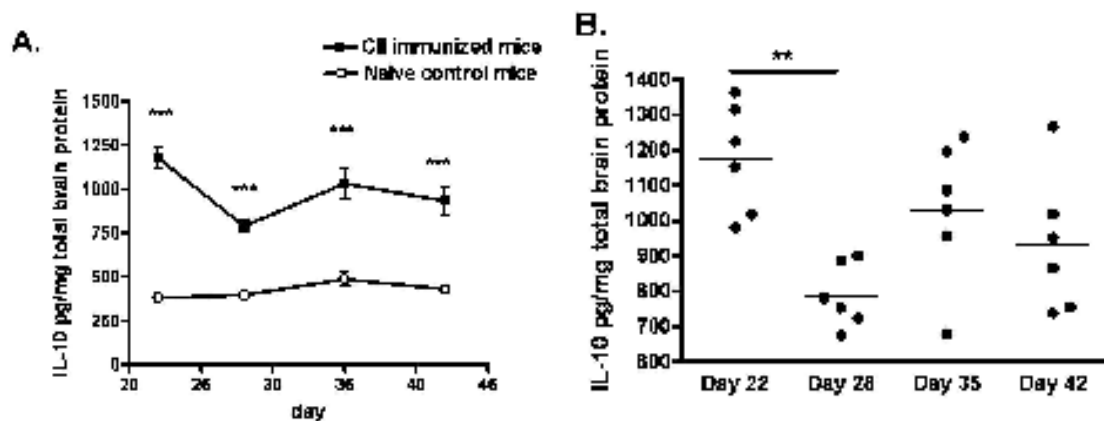


Figure 4.16 Time-course of a Th2 cytokine (IL-10) protein concentrations in brains of CII immunized mice by an ELISA assay

(A) Mice immunized with type II collagen (filled squares) were culled on days 22, 28, 35, 42 and brain from CII immunized mice at all time points were harvested. Brain samples collected from naïve control mice (open circle) culled on the days indicated were used as controls. IL-10 protein concentrations in brain tissue homogenate of mice from all experimental groups were determined using an ELISA assay. IL-10 concentrations in brain tissue, normalized against total brain protein, are expressed as pg/mg total brain protein. Data represent means \pm SEM. ($n = 6$ CII immunised mice/group). Statistical analysis of data was performed using two-way ANOVA compared with naïve control mice: $***P < 0.001$. (B) shows longitudinal changes of brain IL-10 in CII immunized mice culled on the days indicated. Bars represent mean values: (* $P < 05$; ** $P < 01$; *** $P < 001$ by one-way ANOVA analysis).

4.2.4.4 Time-course analysis of chemokine protein concentrations in the brains of CII immunized mice by ELISA assays

CCL2 was the only chemokine that could be detected using ELISA in brain tissue extracts of mice from all experimental groups. Two-way ANOVA analysis followed by Bonferroni posttests demonstrated that brain CCL2 protein concentrations were increased significantly in immunized mice compared to those in control mice on days 22, 28, and 42 ($P < 0.05$). The mean value of brain CCL2 (CII immunized versus naïve control) on day 22 was 268.5 ± 20.1 pg/mg total brain protein versus 102.3 ± 26.7 pg/mg total brain protein ($P = 0.0118$). The mean value of brain CCL2 (CII immunized versus control) on day 28 was 234.8 ± 31.3 pg/mg total brain protein versus 122.1 ± 35.7 pg/mg total brain protein ($P = 0.0238$). The mean value of brain CCL2 (CII immunized versus naïve control) on day 42 was 193.1 ± 48.0 pg/mg total brain protein versus 93.7 ± 74.7 pg/mg total brain protein ($P = 0.0125$) (Figure 4.17A). One-way ANOVA demonstrated that there was also no significant difference in brain CCL2 protein concentrations in different groups of CII immunized mice culled on day 22, day 28, day 35 and day 42 (Figure 4.17B).

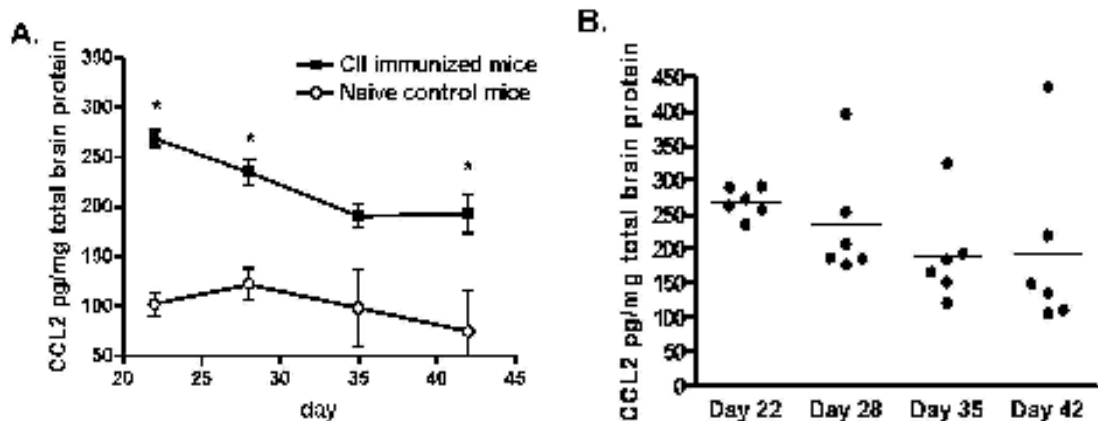


Figure 4.17 Time-course of a chemokine (CCL2) protein concentrations in brains of CII immunized mice by an ELISA assay

(A) Mice immunized with type II collagen (filled squares) were culled on days 22, 28, 35, 42 and brain from CII immunized mice at all time points were harvested. Brain samples collected from naïve control mice (open circle) culled on the days indicated were used as controls. CCL2 protein concentrations in brain tissue homogenate of mice from all experimental groups were determined using an ELISA assay. CCL2 concentrations in brain tissue, normalized against total brain protein, are expressed as pg/mg total brain protein. Data represent means \pm SEM. ($n = 6$ CII immunised mice/group). Statistical analysis of data was performed using two-way ANOVA compared with naïve control mice: $*P < 0.05$. (B) shows longitudinal changes of brain CCL2 in CII immunized mice culled on the days indicated. Bars represent mean values: ($*P < 05$; $**P < 01$; $***P < 001$ by one-way ANOVA analysis).

4.2.4.5 Differences in inflammatory mediator protein concentrations in brain of arthritic mice and non-arthritic mice

3 mice out of 6 mice from immunized mice group 3 and 4, which were culled on day 35 and day 42 respectively, developed arthritis. In order to investigate differences in brain inflammatory mediator gene expression level and protein concentrations between mice with and without arthritis, cytokine, chemokine and growth factor mRNA and protein concentrations in arthritic mice and non-arthritic mice were compared. There was no difference in protein concentrations of IL-1 β , TNF- α , IL-2, IL-12, IL-4, IL-10, CCL2 and FGF2 between brains of arthritic mice and non-arthritic mice. This was consistent with our data of the previous chapter showing non-significant difference in protein concentrations of IL-1 β , IL-1 α , IL-2, IL-5, IL-10, IL-13, CXCL10, VEGF and FGF2 between brains of arthritic mice and non-arthritic mice (Figure 4.18A-Figure 4.18H, Figure 4.19A). However, our data in this chapter showed that there was a significant difference in brain CXCL1 protein concentrations between arthritic and non-arthritic mice on day 42. This was inconsistent to data from the previous chapter showing no significant difference in brain CXCL1 protein between arthritic and non-arthritic mice at the same time point (day 42). The CXCL1 protein concentrations in brains of arthritic mice were significantly higher than those of non-arthritic mice on day 42. The mean value of CXCL1 of CII immunized mice on day 42 (arthritic versus non-arthritic) was 9 ± 0.5 pg/mg total brain protein versus 7 ± 0.6 pg/mg total brain protein ($P = 0.0262$) (Figure 4.19B)

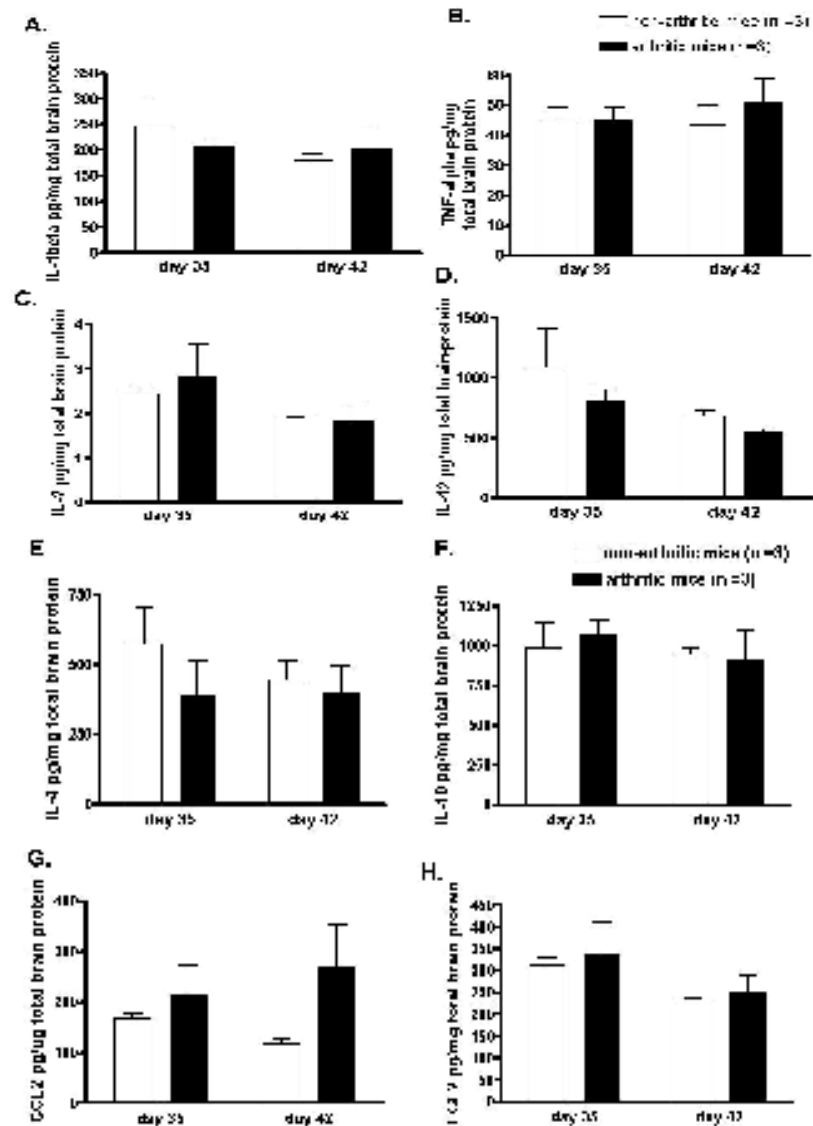


Figure 4.18 Differences in inflammatory mediator protein concentrations in brains of arthritic mice and non-arthritic mice

(A), (B), (C), (D), (E), (F), (G), and (H) show inflammatory mediator protein concentrations (pg/mg total brain protein) in brains of CII immunized mice with and without arthritis (n =3 CII immunised mice/group) on day 35 and day 42. Data are presented as the mean \pm S.D. (*P < 05; **P < 01; ***P < 001 by Student's t test.)

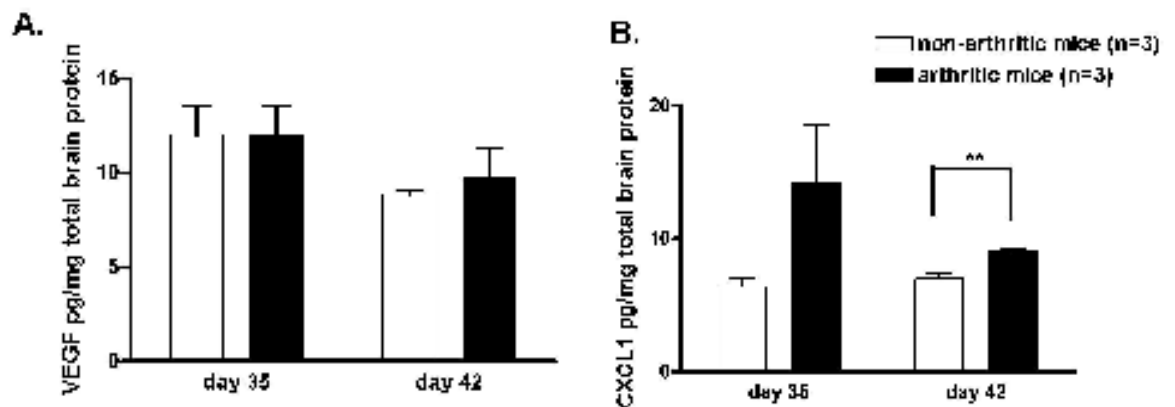


Figure 4.19 Differences in VEGF and CXCL1 protein concentrations in brains of arthritic mice and non-arthritic mice

Brain VEGF and CXCL1 protein concentrations (pg/mg total brain protein) in arthritic (n=3 arthritic mice) and non-arthritic (n=3 non-arthritic mice) were compared on day 35 and day

42. Data are presented as the mean \pm S.D. (* $P < 0.05$; ** $P < 0.02$; *** $P < 0.01$ by Student's *t*-test.)

4.2.5 Cytokine gene expression profiles in CIA mouse brains by Real-time PCR

To further investigate local production of inflammatory mediators in brains of CII immunized mice, real-time PCR was used to quantify the gene expression of the same pro-inflammatory cytokines (IL-6, IL-1 β , TNF- α and IL-1 α), Th1 cytokines (IL-2, IL-12 and IFN- γ), Th2 cytokines (IL-4, IL-5, IL-10 and IL-13), chemokines (CXCL1, CXCL10, CCL2 and CCL3) and growth factors (FGF2 and, VEGF) in one half of the brain tissue of mice from all experimental groups. Longitudinal changes in gene expression of IL-1 α , IL-2, IL-4, IL-5, IL-6, CXCL1, CXCL10 and FGF were observed in brains of CII immunized mice.

4.2.5.1 Time course analysis of pro-inflammatory cytokine mRNA concentrations in the brains of CII immunized mice

The gene expressions of pro-inflammatory cytokines including IL-6, IL-1 β , TNF- α and IL-1 α were determined in brains of mice from all experimental groups. There was no pro-inflammatory cytokine gene expression detectable in brains of CII immunized mice by the real-time PCR assay.

4.2.5.2 Time course analysis of Th1 cytokine mRNA expression levels in the brains of CII immunized mice

Changes in gene expressions of Th-1 cytokines, including IL-12, IL-2 and IFN- γ , over time were determined in the brain of mice from all experimental groups. The expression of IL-12 was the only Th1 cytokine that was up-regulated significantly in CII immunized mouse brains compared to those in naïve control mice. Two-way ANOVA analysis followed by Bonferroni posttests demonstrated that a significant increase in IL-12 gene expression was observed in CII immunized mice on day 35 compared to those in naïve control mice ($P = 0.0190$). The mean value of brain IL-12 gene expression (CII immunized versus naïve control) on day 35 were 6318 ± 4120 versus 4872 ± 2088 ($P = 0.0264$) (Figure 4.20A). One-way ANOVA demonstrated that there was also no significant difference in brain IL-12 gene expression in different groups of CII immunized mice culled on day 22, day 28, day 35 and day 42 (Figure 4.20B).

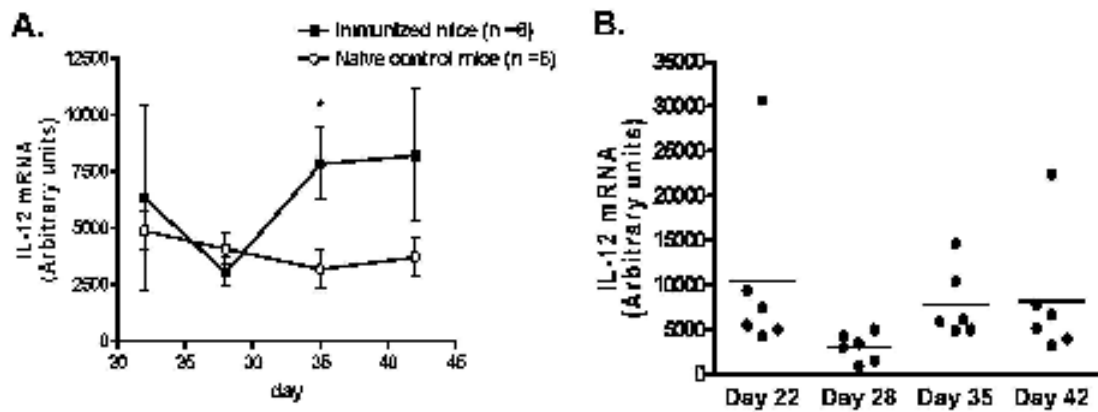


Figure 4.20 Time-course of a Th1 (IL-12) mRNA expression levels in brains of CII immunized mice by Real-time PCR

(A) Mice immunized with type II collagen (filled squares) were culled on days 22, 28, 35, 42 and brain from CII immunized mice at all time points were harvested. Brain samples collected from naïve control mice (open circle) culled on the days indicated were used as controls. IL-12 mRNA levels in brain tissue homogenate of mice from all experimental groups were determined using a real-time PCR assay. The expression levels of IL-12 mRNA were normalized against GAPDH expression and shown as arbitrary units. Data represent means \pm SEM. (n = 6 CII immunised mice/group). Statistical analysis of data was performed using two-way ANOVA compared with naïve control mice: * $P < 0.05$. (B) shows longitudinal changes of brain IL-12 in CII immunized mice culled on the days indicated. Bars represent mean values: (* $P < 0.05$; ** $P < 0.01$; *** $P < 0.001$ by one-way ANOVA analysis).

4.2.5.3 Time course analysis of Th2 cytokine mRNA levels in the brains of CII immunized mice

Th-2 cytokines, including IL-4, IL-5, IL-10 and IL-13 gene expression were determined in the brains of mice from all experimental groups. There was no Th2 cytokine gene expression detectable in brains of CII immunized mice by the real-time PCR assay.

4.2.5.4 Time course analysis of chemokine mRNA levels in the brains of CII immunized mice

CXCL1, CXCL10, CCL-2 and CCL-3 gene expression were determined in the brains of control mice from all experimental groups. Among these chemokines, only brain CXCL1 and CXCL10 mRNA were detectable within the assay detection limit.

Two-way ANOVA analysis followed by Bonferroni posttests demonstrated that brain CXCL1 gene expression levels were elevated in immunized mice compared to those in control mice on day 22 and day 42 ($P < 0.0001$). The mean value of brain CXCL1 gene expression (CII immunized versus naïve control) on day 22 were 13406 ± 5054 versus 6140 ± 1700 ($P < 0.0001$), while the mean value of brain CXCL1 (CII immunized versus naïve control) on day 42 was 15935 ± 8744 versus 6591 ± 2148 ($P = 0.0067$) (Figure 4.21A). One-way ANOVA demonstrated

that there were significant differences in CXCL1 gene expression among the four groups of mice culled on day 22, 28, 35 and 42 ($P = 0.0017$). Post hoc analysis with Bonferroni correction demonstrated that the levels of CXCL1 mRNA in brains of CII immunized mice on day 22 were significantly higher than those of day 28. The mean value of brain CXCL1 gene expression of CII immunized mice (day 22 versus day 28) was 14576 ± 1700 versus 4700 ± 2200 ($P < 0.01$). The levels of CXCL1 mRNA in brains of CII immunized mice on day 28 were significantly lower than those of day 42. The mean value of brain CXCL1 gene expression of CII immunized mice (day 35 versus day 42) was 8115 ± 1916 versus 15935 ± 2148 ($P < 0.01$) (Figure 4.21B).

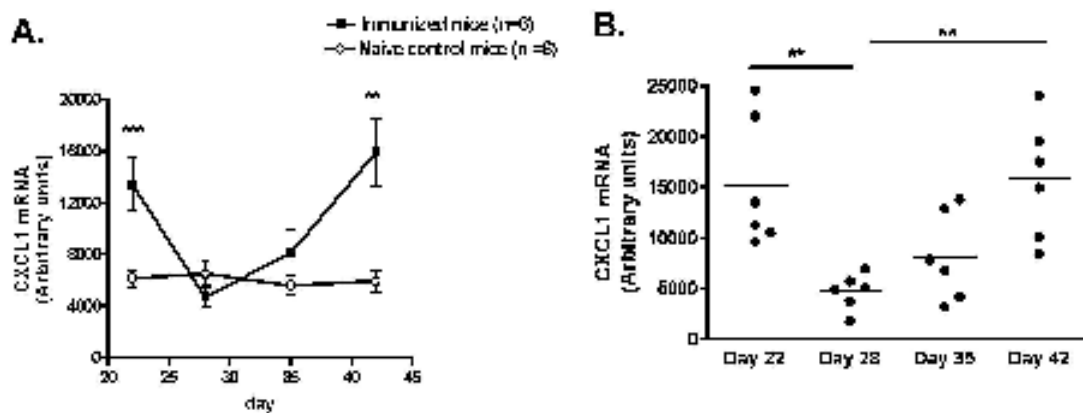


Figure 4.21 Time-course of a chemokine (CXCL1) mRNA levels in brains of CII immunized mice by Real-time PCR

(A) Mice immunized with type II collagen (filled squares) were culled on days 22, 28, 35, 42 and brain from CII immunized mice at all time points were harvested. Brain samples collected from naïve control mice (open circle) culled on the days indicated were used as controls. CXCL1 mRNA levels in brain tissue homogenate of mice from all experimental groups were determined using a real-time PCR assay. The levels of CXCL1 mRNA were normalized against GAPDH expression and shown as arbitrary units. Data represent means \pm SEM. ($n = 6$ CII immunised mice/group). Statistical analysis of data was performed using two-way ANOVA compared with naïve control mice: * $P < 0.05$, ** $P < 0.01$, *** $P < 0.001$. (B) shows longitudinal changes of brain CXCL1 in CII immunized mice culled on the days indicated. Bars represent mean values: (* $P < 0.05$; ** $P < 0.01$; *** $P < 0.001$ by one-way ANOVA analysis).

Two-way ANOVA analysis followed by Bonferroni posttests demonstrated that CII immunized mice showed significant increases in CXCL10 mRNA levels compared to those in control mouse brains on day 28 and day 35 ($P = 0.0118$). The mean value of brain CXCL10 gene expression (CII immunized versus naïve control) on day 28 were 2316 ± 681 versus 1244 ± 588 ($P = 0.0154$), while the mean value of brain CXCL10 gene expression (CII immunized versus naïve control) on day 35 were 4100 ± 2351 versus 1058 ± 289 ($P = 0.0105$) (Figure 4.22A). A peak in mRNA of CXCL10 in brains of CII immunized mice was observed on day 35 after immunization. However, one-way ANOVA demonstrated that there was also no

significant difference in brain CXCL10 gene expression in different groups of CII immunized mice culled on day 22, day 28, day 35 and day 42 (Figure 4.22B).

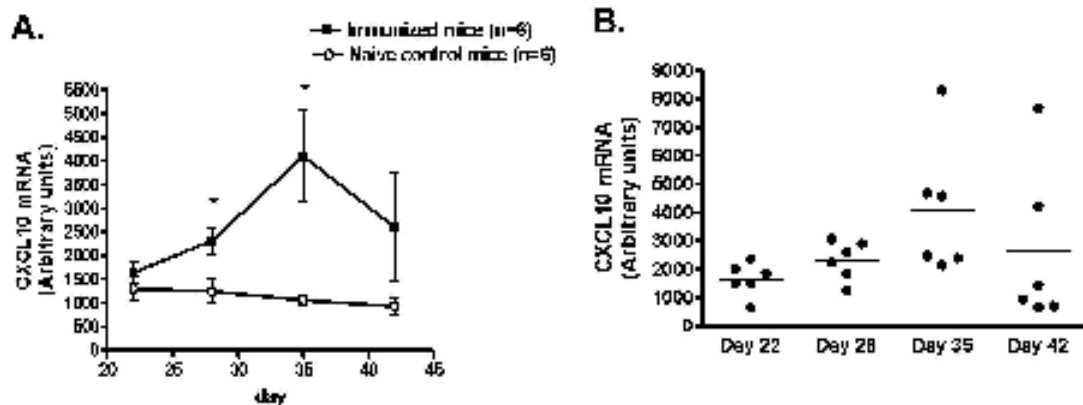


Figure 4.22 Time-course of a chemokine (CXCL10) mRNA concentrations in brains of CII immunized mice by Real-time PCR

(A) Mice immunized with type II collagen (filled squares) were culled on days 22, 28, 35, 42 and brain from CII immunized mice at all time points were harvested. Brain samples collected from naïve control mice (open circle) culled on the days indicated were used as controls. CXCL10 mRNA concentrations in brain tissue homogenate of mice from all experimental groups were determined using a real-time PCR assay. The concentrations of CXCL10 mRNA were normalized against GAPDH expression and shown as arbitrary units. Data represent means \pm SEM. (n = 6 CII immunised mice/group). Statistical analysis of data was performed using two-way ANOVA compared with naïve control mice: *P<0.05. (B) shows longitudinal changes of brain CXCL10 in CII immunized mice culled on the days indicated. Bars represent mean values: (*P < 05; **P < 01; ***P < 001 by one-way ANOVA analysis).

4.2.5.5 Time course analysis of growth factor mRNA levels in the brains of CII immunized mice

Gene expressions of growth factors including FGF2 and VEGF were detectable in the brains of mice from all experimental groups.

Two-way ANOVA analysis demonstrated that there was no significant different in FGF2 gene expression levels in brains of CII immunized mice versus those of naïve control mice (Figure 4.23A). One-way ANOVA demonstrated that FGF2 mRNA levels in brains of CII immunized mice from different time point groups were not significantly different (Figure 4.23B).

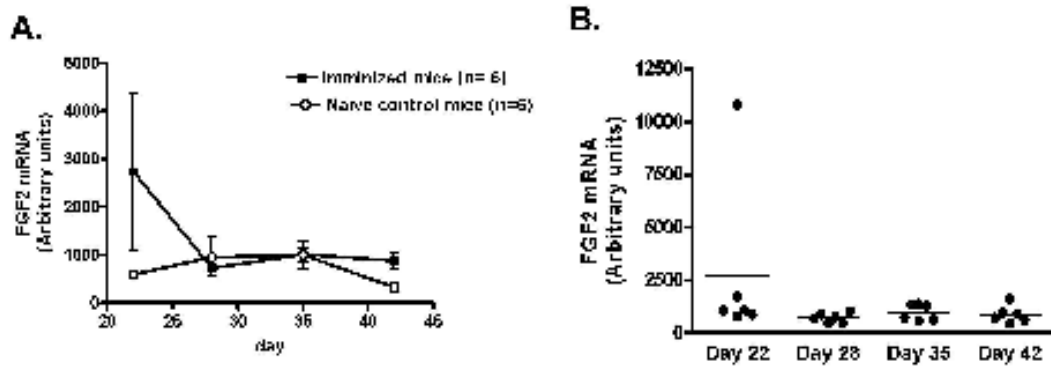


Figure 4.23 Time-course of a growth factor (FGF2) mRNA levels in brains of CII immunized mice by Real-time PCR

(A) Mice immunized with type II collagen (filled squares) were culled on days 22, 28, 35, 42 and brain from CII immunized mice at all time points were harvested. Brain samples collected from naïve control mice (open circle) culled on the days indicated were used as controls. FGF2 mRNA levels in brain tissue homogenate of mice from all experimental groups were determined using a real-time PCR assay. The levels of FGF2 mRNA were normalized against GAPDH expression and shown as arbitrary units. Data represent means \pm SEM. (n = 6 CII immunised mice/group). Statistical analysis of data was performed using two-way ANOVA compared with naïve control mice. (B) shows longitudinal changes of brain FGF2 in CII immunized mice culled on the days indicated. Bars represent mean values: (*P < 05; **P < 01; ***P < 001 by one-way ANOVA analysis).

Two-way ANOVA analysis followed by Bonferroni posttests demonstrated that brain VEGF gene expression levels were elevated in CII immunized mice compared to those in naïve control mice on day 28 and day 35 ($P = 0.0005$). The mean value of brain VEGF gene expression (CII immunized versus naïve control) on day 28 were 10265 ± 3384 versus 4261 ± 2141 ($P = 0.0043$), while the mean value of brain VEGF gene expression (CII immunized versus naïve control) on day 35 were 16860 ± 8380 versus 4829 ± 1158 ($P = 0.0059$) (Figure 4.24A). One-way ANOVA demonstrated that there was no significant difference in brain VEGF mRNA level of immunized mice at different time points (Figure 4.24B).

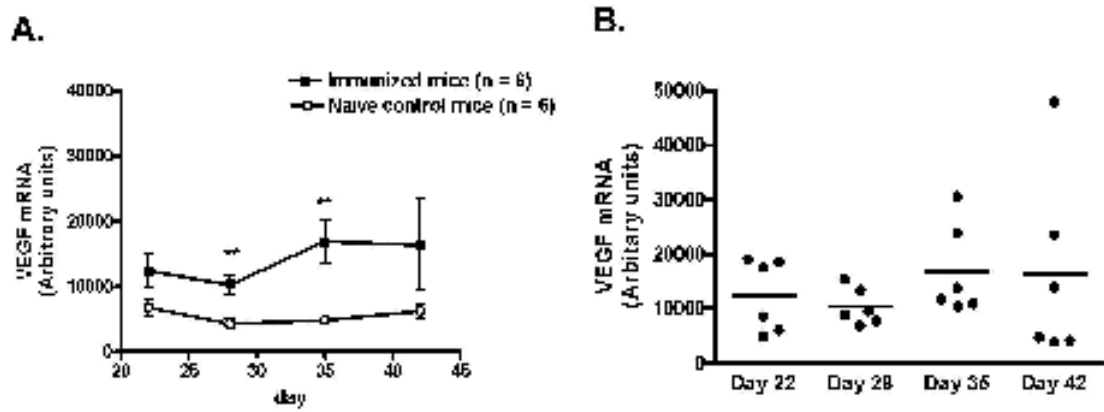


Figure 4.24 Time-course of a growth factor (VEGF) mRNA levels in brains of CII immunized mice by Real-time PCR

(A) Mice immunized with type II collagen (filled squares) were culled on days 22, 28, 35, 42 and brain from CII immunized mice at all time points were harvested. Brain samples collected from naïve control mice (open circle) culled on the days indicated were used as controls. VEGF mRNA levels in brain tissue homogenate of mice from all experimental groups were determined using a real-time PCR assay. The levels of VEGF mRNA were normalized against GAPDH expression and shown as arbitrary units. Data represent means \pm SEM. (n = 6 CII immunised mice/group). Statistical analysis of data was performed using two-way ANOVA compared with naïve control mice: **P<0.01. (B) shows longitudinal changes of brain VEGF in CII immunized mice culled on the days indicated. Bars represent mean values: (*P < 05; **P < 01; ***P < 001 by one-way ANOVA analysis).

4.2.5.6 Differences in inflammatory mediator mRNA levels in brain of arthritic mice and non-arthritic mice

We also compared mRNA levels of inflammatory mediators including IL-12, CXCL1, CXCL10, FGF2 and VEGF. There were no significant differences in brain mRNA levels of IL-12 CXCL10, FGF2 and VEGF between arthritis and non-arthritis mice on day 35 and day 42 (Figure 4.25A-Figure 4.25D).

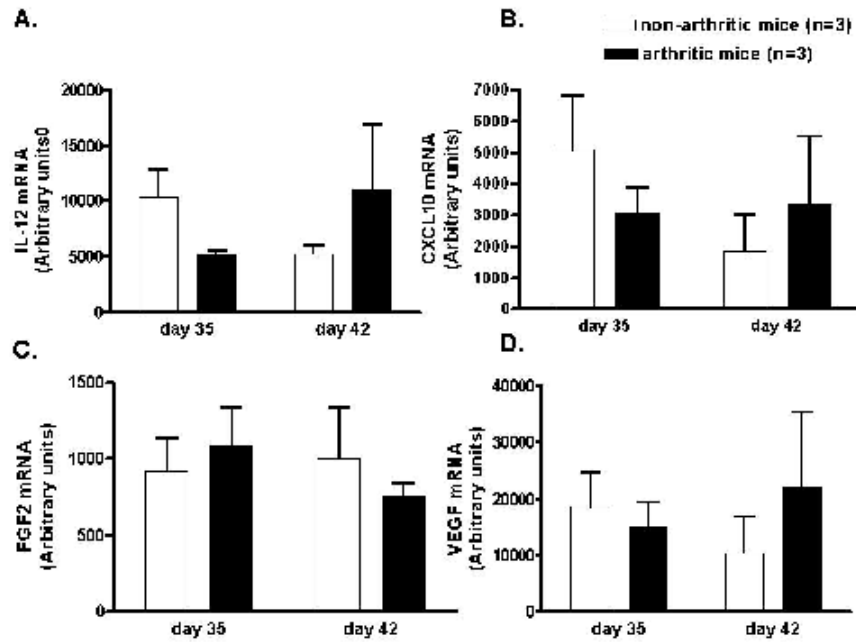


Figure 4.25 Differences in inflammatory mediator mRNA levels in brains of arthritic mice and non-arthritic mice
 (A), (B), (C) and (D) show inflammatory mediator protein levels (pg/mg total brain protein) in brains of CII immunized mice with and without arthritis (n =3 CII immunised mice/group) on day 35 and day 42. Data are presented as the mean \pm S.D. (*P < 05; **P < 01; ***P < 001 by Student's t test.)

Interestingly, a significant difference in brain CXCL1 mRNA levels between arthritic and non-arthritic mice was observed on day 35, which was similar to brain CXCL1 protein profile of arthritic and non-arthritic mice on day 42. Arthritic mice on day 35 showed a significant increase in brains CXCL1 gene expression levels compared to those in brains of non-arthritic mice on day 35. The mean value of brain CXCL1 gene expression (arthritic versus non-arthritic) on day 35 were 6908 ± 1255 versus 4283 ± 1037 ($P = 0.0493$) (Figure 4.26B).

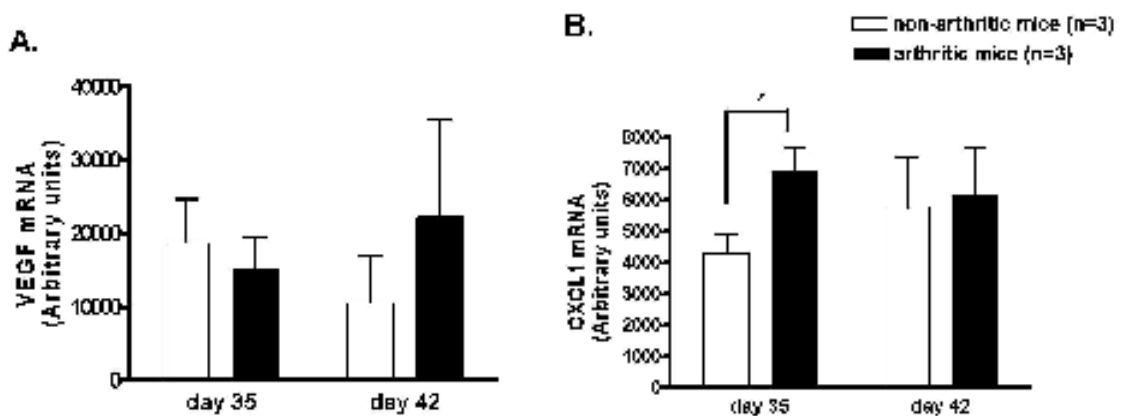


Figure 4.26 Differences in CXCL1 mRNA levels in brains of arthritic mice and non-arthritic mice
 Brain CXCL1 mRNA levels (pg/mg total brain protein) in arthritic (n=3 arthritic mice) and non-arthritic (n=3 non-arthritic mice) were compared on day 35 and day 42. Data are presented as the mean \pm S.D. (*P < 05; **P < 01; ***P < 001 by Student's t test.)

4.2.6 Comparison between time course changes in inflammatory mediator protein and mRNA levels in brain of CII immunized mice

Both mRNA and protein expression of IL-12, CXCL1, VEGF and FGF2 were detectable and longitudinal changes of these inflammatory mediators were observed in brains of immunized mice. The comparison between overall trends in inflammatory mediator protein and mRNA levels may provide some evidence of how the periphery induces central inflammatory mediator production and the possible cellular sources of these inflammatory mediators in the brain of CII immunized mice.

Our data showed that the overall trends of time course profiles of inflammatory mediator protein concentrations were not similar to the time course profiles of the same inflammatory mediator gene expression in brain of immunized mice. However, overlapping or parallel trends of time course profiles of brain inflammatory mediator protein concentrations and brain gene expression were observed at some time points.

4.2.6.1 Comparison between time course changes in Th1 cytokine protein and mRNA expression levels in brain of CII immunized mice

Longitudinal changes of both mRNA expression levels and protein concentrations of IL-12, a Th1 cytokine, were observed in brains of CII immunized mice compared to those of naïve control mice. Parallel trends of time course profiles of brain IL-12 protein concentration and gene expression in CII immunized mouse brains was observed during days 22 to 28 after immunization. Differences between IL-12 protein concentration and gene expression were observed from day 28 onwards. While brain IL-12 protein concentrations continued to decrease gradually, an increase in IL-12 gene expression levels was observed during the same period and this was followed by an unchanged IL-12 gene expression level (Figure 4.27). This data suggest that there may be migration of peripheral Th1 cells into the brain or induction of local production of IL-12 during the period of onset of disease (day 22-day 28 after immunization). The migration of these peripheral Th1 cells may continued throughout the acute and chronic phases of CIA experimental course, indicated by the prolong expression of IL-12 protein during day 28 to day 42 after immunization. However, the concentrations of the

Th1 cytokine migration may be reduced over time during day 28-day 42 and not as much as the period of disease onset. By contrast, mRNA expression levels of IL-12 increased during day 28 to day 42 after immunization, suggesting that there may be induction of the local production of IL-12 in brains of CII immunized mice throughout the period of acute and chronic phases of disease (Figure 4.27).

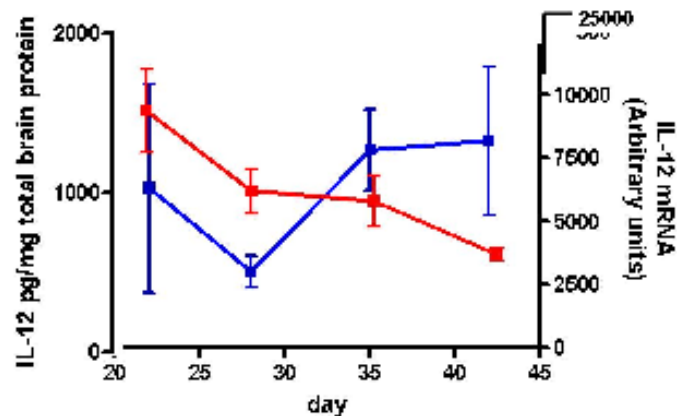


Figure 4.27 Longitudinal changes of a Th1 (IL-12) cytokine protein concentrations and mRNA expression levels in brains of CII immunized mice

Brain samples collected from CII immunized mice culled on the days indicated were harvested. Half brain samples were processed for protein quantification by an ELISA assay (red filled squares), while the other half brain was processed for mRNA quantification and real-time PCR (blue filled squares). Data represent means \pm SEM ($n = 6$ CII immunised mice/group). IL-12 protein concentrations in brain tissue, normalized against total brain protein, are expressed as pg/ μ g total brain protein. IL-12 mRNA levels in brain tissue, normalized against the expression of housekeeping gene GAPDH, are presented as arbitrary units.

4.2.6.2 Comparison between time course changes in chemokine protein and mRNA levels in brain of CII immunized mice

Trends of time course profiles of brain CXCL1 protein concentrations and gene expressions in immunized mouse brains fluctuated during day 22 to day 35 after immunization. Brain CXCL1 protein and gene expression levels decreased on day 28 and then increased back on day 35. However, the divergence in trends of time course profiles of brain CXCL1 protein concentrations and gene expressions was observed during the final period. A gradual increase in CXCL1 gene expression was observed during day 35 to day 42, while CXCL1 protein concentrations in immunized mouse brains decreased slightly during the same period (Figure 4.28). CXCL1 in the brain is produced mainly by microglia (Brown et al., 2010). The overlap between CXCL1 gene and protein expression in brains

of CII immunized mice may suggest the local production of CXCL1 by microglia over the period of onset and acute phase of CIA experimental course. It was also possible there may be the transportation of CXCL1 into the brains of these CII immunized mice, which was reduced during the late disease phase (day 35–day 42 after immunization). However, in that period the gene expression of CXCL1 still increased, suggesting the continuous production of CXCL1 by CNS immune cells in the chronic phase of disease.

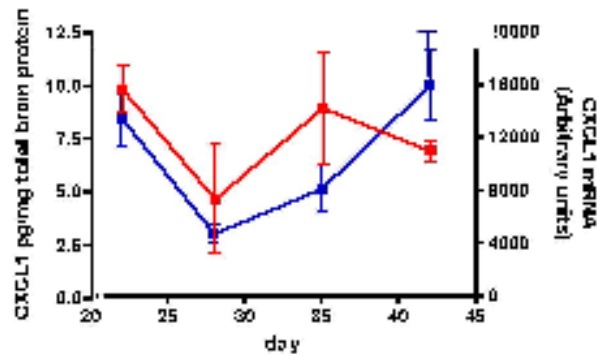


Figure 4.28 Longitudinal changes of a chemokine (CXCL1) protein concentrations and mRNA expression levels in brains of CII immunized mice

Brain samples collected from CII immunized mice (open circle) culled on the days indicated were harvested. Half brain samples were processed for protein quantification by a Luminex assay (red filled squares), while the other half brain was processed for mRNA quantification and real-time PCR (blue filled squares). Data represent means \pm SEM ($n = 6$ CII immunised mice/group). CXCL1 protein concentrations in brain tissue, normalized against total brain protein, are expressed as pg/ μ g total brain protein. CXCL1 mRNA levels in brain tissue, normalized against the expression of housekeeping gene GAPDH, are presented as arbitrary units.

4.2.6.3 Comparison between time course changes in growth factor protein and mRNA levels in brain of CII immunized mice

The overall trends of longitudinal changes of brain FGF2 protein concentrations was similar to those of brain FGF2 gene expression in immunized mice across all the time points. Parallel trends of time course profiles of brain FGF protein concentrations and gene expressions in immunized mouse brains was observed during day 22 to day 28 after immunization. The trend of time course profile of brain FGF protein concentrations remained unchanged during day 28 and day 35, followed by a slight decrease until the terminal day. In contrast, brain FGF2 gene expression levels slightly increased during day 28 and day 35 and then the expression level of FGF mRNA remained unchanged until day 42 (Figure 4.29). The similarity on the overall trends between FGF2 gene and protein expression

throughout the period of CIA experimental period may suggest local production of FGF2 in the brains (Figure 4.29).

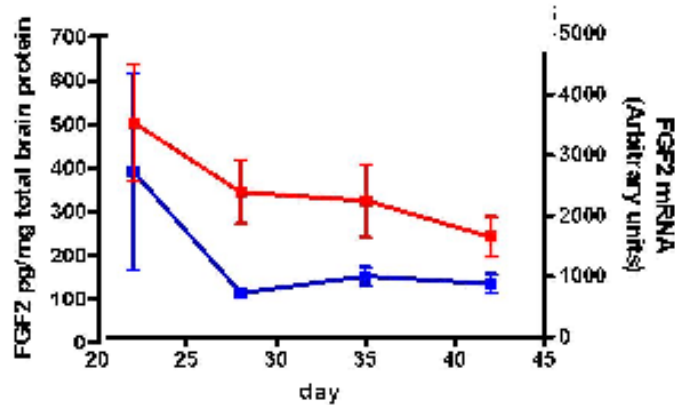


Figure 4.29 Longitudinal changes of a growth factor (FGF2) protein concentrations and mRNA expression levels in brains of CIA immunized mice

Brain samples collected from CIA immunized mice (open circle) culled on the days indicated were harvested. Half brain samples were processed for protein quantification by a Luminex assay (red filled squares), while the other half brain was processed for mRNA quantification and real-time PCR (blue filled squares). Data represent means \pm SEM ($n = 6$ CIA immunised mice/group). FGF2 protein concentrations in brain tissue, normalized against total brain protein, are expressed as pg/ μ g total brain protein. FGF2 mRNA levels in brain tissue, normalized against the expression of housekeeping gene GAPDH, are presented as arbitrary units.

The overall trends of longitudinal changes of VEGF protein concentrations were quite similar to those of time course profiles of VEGF gene expressions in brain of CIA mice across all the time points. The overall trends of time course profiles of VEGF protein concentrations overlapped those of VEGF gene expression levels. Increases in both brain VEGF gene expressions and protein concentrations were observed in immunized mouse brain during day 28 and day 35. However, trends of both brain VEGF gene and protein expression profiles were divergent during the last period. While brain VEGF gene expression levels remained unchanged from day 35 to 42, protein concentrations of VEGF decreased during the same period (Figure 4.30). These data suggest that the majority of VEGF detectable in CIA immunized mice may be produced locally in the brain.

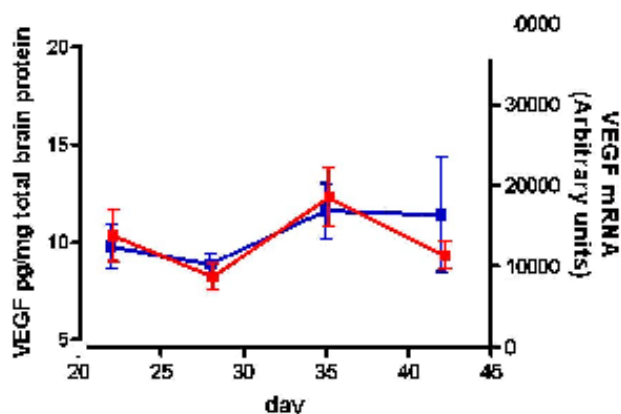


Figure 4.30 Longitudinal changes of a growth factor (VEGF) protein concentrations and mRNA expression levels in brains of CII immunized mice. Brain samples collected from CII immunized mice (open circle) culled on the days indicated were harvested. Half brain samples were processed for protein quantification by a Luminex assay (red filled squares), while the other half brain was processed for mRNA quantification and real-time PCR (blue filled squares). Data represent means \pm SEM ($n = 6$ CII immunised mice/group). VEGF protein concentrations in brain tissue, normalized against total brain protein, are expressed as pg/ μ g total brain protein. VEGF mRNA levels in brain tissue, normalized against the expression of housekeeping gene GAPDH, are presented as arbitrary units.

4.2.7 Summary; longitudinal changes in mRNA and protein concentrations in brain of CII immunized mice

In this experiment we determined changes in inflammatory mediators in brain of arthritic mice in 4 time points, which represented different stages of inflammatory joint disease. Therefore, 42 day period of CIA experimental course was divided into 3 phases. The period of disease onset was defined as day 22-day 28 after immunization, early disease phase was defined as day 28-day 35 after immunization, and the transition to the late disease phase was defined as day 35 to day 42 after immunization. We found elevation of mRNA and protein concentrations of various brain inflammatory mediators, including IL-1 β , TNF- α , IL-4, IL-12, IL-2, IL-10, CCL2, CXCL1, CXCL10, VEGF and FGF2 in different phases of CIA experimental course (Table 4.2).

Cytokines, chemokines Growth factors	Day 22		Day 28		Day 35		Day 42	
	protein	gene	protein	gene	protein	gene	protein	gene
IL-1 β	\uparrow 0.0235	undt	NS	undt	NS	undt	NS	undt
TNF- α	NS	undt	NS	undt	\uparrow 0.0113	undt	\uparrow 0.0075	undt
IL-4	\uparrow 0.0015	undt	\uparrow 0.0037	undt	NS	undt	NS	undt
IL-10	\uparrow <0.0001	undt	\uparrow <0.0001	undt	\uparrow 0.0003	undt	\uparrow 0.0003	undt
IL-2	NS	undt	NS	undt	\uparrow 0.0357	undt	NS	undt
IL-12	\uparrow 0.0018	NS	\uparrow 0.0009	NS	\uparrow 0.02	\uparrow 0.0264	\uparrow <0.0001	NS
CCL2	\uparrow 0.0118	undt	\uparrow 0.0238	undt	NS	undt	\uparrow 0.0125	undt
CXCL1	NS	\uparrow 0.0001	NS	NS	NS	NS	NS	\uparrow 0.007
CXCL10	undt	NS	undt	\uparrow 0.0154	undt	\uparrow 0.0105	undt	NS
VEGF	NS	NS	NS	\uparrow 0.0043	NS	\uparrow 0.0059	\uparrow 0.0219	NS
FGF2	NS	NS	NS	NS	NS	NS	\uparrow 0.0402	NS

Table 4.2 Longitudinal changes in concentrations brain inflammatory mediator profiles in brains of CII immunized mice relative to those of those in control mice
Red arrows represent an increase of inflammatory mediator protein concentrations, while blue arrows represent an increase of inflammatory mediator mRNA expression levels in brains of CII immunized mice compared to those in naïve control mice on day 22, day 28, day 35 and day 42 after immunization. Differences between inflammatory mediator concentrations in CII immunized mouse brains and naïve control groups were analyzed by Student's t- test (*P < 05; **P < 01; ***P < 001). NS = not statistically significant, undt = undetectable.

During the period of onset of arthritis disease (day 22 - day 28 after immunization) in CII immunized mice, we found transient elevation of IL-1 β protein concentrations in brains of these CII immunized mice. IL-1 β has been reported to regulate the production of CXCL in the CNS (Shaftel et al., 2007). Therefore, the increased in concentrations of brain IL-1 β protein may be associated with the elevation of CXCL1 mRNA, which was also increased transiently at the same period of time. From day 22 after immunization onwards, protein concentrations of both Th1 (IL-12 and IL-2) and Th2 (IL-4 and

IL-10) cytokines started to increase. The prolonged elevation of brain IL-12 protein concentrations in CII immunized mice were observed throughout the CIA experimental course (day 22 - day 42 after immunization), while elevation of IL-12 mRNA levels were only observed on day 35. This suggests that the majority of IL-12 protein may be transported from the periphery and may be via the recruitment of peripheral Th1 into the CNS. The concentrations of IL-2 in brains of CII immunized mice also peaked on day 35, at the end of the acute phase of the CIA experimental course. Interestingly, the IL-12 protein concentrations started at the beginning of disease onset before the peak of CXCL10, a potent recruiter of Th1 lymphocytes, during day 28 and day 35 after immunization. This may suggest the influx of Th1 cells may be apparent during the early phase of the disease course. The prolonged elevation of Th2 cytokines, particularly IL-10 were also observed throughout the CIA experimental course (day 22 - day 42 after immunization), although the brain IL-4 protein concentrations were only increased during the period of onset of arthritis disease and the concentrations were reduced towards the end of the CIA experimental course. Interestingly, the prolonged elevation of Th2 cytokines seemed to correspond to the prolonged up-regulations of CCL2 protein in the brains of CII immunized mice throughout the period of the CIA experimental course. CCL2 is known to regulate the trafficking of Th2 cells into the inflamed site. Therefore, the coincidence between CCL2 and Th2 cytokines suggested that there may be recruitment of Th2 lymphocytes from the periphery into the brain. We found increased concentrations of the growth factors FGF2 and VEGF, which are angiogenic factors that have been reported to be associated with BBB breakdown during the neuro-inflammatory process, especially during the early phase of the disease. The coincidental elevation of these growth factors (VEGF, FGF2) and chemokines such as CXCL1 and CXCL10 during day 28 - day 35 after immunization may suggested that BBB breakdown and the recruitment of peripheral immune cells into the brain during the early phase of CIA experimental course may be regulated by peripheral inflammatory cytokine signals.

4.3 Result chapter 4: Summary of major findings.

The aim of this chapter was to investigate longitudinal changes of brain inflammatory mediators that may be associated with longitudinal changes in peripheral inflammatory mediators and the development and the progression of

arthritis disease in CII immunized mice. We determined changes in brain inflammatory mediators in CII immunized mice in 3 phases across the 42-day period of the CIA experimental course. Day 22 - day 28 after immunization was the period of disease onset, day 28 - day 35 after immunization was the acute phase of disease and day 35 - day 42 after immunization was the transition to chronic phase of the disease. We found:-

1. Transient elevation of serum IL-1 β , IL-5, CCL2 and FGF2 protein concentration during the period of onset of disease (day 22 - day 28 after immunization) in CII immunized mice. This was followed by a reduction in these serum inflammatory mediator concentrations during the acute and chronic phases of disease development.
2. Transient elevation of pro-inflammatory cytokine IL-1 β protein concentration during the onset of disease in the brains of CII immunized mice. In contrast, an elevation of brain TNF- α protein concentration was observed in brains of CII immunized mice during the late disease stage (day 35-day 42 after immunization).
3. Prolonged elevation of the Th1 cytokine IL-12 concentration in brains of CII immunized mice throughout the CIA experimental period, while a peak of IL-2 protein in the brains of CII immunized mice was observed on day 35 after immunization.
4. Prolonged elevation of the Th2 cytokine IL-10 protein concentration in brains of CII immunized mice throughout the CIA experimental period, while IL-4 protein concentration was elevated in brains of CII immunized mice only during the period of onset of the disease (day 22 - day 28 after immunization).
5. Transient elevation of brain CXCL1 mRNA expression in brains of CII immunized mice during the onset of the disease (day 22 after immunization) and at the end of the CIA experimental course (day 42 after immunization)
6. Prolonged elevation of the chemokine CCL2 protein concentration in brains of CII immunized mice throughout the CIA experimental period.

7. Coincidental increase of CXCL10 and VEGF mRNA expression levels in brains of CII immunized mice during the acute phase of the disease (day 28-day 35 after immunization).

8. The FGF2 and VEGF protein concentrations and mRNA expression levels in brains of CII immunized mice started to increase from day 28 after immunization onwards.

9. There was no significant difference in brain mRNA expression levels of IL-12, CXCL10, VEGF and FGF2 and protein concentrations of IL-1 β , TNF- α , IL-2, IL-12, IL-4, IL-10, CCL2, VEGF and FGF2 between arthritic and non arthritic mice on day 35 and day 42. However, there were differences in CXCL1 gene expression levels and protein concentrations between arthritic and non-arthritic mice on day 35 and day 42.

10. Overlapping or parallel trends of time course profiles of brain IL-12 and CXCL1 protein concentrations and gene expression in brains of CII immunized mice were observed at some time points across the 42-day period of CIA experimental course. However, the divergence between IL-12 and CXCL1 gene and protein concentrations was observed during the transition to the chronic phase of the disease. The concentrations of brain IL-12 and CXCL1 protein were reduced between day 35 and day 42 after immunization, while mRNA expression levels of IL-12 and CXCL1 in brains of were increased during that period.

11. Overlapping or parallel trends of time course profiles of brain FGF2 and VEGF protein concentrations and gene expression in brains of CII immunized mice were observed at some time points across the 42-day period of CIA disease course.

4.4 Discussion

In this chapter we investigated the possible mechanism by which peripheral inflammation, ie serum cytokines, induced production of brain inflammatory mediators in CII immunized mice. We found increased concentrations of serum IL-1 β , IL-5, CCL2 and FGF2 in CII immunized mice (day 22 - day 28 after immunization), suggesting they provided a possible inflammatory signal during the onset and the early disease period. We also found increased concentrations of these same inflammatory mediators (IL-1 β , CCL2 and FGF2) in the brain during the onset of the disease, suggesting the possible transportation of these inflammatory mediators from the periphery into the brain of CII immunized mice, or alternatively local synthesis. In addition, we demonstrated coincidental increase of serum concentrations and mRNA expression levels of inflammatory mediators, for example, IL-1 β and CXCL1 or FGF2 and VEGF during the same CIA experimental period, and these cytokines can mutually regulate each other. This could be important evidence suggesting that the peripheral inflammatory cytokine signal may induce local production of inflammatory mediators in brains of CII immunized mice during the onset and the early disease period. For example, it is possible that the production of brain CXCL1 and VEGF production may be induced via the peripheral inflammatory cytokine signals of IL-1 β and FGF2 during the onset and the early disease period. We demonstrated the up- and down-regulation of different inflammatory mediators in brains of CII immunized mice at different time point over the CIA disease course. In addition, we also showed a prolonged increase of the concentration of the Th1 inflammatory cytokine IL-12, which was coincidental with down-regulation of Th2 anti-inflammatory cytokine IL-4 in brains of CII immunized mice. These data suggest that there may be an interplay and regulation between brain inflammatory mediators, which indicates the possible immune activation and inflammatory process in the brains of CII immunized mice. We therefore set out to discuss and interpreted our data in detail separately in 3 main aspects; (i) peripheral inflammation signal in CII immunized mice; (ii) peripheral inflammation-induced brain inflammation in CII immunized mice; (iii) the possible interplay between inflammatory mediators in brains of CII immunized mice.

4.4.1 Longitudinal changes in peripheral inflammatory mediators in CII immunized mice.

We analysed changes in inflammatory mediator protein concentrations in the peripheral circulation of CIA mice by using a Luminex multi-analyte assay to determine changes in serum cytokines, chemokines and growth factor protein concentrations in CIA mice across all time points of the disease course. We found increased concentrations of serum IL-1 β , IL-5, CCL2 and FGF2 in CII immunized mice during the onset of disease (day 22 and day 28), suggesting these inflammatory mediators may play crucial roles at different pathological stages in the development of disease. IL-1 β is considered to be a key cytokine in the RA process (Koenders et al., 2008) and up-regulation of IL-1 β has been reported in the joints of CIA mice during the onset of disease. A time course study in joint cytokine expression in CIA mice showed transient expression of pro-inflammatory cytokines IL-6, IL-1 β and TNF- α during the period of 15 days after immunization. mRNA and protein concentrations of IL-6 increased sharply by day 1, while TNF- α concentration showed a significant increase occurring on days 4 to 8. IL-1 β concentration was up-regulated on day 4 and its concentration remained significantly high until the onset of the disease. These data suggest that pro-inflammatory cytokines may induce the disease development in this model shortly after the primary sensitisation / immunization, and that changes in serum cytokines may be observed in this model in the early (onset of the disease) period of time after immunization (Rioja et al., 2004). However, most studies in CIA models showed that the IL-1 β concentrations in serum of CIA mice were low or undetectable. A time course study by Marije et al., showed that IL-1 β serum concentration in CIA mice did not increase over time throughout the CIA experimental course (Koenders et al., 2008). Another study by J-M Kim et al., showed that the IL-1 β serum concentration in CIA mice on day 40 after immunization was undetectable, but there was marked increase of IL-1 β in the joints of CIA mice, suggesting that IL-1 β protein may not necessarily be increased in the blood during the joint inflammatory process, but the increase of IL-1 β in the joint may be more important for the development of arthritis in the CIA model (Kim et al., 2003). We also found an increased concentration of the Th2 cytokine IL-5 in serum of these CII immunized mice during the period of onset of arthritis disease (day 22-day 28) after immunization. Our data was

consistent with a previous study by Schaefer et al., showing up-regulation of IL-5 protein in serum of CIA mice (Schaefer et al., 1999). Our data, combined with this previous report, suggests that IL-5 and Th2 cells may play an important role in the development of arthritis. This premise is supported by clinical studies showing that raised concentrations of Th2 cytokines such as IL-4, IL-5, IL-10 and IL-13 were predominately detected in RA synovial fluid during the early stage of disease (Hitchon et al., 2004); (Hitchon and El-Gabalawy, 2002). A transient increase of serum CCL2 protein concentration was observed in these CII immunized mice during the period of onset of disease (day 22-day 28), followed by a marked decrease over time throughout the early and the late disease phases. A similar longitudinal change in serum CCL2 protein profile has been reported previously in a study in arthritic rats by Stolina *et al.*, (Stolina et al., 2009). CCL2 is chemotactic for monocytes and Th2 cells, and this chemokine has been detected in high concentrations in synovial fibroblasts from RA patients (Szekanecz et al., 2003), especially in response to IL-1 and TNF- α . The main function of CCL2 during the onset of arthritis disease may be the recruitment of Th2 cells into the joint. This premise is supported by our finding showing the coincidental increase of serum CCL2 and IL-5 concentrations in CII immunized mice during the same period of onset of disease. The association between CCL2 and IL-5 has also been demonstrated in CCL2 deficient mice. Lower production of Th2 cytokines including IL-4, IL-5 and IL-10 and an inability to produce specific antibodies were observed in CCL2 deficient mice (Gu et al., 2000). This finding suggests that CCL2 might also regulate the production of Th2 cytokines. The presence of increased concentrations of this serum chemokine in immunized mice during the onset of the disease suggests that there could be increased immune cell migration into the inflamed tissue that may be associated with angiogenesis. We also found significantly increased concentrations of serum FGF2, an angiogenic factor, in immunized mice during the onset and development of disease. This increased concentration of FGF2 may be associated with the process of cartilage and bone erosion including synoviocyte proliferation and osteoclastogenesis, that has been shown to be highly active during the onset of disease (Malemud, 2007); (Stolina et al., 2009).

However, during the early and late disease phase (day 28 - day 35 after immunization), our Luminex data showed reducing serum concentrations of

several inflammatory mediators, including IL-1 β , IL-5, CCL2 and FGF2 in immunized mice. Several studies report the same observation; showing transient increases in serum cytokine concentrations during the onset of disease that became undetectable during the period of clinical manifestation of disease. A study by Tsuji *et al.*, in which time-course changes in serum cytokine profiles in CIA mice were also determined by Luminex over the course of the experimental disease (Tsuji *et al.*, 2009). They reported transient increases of various cytokines, including IL-12, TNF- α , IFN- γ , IL-9, IL-17 and CCL4 in serum of CIA mice after the primary immunization and the concentrations of these serum cytokines reached their peak on day 22. This was followed by a reduction of serum protein concentrations of these cytokines from day 22 onwards (Tsuji *et al.*, 2009). Another study by Asquith *et al.*, 2009 also demonstrated that protein concentrations of several cytokines and chemokines, including IL-1 α , IL-6, IL-17, CCL2, CCL3 and CCL6 in serum of CIA mice on day 31 were at or lower than the detection limits of the assays, and this suggest that there was no elevation of serum inflammatory mediators in CIA mice during the early phase of disease (Asquith *et al.*, 2009a). In addition, several studies demonstrated that serum cytokine concentrations in CIA mouse model were inconsistent and in many cases undetectable as was consistent with our results (Harnett *et al.*, 2008); (Lu *et al.*, 2010); (del Rey *et al.*, 2008). There are several explanations underlying the absence or the undetectable concentrations of serum cytokines in CIA mice during the late disease phase. One possibility is that these inflammatory mediators are generated locally at the inflammatory site and also function locally to induce bone and cartilage destructive process, but may not circulate in the bloodstream. This has been demonstrated by several studies in CIA mice showing high expression of inflammatory mediators in inflamed joints, but undetectable concentrations in the serum (Lu *et al.*, 2010); (Palmlblad *et al.*, 2001). Another possibility is that the distribution of inflammatory mediators and immune cells from inflamed sites to adjacent tissues may be mainly via the lymphatic system rather than via the bloodstream. This is supported by a study of lymphatic vessels draining foot joints of RA patients showing several-fold higher concentrations of lymph cytokines and chemokines than the serum cytokine concentrations. High flow rates of lymphatic vessels containing high cytokine concentrations through the regional lymph nodes observed in RA patients may reflect the activity of lymphatic vessels to transport immune cells

and inflammatory mediators from the inflammation site to the periphery (Olszewski et al., 2001).

4.4.2 Association between peripheral inflammation and increased concentrations of brain inflammatory mediators: possible evidence that peripheral inflammatory cytokine signals induce neuro-inflammation.

The model of systemic LPS challenge showing that peripheral inflammation could induce brain inflammation has been well documented (Datta and Opp, 2008), (Laye et al., 1994); (Quan et al., 1994); (Gatti and Bartfai, 1993); (Breder et al., 1994); (Gabellec et al., 1996); (Grinevich et al., 2001). One study by de Ray *et al* is the only study that demonstrated an association between peripheral joint inflammation and inflammation in the brain of CIA rats, which is an equivalent model of a chronic autoimmune disease to the murine model used in this thesis (del Rey et al., 2008). However, the communication between joint-immune system-brain in the CIA model was not well documented in that study. We first investigated the possibility that peripheral inflammation induced brain inflammation in brains and serum of CII immunized mice by using a Luminex and PCR assays to quantify gene expression and protein concentrations of inflammatory mediators. We found that IL-1 β , CCL2, FGF2 and Th2 cytokine proteins were increased in brains of CII immunized mice as well as in their serum, compared to those in naïve control mice. Our data suggest that the peripheral inflammation may signal brain inflammatory cytokine production via IL-1 β , CCL2, FGF2 and Th2 cells during the course of arthritis.

We found transient increases in brain IL-1 β protein during the onset of disease in CII immunized mice, which corresponded to a transient elevation of serum IL-1 β . A similar coincidental increase of IL-1 β in the periphery and in the brain of CIA rats has been reported previously by del Ray *et al* (del Rey et al., 2008). However, we found no corresponding IL-1 β mRNA expression levels in brains of these CII immunized mice, suggesting there may be no local IL-1 β production in the brain. Our data, combined with the finding of the previous report suggest the possibility that there may be a contribution of IL-1 β from the periphery into the brain of CII immunized mice during the course of disease. There was one study that suggested that IL-1 β can be transported into the brain by a saturable

mechanism, suggesting a specific receptor (Banks et al., 1991). However, the mechanism of how IL-1 β protein could be transported into the brain of CII immunized mice during the period of disease onset needs to be further investigated. The increase of IL-1 β protein concentration in the serum of CII immunized mice was coincidental with transient increases in brain CXCL1 mRNA expression levels during the onset of the disease (day 22 after immunization). It is possible that peripheral IL-1 β may signal brain immune cells such as microglia to produce CXCL1 in brain CII immunized mice. This is supported by *in vivo* and *in vitro* studies demonstrating that increases in concentrations of brain IL-1 β can induce CXCL1 production in the brain by microglia (Shaftel et al., 2007).

TNF- α was another pro-inflammatory cytokine that was up-regulated in the brains of arthritic mice during the early and late stages of disease. However, we could not define the source of this TNF- α protein in the brains of these CII immunized mice, since brain TNF- α mRNA and serum TNF- α were undetectable in CII immunized mice in this study. This is difficult to explain but is similar to a study by de Ray who also reported that TNF- α was detectable in the brain of arthritic rats, despite no detectable serum TNF- α . It has been reported that TNF- α protein was detected in high concentration in the peripheral tissue such as peritoneal cavity and spleen of CIA mice during the early and late stages of disease (Stasiuk et al., 1996); (Mussener et al., 1997). It is still unclear how TNF- α from the periphery might have affected the brain during the period of clinical manifestation of disease, despite no TNF- α detectable in the serum. This problem needs to be further investigated, perhaps by using peripheral administration of TNF-blockade into the CII immunized mice during the early and late stage of disease and determine changes in brain cytokines. These experiments will form Chapter 6 of this thesis.

Prolonged increased concentrations of CCL2 were observed in the brains of CII immunized mice throughout the CIA experimental course, which may be associated with transient increases of serum CCL2 during the period of disease onset (day 22 and day 28). Our data seem to suggest that there may be a contribution of CCL2 from the periphery into the brain during the period of disease onset (day 22 and day 28). The prolonged increased concentration of CCL2 in the brain of CII immunized mice continued until the end of the CIA experimental course, suggesting that there may be local production of CCL2 in

the brain after the onset of disease. However, we found no CCL2 gene expression in brains of CII immunized mice over the period of early and late phases of the disease. This seems to suggest that there may be an accumulation of CCL2 in the brains of CII immunized mice after the period of the disease onset. Prolonged increased concentrations of CCL2, a potent chemotactic factor of Th2 lymphocytes, may potentially be associated with increased concentrations of Th2 cytokines, including IL-4 and IL-10 in the brains of CII immunized mice during the disease process. However, we could not demonstrate the presence of any Th2 cytokine in the brains of CII immunized mice in our study. However, we found a coincidental increase of CCL2 and Th2 cytokines in both serum and in the brains at the same period of time, suggesting that there may be trafficking of Th2 cells, regulated by CCL2, from the periphery into the brain of CII immunized mice. This premise was supported by a study in the mouse model of liver injury showing that peripheral hepatic inflammation induced brain microglia to produce CCL2, which was followed by infiltration of monocytes into the brains (D'Mello et al., 2009). This evidence also suggests that CCL2 up-regulated during the early and late disease phase may be associated with an increase of TNF- α , which is produced mainly by monocytes, during the same period of time. However, the hypothesis that CCL2 recruits Th2 cells and monocytes into the brains of CII immunized mice needs to be further investigated perhaps by using immuno-histochemistry for Th2 cells and monocyte markers in CIA brain tissues.

We also found prolonged increased concentrations of IL-12 in the brains of CII immunized mice across all CIA experimental periods. Increases in IL-12 mRNA expression levels were also observed in these CII immunized mice, particularly at the late phase of the disease. This is in contrast to brain Th2 cytokines, for which their mRNA expression levels were undetectable. This may suggest a difference in the location at which these Th1 and Th2 were activated and the origin of these Th1 and Th2 cells before potentially migrating into the brains of these CII immunized mice. The pathological mechanism of the joint destruction in RA is thought to be driven by Th1 cells and Th1 cytokines, including IL-12, and IL-2 can be detected in lymph node, spleen and joints of CIA mice throughout the period of onset and early disease (Okamoto et al., 2000); (Mussener et al., 1997). However, we found no IL-12 or any Th1 cytokine elevated in the serum of

these CII immunized mice. This suggests that there is a possibility that there was no trafficking of Th1 from the periphery into the brains of CII immunized during the course of arthritis. Instead, up-regulation of IL-12 mRNA in brains of these CII immunized mice suggests that IL-12 may be produced from CNS T cells. The mechanism of CNS T cells activation has been well documented in model of neuro-inflammatory disease such as EAE, where the inflammatory demyelination development is driven by autoreactive Th1 cells (Klein, 2004). Although the pathological mechanism of EAE is thought to be due to autoreactive Th1 T cells that invade the CNS, several studies in EAE suggested that the major source of Th1 cells were activated within the CNS. A study by Greter *et al*, in mice that lacked secondary lymphoid tissue showed that activation of T cells in the presence of a cognate antigen occurred in the brain, and that T-cell trafficking to APCs located in secondary lymphoid tissues was not necessarily to initiate tissue destruction (Greter et al., 2005). This has been confirmed by another study (Juedes and Ruddle, 2001) showing that CNS T cells produce cytokines such as TNF- α and IFN- γ only when stimulated with CNS APCs. These data suggest that the activation of T cells in the presence of a cognate antigen occurred in the secondary lymph node and that trafficking of autoreactive Th1 T cells into the brain may not be the main mechanism of the pathological condition of peripheral inflammation associated with neuro-inflammation. Instead, the activation of T cells in the presence of a cognate antigen is more important. Based on the fact that the aetiology of RA and MS are influenced by genes in the HLA region, particularly the class II genes, therefore, CD4⁺ T cells are thought to play a crucial role in both MS and RA pathogenesis (Zozulya and Wiendl, 2008), (McInnes and Schett, 2007). This, combined with our data showing undetectable Th1 cytokines and highly detectable brain IL-12 mRNA expression levels in CII immunized mice, allowed us to hypothesize that there may be activation of CNS T cells occurring in the brain of CII immunized mice during the course of arthritis. This hypothesis is supported by our finding showing that the increased expression of IL-12 mRNA and protein concentrations occurred from day 22 onwards before the peak of mRNA expression levels of CXCL10, a potent Th1 recruiter, in brains of CII immunized mice on day 35. This suggested that the activation of CNS T cells may have occurred in the CNS before Th1 cells actually trafficking into the brain. Similarly, the peak of IL-12 protein also preceded the peak of VEGF, an angiogenic factor implicated in BBB breakdown. This suggests that the presence

of Th1 cells in brains of CII immunized mice may have occurred before the BBB breakdown. Although the increase in VEGF concentration in the brains has been reported to be associated with BBB breakdown (Argaw et al., 2009) some studies reported that BBB breakdown is not necessary to be the cause of an increase in peripheral immune cells infiltration into the CNS (Carson et al., 2006); (D'Mello et al., 2009); (Shaftel et al., 2007). This raises one important question; how the peripheral cytokines signal to the brain in order to activate the CNS Th1 lymphocytes to produced IL-12 in the brain? The only possibility that we could suggest from our data is that the production of IL-12 by CNS immune cells such as T cells may be induced via the peripheral inflammation signal from IL-1 β that was found to be up-regulated in the serum and brain tissues of CII immunized mice during the onset of the disease (day 22- day28 after immunization). We also found a downward trend in longitudinal changes in brain IL-12, which corresponded to a reduction in serum IL-1 β in CII immunized mice. Important evidence supporting our finding is that IL-1 β can enhance the activation of encephalitogenic T lymphocytes, contributing to the development of EAE (Matsuki et al., 2006). This hypothesis can be tested by using peripheral administration of anti-IL-1 β into the CII immunized mice and determining changes in Th1 cytokines in the brain.

A recent study has shown BBB disruption in CIA mice, characterized by an increase in BBB permeability and changes in the tight junction structure of BBB during the progress of arthritis (Nishioku et al., 2010b). Our data also suggest the possible signs of BBB disruption in brains of CII immunized mice, indicated by increased concentrations of VEGF in the brains of CII immunized mice during the early and late stages of disease (day 28-day 42 after immunization). VEGF is an angiogenic factor that has been implicated in BBB breakdown in several inflammatory conditions of the CNS (Croll et al., 2004a). Our data also showed that both VEGF mRNA expression levels and protein concentrations were up-regulated during the same period (day 35 -day 42 after immunization), suggesting that there may be local production of VEGF in the brain by CNS cells such as astrocytes, vascular endothelium, microglia or neurons (Croll et al., 2004a); (Mani et al., 2005). However, the mechanism underlying how the peripheral inflammatory signals induce VEGF production and BBB breakdown in the brains of CII immunized mice during the early disease stage in our study is

still unclear. One possibility is that VEGF production in the brain may be induced via the peripheral inflammatory signal obtained from FGF2 protein that is up-regulated in the serum of these CII immunized mice during the onset and the early disease stages. This is because FGF2 is considered to be a strong inducer of VEGF in endothelial cells (Seghezzi et al., 1998). FGF2 is detectable at high concentrations in the synovial fluid of RA patients as well as in the joints of arthritic mice (Manabe et al., 1999); (Yamashita et al., 2002). These observations suggest that FGF2 may play a role in the joint destruction by inducing osteoclastogenesis that is strongly increased during the onset of arthritis disease (Stolina et al., 2009). It is also possible that there may be a contribution of FGF2 from the joint into the peripheral circulation, and then from the circulation the FGF2 may be transported to the brain during the onset of disease. This can be seen by the up-regulation of serum FGF2 concentration during the onset of disease (day 22), followed by a reduction of serum FGF2 concentration during the chronic phase as seen in our longitudinal data during disease progression in CII immunized mice. However, this hypothesis needs to be further investigated, perhaps by using peripheral administration of anti-FGF2 into the CII immunized mice during the early and late stage of disease and determine changes in brain cytokines, particularly VEGF.

4.4.3 The potential interplay between inflammatory mediators in brains of CII immunized mice: Possible evidence for ongoing immune activation and inflammatory processes.

The data obtained from this time-course experiment provided interesting observations suggesting that there may be ongoing immune activation and inflammatory process in the brains of CII immunized mice over the course of disease development. We demonstrated up- and down-regulation of different inflammatory mediators in brains of CII immunized mice at different time points across the period of clinical manifestation in the CIA experimental course. These changes in mediators may reflect the biological interaction of brain cytokines during the course of disease. There was a prolonged increase in several brain inflammatory cytokines such as IL-12, IL-10 and CCL2 in brains of CII immunized mice throughout the course of disease. These longitudinal patterns of change in brain cytokine profiles are not common in acute inflammation such as the systemic LPS-challenge model. Several studies in the systemic LPS-challenge

model showed transient increases in brain cytokine, seen as single concentration peaks at different time points in the experimental period in various brain regions (Laye et al., 1994); (Quan et al., 1994); (Gatti and Bartfai, 1993); (Breder et al., 1994); (Gabellec et al., 1996); (Grinevich et al., 2001). We found some brain inflammatory mediators such as IL-1 β , CCL2 and FGF2 that were up-regulated corresponding to the up-regulation of the same cytokines in serum occurring during the onset of disease. However, we also found several inflammatory mediators such as TNF- α that were up-regulated in the brain, but not in the serum during the period of clinical disease (day 35 - day 42 after immunization). This suggests that there may be immune activation and cytokine production within the brains of arthritic mice. Interestingly, our data showing that IL-12 protein concentrations were elevated in the brains of CII immunized mice during the onset of the disease and then were decreased towards the latter stages of the disease. This profile was similar to the longitudinal changes in IL-12 mRNA expression levels in the CNS of EAE model of chronic CNS disease (Issazadeh et al., 1995). This suggests that the inflammatory process in the brain may be chronic rather than acute. This premise is supported by a study by de Ray *et al* showing a prolonged increase of IL-6 mRNA expression levels in brains of CIA rats during the period of onset and early disease period. That study also showed an increase of IL-1 β mRNA expression levels in brains of CIA rats during the period of disease onset; which is similar to our finding in the brains of CII immunized mice. Transient increases in brain IL-1 β protein concentrations during the onset of disease may also be associated with sharp increases in IL-12 protein concentrations observed during the same period. Although we have discussed earlier in this chapter that the increase in IL-12 was possibly generated by CNS activated T cells, the possibility that IL-12 could also be produced from astrocytes and microglia should also be considered. An *in vitro* study suggested that brain astrocytes and microglia can produce IL-12 upon stimulation with pro-inflammatory cytokines such as IL-1 β and TNF- α (Stalder et al., 1997). This may also explain our finding showing a coincidental increase in IL-12 mRNA expression levels and TNF- α protein concentration in the brains of CII immunized mice during the late stage of disease. TNF- α not only activates CNS astrocytes and microglia, but also T cells causing them to produce Th1 cytokines. IL-2, another Th1 cytokine that is up-regulated as a single peak on day 35 may also be associated with the increase in TNF- α protein concentration at the same time

period. This could be explained by an *in vivo* study showing that IL-1 and TNF- α are required for IL-12-induced development of Th1 cells (Shibuya et al., 1998). Further indirect evidence for this was seen by adoptive transfer of antigen (PLP)-primed T cells when pre-treated with TNF- α caused more severe EAE, along with a significant increase in TNF- α production (Leonard et al., 1995). These data together with the data presented in this thesis suggest that pro-inflammatory cytokines and Th1 cytokines may mutually regulate each other and may contribute to the development of cell-mediated immune responses within the central nervous system of CII immunized mice.

A longitudinal shift from a Th1-type to Th2-type response is one of the major characteristics of autoimmune disease. The temporal interplay and mutual inhibition between Th1 and Th2 cytokines has been demonstrated in several CNS inflammatory demyelinating disease models such as EAE and Theiler's murine encephalomyelitis virus (TMEV). However, the specific roles of the Th1 and Th2 cytokines in neuro-inflammation in the CNS have not been fully elucidated. This is mainly because studies using different CNS inflammatory demyelinating models reported different temporal relationships and cytokine expression profiles. For example, IL-2, IL-6, IL-12 and IFN- γ concentrations in EAE mouse brains increased during the relapse stage, while brain concentrations of the Th2 cytokines such as IL-4 and IL-10 were up-regulated during the remission or recovery stages (Issazadeh et al., 1996). In contrast, the coincidental expression of Th1 and Th2 cytokines including IL-2, IFN- γ , IL-4, IL-5 and IL-10 were observed during the remission phase of the TMEV-induced demyelinating disease model (Sato et al., 1997). Therefore, the neuro-inflammation in the CIA model, which could be considered as a model of neuro-inflammation induced by systemic autoimmunity, may demonstrate a different temporal interplay between Th1 and Th2 cytokines. Our data showed increased concentrations of brain Th2 cytokines, including IL-4 and IL-10 which occurred at the same time as up-regulation of Th1 cytokines IL-2 and IL-12, and pro-inflammatory cytokines in CII immunized mouse brain during the course of disease. This suggests that there might be a Th1/Th2 shift that could promote an anti-inflammatory environment, perhaps in the joint in an attempt to suppress or regulate ongoing pro-inflammatory Th1 cell activation. The concentration of brain IL-4 peaked at day 22 and then declined, which was at the same time

as the temporal expression profile of brain IL-1 β in CII immunized mice, suggesting that IL-4 production might be up-regulated to suppress the pro-inflammatory functions of IL-1 β (te Velde et al., 1990). Alternatively, the observed reduction of brain IL-4 concentration could be the result of the up-regulation of Th1 cytokines e.g. IL-2 and IL-12. However, IL-12 has also been reported to stimulate IL-10 production in the EAE model, therefore, the up-regulation of IL-10 in CII immunized mouse brains might be associated with an increased concentration of brain IL-12 (Berghmans et al., 2006).

Pro-inflammatory cytokines are known to stimulate the production of chemokines in the CNS, which may then initiate migration of immune cells from the blood into the CNS parenchyma. Cultured astrocytes stimulated by TNF- α and TGF- β produced CCL2 (Hurwitz et al., 1995), while cultured microglia stimulated by IL-1 β and TNF- α produced CCL2, CCL3, CCL4 and CXCL8 (McManus et al., 1998). Our data showed a prolonged up-regulation of brain CCL2 protein concentration in CII immunized mice during the course of disease. This was coincidental with the up-regulation of brain IL-1 β and TNF- α protein production in CII immunized mice, suggesting that CCL2 in CIA mouse brain may be generated by IL-1 β /TNF-activated microglia/astrocytes. Temporal relations between chemokine and cytokine expression in the CNS have been demonstrated in a model of chronic relapsing experimental autoimmune encephalomyelitis (ChREAE) (Glabinski et al., 2003). During the relapse stage, which involves the migration of new autoantigen-specific T cells into the CNS, TNF- α , IFN- γ and IL-6 production was increased at the same time as various chemokines including CCL1, CCL2, CCL3, CCL4, CCL5 and CXCL2-3 in the brains of mice with ChREAE. Another possibility is that CCL2 may move actively or passively from the periphery, or that peripheral IL-1 β might induce brain production of CCL2 in CII immunized mice. This can be seen by up-regulation of serum IL-1 β and CCL2 during the onset of disease on day 22 and this was followed by a reduction of their serum concentrations over time, while brain protein concentrations of CCL2 remained increased in CIA mice. Our data also showed that the up-regulation of brain CXCL1 mRNA expression levels occurred at the same time as the peak of brain IL-1 β protein production. A similar observation has been reported in a study by Shaftel *et al* showing that chronic IL- β expression in mouse brains resulted in the up-regulation of brain CXCL1 mRNA (Shaftel et al.,

2007). A study using a TNF-induced demyelination (TID) model, which is another MS model, showed that mRNA expression levels of CXCL10 and other chemokines including CCL1 and CXCL2 were up-regulated in the brains of mice with inflammatory demyelination during the acute phase of disease. This also correlated with marked immune cell infiltration into the CNS (Quinones et al., 2008). This study suggested that the increased concentration of brain TNF- α is associated with the up-regulation of brain CXCL10 expression, which may partly explain our finding showing the coincidental expression of brain TNF- α and CXCL10 in CIA mice at day 35. These data collectively with the data presented in this thesis suggest that pro-inflammatory cytokines IL-1 β and TNF- α may regulate chemokine production, which eventually contribute to immune cell trafficking from the periphery to the brains of CII immunized mice. We don't present any supportive evidence for this in this thesis and this topic may be for future studies.

Vascular endothelial growth factor is only not an angiogenic factor, but also functions to induce inflammation. In RA, VEGF can regulate angiogenesis contributing to the proliferation of the inflammatory synovial pannus, and can also promote leukocyte recruitment into the site of neovascularisation by inducing CCL2 production by endothelial cells (Marumo et al., 1999). In addition, VEGF has been reported to modulate T cells response and cytokine IL-8, CCL2, TNF- α and IL-1 β production by peripheral blood monocytes (Selvaraj et al., 2003). Very little is known about the role of VEGF-mediated inflammation in the brain. However, it has been reported that brain VEGF functions to regulate monocyte recruitment into the brain. VEGF has been shown to induce CCL3 production by endothelial and brain parenchyma cells (Croll et al., 2004b). In addition, during the neuro-inflammation process, the production of VEGF in the brains is induced by pro-inflammatory cytokine such as IL-1 β (Li et al., 1995). Our data showed coincidental increases of VEGF, CXCL10, CCL2, and TNF- α in brains of CII immunized mice during the early stage of disease (day 28 - day 35 after immunization), suggesting there may be an association between VEGF and CXCL10, CCL2, and TNF- α that may also involve recruitment of leukocytes and monocytes into the brain. Another inflammatory action of VEGF is to regulate T cells. Administration of anti-VEGF antibody in CIA mice resulted in inhibition T-cells responses and a reduction in the production of IL-6. In addition, VEGF-

blockade also reduced TNF- α and IL-6 concentrations measured in peripheral blood mononuclear cells derived from RA synovial fluid (Yoo et al., 2005). Alternatively, T cells have been reported to produce VEGF after stimulation by IL-2 (Mor et al., 2004). This observation may explain our findings in which we demonstrated coincidental increases in VEGF, IL-2 and IL-12 in the brains of CII immunized mice during the early stage of disease (day 28 - day 35 after immunization). This data suggest that there may be an association between Th1 cells and VEGF. However, this hypothesis needs to be further investigated, perhaps by an *in vitro* study of these CNS T cells and CNS immune cells isolated from CII immunized mice during the early stage of disease. Interestingly, there was no VEGF detectable in brains of CII immunized mice during day 22 to day 28 after immunization, which is the period during which the anti-inflammatory cytokines IL-4 and IL-10 were up-regulated. It is possible that IL-4 and IL-10 suppressed the expression of VEGF during that period since it has been reported that the combination of IL-4 and IL-10 inhibited the production of VEGF in rheumatoid synovial fibroblasts (Hong et al., 2007). The prolonged increase of IL-10 across the whole period of the clinical manifestation of disease may be associated with longitudinal decreases in FGF2 mRNA and protein in brains of CII immunized mice. This may be due to IL-10 which also has an anti-angiogenic effect inhibiting the expression of FGF2 as well as VEGF (Cervenak et al., 2000). However, the actual reason underlying the longitudinal reduction in FGF2 is still unclear. However, our data also showed that brain FGF2 concentrations in both normal and CII immunized mice decreased with the age, suggesting age-related alterations in FGF2 production. This is supported by a study comparing wound repairs of young mice and aged mice in which wounds of aged mice heal more slowly and contained less FGF2 than wounds in the young, indicating that age may be associated with macrophage production of FGF2 during the inflammatory process (Swift et al., 1999).

A summary of the possible brain immune activation induced by peripheral inflammatory signals in CII immunized is shown in Figure 4.31.

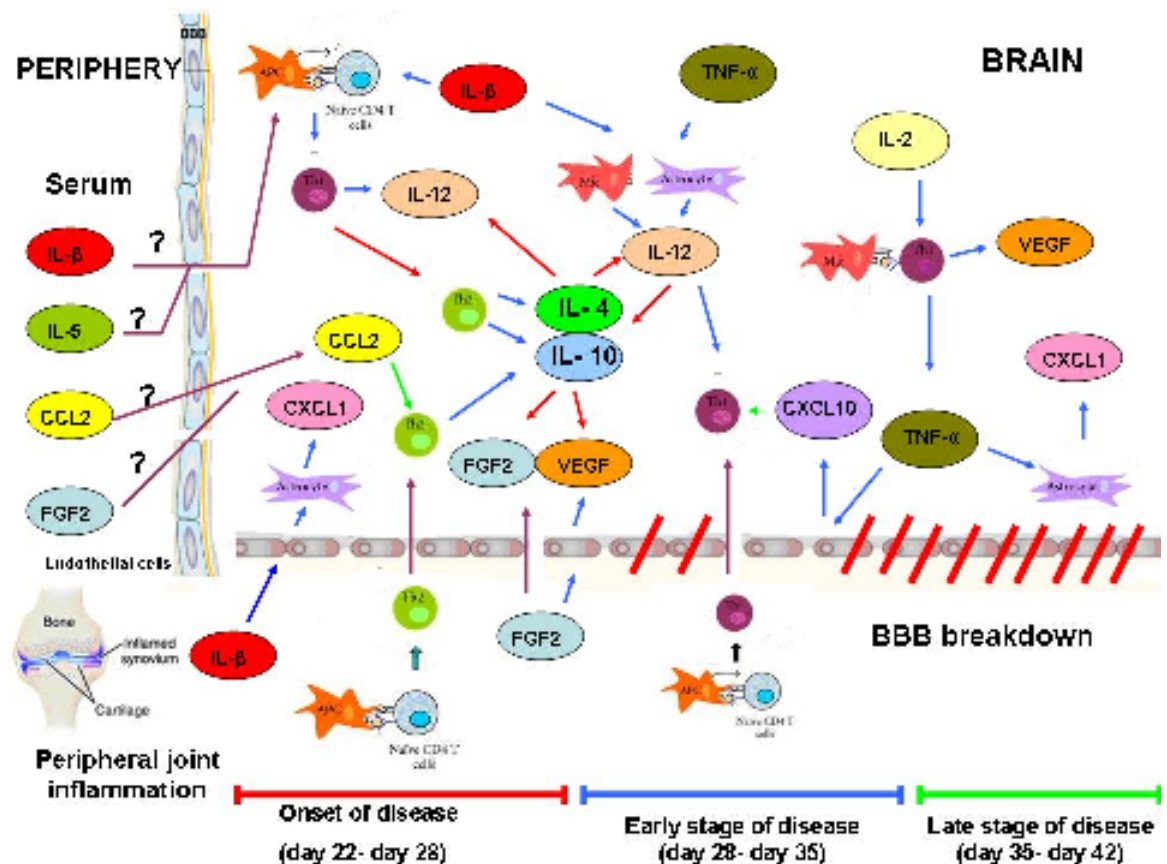


Figure 4.31 Potential mechanisms of immune activation induced by peripheral inflammatory cytokine signals occurring in brains of CII immunized mice

In this chapter we investigated longitudinal changes in brain inflammatory mediators in CII immunized mice during 3 stages of arthritis disease (onset of disease, early stage of disease and late stage of disease). We have shown that longitudinal changes in brain inflammatory mediators in CII immunized mice have been associated with changes in peripheral inflammatory mediators at different stages of disease progression. Increased concentrations of serum IL-1 β , IL-5, CCL2 and FGF2 were observed during the onset of disease (day 22-day 28) at the same time as increased concentrations of brain IL-1 β , CCL2 and FGF2. This suggests that there may be the transudation of IL-1 β , CCL2 and FGF2 from the periphery into the brain by an as yet unknown mechanism. At this early time period of disease, we found increased expression of CXCL1 mRNA, which potentially was generated from astrocytes induced by pro-inflammatory cytokines such as IL-1 β . Up-regulation of both IL-12 mRNA and protein were also observed, suggesting the local production of IL-12 that could be the result of bystander activation of T cells in the brain. The peripheral inflammatory signal of IL-1 β may also play a role to augment the activation of CNS T cells. Th2 cytokines IL-4 and IL-10 were up-regulated by the time of onset of disease, which may be due to the trafficking of Th2 cells into the brain regulated by the chemotactic activity of CCL2. During the early stage of the disease (day 28 – day 35), increased levels of VEGF mRNA expression were observed and may be generated from local CNS cells such as BBB endothelial cells after stimulation by peripheral inflammatory signal from FGF2. Both FGF2 and VEGF may be down-regulated by IL-4 and IL-10 during the onset of disease during which there was no significant increase of FGF2 and VEGF concentrations in brains of CII immunized mice during that period. Also during that period, mRNA and protein concentrations of Th1 cytokines, IL-12 and IL-2 were increased. This could be due to more Th1 cells trafficking from the blood into the brain by the chemotactic activity of CXCL10. Another possibility is that CNS immune cells such as microglia and astrocytes could also produced IL-12 upon stimulation by pro-inflammatory cytokines TNF- α and IL-1 β . IL-12 may also suppress the production of anti-inflammatory IL-4, because there was no further increase in IL-4 protein concentrations after the onset of disease. A prolonged increase of VEGF from the early stage of disease onwards may indicate a breakdown of the BBB during the period of clinical expression of disease. TNF- α may activate astrocytes to produce CXCL1. There may also be the activation of T cells upon stimulation by IL-2, resulting in the production of VEGF in the brain of CII immunized mice during the late stage of disease. Purple arrows denote transportation of peripheral immune cells and inflammatory

mediators. Blue arrows denote activation and production of inflammatory mediators. Red arrows denote inhibition and suppression of productions of inflammatory mediators. Green arrows denote effects of chemokines on immune cells trafficking in brains of CII immunized mice. Mic = microglia.

Summary

In summary, we have demonstrated the possibility that peripheral inflammatory signal derived from the cytokines IL-1 β , IL-5, CCL2 and FGF2 may induce the production of brain inflammatory mediators associated with the onset and early disease stages of arthritis. There may also be trafficking of immune cells from the periphery into brains in response to the increased concentrations of chemokines including CCL2, CXCL10, CXCL1 and angiogenic factors such as VEGF and FGF2. These may be associated with increased permeability of the BBB which may have occurred during the early disease stage indicated by raised levels of VEGF mRNA expression in brains of CII immunized mice during the early and late stages of arthritis.

One important question follows from this. How can inflammatory mediators such as TNF- α be up-regulated in the brain of CII immunized mice during the clinical expression of the arthritis, despite there being no serum inflammatory mediators detectable? In the next chapter, we therefore addressed the issue of the apparent lack of clear association between joint-immune-brain communication by using peripheral administration of TNF-blockade in the CII immunized mice during the early and late stages of disease and determining changes in brain cytokines.

Chapter 5

Effects of tumour necrosis factor (TNF) blockade using recombinant human soluble TNF-receptor (Etanercept) on inflammatory mediator profiles in brains of arthritic model mice

5.1 Introduction

Data described in Chapter 4 (Section 4.2.2, 4.2.4 and 4.2.5) demonstrated various longitudinal changes of inflammatory mediator expression profiles, including IL-1 β , TNF- α , IL-2, IL-10, IL-4, IL-12, CCL2, CXCL1, CXCL10, VEGF and FGF2 in the brains of CII immunized mice throughout the course of disease development from onset, acute and chronic changes. These data suggested that there may be ongoing immune activation in the CNS of these mice, which may be associated with, or caused by peripheral inflammation during development of arthritis. Interestingly, we found increased concentrations of inflammatory mediators, including IL-1 β , IL-5, CCL2 and FGF2 in the serum of these mice during the onset of disease (day 22 to day 28 after immunization). Some of these inflammatory mediators, IL-1 β and CCL2 were also found in increased concentration in brains at the same time period, suggesting that the peripheral inflammatory signals from serum IL-1 β and CCL2, associated with the onset of arthritis disease may induce the production of brain inflammatory mediators. However, during the early and the late stages of arthritis we could no longer detect serum inflammatory mediators (at day 28 to day 42 after immunization), but we could still detect increased concentrations of several inflammatory mediators, including TNF- α , IL-4, IL-10, IL-2, IL-12, CCL2, CXCL1, CXCL10, VEGF and FGF2 in the brains of these CII immunized mice. We could not address the question of how the cytokines associated with peripheral inflammation could signal to the brain in order to produce these inflammatory mediators.

To confirm that the changes in inflammatory mediator profiles were a consequence of the peripheral inflammation during the period of clinical expression of arthritis, we blocked the peripheral inflammation in the CIA model and determined the effect of anti-inflammatory treatment on the brain inflammatory mediator profiles. In the CIA experiment of the present Chapter, we administrated etanercept, a drug that consists of a recombinant human soluble TNF receptor which can cause TNF blockade. It is an extremely effective treatment for RA (Haberhauer et al., 2010), and it can be administered successfully to the murine CIA model as a preventative therapy (Marinova-Mutafchieva et al., 2000). A recent finding by Terrando et al., demonstrated that peripheral administration of TNF blockade to a model of surgery-induced peripheral inflammation could also reverse an increase of brain IL-1 β expression

(Terrando et al., 2010). Clinical evidence also demonstrated an improvement in mood in patients with chronic systemic inflammatory diseases such as psoriasis and RA when receiving etanercept. Psoriasis patients receiving long-term etanercept treatment showed 50% improvement in depression score compared with those receiving placebo as indicated by HAM-D and Beck Depression Inventory (BDI) (Tyring et al., 2006). In addition, a reduction in serotonin transporter (SERT) density and improvement in physical and mental functions have been reported in RA patients receiving anti-TNF- α treatment (Cavanagh et al., 2010). This clinical evidence suggests that etanercept not only inhibits peripheral inflammation at the site of disease, but may also contribute to the suppression of central neuro-inflammation often associated with systemic autoimmune diseases. This eventually inhibits changes in neurobiology contributing to the development of neuropsychiatric disorders such as depression occurring during the course of autoimmune disease.

We hypothesise that 'Using etanercept to treat peripheral inflammation in the CIA model by TNF blockade would affect the brain inflammatory mediator profile by suppressing disease-associated up-regulation of brain inflammatory mediators'. Therefore, the aim of this chapter is to investigate whether systemic etanercept treatment modulates the inflammatory mediator profiles, usually associated with peripheral inflammation, in the brains of mice during the development of arthritis using the experimental CIA model.

5.2 Results

5.2.1 *Effect of etanercept on development of collagen induced arthritis (CIA).*

Data from the previous chapter (Chapter 4; sections 4.2.3, 4.2.4 and 4.2.5) demonstrated up-regulation of production of various inflammatory mediators, including TNF- α , IL-4, IL-10, IL-2, IL-12, CCL2, CXCL10 and VEGF, in the brain of CII immunized mice during the period of clinical expression of arthritis (day 28 to day 35 after immunization). However, we found no inflammatory mediators in the serum of these CII immunized mice during this period. To further test the association between peripheral inflammation and the production of inflammatory mediators in the brain, we used etanercept to block peripheral inflammation during the period of clinical expression of arthritis in CII immunized mice and measured associated changes in brain inflammatory mediators. TNF neutralizing agents have been very effective in ameliorating joint disease and 300ug/mouse of etanercept has been suggested to be the appropriate dose to reduce the severity of joint inflammation in CIA model (Williams et al., 2000b). In this chapter, we investigated the effect of etanercept on the severity of arthritis and production of brain inflammatory mediators at 2 time points during the period of clinical expression of disease (day 32 and day 35 after immunization as time points of early and late stage of disease respectively). We also determine changes in brain inflammatory mediators during the before disease onset (day 14 after immunization) and before etanercept treatment on day 18, as a control time point.

5.2.1.1 Administration of etanercept and induction of arthritis in DBA1 mice

Nineteen DBA1 mice were immunized by intradermal injection of type II collagen in Freund's complete adjuvant on day 0. On day 14, 3 CII (collagen type II) immunized mice (Group 1) were culled and the brains and serum of these mice were harvested for the measurement of inflammatory mediator concentrations before the second immunization on day 21. There was no CII immunized mice in Group 1 that developed arthritis on day 14 after the primary immunization. The other 16 CII immunized mice were randomly divided into 2 groups of 8, namely the treatment and placebo groups. From day 18 onwards, CII immunized mice in

the treatment group received etanercept (300 µg/mice, i.p.) every 3 days, while the placebo group received PBS (i.p.) every 3 days. The signs of arthritis in CII immunized mice were monitored from day 16 after immunization onwards and arthritis severity scores in this experiment were verified independently by Dr. Bernard Leng. CII immunized mice from both groups were re-challenged by intraperitoneal injection of collagen II in PBS on day 21. CII immunized mice of the placebo (PBS treated) group started to show sign of arthritis earlier (day 19 after the primary immunization) than those of the treatment group (day 21 after the primary immunization). 3 CII immunized mice of the treatment group (Group 2) and 3 CII immunized mice of the placebo group (Group 3) were culled and serum and brains of these CII immunized mice were harvested on day 32. CII immunized mice of both treatment and placebo groups (Group 4 and Group 5; 5 CII immunized mice/group) were culled and serum and brains of these CII immunized mice were harvested on day 35; which is the peak day of disease. Another 8 sex- and age-matched untreated DBA1 mice were used as antigen-naïve control mice. These naïve control mice were neither sensitized with type II collagen nor given etanercept treatment. 3 naïve control mice were culled on day 14, and a further 3 and 5 naïve control mice were culled on day 32 and day 35 after the primary immunization respectively. Serum and brains of mice from all experimental groups were harvested on the day indicated and snap-frozen in liquid nitrogen and stored at -80°C. Half of each brain was processed for protein extraction and inflammatory mediator proteins analysed by Luminex; the other half was processed for RNA extraction and the inflammatory mediator gene expression was determined by real-time PCR (Figure 5.1).

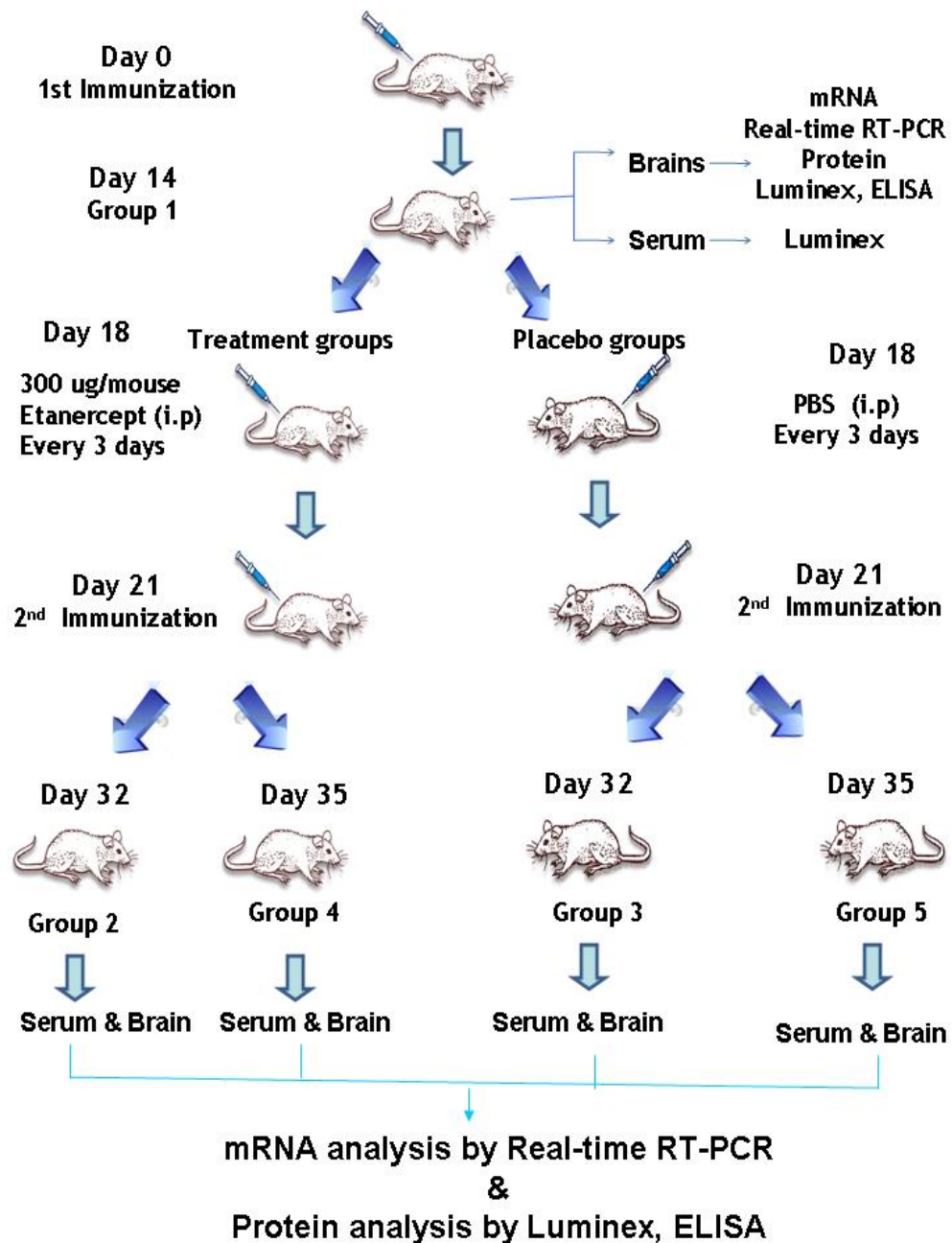


Figure 5.1 Administration of etanercept during the CIA experimental procedure
 19 DBA1 mice at 6-8 weeks of age were immunized with 100 µg type II bovine collagen + complete Freund's adjuvant (CFA) at day 0. On day 14, 3 CII immunized mice in Group 1 were culled and brains and serum of these CII immunized mice from group 1 (3 mice/group) were harvested. At this time point, another 3 naïve control mice, which were neither sensitized nor challenged with type II collagen, were also culled and their brains and serum samples were used as controls to compared changes in brain inflammatory mediators with those of CII immunized mice culled on day 14. On day 18, CII immunized mice were randomly divided into 2 groups (8 CII immunized mice/group), which were a treatment group and a placebo group. From this day onwards, 300 µg/mouse etanercept was administrated (i.p.) to CII immunized mice of the treatment group every 3 days, while PBS was injected to CII immunized mice of the placebo group every 3 days. CII immunized mice of both groups were challenged on day 21 with 200 µg type II collagen. From day 21 onwards, etanercept treated CII immunized mice of etanercept group were randomly divided into 2 groups, namely Group 2 and Group 4. Etanercept treated CII immunized mice in Group 2 (3 CII immunized mice/group) were culled and serum and brains of these CII immunized mice were harvested on day 32, while etanercept treated CII immunized mice in Group 4 (5 CII immunized mice/group) were culled and serum and brains of these CII immunized mice were

harvested on day 35. Similarly, PBS treated CII immunized mice in the placebo group was randomly divided into 2 groups, namely Group 3 and Group 5. PBS treated CII immunized mice in Group 2 (3 CII immunized mice/group) were culled and serum and brains of these CII immunized mice were harvested on day 32, while PBS treated CII immunized mice in Group 4 (5 CII immunized mice/group) were culled and serum and brains of these CII immunized mice were harvested on day 35. Another 8 naïve control mice were culled on the day indicated (3 naïve mice for day 32 and 5 naïve mice for day 35) and their serum and brain were used as controls. Brain and serum from mice of all experimental groups were collected and processed for inflammatory mediator measurements using Luminex, ELISA and real-time PCR.

5.2.1.2 Effect of etanercept on severity of arthritis in CII immunized mice on day 32 and day 35.

To determine the effect of blocking TNF- α during the induction of arthritis, mice were given injections from days 18 onwards (before the second collagen booster immunization) with 300 μ g etanercept every 3 days. Placebo groups received PBS. There were 4 mice in the treatment group 2 and the placebo group 3, both groups of mice were culled on day 32. Mice started to develop arthritis on day 22 days after immunization in the etanercept-treated group 2, compared with 20 days in the PBS treated group 3 (Figure 5.2). There was no significant difference in % incidence, mean paw thickness, and arthritis score between etanercept-treated mice and PBS-treated mice.

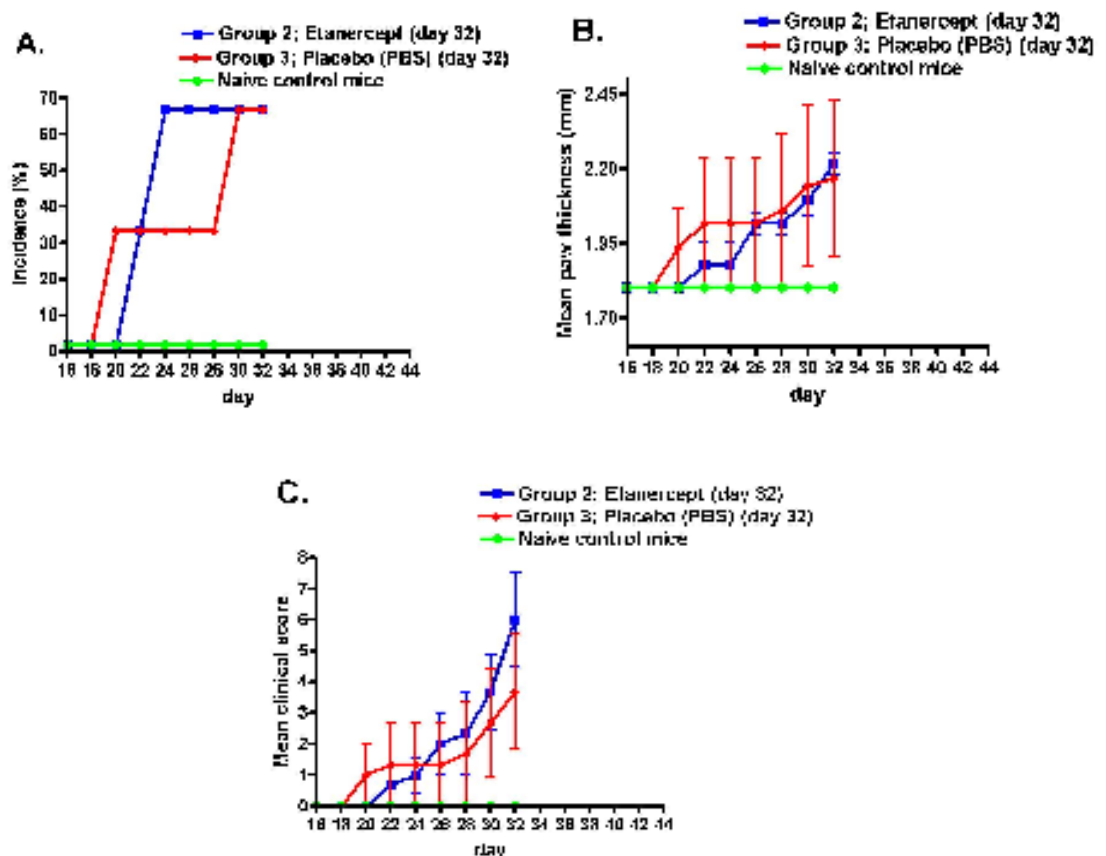


Figure 5.2 Effect of etanercept on severity of arthritis in CII immunized mice on day 32 (groups 1-3)

CII immunized mice in Group 2 (3 etanercept treated CII immunized mice/group; blue line) were given injections from days 18 onwards (before collagen booster immunization) with 300 μ g etanercept every 3 days. 3 CII immunized mice in Group 3 were given PBS as placebo (3 PBS treated CII immunized mice /group; red line). Mice in both Group 2 and Group 3 were culled on day 32. The signs of arthritis in CII immunized mice were monitored from day 16 after immunization onwards. (A) shows the percent of incidence of arthritis in etanercept-treated and PBS-treated CII immunized mice, which was calculated from number of CII immunized mice with arthritis per group/total number of CII immunized mice used per group. Mean clinical arthritis score and mean paw thickness were used as clinical evaluations to measure the severity of joint inflammation in arthritic mice. (B) shows mean paw thickness of etanercept-treated and PBS-treated CII immunized mice which was calculated from the sum of the paw thickness of all mice in each group divided by the number of mice per group. (C) shows mean clinical of etanercept-treated and PBS-treated CII immunized mice which was calculated from the sum of the clinical scores of all mice in the each group divided by the number of mice per group. Mean paw thickness, mean clinical score and % incidence in CII immunised mice (3 CII immunised mice/group) were compared with those values of antigen-naïve control mice (3 naïve mice; green line). These naïve control mice were neither sensitized with type II collagen nor given etanercept treatment. Data represent as mean \pm SEM. (all 19 CII immunised mice in all groups). Statistical analysis of data was performed using two-way ANOVA for multiple comparison, compared with a group of control naïve mice; *P < 05; **P < 01; ***P < 001.

However, the etanercept treatment significantly reduced the severity of arthritis and delayed the start of arthritis in treatment group 4 compared to the placebo group 5. There were 5 mice in the treatment group 4 and the placebo group 5, both groups of mice were culled on day 35. Mice in group 4 started to develop arthritis on day 19 days after immunization in the etanercept-treated group, compared with 27 days in the PBS-treated group 5 (Figure 5.3A). Anti-

TNF- α treatment caused a significant reduction in paw-swelling of etanercept-treated mice in group 4 compared to those in PBS-treated mice in group 5. The mean paw thickness of mice in group 4 and 5 (etanercept-treated versus PBS-treated) was 1.9 ± 0.89 mm versus 2.23 ± 0.33 mm ($P=0.002$) (Figure 5.3B). Mean clinical scores were also significantly reduced in the etanercept-treated mice in group 4, compared to those of PBS-treated mice in group 5. The mean clinical score of mice in group 4 and 5 (etanercept-treated versus PBS-treated) was 1.4 ± 1.4 versus 3.8 ± 2.0 ($P = 0.0014$) (Figure 5.3C).

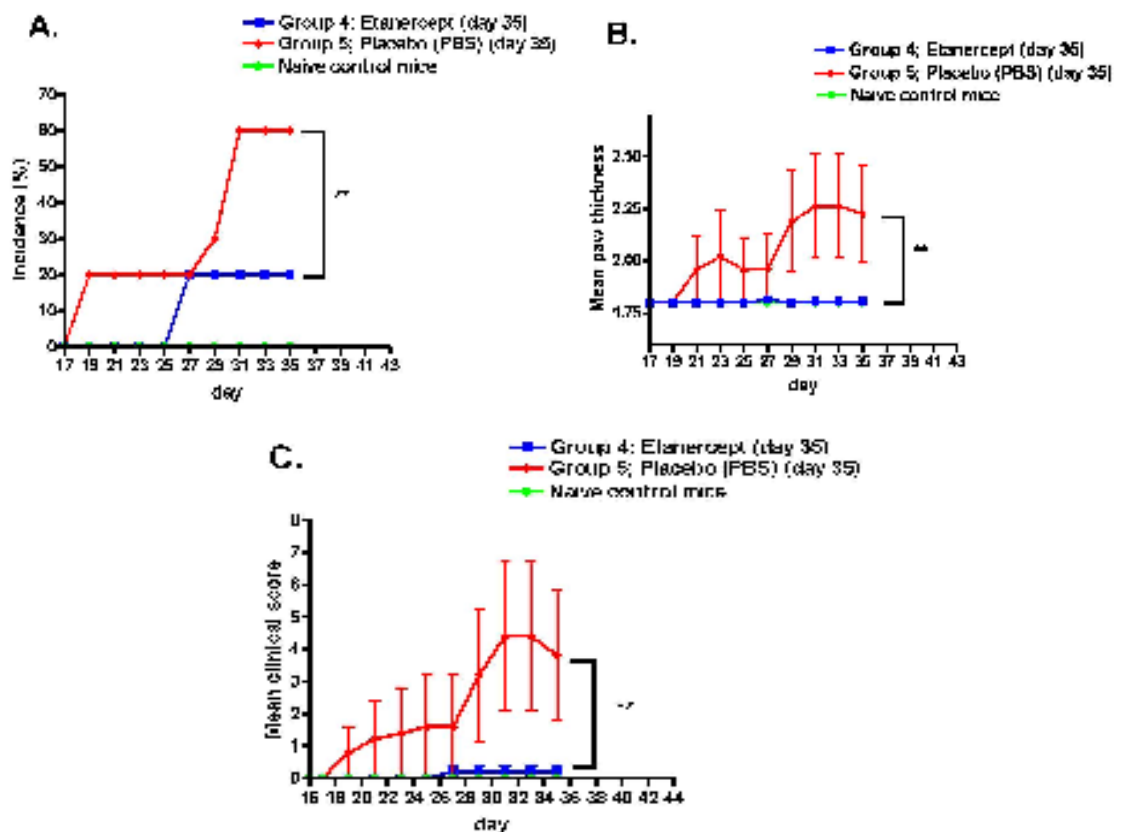


Figure 5.3 Effect of etanercept on severity of arthritis in CII immunized mice on day 35 (groups 4 and 5)

CII immunized mice in Group 4 (5 etanercept treated CII immunized mice /group; blue line) were given injections from days 18 onwards before collagen immunization with 300 μ g etanercept every 3 days. 3 CII immunized mice in Group 5 were given PBS as placebo (5 PBS treated CII immunized mice /group; red line). Mice in both Group 4 and Group 5 were culled on day 35. The signs of arthritis in CII immunized mice were monitored from day 16 after immunization onwards. (A) shows the percent of incidence of arthritis in etanercept-treated and PBS-treated CII immunized mice, which was calculated from number of CII immunized mice with arthritis per group/total number of CII immunized mice used per group. Mean clinical arthritis score and mean paw thickness were used as clinical evaluations to measure the severity of joint inflammation in arthritic mice. (B) shows mean paw thickness of etanercept-treated and PBS-treated CII immunized mice which was calculated from the sum of the paw thickness of all mice in each group divided by the number of mice per group. (C) shows mean clinical of etanercept-treated and PBS-treated CII immunized mice which was calculated from the sum of the clinical scores of all mice in the each group divided by the number of mice per group. Mean paw thickness, mean clinical score and % incidence in CII immunized mice (5 CII immunized mice/group) were compared with those values of naïve control mice (5 naïve mice; green line). These naïve control mice

were neither sensitized with type II collagen nor given etanercept treatment. Data represent as mean \pm SEM. (all 19 CII immunized mice in all groups). Statistical analysis of data was performed using two-way ANOVA for multiple comparison, compared with a group of control naïve mice; * $P < 0.05$; ** $P < 0.01$; *** $P < 0.001$.

Overall, there were 5 out of 8 PBS treated CII immunized mice from Group 3 and Group 5 (~62.5 % incidence) that showed clinical signs of arthritis from day 19. Etanercept treated-CII immunized mice showed a lower disease incidence compared to those in PBS treated-CII immunized mice. 3 out of 8 etanercept treated CII immunized mice from Group 2 and 4 developed arthritis from day 22 (~37.5 % incidence) (Figure 5.4A). Clinical signs of arthritis were observed in PBS-treated CII immunized mice from Group 3 and 5 from day 19 after immunization onward and there were 5 out of 8 PBS-treated CII immunized mice developed arthritis (62.5% incidence). The cumulative mean paw-swelling diameter of all PBS treated CII immunized mice from Group 3 and Group 5 ($n=8$) was 2.2 ± 0.2 mm, which was significantly higher than those in naïve control mice (1.700 ± 0.08 mm; $P= 0.0001$). Etanercept-treated CII immunized mice showed significantly less swelling than PBS treated CII immunized mice (2.0 ± 0.08 mm; $P < 0.0001$). Two-way ANOVA analysis also indicated that the cumulative mean of swelling diameter of etanercept-treated CII immunized mice was significantly higher than those in control mice (1.70 ± 0.08 mm; $P= 0.0005$) (Figure 5.4B). The cumulative mean arthritis score of etanercept-treated CII immunized mice was significantly lower than those of PBS treated CII immunized mice (2.25 ± 1.21 mm versus 3.75 ± 1.35 mm, $p=0.001$) (Figure 5.4C). A summary of number of arthritic mice, mean arthritis score, maximum arthritis score, mean paw diameter of etanercept-treated and PBS-treated CII immunized mice is presented in Table 1.

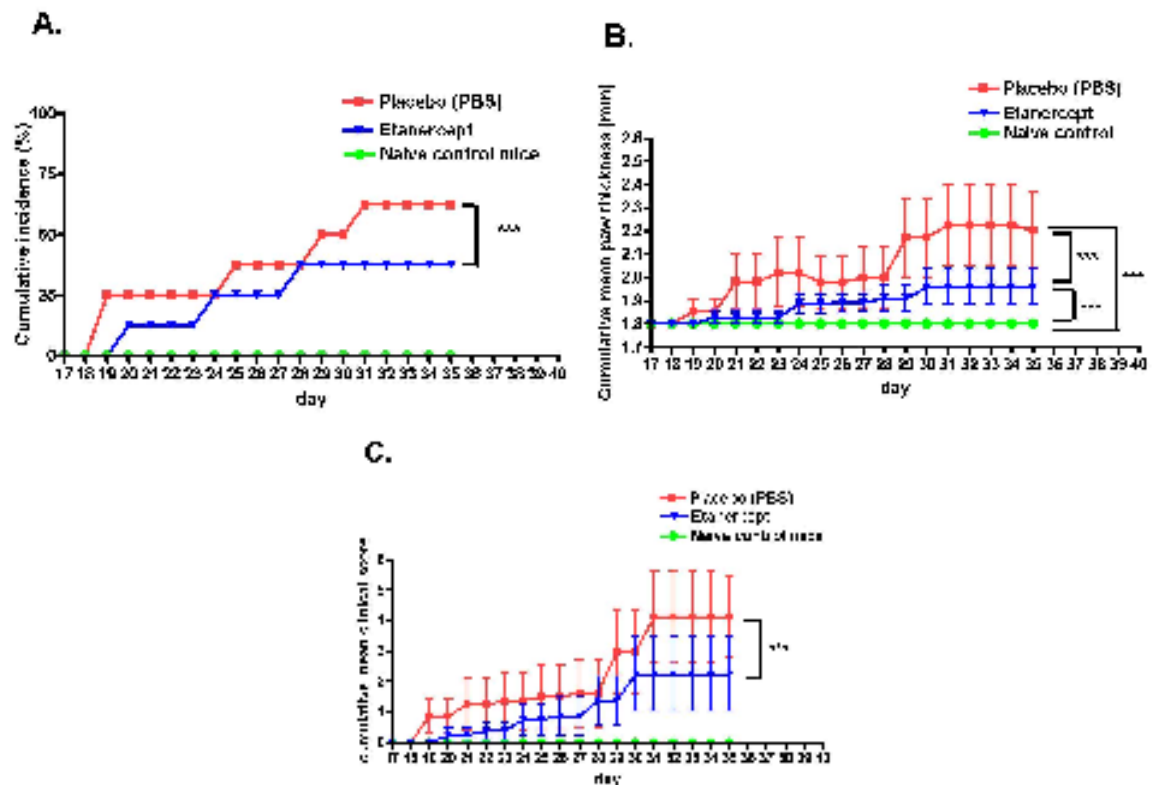


Figure 5.4 Effect of etanercept on severity of arthritis in all CII immunized mice in Group 2, 3, 4 and 5

CII immunized mice in Group 2 and Group 4 ($n=8$ for both groups; blue line) were given injections from days 18 onwards before collagen immunization with 300 μg etanercept every 3 days. 3 CII immunized mice in Group 3 and Group 5 were given PBS as placebo ($n=8$ CII immunized mice /for both groups; red line). Mice in both Group 4 and Group 5 were culled on day 32, while Mice in both Group 4 and Group 5 were culled on day 35. The signs of arthritis in CII immunized mice were monitor from day 16 after immunization onwards. (A) shows the cumulative percent of incidence of arthritis in all etanercept-treated and all PBS-treated CII immunized mice, which was calculated from number of CII immunized mice with arthritis per group/total number of CII immunized mice used per group. Cumulative mean clinical arthritis score and cumulative mean paw thickness were used as clinical evaluations to measure the severity of joint inflammation in arthritic mice. (B) shows cumulative mean paw thickness of all etanercept-treated and all PBS-treated CII immunized mice which was calculated from the sum of the paw thickness of all mice in each group divided by the number of mice per group. (C) shows cumulative mean clinical of all etanercept-treated and all PBS-treated CII immunized mice which was calculated from the sum of the clinical scores of all mice in the each group divided by the number of mice per group. Cumulative mean paw thickness, cumulative mean clinical score and cumulative % incidence in CII immunised mice ($n=3$ CII immunised mice /group) were compared with those values of naïve control mice ($n=8$ naïve control mice; green line). These naïve control mice were neither sensitized with type II collagen nor given etanercept treatment. Data represent as mean \pm SEM. ($n=16$ CII immunized mice). Statistical analysis of data was performed using two-way ANOVA for multiple comparison, compared with a group of control naïve mice; * $P < 05$; ** $P < 01$; *** $P < 001$.

Group	Treatments	Day of harvesting	Arthritic/total number of mice	Mean Arthritis scores	Maximum Arthritis scores	Mean Paw Diameter
2	Etanercept	32	2/3	3.67 ± 2.33	8	2.08 ± 0.23
3	PBS	32	2/3	3.67 ± 1.86	6	2.2 ± 0.3
4	Etanercept	35	1/5	1.4 ± 1.4	7	1.9 ± 0.9
5	PBS	35	3/5	3.8 ± 2.0	10	2.2 ± 0.3

Table 5.1 Numbers of arthritic mice, mean arthritis scores, and mean swelling scores of CIA mice in etanercept-treated and PBS-treated groups.

Etanercept-treated mice and PBS-treated mice (Group 2 and 3) were culled on day 32, while etanercept-treated mice and PBS-treated mice (Group 4 and 5) were culled on day 35.

Numbers of CII immunized mice developed arthritis from each time point group were counted on the harvesting day. Mean arthritis scores (total arthritis score/number of mice in the group), maximum arthritis score and mean swelling of CII immunized mice from each treatment time point group were calculated on the harvesting day.

5.2.2 Effect of etanercept on serum inflammatory mediator protein concentrations in CII immunized mice on day 14, day 32 and day 35 by Luminex cytokine 20-plex assay

The aim of this experiment is to investigate whether etanercept has any effect on peripheral inflammatory mediator protein profiles of CII immunized mice during the early and the late stages of disease in the CIA model. Serum collected from etanercept-treated and PBS-treated control mice on day 32 and day 35 were determined for changes in several cytokines, chemokines and growth factors using a Luminex cytokine 20-plex assay. However, all the inflammatory mediator protein concentrations in serum of mice from all experimental groups were lower than the detection limits of this assay.

5.2.3 *Changes in inflammatory mediator protein concentrations in the brains of etanercept-treated and untreated CII immunized mice on day 14, day 32 and day 35*

Etanercept has shown its protective effect on the joint inflammation in this CIA model by delaying the onset of arthritis and reducing the severity of arthritis in CIA model (Williams et al., 2000b). In this study, etanercept was administered to CII immunized mice as a protective therapy before the disease onset (from day 18 onwards). Results from the previous chapter (Chapter 4; sections 4.2.3 and 4.2.4) demonstrated that longitudinal changes in several inflammatory mediators in brains of CII immunized mice throughout the period of clinical expression of the disease (onset of the disease, early and late phase of disease). Several inflammatory mediators were up-regulated in brains of CII immunized mice during the onset and early disease stage (day 22 - day 35 after immunization), and some of these inflammatory mediators were up-regulated during the late stage of the disease (day 35 - day 42 after immunization). In the previous chapter, we started to measure inflammatory mediators in brains of CII immunized mice from day 22 as a time point of disease onset. However, del Rey et al., reported the upregulation of IL-1 β and IL-6 in brains of CIA rats before the onset of RA disease (during the first 20 days after the primary immunization) (del Rey et al., 2008). In our study, changes in these brain inflammatory cytokine concentrations before the onset of the disease have not been determined. To determine changes in brain inflammatory mediator protein concentrations in CII immunized mice before the onset of RA disease, we measured protein concentrations of brain inflammatory mediator in CII immunized mice on day 14 to represent a reasonable time point before disease-onset and before the etanercept treatment.

We investigated the effects of etanercept on brain inflammatory mediator profiles in treated and un-treated CII immunized mice during the period of clinical expression of the disease, and studied the association with its effect on the amelioration of joint disease during those time points. We determined changes in brain inflammatory mediator protein concentrations on day 32 as the time point of early stage of disease and day 35 as the time point of late stage of the disease. Inflammatory mediators in brains of mice of all experimental groups were determined using a Luminex and ELISA assay. To investigate effects of

etanercept on brain inflammatory mediator protein profiles, half brain tissue homogenates of CII immunized mice treated with etanercept on day 32 and day 35 were determined for inflammatory mediator protein concentrations compared to those in CII immunized mice treated with PBS or control naïve mice.

5.2.3.1 Effects of etanercept on pro-inflammatory cytokine protein profiles in the brain of CII immunized mice on days 14, 32 and 35

The protein concentrations of pro-inflammatory cytokines including IL-6, IL-1 β and TNF- α were determined by ELISA assays in brain homogenates of mice from all experimental groups.

On day 14, the concentrations of brain TNF- α protein of CII immunized mice and naïve control mice were not significantly different (Figure 5.5A). During the period of clinical expression of disease on day 32 and day 35, there was no significant difference in the concentrations of brain TNF- α protein between PBS-treated CII immunized mice and naïve control mice. However, etanercept-treated mice showed a significant reduction in brain TNF- α protein concentrations compared to those in naïve control mice and in PBS-treated CII immunized mice (Figure 5.5A). One-way ANOVA analysis followed by Bonferroni's post-hoc comparison tests demonstrated that there were significant differences in protein concentration of TNF- α among the three groups of mice culled on day 32 ($P = 0.0006$) (Figure 5.5A). The mean value of brain TNF- α protein concentrations on day 32 (etanercept-treated versus PBS-treated CII immunized) was 54.3 ± 2.9 pg/mg total brain protein versus 92.2 ± 8.9 pg/mg total brain protein ($P < 0.01$), while the mean value of brain TNF- α of on day 32 (etanercept-treated versus naïve control) was 54.3 ± 2.9 pg/mg total brain protein versus 79.2 ± 4.2 pg/mg total brain protein ($P < 0.001$). A similar pattern of TNF- α protein concentrations was observed in brain of treated, PBS-treated CII immunized mice compared to those of the naïve control mice on day 35. However, one-way ANOVA analysis showed that there was no significant difference between TNF- α protein concentrations in brains of etanercept-treated, PBS-treated CII immunized mice and naïve control mice on day 35 ($P = 0.1632$) (Figure 5.5A).

During the pre-onset period (day 14) there was no significant difference in brain IL-1 β protein concentrations between naïve control and CII immunized mice (Figure 5.5B). One-way ANOVA analysis showed that there was no significant difference between IL-1 β protein concentrations in brains of etanercept-treated, PBS-treated CII immunized mice and naïve control mice on day 32 ($P = 0.5619$). However, one-way ANOVA analysis followed by Bonferroni's post-hoc comparison tests also demonstrated that there were significant differences in protein concentration of IL-1 β among the three groups of mice culled on day 35 ($P = 0.0030$). The brain IL-1 β protein concentrations of PBS-treated CII immunized mice were significantly lower than those of naïve control mice. The mean value of brain IL-1 β protein concentrations on day 35 (PBS-treated versus naïve control) was 62.6 ± 18.5 pg/mg total brain protein versus 75.9 ± 15.3 pg/mg total brain protein ($P < 0.01$). Similarly, the brain IL-1 β protein concentrations of etanercept-treated CII immunized mice were also lower than those of PBS-treated mice; the mean value of brain IL-1 β protein concentrations on day 35 (etanercept-treated versus naïve control) was 68.2 ± 6.6 pg/mg total brain protein versus 75.9 ± 15.3 pg/mg total brain protein ($P < 0.05$) (Figure 5.5B).

Similar to TNF- α and IL-1 β , there was no significant difference in brain IL-6 protein concentrations between naïve control mice and CII immunized mice on day 14 (Figure 5.5C). One-way ANOVA analysis showed that there was no significant difference between IL-6 protein concentrations in brains of etanercept-treated, PBS-treated CII immunized mice and naïve control mice on day 32 ($P = 0.7684$). One-way ANOVA analysis showed that there was no significant difference between IL-6 protein concentrations in brains of etanercept-treated, PBS-treated CII immunized mice and naïve control mice on day 35 ($P = 0.1368$) (Figure 5.5C).

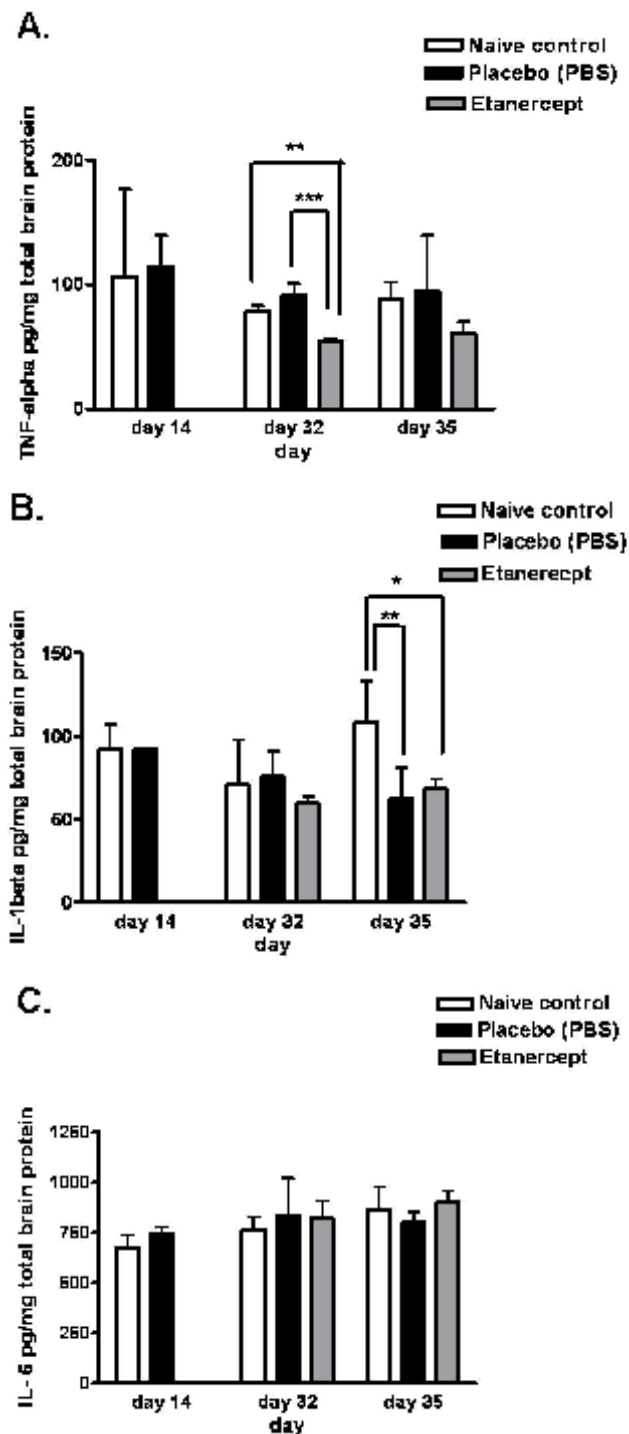


Figure 5.5 Effects of etanercept on brain pro-inflammatory cytokine protein profiles in CII immunized mice on days 14, 32 and 35

CII immunized mice were treated with etanercept (gray bars), or PBS (black bars) from day 18 after immunization onwards. The protein concentrations of brain pro-inflammatory cytokines (TNF- α , IL-1 β and IL-6) of CII immunized mice and naïve control mice were determined on day 14 as a time point of pre-onset of disease and before etanercept treatment. CII immunized mice treated with PBS as a placebo control, were described as PBS-treated CII immunized mice. Etanercept-treated and PBS-treated CII immunized mice were culled on day 32 and day 35, and brains were harvested and processed for inflammatory mediator protein determination. Brain samples collected from antigen-naïve control mice (white bars) culled on the days indicated were used as controls. TNF- α (A), IL-1 β (B) and IL-6 (C) protein concentrations in brain tissue homogenate of mice from all experimental groups were determined using ELISA assays. Pro-inflammatory cytokine protein concentrations in brain tissue, normalized against total brain protein, are expressed as pg/mg total brain protein. Error bars represent means \pm SD ($n = 3$ mice on day 14 and day

32, n = 5 mice on day 35). Statistical analysis of data was performed using one-way ANOVA (* $P < 0.05$; ** $P < 0.01$; *** $P < 0.001$).

5.2.3.2 Effects of etanercept on Th1 cytokine protein profiles in the brain of CII immunized mice on days 14, 32 and 35

IL-2 and IL-12 were the only Th1 cytokines that could be detected using ELISA assays in the brain tissue of mice from all experimental groups. Similar to the profile of pro-inflammatory cytokines, there were no significant changes in Th1 cytokine (IL-2 and IL-12) protein concentrations in brains of CII immunized mice compared to naïve control mice during the pre-onset time point on day 14 (Figure 5.6A and Figure 5.6B)

One-way ANOVA analysis showed that there was no significant difference between IL-2 protein concentrations in brains of treated, PBS-treated CII immunized mice and naïve control mice on day 32 ($P = 0.2046$). One-way ANOVA demonstrated that there was a significant difference in protein concentration of IL-2 among the three groups of mice on day 35 ($P = 0.0222$). Post hoc analysis with Bonferroni correction demonstrated that there was a significant up-regulation in brain IL-2 cytokine concentrations in etanercept-treated CII immunized mice compared to those of PBS-treated CII immunized mice on day 35. The mean value of brain IL-2 protein concentrations on day 35 (etanercept-treated versus PBS-treated) was 422.9 ± 45.4 pg/mg total brain protein versus 337.5 ± 48.3 pg/mg total brain protein ($P < 0.05$) (Figure 5.6A).

One-way ANOVA analysis demonstrated that there was a significant difference in protein concentration of IL-12 among the three groups of mice on day 32 ($P = 0.0110$). Post hoc analysis with Bonferroni correction demonstrated that there was a significant reduction in brain IL-12 protein concentrations in etanercept-treated mice compared with PBS-treated CII immunized mice on day 32. The mean value of brain IL-12 on day 32 (etanercept-treated versus PBS-treated) was 35.0 ± 10.3 pg/mg total brain protein versus 265.6 ± 107.2 pg/mg total brain protein ($P < 0.05$). The similar pattern of brain IL-12 protein concentrations in mice from all experimental groups was also observed on day 35. One-way ANOVA followed by Bonferroni's post-hoc comparison tests demonstrated that there were significant differences in protein concentration of IL-12 among the three groups of mice on day 35 ($P < 0.0001$). Again, brain IL-12 protein concentrations

in etanercept-treated CII immunised mice were significantly lower than those in naïve control and PBS treated mice. The mean value of brain IL-12 protein concentrations on day 35 (etanercept-treated versus naïve control) was 37.9 ± 7.8 pg/mg total brain protein versus 199.8 ± 13.4 pg/mg total brain protein ($P < 0.001$), while the mean value of brain IL-12 protein concentrations on day 35 (etanercept-treated versus PBS-treated) was 37.9 ± 7.8 pg/mg total brain protein versus 197.8 ± 21.7 pg/mg total brain protein ($P < 0.001$) (Figure 5.6B).

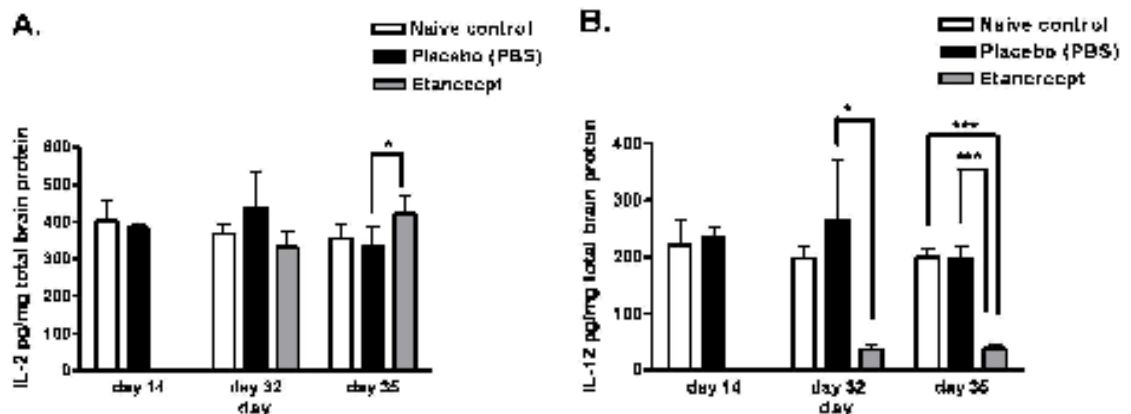


Figure 5.6 Effects of etanercept on brain Th1 cytokine protein profiles in CII immunized mice on day 32 and day 35

CII immunized mice were treated with etanercept (gray bars), or PBS (black bars) from day 18 after immunization onwards; and antigen-naïve control mice (white bars). The protein concentrations of brain Th1 cytokines (IL-2 and IL-12) of CII immunized mice and naïve control mice were determined on day 14 as a time point of pre-onset of disease and before the etanercept treatment. CII immunized mice treated with PBS as a placebo were considered as PBS-treated CII immunized mice. Etanercept-treated and PBS-treated CII immunized mice were culled on day 32 and day 35, and brains were harvested and processed for inflammatory mediator protein determination. Brain samples collected from naïve control mice (white bars) culled on the days indicated were used as controls. IL-2 (A) and IL-12 (B) protein concentrations in brain tissue homogenate of mice from all experimental groups were determined using ELISA assays. Th1 cytokine protein concentrations in brain tissue, normalized against total brain protein, are expressed as pg/mg total brain protein. Error bars represent means \pm SD ($n = 3$ mice on day 14 and day 32, $n = 5$ mice on day 35). Statistical analysis of data was performed using one-way ANOVA (* $P < 0.05$; ** $P < 0.01$; *** $P < 0.001$).

5.2.3.3 Effects of etanercept on Th2 cytokine protein profiles in the brain of CII immunized mice on days 14, 32 and 35

The Th2 cytokines IL-4, IL-5, IL-10 and IL-13 protein concentrations were detectable by ELISA assays in brain tissue of mice from all experimental groups. Again, there was no significant difference in these Th2 cytokine protein concentrations between CII immunized mice and control mice on day 14 before the onset and the etanercept treatment (Figure 5.7A - Figure 5.7D)

One-way ANOVA analysis demonstrated that there was no significant difference between IL-4 protein concentrations in brains of etanercept-treated and PBS-treated-CII immunized mice and naïve control mice on day 32 ($P = 0.7808$). There was no significant difference between IL-4 protein concentrations in brains of etanercept-treated, PBS-treated-CII immunized mice and naïve control mice on day 35 ($P = 0.8415$) (Figure 5.7A).

One-way ANOVA analysis demonstrated that there were significant differences in protein concentration of IL-5 among the three groups of mice on day 32 ($P = 0.0183$). Post hoc analysis with Bonferroni correction demonstrated that there was a significant reduction in brain IL-5 protein concentrations in etanercept-treated mice compared with PBS-treated CII immunized mice on day 32. There was no significant difference in brain IL-5 protein concentrations between PBS-treated CII immunized mice and naïve control mice. Significant reductions in brain IL-5 protein concentrations of etanercept-treated CII immunized mice compared to those in naïve control mice and PBS-treated CII immunized mice were observed on day 32. The mean value of brain IL-5 protein concentrations on day 32 (etanercept-treated versus naïve control) was 4.4 ± 0.9 pg/mg total brain protein versus 9.3 ± 1.7 pg/mg total brain protein ($P < 0.05$), while the mean value of brain IL-5 protein concentrations on day 32 (etanercept-treated versus PBS-treated) was 4.4 ± 0.9 pg/mg total brain protein versus 8.9 ± 2.1 pg/mg total brain protein ($P < 0.05$). One-way ANOVA analysis demonstrated that there were significant differences in protein concentration of IL-5 among the three groups of mice on day 35 ($P = 0.0025$). Post hoc analysis with Bonferroni correction demonstrated that there was a significant reduction in brain IL-5 protein concentrations in etanercept-treated mice compared with PBS-treated CII immunized mice on day 35. PBS-treated CII immunized mice had lower brain IL-5 protein concentrations compared to those of naïve control mice. The mean value of brain IL-5 protein concentrations on day 35 (PBS-treated versus naïve control) was 6.5 ± 1.3 pg/mg total brain protein versus 9.7 ± 2.6 pg/mg total brain protein ($P < 0.05$). Interestingly, etanercept-treated CII immunized mice also show significant reductions in brain IL-5 protein concentrations compared to those in naïve control mice on day 35. The mean value of brain IL-5 protein concentrations on day 35 (etanercept-treated versus naïve control) was 4.8 ± 0.9

pg/mg total brain protein versus 9.7 ± 2.6 pg/mg total brain protein ($P < 0.01$) (Figure 5.7B).

One-way ANOVA analysis demonstrated that there was no significant difference between IL-10 protein concentrations in brains of etanercept-treated, PBS-treated CII immunized mice and naïve control mice on day 32 ($P = 0.6607$). One-way ANOVA analysis also showed that there was no significant difference between IL-10 protein concentrations in brains of etanercept-treated, PBS-treated-CII immunized mice and naïve control mice on day 35 ($P = 0.3533$) (Figure 5.7C).

One-way ANOVA analysis demonstrated that there was no significant difference between IL-13 protein concentrations in brains of etanercept-treated, PBS treated-CII immunized mice and control naïve mice on day 32 ($P = 0.3703$). However, one-way ANOVA demonstrated that there was a significant difference in protein concentration of IL-13 among the three groups of mice on day 35 ($P = 0.0185$). Post hoc analysis with Bonferroni correction demonstrated that there was a significant reduction in brain IL-13 protein level in PBS-treated CII immunized mice compared to those of naïve control mice and treated CII immunized mice on day 35. The mean value of brain IL-13 protein concentrations on day 35 (PBS-treated versus naïve control) was 28.0 ± 15.9 pg/mg total brain protein versus 50.5 ± 9.0 pg/mg total brain protein ($P < 0.05$) (Figure 5.7D).

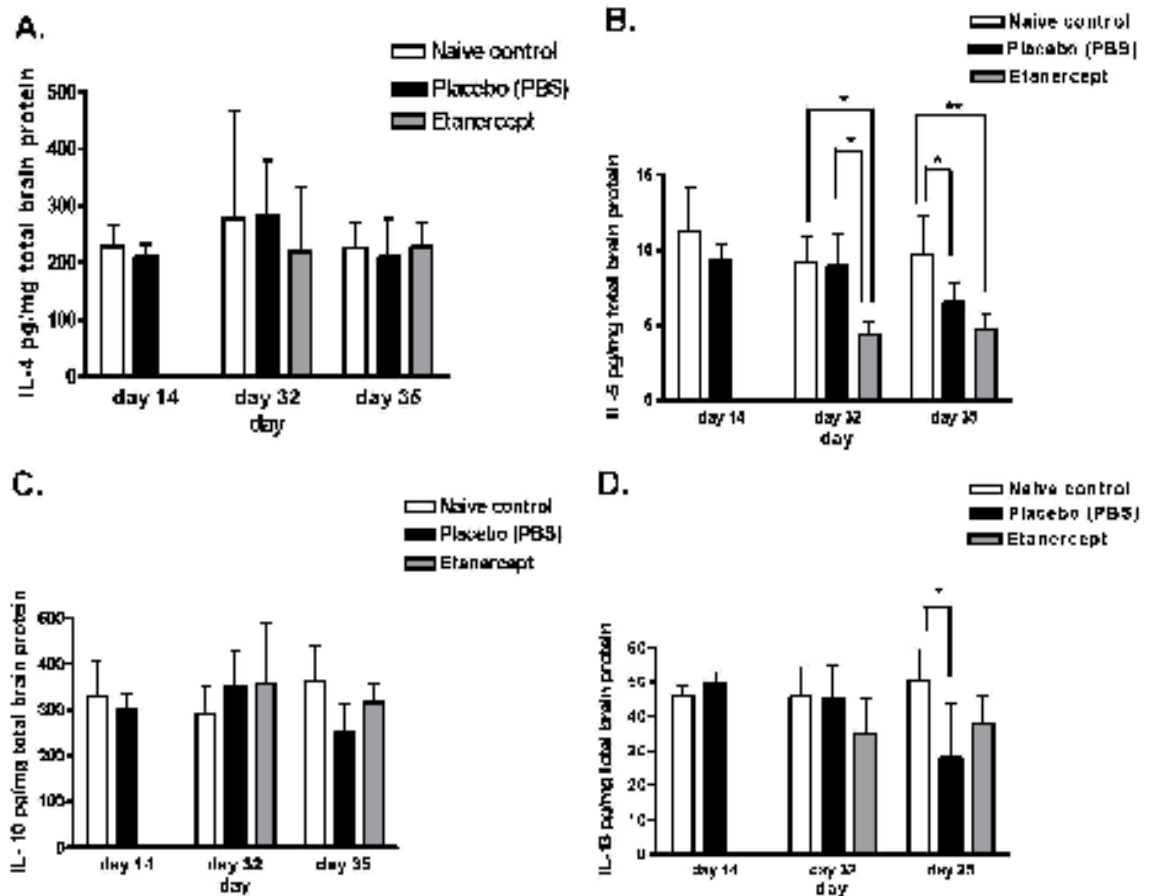


Figure 5.7 Effects of etanercept on brain Th2 cytokine protein profiles in CII immunized mice on day 32 and day 35

CII immunized mice were treated with etanercept (gray bars), or PBS (black bars) from day 18 after immunization onwards; and antigen-naïve control mice (white bars). The protein concentrations of brain Th2 cytokines (IL-4, IL-5, IL-10 and IL-13) of CII immunized mice and naïve control mice were determined on day 14 as the time point of pre-onset and before the etanercept treatment. CII immunized mice treated with PBS as placebo, were considered as PBS-treated CII immunized mice. Etanercept-treated and PBS-treated CII immunized mice were culled on day 32 and day 35, and brains were harvested and processed for inflammatory mediator protein determination. Brain samples collected from naïve control mice (white bars) culled on the days indicated were used as controls. IL-4 (A), IL-5 (B), IL-10 (C) and IL-13 (D) protein concentrations in brain tissue homogenate of mice from all experimental groups were determined using ELISA assays. Th2 cytokine protein concentrations in brain tissue, normalized against total brain protein, are expressed as pg/mg total brain protein. Error bars represent means \pm SD ($n = 3$ mice on day 14 and day 32, $n = 5$ mice on day 35). Statistical analysis of data was performed using one-way ANOVA (* $P < 05$; ** $P < 01$; *** $P < 001$).

5.2.3.4 Effects of etanercept on chemokine protein profiles in the brain of CII immunized mice on days 14, 32 and 35

Changes in CXCL1 protein concentrations in brain tissue extracts of mice from all experimental groups were detected using a Luminex assay. There was no significant difference in brain CXCL1 protein concentrations between naïve control mice and CII immunized mice on day 14 before the onset of disease and the etanercept treatment. In addition, one-way ANOVA analysis demonstrated that there was no significant difference between CXCL1 protein concentrations

in brains of etanercept-treated, PBS-treated CII immunized mice and naïve control mice on day 32 ($P = 0.0798$). One-way ANOVA analysis also demonstrated that there were significant differences in protein concentration of CXCL1 among the three groups of mice on day 35 ($P = 0.0004$). Post hoc analysis with Bonferroni correction demonstrated that there was a significant increase in brain CXCL1 protein concentrations in PBS-treated CII immunized mice compared to those in the naïve control mice on day 35. The mean value of brain CXCL1 protein concentrations on day 35 (PBS-treated versus naïve control) was 51.6 ± 7.0 pg/mg total brain protein versus 26.9 ± 10.8 pg/mg total brain protein ($P < 0.001$). Interestingly, etanercept decreased brain CXCL1 protein concentrations in CII immunized mice as etanercept-treated CII immunized showed a significant reduction in brain CXCL1 protein concentrations compared to those in PBS-treated CII immunized mice. The mean value of brain CXCL1 protein concentrations on day 35 (etanercept-treated versus PBS-treated) was 51.6 ± 7.0 pg/mg total brain protein versus 29.5 ± 6.3 pg/mg total brain protein ($P < 0.01$) (Figure 5.8).

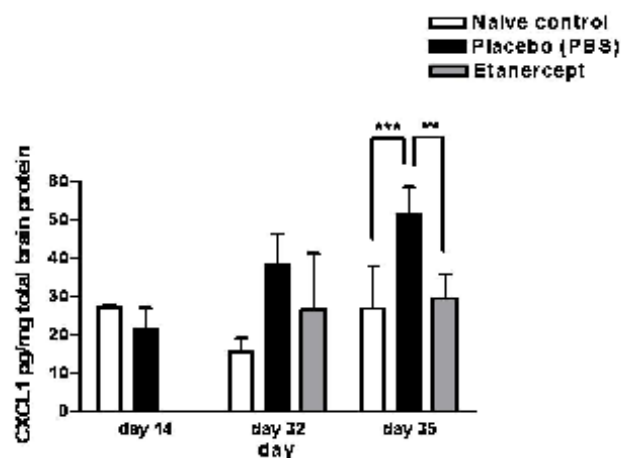


Figure 5.8 Effects of etanercept on brain chemokine (CXCL1) protein profiles in CII immunized mice on day 32 and day 35

CII immunized mice were treated with etanercept (gray bars), or PBS (black bars) from day 18 after immunization onwards; and antigen-naïve control mice (white bars). The protein concentrations of brain a chemokine CXCL1 of CII immunized mice and naïve control mice were determined on day 14 as the time point of pre-onset and before the etanercept treatment. CII immunized mice treated with PBS as a placebo, were considered as PBS-treated CII immunized mice. Etanercept-Treated and PBS-treated CII immunized mice were culled on day 32 and day 35, and brains were harvested and processed for inflammatory mediator protein determination. Brain samples collected from naïve control mice (white bars) culled on the days indicated were used as controls. Chemokine CXCL1 protein concentrations in brain tissue homogenate of mice from all experimental groups were determined using a Luminex assay. Chemokine CXCL1 protein concentrations in brain tissue, normalized against total brain protein, are expressed as pg/mg total brain protein. Error bars represent means \pm SD ($n = 3$ mice on day 14 and day 32, $n = 5$ mice on day 35). Statistical analysis of data was performed using one-way ANOVA ($*P < 0.05$, $**P < 0.01$, $***P < 0.001$).

5.2.3.5 Effects of etanercept on growth factor protein profiles in the brain of CII immunized mice on days 14, 32 and 35

VEGF and FGF2 growth factors were detected using an ELISA assay and a Luminex assay in brain tissue extracts of mice from all experimental groups. One-way ANOVA analysis showed that there was no significant difference between VEGF protein concentrations in brains of etanercept-treated, PBS-treated-CII immunized mice and naïve control naïve mice on day 32 ($P = 0.2730$). However, one-way ANOVA analysis also demonstrated that there was a significant difference in protein concentration of VEGF among the three groups of mice on day 35 ($P = 0.0115$). Post hoc analysis with Bonferroni correction demonstrated that brain VEGF protein level was significantly increased in etanercept-treated CII immunized mice compared to those in PBS-treated CII immunized mice. The mean value of brain VEGF protein concentrations on day 35 (PBS-treated versus etanercept-treated) was 431.6 ± 59.8 pg/mg total brain protein versus 332.6 ± 32.5 pg/mg total brain protein ($P < 0.05$) (Figure 5.9A).

There was no significant difference between FGF2 protein concentrations in brains of etanercept-treated, PBS-treated CII immunized mice and naïve control mice on both day 32 and day 35 (Figure 5.9B).

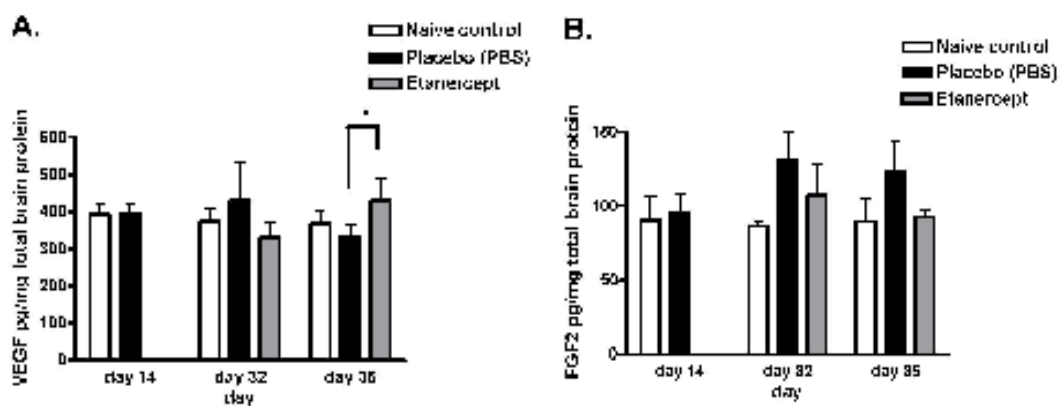


Figure 5.9 Effects of etanercept on brain growth factor protein profiles in CII immunized mice on day 32 and day 35

CII immunized mice were treated with etanercept (gray bars), or PBS (black bars) from day 18 after immunization onwards; and antigen-naïve control mice (white bars). The protein concentrations of brain growth factors (VEGF and FGF2) of CII immunized mice and naïve control mice were determined on day 14 as the time point of pre-onset and before the etanercept treatment. CII immunized mice treated with PBS as a placebo, were considered as PBS-treated CII immunized mice. Etanercept-treated and PBS-treated CII immunized mice were culled on day 32 and day 35, and brains were harvested and processed for inflammatory mediator protein determination. Brain samples collected from naïve control mice (white bars) culled on the days indicated were used as controls. VEGF (A) and FGF2 (B) protein concentrations in brain tissue homogenate of mice from all experimental groups

were determined using ELISA assays. Growth factor protein concentrations in brain tissue, normalized against total brain protein, are expressed as pg/mg total brain protein. Error bars represent means \pm SD ($n = 3$ mice on day 14 and day 32, $n = 5$ mice on day 35). Statistical analysis of data was performed using one-way ANOVA (* $P < 0.05$, ** $P < 0.01$, *** $P < 0.001$).

5.2.4 Changes in inflammatory mediator gene expression in the brains of etanercept treated and PBS treated CII immunized mice on day 14, day 32 and day 35 by real-time PCR

We also investigated the effects of etanercept on the gene expression of inflammatory mediators in CII immunized mice. Real-time PCR was used to quantify the gene expression of the same pro-inflammatory cytokines (IL-6, IL-1 β , TNF- α and IL-1 α), Th1 cytokines (IL-2, IL-12 and IFN- γ), Th2 cytokines (IL-4, IL-5, IL-10 and IL-13), chemokines (CXCL1, CXCL10, CCL2 and CCL3) and growth factors (FGF2 and, VEGF) using one half of the brain tissue of mice from all experimental groups. Gene expression of IL-1 β , CXCL1, CXCL10, FGF2 and VEGF were detectable within the assay detection limits.

5.2.4.1 Effects of etanercept on pro-inflammatory cytokine mRNA profiles in brains of CII immunized mice on days 14, 32 and 35 by Real-time PCR assays

The gene expression of pro-inflammatory cytokines including IL-6, IL-1 β and TNF- α and IL-1 α were determined in brains of mice from all experimental groups. In our study, IL-1 β was the only pro-inflammatory cytokine gene expression levels detectable within the detection limit of the assays.

There was no significant difference in brain IL-1 β mRNA levels between naïve control mice and CII immunized mice on day 14 before the etanercept treatment and onset of the disease. On day 32, one-way ANOVA analysis showed that there was no significant difference between IL-1 β mRNA levels in brains of etanercept-treated, PBS-treated CII immunized mice and naïve control mice ($P = 0.2444$). Brain IL-1 β mRNA levels in PBS-treated CII immunized mice was higher, but not significant, than those of naïve control mice. One-way ANOVA analysis demonstrated that there were significant differences in IL-1 β mRNA levels among the three groups of mice on day 35 ($P = 0.0011$). Post hoc analysis with Bonferroni correction demonstrated that PBS-treated CII immunized mice had a significantly higher brain IL-1 β mRNA level compared to those in naïve control

mice on day 35. The mean value of brain IL-1 β mRNA levels on day 35 (PBS-treated versus naïve control) was 1261 ± 158 versus 702 ± 109 ($P < 0.05$). At this time point, IL-1 β mRNA levels in brains of etanercept-treated CII immunized mice was decreased significantly compared to those of PBS-treated CII immunized mice. The mean value of IL-1 β mRNA levels on day 35 (etanercept-treated versus PBS-treated) was 478 ± 33 versus 1261 ± 158 ($P < 0.01$) (Figure 5.10).

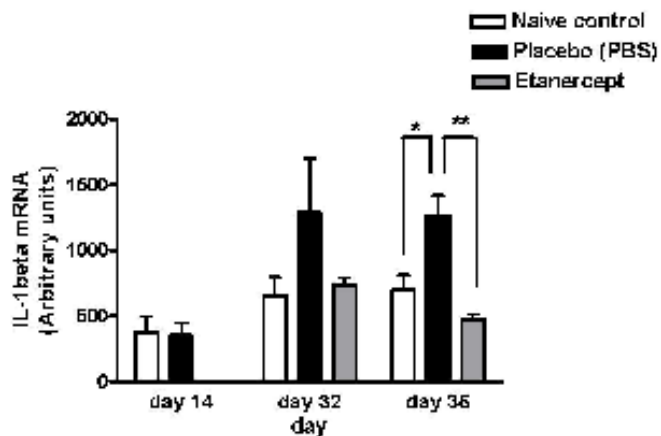


Figure 5.10 Effects of etanercept on a brain pro-inflammatory cytokine gene expression profiles in CII immunized mice on day 32 and day 35

CII immunized mice were treated with etanercept (gray bars), or PBS (black bars) from day 18 after immunization onwards; and antigen-naïve control mice (white bars). The mRNA levels of a brain pro-inflammatory cytokine IL-1 β of CII immunized mice and naïve control mice were determined on day 14 as the time point of pre-onset and before the etanercept treatment. CII immunized mice treated with PBS as a placebo, were considered as PBS-treated CII immunized mice. Etanercept-treated and PBS-treated CII immunized mice were culled on day 32 and day 35, and brains were harvested and processed for inflammatory mediator protein determinations. Brain samples collected from normal mice (white bars) culled on the days indicated were used as controls. IL-1 β mRNA levels in brain tissue homogenate of mice from all experimental groups were determined using Real-time PCR. mRNA levels of pro-inflammatory cytokines in brain tissue, normalized against the housekeeping gene GAPDH, are expressed as arbitrary units. Error bars represent means \pm SD ($n = 3$ mice on day 14 and day 32, $n = 5$ mice on day 35). Statistical analysis of data was performed using one-way ANOVA (* $P < 0.05$, ** $P < 0.01$, *** $P < 0.001$).

5.2.4.2 Effects of etanercept on Th1 cytokine mRNA profiles in brains of CII immunized mice on days 14, 32 and 35 by real-time PCR assays

Changes in gene expression of Th-1 cytokines, including IL-12, IL-2 and IFN- γ , over time were determined in the brains of mice from all experimental groups. However, there was no significant difference between Th-1 cytokines mRNA levels in brains of treated, PBS treated CII immunized mice and control naïve mice on day 32 and day 35.

5.2.4.3 Effects of etanercept on Th2 mRNA profiles in brains of CII immunized mice on days 14, 32 and 35 by real-time PCR assays

Th-2 cytokines, including IL-4, IL-5, IL-10 and IL-13 gene expression were determined in the brains of mice from all experimental groups. However, there was no significant difference between Th-2 cytokines mRNA levels in brains of treated, PBS treated CII immunized mice and control naïve mice on day 32 and day 35.

5.2.4.4 Effects of etanercept on chemokine mRNA profiles in brains of CII immunized mice on days 14, 32 and 35 by real-time PCR assays

CXCL1, CXCL10, CCL2 and CCL3 gene expression levels were determined in the brains of control mice from all experimental groups. Among these chemokines, only CXCL1 and CXCL10 were detectable within the assay limits. During the pre-onset time on day 14, there was no significant difference in CXCL1 and CXCL10 mRNA levels between naïve control mice and CII immunized mice on day 14 before the etanercept treatment.

One-way ANOVA analysis demonstrated that there was no significant difference between CXCL1 mRNA levels in brains of etanercept-treated, PBS-treated CII immunized mice and naïve control mice on day 32 and day 35 ($P = 0.0761$ and $P = 0.2627$ respectively). Increases in brain CXCL1 mRNA levels was observed in PBS-treated CII immunized mice compared to those in naïve control and etanercept-treated CII immunized mice on both time points. However, a statistical analysis using one-way ANOVA analysis showed that the differences were not significant (Figure 5.11A).

One-way ANOVA analysis demonstrated that there was no significant difference between CXCL10 mRNA levels in brains of treated, untreated CII immunized mice and naïve control mice on day 32 and day 35 ($P = 0.5512$ and $P = 0.5347$ respectively) (Figure 5.11B).

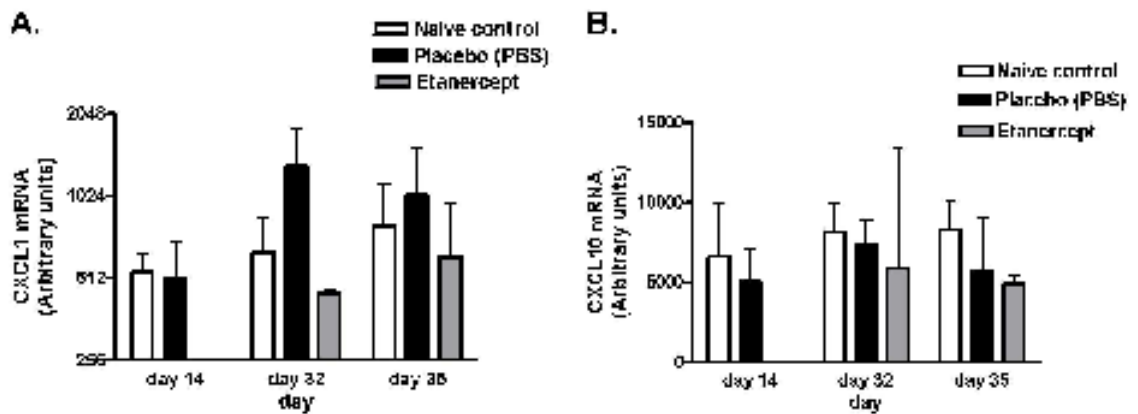


Figure 5.11 Effects of etanercept on a brain chemokine gene expression profiles in CII immunized mice on day 32 and day 35

CII immunized mice were treated with etanercept (gray bars), or PBS (black bars) from day 18 after immunization onwards; and antigen-naïve control mice (white bars). The mRNA levels of a brain chemokine CXCL1 and CXCL10 of CII immunized mice and naïve control mice were determined on day 14 as the time point of pre-onset and before the etanercept treatment. CII immunized mice treated with PBS as a placebo, were considered as PBS-treated CII immunized mice. Etanercept-treated and PBS-treated CII immunized mice were culled on day 32 and day 35, and brains were harvested and processed for inflammatory mediator protein determinations. Brain samples collected from normal mice (white bars) culled on the days indicated were used as controls. CXCL1 (A) and CXCL10 (B) mRNA levels in brain tissue homogenate of mice from all experimental groups were determined using Real-time PCR. mRNA levels of chemokines in brain tissue, normalized against the housekeeping gene GAPDH, are expressed as arbitrary units. Error bars represent means \pm SD ($n = 3$ mice on day 14 and day 32, $n = 5$ mice on day 35). Statistical analysis of data was performed using one-way ANOVA (* $P < 0.05$, ** $P < 0.01$, *** $P < 0.001$).

5.2.4.5 Effects of etanercept on growth factor mRNA profiles in brains of CII immunized mice on days 14, 32 and 35 by real-time PCR assays

Gene expression of growth factor mRNA for FGF2 and VEGF were detectable in the brains of mice from all experimental groups. There was no significant difference in FGF2 and VEGF mRNA levels observed in brains of CII immunized mice and naïve control mice.

One-way ANOVA analysis demonstrated that there was no significant difference between VEGF mRNA levels in brains of treated, PBS-treated CII immunized mice and naïve control mice on day 32 and day 35 ($P = 0.6335$ and $P = 0.6188$ respectively) (Figure 5.12A).

One-way ANOVA analysis demonstrated that, on day 32, there was no significant difference between FGF2 mRNA levels in brains of etanercept-treated, PBS-treated CII immunized mice and naïve control mice ($P = 0.1145$). However, brain FGF2 mRNA levels in both etanercept-treated and PBS-treated CII immunized mice appeared lower than those in naïve control mice at that time point. On day

35, One-way ANOVA analysis also demonstrated that there was no significant difference in brain FGF2 mRNA levels among the three groups of mice on day 35 ($P = 0.0544$) (Figure 5.12B).

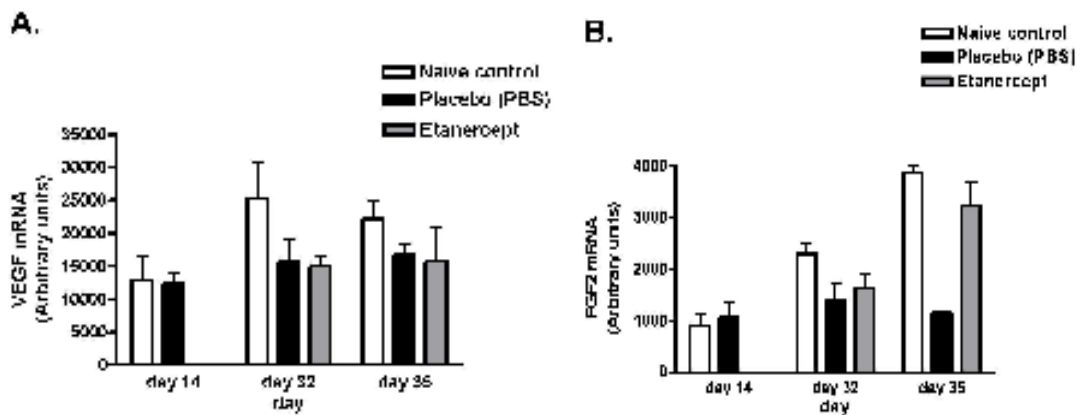


Figure 5.12 Effects of etanercept on a brain growth factor gene expression profiles in CII immunized mice on day 32 and day 35

CII immunized mice were treated with etanercept (gray bars), or PBS (black bars) from day 18 after immunization onwards; and antigen-naïve control mice (white bars). The mRNA levels of a brain chemokine VEGF and FGF2 of CII immunized mice and naïve control mice were determined on day 14 as the time point of pre-onset and before the etanercept treatment. CII immunized mice treated with PBS as a placebo, were considered as PBS-treated CII immunized mice. Etanercept-treated and PBS-treated CII immunized mice were culled on day 32 and day 35, and brains were harvested and processed for inflammatory mediator protein determinations. Brain samples collected from normal mice (white bars) culled on the days indicated were used as controls. VEGF (A) and FGF2 (B) mRNA levels in brain tissue homogenate of mice from all experimental groups were determined using Real-time PCR. mRNA levels of growth factors in brain tissue, normalized against the housekeeping gene GAPDH, are expressed as arbitrary units. Error bars represent means \pm SD ($n = 3$ mice on day 14 and day 32, $n = 5$ mice on day 35). Statistical analysis of data was performed using one-way ANOVA (* $P < 0.05$, ** $P < 0.01$, *** $P < 0.001$).

5.3 Summary; Effects of etanercept on inflammatory mediator mRNA and protein profiles in brains of CII immunized mice

In this chapter, we investigated the effect of TNF-blockade therapy using etanercept on brain inflammatory mediator profiles, comparing etanercept-treated and PBS-treated CII immunized mice during the period of clinical expression of the disease, and studied the association with its effect on the amelioration of joint disease during those time points. We found that etanercept treatment not only alleviated arthritis, but also had effects on inflammatory mediator mRNA and protein profiles in the brains of CII immunized mice. These changes in mRNA expression and protein concentrations of IL-1 β , TNF- α , IL-6, IL-4, IL-5, IL-10, IL-13, IL-2, IL-12, CXCL1, CXCL10, VEGF and FGF2 are summarised in Table 5.2

Inflammatory mediators	Day 32		Day 35	
	Protein	mRNA	Protein	mRNA
IL-1 β	NS	NS	NS	 P < 0.01
TNF- α	 P < 0.01	UD	NS	UD
IL-6	NS	UD	NS	UD
IL-4	NS	UD	NS	UD
IL-5	 P < 0.01	UD	NS	UD
IL-10	NS	UD	NS	UD
IL-13	NS	NS	UD	UD
IL-2	NS	UD	 P < 0.05	UD
IL-12	 P < 0.05	UD	 P < 0.001	UD
CXCL1	NS	NS	 P < 0.01	NS
CXCL10	UD	NS	UD	N
VEGF	NS	NS	 P < 0.05	NS
FGF2	NS	NS	NS	NS

Table 5.2 Effects of etanercept on inflammatory mediator protein and mRNA profiles in brains of etanercept-treated CII immunized mice relative to those of PBS-treated CII immunized mice

Red arrows represent changes in of inflammatory mediator protein concentrations, while blue arrows represent changes in inflammatory mediator mRNA levels in brains of etanercept-treated CII immunized mice compared to PBS-treated CII immunized mice on day 32 and day 35. Differences between inflammatory mediator concentrations in etanercept-treated CII immunized mouse brains and PBS-treated CII immunized mouse brains were analyzed by Student's t- test (*P < 005; **P < 002; ***P < 001). NS = not statistically significant, UD= Undetectable (below assay detection limit).

In this experiment, we investigated effects of etanercept on inflammatory mediator production in brains of CII immunized mice during the early stage of disease (day 32 after immunization) and late stage of disease (day 35 after immunization). We found that, at the early stage of RA disease, etanercept reduced the production of TNF- α and the Th1 cytokine IL-12, which are considered to be the main cytokines that initiate the RA disease process. However, at the late stage etanercept reduced IL-1 β and TNF- α production,

while increasing IL-6 production. Surprisingly, etanercept showed contradictory effects on two different Th1 cytokines, IL-2 and IL-12. Etanercept reduced brain IL-12 protein concentrations, but increased brain IL-2 protein concentrations, suggesting that etanercept may induce different signals on Th1 cells to generate different types of Th1 cytokines, for example IL-2 is an autocrine T-cell growth factor that is produced early in T-cell activation (Lorre et al., 1990), whereas IL-12 is produced later as a functional cytokine after T-cell polarisation (Feili-Hariri et al., 2005). Another possibility is that etanercept not only activated Th1 cells, but also could regulate other type of immune cell populations that can also produce Th1 cytokines in the brain such as astrocytes and microglia. Etanercept seemed to have no effect on brain Th2 cytokine production, including IL-4, IL-13 and IL-10. However, etanercept significantly reduced brain IL-5 protein concentrations in the brains of etanercept-CII immunized mice throughout the period of clinical expression of disease. The most striking data in this section seems to be the effect of etanercept suppressing the increased production of brain CXCL1 and IL-1 β that was seen in control PBS-treated CII immunized mice. These two cytokines are functionally related; IL-1 β is known to be a potent cytokine that stimulates the expression of CXCL1. It has been shown that chronic expression of IL-1 β can induce the expression of CXCL1 in the mouse brain. Therefore, it is possible that etanercept acts by inhibiting IL-1 β production resulting in a reduction of CXCL1 and potentially reducing immune cells influx into the brain. Interestingly, at this stage, etanercept can also activate the production of VEGF and FGF2. These growth factors are known as angiogenic factors that may suggest BBB breakdown in the CIA mouse brain. However, these growth factors may also have other functions in the brain and whether or not etanercept may worsen BBB breakdown in CIA mouse brains via enhancement of these brain growth factors need to be further investigated.

5.4 Result chapter 5: Summary of major findings.

The aim of this chapter was to investigate the effects of etanercept on the production of inflammatory mediators in the brain of CII immunized mice. We compared changes in brain inflammatory mediators among etanercept-treated CII immunized and control PBS-treated CII immunized mice at 3 time points across the 42 day experimental course of CIA. Day 14 after immunization was studied as a representative time-point prior to the onset of disease and before the etanercept treatment. The other 2 time points were during the period of clinical expression on day 32 representing the time point of early disease and at day 35 after immunization representing the time point of the late stage of disease. We found that:

1. There was no significant difference in brain inflammatory mediators between antigen-naïve control mice and CII immunized at day 14 after immunization which is representative of a time point prior to the onset of disease and pre-etanercept treatment.
2. In the first of two experiments, etanercept treatment did not delay the onset of arthritis nor reduce the incidence at day 32. In addition, etanercept treatment did not decreasing the severity of arthritis by reducing the mean paw thickness and the clinical score compared to PBS-treated CII immunized mice. However, etanercept treatment was associated with reductions in TNF- α , IL-5 and IL-12 protein concentrations in brains of etanercept-treated CII immunized mice.
3. In the second experiment, etanercept treatment did delay the onset of arthritis and reduced the incidence at day 35, as well as attenuating the severity of arthritis by reducing the mean paw thickness and the clinical score compared to PBS-treated CII immunized mice. At this time point, etanercept treatment was associated with reductions in IL-12, CXCL1 protein concentrations and with increases in IL-2 and VEGF protein concentrations in brains of etanercept- treated CII immunized mice.

5.5 Discussion

To extend our investigation of the association between peripheral inflammation and changes in brain inflammatory mediator profiles in CII immunized mice, we attempted to reduce the peripheral inflammatory signal using the anti-inflammatory drug etanercept as a preventive therapy for arthritis. We then examined the changes in the brain inflammatory mediator profile during the time course of the development of arthritis in CII immunized mice.

We found that systemic administration of the TNF- α blockade drug etanercept not only had an effect on the amelioration of joint disease by reducing mean paw thickness and incidence of arthritis in CII immunized mice, but also had effects on brain inflammatory mediator profiles in these mice. We found increases in IL-6, IL-2, VEGF protein concentrations and FGF2 mRNA levels, along with decreases in TNF- α , IL-5, IL-12, CXCL1 protein concentrations and IL-1 β mRNA levels in brains of etanercept-treated CII immunized mice compared to those of PBS-treated CII immunized mice. Our data suggest that changes in inflammatory mediators in brains of CII immunized mice may be a consequence of changes in the peripheral inflammatory cytokine signal during the clinical development of arthritis.

5.5.1 *Effect of etanercept on the amelioration of joint disease in CII immunized mice*

Etanercept is a recombinant human soluble p75 TNFR:Fc fusion protein that has been developed for the therapeutic treatment of RA. The administration of etanercept has been reported to attenuate the development of clinical arthritis and, in CIA mouse model, the development of experimental RA. Our data showed that the experimental arthritis disease process could be attenuated when the etanercept treatment was administered therapeutically from day 18 after the immunization, as indicated by significant reductions in mean arthritis scores, in mean paw swelling and in disease percent incidence compared to PBS treated CIA mice. Our finding is in agreement with several reports on the prevention of arthritis in CIA and AIA models of RA by the administration of 300 μ g/mouse/3 days of recombinant human/rodent TNFR:Fc fusion protein. In one of these reports, the administration of a recombinant soluble TNFR in CIA mice from day

14 onwards resulted in the delay of arthritis disease development, along with reduced arthritis disease severity as determined by paw swelling. However, that study did not address the effect on disease incidence (Williams et al., 2000b). The ability to prevent arthritis in the CIA model by peripheral TNF blockade in the days (typically <21 days) before the disease onset might be due to the fact that TNF- α plays a critical role in initiating an immuno-inflammatory cascade leading to the development of arthritis. TNF- α is involved in regulating other cytokine and chemokine release, recruitment of immune cells and expression of endothelial adhesion molecules at the inflamed site. However, the precise action of human soluble p75 TNFR:Fc fusion protein on the immune response to collagen challenge in the CIA model is not currently clear. The few studies in print suggested that recombinant human soluble p75 TNFR inhibited the immune-mediated arthritis by suppressing IgG2a anti-collagen antibody production, this is the dominant antibody subclass in the CIA model and is induced by Th1-type cells (Mukherjee et al., 2003). A study of RA demonstrated that soluble p75 TNFR treated CIA mice had lower concentrations of inflammatory Th1 driven IgG2a antibodies to CII than controls (Mageed et al., 1998). In addition, several studies also suggested that the immunosuppressive effects of this TNF- α blockade are related to inhibition of CD4⁺ activation and to down-regulation of the Th1 response. TNFR-p75 has been shown to be an essential co-stimulator for the survival of CD4⁺ T cells during clonal expansion, and p75-deficient T cells showed a defect in IL-2 production (Kim and Teh, 2004). CIA mice treated with TNF- α blockade also showed reduced number of CD4⁺ T cells in the joint (Marinova-Mutafchieva et al., 2000).

In this experiment, CII immunized mice after day 21 were randomly divided into 4 groups (Group 2 - 5) consisting of 3 - 5 mice per group. Each group of mice were allocated a separate cage and set up as follows;

Group 2: CII immunized mice treated with PBS and culled on day 32

Group 3: CII immunized mice treated with etanercept and culled on day 32

Group 4: CII immunized mice treated with PBS and culled on day 35

Group 4: CII immunized mice treated with etanercept and culled on day 35.

The incidences of RA appear to be around 60% for CII immunized mice in Group 2, 3 and 5. However, the data shown for paw thickness and arthritis score in CII immunized mice in each group were different. This suggests that each group mice developed arthritis in different severity. Therefore the data shown for paw thickness and arthritis score in the mice culled at day 32 and day 35 are different (Figure 5.2Figure 5.3). The different patterns of the arthritis score and paw thickness between CII immunized mice on day 32 and 35 may have been due to the small sample size ($n = 3-5$ CII immunized mice) and the inequality in number of mice culled on day 32 and day 35. The small number of mice per group may help to explain the inconsistency in the data shown for paw thickness and arthritis score in the mice culled on day 32 and day 35. Therefore, repetition of this experiment using a greater group size to increase in statistical power may help to improve the consistency of the data.

5.5.2 *Effects of peripheral etanercept treatment on inflammatory mediators in brains of CII immunized mice; possible evidence of peripheral inflammatory signal inducing neuro-inflammation*

By blocking peripheral inflammatory cytokine signal using etanercept in CII immunized mice, we found interesting evidence of immune activation and inflammation in the brains of CII immunized mice during the development of arthritis. In this study, we also investigated changes in brain inflammatory mediators in CII immunized mice compared to those in naïve control mice during the period before the onset of arthritis disease on day 14 after immunization. That time point was also used as a control time point before the etanercept treatment began on day 18. At that time point, no CII immunized mice developed arthritis and we found no significant difference in brain inflammatory mediator concentrations between CII immunized mice and those in naïve control mice. However, changes in inflammatory mediators in brains of etanercept-treated and PBS-treated CII immunized mice compared to those of naïve control mice were observed on day 32 and day 35 as the CII immunized mice developed arthritis. This finding suggested that the production in inflammatory mediators in brains of CII immunized mice may be stimulated by immune activation and inflammatory signals from cytokines in the peripheral circulation. This also suggests that etanercept may act at the peripheral blood level rather than at

the CNS level to regulate the production of brain inflammatory mediators in CII immunized mice. Another important piece of evidence suggesting that peripheral inflammation induced neuro-inflammation was that etanercept treatment was administered peripherally, but we could still observe changes in inflammatory mediators in the brains of CII-immunized mice. In particular, a reduction of brain TNF- α and IL-12, initiators of the joint destructive pathology of RA, were observed in etanercept-treated CII immunized mice on both day 32 and day 35. This suggested that etanercept may act mainly by inhibition of TNF- α and subsequently Th1 cells. However, we could not detect serum inflammatory mediators in mice from any of the experimental groups in this study, suggesting that the Luminex assay may not have been sufficiently sensitive to detect biologically active concentrations of relevant cytokines in this system. We therefore could not conclude whether or not etanercept actually blocked any specific peripheral inflammatory cytokine signal by reducing serum TNF- α and other inflammatory mediators during the development of arthritis. It is also possible that TNF- α is present in the serum at low concentrations that is sufficient to initiate disease and/or it is transiently cleared after inflammatory challenge. A study by Goto *et al* has demonstrated rapid clearance (120 min) of recombinant TNF- α from the rat circulation following intravenous injection of LPS (Goto *et al.*, 2001). We hypothesized that TNF- α may activate the production of inflammatory mediators in the circulation and that these may be rapidly cleared. This hypothesis is supported by a study in a model of surgical trauma showing that anti-TNF transiently reduced the protein concentrations of serum IL-1 β both at 6 and 24 h following surgery (Terrando *et al.*, 2010). Interestingly, in the brains of etanercept-treated CII immunized mice we found a significant reduction of IL-12, TNF- α , IL-5 on day 32, and a reduction of brain IL-12 on day 35 associated with a significant lower mean clinical score and paw thickness compared to PBS-treated CII immunized mice on day 35.

The transient effect of anti-TNF therapy on CNS cytokine production has also been demonstrated in recent studies; in a model of acute inflammatory brain injury in morphine-tolerant rats (Shen *et al.*, 2011) and in traumatic brain injury (Chio *et al.*, 2010).

5.5.3 Effects of peripheral etanercept treatment on pro-inflammatory cytokines in brains of CII immunized mice

We will now consider how CIA may be associated with brain inflammation. In the CNS, TNF- α and TNFR signalling play crucial roles in neuro-inflammatory processes. The p75 TNFR was shown to be increased on peripheral blood monocytes and lymphocytes of MS patients (Jurewicz et al., 1999). In addition, TNF/TNFR signalling was shown to induce oligodendrocyte apoptosis and primary demyelination in an MS model (Akassoglou et al., 1998). In an EAE model, TNF- α plays an essential role in the initiation of clinical symptoms, and the therapeutic administration of TNFR-IgG could prevent the development of disease (Korner et al., 1997). In experimental cerebral ischemia, p75 TNFR signalling was demonstrated to initiate CNS inflammation as indicated by endothelial cell activation, meningeal inflammation, and vessel fibrosis in p75 TNFR transgenic mice (Akassoglou et al., 2003). Recently, etanercept, TNF blockade, has been shown to be effective treatment for both immune and non-immune-mediated CNS injury. A study by Genovese *et al* showed that the inflammation associated with acute spinal cord injury was significantly decreased by etanercept. Etanercept has shown to attenuate central endotoxin-induced brain injury (Campbell et al., 2007). Our data showing that peripheral administration of etanercept reduced the local concentrations of pro-inflammatory cytokines including TNF- α and IL-1 β in the brains of CII immunized mice are in agreement with recent reports of models of morphine-tolerant rats (Shen et al., 2011) and traumatic brain injury (Chio et al., 2010).

5.5.4 Effects of peripheral etanercept treatment on TNF- α in brains of CII immunized mice

Our data showed down-regulation of brain TNF- α in etanercept treated- CII immunized mice compared to those in PBS treated-CII immunized mice on days 32 and 35. We were not able to define the precise action of etanercept on this suppression of brain TNF- α in CII immunized mice mainly because we could not detect TNF- α protein in serum or mRNA in the brains of etanercept-treated and PBS-treated CII immunized mice in our study. We could therefore speculate that one possible mechanism is that the etanercept binds systemic TNF- α and thereby prevent the transport of TNF- α through the blood brain barrier (Jiang et al.,

2008). This is the most likely mechanism because etanercept does not cross the blood-brain barrier due to its hydrophilic property and high molecular weight (Francis et al., 2004), suggesting that it is unlikely that etanercept could inhibit production of TNF- α in the brains of CII immunized mice. However, in another study, TNF- α transport across the blood-brain barrier is shown to be mediated by p75 TNFR (Pan and Kastin, 2002), which was strongly up-regulated during CNS inflammation and injury (Pan et al., 2003). This suggests that an increase in p75 TNFR may paradoxically enhance the transportation of peripheral TNF- α into the brain. The soluble form of p75 TNFR that is released from monocytes during inflammation is thought to function by modulating the availability and biological activity of TNF- α via neutralization or stabilization (Joyce and Steer, 1996). A study in an LPS-challenge mouse inflammation model suggested that dimeric sTNFR are effective inhibitors of TNF and, under some circumstances, could also function as TNF carriers. Administration of a mortality-reducing dose of sTNFR reduced the rise in serum TNF bioactivity that normally occurred in response to LPS. However, a lower dose of sTNFR resulted in increased serum TNF concentrations compared to mice given LPS but no soluble receptor. The actual role of TNFR signalling and sTNFR as a TNF carrier during peripheral inflammation that could then induce neuro-inflammation has not been resolved. In addition, key sites of anti-inflammatory effects of etanercept on TNF- α transport from the periphery to the brain and the brain TNF- α production in this model needs to be investigated further (Mohler et al., 1993) perhaps by using immuno-histo-chemistry of brain tissue to identify cell producing local TNF- α during the disease process of arthritis.

5.5.5 *Effects of peripheral etanercept treatment on IL-1 β in brains of CII immunized mice*

TNF- α stimulates the production of other pro-inflammatory cytokines such as IL-1 β . It was shown that blockade of TNF- α in CIA mice reduced IL-1 β expression in the joint, suggesting that the production of IL-1 β in the CIA model is driven by TNF- α (Williams et al., 2000b). In the CNS, brain IL-1 β production has been shown to be inducible by peripheral inflammation. In addition, brain IL-1 β has been reported to play a crucial role in cognitive decline and symptoms of sickness behaviour. Our data showed that brain IL-1 β mRNA expression levels

were up-regulated significantly on day 35 in CII immunized mice compared to control mice. The increased brain IL-1 β mRNA levels in these CII immunized mice were likely to be suppressed by etanercept, as indicated by a significant reduction in brain IL-1 β mRNA levels in etanercept treated-CII immunized mice. Our finding suggested that TNF- α blockade may inhibit peripheral inflammation-mediated brain IL-1 β production. However, whether TNF- α blockade inhibits IL-1 β initially at the peripheral level or at the CNS level was not addressed in our study. A recent study in a model of surgical trauma suggested that TNF- α blockade may inhibit the production of IL-1 β at the peripheral level. The administration of TNF- α blockade was demonstrated to reduce serum IL-1 β after surgical trauma. The inhibition of brain IL-1 β by TNF- α blockade during peripheral inflammation observed in our study was also seen in this study. The administration of TNF- α blockade resulted in a reduction in brain IL-1 β protein caused by surgery-induced inflammation (Terrando et al., 2010). In addition, the effect of etanercept reversing IL-1 β -induced depressive-like and sickness behaviour has been previously reported by (Jiang et al., 2008). In that study, etanercept inhibited peripheral TNF- α production following IL-1 β challenge. In addition, the anhedonic effects of IL-1 β in the brain were blocked by pre-treatment with etanercept. However, that study did not address the effect of etanercept on brain IL-1 β production (Jiang et al., 2008). The combined evidence of our results and these reports demonstrated that TNF- α may be the main regulator for brain IL-1 β production and action. However, the precise action of etanercept on the brain IL-1 β production by local brain immune cells such as microglia in this CIA model needs to be further investigated perhaps by using immuno-histochemistry of brain tissue to identify cells producing local TNF- α as well as IL-1 β to examine the dynamics of this response of these two cytokines during the development of arthritis.

5.5.6 *Effects of peripheral etanercept treatment on Th1 cytokines in brains of CII immunized mice*

TNF/TNFR signalling plays a role in CD4⁺ activation and regulation of the Th1 response via the production of IFN- γ and IL-12 (Marinova-Mutafchieva et al., 2000). Our data showed a significant reduction in brain IL-12 concentration in etanercept treat-CII immunized mice compared to those in PBS treated-CII

immunized mice on days 32 and 35. To date, the precise role of p75 TNFR on Th1 immune responses in the CNS has not been well addressed. A study by Becher and Dodelet 1996 showed that p75 TNFR could inhibit IL-12 production by activated human adult microglial cells (Becher et al., 1996). In addition, p75 TNFR was shown to act on antigen presenting cell-derived IL-12 to inhibit Th1 polarization in the EAE model (Becher et al., 1999). In contrast, TNFR-p75 has been reported to function as an essential co-stimulator for CD4⁺ T cell responses to cognate antigen (Kim et al., 2006). The effect of etanercept on Th1 immune responses in the CNS may also be associated with the role of TNF/TNFR signalling in recruiting T cells from the periphery into the CNS during neuro-inflammation, the mechanism of which has not been elucidated. Animals treated with TNFR:Fc after immunization with myelin basic protein or proteolipid protein in adjuvant, but before onset of clinical symptoms, did not develop disease but have continued inflammation as indicated by the number of CNS infiltrating T cells (Korner et al., 1997). Another study reported that p75 TNFR gene knockout mice exhibited exacerbated EAE, enhanced Th1 cytokine production, and enhanced CD4⁺T cell infiltration to the CNS (Suvannavejh et al., 2000). This evidence could help explain our finding that on the early time point of disease (day 32), TNF-blockade may inhibit the biologic activities of TNF on Th1 response, whereas at the later time point (day 35), p75 TNFR may function to activate CD4 T cells and enhance CD4 T cell recruitment into the CNS by an as-yet unknown mechanism. Therefore, the role of TNF/TNFR signalling in Th1 immune responses in the CNS during peripheral inflammation in CIA model needs to be further investigated perhaps by using separate p75 and p55 TNFR gene-deleted mice to study the effects of etanercept on development arthritis in CIA mice.

5.5.7 Effects of peripheral etanercept treatment on Th2 cytokines in brains of CII immunized mice

In considering the effects of etanercept on Th2 cytokine profiles in brains of CII immunized mice, we found that etanercept treatment had no effect on brain IL-4 and IL-10 concentrations. However, etanercept reduced IL-5 concentrations in brains of CII immunized mice on days 35. To date, the details of any precise mutual regulation between TNF- α and Th2 cytokines is still not well understood in the CNS. IL-10 and IL-4 are known to inhibit TNF- α production by monocytes (Joyce et al., 1994). In addition, TNF blockade in RA patients resulted in an

increase in the production of Th2 cytokine such as IL-10 by monocytes (Schuerwegh et al., 2003). However, the regulation between TNF- α and Th2 cytokines could be divergent in the different cell types and tissue. In the CNS, TNF- α has been reported to stimulate the production of IL-10 by human microglia (Sheng et al., 1995). In a model of airway hyper-responsiveness, TNF- α has been shown to enhance Th2 responses, to up-regulate IL-5 and increase eosinophil recruitment in pulmonary fibrosis, a non-allergic model of lung inflammation (Zhang et al., 1997). In contrast, a recent study in model of allergic hyper-reactivity showed that etanercept treatment reduced eosinophil recruitment into the lungs (Nie et al., 2009), which may be associated with a reduced production of Th2 cytokine IL-5 essential for the bone marrow production, recruitment and activation of eosinophils (Holgate, 2004). Our data also showed a similar inhibitory effect of etanercept on IL-5 in the brains of CII immunized mice. However, the question of how etanercept regulated the production of IL-5 in the brain of CII immunized mice is still unclear and needs further investigation. We could not identify the cellular source of brain IL-5 in our experiments because this was beyond the scope of our work, but this might be important and could be done by immuno-histochemistry.

In RA, IL-5 plays a role in the pathological mechanism of arthritis by promoting the production of specific IgG and IgE that can bind and activate mast cell degranulation and form immune complex with antigen, leading to the exacerbation of joint destruction (Xu et al., 2008). Since we could not detect IL-5 mRNA in brains of mice from all experimental groups, but we could measure IL-5 protein in some, we concluded that there may be a contribution of IL-5 from the periphery into the brains of these CII immunized mice during the course of disease. It is also possible that etanercept may inhibit the peripheral production of IL-5. Although we could not detect IL-5 mRNA in the brain of CII immunized mice, the possibility that etanercept may inhibit the local production of IL-5 in the brain by CNS immune cells such as astrocyte should not be ignored. A study in CIA model also showed that anti-TNF- α therapy reduced astrocyte activity in the spinal cord of CIA mice (Inglis et al., 2007). To test these hypotheses, *in vitro* experiments of both peripheral and CNS immune cell cultures derived from CII immunized mice are required to investigate the regulatory effect of etanercept on the production of IL-5 in CIA model.

5.5.8 *Effects of peripheral etanercept treatment on chemokines in brains of CII immunized mice*

TNF- α plays a critical role in inducing chemokine production and leukocyte trafficking. TNF blockade therapy in RA was shown to reduce the leukocyte migration to the joints and the expression of chemokines such as MCP-1 (Taylor et al., 2000). The inhibitory effect of TNF blockade therapy on chemokine expression has also been reported in neuro-inflammation. In the EAE murine model, p75 TNFR treatment decreased the expression of various chemokines including CCL3, CCL4, CXCL1 and CXCL2 in the CNS (Glabinski et al., 2003). Our data also showed that increased concentrations of brain CXCL1 protein in CIA mice was suppressed by etanercept treatment. TNF- α could induce the production of CXCL1 by brain microglia (Hayashi et al., 1995), astrocytes (Guo et al., 1998) and peripheral blood monocytes (Shea-Donohue et al., 2008) during peripheral inflammation. However, we could not determine the origin of the CXCL1 detected in the brain of CII immunized mice in our study. This could be done by appropriate immuno-histochemistry. In addition, an *in vitro* study of the effect of etanercept on the production of the immune cells isolate from CII immunized mice may help to address the underlying mechanism of the reduction in CXCL1 concentrations in the brains of CII immunized mice.

5.5.9 *Effects of peripheral etanercept treatment on growth factors in brains of CII immunized mice*

Angiogenesis and neovascularisation in inflammation, characterized by increases in several angiogenic factors such as VEGF and FGF, have been recently considered as a potential therapeutic target mechanisms of TNF blockade (Paleolog, 2002). In RA patients, a decline in vascular permeability, along with a rapid reduction of VEGF concentration in serum were observed during early attenuation of joint swelling after anti-TNF therapy (Paleolog et al., 1998). Etanercept has also been reported to reduce VEGF concentrations in psoriatic lesions of psoriasis. However, the angiogenesis associated with changes in BBB permeability during neuroinflammatory processes has not been well elucidated. A recent report by (Wilson et al., 2009), showed TNF blockade resulted in a reduction in BBB permeability, suggesting a protective role of TNF blockade on BBB damage. However, that study did not address the effect of TNF blockade on changes in angiogenic factor concentrations. Our data showed significant

increases in brain VEGF protein concentrations in etanercept treated-CII immunized mice compared to those in control PBS treated-CII immunized mice. In addition, although the ANOVA did not detect a significant difference in FGF2 gene expression levels between etanercept treated-CII immunized mice and those in control PBS treated-CII immunized mice, the FGF2 gene expression levels in etanercept treated-CII immunized mice were lower than to those in control PBS treated-CII immunized mice. This may be explained by the divergent effect of TNF- α that can be both a pro-angiogenic and an anti-angiogenic factor, depending on the TNF- α concentration and the duration of the exposure in the pathological conditions. These divergent roles for p55 and p75 TNFR contribute to different angiogenic signalling as described in a recent study. This report by Goukassian *et al* showed that p75 TNFR gene deficient mice failed to develop neovascularisation during post-ischemic recovery, along with reductions in VEGF and FGF2 concentrations (Goukassian et al., 2007). This finding suggested that p75 TNFR may be essential for the production of angiogenic factors during angiogenesis and neovascularisation. The data from that study implies that an increase in p75 TNFR level (etanercept) could possibly enhance the production of VEGF and FGF2 in the brain, rather than suppressing the production of these angiogenic growth factors.

Summary

In this section we demonstrated the effect of peripheral administration of etanercept on changes in inflammatory mediator profile associated with peripheral and local brain inflammation in the CIA arthritis model.

This may provide preliminary evidence to support the clinical observation that etanercept could improve cognitive decline and depression in patients with chronic inflammatory diseases. However, a limitation of this study is that, because of its complexity, the experiment was conducted using small sample sizes (3-5 mice/group). Smaller samples yield larger standard errors and wider confidence intervals, which may impact the interpretation of the data by making it more difficult to determine significant differences between groups. In future studies, this experiment could be repeated using a greater group size to increase in statistical power, resulting in better biological interpretation. In addition, the

effect of etanercept on specific immune cell types involved in the production of these brain mediators associated with the inflammation in the CIA model is worthy of further study.

Chapter 6

Effect of peripheral inflammation and etanercept on hippocampal neurogenesis in arthritis model mice

6.1 Introduction

In Chapter 3 we reported increased concentrations of several inflammatory mediators that were observed in brains of CII immunized mice, particularly those with arthritis. In Chapter 4, we demonstrated that up-regulation of these inflammatory mediators in brains of arthritic mice may be associated with peripheral inflammation during the CIA experimental course. In Chapter 5, we reported that peripheral administration of etanercept treatment profoundly reduced the concentration of inflammatory cytokines in brains of CII immunized mice during the period of clinical manifestation of arthritis. One important question remains; do these inflammatory mediators up-regulated in the brain have biological functions and contribute to neurobiological changes in brains of CII immunized mice? To test this hypothesis, we investigated changes in hippocampal neurogenesis in CII immunized mice during the period of clinical manifestation. We also investigated whether TNF-blockade using the anti-inflammatory drug etanercept (recombinant human soluble TNFR), could reverse the effects of peripheral inflammation on hippocampal neurogenesis.

Accumulating evidence suggests that peripheral inflammation can contribute to neurobiological changes the brain. One neurobiological change that has been reported to be affected by peripheral inflammation is neurogenesis. Although the role of neurogenesis as part of hippocampal function is still unclear, some experimental evidence suggests it is involved in memory formation and in mood regulation. Impairment of hippocampal neurogenesis has been associated with cognitive decline in Alzheimer's disease (AD), and in major depression (Ekdahl et al., 2003). Several studies have shown that peripheral inflammation generated by systemic administration of the innate immune response activator LPS, or by pro-inflammatory cytokines such as IL-1 β , could cause impairment of hippocampal neurogenesis, leading to progressive cognitive deterioration (Monje et al., 2003); (Ekdahl et al., 2003); (Kaneko et al., 2006). However, less is known about the effect of peripheral inflammation on hippocampal neurogenesis in chronic inflammatory disease models.

In this study, our hypothesis is that the activation of an immune response and systemic inflammation generated during the course of experimental arthritis may cause impairment in hippocampus neurogenesis. Data from the previous

result chapters (Chapter 4; Section 4.2.3, Section 4.2.4 and Section 4.2.5) has highlighted up-regulation of several inflammatory mediators, including TNF- α , IL-1 β and IL-12 in the brains of CIA immunized mice throughout the CIA experimental course. These brain inflammatory mediators, presumably generated by activated microglia, have been reported to promote the death of hippocampal progenitor cells in vitro (Monje et al., 2003). To investigate whether the impairment of neurogenesis observed during the development of arthritis is induced by a mechanism involving activation of the cytokine cascade, we applied TNF blockade using therapeutic recombinant soluble TNF receptor (Etanercept) peripherally into CIA mice. TNF- α is a potent pro-inflammatory cytokine that is thought to be an inducer of other inflammatory mediators in the inflammatory response. Data from our previous Chapter 5 (Chapter 5; Section 5.2.3, Section 5.2.4) demonstrated that TNF blockade suppressed the up-regulation of brain inflammatory mediators such as IL-1 β and CXCL1. In addition, recent experimental evidence suggests that TNF- α may influence the survival of new neurons generated from the neural stem cells of the adult brain in the dentate gyrus subgranular zone (SGZ) and in the subventricular zone, lining the lateral ventricles (Iosif et al., 2006). TNF- α can trigger apoptosis and excitotoxicity of dentate granule neurons through its receptor and intracellular signalling (Harry et al., 2008). Interestingly, Etanercept treatment has been shown to improve cognitive decline and depression symptoms in patients with chronic inflammatory diseases such as psoriasis, suggesting that Etanercept possibly reverses the impairment of hippocampal neurogenesis associated with chronic systemic inflammation (Tyring et al., 2006). Based on this experimental and clinical evidence, we propose a further hypothesis that TNF blockade may have a protective effect on dentate granule neurons by inhibiting the neurotoxic action of TNF- α and/or suppressing the neuro-inflammatory cascade initiated by TNF- α . Therefore, one aim of this chapter is to investigate whether systemic Etanercept treatment can reverse the impairment of hippocampal neurogenesis induced by peripheral inflammation in the brain of CIA mice during the course of experimental arthritis.

The study in this Results chapter will be in 3 main stages.

In the first stage we will evaluate the immunohistochemical expression of doublecortin (DCX), the neuronal marker for hippocampal neurogenesis in brain

tissue of a normal DBA1 mouse. The optimal DCX antibody concentrations for both immunofluorescent staining and avidin-biotin-peroxidase immunohistochemistry were successfully evaluated. The biotin-peroxidase immunohistochemistry was used for quantitative analysis of hippocampal neurogenesis.

In the second stage, we conducted a CIA experiment using 10 DBA1 mice and performed DCX-immunohistochemistry of brain of these CIA immunized mice culled on day 42, using a biotin-peroxidase immunohistochemistry technique. To investigate the changes in hippocampal neurogenesis that may be effect of peripheral inflammation, we then compared the number of DCX-positive cells the dentate gyrus of CIA immunized mice and those of naïve control mice sacrificed on the same day.

In the third stage, we will investigate the effect of etanercept treatment on changes in hippocampal neurogenesis in CIA immunized mice to test whether any changes may be associated with the peripheral inflammation.

6.2 Immunohistochemistry of Doublecortin (DCX) in mouse hippocampus

Neurogenesis is the ongoing process of neuronal turnover in the dentate gyrus that regulates hippocampus-dependent learning and memory formation. The change in the number of proliferative and immature neurons during neuronal proliferation and maturation stages in the dentate gyrus reflects the level of hippocampal neurogenesis. In this study, we quantitatively evaluated neurogenesis by doublecortin (DCX) immuno-histochemistry. The first step was to optimize the concentration of DCX antibody for immuno-histochemistry to visualise the specific staining of DCX-positive neurons in the mouse dentate gyrus.

6.2.1 Optimization of Doublecortin Immuno-histochemistry

The concentration of DCX antibody for both immunofluorescent and avidin-biotin-peroxidase immuno-histochemistry was optimized for the specificity of DCX immunostaining in mouse brains.

Histologically, approximately 60% of the brain is fat, due to the myelin insulating the axons of neurons and glia. This high fat content may block the penetration of antibodies and thus lower the chance to identify target proteins. Therefore, in order to obtain successful staining, it is essential to optimize the ability of antibody to penetrate through the brain tissue. In the normal immuno-histochemistry approach, the section mounted on the slide has only one side exposed, which limits the opportunity for reagents to penetrate the tissue completely. In contrast, the free-floating method enhances the permeability of antibody by exposing both sides of the section. Briefly, brain tissues from DBA1 mice were cut using a cryostat machine set at 60 μm . All the sections containing the hippocampus region were kept freely floating in an appropriate glass container during the staining process.

6.2.1.1 Immunofluorescent staining in mouse brain tissue

A study suggested that 1:500 is the appropriate dilution of DCX antibody used to develop an immunofluorescent staining in mouse brain tissue (Couillard-Despres et al., 2005). Thus, to optimize the concentration for staining, the DCX antibody

was diluted around this concentration; from 1:100, 1:200, 1:500 to 1:1000. The secondary antibody (1:500) containing Green Alexa fluor dye was added. Consistent with a previous report by Couillard-Despres et al., our results from confocal microscopy showed that 1:500 was the optimal dilution of DCX antibody because the best image of granule cell dendritic morphology was exhibited. As DCX is a cytoskeleton protein, the attached green fluorescent dye could be visualized in the cytoplasm of the soma and dendrite (Figure 6.1A). These DCX-labelled cells, depicted by a neuronal cell body with extensive dendrites, gathered along the dentate gyrus (Figure 6.1B)

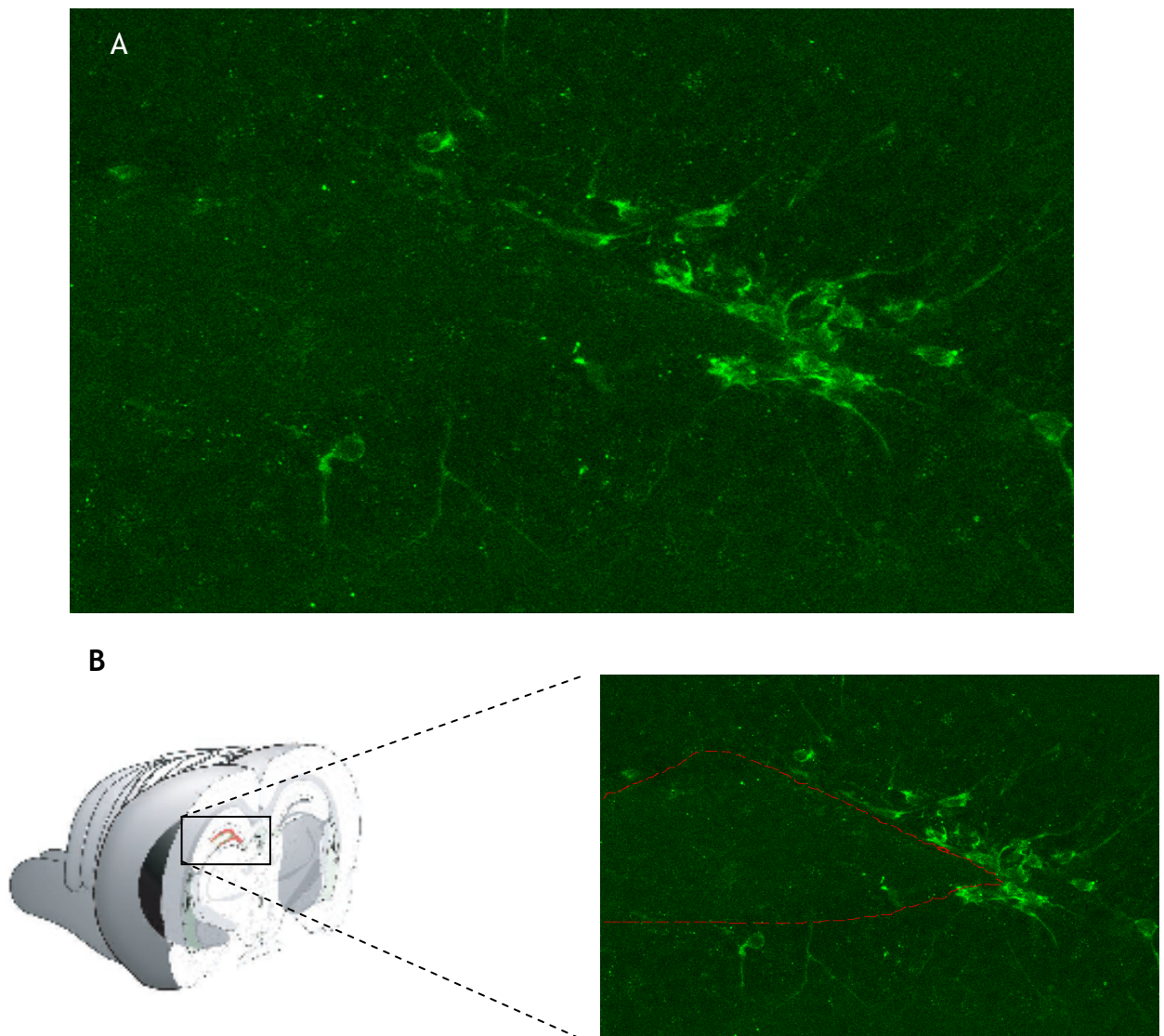


Figure 6.1 Immunofluorescent staining of DCX
(A) Confocal images (10 x magnification) of immature (doublecortin positive) neurons in the dentate gyrus of a DBA1 mouse labeled by Green AlexaFluor 488. (B) illustrates the anatomic location of dentate gyrus and the location of DCX staining. The red dashed lines showed the hippocampal region.

6.2.1.1.1 Triple immunofluorescent staining to define immature neuronal cells

DCX is exclusively expressed on immature neurons, particularly during the maturation and differentiation stages, and has been widely used as an immature neuronal marker (Brown et al., 2003); (Rao and Shetty, 2004); (Couillard-Despres et al., 2005). Toward the final stage of neuronal maturation, precursor cells begin to express proteins typically present in mature neurons such as the nuclear neuronal marker NeuN (Brown et al., 2003). Neuronal precursor cells in the dentate gyrus of hippocampus begin to express DCX while actively dividing, and the expression of DCX lasts for up to 3 weeks as these neuronal precursor cells develop to be mature neurons. A reduction of DCX expression in these precursor cells begins after 2 weeks, and occurs at the same time that these cells begins to express NeuN, a marker for mature neurons (Brown et al., 2003). This suggests that neuronal precursor cells express different neuronal markers at different stages throughout the process of neurogenesis. For that reason, we used co-immunofluorescence of DCX and NeuN to distinguish the population of immature neurons in the dentate gyrus. Neurons in the immature differentiation stage should express only DCX, but not NeuN.

Anti-DCX-Alexa green was used to define the morphology of immature neuron progenitor cells as mentioned. Anti-NeuN-Cy5, a nuclear antigen present in mature cells, was employed to identify the morphology of mature neuron cells. Thirdly, propidium iodide (PI) a fluorescent molecule that can bind DNA was used to stain the DNA inside the nucleus independent of the type and developing stage of cells. Therefore, overlapping PI staining with either DCX-Alexa green or NeuN-Cy5 demonstrates immature neuron cells and mature neuron cells, respectively. By this triple immunofluorescent staining, immature neuron cells can be clearly identified. DCX-Alexa green staining shows a few immature neuron cells, characterized by a neuronal cell body with extensive dendrites (Figure 6.2A). The NeuN-Cy5 positive staining also shows a number of mature neuron cells (in blue) locating along the dentate gyrus and in the hippocampus (Figure 6.2B). The same population of these neurons was also stained positive for the nuclear DNA dye (propidium iodide) (Figure 6.2C).

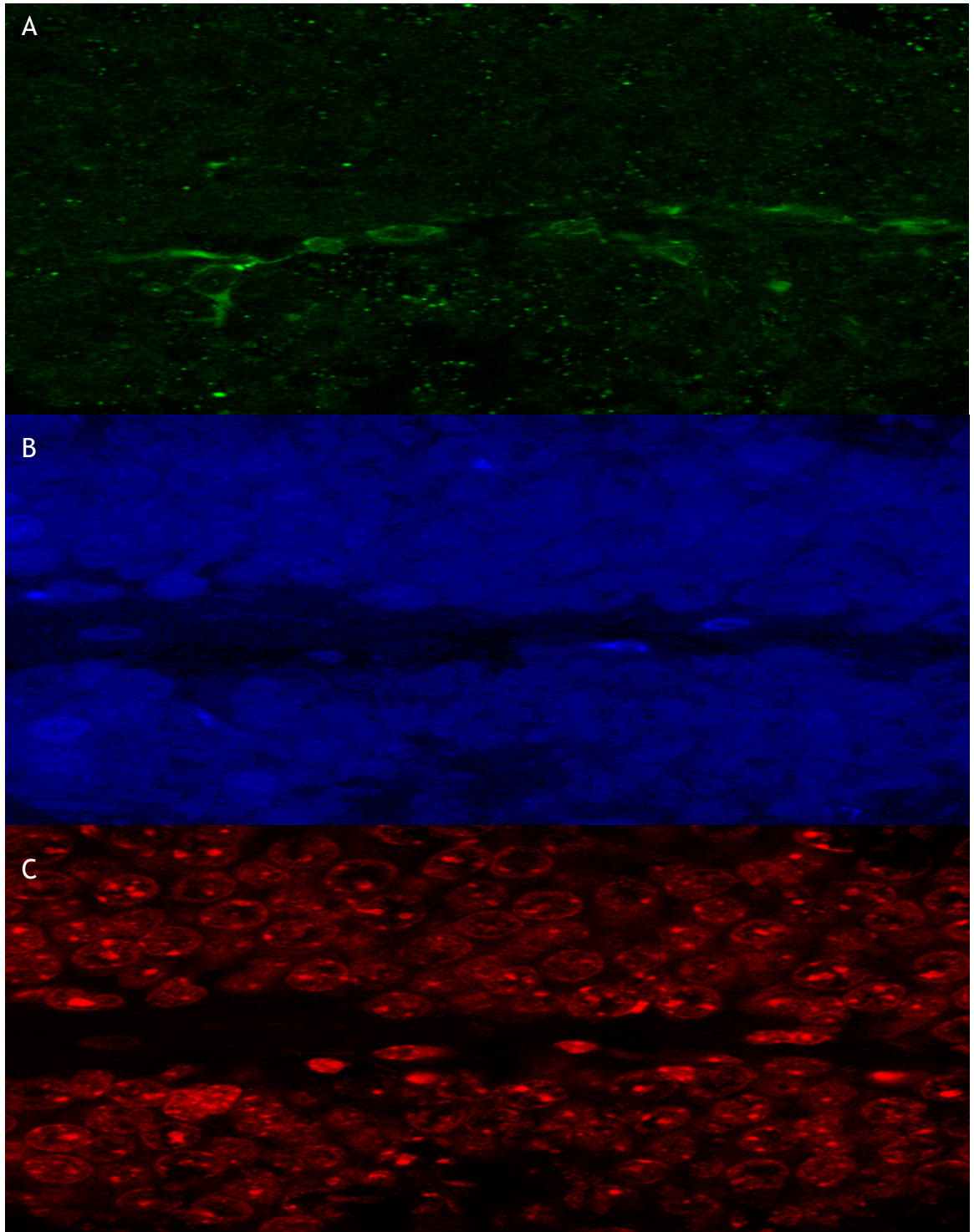


Figure 6.2 Immunofluorescent staining of DCX, NeuN and PI
(A) Confocal images (40 x magnification) show expression patterns of three neuronal markers in the dentate gyrus of a DBA1 mouse. Sections show the expression of doublecortin visualized with green fluorescence (A), the presence of NeuN was seen in blue (B), and the DNA staining by propidium iodide was detected as red (C).

When these images are overlapped (Figure 6.3), it is clear that i) immature neuron cells doubly stained by DCX-Alexa green (green) and PI (red) exclusively distribute along the dentate gyrus; ii) mature neuron cells with dual staining of NeuN-Cy5 (blue) and PI (red) locate in the same area; iii) the absence of co-

localization of DCX-Alexa (green) and NeuN-Cy5 (blue) demonstrates that DCX is not on mature neuron cells, and may identify immature neurons.

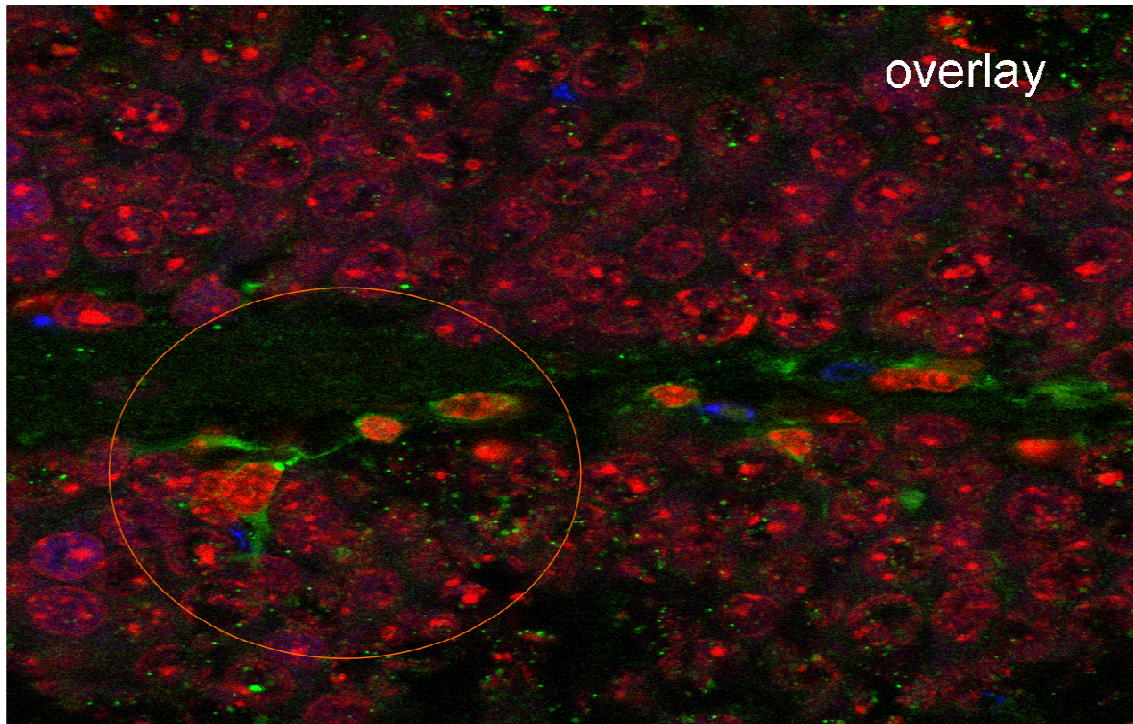


Figure 6.3 An overlay image of triple immunofluorescent staining of DCX, NeuN and PI in the dentate gyrus of a DBA1 mouse
A confocal image (40 x magnification) shows co-expression of DCX together with PI observed in cells with no expression of NeuN, a mature neuronal marker. The circle surrounds a neuron that expresses both DCX and PI. However, this cell is negative for NeuN.

6.2.1.2 Optimization of avidin-biotin-peroxidase immunohistochemistry

Although these specific fluorescence labels successfully defined immature neuron cells and their distribution, it is necessary to conduct a further peroxidase staining to confirm that they locate in the dentate gyrus of the brain. Preliminary experiments demonstrated that the dilution (1:500) used in the fluorescence IHC protocol successfully detected DCX-positive cells. A further 10 times dilution (1:5000) was suggested to identify DCX in the Avidin-biotin-peroxidase immuno-histochemistry protocol to avoid non-specific binding and minimise background staining.

The test dilutions of anti-DCX antibody have been varied from 1:1000, 1:5000, 1:10,000. Normal goat IgG of the same concentrations as the primary antibody was used to generate negative controls for the immuno-histochemistry. The results from the light electron microscopy demonstrated that the DCX antibody

dilution at 1:1000 was the optimal for the Avidin-biotin-peroxidase immunohistochemistry protocol. However, at dilution 1:1000, there was some non-specific staining of red blood cells and blood vessels observed on the slides (data not shown). This was the result of endogenous peroxidase in the blood vessels which reacts with the substrate DAB (3,3-diaminobenzidine). Therefore, to block the endogenous peroxidase in the brain sections, the treatment of 0.3% H_2O_2 in phosphate buffer for 30 min was used before primary antibody incubation. Consequently, most of the non-specific staining was eliminated and a higher intensity of DCX staining in the dentate gyrus was observed (Figure 6.4). DCX-positive cells were distributed throughout the extent of the DG in normal DBA 1 mice (Figure 6.5A). By contrast, the negative control antibody for immunohistochemistry did not show any non-specific binding (Figure 6.5B). DCX positive neurons in the DG exhibited the phenotype of immature neurons in their maturation stage (Jones et al., 2003). The cell bodies of DCX positive neurons were located in either the subgranular zone (SGZ) or granular cell layer (GCL) of the DG. Apical dendrites of these DCX positive neurons extend their delicate dendritic tree branching into the molecular layer (ML) (Figure 6.6).

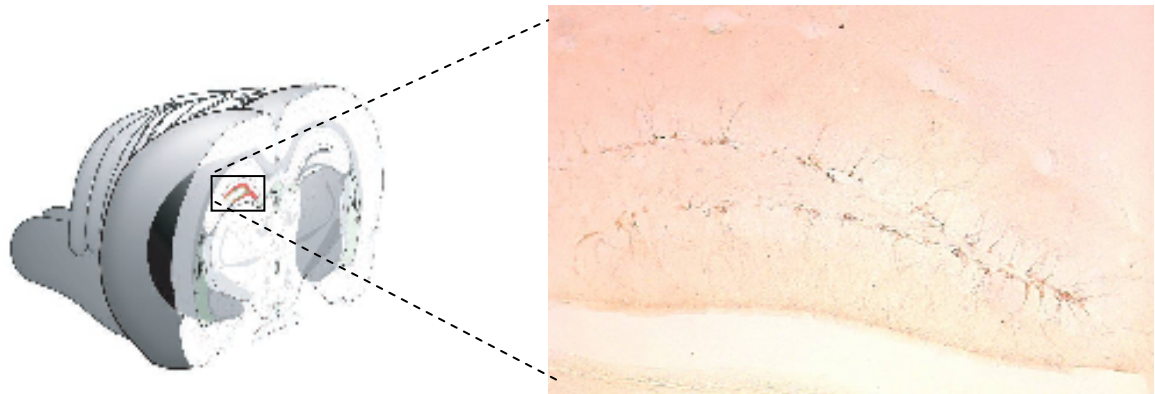


Figure 6.4 Avidin-biotin-peroxidase immunohistochemistry of DCX
(A) An image (10 x magnification) from a light electron microscope shows immunoperoxidase-staining of DCX of immature (DCX-positive) neurons in the dentate gyrus of a DBA1. (B) Illustrates the anatomic location of dentate gyrus and the location of DCX staining.

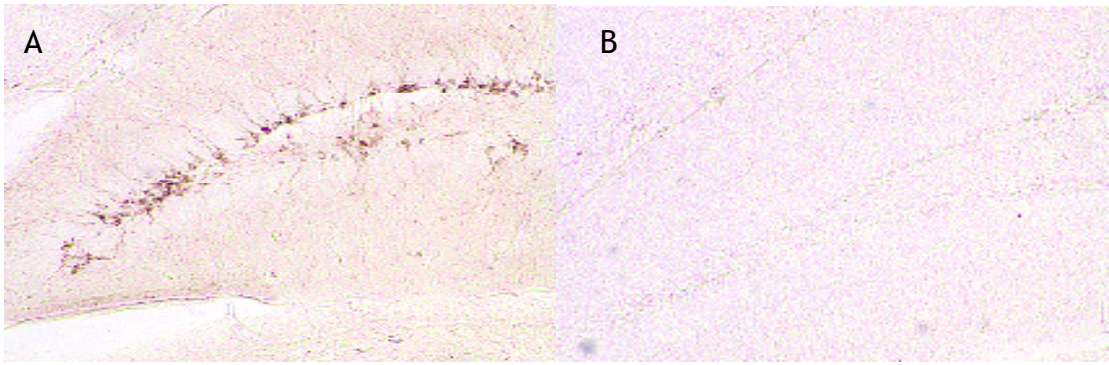


Figure 6.5 Avidin-biotin-peroxidase immuno-histochemistry of DCX in the dentate gyrus of a DBA 1 mouse

An image (10 x magnification) represents the immunoperoxidase-staining for DCX and the distribution of DCX-positive neurons in the adult dentate gyrus of a DBA1 mouse (A). (B) shows a negative control of immuno-histochemistry generated by replacing DCX primary antibody with the same amount of normal goat IgG.

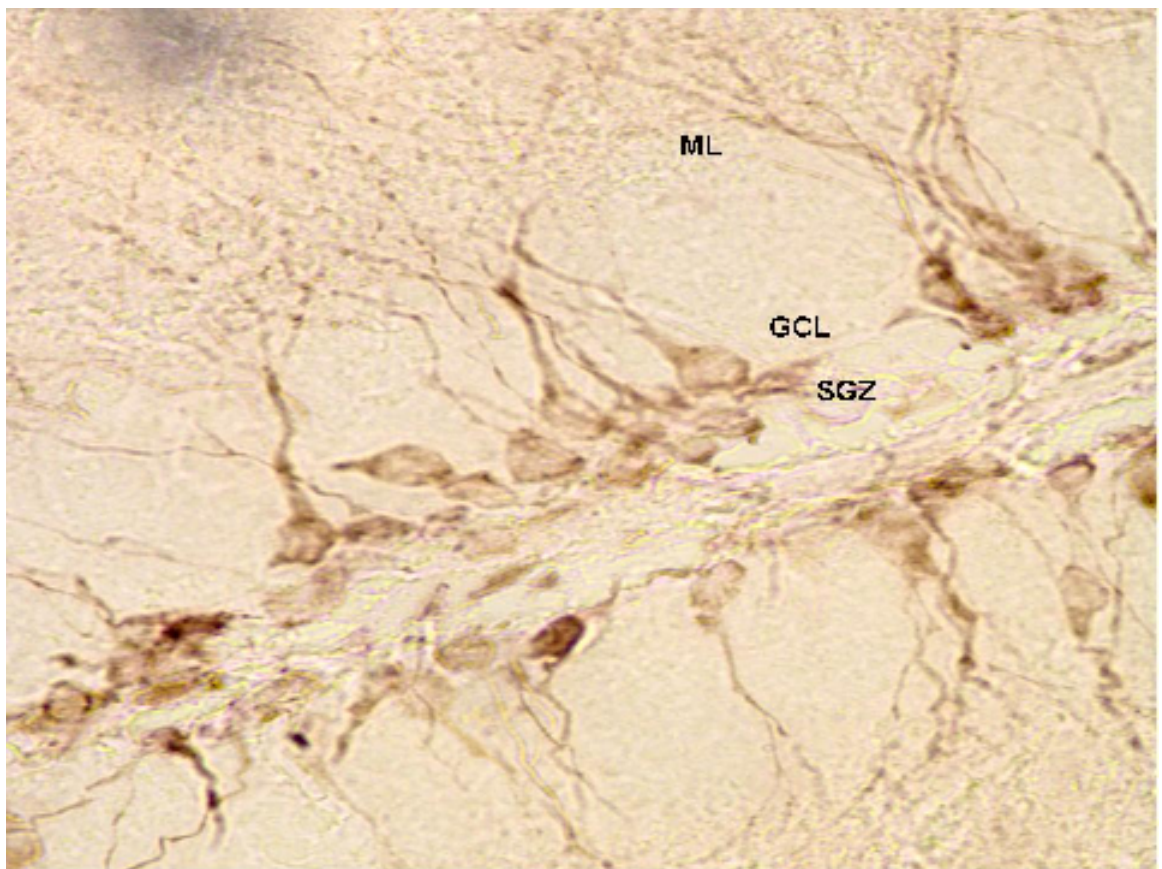


Figure 6.6 High magnification of a representative image of DCX immuno-histochemistry in the dentate gyrus of a DBA1 mouse

An image (20 x magnification) presents the morphology of DCX-positive neurons which have their cell bodies located either in the subgranular zone (SGZ) or the granular cell layer (GCL) of the dentate gyrus. These DCX-positive neurons extend their delicate dendritic tree branching into the molecular layer (ML)

6.3 Induction of arthritis in DBA1 mice

6.3.1 CIA experimental procedure

The aim of this experiment is to investigate whether the peripheral immune/inflammatory response occurring during arthritis in DBA1 mice induced by type II collagen can change hippocampal neurogenesis in the brain. In the second stage of this chapter, we conducted another CIA experiment and brains of these CII immunized mice were processed for doublecortin (DCX) immunohistochemistry in order to determine changes in the number of DCX-positive neurons. Since DCX expression in neuronal precursor cells in the dentate gyrus is transient and persists for up to 3-4 weeks (Brown et al., 2003), it is difficult to estimate the optimal time point during the experimental course to determine changes in hippocampal neurogenesis in a chronic inflammatory model like the CIA model. However, a study by Wolf *et al.*, in an AIA model showed that an increase in hippocampal neurogenesis was observed during the massive infiltration of inflammatory cells into the knee joint of arthritic mice. That study also showed a significant positive correlation between paw swelling and neuronal cell proliferation in these arthritic mice (Wolf et al., 2009b). These data suggest that change in hippocampal neurogenesis may occur during the clinical manifestation of arthritis in AIA mice. For that reason, we chose to determine changes in hippocampal neurogenesis on day 42 of the CIA experimental course. This time point is during the maximum clinical manifestation of disease. In addition, we determined changes in brain inflammatory mediator concentrations in CII immunized mice on day 42 in Chapter 3 (Section 3.2.3 and Section 3.2.4), and we found increases in several inflammatory mediator concentrations in brains of CII immunized mice at that time point. Therefore, we conducted another CIA experimental identical to the one in Chapter 3 (Section 3.2.1), but brains of mice in this CIA experiment were processed for DCX-immunohistochemistry. In doing so, we may be able to use the data of Chapter 3 (Section 3.2.3 and Section 3.2.4) section to explain our data of changes in hippocampal neurogenesis in CII immunized mice at the same time point.

10 DBA1 mice were immunized by intradermal injection of type II collagen in complete Freund's adjuvant on day 0. On day 21, mice were given an i.p. booster injection of type II collagen dissolved in PBS. 6 DBA1 sex- and age-

matched DBA1 mice were used as the antigen-naïve control group and were neither immunized nor challenged with type II collagen. Groups of both CII immunized and naïve control mice were sacrificed on day 42 and the brain of each mouse was fixed in formalin and cryoprotected in 30% sucrose buffer. Serial sections throughout the hippocampus were cut at 60-um and immunostained for DCX using the free-floating technique (Figure 6.7).

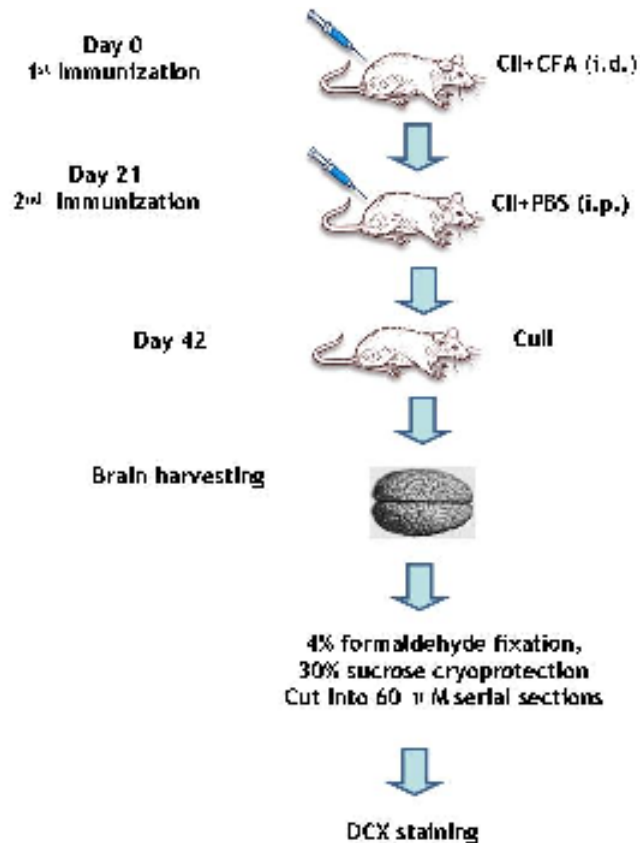


Figure 6.7 The experimental procedure of collagen II-induced experimental arthritis model for hippocampal neurogenesis analysis

DBA1 mice at 6-8 weeks of age were separated into two groups: i) naïve control, n=6 naïve control; ii) immunized mice, n=10 immunized mice. Mice were immunized with 100 μ g type II bovine collagen + complete Freund's adjuvant (CFA) at day 0 and then challenged on day 21 with 200 μ g type II collagen. A group of 6 naïve DBA1 mice which were not immunized and not treated with type II collagen was use as a control group. Serum and brains from control and CII-immunized mice were harvested at Day 42. The brain of each mouse from all experimental groups was fixed in formalin and cryoprotected in 30% sucrose buffer. Serial sections throughout the hippocampus were cut into 60-um sections and immunostained for DCX using the free-floating technique.

6.3.2 Clinical response

Some of CII-immunized mice started to show clinical signs of arthritis from day 20 onwards and there were 6 out of the total 10 CII immunized mice that developed arthritis (60% incidence) on day 42 (Figure 6.8A). 4 of the 10 mice did not develop arthritis after immunization and challenge, and these formed a separate immunised but non-arthritis study group. CII immunized mice showed a significant increase in paw thickness compared to the naïve control mice ($P < 0.0001$). The mean paw thickness and the mean arthritis score for the whole group of CII-immunized mice ($n=10$) on day 42 were 2.0 ± 0.08 mm and 3.9 ± 1.4 respectively (Figure 6.8B), (Figure 6.8C).

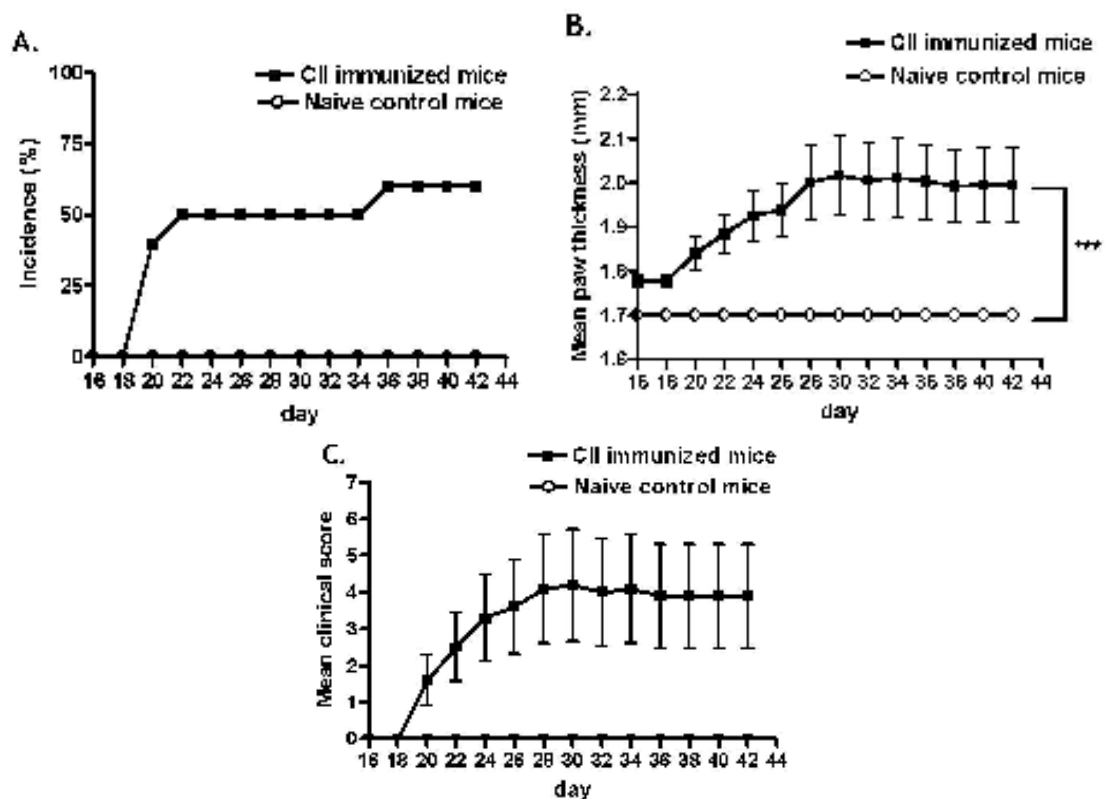


Figure 6.8 Development and severity of arthritis disease in CII immunized mice over 42 days of experimental arthritis course

The signs of arthritis in CII immunized mice were monitored from day 16 after immunization onwards. (A) shows the percent incidence of arthritis in CII immunized mice, which was calculated from number of CII immunized mice with arthritis/total number of CII immunized mice used. The signs of arthritis were observed in CII immunized mice from day 20 onwards and there were 6 out of total 10 CII immunized mice developed arthritis on day 42. The mean clinical arthritis score and mean paw thickness were used as a clinical evaluation to measure the severity of joint inflammation in arthritic mice. (B) shows mean paw thickness of CII immunized mice which was calculated from the sum of the paw thickness of all mice divided by the number of mice. (C) shows mean clinical of CII immunized mice which was calculated from the sum of the clinical scores of all mice divided by the number of mice. Mean paw thickness, mean clinical score and %incidence in CII immunised mice ($n=10$ CII immunised mice; filled squares) were compared with those values of naïve control mice ($n=6$ naïve control mice; open circles). Data represented as mean \pm SEM. ($n=10$ CII immunized

mice). Statistical analysis of data was performed using two-way ANOVA for multiple comparison, compared with a group of control naïve mice; * $P < 0.05$, ** $P < 0.01$, *** $P < 0.001$.

6.4 Changes in number of DCX-positive neurons in the dentate gyrus in CII immunized mice

To investigate whether peripheral inflammation affects changes in the neurogenesis, quantitative immuno-histochemistry of DCX positive neurons was performed in the brain sections containing the hippocampus region from mice of all experimental groups to determine changes in the number and the morphology of DCX-positive neurons in dentate gyrus of immunized mice compared to those in the control mice.

6.4.1 Changes in number of DCX-positive neurons in the dentate gyrus in arthritic mice

In this CIA experiment, there were 6 mice that developed arthritis. DCX-positive cells were detected in the dentate gyrus of both naïve control and arthritic mice. However, the light microscopy image showed that there were differences in the number of DCX-positive neurons between arthritic mice and naïve control mice (Figure 6.9A - Figure 6.9H and Figure 6.10A - Figure 6.10D). A reduction in the number of DCX-positive cells was observed in dentate gyrus of arthritic mice compared to those in naïve control mice. Figures 9A-9H and 10A-10D show the representative images of DCX-immuno-histochemistry in the dentate gyrus of arthritic mice with different arthritis scores. This was confirmed by the cell count data showing that the number of DCX-positive neurons in the dentate gyrus of arthritic mice was significantly decreased; the mean number of DCX-positive neurons in the dentate gyrus (arthritic versus naïve control) was 1322 ± 285 cells versus 5417 ± 1673 cells ($P = 0.0001$) (Figure 6.11A). However, the reduction in DCX-positive neurons did not correlate with the arthritis score ($r^2 = 0.06948$; $P = 0.6138$) (Figure 6.11B).

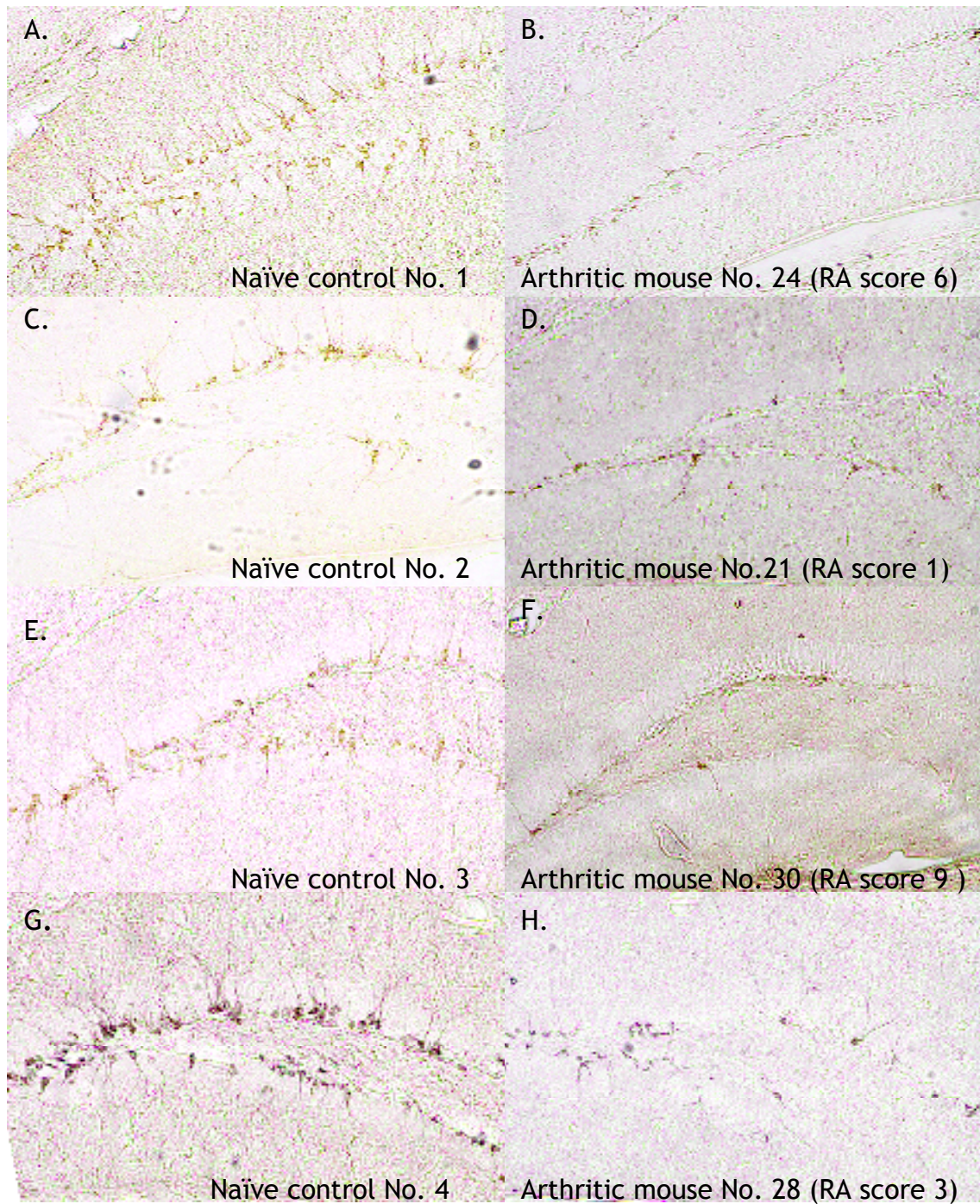


Figure 6.9 Changes in hippocampal neurogenesis in arthritic mice on day 42
 DCX-immuno-histochemistry in dentate gyrus of arthritic mice were randomly compared to those of naïve control mice. (A), (C), (E) and (G) show representative images of DCX immuno-histochemistry in the dentate gyrus of naïve control mice no 1, 2, 3 and 4 respectively. (B), (D), (F) and (H) show representative images of DCX immuno-histochemistry in the dentate gyrus of different arthritic mice (No. 24, 21, 30 and 28) with different arthritis scores (score 1, 6, 9 and 3 respectively). Clinical scores (RA scores) were calculated on the cull day 42. All images were at 10X magnification.

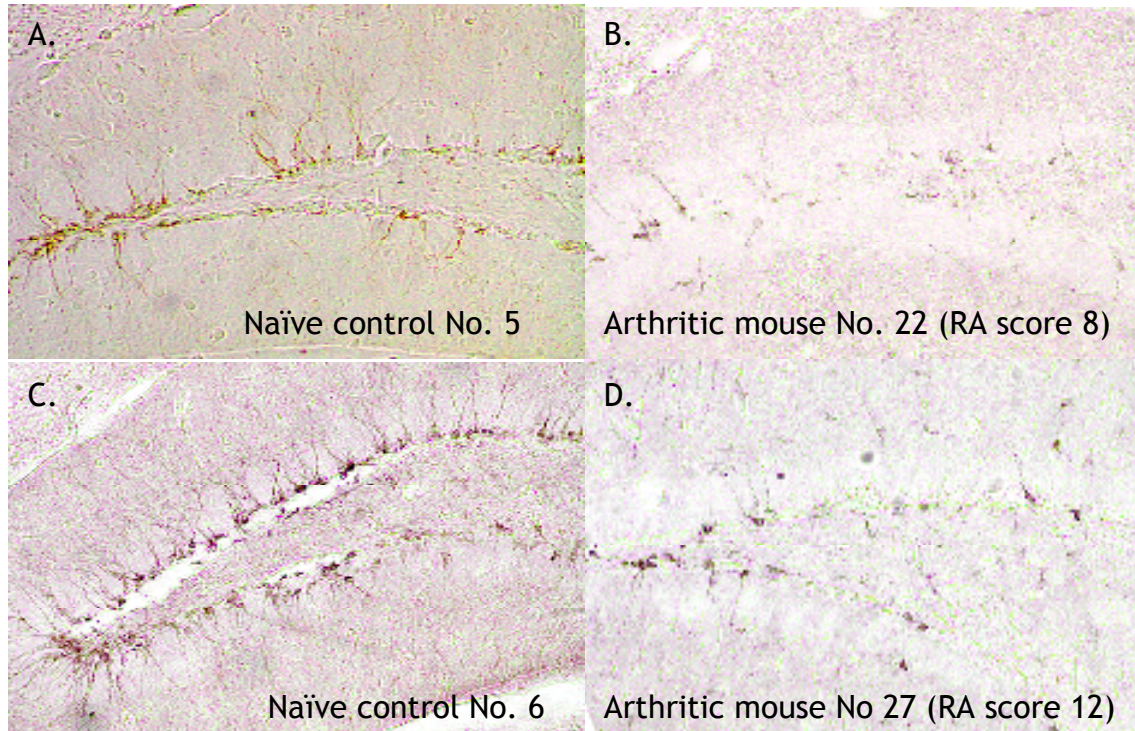


Figure 6.10 Changes in hippocampal neurogenesis in arthritic mice on day 42
DCX-immuno-histochemistry images in the dentate gyrus of arthritic mice were randomly compared to those of naïve mice. (A) and (C) show representative images of DCX immuno-histochemistry in the dentate gyrus of naïve control mice no 5 and 6 respectively. (B) and (D) show representative images of DCX immuno-histochemistry in the dentate gyrus of different arthritic mice (No. 22 and 27) with different arthritis scores (score 8 and 12 respectively). Clinical scores (RA scores) were calculated on the cull day 42. All images were at 10X magnification.

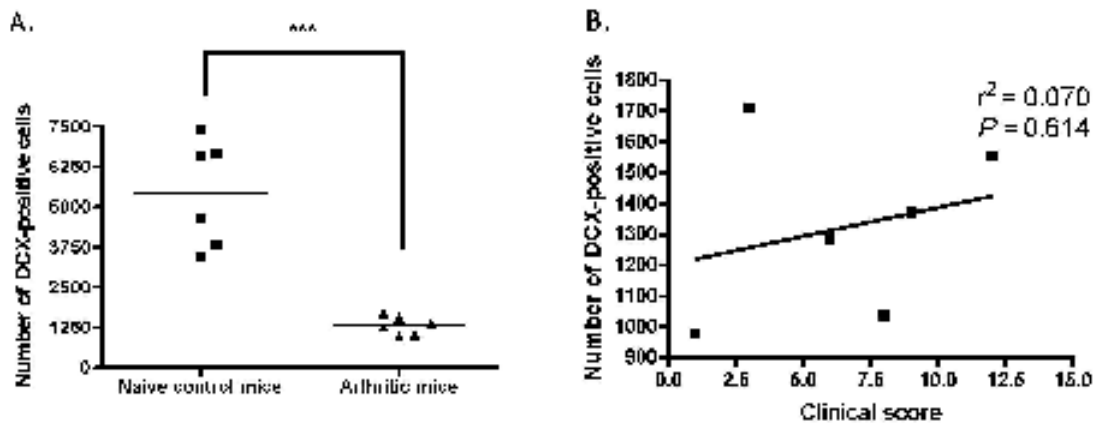


Figure 6.11 Changes in number of DCX-positive cells in dentate gyrus of arthritic mice on day 42
(A) The dots represent the number of DCX positive cells in the hippocampus of individual naïve control mice (filled squares; n=6 naïve control mice) and arthritic mice (filled triangles; n=6 arthritic mice). The number of DCX positive cells in the hippocampus of mice from both naïve control and arthritic groups all experimental groups was determined by counting DCX-positive cells in every sixth serial brain section containing DCX immuno-histochemistry in the dentate gyrus. Bars represent the mean values (***) $P < 0.01$ by Student's t-test). (B) Correlations of the number of DCX-positive cells and clinical (RA) score. Plots show relationships between the number of DCX-positive cells in the dentate gyrus of arthritic mice and their arthritic score (RA score) on day 42 analysed by Pearson's correlation coefficient analysis.

6.4.2 *Changes in number of DCX-positive neurons in the dentate gyrus in non-arthritic mice*

Interestingly, immunized mice that did not develop arthritis (non-arthritic mice) also showed differences in the number of DCX-positive neurons compared to those in the naïve control mice. Figure 12A - 12I show the representative images of DCX-immuno-histochemistry in the dentate gyrus of non-arthritic mice compared to those in the control mice (Figure 6.12A - Figure 6.12I). Similar to arthritic mice, a reduction in hippocampal neurogenesis was also observed in non-arthritic mice. The mean number of DCX-positive neurons in the dentate gyrus (non-arthritic versus naïve control mice) was 1668 ± 329 cells versus 5417 ± 1673 cells ($P = 0.0025$) (Figure 6.13).

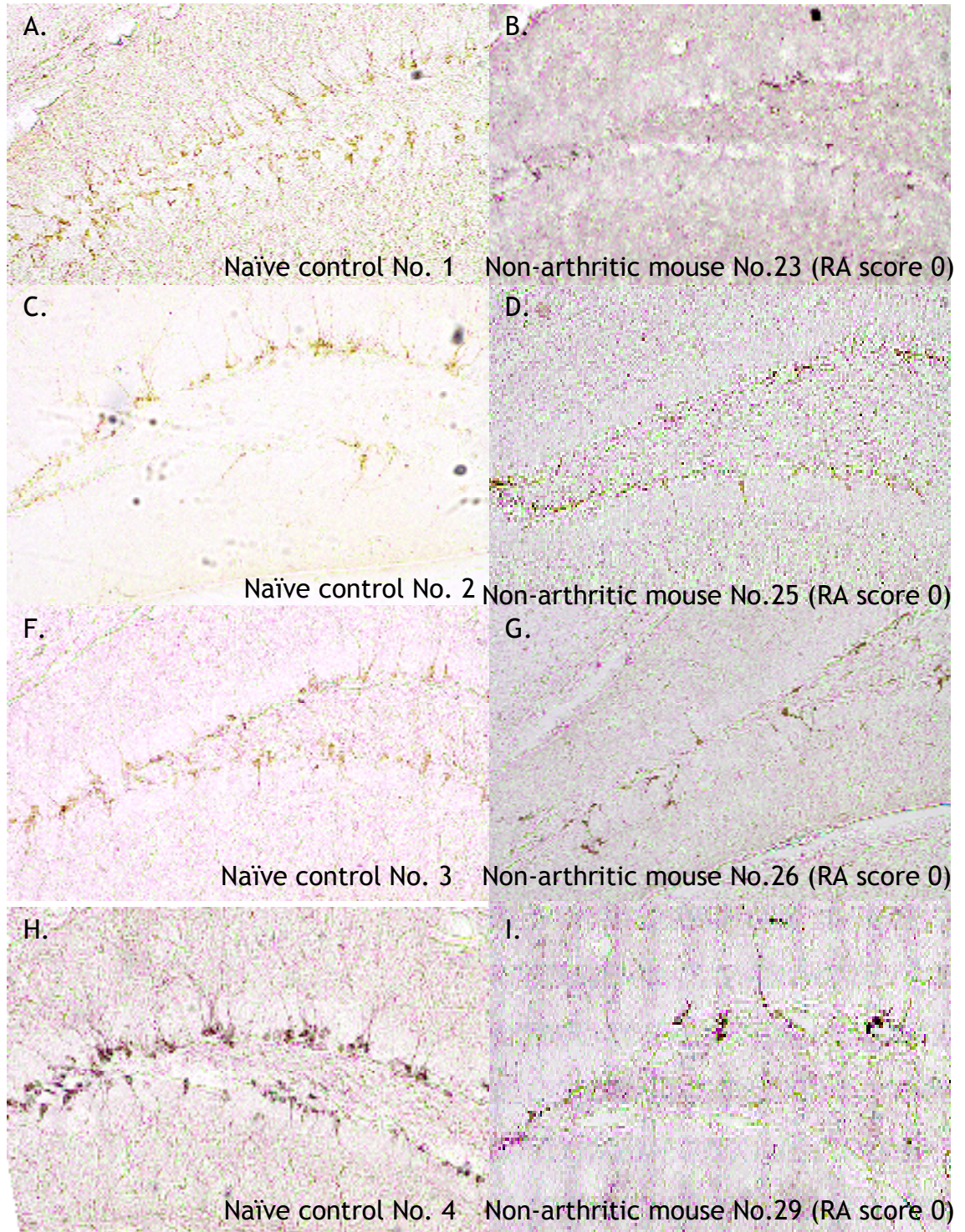


Figure 6.12 Changes in hippocampal neurogenesis in non-arthritic mice on day 42 DCX-immuno-histochemistry images of the dentate gyrus of non-arthritic mice were randomly compared to those of naïve control mice. (A), (C), (F) and (H) show representative images of DCX immuno-histochemistry in the dentate gyrus of naïve control mice no 1, 2, 3 and 4 respectively. (B), (D), (G) and (I) show representative images of DCX immuno-histochemistry in the dentate gyrus of different non-arthritic mice (No. 23, 25, 26 and 29) with clinical (RA) score 0. Clinical scores (RA scores) were calculated on the cull day 42. All images were at 10X magnification.

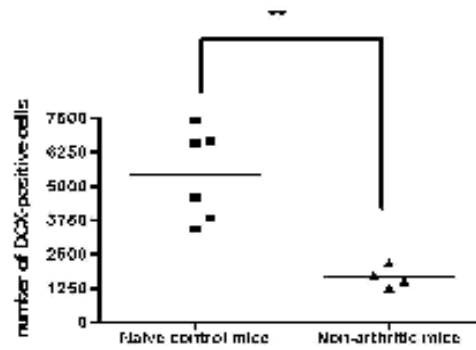


Figure 6.13 Change in number of DCX-positive cells in dentate gyrus of non-arthritic mice on day 42

The dots represent the number of DCX positive cells in the hippocampus of individual naïve control mice (filled squares; n=6 naïve control mice) and arthritic mice (filled triangles; n=4 arthritic mice). The number of DCX positive cells in the hippocampus of mice from both naïve control and non-arthritic groups was determined by counting DCX-positive cells in every sixth serial brain section containing DCX immuno-histochemistry in the dentate gyrus. Bars represent the mean values (*P < 05; **P < 01; ***P < 001 by Student's t-test)

6.4.3 Comparison of changes in number of DCX-positive neurons in the dentate gyrus between naïve control, arthritic and non-arthritic mice

A reduction in hippocampal neurogenesis indicated by decrease in number of DCX-positive neurons was observed in the dentate gyrus of both arthritic and non-arthritic mice compared to those of control naïve mice. One-way ANOVA followed by Bonferroni's post-hoc comparison tests demonstrated that there were significant differences in the number of DCX-positive neurons in the dentate gyrus among the three groups of mice ($P < 0.0001$) (Figure 6.14). The mean number of DCX-positive neurons in the dentate gyrus (arthritic versus naïve control) was 1322 ± 285 cells versus 5417 ± 1673 cells ($P = 0.0001$), while the mean number of DCX-positive neurons in the dentate gyrus (non-arthritic versus naïve control) was 1668 ± 329 cells versus 5417 ± 1673 cells ($P = 0.0025$). However, there was no significant difference in number of DCX-positive cells between arthritic and non-arthritic mice (Figure 6.14). This finding suggests that the immunization with CII/CFA may itself affect Hippocampal neurogenesis in a different mechanism of that affecting the joint in CII immunized mice.

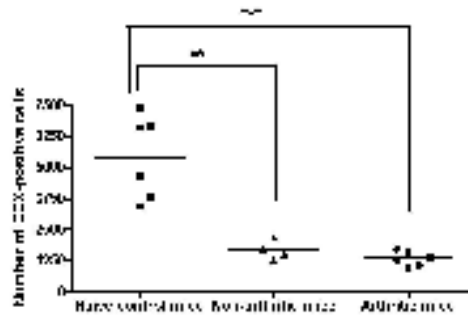


Figure 6.14 Changes in number of DCX-positive cells in dentate gyrus of arthritic and non-arthritic mice on day 42

The dots represent the number of DCX positive cells in the hippocampus of individual naïve control mice (filled squares; n=6 naïve control mice), non-arthritic mice (filled triangles; n=4 non-arthritic mice) and arthritic mice (filled circles; n=6 arthritic mice). The number of DCX positive cells in the hippocampus of mice from all experimental groups was determined by counting DCX-positive cells in every sixth serial brain section containing DCX immunohistochemistry in the dentate gyrus. Bars represent the mean values (*P < 0.05; **P < 0.01; ***P < 0.001 by one-way ANOVA.)

6.5 Effect of etanercept on hippocampal neurogenesis in CII immunized mice

Data from the previous section of this Chapter 6 (section 6.4) showed a reduction of neurogenesis, indicated by a decrease in number of DCX-positive cells in the dentate gyrus of CII immunized mice on day 42. In Chapter 3 (Section 3.2.3 and Section 3.2.4), we demonstrated up-regulation of several inflammatory mediators, including of IL-1 α , IL-2, IL-5, IL-10, IL-13, CXCL1, CXCL10, VEGF and FGF2 in the brain of CII immunized mice at the same time point (day 42). This data from Chapter 3 combined with data in this chapter suggested that the reduction in neurogenesis in CII immunized mice may be associated with up-regulation of inflammatory mediators in the brain of CII immunized mice. In Chapter 5 (Section 5.2.3 and Section 5.2.4), we demonstrated that peripheral administration of etanercept treatment profoundly inhibited the production of inflammatory mediators, including TNF- α , IL-12 in brains of CII immunized mice during the period of clinical manifestation of arthritis. We hypothesized that the inhibitory effect of etanercept on inflammatory mediator production in the brain may also contribute to the protective effect against a reduction in hippocampal neurogenesis in CII immunized mice. We therefore conducted another CIA experiment, similar to the CIA experiment in Chapter 5 (Section 5.2.1). In this third stage of this chapter, we analysed changes in hippocampal neurogenesis in etanercept-treated immunized mice compared to those of PBS-treated immunized mice and

control naïve mice on day 14 (pre-onset and pre-etanercept treatment time point), day 32 and day 35 (2 time points during the period of development of arthritis).

6.5.1 Administration of etanercept and induction of arthritis in DBA1 mice; CIA experimental procedure

Nineteen DBA1 mice were immunized by intradermal injection of type II collagen in Freund's complete adjuvant on day 0. On day 14, 3 CII (collagen type II) immunized mice (Group 1) were sacrificed and the brains and serum of these mice were harvested for the measurement of inflammatory mediator levels before the second immunization on day 21. There was no CII immunized mice in Group 1 that developed arthritis on day 14. The other 16 CII immunized mice were randomly divided into 2 groups of 8, namely the treatment and placebo groups. From day 18 onwards, CII immunized mice of the treatment group received Etanercept (300 µg/mice, i.p.) every 3 days, while the placebo group received PBS (i.p.) every 3 days. The signs of arthritis in CII immunized mice were monitored from day 16 after immunization onwards and arthritis severity scores in this experiment were verified independently by Dr. Bernard Leng. CII immunized mice from both groups were re-challenged by intraperitoneal injection of collagen II in PBS on day 21. CII immunized mice in the placebo group started to show sign of arthritis earlier (day 19) than those of the treatment group (day 21). 3 CII immunized mice of the treatment group (Group 2) and 3 CII immunized mice of the placebo group (Group 3) were sacrificed and serum and brains of these CII immunized mice were harvested on day 32. CII immunized mice of both treatment and placebo groups (Group 4 and Group 5; 5 CII immunized mice/group) were sacrificed and serum and brains of these CII immunized mice were harvested on day 35; which is the peak day of disease. Another 11 sex- and age-matched untreated DBA1 mice were used as antigen-naïve control mice. These naïve control mice were neither sensitized with type II collagen nor given etanercept treatment. 3 naïve control mice were sacrificed on day 14, and a further 3 and 5 naïve control mice were sacrificed on day 32 and day 35 respectively. The brains of all experimental groups of mice were harvested and fixed in formalin and cryoprotected in 30% sucrose buffer. Serial 60-µm sections throughout the hippocampus were cut and immunostained for DCX using the free-floating technique (Figure 6.15).

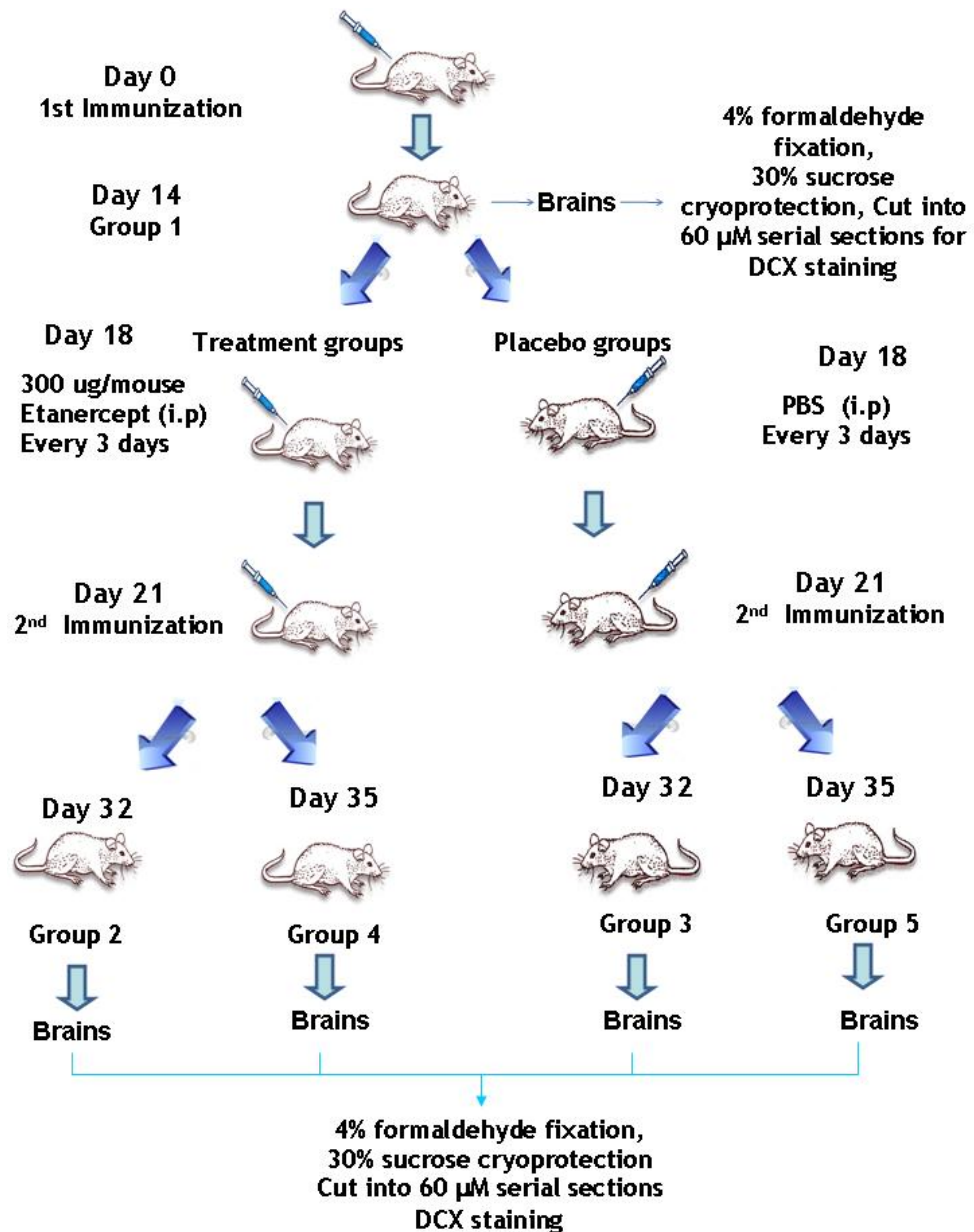


Figure 6.15 Administration of etanercept and CIA experimental procedure for hippocampal neurogenesis analysis

19 DBA1 mice at 6-8 weeks of age were immunized with 100µg type II bovine collagen + complete Freund's adjuvant (CFA) at day 0. On day 14, 3 CII immunized mice in Group 1 were culled and brains and serum of these CII immunized mice from group 1 (3 mice/group) were harvested. At this time point, another 3 naïve control mice, which were given neither sensitized with type II collagen, were also culled and their brains and serum samples were used as controls to compared changes in brain inflammatory mediators with those of CII immunized mice culled on day 14. On day 18, CII immunized mice were randomly divided into 2 groups (8 CII immunized mice/group), which were a treatment group and a placebo group. From this day onwards, 300 µg/mouse etanercept was administrated (i.p.) to CII immunized mice of the treatment group every 3 days, while PBS was injected to CII immunized mice of the placebo group every 3 days. CII immunized mice of both groups were challenged on day 21 with 200µg type II collagen. From day 21 onwards, etanercept treated CII immunized mice of etanercept group were randomly divided into 2 groups, namely Group 2 and Group 4. etanercept treated CII immunized mice in Group 2 (3 CII immunized mice/group) were culled and brains of these CII immunized mice were harvested on day 32, while etanercept treated CII immunized mice in Group 4 (5 CII immunized mice/group) were culled and brains of these CII immunized mice were harvested on day 35. Similarly, PBS treated CII immunized mice in the placebo group was randomly divided into 2

groups, namely Group 3 and Group 5. PBS treated CII immunized mice in Group 2 (3 CII immunized mice/group) were culled and brains of these CII immunized mice were harvested on day 32, while PBS treated CII immunized mice in Group 4 (5 CII immunized mice/group) were culled and brains of these CII immunized mice were harvested on day 35. Another 8 naïve control mice were culled on the day indicated (3 naïve mice for day 32 and 5 naïve mice for day 35) and their serum and brain were used as controls. Brains from mice of all experimental groups were collected and brains processed for DCX immuno-histochemistry.

6.5.2 Effect of etanercept on the development of collagen induced arthritis (CIA)

6.5.2.1 Effect of etanercept on the severity of arthritis in CII immunized mice on day 32

CII immunized mice in the treatment Group 2 (n=3) and the placebo Group 3 were given etanercept (300 µg/mouse every 3 day) and PBS (placebo) respectively from day 18 after immunization onwards. Mice of both Group 2 and Group 3 were sacrificed on day 32. Some CII immunized mice in both Group 2 and Group 3 started to show signs of arthritis from day 18 onwards. In addition, by day 32, there were 2 etanercept-treated CII immunized in Group 2 (66.66 % incidence), and 2 PBS-treated CII immunized mice in Group 3 (66.66 % incidence) developed arthritis. In this very small study sub-group, this suggests that etanercept treatment did not have an effect on the onset of disease and the incidence of disease in CII immunized mice in treatment Group 2 (Figure 6.16A). However, a significant reduction in mean paw thickness was observed in etanercept-treated mice in Group 2 compared to those in PBS-treated CII immunized mice (Figure 6.16B). The mean paw thickness of mice in Group 2 and 3 (etanercept-treated versus PBS-treated) was 2.0 ± 0.1 mm versus 2.3 ± 0.3 mm ($P = 0.084$), while the mean clinical score of mice in Group 2 and 3 (etanercept-treated versus PBS-treated) was 4 ± 2.1 versus 8 ± 4.2 ($P = 0.029$) (Figure 6.16C). However, the mean paw thickness and mean arthritis score of etanercept-treated immunized mice was also significantly higher than those in naïve control mice. The mean paw thickness of mice (etanercept-treated versus control naïve) was 2.0 ± 0.1 mm versus 1.8 ± 0.0 mm ($P = 0.0008$). This suggests that etanercept treatment seemed to ameliorate joint inflammation in CII immunized mice, but not completely inhibit the onset and progression of arthritis on day 32, at least as seen in this small subset.

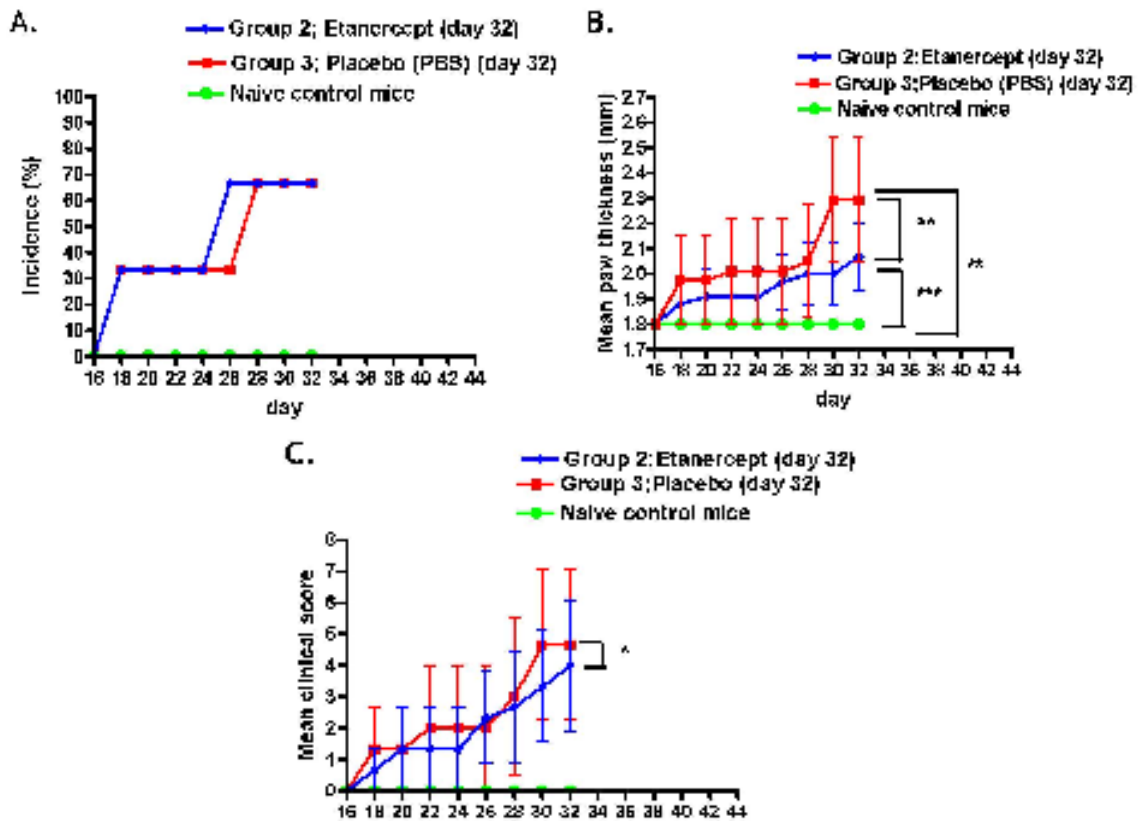


Figure 6.16 Effect of etanercept on severity of arthritis in CII immunized mice on day 32. CII immunized mice in Group 2 ($n=3$ CII immunized mice/group blue line) were given injections from days 18 onwards before collagen immunization with $300\ \mu\text{g}$ etanercept every 3 days. 3 CII immunized mice in Group 3 were given PBS as placebo ($n=3$ CII immunized mice/group red line). Mice in both Group 2 and Group 3 were sacrificed on day 32. The signs of arthritis in CII immunized mice were monitored from day 16 after immunization onwards. (A) shows the percent of incidence of arthritis in etanercept-treated and PBS-treated CII immunized mice, which was calculated from number of CII immunized mice with arthritis per group/total number of CII immunized mice used per group. Mean clinical arthritis score and mean paw thickness were used as a clinical evaluation to measure the severity of joint inflammation in arthritic mice. (B) shows mean paw thickness of etanercept-treated and PBS-treated CII immunized mice which was calculated from the sum of the paw thickness of all mice in each group divided by the number of mice per group. (C) shows mean clinical score of etanercept-treated and PBS-treated CII immunized mice which was calculated from the sum of the clinical scores of all mice in the each group divided by the number of mice per group. Mean paw thickness, mean clinical score and %incidence in CII immunized mice ($n=3$ /group) were compared with those values of naïve control mice ($n=3$ naïve control mice; green line). These naïve control mice were neither sensitized with type II collagen nor given etanercept treatment. Data represented as mean \pm SEM. ($n=6$ CII immunized mice). Statistical analysis of data was performed using two-way ANOVA for multiple comparison, compared with a group of control naïve mice; * $P<0.05$, ** $P<0.01$, *** $P<0.001$.

6.5.2.2 Effect of etanercept on severity of arthritis in CII immunized mice on day 35.

By day 35, the etanercept treatment seemed to prevent the arthritis disease progression in the etanercept-treated CII immunized mice in Group 4.

Firstly, etanercept treatment delayed the disease onset and significantly reduced disease incidence compared with the PBS-treated arthritis controls ($P=0.0002$). Mice in Group 4 ($n=5$) started to develop arthritis on day 19 days after immunization in the PBS-treated group, compared with 33 days after immunization in the etanercept-treated Group 5 ($n=5$) (Figure 6.17A). There was only 1 etanercept-treated CII immunized mouse that developed arthritis (20% incidence), compared with 3 arthritic mice in the PBS-treated group (60% incidence).

Secondly, etanercept significantly decreased mean paw thickness of etanercept-treated CII immunized mice compared to those of PBS-treated CII immunized mice. The mean paw thickness of mice in Group 4 and 5 (etanercept-treated versus PBS-treated) was 2.1 ± 0.2 mm versus 2.8 ± 2.1 mm ($P < 0.0001$) (Figure 6.17B).

Thirdly, a significant reduction in mean clinical score was observed in etanercept-treated CII immunized mice compared to those of PBS-treated CII immunized mice. The mean clinical score of mice in Group 4 and 5 (etanercept-treated versus PBS-treated) was 2.8 ± 2.1 versus 0.4 ± 0.4 ($P < 0.0001$) (Figure 6.17C). There was no significant difference in mean clinical score between etanercept-treated mice and naïve control mice. There was no significant difference in mean paw thickness and mean clinical score between etanercept-treated CII immunized mice Group 4 and naïve control mice on day 35.

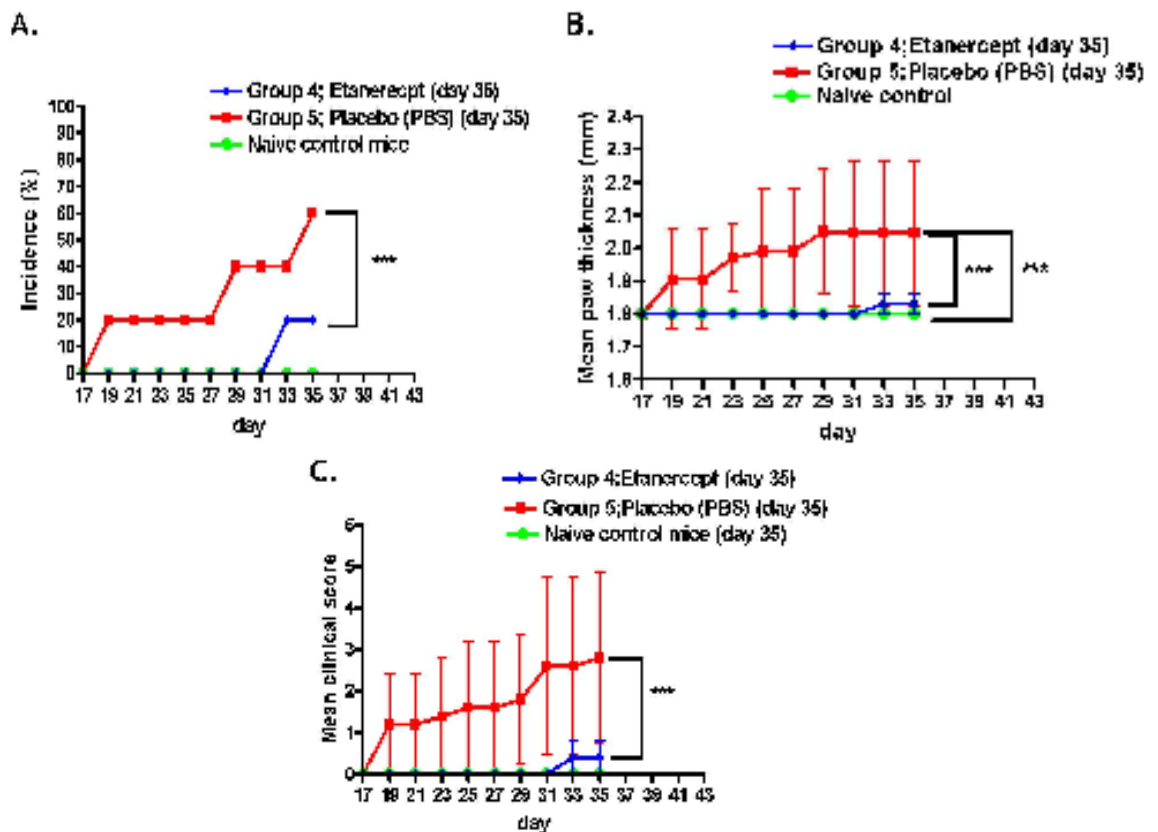


Figure 6.17 Effect of etanercept on severity of arthritis in CII immunized mice on day 35. CII immunized mice in Group 4 ($n=5$ CII immunized mice/group blue line) were given injections from days 18 onwards before collagen immunization with 300 μg etanercept every 3 days. 5 CII immunized mice in Group 5 were given PBS as placebo ($n=5$ CII immunized mice/group red line). Mice in both Group 4 and Group 5 were sacrificed on day 35. The signs of arthritis in CII immunized mice were monitored from day 16 after immunization onwards. (A) shows the percent incidence of arthritis in etanercept-treated and PBS-treated CII immunized mice, which was calculated as number of CII immunized mice with arthritis per group/total number of CII immunized mice used per group. Mean clinical arthritis score and mean paw thickness were used as a clinical evaluation to measure the severity of joint inflammation in arthritic mice. (B) shows mean paw thickness of etanercept-treated and PBS-treated CII immunized mice which was calculated from the sum of the paw thickness of all mice in each group divided by the number of mice per group. (C) shows mean clinical of etanercept-treated and PBS-treated CII immunized mice which was calculated from the sum of the clinical scores of all mice in the each group divided by the number of mice per group. Mean paw thickness, mean clinical score and %incidence in CII immunised mice ($n=5$ CII immunized mice/group) were compared with those values of naïve control mice ($n=5$; green line). These naïve control mice were neither sensitized with type II collagen nor given etanercept treatment. Data represented as mean \pm SEM. ($n=10$ CII immunised mice). Statistical analysis of data was performed using two-way ANOVA for multiple comparison, compared with a group of control naïve mice; * $P < 0.05$; ** $P < 0.01$; *** $P < 0.001$.

6.5.2.3 Overall severity of arthritis in etanercept-treated groups to PBS-treated groups

Overall, there were 5 out of 8 PBS treated CII immunized mice from Group 3 and Group 5 (~62.5 % incidence) that showed clinical signs of arthritis from day 18. Etanercept treated-CII immunized mice showed a lower disease incidence compared to those in PBS treated-CII immunized mice. 3 out of 8 Etanercept treated CII immunized mice from Group 2 and 4 developed arthritis from day 18

(~37.5 % incidence) (Figure 6.18A). Clinical signs of arthritis were observed in PBS-treated CII immunized mice from Group 3 and 5 from day 19 after immunization onward and there were 5 out of 8 PBS-treated CII immunized mice developed arthritis (62.5% incidence). The cumulative mean paw-swelling diameter of all PBS-treated CII immunized mice from Group 3 and Group 5 (n=8) was 2.1 ± 0.2 mm, which was significantly higher than those in naïve control mice (1.8 ± 0.0 mm; $P < 0.0001$). Etanercept-treated CII immunized mice showed significantly less swelling than PBS treated CII immunized mice (2.1 ± 0.2 mm; $P < 0.0001$). Two-way ANOVA analysis also indicated that the cumulative mean of swelling diameter of Etanercept-treated CII immunized mice was significantly higher than those in control mice (1.8 ± 0.0 mm; $P = P < 0.0001$) (Figure 6.18B). The cumulative mean arthritis score of Etanercept-treated CII immunized mice was significantly lower than those of PBS treated CII immunized mice (2.25 ± 1.21 versus 3.75 ± 1.35) (Figure 6.18C). A summary of number of arthritic mice, mean arthritis score, maximum arthritis score, mean paw diameter of etanercept-treated and PBS-treated CII immunized mice is presented in Table 1. Overall, our data suggest that etanercept treatment before the onset of disease attenuated arthritis disease severity in CII immunized mice.

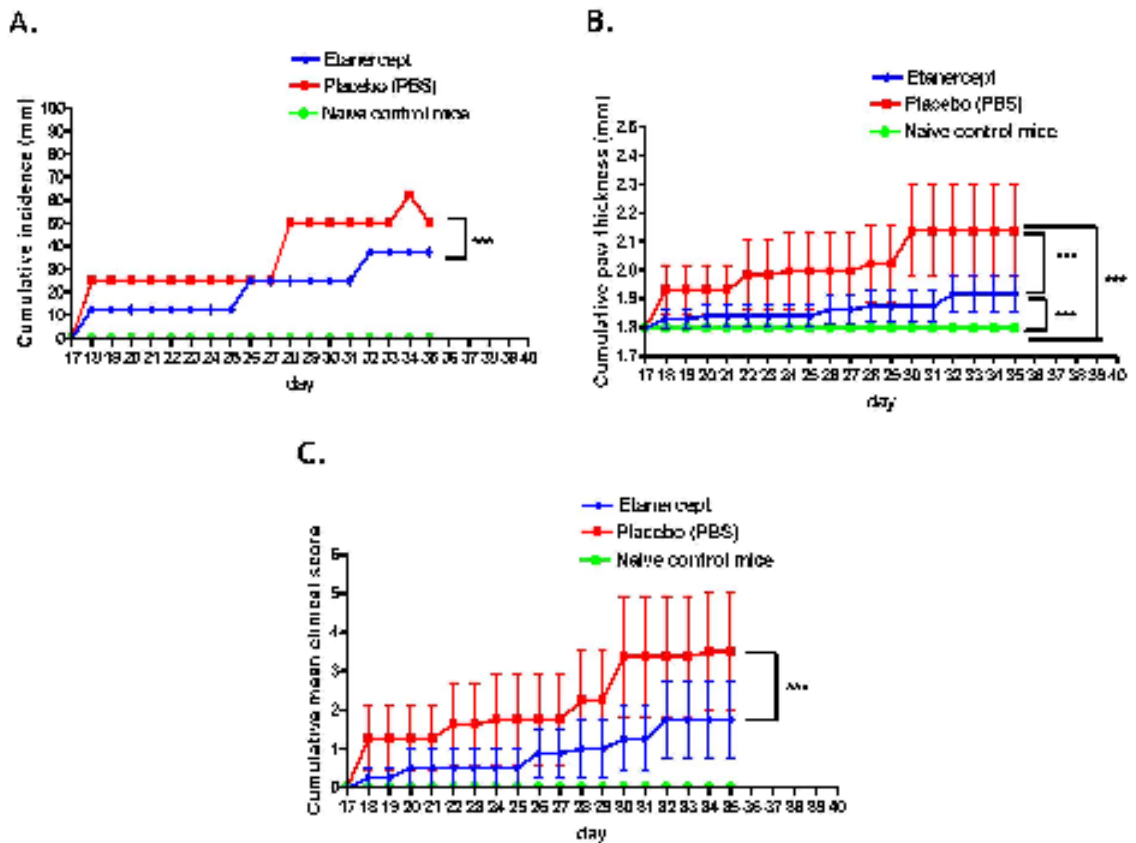


Figure 6.18 Effect of etanercept on severity of arthritis in all CII immunized mice in Group 2, 3, 4 and 5

CII immunized mice in Group 2 and Group 4 ($n=8$ CII immunized mice for both groups; blue line) were given injections of 300 μg etanercept every 3 days from days 18 onwards, before collagen immunization. 3 CII immunized mice in Group 3 and Group 5 were given PBS as placebo treatment ($n=8$ CII immunized mice for both groups; red line). Mice in both Group 4 and Group 5 were sacrificed on day 32, while mice in both Group 4 and Group 5 were sacrificed on day 35. The signs of arthritis in CII immunized mice were monitored from day 16 after immunization onwards. (A) shows the cumulative percent of incidence of arthritis in all etanercept-treated and all PBS-treated CII immunized mice, which was calculated from number of CII immunized mice with arthritis per group/total number of CII immunized mice used per group. Cumulative mean clinical arthritis score and cumulative mean paw thickness were used as a clinical evaluation to measure the severity of joint inflammation in arthritic mice. (B) shows cumulative mean paw thickness of all etanercept-treated and all PBS-treated CII immunized mice which was calculated from the sum of the paw thickness of all mice in each group divided by the number of mice per group. (C) shows cumulative mean clinical of all etanercept-treated and all PBS-treated CII immunized mice which was calculated from the sum of the clinical scores of all mice in the each group divided by the number of mice per group. Cumulative mean paw thickness, cumulative mean clinical score and cumulative %incidence in CII immunised mice ($n= 8$ CII immunised mice/group) were compared with those values of naïve control mice ($n = 8$; green line). These naïve control mice were neither sensitized with type II collagen nor given etanercept treatment. Data represented as mean \pm SEM. ($n=16$ CII immunized mice). Statistical analysis of data was performed using two-way ANOVA for multiple comparison, compared with a group of control naïve mice; * $P < 05$; ** $P < 01$; *** $P < 001$.

Group	Treatment	Day of harvesting	Arthritic/total number of mice	Mean Arthritis scores	Maximum Arthritis scores	Mean Paw Diameter (mm)
2	Etanercept	32	2/3	4.0 ± 2.1	7	2.1 ± 0.1
3	PBS	32	2/3	4.7 ± 2.4	8	2.1 ± 0.3
4	Etanercept	35	1/5	0.4 ± 0.4	2	1.9 ± 0.0
5	PBS	35	3/5	2.8 ± 2.1	11	2.1 ± 0.2

Table 6.1 Numbers of arthritic mice, mean arthritis scores, and mean swelling scores of CIA mice in etanercept-treated and PBS-treated groups. Etanercept-treated mice and PBS-treated mice (Group 2 and 3) were sacrificed on day 32, while etanercept-treated mice and PBS-treated mice (Group 4 and 5) were sacrificed on day 35. Numbers of immunized mice developed arthritis from each time point group were counted on the harvesting day. Mean arthritis scores (total arthritis score/number of mice in the group), maximum arthritis score and mean swelling of immunized mice from each treatment time point group were calculated on the cull day.

6.5.3 Changes in hippocampal neurogenesis in CII immunized mice before the onset of arthritis on day 14.

Data from the previous section of this Chapter 6 (Section 6.4) showed a reduction in neurogenesis in CII immunized mice on day 42; during the period of clinical disease. However, it still remained unclear whether the reduction in neurogenesis is actually associated with peripheral inflammation. We therefore analysed the change in neurogenesis in CII immunized mice compared to those in naïve control mice before the disease onset. 14 days after the primary immunization on day 1, there were no CII immunized mice (n=19) that developed arthritis. We randomly sacrificed 3 CII immunized mice and the brains of these

mice were processed for DCX-immuno-histochemistry to investigate any change in hippocampal neurogenesis compared to brains from 3 naïve control mice harvested on the same day. Etanercept treatment (300 ug/animal i.p., every 3 days) was not administered to CII immunized mice until day 18 after immunization. Therefore, day 14 is also the control time point before etanercept treatment. The quantitative immuno-histochemistry of DCX positive neurons was performed on the brain sections from CII immunized mice and naïve control mice harvested on day 14 to investigate changes in hippocampal neurogenesis before etanercept treatment which was started on day 18. The microscopy images of stained brain sections showed no changes in the number of DCX positive neurons in the hippocampus of immunized mice compared to those of control untreated mice (Figure 6.19A - Figure 6.19F). This was confirmed by the cell count data showing that the number of DCX-positive neurons in the dentate gyrus of arthritic mice was not significantly different from those in naïve control mice on day 14. The mean number of DCX-positive neurons in the dentate gyrus (CII immunized versus control) was 9528 ± 2040 cells versus 10938 ± 2244 cells ($P = 0.4643$; $n=3$) (Figure 6.20). These data suggested that the changes in the hippocampal neurogenesis seen at day 42 may be associated with the subsequent peripheral inflammation. This also corresponded with data from Chapter 5 (Section 5.2.3 and Section 5.2.4) also showing that there was no significant difference in brain inflammatory mediator concentrations in CII immunized mice on day 14 compared to those in naïve control mice. Our data from the previous chapter (Chapter 5 ; Section 5.2.3 and Section 5.2.4) combined with this hippocampal neurogenesis data of CII immunized mice on day 14 in this section suggest that brain inflammatory mediators in CII immunized mice may contribute to the reduction in hippocampal neurogenesis.

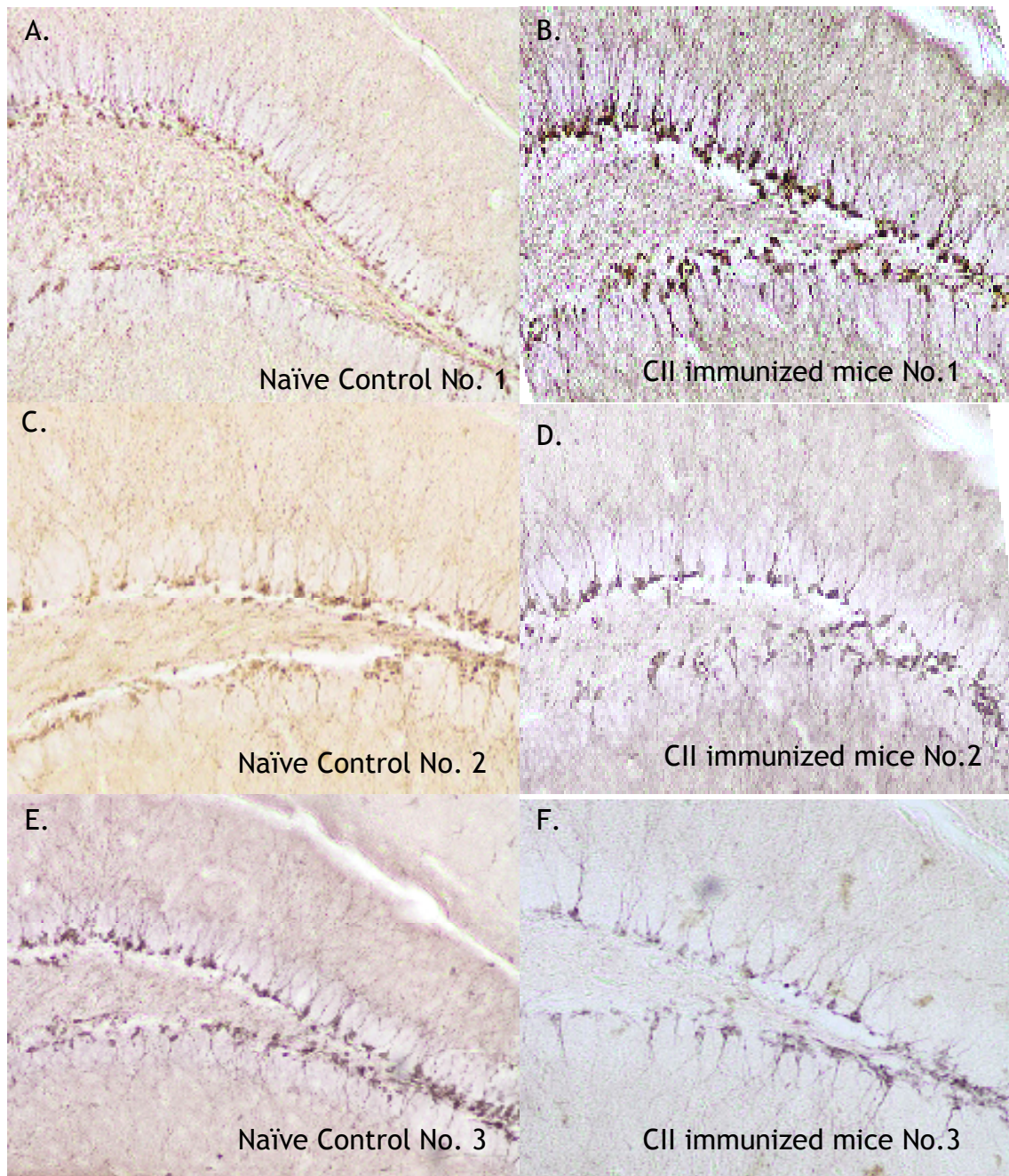


Figure 6.19 DCX immuno-histochemistry in the dentate gyrus of control untreated mice and CII immunized mice on day 14

Control and CII immunized mice (3 mice/group) were sacrificed on day 14 and the brains of these were processed for DCX immuno-histochemistry. (A), (C) and (E) show representative images of DCX immuno-histochemistry in the dentate gyrus of control mice (numbers 1, 2 and 3 respectively). (B), (D), (F) show representative images of DCX immuno-histochemistry in the dentate gyrus of CII Immunized mice. All images were 10X magnification.

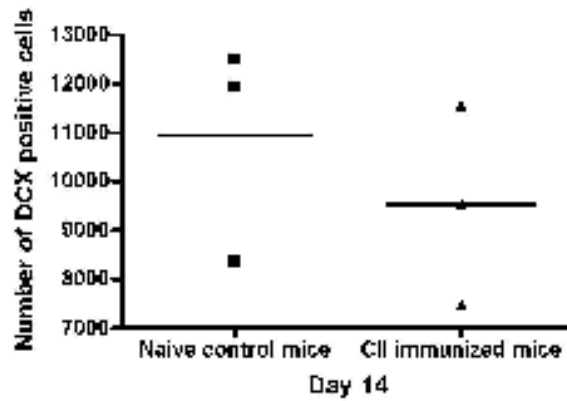


Figure 6.20 Changes in number of DCX-positive cells in dentate gyrus of CII immunized mice on day 14

The dots represent the number of DCX positive cells in the hippocampus of individual naïve control mice (filled squares; n=3 naïve control mice) and CII immunized mice (filled triangles; n=3 CII immunized mice) on day 14. Numbers of DCX positive cells in the hippocampus of mice from both naïve control and CII immunized groups were determined by counting DCX-positive cells in every sixth serial brain section containing hippocampal tissue. Bars represent the mean values. (*P < 05; **P < 01; ***P < 001 by Student's t-test).

6.5.4 Effect of etanercept on hippocampal neurogenesis during period of clinical manifestation of arthritis

Data from Chapter 3 (section 3.2.3 and section 3.2.4) suggest that a reduction in hippocampal neurogenesis may be associated with peripheral joint inflammation that may be due to inflammatory mediators that are up-regulated in brains of CII immunized mice during the period of clinical manifestation of arthritis on day 42. In Chapter 5 (Section 5.2.3 and Section 5.2.4), we demonstrated that peripheral administration of etanercept resulted in decreases in brain inflammatory mediators, including TNF- α , IL-12 and IL-5. We therefore hypothesised that the reductions of these brain inflammatory mediators resulting from peripheral etanercept treatment may have the protective effect against the impairment of hippocampal neurogenesis in CII immunized mice.

To determine whether the reduction in hippocampus neurogenesis in CII immunized mice could be prevented by anti-inflammatory drug therapy, etanercept (300 ug/animal i.p., every 3 days) was peripherally administered to CII immunized mice from day 18 onwards. Etanercept-treated immunized mice (Group 2 and 4), PBS-treated CII immunized mice (Group 3 and 5), and naïve control mice were sacrificed on day 32 and day 35, which is typically during the period of clinical manifestation of arthritis. Brains of mice from all experimental groups were processed and immuno-histochemistry stained for DCX. In order to

compare the DCX staining pattern we used a strategy to compare subgroups using random images from one mouse in each group of naïve control mice, PBS-treated and Etanercept treated CII immunized mice at each of the time points on day 32 and day 35. Each subgroup was labelled study groups A, B, C etc. A summary of the data showing arthritis score, paw diameter and number of DCX-positive cells of individual mouse from each subgroup on each day is added at the end.

6.5.4.1 Effect of etanercept on hippocampal neurogenesis in CII immunized mice on day 32

There were 2 etanercept-treated CII immunized mice from Group 2 that developed arthritis on day 32. At that time point, there was 1 etanercept-treated CII immunized mouse with no arthritis in that group. In Group 3, there were 2 PBS-treated CII immunized mice developed arthritis and 1 PBS-treated CII immunized mice that did not develop arthritis. We compared subgroups of images from one mouse in each group of naïve control mice, PBS-treated and etanercept-treated CII immunized mice. Each subgroup was labelled study groups as Set A, Set B and Set C. Since we had the same number of PBS-treated and etanercept-treated CII immunized mice that developed arthritis (n=2) on day 32, we decided to compare DCX immuno-histochemistry images from PBS-treated mice with arthritis and etanercept-treated CII immunized mice that developed arthritis. Therefore, Set A and Set B consisted of DCX-staining images from etanercept-treated and PBS-treated CII immunized mice with arthritis and naïve control mice. Set C consisted of DCX-staining images from one etanercept-treated mouse and one PBS-treated CII immunized mouse with arthritis and one naïve control mouse. The analysis plan of DCX immuno-histochemistry images of mice from all experimental groups is shown in Figure 6.21.

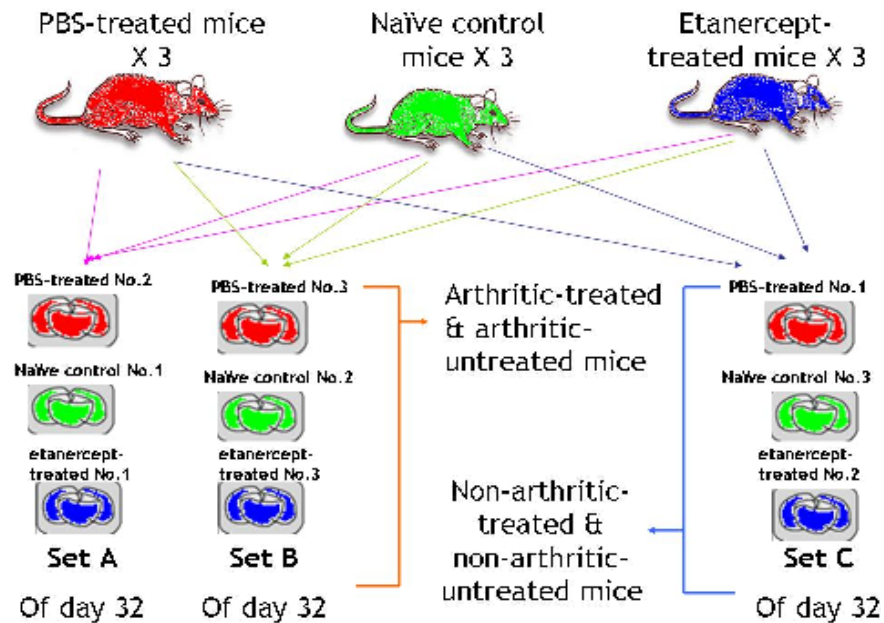


Figure 6.21 Analysis plan to compare DCX staining pattern in brains of PBS-treated, etanercept-treated CII immunized mice and naïve control mice on day 32

DCX staining images from one mouse in each group of PBS-treated mice ($n=3$ PBS-treated mice; red mouse), naïve control mouse ($n=3$ naïve control mouse; green mouse) and etanercept-treated mice ($n=3$ etanercept-treated mice; blue mouse) were compared. DCX staining images of one PBS-treated mouse (red), one naïve control mouse (green) and one etanercept-treated mouse (blue) and were organized as subgroups, namely Set A, B and C. Set A and B consisted of DCX-staining images from PBS-treated, etanercept-treated CII immunized mice with arthritis and naïve control mice. Set C consisted of DCX-staining images from PBS-treated, etanercept-treated CII immunized mice without arthritis and a naïve control mouse.

6.5.4.1.1 *Effect of etanercept on the number of DCX-positive cells in CII immunized mice with arthritis on day 32*

Set A consisted of control mouse No.1, the PBS-treated arthritis mouse No.2 (clinical score 8), and an etanercept-treated arthritis mouse No.1 (clinical score 1). The microscopy images in Figure 6.22 showed differences in the number of DCX-positive neurons between the hippocampi of treated, untreated arthritic mice and control mice. A result from the cell count demonstrated that the hippocampus of the PBS-treated arthritis mouse No. 2 (clinical score 8) showed fewer DCX-positive cells compared to those of the naïve control mouse No. 1 (4176 versus 8310 cells). Interestingly, the etanercept-treated mouse No.1 showed a higher number of DCX-positive cells (10416 cells) compared to those of a naïve control mouse No.1 and PBS-treated arthritis mouse No.2 (Figure 6.22A - Figure 6.22C).

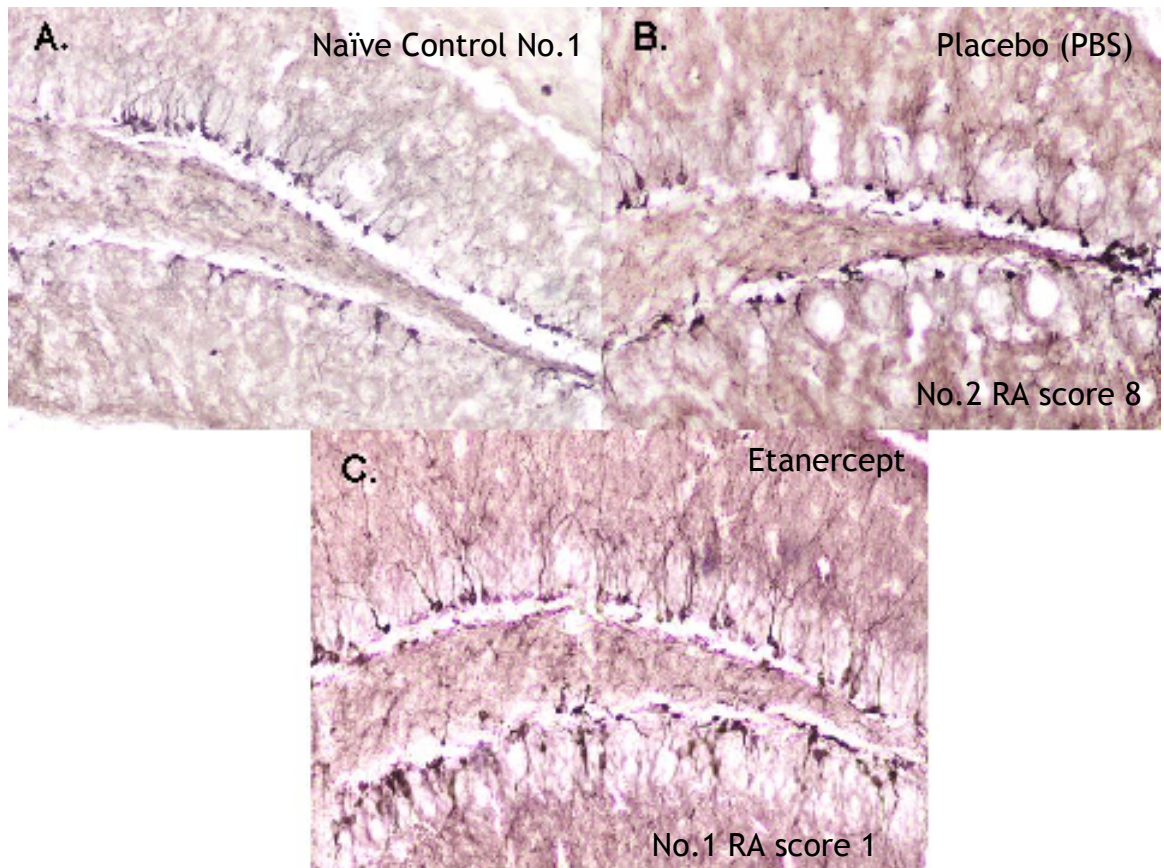


Figure 6.22 DCX immuno-histochemistry in the dentate gyrus of one naïve control, one PBS-treated and one etanercept-treated CII immunized mouse in set A. All the mouse brains from mice of set A were harvested on day 32. (A) shows a representative image of DCX immuno-histochemistry in the dentate gyrus of control mice No.1. (B) shows a representative image of DCX of PBS-treated CII immunized mice No.2 (clinical score 8). (C) shows a representative image of DCX of Etanercept-treated CII immunized mice No.1 (clinical score 1). RA score = clinical score. All images at 10X magnification.

A similar pattern of changes in the number of DCX-positive cells in the dentate gyrus was observed in DCX staining images from naïve control, PBS-treated and etanercept-treated arthritic mice in Set B. The PBS-treated-arthritic mouse No 3 (clinical score 6) had less number of DCX-positive cells in the dentate gyrus compared those of naïve control mouse No 2 (Figure 6.23A and Figure 6.23B). The number of DCX-positive cells in dentate gyrus of the naïve control mouse was 9222 cells, while the number of DCX-positive cells in the dentate gyrus of the PBS-treated arthritis mouse No.3 was 2310 cells. The etanercept treated arthritic mouse No 3 (clinical score 6) showed a similar number of DCX-positive cells in the dentate gyrus (n=9204) compared to the naïve control mouse No.2, which higher than those of the PBS-treated CII immunized mice No.3 (Figure 6.23A and Figure 6.23C).

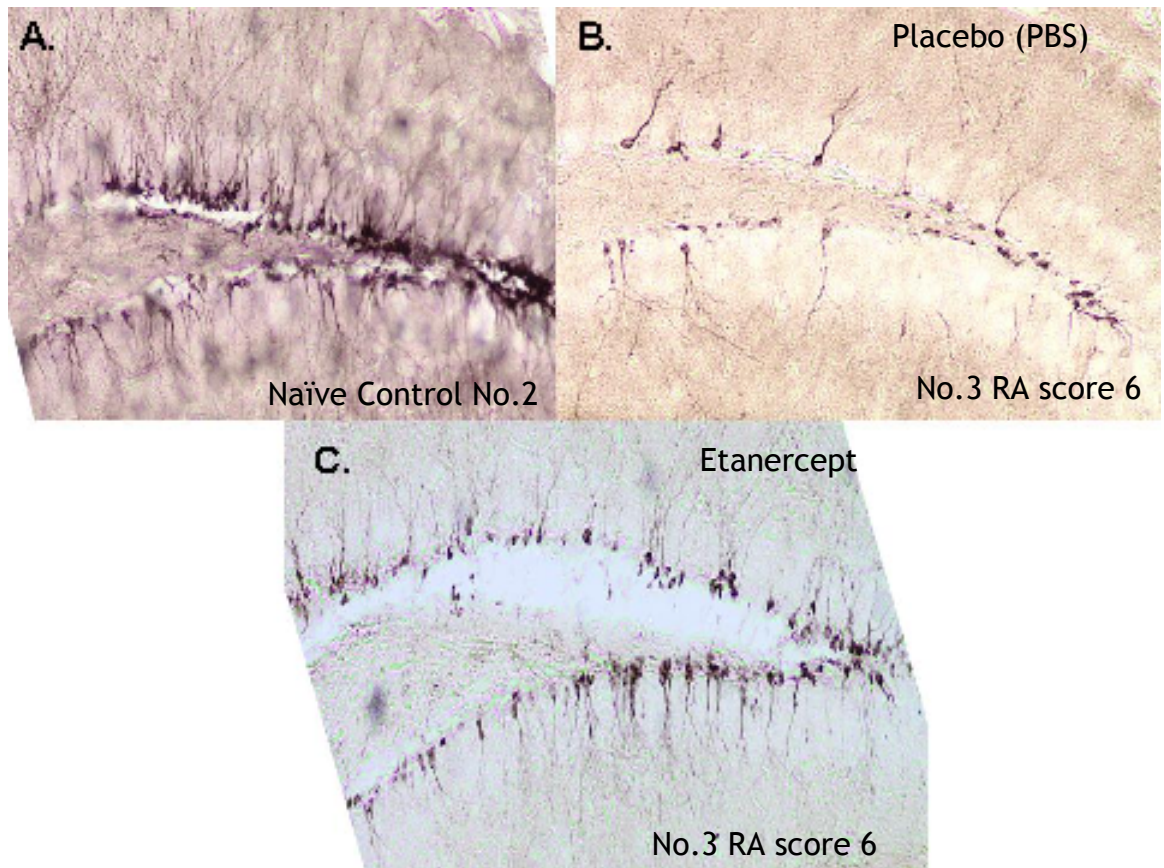


Figure 6.23 DCX immuno-histochemistry in the dentate gyrus of one naïve control, one PBS-treated arthritic and one etanercept-treated arthritic mouse in set B
 All mouse brains from mice of set B were harvested on day 32 and processed for DCX immuno-histochemistry. (A) shows a representative image of DCX immuno-histochemistry in the dentate gurus of the naïve control mice No.2. (B) shows a representative image of DCX immuno-histochemistry in the dentate gurus of untreated CII immunized mice No.3 (clinical score 6). (C) shows a representative image of DCX immuno-histochemistry in the dentate gurus of the etanercept-treated CII immunized mice No.3, (clinical score 6). RA score = clinical score. All images 10X magnification.

A summary of the number of DCX-positive neurons in the hippocampus of individual naïve control mice, PBS-treated-arthritic mice and etanercept-treated arthritic mice and their arthritis scores is presented in Table 6.2.

Mouse	Individual Clinical scores	Individual paw diameter (mm)	Number of DCX-positive neurons
Set A mice			
Naïve control mouse No.1	0	1.8	8310
PBS-treated mouse No.2	8	2.5	4176
Etanercept-treated mouse No.1	1	2.2	10416
Set B mice			
Naïve control mouse No.2	0	1.8	9222
PBS-treated mouse No.3	6	2.6	2310
Etanercept-treated mouse No.3	6	2.5	9204

Table 6.2 Individual arthritis score, individual paw swelling scores and number of DCX-positive neurons of arthritic mice in etanercept-treated and PBS-treated groups
Each set of mice (set A and set B) consisted of a naïve control mouse, a PBS treated arthritic mouse and an etanercept-treated arthritic mouse, which were sacrificed on day 32. DCX immuno-histochemistry and number of DCX-positive neurons in the dentate gyrus of mice in each set were compared. Individual arthritis score, paw diameter (sum of all 4 paws of each mouse divided by 4) and number of DCX positive neurons in the dentate gyrus of mice were calculated and measured on the cull day.

6.5.4.1.2 Effect of etanercept on hippocampal neurogenesis of non-arthritic mice on day 32

Set C of mice consisted of a naïve control mouse No. 3, a PBS-treated CII immunized mouse No.1 and an etanercept-treated CII immunized mouse No. 2. Both the PBS-treated and the etanercept-treated CII immunized mice did not develop arthritis by day 32. Despite this, there was a difference in the number of DCX-positive neurons observed in the dentate gyrus of both PBS-treated and etanercept-treated CII immunized mice with no arthritis compared to those of the naïve control mouse (Figure 6.24A - Figure 6.24B). PBS-treated non-arthritic mouse No 1 had less DCX-positive cells in its dentate gyrus as compared with DCX-positive cells in the dentate gyrus of the naïve control mouse No 3 (n=2136 cells versus 8904 cells). Interestingly, the dentate gyrus of the etanercept-treated non arthritic mouse No 2 had a higher number of DCX-positive cells (n=7428) than those of the PBS-treated non arthritic mouse No 1 (Figure 6.24B - Figure 6.24C). A summary of number DCX-positive neurons in the dentate gyrus of individual mice PBS-treated non arthritic mouse, etanercept-treated non

arthritic mouse and the naïve control mouse in Set C and their clinical scores and paw diameters is presented in Table 6.3.

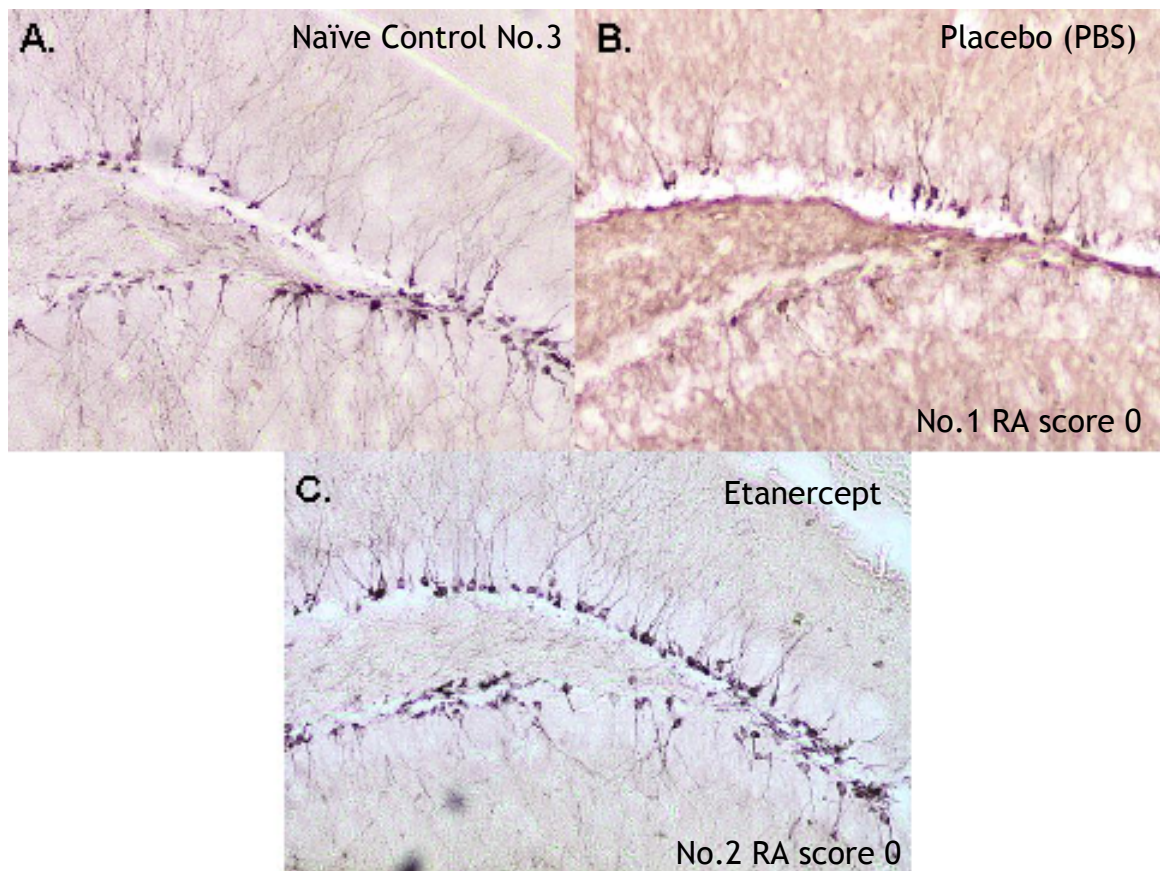


Figure 6.24 DCX immuno-histochemistry in the dentate gyrus of one control, one PBS-treated and one etanercept-treated CII immunized mouse in Set C (neither developed arthritis)

All the mouse brains from the mice of Set C were harvested on day 32 and processed for DCX immuno-histochemistry. (A) shows a representative image of DCX immuno-histochemistry in the dentate gurus of the naïve control mice No.3. (B) shows a representative image of DCX immuno-histochemistry in the dentate gurus of PBS-treated CII immunized mice No.1 (clinical score 0). (C) shows a representative image of DCX immuno-histochemistry in the dentate gurus of the etanercept-treated CII immunized mice No.2 (clinical score 0). RA score = clinical score. All images at 10X magnification.

Mouse	clinical scores	paw diameter (mm)	Number of DCX-positive neurons
Naïve control mouse No.3	0	1.8	8904
PBS-treated mouse No.1	0	1.8	2136
Etanercept-treated mouse No.2	0	1.8	7428

Table 6.3 Individual arthritis score, individual paw swelling scores and number of DCX-positive neurons of non-arthritic mice in etanercept-treated and PBS-treated CII immunized groups on day 32

Set C consisted of a naïve control mouse No.3, PBS-treated non-arthritic mouse No.1 and etanercept-treated non-arthritic mouse No.2, which were sacrificed on day 32. DCX immuno-histochemistry and number of DCX-positive neurons in the dentate gyrus of mice in each

set were compared. Individual arthritis score, paw diameter (*sum of all 4 paws of each mouse divided by 4*) and number of DCX positive neurons in the dentate gyrus of mice were calculated and measured on the cull day 32.

6.5.4.1.3 Comparison of numbers of DCX-positive cells between etanercept-treated and PBS-treated groups on day 32

Overall, the cell count data showed that DCX-positive neurons in the dentate gyrus of PBS-treated CII immunized mice on day 32 were significantly decreased compared to those in the naïve control mice on day 32. One-way ANOVA followed by Bonferroni's post-hoc comparison tests demonstrated that there were significant differences in the number of DCX-positive neurons in the dentate gyrus among the three groups of mice culled on day 32 ($P = 0.0008$) (Figure 6.25). The mean number of DCX-positive neurons in the dentate gyrus (PBS-treated CII immunized versus naïve control) was 2874 ± 1128 cells versus 8814 ± 462 cells ($P = 0.0011$) (Figure 6.25). The number of DCX-positive neurons in the dentate gyrus of etanercept-treated CII immunized mice was significantly increased compared to those in the PBS-treated-arthritic mice on day 32. The mean number of DCX-positive neurons in the dentate gyrus (etanercept-treated CII immunized versus PBS-treated CII immunized) was 9018 ± 1218 cells versus 2874 ± 1128 cells ($P = 0.0048$) (Figure 6.25). However, there was no significant difference between the numbers of DCX-positive neurons in the dentate gyrus of etanercept-treated CII immunized compared to those of naïve control mice on day 32 (Figure 6.25). This finding suggests that etanercept treatment may have a protective effect against the impairment of hippocampal neurogenesis in CII immunized mice on day 32

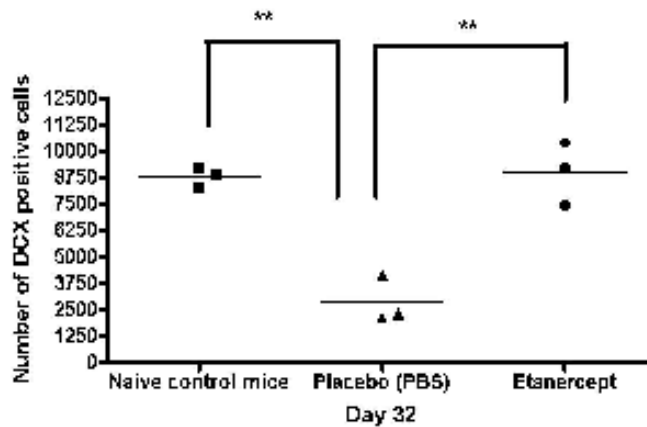


Figure 6.25 Number of DCX-positive cells in dentate gyrus of PBS-treated and etanercept-treated CII immunized mice on day 32

The dots represent the number of DCX positive cells in the hippocampus of individual control untreated mice (filled squares; n=3 control untreated mice), CII immunized mice treated with PBS as the placebo group (filled triangles; n=3 CII immunized mice), and immunised etanercept-treated mice (filled circles; n=3 immunised etanercept-treated mice) on day 32. The number of DCX positive cells in the hippocampus of mice from all experimental groups was determined by counting DCX-positive cells in every sixth serial brain section containing DCX immuno-histochemistry in the dentate gyrus. Bars represent the mean values: Statistical analysis of data was performed using one-way ANOVA (* $P < 0.05$, ** $P < 0.01$, *** $P < 0.001$).

6.5.4.2 Effect of Etanercept on hippocampal neurogenesis of CII immunized mice on day 35

Quantitative immuno-histochemistry of DCX positive neurons was performed in the brain sections from immunized mice of the etanercept-treated Group 4 (n=5), the PBS-treat Group 5 (n=5) and the naïve control group (n=5) on day 35 to investigate the effect of etanercept on changes in hippocampal neurogenesis. At this time point, there were 3 out of 5 immunized mice from the PBS-treated Group 5 that developed arthritis. There was one out of 5 Etanercept-treated mouse that developed arthritis. Again, to compare DCX-staining pattern the dentate gyrus between PBS-treated, etanercept-treated and antigen-naïve control mice. Images of DCX immuno-histochemistry from one mouse in each group of naïve control, etanercept-treated and PBS-treated mice were randomly organized as subgroups, namely Set D, E, F, G and H. A summary of the data showing arthritis score, paw diameter and number of DCX-positive cells of individual mouse from each subgroup on each day is added at the end. The analysis plan for images of DCX-staining of mice from all experimental groups on day 35 is shown in Figure 6.26.

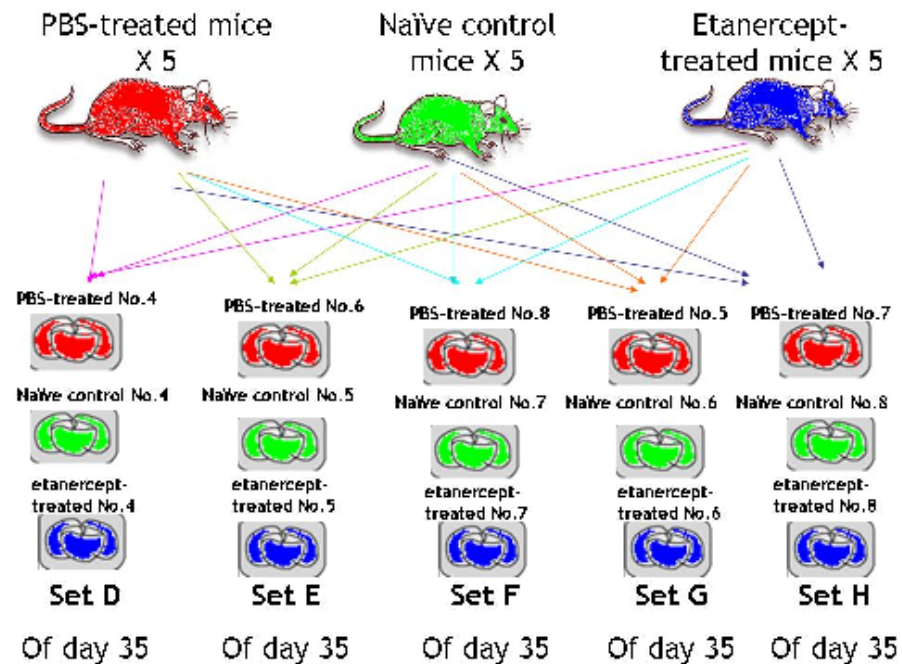


Figure 6.26 Analysis plan to compare DCX staining pattern in brains of PBS-treated, etanercept-treated CII immunized mice and naïve control mice on day 35

DCX staining images from one mouse in each group of PBS-treated mice (n=5 PBS-treated mice; red mouse), naïve control mouse (n=5 naïve control mouse; green mouse) and etanercept-treated mice (n=5 etanercept-treated mice; blue mouse) were compared. DCX staining images of one PBS-treated mouse (red), one naïve control mouse (green) and one etanercept-treated mouse (blue) and were randomly organized as subgroups, namely Set D, E, F, G and H.

Brain slices containing hippocampus from mice of all experimental groups on day 35 were stained for DCX, and the differences in numbers of DCX positive cells between control, treated and untreated mice compared. The microscopy images showed that there were differences in the numbers of DCX-positive neurons between dentate gyrus of PBS-treated-arthritis mice and naïve control mice (Figure 6.27A - Figure 6.31A and Figure 6.27B - Figure 6.31B). PBS-treated CII immunized mice were likely to have less DCX-positive cells in their dentate gyrus compared to those of naïve control mice. Interestingly, PBS-treated-immunized mice, which did not develop arthritis also showed reduced numbers of DCX-positive neurons compared to those of the naïve control mice (Figure 6.27A - Figure 6.31A and Figure 6.27B - Figure 6.31B). In comparison to PBS-treated CII immunized mice, etanercept-treated mice had a trend for more DCX-positive cells in their dentate gyrus (Figure 6.27B - Figure 6.31C). However, the number DCX-positive neurons in dentate gyrus of some etanercept-treated immunized mice were less than those of the naïve control mice (Figure 6.27A - Figure 6.31C).

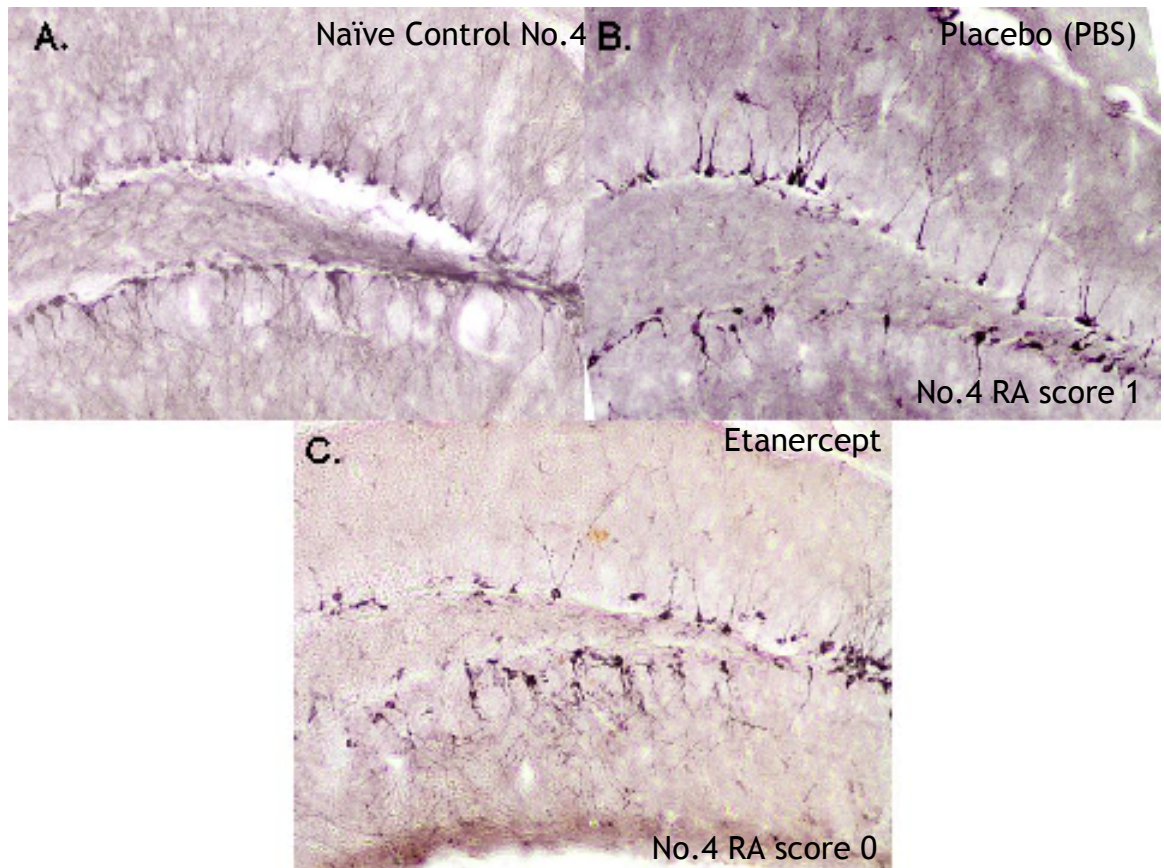


Figure 6.27 DCX immuno-histochemistry in the dentate gyrus of one naïve control, one PBS-treated arthritic and one etanercept non-arthritic mouse in set D
All the mouse brains from mice of Set D were harvested on day 35 and processed for DCX immuno-histochemistry. (A) shows a representative image of DCX immuno-histochemistry in the dentate gurus of a naïve control mouse No.4. (B) shows a representative image of DCX immuno-histochemistry in the dentate gurus of the PBS-treated arthritic CII immunized mouse No.4, (clinical score 1). (C) shows a representative image of DCX immuno-histochemistry in the dentate gurus of the Etanercept-treated non-arthritic mouse No.4, (clinical score 0). RA score = clinical score. All images at 10X magnification.

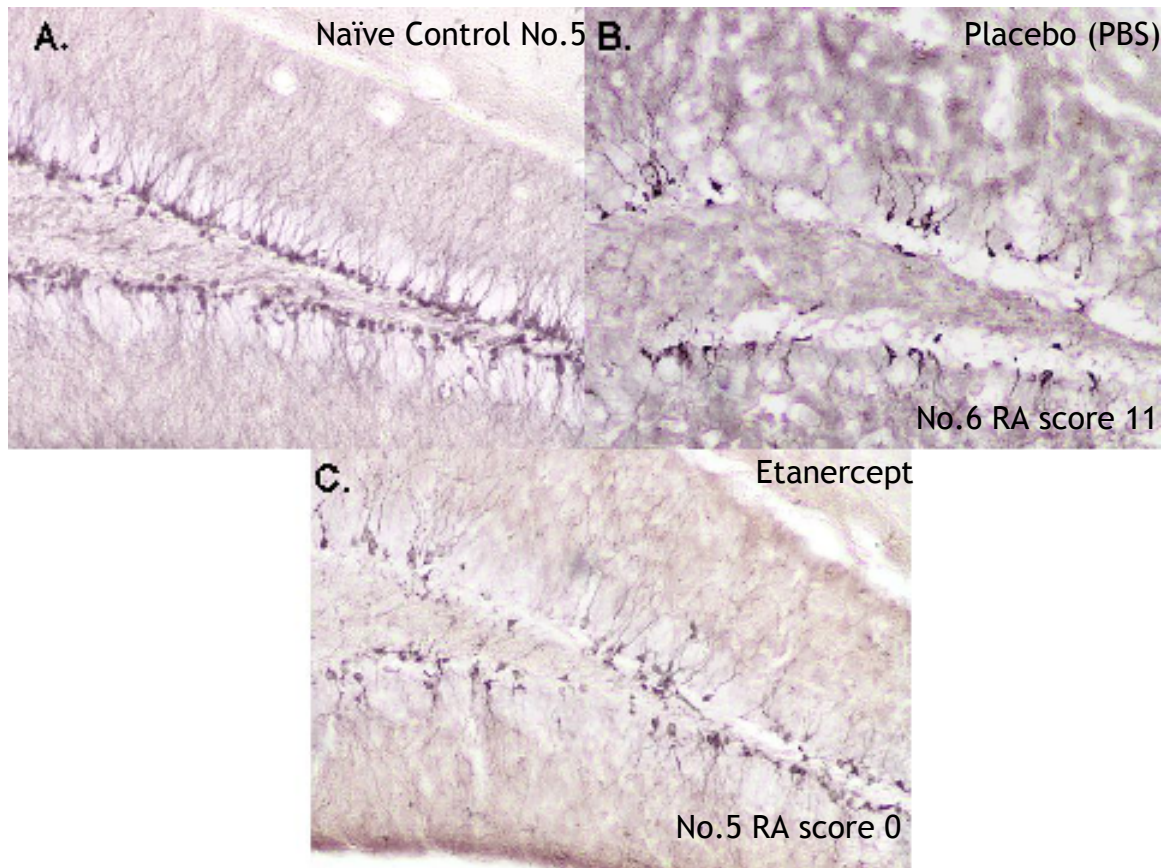


Figure 6.28 DCX immuno-histochemistry in the dentate gyrus of one naïve control, one PBS-treated arthritic and one etanercept-treated non-arthritic mouse in Set E
All the mouse brains from mice of Set E were harvested on day 35 and processed for DCX immuno-histochemistry. (A) shows a representative image of DCX immuno-histochemistry in the dentate gurus of the naïve control mice No.5. (B) shows a representative image of DCX immuno-histochemistry in the dentate gurus of the PBS-treated arthritic untreated mouse No.6 (clinical score 11). (C) shows a representative image of DCX immuno-histochemistry in the dentate gurus of etanercept-treated non-arthritic mouse No.5, (clinical arthritis score 0). RA score = clinical score. All images 10X magnification.

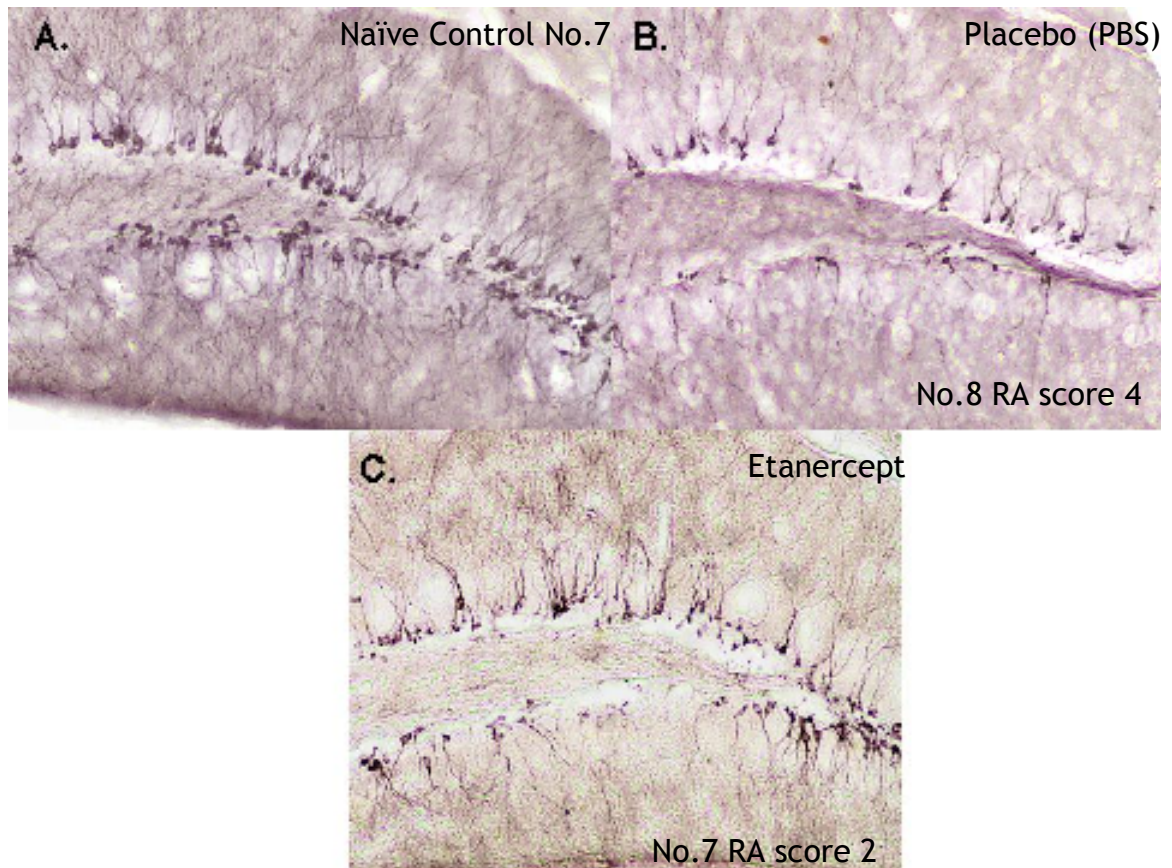


Figure 6.29 DCX immuno-histochemistry in the dentate gyrus of one naïve control, one PBS-treated arthritic and one etanercept arthritic mice in Set F

All the mouse brains from mice of Set F were harvested on day 35 and processed for DCX immuno-histochemistry. (A) shows a representative image of DCX immuno-histochemistry in the dentate gurus of the naïve control mouse No.7. (B) shows a representative image of DCX immuno-histochemistry in the dentate gurus of the PBS-treated arthritic mouse No.8, (clinical score 4). (C) shows a representative image of DCX immuno-histochemistry in the dentate gurus of the etanercept-treated arthritic mouse No.7, (clinical score 2). RA score = clinical score. All images at 10X magnification.

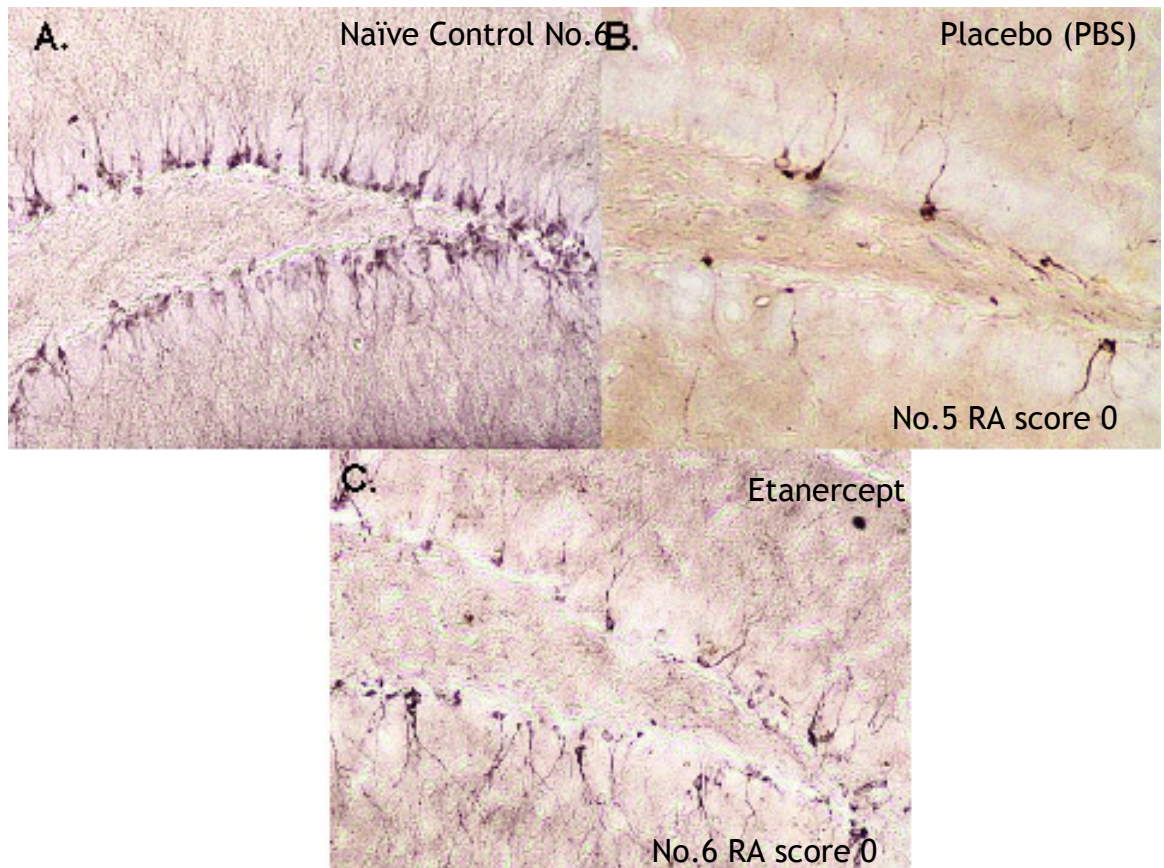


Figure 6.30 DCX immuno-histochemistry in the dentate gyrus of one naïve control, one PBS-treated non-arthritis and one etanercept non-arthritis mouse in Set G
All the mouse brains from mice of Set G were harvested on day 35 and processed for DCX immuno-histochemistry. (A) shows a representative image of DCX immuno-histochemistry in the dentate gurus of the naïve control mouse No.6. (B) shows a representative image of DCX immuno-histochemistry in the dentate gurus of PBS-treated non-arthritis mouse No.5, (clinical score 0). (C) shows a representative image of DCX immuno-histochemistry in the dentate gurus of the etanercept-treated non-arthritis mouse No.6, (clinical score 0). RA score = clinical score. All images at 10X magnification.

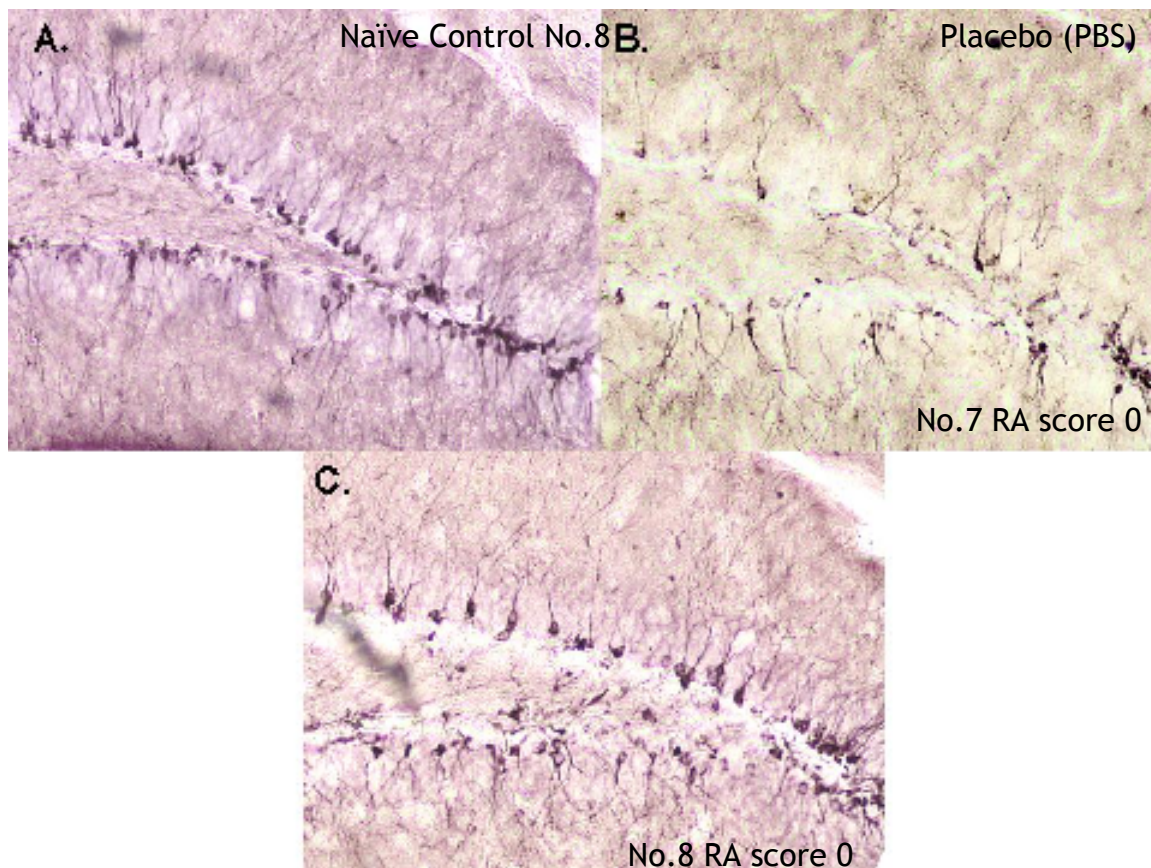


Figure 6.31 DCX immuno-histochemistry in the dentate gyrus of one naïve control, one PBS-treated non-arthritis and one etanercept non-arthritis mouse in Set H
All the mouse brains from mice of Set H were harvested on day 35 and processed for DCX immuno-histochemistry. (A) shows a representative image of DCX immuno-histochemistry in the dentate gyrus of the naïve control mice No.8. (B) shows a representative image of DCX immuno-histochemistry in the dentate gyrus of the PBS-treated non-arthritis mouse No.7, (clinical score 0). (C) shows a representative image of DCX immuno-histochemistry in the dentate gyrus of the etanercept-treated non-arthritis mouse No.8, (clinical score 0). RA score = clinical score. All images at 10X magnification.

A summary of the number of DCX-positive neurons in the dentate gyrus of individual naïve control mice, PBS-treated-arthritis mice and etanercept-treated CII immunized mice, their clinical scores and paw diameters is presented in Table 6.4.

Mouse	Individual clinical scores	Individual paw diameter (mm)	Number of DCX-positive neurons
Set D mice			
Naïve control mouse No.4	0	1.8	7422
PBS-treated mouse No.4	1	1.8	4638
Etanercept-treated mouse No. 4	0	1.8	5556
Set E mice			
Control mouse No.2	0	1.8	13860
Untreated mouse No.2	11	2.9	2640
Etanercept-treated mouse No. 2	0	1.8	5034
Set F mice			
Control mouse No.3	0	1.8	7146
Untreated mouse No.5	0	1.8	1680
Etanercept-treated mouse No. 3	0	1.8	3438
Set G mice			
Control mouse No.1	0	1.8	9276
Untreated mouse No. 5	4	2.1	3414
Etanercept-treated mouse No. 4	2	1.9	7422
Set H mice			
Control mouse No.1	0	1.8	10998
Untreated mouse No.3	0	1.8	3108
Etanercept-treated mouse No.3.1	0	1.8	7056

Table 6.4 Individual arthritis score, individual swelling scores and number of DCX-positive neurons of CII immunized mice in etanercept-treated and PBS-treated groups on day 35 Each set of mice (Set D to H) consisted of one antigen-naïve control mouse, one PBS-treated CII immunized mouse and one etanercept-treated CII immunized mouse, which were sacrificed on day 35. DCX immuno-histochemistry and number of DCX-positive neurons in the dentate gyrus of mice in each set were compared. Individual arthritis scores, paw diameters (sum of all 4 paws of each mouse divided by 4) and numbers of DCX positive neurons in the dentate gyrus of mice were calculated and measured on the cull day.

6.5.4.2.1 Comparison of numbers of DCX-positive cells between etanercept-treated and PBS-treated groups on day 35

Overall, the cell count data demonstrated that DCX-positive neurons in the dentate gyrus of PBS-treated CII immunized mice were significantly decreased compared to those in of naïve control mice on day 35. One-way ANOVA followed by Bonferroni's post-hoc comparison tests demonstrated that there were significant differences in the number of DCX-positive neurons in the dentate gyrus among the three groups of mice on day 35 ($P = 0.0005$). The mean number of DCX-positive neurons in the dentate gyrus (PBS-treated CII immunized versus naïve control) was 516 ± 181 cells versus 1631 ± 456 cells ($P < 0.001$) (Figure 6.32). The number of DCX-positive neurons in the dentate gyrus of etanercept-treated CII immunized mice tended to be higher compared to those in the PBS-treated CII immunized mice. The mean number of DCX-positive neurons in the dentate gyrus (etanercept-treated CII immunized versus PBS-treated CII immunized) was 5700 ± 1614 cells versus 3096 ± 1086 cells (Figure 6.32). However, post hoc analysis with Bonferroni correction showed that the difference in mean number of DCX-positive neurons in the dentate gyrus between etanercept-treated CII immunized and PBS-treated CII immunized was not statistically significant. Interestingly, the number of DCX-positive neurons in the dentate gyrus of etanercept-treated CII immunized mice was significantly lower compared to those in the naïve control mice. The mean number of DCX-positive neurons in the dentate gyrus (etanercept treated CII immunized versus control) was 5700 ± 1614 cells versus 9786 ± 2736 cells ($P < 0.05$) (Figure 6.32). This data suggest that TNF-blockade therapy using etanercept showed no preventative effect on the impairment of hippocampal neurogenesis in the group of CII immunized mice on day 35.

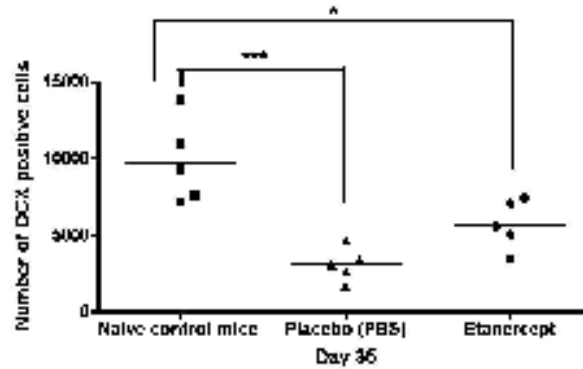


Figure 6.32 Number of DCX-positive cells in the dentate gyrus of PBS-treated and etanercept-treated CII immunized mice on day 35, compared with antigen-naïve control mice. The dots represent the number of DCX positive cells in the hippocampus of individual naïve control mice (filled squares; n=5), CII immunized mice treated with PBS as the placebo (filled triangles; n=5), and etanercept-treated mice (filled circles; n=5) on day 35. The number of DCX positive cells in the hippocampus of mice from all experimental groups was determined by counting of DCX-positive cells in every sixth serial brain section containing DCX immuno-histochemistry in the dentate gyrus. Bars represent the means values: Statistical analysis of data was performed using one-way ANOVA (*P<0.05, **P<0.01, ***P<0.001).

6.5.4.2.2 *Correlation between hippocampal neurogenesis and arthritis score of PBS-treated CII immunized mice on day 35*

We investigated whether there was an association between the numbers of DCX-positive neuron in the dentate gyrus of arthritic mice and their clinical score (RA score) on day 35. Using Pearson's correlation coefficient, we showed that the reduction in DCX-positive neurons did not correlated with the arthritis score ($r^2=0.868$; $P = 0.236$) (Figure 6.33). This data is consistent with our data in the previous section of this Chapter 6 (section 6.4) showing that there was no significant correlation between the number of DCX-positive neurons in the dentate gyrus of arthritic mice and their RA score on day 42. We recognise that the low numbers of mice used in these experiments is likely to be a major limiting factor to this interpretation and would recommend that this is repeated with a sufficient number.

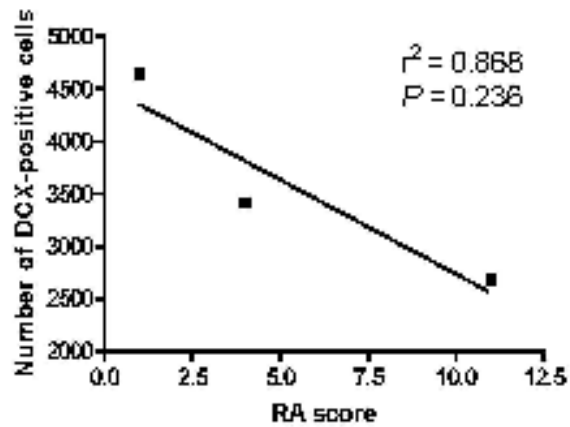


Figure 6.33 Correlation of the number of DCX-positive cells and RA score
Plot showing the relationship between the number of DCX-positive cells in the dentate gyrus of arthritic mice and their clinical score (RA score) on day 35 analysed by Pearson's correlation coefficient analysis.

6.5.5 Longitudinal changes of hippocampal neurogenesis in PBS-treated CII immunized mice.

We compared the number of DCX-positive cells in the dentate gyrus of untreated CII immunized mice and control mice at different time points in order to investigate the association between the development of inflammatory joint disease and changes in hippocampal neurogenesis. Significant reductions in the number of DCX-positive cells were observed in PBS-treated CII-immunized mice compared to those in the naïve control mice on day 32 and day 35. The mean numbers of DCX-positive cells in mice on day 32 (PBS-treated CII-immunized versus naïve control mice) were 2850 ± 1128 cells versus 8814 ± 462 cells ($P = 0.0011$), while the mean numbers of DCX-positive cells on day 35 (PBS-treated CII-immunized versus naïve control mice) was 3096 ± 1086 cells versus 9786 ± 2736 cells ($P = 0.0009$) (Figure 6.34). This suggests that the impairment in hippocampal neurogenesis occurred during the period of clinical manifestation of arthritis disease in CII immunized mice, but not during the period prior to the onset of disease.

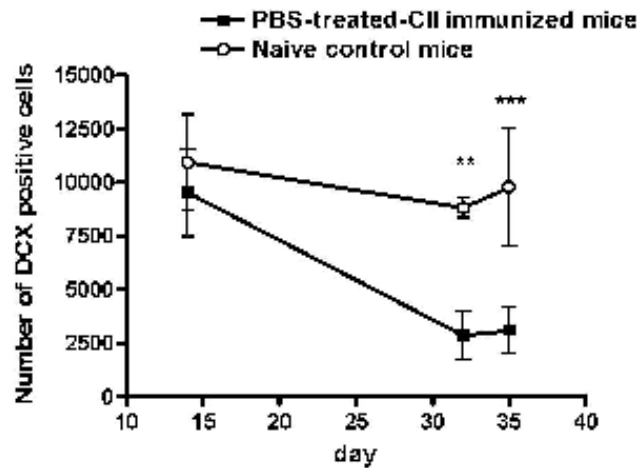


Figure 6.34 Time-course of the number of DCX-positive neurons in the dentate gyrus of CII immunized mice

Mice immunized with type II collagen (filled squares) were sacrificed on days 14 ($n = 3$ CII immunized mice), 32 ($n = 3$ CII immunized mice) and 35 ($n = 5$ CII immunized mice) and brains from CII immunized mice at all time points were harvested. Brain samples collected from untreated naïve mice (open circle) sacrificed on the days indicated were used as controls. Immuno-histochemistry of DCX was performed in brain tissue containing the hippocampus, and the number of DCX positive cells in the hippocampus of mice from all experimental groups was determined by counting DCX-positive cells in every sixth serial brain section containing DCX immuno-histochemistry in the dentate gyrus. Data represent means \pm S.E.M. ($n = 3-5$ mice/group). Statistical analysis of data was performed using two-way ANOVA compared with naïve control mice: (* $P < 0.05$; ** $P < 0.01$; *** $P < 0.001$).

We compared the number of DCX-positive cells in the dentate gyrus of CII immunized mice to investigate longitudinal changes in hippocampal neurogenesis within the group of CII immunized mice. One-way ANOVA followed by Bonferroni's post-hoc comparison tests demonstrated that there were significant differences in the number of DCX-positive neurons in the dentate gyrus among the three groups of mice culled on day 14, day 32 and day 35 ($P = 0.0004$) (Figure 6.35). A decrease in the number of DCX-positive cells in the dentate gyrus was observed in CII immunized mice on day 32 and day 35 compared to those on day 14. The mean number of DCX-positive cells in CII immunized mice (day 32 versus day 14) was 2874 ± 1128 cells versus 9528 ± 2040 cells ($P = 0.0078$), while the mean number of DCX-positive cells in CII immunized mice (day 35 versus day 14) was 3108 ± 1086 cells versus 9528 ± 2040 cells ($P = 0.001$) (Figure 6.35). There was a significant reduction in hippocampus neurogenesis on day 32 and day 35, which correspond to the development stage and the peak of arthritis in the CIA model respectively. There was no significant difference in the hippocampal neurogenesis between control mice and CII immunized mice on day 14, suggesting that the reduction of hippocampus neurogenesis occurred after

the onset of arthritis and that this may be associated with the development peripheral joint inflammation.

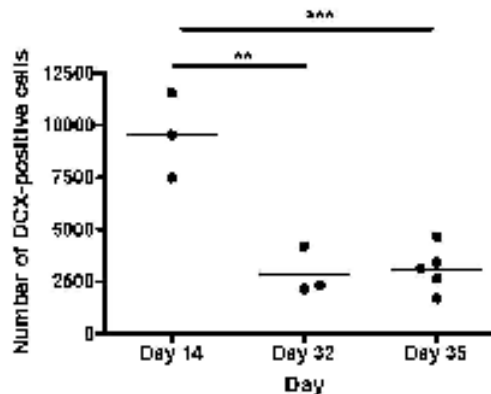


Figure 6.35 Longitudinal changes of DCX-positive neurons in dentate gyrus of CII immunized mice sacrificed on the day 14, 32 and 35
 Bars represent mean values: Statistical analysis of data was performed using one-way ANOVA (* $P < 0.05$, ** $P < 0.01$, *** $P < 0.001$).

6.5.6 Longitudinal changes of hippocampal neurogenesis in antigen-naïve control mice.

Time course experiments of doublecortin (DCX) expression in immature neurons of mouse adult dentate gyrus showed that hippocampal neurogenesis decreases with age (Kuhn et al., 1996). The dentate gyrus of mice sacrificed on day 28 after administration of bromodeoxyuridine (BrdU), a synthetic thymidine analogue which can be used as a marker of proliferation showed a significant reduction in BrdU positive neurons compared to those on day 14 (Couillard-Despres et al., 2005). In addition, a study by Brown et al., 2003 showed a transient expression of DCX-positive neurons during adult neurogenesis, and the number of DCX-positive neurons was also decreased over time (Brown et al., 2003).

The expression of DCX in neurons persists for up to 3 weeks (Brown et al., 2003), which could be a limitation of using DCX as the neuronal marker for testing changes in hippocampal neurogenesis and the effect of etanercept treatment on hippocampal neurogenesis in a chronic inflammatory disease like CIA model. We therefore compared the number of DCX-positive cells in the dentate gyrus of control mice to investigate the effect of age on hippocampal neurogenesis within the group of control mice.

We found no significant difference in the number of DCX-positive cells in the dentate gyrus of control mice at different time points ($P = 0.5361$ by one-way ANOVA analysis) (Figure 6.36). This suggests that there was no effect of age on number of DCX-positive cells in the dentate gyrus, and therefore hippocampal neurogenesis of naïve control mice. This also confirms that the reduction in numbers of DCX-positive neurons observed in the dentate gyrus of PBS-treated CII immunized mice may be due the effect of peripheral inflammation. Therefore we conclude that there is likely to be no effect of age affecting the result showing the impairment in hippocampal neurogenesis in CII immunized mice in the previous sections of this Chapter 6 (Section 6.4 and Section 6.5.4).

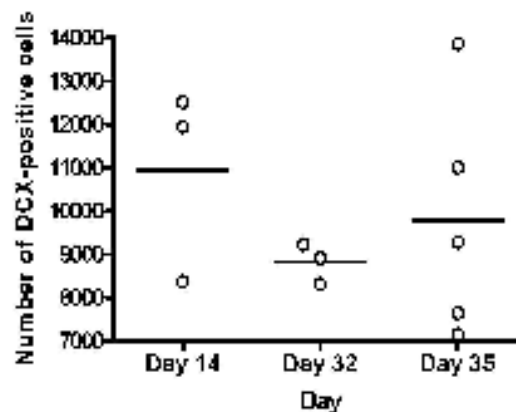


Figure 6.36 Longitudinal changes of DCX-positive neurons in dentate gyrus of control mice sacrificed on the day 14, 32 and 35
 Bars represent mean values: there were no significant differences.

6.6 Result chapter 6: Summary of major findings.

This aim of the chapter is to investigate changes in hippocampal neurogenesis in a murine chronic inflammatory disease model of rheumatoid arthritis, the collagen-induced arthritis (CIA) model. To investigate whether changes in hippocampal neurogenesis in collagen-II (CII) immunized mice is associated with peripheral inflammation, we tested the effects of anti-inflammatory treatment, using therapeutic TNF-blockade using recombinant human soluble TNF-receptor (etanercept) on changes of hippocampal neurogenesis in CII immunized mice. We found;

1. An impairment in hippocampal neurogenesis was observed in CII immunized mice. This was observed by a reduction in number of DCX-positive cells in the dentate gyrus compared with healthy age-matched antigen-naïve control mice.

2. This reduction in the number of DCX-positive cells in the dentate gyrus was observed in CII immunized mice irrespective of whether they developed arthritis. In addition, there was no significant difference in the reduced number of DCX-positive cells in the dentate gyrus between arthritis and non-arthritis mice.
3. There was no significant correlation between the number of DCX-positive cells in the dentate gyrus and clinical scores of the CII immunized mice.
4. There was no significant change in hippocampal neurogenesis as estimated by the number of DCX-positive cells in the dentate gyrus in CII immunized mice before the onset of arthritis (day 14) compared to those in antigen-naïve control mice.
5. In the first of two experiments, etanercept treatment did not delay the onset of arthritis nor reduce the incidence at day 32, but attenuated the severity of arthritis by reducing the mean paw thickness and the clinical score compared to PBS-treated CII immunized mice. At this time point the etanercept treatment protected against impairment of neurogenesis; there was no significant difference in the number of DCX-positive cells in the dentate gyrus between etanercept-treated CII immunized mice and antigen-naïve control mice.

In the second experiment, etanercept treatment did delay the onset of arthritis and reduced the incidence at day 35, as well as attenuating the severity of arthritis by reducing the mean paw thickness and the clinical score compared to PBS-treated CII immunized mice. At this time point the etanercept treatment did not protect against impairment of neurogenesis; there was a significant decrease in the number of DCX-positive cells in the dentate gyrus between etanercept-treated CII immunized mice and antigen-naïve control mice. However, a difference in the number of DCX-positive cells in the dentate gyrus between etanercept-treated CII immunized mice and PBS-treated CII-immunized mice was not statistically significant.

6. Etanercept treatment seemed to have a protective effect on the brain and on the joints that appeared to be different at days 32 and 35. It may be that the disease process changes between these two time points. This aspect will require further experiments.

8. There was no effect of age involved in the reduction of hippocampal neurogenesis in CII immunized mice.

6.7 Discussion

For clarity, I will set out the discussion in logical sections interpreting the results in sequence. I will summarise and draw conclusions from these at the end.

6.7.1 *The role of Doublecortin (DCX) in neuronal maturation in the adult hippocampus*

Doublecortin (DCX) is widely used as a marker in studies of hippocampal neurogenesis in both rodents and humans. Our data demonstrated the presence of DCX-positive cells with a neuronal-like morphology in the hippocampus of both antigen-naïve control and CII immunized mice. Triple-immunofluorescent staining demonstrated a lack of co-localization of DCX with NeuN, a neuronal marker of maturity, indicated an undifferentiated or immature phenotype, and this suggests that DCX-positive neurons are immature. These immature neurons developed during the process of hippocampus neurogenesis and have been demonstrated to play major roles in the induction of synaptic plasticity, leading to the encoding of new hippocampus-dependent memories. DCX is a microtubule-associated protein which is considered to be an important regulator of several steps in the process of neuronal maturation during neurogenesis.

Neurogenesis in the dentate gyrus involves neural progenitor proliferation, neural cell production/differentiation/maturation, and final integration into the neuronal circuit network in the hippocampus (Li and Pleasure, 2010). The duration of the development of hippocampal granule neurons is usually about one or two months. Neuronal precursor cells are generated from neural stem cells in the subgranular zone of the dentate gyrus and continue to proliferate for a few more days. These neuronal precursor cells are characterized by the expression of the intermediate filament proteins glial fibrillary acidic protein (GFAP) and nestin. At approximately two weeks after mitosis, progenitors develop into either neuroblast or non-neuronal cells. Neuroblasts continue to elongate neurites and axons, and migrate from the subgranular zone to the granular layer of the dentate gyrus. Migrating neurons no longer express nestin, but the expression of DCX is up-regulated (Perera et al., 2008). DCX functions to regulate neuronal migration during development. DCX expression has been associated with neurite and axon elongation, and the generation of synapses

(Rao and Shetty, 2004). DCX gene-deficient mice showed morphological abnormalities in migrating neurons, including neuronal branching defects and shorter length of neuronal processes (Kappeler et al., 2006). At this stage, immature neurons develop primary apical dendrites and GABAergic synapses expressed on apical dendrite become excitatory. GABAergic synapses initially depolarize immature neurons and then gradually convert to hyperpolarization over a period of 2-3 weeks (Perera et al., 2008). Excitatory dendritic GABAergic synaptic activation during hippocampal neurogenesis plays a major role in the neuronal maturation and the encoding of new memory. The level of excitatory GABA signal indicates of the dynamic neuronal network activity, while GABAergic activation encodes input specific information (Ming and Song, 2005). In addition, GABAergic activation is also thought to be the initial step of immature neurons to integrate into the hippocampal neuronal circuit and extend their axonal projections along mossy fiber pathways to the CA3 pyramidal cell layer (Lledo et al., 2006). This is considered to be the most critical period of hippocampal neurogenesis since these immature neurons are selected for activation by external stimuli including environmental enrichment and spatial learning. These excitable immature neurons up-regulate NMDA receptors with the NR2B subunit and the presence of T-type Ca²⁺ channels and thus develop stronger electrical property for long-term potentiation (LTP), which is essential for encoding memory. DCX has been demonstrated to play a role in regulating the electrical property in the hippocampal immature neurons (Perera et al., 2008). DCX deficient mice showed a reduction in GABA-mediated synaptic activity in hippocampus neurons (Kerjan et al., 2009). This also suggests that DCX deficiency may also affect hippocampal-dependent memory function. Nyffeler *et al* demonstrated that an increase in the numbers of doublecortin (DCX) positive neurons in both subgranular zone and granule cell layers (SGZ-GCL) was associated with improvement in the working memory performance in rats (Nyffeler et al., 2010). This evidence suggests that DCX could be an efficient neuronal marker to analyse the absolute number and dendritic growth of immature neuron in the dentate gurus in the adult brain which reflects neurogenesis, memory formation, and cognitive function of the hippocampus. This is supported by several publications suggesting that DCX is a reliable and specific marker that reflects levels of adult neurogenesis and its modulation, since DCX is transiently expressed during the migration of immature neurons

(Brown et al., 2003); (Rao and Shetty, 2004); (Couillard-Despres et al., 2005). Using DCX-immuno-staining also provides the absolute number, the distribution and the differences in dendritic features of these immature neurons, which can reflect the pattern and dynamics of dendrite development (Plumpe et al., 2006). Several studies report the expression patterns of DCX in numerous combinations with markers of proliferation such as BrdU incorporation in the hippocampal dentate gyrus (DG) of animals. The *in-vivo* BrdU injection is the most commonly used method to study cell proliferation and survival in neurogenesis studies. However, there are several limitations using this approach to detect changes in neurogenesis. Firstly, the administration of BrdU can be toxic to animals since BrdU can interfere with DNA replication. Secondly, BrdU can be incorporated during DNA repair, resulting in inconsistent or partial labelling of proliferating cells (Ming and Song, 2005). Thirdly, BrdU can be non-specific to all types of proliferative cells, including neural stem cells, glial precursors or glial cells (Couillard-Despres et al., 2005). Thus, it is necessary to use other specific marker for the neuronal lineage to identify granular neurons in the hippocampus. This could be another advantage of using DCX-immuno-histochemistry to study hippocampal neurogenesis in comparison of the *in-vivo* BrdU staining. This is because DCX specifically labels immature neurons in the dentate gyrus, which allows us to see the clear morphology of pyramidal neurons without co-staining with other markers.

6.7.2 *Reduction in hippocampal neurogenesis in CII immunized mice.*

An impairment in hippocampal neurogenesis has been implicated in mood and cognition disorders (Sahay and Hen, 2007); (Sahay et al., 2007). Several studies have demonstrated that antidepressants increase hippocampal neurogenesis in both animals and humans (Wang et al., 2008); (Malberg et al., 2000); (Boldrini et al., 2009); (Jacobs et al., 2000). In addition, impairment in hippocampal neurogenesis may underlie the cognitive deficits seen in depression. Several animal behavioural studies showed that reduction or ablation of hippocampal neurogenesis in rodents had detrimental effects on hippocampus-dependent forms of cognition such as fear conditioning, long-term spatial memory and working memory (Saxe et al., 2006); (Winocur et al., 2006); (Snyder et al., 2005). Accumulating evidence suggests that the patho-physiology of depression

might be associated with inflammation. Depression is common in chronic inflammatory diseases such as RA, multiple sclerosis (MS) and psoriasis. In addition, increases of pro-inflammatory cytokines including interleukin (IL)-1, IL-6, IL-8, IL-12, interferon (IFN)- γ and tumor necrosis factor (TNF)- α have been reported in patients with depression (Schiepers et al., 2005); (Raison et al., 2006). In animal models, peripheral inflammation induced by LPS has been shown to activate microglia to produce various brain inflammatory mediators, including IL-1 β and IL-10 (Henry et al., 2009). The activation of microglia in the LPS-induced inflammation model has been reported to induce a reduction in hippocampal neurogenesis, which is associated with a cognitive decline in learning and memory (Ekdahl et al., 2003); (Monje et al., 2003). Taken together, this evidence suggests that suppression of hippocampal neurogenesis by inflammation may underlie the depression in chronic inflammatory disease.

The data in this chapter demonstrated a significant reduction in a number of DCX-positive neurons in the dentate gyrus of collagen (CII)-immunized mice compared to those in antigen-naïve control mice on day 42. In addition, our longitudinal study showed that the reduction in hippocampal neurogenesis in these CII immunized mice occurred during the period of clinical manifestation of arthritis (day 32 and day 35), but not before the onset of disease on day 14. These findings suggest that the reduction in hippocampal neurogenesis may be associated with the peripheral inflammation associated with joint disease. The reduction in DCX positive cells in the dentate gyrus was described in several autoimmune disease models, including type II diabetic rats (Hwang et al., 2008) and autoimmune-prone cytokine B-cell-activating factor (Capuzzi et al.) transgenic mice (Crupi et al., 2010). However, our findings contrast with one previous study which demonstrated a transient increased in DCX positive cells in the dentate gyrus of antigen-induced arthritis (AIA) mice (Wolf et al., 2009b). In that study, an increase in hippocampal neurogenesis was observed during a particularly marked infiltration of inflammatory cells into the knee joint and the author suggested that this may be associated with the systemic activation of CD4-positive cells during the course of arthritis (Wolf et al., 2009b). There are several possible explanations that might underlie this contradictory data. Firstly, differences in the procedure for inducing arthritis and immuno-pathogenesis may account for contradictory results from the literature. Adjuvant induced arthritis

(AIA) is an arthritis model, induced by a single intradermal injection of complete Freund's adjuvant (CFA) consisting of heat-killed *Mycobacterium tuberculosis* (Mt) in an oil-in water emulsion (Hossain et al., 2001). Unlike CIA, AIA is a transient model of arthritis in which antigens activate acute inflammation, leading to joint destruction. Polyarthritis rapidly develops around 10 days after immunization using adjuvant and the whole course of the disease lasts for 21 days (Bendele, 2001). In addition, the AIA model is Th1-cell and neutrophil dependent, and complement-independent. There is no evidence demonstrating that B-cells play a role in the pathogenesis of AIA. By contrast, the immune response of CIA involves both CII-specific T-cells and B-cells, which produce antibodies to type II collagen. The difference in humoral immune response between the 2 arthritis models can be another explanation of the contradictory data. This is supported by evidence showing a reduction in DCX-positive cells in the dentate gyrus of transgenic mice over-expressing BAFF, which develop autoantibodies leading to an autoimmune syndrome of systemic lupus erythematosus, rheumatoid arthritis and Sjögren's syndrome (Crupi et al., 2010). However, the role of B cells in neurogenesis needs to be further investigated. In addition, the precise effect of T cells on hippocampal neurogenesis is still controversial. A study by Wolf et al., suggested that T cells enhance hippocampal neurogenesis in AIA model (Wolf et al., 2009b), which is supported by a study in transgenic mice lacking T cells (Ziv et al., 2006). However, it has also been reported that T cells could support and inhibit hippocampal neurogenesis (Wang et al., 2010). Secondly, the differences in the immuno-pathological mechanism of both arthritic models may cause different peripheral inflammatory mediator profiles. TNF, IFN- γ , IL-1, IL-6 and IL-17A are dominant in the circulation of AIA model, while several pro- and anti-inflammatory cytokines, including TNF- α and IL-1 β , IL-6, IL-12, IL-1Ra, IL-10 and TGF- β , are highly expressed in the periphery of mice with CIA (Hegen et al., 2008). Different inflammatory mediator profiles may cause different effects on hippocampal neurogenesis, therefore the effect of peripheral inflammation inducing changes in hippocampal neurogenesis may be contradictory in different arthritis models.

Inflammation and inflammatory cytokines can affect hippocampal neurogenesis directly (Vallieres et al., 2002); (Monje et al., 2003); (Ekdahl et al., 2003). Our data in Chapter 1 and 2 showed increased in various inflammatory mediators

including TNF- α , IL-1 α , IL-1 β , IFN- γ , IL-2, IL-4, IL-5, IL-10, IL-13, CXCL1, CXCL10, VEGF and FGF2 in brains of CII immunized mice. It is possible that the reduction of neurogenesis observed in the CIA mice may be the result of the up-regulation of brain inflammatory mediators during the course of arthritis. Some of the inflammatory mediators, including IL-1 α and IL-1 β , that are increased in the brains of CII immunized mice in our study have been reported to have different regulatory effects on hippocampal neurogenesis. TNF- α (Seguin et al., 2009), IL-1 β (Kaneko et al., 2006) and IL-2 (Beck et al., 2005) have been demonstrated to be inhibitors of neurogenesis. CXCL10 not only exaggerates the brain inflammation by recruiting activated T cells into the brain, but also functions as a neuromodulator for immature neurons in the hippocampus (Muzio et al., 2010). CXCL10 has been shown to suppress hippocampal neurogenesis by inhibiting long-term potentiation (LTP) in immature hippocampal neurons, probably via changing expression levels of synaptic proteins involved in synaptic transmission such as GABA receptor and NMDA receptor (Vlkolinsky et al., 2004); (Cho et al., 2009). In contrast, IL-1 α (Greco and Rameshwar, 2007), IL-4, IFN- γ (Butovsky et al., 2006), VEGF (Wang et al., 2007) and FGF2 (Jin et al., 2005) have been reported to support hippocampal neurogenesis. Therefore, the reduction in hippocampal neurogenesis observed in our CIA model may be due to the complex interplay between activated immune cells and inflammatory mediators. For example, an increase in hippocampal neurogenesis was observed in IL-2 deficient mice, along with up-regulation of brain IL-15, IL-12, CXCL10 and CCL2 (Beck et al., 2005). This finding suggests that IL-2 may either suppress hippocampal neurogenesis directly or via the production of other cytokines such as IL-15, IL-12, CXCL10 and CCL2. Likewise, the detrimental effect of IL-1 β on hippocampal neurogenesis may be regulated by IFN- α (Kaneko et al., 2006). However, it is not clear to what extent each individual cytokine contributes to the overall reduced hippocampal neurogenesis in CII immunized mice. Different concentrations of the same cytokines in the brain may also result in different effects on hippocampal neurogenesis. IFN- γ has been associated with pathology of CNS inflammation. IFN- γ (1000 ng/ml) activates the production of CXCL10 in microglia which could be detrimental to hippocampal neurogenesis (Ellis et al., 2010). In contrast, activation of microglia by low concentrations of IFN- γ (20 ng/ml) has been shown to support neurogenesis (Butovsky et al., 2006). Therefore, it will be necessary to conduct an *in vitro* study of hippocampal

neuronal progenitor cell culture and test the effects of different concentrations of cytokines on the differentiation and maturation of these cells.

The mechanism, function and significance of the modulation of neurogenesis during inflammatory processes remain to be elucidated. It has been hypothesized that the same CNS immune response that blocks neurogenesis in the adult CNS under neurodegenerative conditions can also paradoxically support neurogenesis. This is supported by a study showing that neurogenesis is inhibited by LPS-activated microglia, but induced by the same microglia activated by IL-4 or low concentration of IFN- γ (Butovsky et al., 2006). This could be a protective mechanism of the CNS against excessive inflammation in the brain, which may eventually cause irreversible neuronal loss or damage. In addition, peripheral and central cytokine signals have been shown to have different influences on hippocampal neurogenesis. A study has shown that peripheral administration of TNF- α resulted in suppression of neurogenesis, while intra-hippocampal injection of IL-1 β and IL-6 caused increased neurogenesis (Seguin et al., 2009). This data suggest that cytokines produced locally in the brain under the condition of neuro-inflammation may play a protective role against excessive brain inflammation. Therefore, it is important to know the cellular source of inflammatory mediators up-regulated in brains of CII immunized mice in our study since cytokines from different sources (either peripheral circulation or CNS) may regulate neurogenesis differently.

6.7.3 Effect of etanercept on impairment of hippocampal neurogenesis in CII immunized mice

TNF- α has been implicated in the development of depressive disorders. A significant increase in serum TNF- α has been reported in depression patients. Etanercept is an anti-TNF agent that has been associated with the improvement of mood and anxiety disorders in patients with chronic inflammatory diseases such as psoriasis and RA (Uguz et al., 2009); (Tyring et al., 2006). In addition, one well known study by Tobinick *et al* demonstrated an immediate effect improving cognition in Alzheimer's disease (Tobinick and Gross, 2008). The mechanism that underlies the effects of etanercept on neurobiological functions that contribute to the improvement in psychiatric and cognitive problems in patients with chronic inflammatory diseases remains unclear. A recent study by

Terrando et al., showed that TNF-blockade can improve a hippocampal-dependent form of cognitive decline induced by surgery-induced Inflammation (Terrando et al., 2010). In that study, etanercept also reduced IL-1 β protein levels in both brain and periphery (Terrando et al., 2010). This suggests that etanercept can improve cognitive decline by inhibiting IL-1 β , which may be associated with the improvement of hippocampal function. However, that study did not address the issue of the effects of etanercept on hippocampal neurogenesis, which may be associated with the improvement of the cognitive function of the hippocampus. To date, there are no animal studies that report the molecular mechanism of etanercept on hippocampal neurogenesis. We first demonstrated that peripheral etanercept treatment reversed impairment of neurogenesis in CII immunized mice. Our findings may help explain the mechanism by which etanercept improves cognitive decline observed in both human and animal studies.

The combination of our data in Chapter 3 (Section 3.2.3 and Section 3.2.4), Chapter 4 (Section 4.2.3, Section 4.2.4 and Section 4.2.5) and this chapter suggests that the reduction in neurogenesis in CII immunized mice may be associated with increases in brain inflammatory mediators. Our data also showed that etanercept-treated CII immunized mice had more DCX-positive cells in their hippocampus compared to untreated CII immunized mice during the peak of the disease, whereas the severity of arthritic disease of these etanercept-treated CII immunized mice was lower compared to control PBS-treated CII immunized mice. This suggests that the neuro-protective effect of etanercept on hippocampal neurogenesis during disease development of inflammatory arthritis could be due to its anti-inflammatory effect on peripheral inflammation. We could not address the mechanism of how peripheral etanercept treatment could prevent the reduction of hippocampal neurogenesis in CII immunized mice during the period of clinical manifestation of arthritis. Etanercept may directly inhibit the peripheral inflammatory signal of TNF- α , which has been shown to be detrimental to neurogenesis (Seguin et al., 2009). This is also supported by a study by Jiang *et al* showing that the effect of peripheral treatment of etanercept on sickness behaviour induced centrally by IL-1 β did not require transportation of the etanercept molecules across the blood-brain barrier into the brain. Instead, the peripheral etanercept treatment reversed sickness

behaviour in mice by suppressing the expression of IL-1 β in the peripheral organs (Jiang et al., 2008). Another possibility is that peripheral etanercept treatment may prevent the reduction of hippocampal neurogenesis via the suppression of brain cytokine production. This possibility is supported by our data in Chapter 5 (Section 5.2.3 and Section 5.2.4) showing that peripheral treatment of etanercept reduced brain inflammatory mediators, including TNF- α , IL-1 β , IL-12 and IL-5 in brains of CII immunized mice. As discussed previously, some of these inflammatory mediators including TNF- α , IL-1 β and IL-12 have been reported to have detrimental effects on hippocampus neurogenesis. Some of our data in that section is consistent with a recent report showing that peripheral treatment using etanercept reduced IL-1 β protein levels in brains of the mouse model of surgery-induced brain inflammation (Terrando et al., 2010). A study by the same group also showed that IL-1 β is a potent regulator of the hippocampus-dependent form of cognition. Taken together, data from recent reports suggest that IL-1 β may be the target for the action of etanercept to improve the function of the hippocampus.

Interestingly, our data also demonstrated that the suppression of brain inflammatory mediators by etanercept may not be the only mechanism by which etanercept treatment protects against the reduction of hippocampal neurogenesis. In this chapter, we had 2 etanercept-treated CII immunized mice and PBS-treated CII immunized mice sacrificed on day 32 and day 35. On day 32, etanercept treatment attenuated severity of arthritis and prevented impairment of hippocampal neurogenesis in CII immunized mice. In contrast, etanercept treatment inhibited the progression of arthritis in etanercept-treated CII immunized mice, but the effect to prevent the impairment of hippocampus neurogenesis seemed to be weaker compared to those etanercept-treated CII immunized mice on day 35. Etanercept treatment only attenuated, but did not prevent the reduction of hippocampal neurogenesis in etanercept-treated CII immunized mice on day 35. These data suggest that the effect of etanercept treatment on impairment of hippocampal neurogenesis may not be associated with the therapeutic effect of etanercept on peripheral joint inflammation of arthritis. Considering the brain inflammatory mediator profiles of etanercept-treated CII immunized mice on day 35 and day 32 (Chapter 5; Section 5.2.3 and Section 5.2.4), we found that etanercept treatment reduced TNF- α , IL-5 and IL-

12, which have detrimental effects on hippocampal neurogenesis in etanercept-treated CII immunized mice on day 32. We could not measure changes in brain inflammatory mediators and hippocampal neurogenesis in the same brain since brain samples for both analyses were processed differently. However, data of both brain inflammatory mediator profiles and hippocampal neurogenesis in etanercept-treated CII immunized mice on the same time point (day 32 and day 35 after immunization) seemed to correspond and support each other. It is possible that the prevention of the reduction of hippocampal neurogenesis by etanercept may be due to the reduction of these brain inflammatory mediators. Surprisingly, brains of etanercept-treated CII immunized mice on day 35 not only showed a reduction of IL-1 β , CXCL1 and IL-12, but also showed increases in IL-2, VEGF and FGF2. VEGF and FGF2 have been reported to support hippocampal neurogenesis. These inflammatory mediators may enhance the action of etanercept, leading the greater effects of etanercept to prevent impairment of hippocampal neurogenesis. However, we found that etanercept did not prevent hippocampal neurogenesis in etanercept-treated CII immunized mice on day 35. These data suggest that changes in hippocampal neurogenesis may not only depend on direct effects of cytokines in the brain. There may be several explanations for this observation. Firstly, we do not know the actual function of these inflammatory mediators in the brain. Although VEGF and FGF2 have been shown to play neuroprotective roles, they could also have detrimental immunological effects on neurogenesis. For example, VEGF has been reported to be a neuronal growth factor supporting growth of neurons (Rosenstein et al., 2003). However, it is also an angiogenic factor and has been implicated in BBB breakdown (Sasaki et al., 2010) that is associated with more recruitment of immune cells into the brain, which could suppress hippocampal neurogenesis. Secondly, the effect of etanercept on hippocampal neurogenesis may be transient. This hypothesis is supported by a study in Alzheimer's disease showing that etanercept can improve mood within minutes (Tobinick and Gross, 2008). This could be the reason why the effect of etanercept on impairment of hippocampal neurogenesis was observed at the earlier time point (day 32) but not the later (day 35). However, this hypothesis needs to be further investigated by determining changes of hippocampal neurogenesis in etanercept-treated CII immunized mice in more time points across the CIA experimental period. Thirdly, etanercept may indirectly affect hippocampal neurogenesis via other

systems that regulate systemic inflammation such as HPA axis. The hypothalamo-pituitary-adrenal (HPA) system is a combined regulatory system between the endocrine system and the immune system (Heiser et al., 2008). Peripheral inflammatory signals activate the HPA axis by stimulating the anterior pituitary gland to release adrenocorticotrophic hormone (ACTH) into the circulation. Adrenocorticotrophic hormone (ACTH) in turn activates the production of glucocorticoid-producing cortex cells in adrenal glands to release corticosteroid hormones including cortisol (in humans) (Lanfumey et al., 2008). These corticosteroids function as anti-inflammatory hormones and their levels are normally upregulated during inflammation and infection (Hadid et al., 1999). Chronic administration of corticosteroid hormones was shown to inhibit hippocampal neurogenesis and reduce hippocampal volume, along with increased anxiety (light dark box test) and depression (forced swim test)-like behaviour, suggesting that corticosterone not only induces depression via the serotonergic system, but also via neurogenesis (Murray et al., 2008). A recent study showed that after TNF-blockade, a rapid increase in corticosteroid hormones in RA patients during the first 12 week period of treatment, following by the reduction of corticosteroid hormones in the later period as the result of HPA adaptation (Straub et al., 2003). Based on this evidence, we hypothesized that etanercept may effect the level of peripheral corticosteroid hormones, which eventually effect changes in hippocampal neurogenesis. To test this hypothesis we could measure the level of corticosteroid hormones during the treatment of etanercept that may provide additional information underlying the protective effect of etanercept against impairment of hippocampal neurogenesis.

6.7.4 Severity of arthritis was not associated changes in hippocampal neurogenesis in arthritic mice, and the reduction in hippocampal neurogenesis in non-arthritic mice

Our data also showed that there was no significant correlation between clinical score and the number of DXC-positive cells in both untreated arthritic CII immunized mice and etanercept-treated arthritic CII immunized mice. Our data suggest that the reduction in hippocampal neurogenesis in arthritic mice and the preventive effect of etanercept against impairment in hippocampal neurogenesis

were not associated with severity of arthritis. This observation also contrasts with a previous study using AIA mice showing a significant correlation between degree of joint swelling and cell proliferation indicated by the number of BrdU-positive cells (Wolf et al., 2009b). However, there was no significant correlation between the number of DCX-positive cells and joint swelling reported in that study, suggesting that the increase in proliferative brain immune cells such as microglia and astrocytes may reflect the increase inflammatory cells in the joint that may distribute to the brain. Our data also showed significant reduction in neurogenesis in immunized mice that did not develop arthritis (non-arthritic mice). In addition, the etanercept treatment also showed similar effects preventing the reduction in hippocampal neurogenesis in these non-arthritic mice as well as arthritic mice. This finding suggests that the impairment in hippocampal neurogenesis may be independent to inflammatory joint disease. There may be ongoing immune activation in the peripheral of non-arthritic mice that could signal the suppression of neurogenesis, but could not initiate joint inflammation due to difference in immune-tolerance mechanisms in individual mice. This premise is supported by our data in Chapter 3 (Section 3.2.3 and Section 3.2.4) and Chapter 4 (Section 4.2.3, Section 4.2.4 and Section 4.2.5) showing that there was no significant difference in brain inflammatory mediator concentrations between arthritic and non-arthritic mice. There are several explanation underlying these observations. One possible explanation is that the CFA given to the non-arthritic mice during the immunization may itself cause a reduction in hippocampal neurogenesis without development of arthritis. Peripheral administration of CFA alone has been reported to activate brain immune response (Raghavendra et al., 2004), suggesting that the inhibition of hippocampal neurogenesis in non-arthritic mice may be the result of CFA itself that can induce brain inflammation. Our data also suggests that brain inflammation can cause a reduction in neurogenesis even at the subclinical level. So the presence of inflammatory phenotypes in terms of illness [manifestation of frank arthritis or not (sub-clinical) in CIA model] is not necessary directly connected with the depression (Tyring et al., 2006), where there is a separation of the effect of anti-inflammatory drug (TNF-blockade) between the arthritis and the depression. So inflammatory mediators can impact on neurogenesis negatively even though the illness is not manifested. In addition, peripheral administration of CFA has also been reported to reduce hippocampal

neurogenesis via suppressing the gene expression of brain-derived growth factor (BDNF) in the hippocampus (Duric and McCarson, 2006). BDNF is a nerve growth factor that is constitutively expressed across subregions of the hippocampus and the adult forebrain (Lu et al., 2008) that has been implicated in the regulation of hippocampal neurogenesis. Interestingly, ablation of BDNF in the hippocampus resulted in a reduction in hippocampus neurogenesis, along with increased behaviour associated with depression, suggesting a role for BDNF-induced neurogenesis in the psychological aspect of depression (Taliaz et al., 2010). The production of BDNF in the brain could be suppressed by cytokines such as IL- β or LPS (Guan and Fang, 2006). This evidence suggests another indirect pathway of peripheral inflammation to modulate hippocampal neurogenesis via the production of brain neurotrophic factors. Therefore, it would be of interest to determine the concentrations of BDNF in the hippocampus in brains of CII immunized mice, which may be associated with brain cytokine concentrations and number of DCX-positive cells in dentate gyrus.

Summary

We demonstrated a reduction in hippocampal neurogenesis in CII immunized mice that may be induced by peripheral inflammation, which may/ may not be directly associated with peripheral joint inflammation. In addition, we also showed that peripheral treatment with etanercept prevented / attenuated the impairment of hippocampal neurogenesis in CII immunized mice. This could be important evidence suggesting that the reduction in hippocampal neurogenesis may be caused by peripheral inflammation in this chronic inflammatory disease model of arthritis. However, it would be of interest to conduct behavioural tests of hippocampal-dependent forms of cognition for the functional analysis of changes in hippocampal neurogenesis in both treated and etanercept-treated CII immunized mice. Our findings could also help explain the cognitive decline and depression associated with chronic inflammatory diseases like RA. In addition our findings could help explain the underlying mechanism of etanercept in transient improvement of mood in patients with chronic inflammatory diseases.

Chapter 7

General discussion and conclusion

7 General discussion and conclusion

Several lines of evidence have demonstrated that peripheral inflammation could induce neuro-inflammation, indicated by up-regulation of inflammatory mediator profiles. The model of systemic challenge with LPS showed increases in expression of several cytokines, including IL-1 β , IL-6 and TNF- α in various regions of the brain (Henry et al., 2009); (Datta and Opp, 2008). These pro-inflammatory cytokines have been reported to be up-regulated in the spinal cord and brains of animal models of chronic inflammatory disease such as adjuvant-induced arthritis (Bao et al., 2001); (del Rey et al., 2008). IL-1 β was increased in the hippocampus in a model of surgery-induced peripheral inflammation (Terrando et al., 2010a). Other inflammatory mediators such as CCL2 were shown to be up-regulated in the brain of mice with liver injury (D'Mello et al., 2009). Importantly, this neuro-inflammation induced by peripheral inflammation may also contribute to changes in neurobiology, resulting in psychological disorder such as depression and cognitive dysfunction. A high rate of depression is commonly found in patients with RA (Isik et al., 2007), psoriasis (Biljan et al., 2009) and MS (Lo Fermo et al., 2010), which is presumably associated with chronic inflammation. A reduction in serotonin transporter (SERT) density and an improvement in physical and mental function were observed in RA patients after receiving anti-TNF- α treatment (Cavanagh et al., 2010). Animal studies also showed that up-regulation of cytokines induced by peripheral inflammation caused a decline in hippocampal neurogenesis, resulting in cognitive decline and changes in emotional behaviour (Crupi et al., 2010); (Ek Dahl et al., 2003), (Kaneko et al., 2006); (Terrando et al., 2010b); (Ziv et al., 2006). Interestingly, peripheral administration of anti-inflammatory drugs and the blockade of cytokines can inhibit production of some of the brain inflammatory mediators such as IL-1 β that is generated during peripheral inflammation (Terrando et al., 2010). Clinical and animal studies also showed that anti-inflammatory therapy and TNF-blockade can result in a reduction in hippocampal neurogenesis and improve cognitive impairment and depression symptoms in patients with chronic inflammatory diseases (Monje et al., 2003); (Tyring et al., 2006); (Tobinick and Gross, 2008); (Tobinick and Gross, 2008b). These data provide important evidence showing that the impairment of hippocampal neurogenesis and

cognition may be associated with and regulated by increases in brain inflammatory mediators during peripheral inflammation.

Based on this evidence we hypothesized that the peripheral immune/inflammatory response during arthritis can affect the brain inflammatory mediator profiles and hippocampal neurogenesis which might help explain the psychological illness associated with RA. To explore this possibility, firstly, we determined changes in brain inflammatory mediators and the interplay between production of cytokines, chemokines and growth factors during experimental arthritis induced by type II collagen (CIA mice), a model of arthritis. Secondly, we investigate changes in hippocampal neurogenesis in this arthritis model. Finally, to confirm that all changes in brain inflammatory mediators and hippocampal neurogenesis are associated with inflammation, the effect of Etanercept, a recombinant humanised soluble TNF-receptor, on peripheral inflammation-induced neuro-inflammation and impairment in hippocampal neurogenesis in this CIA model was also investigated.

The major findings from this thesis are summarised in Figure 7.1

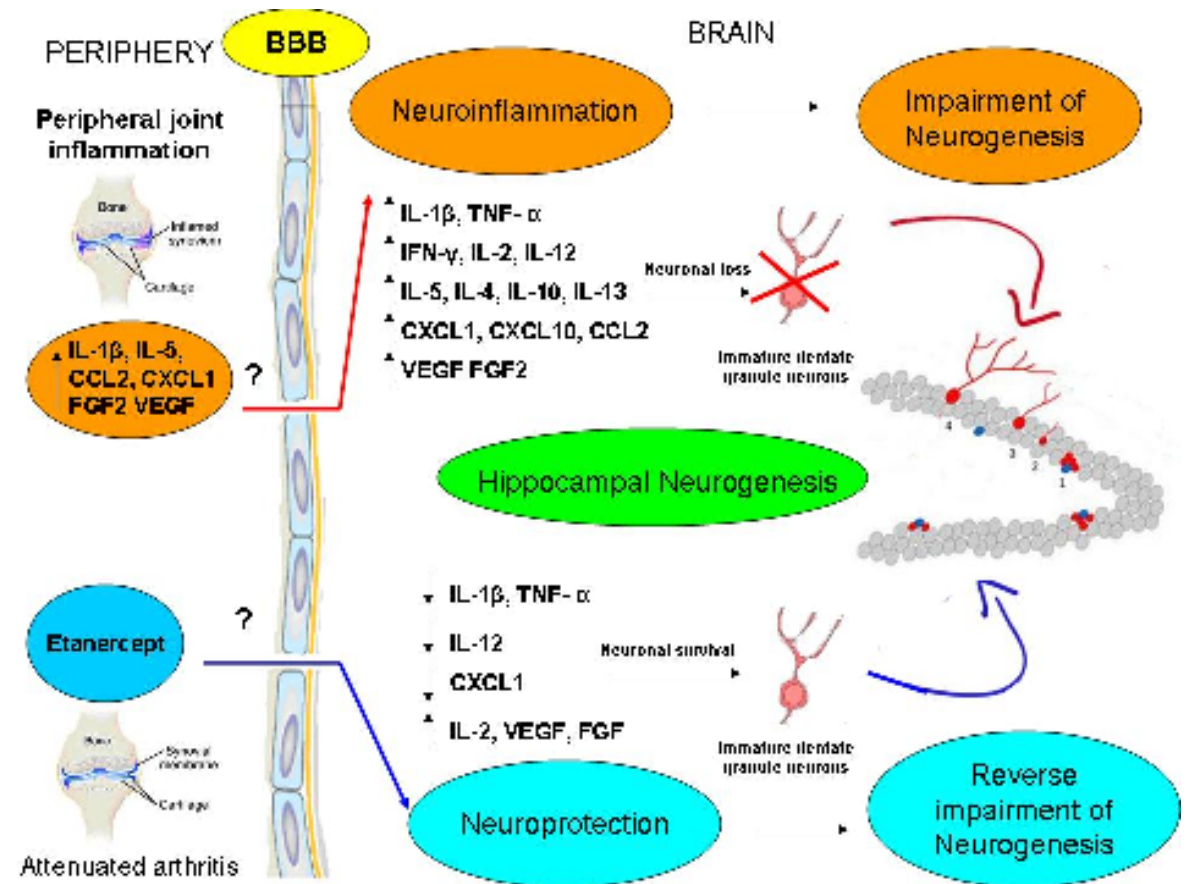


Figure 7.1 Summary of the major findings from this thesis entitled; ‘Peripheral autoimmunity induces central neuro-inflammation and hippocampal neurogenesis impairment in a murine model of collagen induced Rheumatoid Arthritis’.

Peripheral joint inflammation was induced by type II collagen in a mouse model of Rheumatoid Arthritis (CIA mice). Several inflammatory mediators were detected in the periphery (serum) during the course of arthritis and they may be transported through the blood brain barrier (BBB) into the brain by unknown mechanisms and induced neuro-inflammation. Up-regulation of both gene and protein expression of inflammatory mediators observed in the brain of these collagen II immunized mice may be associated with impairment in hippocampal neurogenesis. Peripheral TNF blockade treatment with Etanercept attenuated the arthritis in arthritic mice, along with a reduction of several inflammatory cytokines (including IL-1 β , TNF- α , IL-12), chemokine (including CXCL1), and an increase of some inflammatory and remodelling mediators (including IL-2, FGF2, VEGF) in the brain of arthritic mice. Etanercept treatment was also associated with a reversal of the disease-associated reduction in hippocampal neurogenesis. The anti-inflammatory effect of Etanercept on neuro-inflammation may contribute to neuroprotection against impairment of hippocampal neurogenesis.

We demonstrated that changes in inflammatory mediator profiles in brains of CII immunized mice may be associated with peripheral inflammation. Our time course data showed that there was no significant difference in levels of brain inflammatory mediators in CII immunized mice compared to those in the control mice on day 14, which is the time point typically just before the onset of arthritis which usually starts on day 19. However, changes in various inflammatory mediator profiles were observed after the onset of arthritis; on day 22, and towards the end of the course of arthritis disease at day 42. In addition, our time-course experiment showed longitudinal changes in various

inflammatory mediator gene/protein concentrations including IL-1 β , TNF- α , IL-4, IL-2, CXCL1, CXCL10, VEGF and FGF2 in brains of CII immunized mice during the whole period of onset and clinical manifestation of arthritis disease. In addition, prolonged increases in protein concentrations of IL-12 and IL-4 were observed in brains of CII immunized mice during the onset and disease development periods of experimental arthritis. These data suggest that there may be immune activation and inflammation occurring in the brain of CII immunized mice during the developmental process of peripheral joint inflammatory disease. A previous study by del Rey *et al* is consistent with our findings by showing longitudinal changes in brain cytokines such as IL-1 β , IL-6 and TNF- α and the up-regulation of some cytokines such as IL-6 during the ongoing stage and the peak of the arthritic disease in an adjuvant induced arthritis model (AIA) (del Rey *et al.*, 2008). Importantly, our data also showed that the anti-inflammatory effect of Etanercept could also suppress the up-regulations of some inflammatory mediators, including TNF- α , IL-1 β , IL-12 and CXCL1 in the brain of CII immunized mice. These inflammatory mediators play important roles in initiating the immune response and the development of joint inflammation in RA. Similar findings were reported recently by Terrando *et al.*, showing that anti-TNF- α could suppress up-regulation of brain IL-1 β during peripheral inflammation induced by surgery in a model of surgical trauma (Terrando *et al.*, 2010a).

Up-regulation of inflammatory mediators in the brain of CII immunized mice may reflect immune activation and neuro-inflammatory processes. Increases in the levels of pro-inflammatory cytokines TNF- α and IL-1 β may indicate microglial activation and innate immune responses in the brain of CII immunized mice. Up-regulation of Th1 cytokines (IL-12, IL-2, IFN- γ) and Th2 cytokines may suggest the potential for adaptive immunity in the brain of CII immunized mice. Increases in chemokines, including CXCL1, CCL2 and CXCL10, and angiogenic factors such as FGF and VEGF may implicate trafficking of immune cells and blood brain barrier leakage in the brain of CII immunized mice. One of the most striking findings in this study is the up-regulation of CXCL10 in CII immunized mouse brains during the ongoing stage and peak of arthritis. Interestingly, mRNA levels of brain CXCL10 were higher in arthritic mice compared to those in similarly CII immunized mice but with no arthritis. The CXCL10 is thought to play an important role in neuro-inflammatory diseases because, during CNS neuro-

inflammation, expression of CXCL10 is elevated several fold (Bajova et al., 2008). In the CNS, CXCL10 regulates trafficking of Th1 cells into the CNS, which is thought to be the initiation of the development of inflammatory demyelination in MS and EAE (Klein, 2004). The lesions of CNS inflammatory demyelination have also been reported in brains of RA patients (Tsai et al., 2008); (Tajima et al., 2004). It is possible that peripheral Th1 cells are recruited into the CNS by CXCL10 chemotactic signals which can then induce the development of inflammatory demyelination in the brain during the course of arthritis in these RA patients. This rationale is feasible because of several similarities in pathological mechanisms of MS and RA. Particularly, CD4⁺T cells are thought to have a crucial role in both MS and RA pathogenesis (Zozulya and Wiendl, 2008); (McInnes and Schett, 2007). Therefore, the elevation of CXCL10 in arthritic mouse brains may be the most important indicator of the presence of neuro-inflammation in the brain of arthritic mice, and this may be strongly associated with peripheral joint inflammation.

Our longitudinal data of inflammatory mediators in the brain of CII immunized mice demonstrated some interesting observations about brain-immune system-joint communication. The concentrations of brain inflammatory mediators such as TNF- α and IL-13 increased in parallel with arthritis development, while prolonged expressions of some brain inflammatory mediators such as IL-6, IL-10, IL-13, IL-12 and CXCL2 were observed over the course of arthritis. These data seem to suggest that inflammatory mediators can access the brain from the periphery during the development of “peripheral” chronic joint inflammatory diseases. However, our data of serum inflammatory mediators showed that the concentrations of several inflammatory mediators such as IL-5, IL-1 β , CCL2 and FGF were elevated in serum immediately after the onset of arthritis and the concentrations then decreased in parallel with disease development. These data suggest a disruption in communication between the peripheral immune system and CNS during the course of arthritis. We cannot define a precise mechanism of how the inflamed joint signalled to the brain in order to produce inflammatory mediators. A similar finding was reported by del Rey *et al* in CIA rats. In that study, there were no significant serum cytokines detected, but the brains of these CIA rats showed elevations of IL-1 β and IL-6 during the course of arthritis (del Rey et al., 2008). Two main questions remain: first, how can these

inflammatory mediators access the brain, and second, what are the cellular sources in the brain that produce these inflammatory mediators? Several studies suggest various mechanisms of how peripheral inflammation signals the CNS to produce inflammatory mediators. One putative mechanism is that the trafficking of the peripheral immune cells into the brain occurs during the blood brain barrier breakdown that is induced by the peripheral inflammation (Carson et al., 2006). Our data showed that various inflammatory mediators were up-regulated in the brain of CII immunized mice, including IL-1 β , TNF- α , IL-4, IL-10, IL-12 and CXCL1, on day 22, whereas VEGF and FGF, which are angiogenic factors that could be indicators of blood brain barrier damage, are elevated in the brain later on day 28. These data suggest that the brains of these CII immunized mice may be signalled to produce inflammatory mediators before the integrity of the blood brain barrier is compromised. Several pieces of experimental evidence supported this observation by showing that blood brain barrier breakdown during neuro-inflammation is not a simple case of increase recruitment of peripheral immune cells into the brain (Carson et al., 2006); (D'Mello et al., 2009); (Shaftel et al., 2007) . Brains of transgenic mice over-expressing IL-1 β showed blood-brain barrier leakage, along with elevations of CXCL1 and CCL2, and dramatic infiltration of CD45⁺ leukocytes. However, transgene induction of IL-1 β in brains of mice lacking CXCR2, a chemokine receptor that regulates neutrophil recruitment, showed disruption in neutrophil infiltration into the brain but failed to reduce leakage of the blood- brain barrier (Shaftel et al., 2007). The data of this study suggest that blood brain barrier breakdown is not associated with increased rate of leukocyte accumulation in the brain.

We also found prolonged expression of Th2 cytokines including IL-4 and IL-10 in the brains of CII -immunized mice throughout the onset of disease (day 22), the ongoing stage of the disease (day 28) and during the peak of the disease (day 35). However, in the periphery, during the onset of disease (day 19 to day 22) and on to the peak of the disease (day 35), the course of the arthritis in the CIA model is thought to be regulated predominantly by Th1 cells, whereas the Th2 response is dominant during the remission phase (day 35 - day 42). This finding suggests there may be local production of IL-4 and IL-10 by CNS immune cells such as astrocytes and microglia. Several studies reported that inflamed peripheral organs can signal brain microglia and astrocytes to produce

inflammatory mediators in the brain by an unknown mechanism (D'Mello et al., 2009); (Riazi et al., 2008). A study using a model of liver inflammation showed that microglia were activated to produce CCL2 before monocytes could migrate into the brain. This study also demonstrated that the inflamed liver signalled to the brain microglia to produce CCL2 and as a consequence cause monocyte trafficking to the brain via systemic TNFR signalling (D'Mello et al., 2009). We also showed similar observation in our study; systemic administration of Etanercept, which effectively induced TNF blockade, demonstrated reductions in various inflammatory mediators, including TNF- α , IL-1 β , IL-12 and CXCL1 in the brain of CII immunized mice.

Taken together, our data combined with findings from previous reports suggest that peripheral joint inflammation may provide a signal to the brain to produce inflammatory mediators by local CNS immune cells such as microglia and astrocytes. This is shown in the brains of CII immunized mice during the elevation of serum inflammatory mediators at the onset and clinical manifestation stages of the disease (day 22 - day 28 after immunization). The initial signal from the periphery may further activate the immune and inflammation response in the brain and recruit more peripheral immune cells into the brain.

We also demonstrated that these inflammatory mediators that were elevated in the brains of CII immunized mice may contribute to neurobiological changes in the brain. This is demonstrated by the impairment in hippocampal neurogenesis, characterized by a decline in DCX-positive cells in the dentate gyrus that was observed in brains of CII immunized mice. This was reversed by the anti-inflammatory effect of TNF blockade using Etanercept. Our data raised an important question; does neuro-inflammation in brains of CII -immunized mice contribute to neuron loss in the dentate gyrus by suppression of hippocampal neurogenesis, or by enhancing neurodegeneration? Several experimental studies reported various roles of innate immunity, adaptive immunity, cytokines, chemokines and growth factors, which contribute to different aspects of the regulation of hippocampal neurogenesis. For example, TLR2 agonists enhance neurogenesis, while TLR4 agonists suppress hippocampal neuronal proliferation (Rolls et al., 2007). T cells have been reported to maintain neurogenesis (Ziv et al., 2006), whereas B cells were shown to inhibit neurogenesis (Crupi et al.,

2010). Chemokines such as CXCL12 acts as a neuromodulator to support maturation and neurite extension of hippocampal neurons (Chalasanani et al., 2003). In contrast, IFN- α has been reported to inhibit neuronal proliferation in the dentate gyrus via IL-1 β signalling (Kaneko et al., 2006). Therefore, brain inflammatory mediators up-regulated in brains of CII-immunized mice may function in a complex network to regulate hippocampal neurogenesis. Interestingly, a recent study by Julie Anne Seguin 2009 *et al* demonstrated different regulation of various pro-inflammatory cytokines on hippocampal neurogenesis depending upon the route and duration of administration. Systemic administration of TNF- α reduces hippocampal neurogenesis, while intra-hippocampal infusion of IL-6 and IL-1 β enhances neuronal proliferation. These data suggest that the inflammatory signals from the periphery are detrimental to hippocampal neurogenesis, whereas local inflammatory signals paradoxically play a protective role in hippocampal neurogenesis (Seguin et al., 2009). This would also explain our finding showing that peripheral treatment using TNF blockade could reverse the impairment of hippocampus neurogenesis in CII immunized mice, probably via the inhibition of inflammatory signals from the periphery. Preventing the TNF-induced apoptosis pathway could be another mechanism by which Etanercept could inhibit neuronal loss in the hippocampus. However, it is difficult to conclude the precise effect of TNF blockade on apoptosis-induced neuronal death in this study. This is because the two TNF receptor chains; p55 TNFR and p75 TNFR can play divergent roles in hippocampal neurogenesis. p55 TNFR (TNFR1) contains an intracellular “death domain” and activation of this receptor leads to apoptosis and neuronal death. In contrast, p75 TNFR (TNFR2) can be either neuroprotective (Marchetti et al., 2004) or induce apoptosis (Depuydt et al., 2005). Therefore, blocking TNFR signal by Etanercept can possibly prevent apoptosis and neuronal death as well as reduced neuroprotection.

Our study has a number of strengths. Firstly, we used a CIA mouse model of arthritis, which shares similar immunopathology with human RA. This is also one of the best validated models of a chronic inflammatory disease. Secondly, we employed a novel high-throughput screening method, Luminex, to detect protein expression of multiple inflammatory mediators which allows analysis of the small volumes obtained from serum and brain homogenate samples. We also used a

highly sensitive real-time PCR for specific detection and quantification of mRNA levels of brain inflammatory mediators. Thirdly, we chose DCX as a neuronal marker for hippocampal neurogenesis because it specifically labels immature neurons in the dentate gyrus. It also allows us to see the clear morphology of pyramidal neurons without co-staining with other markers. However, it also had several important limitations.

1. There were apparent inconsistencies in several concentrations of brain inflammatory mediators in the CII immunized mice. Part of this was because we used different number of mice and measured levels of brain inflammatory mediators in experimental time points in different CIA experiments. Therefore, increase statistical power by increasing number of mice per group per time point would have helped to improve the consistency of the data.
2. The etanercept experiments in chapter 5 and 6, conducted using small sample size (3-5 mice/ group), are considered to be pilot studies which belongs to the exploratory phase of the research project. The preliminary data generated from small groups of mice may affect the power of statistical analysis and thus impact the ability to interpret the results. However, these pilot data can be very valuable and can guide to a more extensive experiment. Therefore, it is worthwhile to repeat these experiments using the larger numbers of animals.
3. Most of our data, particularly in Chapter 3 and 4, demonstrated that there was a significant difference in increased inflammatory mediator gene/protein levels in arthritic compared with non-arthritic mouse brains; both groups received CFA. In addition, we also found that there was no significant correlation between inflammatory mediator gene/protein levels and arthritis scores of arthritic mice, suggesting that the subclinical systemic inflammation may also be important in neurological response as seen in psoriasis (Tyring et al., 2006). Our neurogenesis study also showed that there was no significant different in the reduced number of DCX-positive cells in the dentate gurus between arthritis

and non-arthritis mice. Again, there is no correlation between number of DCX-positive cells in the dentate gyrus of arthritic mice and their arthritis score. Based on our data, it is difficult to conclude whether or not up-regulations of inflammatory mediator gene/protein levels and the reduction in neurogenesis are directly associated with clinical manifestations of rheumatoid arthritis. We hypothesized that the CFA given to the non-arthritic mice during the immunization may itself cause a reduction in hippocampal neurogenesis and the activation of brain immune response in the subclinical level of rheumatoid arthritis. Therefore, it is important to include another control consisting of DBA1 mice that receive only CFA in the future study to investigate the extent of CFA in induction of inflammatory mediator gene/protein expression and of the reduction in neurogenesis in the subclinical level in this CIA model.

4. In an attempt to investigate the inflammatory signals from the periphery, we measured inflammatory mediator proteins in serum of CII immunized mice. However, we only detected increases in serum inflammatory mediator proteins during the earlier time points of the disease progression period (day 22-day 28 after immunization) but not during the period that the arthritis was manifested (day 35-day 42 after immunization) in CII immunized mice. Our results were consistent with previous studies showing that serum cytokine concentrations in CIA model were inconsistent and in many cases undetectable at the arthritis phase (Harnett et al., 2008); (Lu et al., 2010); (del Rey et al., 2008). This may be explained by several studies showing that rheumatoid arthritis is a tissue specific autoimmune disease where inflammatory mediators are generated locally and induce bone and cartilage destructive process, but may not circulate in the bloodstream (Lu et al., 2010); (Palmlblad et al., 2001). In addition, clinical evidence also suggests that the localization of inflammatory mediators from the inflamed sites to other peripheral organs may be mainly via the lymphatic system rather than the bloodstream (Olszewski et al., 2001). This

was also supported by several CIA studies revealing increases of various inflammatory mediators in several peripheral organs such as paws, draining lymph nodes and spleen during the period of clinical manifestation of arthritis (Thornton et al., 1999);(Rioja et al., 2004);(Mauri et al., 1996). Therefore, to further investigate the communication between peripheral inflammatory signal and brain inflammation in CIA model, it would be important to measure expression of inflammatory mediators in other peripheral organs such as paws, draining lymph nodes and spleen which may be associated with the expression of these inflammatory mediators in the brain of CIA mice.

In summary, our study demonstrated that peripheral inflammation in CII-immunized mice induced changes in brain inflammatory mediator profiles and impairment in hippocampal neurogenesis. We also showed that peripheral treatment of TNF-blockade using Etanercept could inhibit cytokine production and activity within the brain of CII-immunized mice, resulting in the reversal of the arthritis-associated impairment in hippocampal neurogenesis. These observations suggest that inflammatory signals from the periphery can activate immune and inflammatory responses in the brain, which may contribute to neurobiological changes such as alterations in hippocampal function. This scenario may help explain the clinical observations of psychiatric disorders such as depression and cognitive impairment in chronic inflammatory diseases such as RA and psoriasis. Our findings also suggest that TNF-blockade may be a possible novel strategy to alleviate symptoms of depression and cognitive impairment associated with chronic inflammatory diseases. Studies have shown that depression in rheumatoid arthritis has an important impact on health-related quality of life. Therefore, further investigations of Etanercept as a novel approach to both the anti-inflammatory and antidepressant treatments are worthy.

7.1 Suggestions for future studies

Based on the results of this thesis we propose the following hypotheses and studies that might address them:

7.1.1 Hypothesis; there is migration of immune cells from the periphery into the brain of CII immunized mice.

We found up-regulation of inflammatory mediators in the brain of CII immunized mice, which may be produced from immune cells migrating from the periphery.

7.1.1.1 Investigate the migration of immune cells from the periphery into the brain of the CIA mouse model of arthritis.

The questions of how peripheral joint inflammation signals to the brain to produce inflammatory mediators, and does that process involve migration of immune cells from the periphery into the brain remains unresolved. We suggest using an *ex-vivo* technique called ‘adaptive transfer’ to track the migration of labelled immune cells from the periphery into the CNS (D’Mello et al., 2009). This technique is commonly used to study the pathological mechanism of MS, in which inflammatory demyelination is thought to be induced by peripheral immune cells. The principle of this technique involves isolation of monocytes from peripheral blood and/or leukocytes from lymph nodes in the donor animals. Each type of peripheral immune cell is isolated and purified by magnetic beads linked to cell-specific antibodies. For example, beads with anti-CD11b can be used to purify monocytes (D’Mello et al., 2009), while CD45 and TCR can be used for the isolation of T cells (Lees et al., 2008). These CD11b⁺ monocytes and/or CD45⁺ T cells are then labelled with fluorescent dyes. These labelled immune cells are then adoptively transferred by i.v. injection into the recipient animals. The presence of these adoptively transferred immune cells is then detected in the brains of these recipient animals using fluorescent immunohistochemistry. This technique can also be used for measuring the cytokine production capabilities of immune cells present within the CNS at various time points following adoptive transfer.

7.1.2 Hypothesis; there is local production of inflammatory mediators by astrocytes and microglia in the brain of CII immunized mice.

We found up-regulation of protein and gene of inflammatory mediators in the brain of CII immunized mice, which may be produced from CNS immune cells such as astrocytes and microglia.

7.1.2.1 Investigate the local production of inflammatory mediators by CNS immune cells such as astrocytes and microglia.

Previous reports suggest that peripheral inflammation can signal to the local immune cells in the brain to produce inflammatory mediators by an unknown mechanism. Although we demonstrated an increase of both protein and mRNA levels of some inflammatory mediators in the brain of CII immunized mice, it is still difficult to conclude the cellular sources of these inflammatory mediators. The activation of astrocytes and microglia and their cytokine production capabilities during the peripheral inflammatory process can be investigated by double staining for each cytokine and the microglia or astrocytic markers. We can use GFAP to label astrocytes and determine any increase in astrocyte number in the brain (Sofroniew and Vinters, 2010). Studies also showed that peripheral inflammation can induce cytokine production via microglial activation in the brain (D'Mello et al., 2009); (Riazi et al., 2008). CD11b and CD45 are commonly used as markers for microglia (Yang et al., 2010). Microglia activation is indicated by the change in morphology of microglia from inactive ramified microglia to active amoeboid microglia (Riazi et al., 2008).

7.1.3 Hypothesis; different inflammatory mediators play different role in hippocampal neurogenesis.

Up-regulation of protein and genes of various inflammatory mediators including IL-1 α , IL-5, CXCL1, CXCL10, IL-10, IL-13, FGF2 and VEGF in brains of CII immunized mice on day 42. At that time point, we also found an impairment in hippocampal neurogenesis in the brains of CII immunized mice. Different inflammatory mediators play different roles in regulation of hippocampal neurogenesis. Therefore, it is interesting to define the extent to which inflammatory mediators regulate hippocampal neurogenesis.

7.1.3.1 Investigate roles of inflammatory mediators in hippocampal neurogenesis using in vitro experiments.

Different regulations of various inflammatory mediators on hippocampal neurogenesis are also worth investigating. We can generate an in vitro model of hippocampal neurogenesis by deriving and culturing neuronal progenitor cells from the adult hippocampal dentate gyrus. Single or multiple inflammatory mediators can be added into the culture of neuronal progenitor cells to determine the effect of individual or combined inflammatory mediators on the proliferation and maturation of dentate gyrus neurons. The hippocampal neurogenesis after the cytokine treatment can be analysed by labelling these dentate gyrus neurons with various neuronal markers identifying different stages of neurogenesis. For example, DCX is used to label neurons in the immature stage, while NeuN is used to label neurons in the mature stage. FACS (fluorescence activated cell sorting) can then be used to determine the level of neurogenesis by analysing the number of neurons that are positive to immature neuronal markers such as DCX and Brdu (Ming and Song, 2005).

7.1.4 Hypothesis; the reduction in the number of neurons in the hippocampus of CII immunized mice could be the result of neurodegeneration.

We demonstrated that the reduction in the number of neurons in dentate gyrus of CII immunized mice was the result of the inhibition of neurogenesis using neuronal marker DCX. However, the neuronal loss in dentate gyrus of CII immunized mice may possibly be the result of neurodegeneration process such as apoptosis.

7.1.4.1 Investigate neurodegenerative effects of peripheral inflammation on neurons in the hippocampal dentate gyrus.

We demonstrated the suppression in hippocampal neurogenesis in CII immunized mice using DCX, a neuronal marker for immature neurons in the maturation stage. This was indicated by a reduction in the number of DCX-positive neurons in the dentate gyrus. However, it is also possible that peripheral inflammation can induce neuronal loss in the hippocampal dentate gyrus via neurodegenerative pathways. We showed that TNF-blockade can reverse this neurogenesis impairment. The neuroprotective effect of Etanercept may involve

blocking the apoptosis pathway induced by TNF receptor. Therefore, using markers for apoptosis such as TUNEL may lead to better understanding of another mechanism underlying the process of neuronal loss in the hippocampal dentate gyrus by peripheral inflammation.

7.1.5 Hypothesis; Peripheral inflammation has effects on neurotransmitter and neurotropic factors in brains of CII immunized mice, that are associated with the pathological mechanism of depression.

We demonstrated that peripheral inflammation had a detrimental effect on hippocampal neurogenesis. Inflammatory mediators up-regulated in brains of CII immunized mice may have actions on neurochemical or neurotropic factors, which may be associated with the development of depression.

7.1.5.1 Investigate effects of peripheral inflammation in other pathological mechanisms of depression.

Animal studies suggest that peripheral inflammation can induce cognitive impairment and depressive-like symptoms via suppression of hippocampal neurogenesis. However, the implication of neurogenesis and neural network disturbance in the patho-physiology of depression is still a novel theory. The effect of peripheral inflammation on other classical pathological mechanisms, monoamine (eg., serotonin, dopamine), HPA axis, and neuronal growth factors (eg., BDNF) should not be ignored. A study by del Rey *et al.*, showed an increase in serotonin levels in the hypothalamus of the CIA rat model. Interestingly, that study also showed an increase in noradrenaline (NA), corresponding to reduced glucocorticoid levels in the hypothalamus of CIA rat. The author suggests that this data demonstrated a reduction in HPA axis activity, which has also been reported in RA patients (del Rey *et al.*, 2008). However, an increase in HPA axis activity and a decrease in brain serotonin level have been reported in depression patients (Lanfumeijer *et al.*, 2008). Therefore, it is better to use anatomical analysis such as *in situ* hybridization and autoradiography to determine changes in monoamine levels and neurotransmitter receptors in various areas in the brain. It may also be interesting to study changes in animal behaviour in the CIA mouse model using animal behavioural tests to investigate changes in cognition

and depressive-like behaviour during different phases of disease; to quantify associated inflammatory mediators and to test the effects of TNF blockade.

8 References

- ABBOTT, N. J., PATABENDIGE, A. A., DOLMAN, D. E., YUSOF, S. R. & BEGLEY, D. J. 2010. Structure and function of the blood-brain barrier. *Neurobiol Dis*, 37, 13-25.
- ABBOTT, N. J., RONNBACK, L. & HANSSON, E. 2006. Astrocyte-endothelial interactions at the blood-brain barrier. *Nat Rev Neurosci*, 7, 41-53.
- ABRAMSON, S. B. & AMIN, A. 2002. Blocking the effects of IL-1 in rheumatoid arthritis protects bone and cartilage. *Rheumatology (Oxford)*, 41, 972-80.
- ADAMS, D. H. & LLOYD, A. R. 1997. Chemokines: leucocyte recruitment and activation cytokines. *Lancet*, 349, 490-5.
- AFONSO, P. V., OZDEN, S., PREVOST, M. C., SCHMITT, C., SEILHEAN, D., WEKSLER, B., COURAUD, P. O., GESSAIN, A., ROMERO, I. A. & CECCALDI, P. E. 2007. Human blood-brain barrier disruption by retroviral-infected lymphocytes: role of myosin light chain kinase in endothelial tight-junction disorganization. *J Immunol*, 179, 2576-83.
- AFUWAPE, A. O., FELDMANN, M. & PALEOLOG, E. M. 2003. Adenoviral delivery of soluble VEGF receptor 1 (sFlt-1) abrogates disease activity in murine collagen-induced arthritis. *Gene Ther*, 10, 1950-60.
- AGRAWAL, S., MISRA, R. & AGGARWAL, A. 2007. Autoantibodies in rheumatoid arthritis: association with severity of disease in established RA. *Clin Rheumatol*, 26, 201-4.
- AIMONE, J. B., WILES, J. & GAGE, F. H. 2006. Potential role for adult neurogenesis in the encoding of time in new memories. *Nat Neurosci*, 9, 723-7.
- AKAMA, K. T. & VAN ELDIK, L. J. 2000. Beta-amyloid stimulation of inducible nitric-oxide synthase in astrocytes is interleukin-1beta- and tumor necrosis factor-alpha (TNFalpha)-dependent, and involves a TNFalpha receptor-associated factor- and NFkappaB-inducing kinase-dependent signaling mechanism. *J Biol Chem*, 275, 7918-24.
- AKASSOGLU, K., BAUER, J., KASSIOTIS, G., PASPARAKIS, M., LASSMANN, H., KOLLIAS, G. & PROBERT, L. 1998. Oligodendrocyte apoptosis and primary demyelination induced by local TNF/p55TNF receptor signaling in the central nervous system of transgenic mice: models for multiple sclerosis with primary oligodendroglipathy. *Am J Pathol*, 153, 801-13.
- AKASSOGLU, K., DOUNI, E., BAUER, J., LASSMANN, H., KOLLIAS, G. & PROBERT, L. 2003. Exclusive tumor necrosis factor (TNF) signaling by the p75TNF receptor triggers inflammatory ischemia in the CNS of transgenic mice. *Proc Natl Acad Sci U S A*, 100, 709-14.
- ALBERT, L. J. & INMAN, R. D. 1999. Molecular mimicry and autoimmunity. *N Engl J Med*, 341, 2068-74.
- ALLAN, S. M., TYRRELL, P. J. & ROTHWELL, N. J. 2005. Interleukin-1 and neuronal injury. *Nat Rev Immunol*, 5, 629-40.
- ALLAVENA, R., NOY, S., ANDREWS, M. & PULLEN, N. 2010. CNS elevation of vascular and not mucosal addressin cell adhesion molecules in patients with multiple sclerosis. *Am J Pathol*, 176, 556-62.
- ALON, R. & DUSTIN, M. L. 2007. Force as a facilitator of integrin conformational changes during leukocyte arrest on blood vessels and antigen-presenting cells. *Immunity*, 26, 17-27.
- ALON, R. & LEY, K. 2008. Cells on the run: shear-regulated integrin activation in leukocyte rolling and arrest on endothelial cells. *Curr Opin Cell Biol*, 20, 525-32.

- ALT, C., LASCHINGER, M. & ENGELHARDT, B. 2002. Functional expression of the lymphoid chemokines CCL19 (ELC) and CCL 21 (SLC) at the blood-brain barrier suggests their involvement in G-protein-dependent lymphocyte recruitment into the central nervous system during experimental autoimmune encephalomyelitis. *Eur J Immunol*, 32, 2133-44.
- AMREIN, I. & LIPP, H. P. 2009. Adult hippocampal neurogenesis of mammals: evolution and life history. *Biol Lett*, 5, 141-4.
- ANACKER, C., ZUNSZAIN, P. A., CATTANEO, A., CARVALHO, L. A., GARABEDIAN, M. J., THURET, S., PRICE, J. & PARIANTE, C. M. 2011. Antidepressants increase human hippocampal neurogenesis by activating the glucocorticoid receptor. *Mol Psychiatry*.
- ANDERSEN, C. L., JENSEN, J. L. & ORNTOFT, T. F. 2004. Normalization of real-time quantitative reverse transcription-PCR data: a model-based variance estimation approach to identify genes suited for normalization, applied to bladder and colon cancer data sets. *Cancer Res*, 64, 5245-50.
- ANG, D. C., CHOI, H., KROENKE, K. & WOLFE, F. 2005. Comorbid depression is an independent risk factor for mortality in patients with rheumatoid arthritis. *J Rheumatol*, 32, 1013-9.
- ARAKAWA, Y., BITO, H., FURUYASHIKI, T., TSUJI, T., TAKEMOTO-KIMURA, S., KIMURA, K., NOZAKI, K., HASHIMOTO, N. & NARUMIYA, S. 2003. Control of axon elongation via an SDF-1alpha/Rho/mDia pathway in cultured cerebellar granule neurons. *J Cell Biol*, 161, 381-91.
- ARGAW, A. T., GURFEIN, B. T., ZHANG, Y., ZAMEER, A. & JOHN, G. R. 2009. VEGF-mediated disruption of endothelial CLN-5 promotes blood-brain barrier breakdown. *Proc Natl Acad Sci U S A*, 106, 1977-82.
- ARGAW, A. T., ZHANG, Y., SNYDER, B. J., ZHAO, M. L., KOPP, N., LEE, S. C., RAINE, C. S., BROSNAN, C. F. & JOHN, G. R. 2006. IL-1beta regulates blood-brain barrier permeability via reactivation of the hypoxia-angiogenesis program. *J Immunol*, 177, 5574-84.
- ARTIS, D., HUMPHREYS, N. E., BANCROFT, A. J., ROTHWELL, N. J., POTTEN, C. S. & GRENCIS, R. K. 1999. Tumor necrosis factor alpha is a critical component of interleukin 13-mediated protective T helper cell type 2 responses during helminth infection. *J Exp Med*, 190, 953-62.
- ASAHARA, T., TAKAHASHI, T., MASUDA, H., KALKA, C., CHEN, D., IWAGURO, H., INAI, Y., SILVER, M. & ISNER, J. M. 1999. VEGF contributes to postnatal neovascularization by mobilizing bone marrow-derived endothelial progenitor cells. *EMBO J*, 18, 3964-72.
- ASQUITH, D. L., MILLER, A. M., HUEBER, A. J., MCKINNON, H. J., SATTAR, N., GRAHAM, G. J. & MCINNES, I. B. 2009a. Liver X receptor agonism promotes articular inflammation in murine collagen-induced arthritis. *Arthritis Rheum*, 60, 2655-65.
- ASQUITH, D. L., MILLER, A. M., MCINNES, I. B. & LIEW, F. Y. 2009b. Animal models of rheumatoid arthritis. *Eur J Immunol*, 39, 2040-4.
- ATLANTIS, E., GOLDNEY, R. D. & WITTERT, G. A. 2009. Obesity and depression or anxiety. *BMJ*, 339, b3868.
- BACHIS, A. & MOCCHETTI, I. 2004. The chemokine receptor CXCR4 and not the N-methyl-D-aspartate receptor mediates gp120 neurotoxicity in cerebellar granule cells. *J Neurosci Res*, 75, 75-82.
- BADIE, B., BARTLEY, B. & SCHATNER, J. 2002. Differential expression of MHC class II and B7 costimulatory molecules by microglia in rodent gliomas. *J Neuroimmunol*, 133, 39-45.

- BAGRI, A., GURNEY, T., HE, X., ZOU, Y. R., LITTMAN, D. R., TESSIER-LAVIGNE, M. & PLEASURE, S. J. 2002. The chemokine SDF1 regulates migration of dentate granule cells. *Development*, 129, 4249-60.
- BAHBOUHI, B., BERTHELOT, L., PETTRE, S., MICHEL, L., WIERTLEWSKI, S., WEKSLER, B., ROMERO, I. A., MILLER, F., COURAUD, P. O., BROUARD, S., LAPLAUD, D. A. & SOULILLOU, J. P. 2009. Peripheral blood CD4+ T lymphocytes from multiple sclerosis patients are characterized by higher PSGL-1 expression and transmigration capacity across a human blood-brain barrier-derived endothelial cell line. *J Leukoc Biol*, 86, 1049-63.
- BAILEY, S. L., SCHREINER, B., MCMAHON, E. J. & MILLER, S. D. 2007. CNS myeloid DCs presenting endogenous myelin peptides 'preferentially' polarize CD4+ T(H)-17 cells in relapsing EAE. *Nat Immunol*, 8, 172-80.
- BANASR, M., SOUMIER, A., HERY, M., MOCAER, E. & DASZUTA, A. 2006. Agomelatine, a new antidepressant, induces regional changes in hippocampal neurogenesis. *Biol Psychiatry*, 59, 1087-96.
- BANISADR, G., GOSSELIN, R. D., MECHIGHHEL, P., ROSTENE, W., KITABGI, P. & MELIK PARSADANIANTZ, S. 2005. Constitutive neuronal expression of CCR2 chemokine receptor and its colocalization with neurotransmitters in normal rat brain: functional effect of MCP-1/CCL2 on calcium mobilization in primary cultured neurons. *J Comp Neurol*, 492, 178-92.
- BANISADR, G., QUERAUD-LESAUX, F., BOUTTERIN, M. C., PELAPRAT, D., ZALC, B., ROSTENE, W., HAOUR, F. & PARSADANIANTZ, S. M. 2002. Distribution, cellular localization and functional role of CCR2 chemokine receptors in adult rat brain. *J Neurochem*, 81, 257-69.
- BANISADR, G., SKRZYDELSKI, D., KITABGI, P., ROSTENE, W. & PARSADANIANTZ, S. M. 2003. Highly regionalized distribution of stromal cell-derived factor-1/CXCL12 in adult rat brain: constitutive expression in cholinergic, dopaminergic and vasopressinergic neurons. *Eur J Neurosci*, 18, 1593-606.
- BANKS, W. A. 2010. Blood-brain barrier as a regulatory interface. *Forum Nutr*, 63, 102-10.
- BANKS, W. A., KASTIN, A. J. & EHRENSING, C. A. 1994a. Blood-borne interleukin-1 alpha is transported across the endothelial blood-spinal cord barrier of mice. *J Physiol*, 479 (Pt 2), 257-64.
- BANKS, W. A., KASTIN, A. J. & GUTIERREZ, E. G. 1994b. Penetration of interleukin-6 across the murine blood-brain barrier. *Neurosci Lett*, 179, 53-6.
- BANKS, W. A., NIEHOFF, M. L. & ZALCMAN, S. S. 2004. Permeability of the mouse blood-brain barrier to murine interleukin-2: predominance of a saturable efflux system. *Brain Behav Immun*, 18, 434-42.
- BANKS, W. A., ORTIZ, L., PLOTKIN, S. R. & KASTIN, A. J. 1991. Human interleukin (IL) 1 alpha, murine IL-1 alpha and murine IL-1 beta are transported from blood to brain in the mouse by a shared saturable mechanism. *J Pharmacol Exp Ther*, 259, 988-96.
- BAO, L., ZHU, Y., ELHASSAN, A. M., WU, Q., XIAO, B., ZHU, J. & LINDGREN, J. U. 2001. Adjuvant-induced arthritis: IL-1 beta, IL-6 and TNF-alpha are up-regulated in the spinal cord. *Neuroreport*, 12, 3905-8.
- BARCELOS, L. S., TALVANI, A., TEIXEIRA, A. S., CASSALI, G. D., ANDRADE, S. P. & TEIXEIRA, M. M. 2004. Production and in vivo effects of chemokines CXCL1-3/KC and CCL2/JE in a model of inflammatory angiogenesis in mice. *Inflamm Res*, 53, 576-84.
- BARICHELLO, T., DOS SANTOS, I., SAVI, G. D., FLORENTINO, A. F., SILVESTRE, C., COMIM, C. M., FEIER, G., SACHS, D., TEIXEIRA, M. M., TEIXEIRA, A. L. & QUEVEDO, J. 2009. Tumor necrosis factor alpha (TNF-alpha) levels in the

- brain and cerebrospinal fluid after meningitis induced by *Streptococcus pneumoniae*. *Neurosci Lett*, 467, 217-9.
- BARICHELLO, T., DOS SANTOS, I., SAVI, G. D., SIMOES, L. R., SILVESTRE, T., COMIM, C. M., SACHS, D., TEIXEIRA, M. M., TEIXEIRA, A. L. & QUEVEDO, J. 2010. TNF-alpha, IL-1beta, IL-6, and cinc-1 levels in rat brain after meningitis induced by *Streptococcus pneumoniae*. *J Neuroimmunol*, 221, 42-5.
- BARNES, P. J. & ADCOCK, I. M. 2009. Glucocorticoid resistance in inflammatory diseases. *Lancet*, 373, 1905-17.
- BARNUM, S. R. 1999. Inhibition of complement as a therapeutic approach in inflammatory central nervous system (CNS) disease. *Mol Med*, 5, 569-82.
- BARRIENTOS, R. M., SPRUNGER, D. B., CAMPEAU, S., HIGGINS, E. A., WATKINS, L. R., RUDY, J. W. & MAIER, S. F. 2003. Brain-derived neurotrophic factor mRNA downregulation produced by social isolation is blocked by intrahippocampal interleukin-1 receptor antagonist. *Neuroscience*, 121, 847-53.
- BARSANTE, M. M., CUNHA, T. M., ALLEGRETTI, M., CATTANI, F., POLICANI, F., BIZZARRI, C., TAFURI, W. L., POOLE, S., CUNHA, F. Q., BERTINI, R. & TEIXEIRA, M. M. 2008. Blockade of the chemokine receptor CXCR2 ameliorates adjuvant-induced arthritis in rats. *Br J Pharmacol*, 153, 992-1002.
- BARTHOLOME, B., SPIES, C. M., GABER, T., SCHUCHMANN, S., BERKI, T., KUNKEL, D., BIENERT, M., RADBRUCH, A., BURMESTER, G. R., LAUSTER, R., SCHEFFOLD, A. & BUTTGEREIT, F. 2004. Membrane glucocorticoid receptors (mGCR) are expressed in normal human peripheral blood mononuclear cells and up-regulated after in vitro stimulation and in patients with rheumatoid arthritis. *FASEB J*, 18, 70-80.
- BARTOK, B. & FIRESTEIN, G. S. 2010. Fibroblast-like synoviocytes: key effector cells in rheumatoid arthritis. *Immunol Rev*, 233, 233-55.
- BAUER, B., HARTZ, A. M. & MILLER, D. S. 2007. Tumor necrosis factor alpha and endothelin-1 increase P-glycoprotein expression and transport activity at the blood-brain barrier. *Mol Pharmacol*, 71, 667-75.
- BAUER, M., BRAKEBUSCH, C., COISNE, C., SIXT, M., WEKERLE, H., ENGELHARDT, B. & FASSLER, R. 2009. Beta1 integrins differentially control extravasation of inflammatory cell subsets into the CNS during autoimmunity. *Proc Natl Acad Sci U S A*, 106, 1920-5.
- BECHER, B., BLAIN, M., GIACOMINI, P. S. & ANTEL, J. P. 1999. Inhibition of Th1 polarization by soluble TNF receptor is dependent on antigen-presenting cell-derived IL-12. *J Immunol*, 162, 684-8.
- BECHER, B., DODELET, V., FEDOROWICZ, V. & ANTEL, J. P. 1996. Soluble tumor necrosis factor receptor inhibits interleukin 12 production by stimulated human adult microglial cells in vitro. *J Clin Invest*, 98, 1539-43.
- BECHMANN, I., PRILLER, J., KOVAC, A., BONTERT, M., WEHNER, T., KLETT, F. F., BOHSUNG, J., STUSCHKE, M., DIRNAGL, U. & NITSCH, R. 2001. Immune surveillance of mouse brain perivascular spaces by blood-borne macrophages. *Eur J Neurosci*, 14, 1651-8.
- BECK, R. D., JR., WASSERFALL, C., HA, G. K., CUSHMAN, J. D., HUANG, Z., ATKINSON, M. A. & PETITTO, J. M. 2005. Changes in hippocampal IL-15, related cytokines, and neurogenesis in IL-2 deficient mice. *Brain Res*, 1041, 223-30.
- BEGOVIĆ, A. B., CARLTON, V. E., HONIGBERG, L. A., SCHRODI, S. J., CHOKKALINGAM, A. P., ALEXANDER, H. C., ARDLIE, K. G., HUANG, Q., SMITH, A. M., SPOERKE, J. M., CONN, M. T., CHANG, M., CHANG, S. Y.,

- SAIKI, R. K., CATANESE, J. J., LEONG, D. U., GARCIA, V. E., MCALLISTER, L. B., JEFFERY, D. A., LEE, A. T., BATLIWALLA, F., REMMERS, E., CRISWELL, L. A., SELDIN, M. F., KASTNER, D. L., AMOS, C. I., SNINSKY, J. J. & GREGERSEN, P. K. 2004. A missense single-nucleotide polymorphism in a gene encoding a protein tyrosine phosphatase (PTPN22) is associated with rheumatoid arthritis. *Am J Hum Genet*, 75, 330-7.
- BELMAKER, R. H. & AGAM, G. 2008. Major depressive disorder. *N Engl J Med*, 358, 55-68.
- BEN MENACHEM-ZIDON, O., GOSHEN, I., KREISEL, T., BEN MENAHEM, Y., REINHARTZ, E., BEN HUR, T. & YIRMIYA, R. 2008. Intrahippocampal transplantation of transgenic neural precursor cells overexpressing interleukin-1 receptor antagonist blocks chronic isolation-induced impairment in memory and neurogenesis. *Neuropsychopharmacology*, 33, 2251-62.
- BENDELE, A. M. 2001. Animal models of osteoarthritis. *J Musculoskelet Neuronal Interact*, 1, 363-76.
- BERGER, J., SPRAGUE, S. M., WU, Y., DAVIS, W. W., JIMENEZ, D. F., BARONE, C. M. & DING, Y. 2007. Peripheral thermal injury causes early blood-brain barrier dysfunction and matrix metalloproteinase expression in rat. *Neurol Res*, 29, 610-4.
- BERGHMANS, N., DILLEN, C. & HEREMANS, H. 2006. Exogenous IL-12 suppresses experimental autoimmune encephalomyelitis (EAE) by tuning IL-10 and IL-5 levels in an IFN-gamma-dependent way. *J Neuroimmunol*, 176, 63-75.
- BERNER, B., AKCA, D., JUNG, T., MULLER, G. A. & REUSS-BORST, M. A. 2000. Analysis of Th1 and Th2 cytokines expressing CD4+ and CD8+ T cells in rheumatoid arthritis by flow cytometry. *J Rheumatol*, 27, 1128-35.
- BESSA, J. M., FERREIRA, D., MELO, I., MARQUES, F., CERQUEIRA, J. J., PALHA, J. A., ALMEIDA, O. F. & SOUSA, N. 2009. The mood-improving actions of antidepressants do not depend on neurogenesis but are associated with neuronal remodeling. *Mol Psychiatry*, 14, 764-73, 739.
- BILBO, S. D., BARRIENTOS, R. M., EADS, A. S., NORTH CUTT, A., WATKINS, L. R., RUDY, J. W. & MAIER, S. F. 2008. Early-life infection leads to altered BDNF and IL-1beta mRNA expression in rat hippocampus following learning in adulthood. *Brain Behav Immun*, 22, 451-5.
- BILJAN, D., LAUFER, D., FILAKOVIC, P., SITUM, M. & BRATALJENOVIC, T. 2009. Psoriasis, mental disorders and stress. *Coll Antropol*, 33, 889-92.
- BISCHOFF, D. S., ZHU, J. H., MAKHIJANI, N. S. & YAMAGUCHI, D. T. 2005. KC chemokine expression by TGF-beta in C3H10T1/2 cells induced towards osteoblasts. *Biochem Biophys Res Commun*, 326, 364-70.
- BLACKBURN, D., SARGSYAN, S., MONK, P. N. & SHAW, P. J. 2009. Astrocyte function and role in motor neuron disease: a future therapeutic target? *Glia*, 57, 1251-64.
- BLAMIRE, A. M., ANTHONY, D. C., RAJAGOPALAN, B., SIBSON, N. R., PERRY, V. H. & STYLES, P. 2000. Interleukin-1beta -induced changes in blood-brain barrier permeability, apparent diffusion coefficient, and cerebral blood volume in the rat brain: a magnetic resonance study. *J Neurosci*, 20, 8153-9.
- BLISS, T. V. & GARDNER-MEDWIN, A. R. 1973. Long-lasting potentiation of synaptic transmission in the dentate area of the unanaesthetized rabbit following stimulation of the perforant path. *J Physiol*, 232, 357-74.
- BLUTHE, R. M., CASTANON, N., POUSET, F., BRISTOW, A., BALL, C., LESTAGE, J., MICHAUD, B., KELLEY, K. W. & DANTZER, R. 1999. Central injection of

- IL-10 antagonizes the behavioural effects of lipopolysaccharide in rats. *Psychoneuroendocrinology*, 24, 301-11.
- BOCHE, D., CUNNINGHAM, C., GAULDIE, J. & PERRY, V. H. 2003. Transforming growth factor-beta 1-mediated neuroprotection against excitotoxic injury in vivo. *J Cereb Blood Flow Metab*, 23, 1174-82.
- BOLDRINI, M., UNDERWOOD, M. D., HEN, R., ROSOKLIJA, G. B., DWORK, A. J., JOHN MANN, J. & ARANGO, V. 2009. Antidepressants increase neural progenitor cells in the human hippocampus. *Neuropsychopharmacology*, 34, 2376-89.
- BOLTON, M. M. & EROGLU, C. 2009. Look who is weaving the neural web: glial control of synapse formation. *Curr Opin Neurobiol*, 19, 491-7.
- BOLTON, S. J., ANTHONY, D. C. & PERRY, V. H. 1998. Loss of the tight junction proteins occludin and zonula occludens-1 from cerebral vascular endothelium during neutrophil-induced blood-brain barrier breakdown in vivo. *Neuroscience*, 86, 1245-57.
- BONACCORSO, S., PUZELLA, A., MARINO, V., PASQUINI, M., BIONDI, M., ARTINI, M., ALMERIGHI, C., LEVRERO, M., EGYED, B., BOSMANS, E., MELTZER, H. Y. & MAES, M. 2001. Immunotherapy with interferon-alpha in patients affected by chronic hepatitis C induces an intercorrelated stimulation of the cytokine network and an increase in depressive and anxiety symptoms. *Psychiatry Res*, 105, 45-55.
- BORZI, R. M., MAZZETTI, I., CATTINI, L., UGUCCIONI, M., BAGGIOLINI, M. & FACCHINI, A. 2000. Human chondrocytes express functional chemokine receptors and release matrix-degrading enzymes in response to C-X-C and C-C chemokines. *Arthritis Rheum*, 43, 1734-41.
- BOUFIDOU, F., LAMBRINOUDAKI, I., ARGEITIS, J., ZERVAS, I. M., PLIATSIKA, P., LEONARDOU, A. A., PETROPOULOS, G., HASIAKOS, D., PAPADIAS, K. & NIKOLAOU, C. 2009. CSF and plasma cytokines at delivery and postpartum mood disturbances. *J Affect Disord*, 115, 287-92.
- BOURGUIGNON, C., LABYAK, S. E. & TAIBI, D. 2003. Investigating sleep disturbances in adults with rheumatoid arthritis. *Holist Nurs Pract*, 17, 241-9.
- BRAND, D. D., KANG, A. H. & ROSLONIEC, E. F. 2003. Immunopathogenesis of collagen arthritis. *Springer Semin Immunopathol*, 25, 3-18.
- BRAND, D. D., MARION, T. N., MYERS, L. K., ROSLONIEC, E. F., WATSON, W. C., STUART, J. M. & KANG, A. H. 1996. Autoantibodies to murine type II collagen in collagen-induced arthritis: a comparison of susceptible and nonsusceptible strains. *J Immunol*, 157, 5178-84.
- BREDER, C. D., HAZUKA, C., GHAYUR, T., KLUG, C., HUGININ, M., YASUDA, K., TENG, M. & SAPER, C. B. 1994. Regional induction of tumor necrosis factor alpha expression in the mouse brain after systemic lipopolysaccharide administration. *Proc Natl Acad Sci U S A*, 91, 11393-7.
- BRENCHLEY, P. E. 2001. Antagonising angiogenesis in rheumatoid arthritis. *Ann Rheum Dis*, 60 Suppl 3, iii71-4.
- BRENNAN, F. M., CHANTRY, D., JACKSON, A., MAINI, R. & FELDMANN, M. 1989. Inhibitory effect of TNF alpha antibodies on synovial cell interleukin-1 production in rheumatoid arthritis. *Lancet*, 2, 244-7.
- BRENNAN, F. M. & MCINNES, I. B. 2008. Evidence that cytokines play a role in rheumatoid arthritis. *J Clin Invest*, 118, 3537-45.
- BRIOLAY, J., DECHANET, J., BLANCHARD, D., BANCHEREAU, J. & MIOSSEC, P. 1992. Interleukin 4 inhibits polyclonal immunoglobulin secretion and cytokine production by peripheral blood mononuclear cells from rheumatoid arthritis patients. *J Clin Immunol*, 12, 36-44.

- BROWN, C. M., MULCAHEY, T. A., FILIPEK, N. C. & WISE, P. M. 2010. Production of proinflammatory cytokines and chemokines during neuroinflammation: novel roles for estrogen receptors alpha and beta. *Endocrinology*, 151, 4916-25.
- BROWN, J. P., COUILLARD-DESPRES, S., COOPER-KUHN, C. M., WINKLER, J., AIGNER, L. & KUHN, H. G. 2003. Transient expression of doublecortin during adult neurogenesis. *J Comp Neurol*, 467, 1-10.
- BRUEL-JUNGERMAN, E., DAVIS, S. & LAROCHE, S. 2007. Brain plasticity mechanisms and memory: a party of four. *Neuroscientist*, 13, 492-505.
- BRUMMELTE, S. & GALEA, L. A. 2010. Chronic high corticosterone reduces neurogenesis in the dentate gyrus of adult male and female rats. *Neuroscience*, 168, 680-90.
- BSIBSI, M., PERSOON-DEEN, C., VERWER, R. W., MEEUWSEN, S., RAVID, R. & VAN NOORT, J. M. 2006. Toll-like receptor 3 on adult human astrocytes triggers production of neuroprotective mediators. *Glia*, 53, 688-95.
- BSIBSI, M., RAVID, R., GVERIC, D. & VAN NOORT, J. M. 2002. Broad expression of Toll-like receptors in the human central nervous system. *J Neuropathol Exp Neurol*, 61, 1013-21.
- BURGESS, N., MAGUIRE, E. A. & O'KEEFE, J. 2002. The human hippocampus and spatial and episodic memory. *Neuron*, 35, 625-41.
- BUTOVSKY, O., ZIV, Y., SCHWARTZ, A., LANDA, G., TALPALAR, A. E., PLUCHINO, S., MARTINO, G. & SCHWARTZ, M. 2006. Microglia activated by IL-4 or IFN-gamma differentially induce neurogenesis and oligodendrogenesis from adult stem/progenitor cells. *Mol Cell Neurosci*, 31, 149-60.
- BYRAM, S. C., CARSON, M. J., DEBOY, C. A., SERPE, C. J., SANDERS, V. M. & JONES, K. J. 2004. CD4-positive T cell-mediated neuroprotection requires dual compartment antigen presentation. *J Neurosci*, 24, 4333-9.
- CAMPBELL, I. K., HAMILTON, J. A. & WICKS, I. P. 2000. Collagen-induced arthritis in C57BL/6 (H-2b) mice: new insights into an important disease model of rheumatoid arthritis. *Eur J Immunol*, 30, 1568-75.
- CAMPBELL, S. J., JIANG, Y., DAVIS, A. E., FARRANDS, R., HOLBROOK, J., LEPPERT, D. & ANTHONY, D. C. 2007. Immunomodulatory effects of etanercept in a model of brain injury act through attenuation of the acute-phase response. *J Neurochem*, 103, 2245-55.
- CANETE, J. D., MARTINEZ, S. E., FARRAS, J., SANMARTI, R., BLAY, M., GOMEZ, A., SALVADOR, G. & MUNOZ-GOMEZ, J. 2000. Differential Th1/Th2 cytokine patterns in chronic arthritis: interferon gamma is highly expressed in synovium of rheumatoid arthritis compared with seronegative spondyloarthropathies. *Ann Rheum Dis*, 59, 263-8.
- CAPURON, L., RAVAUD, A., NEVEU, P. J., MILLER, A. H., MAES, M. & DANTZER, R. 2002. Association between decreased serum tryptophan concentrations and depressive symptoms in cancer patients undergoing cytokine therapy. *Mol Psychiatry*, 7, 468-73.
- CAPUZZI, D., SANTORO, E., HAUCK, W. W., KOVATICH, A. J., ROSATO, F. E., BAFFA, R., HUEBNER, K. & MCCUE, P. A. 2000. Fhit expression in gastric adenocarcinoma: correlation with disease stage and survival. *Cancer*, 88, 24-34.
- CARACI, F., BATTAGLIA, G., BUSCETI, C., BIAGIONI, F., MASTROIACOVO, F., BOSCO, P., DRAGO, F., NICOLETTI, F., SORTINO, M. A. & COPANI, A. 2008. TGF-beta 1 protects against Abeta-neurotoxicity via the phosphatidylinositol-3-kinase pathway. *Neurobiol Dis*, 30, 234-42.

- CARPENTIER, P. A., DUNCAN, D. S. & MILLER, S. D. 2008. Glial toll-like receptor signaling in central nervous system infection and autoimmunity. *Brain Behav Immun*, 22, 140-7.
- CARSON, M. J. 2002. Microglia as liaisons between the immune and central nervous systems: functional implications for multiple sclerosis. *Glia*, 40, 218-31.
- CARSON, M. J., DOOSE, J. M., MELCHIOR, B., SCHMID, C. D. & PLOIX, C. C. 2006. CNS immune privilege: hiding in plain sight. *Immunol Rev*, 213, 48-65.
- CARTER, J. H. 2000. The immune system as a model for pattern recognition and classification. *J Am Med Inform Assoc*, 7, 28-41.
- CARTER, S. L., MULLER, M., MANDERS, P. M. & CAMPBELL, I. L. 2007. Induction of the genes for Cxcl9 and Cxcl10 is dependent on IFN-gamma but shows differential cellular expression in experimental autoimmune encephalomyelitis and by astrocytes and microglia in vitro. *Glia*, 55, 1728-39.
- CASTANEDA, A. E., TUULIO-HENRIKSSON, A., MARTTUNEN, M., SUVISAARI, J. & LONNQVIST, J. 2008. A review on cognitive impairments in depressive and anxiety disorders with a focus on young adults. *J Affect Disord*, 106, 1-27.
- CAVANAGH, J., PATERSON, C., MCLEAN, J., PIMLOTT, S., MCDONALD, M., PATTERSON, J., WYPER, D. & MCINNES, I. 2010. Tumour necrosis factor blockade mediates altered serotonin transporter availability in rheumatoid arthritis: a clinical, proof-of-concept study. *Ann Rheum Dis*, 69, 1251-2.
- CERVENAK, L., MORBIDELLI, L., DONATI, D., DONNINI, S., KAMBAYASHI, T., WILSON, J. L., AXELSON, H., CASTANOS-VELEZ, E., LJUNGGREN, H. G., MALEFYT, R. D., GRANGER, H. J., ZICHE, M. & BEJARANO, M. T. 2000. Abolished angiogenicity and tumorigenicity of Burkitt lymphoma by interleukin-10. *Blood*, 96, 2568-73.
- CHAKRAVARTY, S. & HERKENHAM, M. 2005. Toll-like receptor 4 on nonhematopoietic cells sustains CNS inflammation during endotoxemia, independent of systemic cytokines. *J Neurosci*, 25, 1788-96.
- CHALASANI, S. H., SABELKO, K. A., SUNSHINE, M. J., LITTMAN, D. R. & RAPER, J. A. 2003. A chemokine, SDF-1, reduces the effectiveness of multiple axonal repellents and is required for normal axon pathfinding. *J Neurosci*, 23, 1360-71.
- CHARO, I. F. & RANSOHOFF, R. M. 2006. The many roles of chemokines and chemokine receptors in inflammation. *N Engl J Med*, 354, 610-21.
- CHEN, Z. Y., JING, D., BATH, K. G., IERACI, A., KHAN, T., SIAO, C. J., HERRERA, D. G., TOTH, M., YANG, C., MCEWEN, B. S., HEMPSTEAD, B. L. & LEE, F. S. 2006. Genetic variant BDNF (Val66Met) polymorphism alters anxiety-related behavior. *Science*, 314, 140-3.
- CHIKAZU, D., HAKEDA, Y., OGATA, N., NEMOTO, K., ITABASHI, A., TAKATO, T., KUMEGAWA, M., NAKAMURA, K. & KAWAGUCHI, H. 2000. Fibroblast growth factor (FGF)-2 directly stimulates mature osteoclast function through activation of FGF receptor 1 and p42/p44 MAP kinase. *J Biol Chem*, 275, 31444-50.
- CHIO, C. C., LIN, J. W., CHANG, M. W., WANG, C. C., KUO, J. R., YANG, C. Z. & CHANG, C. P. 2010. Therapeutic evaluation of etanercept in a model of traumatic brain injury. *J Neurochem*, 115, 921-9.
- CHO, J., NELSON, T. E., BAJOVA, H. & GRUOL, D. L. 2009. Chronic CXCL10 alters neuronal properties in rat hippocampal culture. *J Neuroimmunol*, 207, 92-100.

- CHO, Y. G., CHO, M. L., MIN, S. Y. & KIM, H. Y. 2007. Type II collagen autoimmunity in a mouse model of human rheumatoid arthritis. *Autoimmun Rev*, 7, 65-70.
- CHOI, S. H., LI, Y., PARADA, L. F. & SISODIA, S. S. 2009. Regulation of hippocampal progenitor cell survival, proliferation and dendritic development by BDNF. *Mol Neurodegener*, 4, 52.
- CHOI, W. T., KAUL, M., KUMAR, S., WANG, J., KUMAR, I. M., DONG, C. Z., AN, J., LIPTON, S. A. & HUANG, Z. 2007. Neuronal apoptotic signaling pathways probed and intervened by synthetically and modularly modified (SMM) chemokines. *J Biol Chem*, 282, 7154-63.
- CHOU, W. H. & MESSING, R. O. 2008. Hypertensive encephalopathy and the blood-brain barrier: is deltaPKC a gatekeeper? *J Clin Invest*, 118, 17-20.
- CHOURBAJI, S., HELLWEG, R., BRANDIS, D., ZORNER, B., ZACHER, C., LANG, U. E., HENN, F. A., HORTNAGL, H. & GASS, P. 2004. Mice with reduced brain-derived neurotrophic factor expression show decreased choline acetyltransferase activity, but regular brain monoamine levels and unaltered emotional behavior. *Brain Res Mol Brain Res*, 121, 28-36.
- COISNE, C., MAO, W. & ENGELHARDT, B. 2009. Cutting edge: Natalizumab blocks adhesion but not initial contact of human T cells to the blood-brain barrier in vivo in an animal model of multiple sclerosis. *J Immunol*, 182, 5909-13.
- COLUMBA-CABEZAS, S., SERAFINI, B., AMBROSINI, E. & ALOISI, F. 2003. Lymphoid chemokines CCL19 and CCL21 are expressed in the central nervous system during experimental autoimmune encephalomyelitis: implications for the maintenance of chronic neuroinflammation. *Brain Pathol*, 13, 38-51.
- CONNOR, T. J., STARR, N., O'SULLIVAN, J. B. & HARKIN, A. 2008. Induction of indolamine 2,3-dioxygenase and kynurenine 3-monooxygenase in rat brain following a systemic inflammatory challenge: a role for IFN-gamma? *Neurosci Lett*, 441, 29-34.
- CONSTAM, D. B., PHILIPP, J., MALIPIERO, U. V., TEN DIJKE, P., SCHACHNER, M. & FONTANA, A. 1992. Differential expression of transforming growth factor-beta 1, -beta 2, and -beta 3 by glioblastoma cells, astrocytes, and microglia. *J Immunol*, 148, 1404-10.
- CONSTANTIN, G. 2008. Chemokine signaling and integrin activation in lymphocyte migration into the inflamed brain. *J Neuroimmunol*, 198, 20-6.
- CONSTANTINESCU, C. S., TANI, M., RANSOHOFF, R. M., WYSOCKA, M., HILLIARD, B., FUJIOKA, T., MURPHY, S., TIGHE, P. J., DAS SARMA, J., TRINCHIERI, G. & ROSTAMI, A. 2005. Astrocytes as antigen-presenting cells: expression of IL-12/IL-23. *J Neurochem*, 95, 331-40.
- COPE, A. P., ADERKA, D., DOHERTY, M., ENGELMANN, H., GIBBONS, D., JONES, A. C., BRENNAN, F. M., MAINI, R. N., WALLACH, D. & FELDMANN, M. 1992. Increased levels of soluble tumor necrosis factor receptors in the sera and synovial fluid of patients with rheumatic diseases. *Arthritis Rheum*, 35, 1160-9.
- CORREALE, J. & VILLA, A. 2009. Cellular elements of the blood-brain barrier. *Neurochem Res*, 34, 2067-77.
- COUILLARD-DESPRES, S., WINNER, B., SCHAUBECK, S., AIGNER, R., VROEMEN, M., WEIDNER, N., BOGDHORN, U., WINKLER, J., KUHN, H. G. & AIGNER, L. 2005. Doublecortin expression levels in adult brain reflect neurogenesis. *Eur J Neurosci*, 21, 1-14.

- COURTENAY, J. S., DALLMAN, M. J., DAYAN, A. D., MARTIN, A. & MOSEDALE, B. 1980. Immunisation against heterologous type II collagen induces arthritis in mice. *Nature*, 283, 666-8.
- CROLL, S. D., GOODMAN, J. H. & SCHARFMAN, H. E. 2004a. Vascular endothelial growth factor (VEGF) in seizures: a double-edged sword. *Adv Exp Med Biol*, 548, 57-68.
- CROLL, S. D., RANSOHOFF, R. M., CAI, N., ZHANG, Q., MARTIN, F. J., WEI, T., KASSELMAN, L. J., KINTNER, J., MURPHY, A. J., YANCOPOULOS, G. D. & WIEGAND, S. J. 2004b. VEGF-mediated inflammation precedes angiogenesis in adult brain. *Exp Neurol*, 187, 388-402.
- CRUPI, R., CAMBIAGHI, M., SPATZ, L., HEN, R., THORN, M., FRIEDMAN, E., VITA, G. & BATTAGLIA, F. 2010. Reduced adult neurogenesis and altered emotional behaviors in autoimmune-prone B-cell activating factor transgenic mice. *Biol Psychiatry*, 67, 558-66.
- CSOLLE, C. & SPERLAGH, B. 2010. Peripheral origin of IL-1beta production in the rodent hippocampus under in vivo systemic bacterial lipopolysaccharide (LPS) challenge and its regulation by P2X(7) receptors. *J Neuroimmunol*, 219, 38-46.
- CUMBERBATCH, M., GOULD, S. J., PETERS, S. W. & KIMBER, I. 1991. MHC class II expression by Langerhans' cells and lymph node dendritic cells: possible evidence for maturation of Langerhans' cells following contact sensitization. *Immunology*, 74, 414-9.
- CZEH, B. & LUCASSEN, P. J. 2007. What causes the hippocampal volume decrease in depression? Are neurogenesis, glial changes and apoptosis implicated? *Eur Arch Psychiatry Clin Neurosci*, 257, 250-60.
- CZEH, B., MICHAELIS, T., WATANABE, T., FRAHM, J., DE BIURRUN, G., VAN KAMPEN, M., BARTOLOMUCCI, A. & FUCHS, E. 2001. Stress-induced changes in cerebral metabolites, hippocampal volume, and cell proliferation are prevented by antidepressant treatment with tianeptine. *Proc Natl Acad Sci U S A*, 98, 12796-801.
- D'MELLO, C., LE, T. & SWAIN, M. G. 2009. Cerebral microglia recruit monocytes into the brain in response to tumor necrosis factor alpha signaling during peripheral organ inflammation. *J Neurosci*, 29, 2089-102.
- DAI, W. & GUPTA, S. L. 1990. Regulation of indoleamine 2,3-dioxygenase gene expression in human fibroblasts by interferon-gamma. Upstream control region discriminates between interferon-gamma and interferon-alpha. *J Biol Chem*, 265, 19871-7.
- DANTZER, R., O'CONNOR, J. C., FREUND, G. G., JOHNSON, R. W. & KELLEY, K. W. 2008. From inflammation to sickness and depression: when the immune system subjugates the brain. *Nat Rev Neurosci*, 9, 46-56.
- DAS, M. P., NICHOLSON, L. B., GREER, J. M. & KUCHROO, V. K. 1997. Autoantigenic T helper cell type 1 (Th1) and protective Th2 clones differ in their recognition of the autoantigenic peptide of myelin proteolipid protein. *J Exp Med*, 186, 867-76.
- DATTA, S. C. & OPP, M. R. 2008. Lipopolysaccharide-induced increases in cytokines in discrete mouse brain regions are detectable using Luminex xMAP technology. *J Neurosci Methods*, 175, 119-24.
- DAVID, D. J., SAMUELS, B. A., RAINER, Q., WANG, J. W., MARSTELLER, D., MENDEZ, I., DREW, M., CRAIG, D. A., GUIARD, B. P., GUILLOUX, J. P., ARTYMYSHYN, R. P., GARDIER, A. M., GERALD, C., ANTONIJEVIC, I. A., LEONARDO, E. D. & HEN, R. 2009. Neurogenesis-dependent and -independent effects of fluoxetine in an animal model of anxiety/depression. *Neuron*, 62, 479-93.

- DAYER, J. M. & CHOY, E. 2010. Therapeutic targets in rheumatoid arthritis: the interleukin-6 receptor. *Rheumatology (Oxford)*, 49, 15-24.
- DAYER, J. M. & FENNER, H. 1992. The role of cytokines and their inhibitors in arthritis. *Baillieres Clin Rheumatol*, 6, 485-516.
- DE JONG, E. K., DIJKSTRA, I. M., HENSENS, M., BROUWER, N., VAN AMERONGEN, M., LIEM, R. S., BODDEKE, H. W. & BIBER, K. 2005. Vesicle-mediated transport and release of CCL21 in endangered neurons: a possible explanation for microglia activation remote from a primary lesion. *J Neurosci*, 25, 7548-57.
- DE JONG, E. K., VINET, J., STANULOVIC, V. S., MEIJER, M., WESSELING, E., SJOLLEMA, K., BODDEKE, H. W. & BIBER, K. 2008. Expression, transport, and axonal sorting of neuronal CCL21 in large dense-core vesicles. *FASEB J*, 22, 4136-45.
- DE VOS, A. F., VAN MEURS, M., BROK, H. P., BOVEN, L. A., HINTZEN, R. Q., VAN DER VALK, P., RAVID, R., RENSING, S., BOON, L., T HART, B. A. & LAMAN, J. D. 2002. Transfer of central nervous system autoantigens and presentation in secondary lymphoid organs. *J Immunol*, 169, 5415-23.
- DE WAAL MALEFYT, R., ABRAMS, J., BENNETT, B., FIGDOR, C. G. & DE VRIES, J. E. 1991. Interleukin 10(IL-10) inhibits cytokine synthesis by human monocytes: an autoregulatory role of IL-10 produced by monocytes. *J Exp Med*, 174, 1209-20.
- DEL REY, A., WOLFF, C., WILDMANN, J., RANDOLF, A., HAHNEL, A., BESEDOVSKY, H. O. & STRAUB, R. H. 2008. Disrupted brain-immune system-joint communication during experimental arthritis. *Arthritis Rheum*, 58, 3090-9.
- DELVES, P. J. & ROITT, I. M. 2000a. The immune system. First of two parts. *N Engl J Med*, 343, 37-49.
- DELVES, P. J. & ROITT, I. M. 2000b. The immune system. Second of two parts. *N Engl J Med*, 343, 108-17.
- DENG, W., AIMONE, J. B. & GAGE, F. H. 2010. New neurons and new memories: how does adult hippocampal neurogenesis affect learning and memory? *Nat Rev Neurosci*, 11, 339-50.
- DEPUYDT, B., VAN LOO, G., VANDENABEELE, P. & DECLERCQ, W. 2005. Induction of apoptosis by TNF receptor 2 in a T-cell hybridoma is FADD dependent and blocked by caspase-8 inhibitors. *J Cell Sci*, 118, 497-504.
- DHABHAR, F. S., BURKE, H. M., EPEL, E. S., MELLON, S. H., ROSSER, R., REUS, V. I. & WOLKOWITZ, O. M. 2009. Low serum IL-10 concentrations and loss of regulatory association between IL-6 and IL-10 in adults with major depression. *J Psychiatr Res*, 43, 962-9.
- DICKENS, C., MCGOWAN, L., CLARK-CARTER, D. & CREED, F. 2002. Depression in rheumatoid arthritis: a systematic review of the literature with meta-analysis. *Psychosom Med*, 64, 52-60.
- DIMITRIJEVIC, O. B., STAMATOVIC, S. M., KEEP, R. F. & ANDJELKOVIC, A. V. 2006. Effects of the chemokine CCL2 on blood-brain barrier permeability during ischemia-reperfusion injury. *J Cereb Blood Flow Metab*, 26, 797-810.
- DINGES, D. F., DOUGLAS, S. D., ZAUGG, L., CAMPBELL, D. E., MCMANN, J. M., WHITEHOUSE, W. G., ORNE, E. C., KAPOOR, S. C., ICAZA, E. & ORNE, M. T. 1994. Leukocytosis and natural killer cell function parallel neurobehavioral fatigue induced by 64 hours of sleep deprivation. *J Clin Invest*, 93, 1930-9.
- DOLHAIN, R. J., VAN DER HEIDEN, A. N., TER HAAR, N. T., BREEDVELD, F. C. & MILTENBURG, A. M. 1996. Shift toward T lymphocytes with a T helper 1

- cytokine-secretion profile in the joints of patients with rheumatoid arthritis. *Arthritis Rheum*, 39, 1961-9.
- DONG, Y. & BENVENISTE, E. N. 2001. Immune function of astrocytes. *Glia*, 36, 180-90.
- DOWLATI, Y., HERRMANN, N., SWARDFAGER, W., LIU, H., SHAM, L., REIM, E. K. & LANCTOT, K. L. 2010. A meta-analysis of cytokines in major depression. *Biol Psychiatry*, 67, 446-57.
- DUPRET, D., REVEST, J. M., KOEHL, M., ICHAS, F., DE GIORGI, F., COSTET, P., ABROUS, D. N. & PIAZZA, P. V. 2008. Spatial relational memory requires hippocampal adult neurogenesis. *PLoS One*, 3, e1959.
- DURIC, V. & MCCARSON, K. E. 2006. Persistent pain produces stress-like alterations in hippocampal neurogenesis and gene expression. *J Pain*, 7, 544-55.
- EKDAHL, C. T., CLAASEN, J. H., BONDE, S., KOKAIA, Z. & LINDVALL, O. 2003. Inflammation is detrimental for neurogenesis in adult brain. *Proc Natl Acad Sci U S A*, 100, 13632-7.
- EL-ZAYADI, A. R. 2009. Hepatitis C comorbidities affecting the course and response to therapy. *World J Gastroenterol*, 15, 4993-9.
- ELLER, T., ALUOJA, A., MARON, E. & VASAR, V. 2009. Soluble interleukin-2 receptor and tumor necrosis factor levels in depressed patients in Estonia. *Medicina (Kaunas)*, 45, 971-7.
- ELLIS, S. L., GYSBERS, V., MANDERS, P. M., LI, W., HOFER, M. J., MULLER, M. & CAMPBELL, I. L. 2010. The cell-specific induction of CXC chemokine ligand 9 mediated by IFN-gamma in microglia of the central nervous system is determined by the myeloid transcription factor PU.1. *J Immunol*, 185, 1864-77.
- ENGELHARDT, B. 2006. Regulation of immune cell entry into the central nervous system. *Results Probl Cell Differ*, 43, 259-80.
- ENGELHARDT, B., CONLEY, F. K. & BUTCHER, E. C. 1994. Cell adhesion molecules on vessels during inflammation in the mouse central nervous system. *J Neuroimmunol*, 51, 199-208.
- ENGELHARDT, B., MARTIN-SIMONET, M. T., ROTT, L. S., BUTCHER, E. C. & MICHIE, S. A. 1998. Adhesion molecule phenotype of T lymphocytes in inflamed CNS. *J Neuroimmunol*, 84, 92-104.
- ENGUM, A., MYKLETUN, A., MIDTHJELL, K., HOLEN, A. & DAHL, A. A. 2005. Depression and diabetes: a large population-based study of sociodemographic, lifestyle, and clinical factors associated with depression in type 1 and type 2 diabetes. *Diabetes Care*, 28, 1904-9.
- FABIS, M. J., SCOTT, G. S., KEAN, R. B., KOPROWSKI, H. & HOOPER, D. C. 2007. Loss of blood-brain barrier integrity in the spinal cord is common to experimental allergic encephalomyelitis in knockout mouse models. *Proc Natl Acad Sci U S A*, 104, 5656-61.
- FABRIEK, B. O., ZWEMMER, J. N., TEUNISSEN, C. E., DIJKSTRA, C. D., POLMAN, C. H., LAMAN, J. D. & CASTELIJNS, J. A. 2005. In vivo detection of myelin proteins in cervical lymph nodes of MS patients using ultrasound-guided fine-needle aspiration cytology. *J Neuroimmunol*, 161, 190-4.
- FAN, M. M. & RAYMOND, L. A. 2007. N-methyl-D-aspartate (NMDA) receptor function and excitotoxicity in Huntington's disease. *Prog Neurobiol*, 81, 272-93.
- FARINA, C., ALOISI, F. & MEINL, E. 2007. Astrocytes are active players in cerebral innate immunity. *Trends Immunol*, 28, 138-45.
- FARIOLI-VECCHIOLI, S., SARAULLI, D., COSTANZI, M., LEONARDI, L., CINA, I., MICHELI, L., NUTINI, M., LONGONE, P., OH, S. P., CESTARI, V. & TIRONE,

- F. 2009. Impaired terminal differentiation of hippocampal granule neurons and defective contextual memory in PC3/Tis21 knockout mice. *PLoS One*, 4, e8339.
- FARIOLI-VECCHIOLI, S., SARAULLI, D., COSTANZI, M., PACIONI, S., CINA, I., ACETI, M., MICHELI, L., BACCI, A., CESTARI, V. & TIRONE, F. 2008. The timing of differentiation of adult hippocampal neurons is crucial for spatial memory. *PLoS Biol*, 6, e246.
- FARRAR, M. A. & SCHREIBER, R. D. 1993. The molecular cell biology of interferon-gamma and its receptor. *Annu Rev Immunol*, 11, 571-611.
- FASTH, A. E., SNIR, O., JOHANSSON, A. A., NORDMARK, B., RAHBAR, A., AF KLINT, E., BJORKSTROM, N. K., ULFGREN, A. K., VAN VOLLENHOVEN, R. F., MALMSTROM, V. & TROLLMO, C. 2007. Skewed distribution of proinflammatory CD4+CD28null T cells in rheumatoid arthritis. *Arthritis Res Ther*, 9, R87.
- FEILI-HARIRI, M., FALKNER, D. H. & MOREL, P. A. 2005. Polarization of naive T cells into Th1 or Th2 by distinct cytokine-driven murine dendritic cell populations: implications for immunotherapy. *J Leukoc Biol*, 78, 656-64.
- FELGER, J. C., ALAGBE, O., HU, F., MOOK, D., FREEMAN, A. A., SANCHEZ, M. M., KALIN, N. H., RATTI, E., NEMEROFF, C. B. & MILLER, A. H. 2007. Effects of interferon-alpha on rhesus monkeys: a nonhuman primate model of cytokine-induced depression. *Biol Psychiatry*, 62, 1324-33.
- FERNANDEZ, E. J. & LOLIS, E. 2002. Structure, function, and inhibition of chemokines. *Annu Rev Pharmacol Toxicol*, 42, 469-99.
- FERNSTROM, M. H., MASSOUDI, M. S. & FERNSTROM, J. D. 1990. Effect of 8-hydroxy-2-(di-n-propylamino)-tetralin on the tryptophan-induced increase in 5-hydroxytryptophan accumulation in rat brain. *Life Sci*, 47, 283-9.
- FERRACCIOLI, G., BRACCI-LAUDIERO, L., ALIVERNINI, S., GREMESE, E., TOLUSSO, B. & DE BENEDETTI, F. 2010. Interleukin-1beta and interleukin-6 in arthritis animal models: roles in the early phase of transition from acute to chronic inflammation and relevance for human rheumatoid arthritis. *Mol Med*, 16, 552-7.
- FINKELMAN, F. D., KATONA, I. M., MOSMANN, T. R. & COFFMAN, R. L. 1988. IFN-gamma regulates the isotypes of Ig secreted during in vivo humoral immune responses. *J Immunol*, 140, 1022-7.
- FOROUZANDEH, F., JALILI, R. B., GERMAIN, M., DURONIO, V. & GHAHARY, A. 2008. Differential immunosuppressive effect of indoleamine 2,3-dioxygenase (IDO) on primary human CD4+ and CD8+ T cells. *Mol Cell Biochem*, 309, 1-7.
- FRANCIS, J., CHU, Y., JOHNSON, A. K., WEISS, R. M. & FELDER, R. B. 2004. Acute myocardial infarction induces hypothalamic cytokine synthesis. *Am J Physiol Heart Circ Physiol*, 286, H2264-71.
- FRANZEN, P. L., BUYSSE, D. J., RABINOVITZ, M., POLLOCK, B. G. & LOTRICH, F. E. 2010. Poor sleep quality predicts onset of either major depression or subsyndromal depression with irritability during interferon-alpha treatment. *Psychiatry Res*, 177, 240-5.
- FRODL, T., SCHAUB, A., BANAC, S., CHARYPAR, M., JAGER, M., KUMMLER, P., BOTTLENDER, R., ZETZSCHE, T., BORN, C., LEINSINGER, G., REISER, M., MOLLER, H. J. & MEISENZAHL, E. M. 2006. Reduced hippocampal volume correlates with executive dysfunctioning in major depression. *J Psychiatry Neurosci*, 31, 316-23.
- FURTADO, G. C., MARCONDES, M. C., LATKOWSKI, J. A., TSAI, J., WENSKY, A. & LAFAILLE, J. J. 2008. Swift entry of myelin-specific T lymphocytes into

- the central nervous system in spontaneous autoimmune encephalomyelitis. *J Immunol*, 181, 4648-55.
- GABELLEC, M. M., GRIFFAIS, R., FILLION, G. & HAOUR, F. 1996. Interleukin-1 receptors type I and type II in the mouse brain: kinetics of mRNA expressions after peripheral administration of bacterial lipopolysaccharide. *J Neuroimmunol*, 66, 65-70.
- GALEA, I., BERNARDES-SILVA, M., FORSE, P. A., VAN ROOIJEN, N., LIBLAU, R. S. & PERRY, V. H. 2007. An antigen-specific pathway for CD8 T cells across the blood-brain barrier. *J Exp Med*, 204, 2023-30.
- GALLO, R. C. 1972. RNA-dependent DNA polymerase in viruses and cells: views on the current state. *Blood*, 39, 117-37.
- GARCIA-VICUNA, R., GOMEZ-GAVIRO, M. V., DOMINGUEZ-LUIS, M. J., PEC, M. K., GONZALEZ-ALVARO, I., ALVARO-GRACIA, J. M. & DIAZ-GONZALEZ, F. 2004. CC and CXC chemokine receptors mediate migration, proliferation, and matrix metalloproteinase production by fibroblast-like synoviocytes from rheumatoid arthritis patients. *Arthritis Rheum*, 50, 3866-77.
- GATTI, S. & BARTFAI, T. 1993. Induction of tumor necrosis factor-alpha mRNA in the brain after peripheral endotoxin treatment: comparison with interleukin-1 family and interleukin-6. *Brain Res*, 624, 291-4.
- GELENBERG, A. J. 2010. The prevalence and impact of depression. *J Clin Psychiatry*, 71, e06.
- GENG, H., CARLSEN, S., NANDAKUMAR, K. S., HOLMDAHL, R., ASPBERG, A., OLDBERG, A. & MATTSSON, R. 2008. Cartilage oligomeric matrix protein deficiency promotes early onset and the chronic development of collagen-induced arthritis. *Arthritis Res Ther*, 10, R134.
- GERLI, R., SCHILLACI, G., GIORDANO, A., BOCCI, E. B., BISTONI, O., VAUDO, G., MARCHESI, S., PIRRO, M., RAGNI, F., SHOENFELD, Y. & MANNARINO, E. 2004. CD4+CD28- T lymphocytes contribute to early atherosclerotic damage in rheumatoid arthritis patients. *Circulation*, 109, 2744-8.
- GIRVIN, A. M., DAL CANTO, M. C. & MILLER, S. D. 2002. CD40/CD40L interaction is essential for the induction of EAE in the absence of CD28-mediated co-stimulation. *J Autoimmun*, 18, 83-94.
- GIULIAN, D., BAKER, T. J., SHIH, L. C. & LACHMAN, L. B. 1986. Interleukin 1 of the central nervous system is produced by ameboid microglia. *J Exp Med*, 164, 594-604.
- GLABINSKI, A. R., BIELECKI, B. & RANSOHOFF, R. M. 2003. Chemokine upregulation follows cytokine expression in chronic relapsing experimental autoimmune encephalomyelitis. *Scand J Immunol*, 58, 81-8.
- GOLDMANN, J., KWIDZINSKI, E., BRANDT, C., MAHLO, J., RICHTER, D. & BECHMANN, I. 2006. T cells traffic from brain to cervical lymph nodes via the cribroid plate and the nasal mucosa. *J Leukoc Biol*, 80, 797-801.
- GOTLIB, I. H. & JOORMANN, J. 2010. Cognition and depression: current status and future directions. *Annu Rev Clin Psychol*, 6, 285-312.
- GOTO, M., DERIY, L. V., CHEN, Y. J., BENO, D. W., UHING, M. R., JIYAMAPA-SERNA, V. A. & KIMURA, R. E. 2001. TNF-alpha increases sensitivity to LPS in chronically catheterized rats. *Am J Physiol Heart Circ Physiol*, 280, H2857-62.
- GOUKASSIAN, D. A., QIN, G., DOLAN, C., MURAYAMA, T., SILVER, M., CURRY, C., EATON, E., LUEDEMANN, C., MA, H., ASAHARA, T., ZAK, V., MEHTA, S., BURG, A., THORNE, T., KISHORE, R. & LOSORDO, D. W. 2007. Tumor necrosis factor-alpha receptor p75 is required in ischemia-induced neovascularization. *Circulation*, 115, 752-62.

- GOVERMAN, J. 2009. Autoimmune T cell responses in the central nervous system. *Nat Rev Immunol*, 9, 393-407.
- GRAEBER, M. B. & STREIT, W. J. 2010. Microglia: biology and pathology. *Acta Neuropathol*, 119, 89-105.
- GRAHAM, G. J. 2009. D6 and the atypical chemokine receptor family: Novel regulators of immune and inflammatory processes. *European Journal of Immunology*, 39, 342-351.
- GRALINSKI, L. E., ASHLEY, S. L., DIXON, S. D. & SPINDLER, K. R. 2009. Mouse adenovirus type 1-induced breakdown of the blood-brain barrier. *J Virol*, 83, 9398-410.
- GRASSI-OLIVEIRA, R., BRIETZKE, E., PEZZI, J. C., LOPES, R. P., TEIXEIRA, A. L. & BAUER, M. E. 2009. Increased soluble tumor necrosis factor-alpha receptors in patients with major depressive disorder. *Psychiatry Clin Neurosci*, 63, 202-8.
- GREBE, K. M., HICKMAN, H. D., IRVINE, K. R., TAKEDA, K., BENNINK, J. R. & YEWDELL, J. W. 2009. Sympathetic nervous system control of anti-influenza CD8+ T cell responses. *Proc Natl Acad Sci U S A*, 106, 5300-5.
- GRECO, S. J. & RAMESHWAR, P. 2007. Enhancing effect of IL-1alpha on neurogenesis from adult human mesenchymal stem cells: implication for inflammatory mediators in regenerative medicine. *J Immunol*, 179, 3342-50.
- GREER, J. M., CSURHES, P. A., MULLER, D. M. & PENDER, M. P. 2008. Correlation of blood T cell and antibody reactivity to myelin proteins with HLA type and lesion localization in multiple sclerosis. *J Immunol*, 180, 6402-10.
- GREGORY, B., KIRCHEM, A., PHIPPS, S., GEVAERT, P., PRIDGEON, C., RANKIN, S. M. & ROBINSON, D. S. 2003. Differential regulation of human eosinophil IL-3, IL-5, and GM-CSF receptor alpha-chain expression by cytokines: IL-3, IL-5, and GM-CSF down-regulate IL-5 receptor alpha expression with loss of IL-5 responsiveness, but up-regulate IL-3 receptor alpha expression. *J Immunol*, 170, 5359-66.
- GRETER, M., HEPPNER, F. L., LEMOS, M. P., ODERMATT, B. M., GOEBELS, N., LAUFER, T., NOELLE, R. J. & BECHER, B. 2005. Dendritic cells permit immune invasion of the CNS in an animal model of multiple sclerosis. *Nat Med*, 11, 328-34.
- GRINEVICH, V., MA, X. M., HERMAN, J. P., JEZOVA, D., AKMAYEV, I. & AGUILERA, G. 2001. Effect of repeated lipopolysaccharide administration on tissue cytokine expression and hypothalamic-pituitary-adrenal axis activity in rats. *J Neuroendocrinol*, 13, 711-23.
- GU, L., TSENG, S., HORNER, R. M., TAM, C., LODA, M. & ROLLINS, B. J. 2000. Control of TH2 polarization by the chemokine monocyte chemoattractant protein-1. *Nature*, 404, 407-11.
- GUAN, Z. & FANG, J. 2006. Peripheral immune activation by lipopolysaccharide decreases neurotrophins in the cortex and hippocampus in rats. *Brain Behav Immun*, 20, 64-71.
- GUDBJORNSSON, B. & HETTA, J. 2001. Sleep disturbances in patients with systemic lupus erythematosus: a questionnaire-based study. *Clin Exp Rheumatol*, 19, 509-14.
- GUO, H., JIN, Y. X., ISHIKAWA, M., HUANG, Y. M., VAN DER MEIDE, P. H., LINK, H. & XIAO, B. G. 1998. Regulation of beta-chemokine mRNA expression in adult rat astrocytes by lipopolysaccharide, proinflammatory and immunoregulatory cytokines. *Scand J Immunol*, 48, 502-8.

- GUTIERREZ, E. G., BANKS, W. A. & KASTIN, A. J. 1993. Murine tumor necrosis factor alpha is transported from blood to brain in the mouse. *J Neuroimmunol*, 47, 169-76.
- HABERHAUER, G., STREHLOW, C. & FASCHING, P. 2010. Observational study of switching anti-TNF agents in ankylosing spondylitis and psoriatic arthritis versus rheumatoid arthritis. *Wien Med Wochenschr*, 160, 220-4.
- HADDAD, J. J. 2002. Cytokines and related receptor-mediated signaling pathways. *Biochem Biophys Res Commun*, 297, 700-13.
- HADID, R., SPINEDI, E., CHAUTARD, T., GIACOMINI, M. & GAILLARD, R. C. 1999. Role of several mediators of inflammation on the mouse hypothalamo-pituitary-adrenal axis response during acute endotoxemia. *Neuroimmunomodulation*, 6, 336-43.
- HAFEZI-MOGHADAM, A., THOMAS, K. L. & WAGNER, D. D. 2007. ApoE deficiency leads to a progressive age-dependent blood-brain barrier leakage. *Am J Physiol Cell Physiol*, 292, C1256-62.
- HANSEN, M. K., TAISHI, P., CHEN, Z. & KRUEGER, J. M. 1998. Vagotomy blocks the induction of interleukin-1beta (IL-1beta) mRNA in the brain of rats in response to systemic IL-1beta. *J Neurosci*, 18, 2247-53.
- HARNETT, M. M., KEAN, D. E., BOITELLE, A., MCGUINNESS, S., THALHAMER, T., STEIGER, C. N., EGAN, C., AL-RIYAMI, L., ALCOCER, M. J., HOUSTON, K. M., GRACIE, J. A., MCINNES, I. B. & HARNETT, W. 2008. The phosphorycholine moiety of the filarial nematode immunomodulator ES-62 is responsible for its anti-inflammatory action in arthritis. *Ann Rheum Dis*, 67, 518-23.
- HARRY, G. J., LEFEBVRE D'HELLEN COURT, C., MCPHERSON, C. A., FUNK, J. A., AOYAMA, M. & WINE, R. N. 2008. Tumor necrosis factor p55 and p75 receptors are involved in chemical-induced apoptosis of dentate granule neurons. *J Neurochem*, 106, 281-98.
- HASHIOKA, S., KLEGERIS, A., MONJI, A., KATO, T., SAWADA, M., MCGEER, P. L. & KANBA, S. 2007. Antidepressants inhibit interferon-gamma-induced microglial production of IL-6 and nitric oxide. *Exp Neurol*, 206, 33-42.
- HATTERER, E., DAVOUST, N., DIDIER-BAZES, M., VUAILLAT, C., MALCUS, C., BELIN, M. F. & NATAF, S. 2006. How to drain without lymphatics? Dendritic cells migrate from the cerebrospinal fluid to the B-cell follicles of cervical lymph nodes. *Blood*, 107, 806-12.
- HATTERER, E., TOURET, M., BELIN, M. F., HONNORAT, J. & NATAF, S. 2008. Cerebrospinal fluid dendritic cells infiltrate the brain parenchyma and target the cervical lymph nodes under neuroinflammatory conditions. *PLoS One*, 3, e3321.
- HAWKINS, B. T., LUNDEEN, T. F., NORWOOD, K. M., BROOKS, H. L. & EGLETON, R. D. 2007. Increased blood-brain barrier permeability and altered tight junctions in experimental diabetes in the rat: contribution of hyperglycaemia and matrix metalloproteinases. *Diabetologia*, 50, 202-11.
- HAYASHI, M., LUO, Y., LANING, J., STRIETER, R. M. & DORF, M. E. 1995. Production and function of monocyte chemoattractant protein-1 and other beta-chemokines in murine glial cells. *J Neuroimmunol*, 60, 143-50.
- HEGEN, M., KEITH, J. C., JR., COLLINS, M. & NICKERSON-NUTTER, C. L. 2008. Utility of animal models for identification of potential therapeutics for rheumatoid arthritis. *Ann Rheum Dis*, 67, 1505-15.
- HEINISCH, S. & KIRBY, L. G. 2009. Fractalkine/CX3CL1 enhances GABA synaptic activity at serotonin neurons in the rat dorsal raphe nucleus. *Neuroscience*, 164, 1210-23.

- HEINISCH, S. & KIRBY, L. G. 2010. SDF-1 α /CXCL12 enhances GABA and glutamate synaptic activity at serotonin neurons in the rat dorsal raphe nucleus. *Neuropharmacology*, 58, 501-14.
- HEINZEL, K., BENZ, C. & BLEUL, C. C. 2007. A silent chemokine receptor regulates steady-state leukocyte homing in vivo. *Proc Natl Acad Sci U S A*, 104, 8421-6.
- HEISER, P., LANQUILLON, S., KRIEG, J. C. & VEDDER, H. 2008. Differential modulation of cytokine production in major depressive disorder by cortisol and dexamethasone. *Eur Neuropsychopharmacol*, 18, 860-70.
- HENRY, C. J., HUANG, Y., WYNNE, A. M. & GODBOUT, J. P. 2009. Peripheral lipopolysaccharide (LPS) challenge promotes microglial hyperactivity in aged mice that is associated with exaggerated induction of both pro-inflammatory IL-1 β and anti-inflammatory IL-10 cytokines. *Brain Behav Immun*, 23, 309-17.
- HERVE, F., GHINEA, N. & SCHERRMANN, J. M. 2008. CNS delivery via adsorptive transcytosis. *AAPS J*, 10, 455-72.
- HICKEY, W. F. 1999. Leukocyte traffic in the central nervous system: the participants and their roles. *Semin Immunol*, 11, 125-37.
- HIGGINS, G. A. & OLSCHOWKA, J. A. 1991. Induction of interleukin-1 beta mRNA in adult rat brain. *Brain Res Mol Brain Res*, 9, 143-8.
- HITCHON, C. A., ALEX, P., ERDILE, L. B., FRANK, M. B., DOZMOROV, I., TANG, Y., WONG, K., CENTOLA, M. & EL-GABALAWY, H. S. 2004. A distinct multicytokine profile is associated with anti-cyclical citrullinated peptide antibodies in patients with early untreated inflammatory arthritis. *J Rheumatol*, 31, 2336-46.
- HITCHON, C. A. & EL-GABALAWY, H. S. 2002. Immune features of seronegative and seropositive arthritis in early synovitis studies. *Curr Opin Rheumatol*, 14, 348-53.
- HOFSTETTER, H. H., SEWELL, D. L., LIU, F., SANDOR, M., FORSTHUBER, T., LEHMANN, P. V. & FABRY, Z. 2003. Autoreactive T cells promote post-traumatic healing in the central nervous system. *J Neuroimmunol*, 134, 25-34.
- HOLGATE, S. T. 2004. Cytokine and anti-cytokine therapy for the treatment of asthma and allergic disease. *Cytokine*, 28, 152-7.
- HOLMDAHL, R., BOCKERMANN, R., BACKLUND, J. & YAMADA, H. 2002. The molecular pathogenesis of collagen-induced arthritis in mice--a model for rheumatoid arthritis. *Ageing Res Rev*, 1, 135-47.
- HOLMDAHL, R., JONSSON, R., LARSSON, P. & KLARESKOG, L. 1988. Early appearance of activated CD4⁺ T lymphocytes and class II antigen-expressing cells in joints of DBA/1 mice immunized with type II collagen. *Lab Invest*, 58, 53-60.
- HOLOSHITZ, J. 2010. The rheumatoid arthritis HLA-DRB1 shared epitope. *Curr Opin Rheumatol*, 22, 293-8.
- HONG, K. H., CHO, M. L., MIN, S. Y., SHIN, Y. J., YOO, S. A., CHOI, J. J., KIM, W. U., SONG, S. W. & CHO, C. S. 2007. Effect of interleukin-4 on vascular endothelial growth factor production in rheumatoid synovial fibroblasts. *Clin Exp Immunol*, 147, 573-9.
- HOSOI, T., OKUMA, Y. & NOMURA, Y. 2000. Electrical stimulation of afferent vagus nerve induces IL-1 β expression in the brain and activates HPA axis. *Am J Physiol Regul Integr Comp Physiol*, 279, R141-7.
- HOSSAIN, A., ZHENG, C. L., KUKITA, A. & KOHASHI, O. 2001. Balance of Th1/Th2 cytokines associated with the preventive effect of incomplete Freund's

- adjuvant on the development of adjuvant arthritis in LEW rats. *J Autoimmun*, 17, 289-95.
- HOWLAND, J. G. & WANG, Y. T. 2008. Synaptic plasticity in learning and memory: stress effects in the hippocampus. *Prog Brain Res*, 169, 145-58.
- HUANG, G. J., BANNERMAN, D. & FLINT, J. 2008. Chronic fluoxetine treatment alters behavior, but not adult hippocampal neurogenesis, in BALB/cJ mice. *Mol Psychiatry*, 13, 119-21.
- HUANG, T. L. & LEE, C. T. 2007. T-helper 1/T-helper 2 cytokine imbalance and clinical phenotypes of acute-phase major depression. *Psychiatry Clin Neurosci*, 61, 415-20.
- HUBER, J. D., WITT, K. A., HOM, S., EGLETON, R. D., MARK, K. S. & DAVIS, T. P. 2001. Inflammatory pain alters blood-brain barrier permeability and tight junctional protein expression. *Am J Physiol Heart Circ Physiol*, 280, H1241-8.
- HUGGETT, J., DHEDA, K., BUSTIN, S. & ZUMLA, A. 2005. Real-time RT-PCR normalisation; strategies and considerations. *Genes Immun*, 6, 279-84.
- HURWITZ, A. A., LYMAN, W. D. & BERMAN, J. W. 1995. Tumor necrosis factor alpha and transforming growth factor beta upregulate astrocyte expression of monocyte chemoattractant protein-1. *J Neuroimmunol*, 57, 193-8.
- HWANG, I. K., YI, S. S., KIM, Y. N., KIM, I. Y., LEE, I. S., YOON, Y. S. & SEONG, J. K. 2008. Reduced hippocampal cell differentiation in the subgranular zone of the dentate gyrus in a rat model of type II diabetes. *Neurochem Res*, 33, 394-400.
- ICHIMURA, T., FRASER, P. A. & CSERR, H. F. 1991. Distribution of extracellular tracers in perivascular spaces of the rat brain. *Brain Res*, 545, 103-13.
- INGLIS, J. J., NOTLEY, C. A., ESSEX, D., WILSON, A. W., FELDMANN, M., ANAND, P. & WILLIAMS, R. 2007. Collagen-induced arthritis as a model of hyperalgesia: functional and cellular analysis of the analgesic actions of tumor necrosis factor blockade. *Arthritis Rheum*, 56, 4015-23.
- INGLIS, J. J., SIMELYTE, E., MCCANN, F. E., CRIADO, G. & WILLIAMS, R. O. 2008. Protocol for the induction of arthritis in C57BL/6 mice. *Nat Protoc*, 3, 612-8.
- IOSIF, R. E., EKDAHL, C. T., AHLENIUS, H., PRONK, C. J., BONDE, S., KOKAIA, Z., JACOBSEN, S. E. & LINDVALL, O. 2006. Tumor necrosis factor receptor 1 is a negative regulator of progenitor proliferation in adult hippocampal neurogenesis. *J Neurosci*, 26, 9703-12.
- ISIK, A., KOCA, S. S., OZTURK, A. & MERMI, O. 2007. Anxiety and depression in patients with rheumatoid arthritis. *Clin Rheumatol*, 26, 872-8.
- ISSAZADEH, S., LJUNGDAHL, A., HOJEBERG, B., MUSTAFA, M. & OLSSON, T. 1995. Cytokine production in the central nervous system of Lewis rats with experimental autoimmune encephalomyelitis: dynamics of mRNA expression for interleukin-10, interleukin-12, cytolytic, tumor necrosis factor alpha and tumor necrosis factor beta. *J Neuroimmunol*, 61, 205-12.
- ISSAZADEH, S., LORENTZEN, J. C., MUSTAFA, M. I., HOJEBERG, B., MUSSENER, A. & OLSSON, T. 1996. Cytokines in relapsing experimental autoimmune encephalomyelitis in DA rats: persistent mRNA expression of proinflammatory cytokines and absent expression of interleukin-10 and transforming growth factor-beta. *J Neuroimmunol*, 69, 103-15.
- ISSAZADEH, S., NAVIKAS, V., SCHAUB, M., SAYEGH, M. & KHOURY, S. 1998. Kinetics of expression of costimulatory molecules and their ligands in murine relapsing experimental autoimmune encephalomyelitis in vivo. *J Immunol*, 161, 1104-12.

- IWAMOTO, T., OKAMOTO, H., TOYAMA, Y. & MOMOHARA, S. 2008. Molecular aspects of rheumatoid arthritis: chemokines in the joints of patients. *Febs J*, 275, 4448-55.
- JACOBS, B. L., VAN PRAAG, H. & GAGE, F. H. 2000. Adult brain neurogenesis and psychiatry: a novel theory of depression. *Mol Psychiatry*, 5, 262-9.
- JAECKEL, E., CORNBERG, M., WEDEMEYER, H., SANTANTONIO, T., MAYER, J., ZANKEL, M., PASTORE, G., DIETRICH, M., TRAUTWEIN, C. & MANN, M. P. 2001. Treatment of acute hepatitis C with interferon alfa-2b. *N Engl J Med*, 345, 1452-7.
- JAHN, B., BURMESTER, G. R., SCHMID, H., WESELOH, G., ROHWER, P. & KALDEN, J. R. 1987. Changes in cell surface antigen expression on human articular chondrocytes induced by gamma-interferon. Induction of Ia antigens. *Arthritis Rheum*, 30, 64-74.
- JANSON, C., DE BACKER, W., GISLASON, T., PLASCHKE, P., BJORNSSON, E., HETTA, J., KRISTBJARNARSON, H., VERMEIRE, P. & BOMAN, G. 1996. Increased prevalence of sleep disturbances and daytime sleepiness in subjects with bronchial asthma: a population study of young adults in three European countries. *Eur Respir J*, 9, 2132-8.
- JIANG, Y., DEACON, R., ANTHONY, D. C. & CAMPBELL, S. J. 2008. Inhibition of peripheral TNF can block the malaise associated with CNS inflammatory diseases. *Neurobiol Dis*, 32, 125-32.
- JIN, A. Y., TUOR, U. I., RUSHFORTH, D., KAUR, J., MULLER, R. N., PETTERSON, J. L., BOUTRY, S. & BARBER, P. A. 2010. Reduced blood brain barrier breakdown in P-selectin deficient mice following transient ischemic stroke: a future therapeutic target for treatment of stroke. *BMC Neurosci*, 11, 12.
- JIN, K., LAFEVRE-BERNT, M., SUN, Y., CHEN, S., GAFNI, J., CRIPPEN, D., LOGVINOVA, A., ROSS, C. A., GREENBERG, D. A. & ELLERBY, L. M. 2005. FGF-2 promotes neurogenesis and neuroprotection and prolongs survival in a transgenic mouse model of Huntington's disease. *Proc Natl Acad Sci U S A*, 102, 18189-94.
- JOHNSON, A. K. & GROSS, P. M. 1993. Sensory circumventricular organs and brain homeostatic pathways. *FASEB J*, 7, 678-86.
- JOICE, S. L., MYDEEN, F., COURAUD, P. O., WEKSLER, B. B., ROMERO, I. A., FRASER, P. A. & EASTON, A. S. 2009. Modulation of blood-brain barrier permeability by neutrophils: in vitro and in vivo studies. *Brain Res*, 1298, 13-23.
- JONES, A. R. & SHUSTA, E. V. 2007. Blood-brain barrier transport of therapeutics via receptor-mediation. *Pharm Res*, 24, 1759-71.
- JONES, M. R., QUINTON, L. J., SIMMS, B. T., LUPA, M. M., KOGAN, M. S. & MIZGERD, J. P. 2006. Roles of interleukin-6 in activation of STAT proteins and recruitment of neutrophils during *Escherichia coli* pneumonia. *J Infect Dis*, 193, 360-9.
- JONES, S. P., RAHIMI, O., O'BOYLE, M. P., DIAZ, D. L. & CLAIBORNE, B. J. 2003. Maturation of granule cell dendrites after mossy fiber arrival in hippocampal field CA3. *Hippocampus*, 13, 413-27.
- JOOSTEN, L. A., LUBBERTS, E., DUREZ, P., HELSEN, M. M., JACOBS, M. J., GOLDMAN, M. & VAN DEN BERG, W. B. 1997. Role of interleukin-4 and interleukin-10 in murine collagen-induced arthritis. Protective effect of interleukin-4 and interleukin-10 treatment on cartilage destruction. *Arthritis Rheum*, 40, 249-60.
- JOYCE, D. A., GIBBONS, D. P., GREEN, P., STEER, J. H., FELDMANN, M. & BRENNAN, F. M. 1994. Two inhibitors of pro-inflammatory cytokine

- release, interleukin-10 and interleukin-4, have contrasting effects on release of soluble p75 tumor necrosis factor receptor by cultured monocytes. *Eur J Immunol*, 24, 2699-705.
- JOYCE, D. A. & STEER, J. H. 1996. IL-4, IL-10 and IFN-gamma have distinct, but interacting, effects on differentiation-induced changes in TNF-alpha and TNF receptor release by cultured human monocytes. *Cytokine*, 8, 49-57.
- JUEDES, A. E. & RUDDLE, N. H. 2001. Resident and infiltrating central nervous system APCs regulate the emergence and resolution of experimental autoimmune encephalomyelitis. *J Immunol*, 166, 5168-75.
- JUREWICZ, A. M., WALCZAK, A. K. & SELMAJ, K. W. 1999. Shedding of TNF receptors in multiple sclerosis patients. *Neurology*, 53, 1409-14.
- JURGENS, B., HAINZ, U., FUCHS, D., FELZMANN, T. & HEITGER, A. 2009. Interferon-gamma-triggered indoleamine 2,3-dioxygenase competence in human monocyte-derived dendritic cells induces regulatory activity in allogeneic T cells. *Blood*, 114, 3235-43.
- KANEKO N, KUDO K, MABUCHI T, TAKEMOTO K, FUJIMAKI K, WATI H, IGUCHI H, TEZUKA H & KANBA S 2006. Suppression of cell proliferation by interferon-alpha through interleukin-1 production in adult rat dentate gyrus. *Neuropsychopharmacology*, 31, 2619-26.
- KANEKO, N., KUDO, K., MABUCHI, T., TAKEMOTO, K., FUJIMAKI, K., WATI, H., IGUCHI, H., TEZUKA, H. & KANBA, S. 2006. Suppression of cell proliferation by interferon-alpha through interleukin-1 production in adult rat dentate gyrus. *Neuropsychopharmacology*, 31, 2619-26.
- KANG, C. P., LEE, K. W., YOO, D. H., KANG, C. & BAE, S. C. 2005. The influence of a polymorphism at position -857 of the tumour necrosis factor alpha gene on clinical response to etanercept therapy in rheumatoid arthritis. *Rheumatology (Oxford)*, 44, 547-52.
- KANNAN, K., ORTMANN, R. A. & KIMPEL, D. 2005. Animal models of rheumatoid arthritis and their relevance to human disease. *Pathophysiology*, 12, 167-81.
- KAPPELER, C., SAILLOUR, Y., BAUDOIN, J. P., TUY, F. P., ALVAREZ, C., HOUBRON, C., GASPARD, P., HAMARD, G., CHELLY, J., METIN, C. & FRANCIS, F. 2006. Branching and nucleokinesis defects in migrating interneurons derived from doublecortin knockout mice. *Hum Mol Genet*, 15, 1387-400.
- KARMAN, J., LING, C., SANDOR, M. & FABRY, Z. 2004. Initiation of immune responses in brain is promoted by local dendritic cells. *J Immunol*, 173, 2353-61.
- KASAMA, T., STRIETER, R. M., LUKACS, N. W., LINCOLN, P. M., BURDICK, M. D. & KUNKEL, S. L. 1995. Interleukin-10 expression and chemokine regulation during the evolution of murine type II collagen-induced arthritis. *J Clin Invest*, 95, 2868-76.
- KATSCHKE, K. J., JR., ROTTMAN, J. B., RUTH, J. H., QIN, S., WU, L., LAROSA, G., PONATH, P., PARK, C. C., POPE, R. M. & KOCH, A. E. 2001. Differential expression of chemokine receptors on peripheral blood, synovial fluid, and synovial tissue monocytes/macrophages in rheumatoid arthritis. *Arthritis Rheum*, 44, 1022-32.
- KATZ, P. P. & YELIN, E. H. 1993. Prevalence and correlates of depressive symptoms among persons with rheumatoid arthritis. *J Rheumatol*, 20, 790-6.
- KAUL, M. 2009. HIV-1 associated dementia: update on pathological mechanisms and therapeutic approaches. *Curr Opin Neurol*, 22, 315-20.

- KAUL, M. & LIPTON, S. A. 1999. Chemokines and activated macrophages in HIV gp120-induced neuronal apoptosis. *Proc Natl Acad Sci U S A*, 96, 8212-6.
- KAVELAARS, A. 2002. Regulated expression of alpha-1 adrenergic receptors in the immune system. *Brain Behav Immun*, 16, 799-807.
- KAWANOKUCHI, J., SHIMIZU, K., NITTA, A., YAMADA, K., MIZUNO, T., TAKEUCHI, H. & SUZUMURA, A. 2008. Production and functions of IL-17 in microglia. *J Neuroimmunol*, 194, 54-61.
- KAWASAKI, Y., ZHANG, L., CHENG, J. K. & JI, R. R. 2008. Cytokine mechanisms of central sensitization: distinct and overlapping role of interleukin-1beta, interleukin-6, and tumor necrosis factor-alpha in regulating synaptic and neuronal activity in the superficial spinal cord. *J Neurosci*, 28, 5189-94.
- KEBIR, H., KREYMBORG, K., IFERGAN, I., DODELET-DEVILLERS, A., CAYROL, R., BERNARD, M., GIULIANI, F., ARBOUR, N., BECHER, B. & PRAT, A. 2007. Human TH17 lymphocytes promote blood-brain barrier disruption and central nervous system inflammation. *Nat Med*, 13, 1173-5.
- KEEFER, L., STEPANSKI, E. J., RANJBARAN, Z., BENSON, L. M. & KESHAVARZIAN, A. 2006. An initial report of sleep disturbance in inactive inflammatory bowel disease. *J Clin Sleep Med*, 2, 409-16.
- KEENE, C. D., CHANG, R., STEPHEN, C., NIVISON, M., NUTT, S. E., LOOK, A., BREYER, R. M., HORNER, P. J., HEVNER, R. & MONTINE, T. J. 2009. Protection of hippocampal neurogenesis from toll-like receptor 4-dependent innate immune activation by ablation of prostaglandin E2 receptor subtype EP1 or EP2. *Am J Pathol*, 174, 2300-9.
- KERJAN, G., KOIZUMI, H., HAN, E. B., DUBE, C. M., DJAKOVIC, S. N., PATRICK, G. N., BARAM, T. Z., HEINEMANN, S. F. & GLEESON, J. G. 2009. Mice lacking doublecortin and doublecortin-like kinase 2 display altered hippocampal neuronal maturation and spontaneous seizures. *Proc Natl Acad Sci U S A*, 106, 6766-71.
- KERN, S., OAKES, T. R., STONE, C. K., MCAULIFF, E. M., KIRSCHBAUM, C. & DAVIDSON, R. J. 2008. Glucose metabolic changes in the prefrontal cortex are associated with HPA axis response to a psychosocial stressor. *Psychoneuroendocrinology*, 33, 517-29.
- KIM, B., JEONG, H. K., KIM, J. H., LEE, S. Y., JOU, I. & JOE, E. H. 2011. Uridine 5'-diphosphate induces chemokine expression in microglia and astrocytes through activation of the P2Y6 receptor. *J Immunol*, 186, 3701-9.
- KIM, E. Y., PRIATEL, J. J., TEH, S. J. & TEH, H. S. 2006. TNF receptor type 2 (p75) functions as a costimulator for antigen-driven T cell responses in vivo. *J Immunol*, 176, 1026-35.
- KIM, E. Y. & TEH, H. S. 2004. Critical role of TNF receptor type-2 (p75) as a costimulator for IL-2 induction and T cell survival: a functional link to CD28. *J Immunol*, 173, 4500-9.
- KIM, H. Y., KIM, W. U., CHO, M. L., LEE, S. K., YOUN, J., KIM, S. I., YOO, W. H., PARK, J. H., MIN, J. K., LEE, S. H., PARK, S. H. & CHO, C. S. 1999. Enhanced T cell proliferative response to type II collagen and synthetic peptide CII (255-274) in patients with rheumatoid arthritis. *Arthritis Rheum*, 42, 2085-93.
- KIM, I., MOON, S. O., PARK, S. K., CHAE, S. W. & KOH, G. Y. 2001. Angiotensin-1 reduces VEGF-stimulated leukocyte adhesion to endothelial cells by reducing ICAM-1, VCAM-1, and E-selectin expression. *Circ Res*, 89, 477-9.
- KIM, J. M., JEONG, J. G., HO, S. H., HAHN, W., PARK, E. J., KIM, S., YU, S. S. & LEE, Y. W. 2003. Protection against collagen-induced arthritis by intramuscular gene therapy with an expression plasmid for the interleukin-1 receptor antagonist. *Gene Ther*, 10, 1543-50.

- KIM, W. U., CHO, M. L., JUNG, Y. O., MIN, S. Y., PARK, S. W., MIN, D. J., YOON, J. H. & KIM, H. Y. 2004. Type II collagen autoimmunity in rheumatoid arthritis. *Am J Med Sci*, 327, 202-11.
- KIM, Y. J., BRIDWELL, K. H., LENKE, L. G., RINELLA, A. S. & EDWARDS, C., 2ND 2005. Pseudarthrosis in primary fusions for adult idiopathic scoliosis: incidence, risk factors, and outcome analysis. *Spine (Phila Pa 1976)*, 30, 468-74.
- KIM, Y. K., LEE, S. W., KIM, S. H., SHIM, S. H., HAN, S. W., CHOI, S. H. & LEE, B. H. 2008. Differences in cytokines between non-suicidal patients and suicidal patients in major depression. *Prog Neuropsychopharmacol Biol Psychiatry*, 32, 356-61.
- KIN, N. W. & SANDERS, V. M. 2006. It takes nerve to tell T and B cells what to do. *J Leukoc Biol*, 79, 1093-104.
- KIRK, S. L. & KARLIK, S. J. 2003. VEGF and vascular changes in chronic neuroinflammation. *J Autoimmun*, 21, 353-63.
- KLARESKOG, L., CATRINA, A. I. & PAGET, S. 2009. Rheumatoid arthritis. *Lancet*, 373, 659-72.
- KLARESKOG, L., STOLT, P., LUNDBERG, K., KALLBERG, H., BENGTSSON, C., GRUNEWALD, J., RONNELID, J., HARRIS, H. E., ULFGREN, A. K., RANTAPAA-DAHLQVIST, S., EKLUND, A., PADYUKOV, L. & ALFREDSSON, L. 2006. A new model for an etiology of rheumatoid arthritis: smoking may trigger HLA-DR (shared epitope)-restricted immune reactions to autoantigens modified by citrullination. *Arthritis Rheum*, 54, 38-46.
- KLEIN, R. S. 2004. Regulation of neuroinflammation: the role of CXCL10 in lymphocyte infiltration during autoimmune encephalomyelitis. *J Cell Biochem*, 92, 213-22.
- KOCH, A. E. 2005. Chemokines and their receptors in rheumatoid arthritis: future targets? *Arthritis Rheum*, 52, 710-21.
- KOCH, A. E., KUNKEL, S. L., SHAH, M. R., HOSAKA, S., HALLORAN, M. M., HAINES, G. K., BURDICK, M. D., POPE, R. M. & STRIETER, R. M. 1995. Growth-related gene product alpha. A chemotactic cytokine for neutrophils in rheumatoid arthritis. *J Immunol*, 155, 3660-6.
- KOENDERS, M. I., DEVESA, I., MARIJNISSEN, R. J., ABDOLLAHI-ROODSAZ, S., BOOTS, A. M., WALGREEN, B., DI PADOVA, F. E., NICKLIN, M. J., JOOSTEN, L. A. & VAN DEN BERG, W. B. 2008. Interleukin-1 drives pathogenic Th17 cells during spontaneous arthritis in interleukin-1 receptor antagonist-deficient mice. *Arthritis Rheum*, 58, 3461-70.
- KOH, L., ZAKHAROV, A. & JOHNSTON, M. 2005. Integration of the subarachnoid space and lymphatics: is it time to embrace a new concept of cerebrospinal fluid absorption? *Cerebrospinal Fluid Res*, 2, 6.
- KOJIMA, M., KOJIMA, T., SUZUKI, S., OGUCHI, T., OBA, M., TSUCHIYA, H., SUGIURA, F., KANAYAMA, Y., FURUKAWA, T. A., TOKUDOME, S. & ISHIGURO, N. 2009. Depression, inflammation, and pain in patients with rheumatoid arthritis. *Arthritis Rheum*, 61, 1018-24.
- KORNER, H., LEMCKERT, F. A., CHAUDHRI, G., ETTELDORF, S. & SEDGWICK, J. D. 1997. Tumor necrosis factor blockade in actively induced experimental autoimmune encephalomyelitis prevents clinical disease despite activated T cell infiltration to the central nervous system. *Eur J Immunol*, 27, 1973-81.
- KOZANIDOU, V. I., THEOCHARIS, A. D., GEORGIADIS, A., VOULGARI, P. V., DROSOS, A. A. & KARAMANOS, N. K. 2005. Signal transduction by IL-2 and its receptors as target in treatment of rheumatoid arthritis. *Curr Drug Targets Immune Endocr Metabol Disord*, 5, 41-50.

- KRAAN, M. C., PATEL, D. D., HARINGMAN, J. J., SMITH, M. D., WEEDON, H., AHERN, M. J., BREEDVELD, F. C. & TAK, P. P. 2001. The development of clinical signs of rheumatoid synovial inflammation is associated with increased synthesis of the chemokine CXCL8 (interleukin-8). *Arthritis Res*, 3, 65-71.
- KREUTZBERG, G. W. 1996. Microglia: a sensor for pathological events in the CNS. *Trends Neurosci*, 19, 312-8.
- KUAN, W. P., TAM, L. S., WONG, C. K., KO, F. W., LI, T., ZHU, T. & LI, E. K. 2010. CXCL 9 and CXCL 10 as Sensitive markers of disease activity in patients with rheumatoid arthritis. *J Rheumatol*, 37, 257-64.
- KUHN, H. G., DICKINSON-ANSON, H. & GAGE, F. H. 1996. Neurogenesis in the dentate gyrus of the adult rat: age-related decrease of neuronal progenitor proliferation. *J Neurosci*, 16, 2027-33.
- KULLMANN, D. M. & LAMSA, K. P. 2007. Long-term synaptic plasticity in hippocampal interneurons. *Nat Rev Neurosci*, 8, 687-99.
- KUPPERS, R. 2005. Mechanisms of B-cell lymphoma pathogenesis. *Nat Rev Cancer*, 5, 251-62.
- KUROWSKA-STOLARSKA, M., KEWIN, P., MURPHY, G., RUSSO, R. C., STOLARSKI, B., GARCIA, C. C., KOMAI-KOMA, M., PITMAN, N., LI, Y., NIEDBALA, W., MCKENZIE, A. N., TEIXEIRA, M. M., LIEW, F. Y. & XU, D. 2008. IL-33 induces antigen-specific IL-5+ T cells and promotes allergic-induced airway inflammation independent of IL-4. *J Immunol*, 181, 4780-90.
- KUSABA, M., HONDA, J., FUKUDA, T. & OIZUMI, K. 1998. Analysis of type 1 and type 2 T cells in synovial fluid and peripheral blood of patients with rheumatoid arthritis. *J Rheumatol*, 25, 1466-71.
- KWAK, H. B., HA, H., KIM, H. N., LEE, J. H., KIM, H. S., LEE, S., KIM, H. M., KIM, J. Y., KIM, H. H., SONG, Y. W. & LEE, Z. H. 2008. Reciprocal cross-talk between RANKL and interferon-gamma-inducible protein 10 is responsible for bone-erosive experimental arthritis. *Arthritis Rheum*, 58, 1332-42.
- KWIDZINSKI, E. & BECHMANN, I. 2007. IDO expression in the brain: a double-edged sword. *J Mol Med*, 85, 1351-9.
- LAFLAMME, N., ECHCHANNAOUI, H., LANDMANN, R. & RIVEST, S. 2003. Cooperation between toll-like receptor 2 and 4 in the brain of mice challenged with cell wall components derived from gram-negative and gram-positive bacteria. *Eur J Immunol*, 33, 1127-38.
- LAFLAMME, N. & RIVEST, S. 2001. Toll-like receptor 4: the missing link of the cerebral innate immune response triggered by circulating gram-negative bacterial cell wall components. *FASEB J*, 15, 155-163.
- LAFLAMME, N., SOUCY, G. & RIVEST, S. 2001. Circulating cell wall components derived from gram-negative, not gram-positive, bacteria cause a profound induction of the gene-encoding Toll-like receptor 2 in the CNS. *J Neurochem*, 79, 648-57.
- LANFUMEY, L., MONGEAU, R., COHEN-SALMON, C. & HAMON, M. 2008. Corticosteroid-serotonin interactions in the neurobiological mechanisms of stress-related disorders. *Neurosci Biobehav Rev*, 32, 1174-84.
- LAPCHAK, P. A., ARAUJO, D. M. & HEFTI, F. 1993. Systemic interleukin-1 beta decreases brain-derived neurotrophic factor messenger RNA expression in the rat hippocampal formation. *Neuroscience*, 53, 297-301.
- LATHIA, J. D., OKUN, E., TANG, S. C., GRIFFIOEN, K., CHENG, A., MUGHAL, M. R., LARYEA, G., SELVARAJ, P. K., FFRENCH-CONSTANT, C., MAGNUS, T., ARUMUGAM, T. V. & MATTSON, M. P. 2008. Toll-like receptor 3 is a negative regulator of embryonic neural progenitor cell proliferation. *J Neurosci*, 28, 13978-84.

- LAURO, C., DI ANGELANTONIO, S., CIPRIANI, R., SOBRERO, F., ANTONILLI, L., BRUSADIN, V., RAGOZZINO, D. & LIMATOLA, C. 2008. Activity of adenosine receptors type 1 Is required for CX3CL1-mediated neuroprotection and neuromodulation in hippocampal neurons. *J Immunol*, 180, 7590-6.
- LAYE, S., BLUTHE, R. M., KENT, S., COMBE, C., MEDINA, C., PARNET, P., KELLEY, K. & DANTZER, R. 1995. Subdiaphragmatic vagotomy blocks induction of IL-1 beta mRNA in mice brain in response to peripheral LPS. *Am J Physiol*, 268, R1327-31.
- LAYE, S., PARNET, P., GOUJON, E. & DANTZER, R. 1994. Peripheral administration of lipopolysaccharide induces the expression of cytokine transcripts in the brain and pituitary of mice. *Brain Res Mol Brain Res*, 27, 157-62.
- LEE, E. Y., LEE, Z. H. & SONG, Y. W. 2009. CXCL10 and autoimmune diseases. *Autoimmun Rev*, 8, 379-83.
- LEE, J. S., CHO, M. L., JHUN, J. Y., MIN, S. Y., JU, J. H., YOON, C. H., MIN, J. K., PARK, S. H., KIM, H. Y. & CHO, Y. G. 2006. Antigen-specific expansion of TCR Vbeta3+ CD4+ T cells in the early stage of collagen-induced arthritis and its arthritogenic role in DBA/1J mice. *J Clin Immunol*, 26, 204-12.
- LEHNARDT, S., HENNEKE, P., LIEN, E., KASPER, D. L., VOLPE, J. J., BECHMANN, I., NITSCH, R., WEBER, J. R., GOLENBOCK, D. T. & VARTANIAN, T. 2006. A mechanism for neurodegeneration induced by group B streptococci through activation of the TLR2/MyD88 pathway in microglia. *J Immunol*, 177, 583-92.
- LEHNARDT, S., LACHANCE, C., PATRIZI, S., LEFEBVRE, S., FOLLETT, P. L., JENSEN, F. E., ROSENBERG, P. A., VOLPE, J. J. & VARTANIAN, T. 2002. The toll-like receptor TLR4 is necessary for lipopolysaccharide-induced oligodendrocyte injury in the CNS. *J Neurosci*, 22, 2478-86.
- LEHNARDT, S., MASSILLON, L., FOLLETT, P., JENSEN, F. E., RATAN, R., ROSENBERG, P. A., VOLPE, J. J. & VARTANIAN, T. 2003. Activation of innate immunity in the CNS triggers neurodegeneration through a Toll-like receptor 4-dependent pathway. *Proc Natl Acad Sci U S A*, 100, 8514-9.
- LEHTO, S. M., HUOTARI, A., NISKANEN, L., HERZIG, K. H., TOLMUNEN, T., VIINAMAKI, H., KOIVUMAA-HONKANEN, H., HONKALAMPI, K., SINIKALLIO, S., RUOTSALAINEN, H. & HINTIKKA, J. 2010a. Serum IL-7 and G-CSF in major depressive disorder. *Prog Neuropsychopharmacol Biol Psychiatry*, 34, 846-51.
- LEHTO, S. M., NISKANEN, L., HERZIG, K. H., TOLMUNEN, T., HUOTARI, A., VIINAMAKI, H., KOIVUMAA-HONKANEN, H., HONKALAMPI, K., RUOTSALAINEN, H. & HINTIKKA, J. 2010b. Serum chemokine levels in major depressive disorder. *Psychoneuroendocrinology*, 35, 226-32.
- LEKANDER, M., AXEN, J., KNUTSSON, U., OLGART HOGLUND, C., WERNER, S., WIKSTROM, A. C. & STIERNA, P. 2009. Cytokine inhibition after glucocorticoid exposure in healthy men with low versus high basal cortisol levels. *Neuroimmunomodulation*, 16, 245-50.
- LENCZOWSKI, M. J., VAN DAM, A. M., POOLE, S., LARRICK, J. W. & TILDERS, F. J. 1997. Role of circulating endotoxin and interleukin-6 in the ACTH and corticosterone response to intraperitoneal LPS. *Am J Physiol*, 273, R1870-7.
- LEONARD, J. P., WALDBURGER, K. E. & GOLDMAN, S. J. 1995. Prevention of experimental autoimmune encephalomyelitis by antibodies against interleukin 12. *J Exp Med*, 181, 381-6.

- LI, G. & PLEASURE, S. J. 2010. Ongoing interplay between the neural network and neurogenesis in the adult hippocampus. *Curr Opin Neurobiol*, 20, 126-33.
- LI, J., PERRELLA, M. A., TSAI, J. C., YET, S. F., HSIEH, C. M., YOSHIZUMI, M., PATTERSON, C., ENDEGE, W. O., ZHOU, F. & LEE, M. E. 1995. Induction of vascular endothelial growth factor gene expression by interleukin-1 beta in rat aortic smooth muscle cells. *J Biol Chem*, 270, 308-12.
- LI, Y., XIAO, B., QIU, W., YANG, L., HU, B., TIAN, X. & YANG, H. 2010. Altered expression of CD4(+)CD25(+) regulatory T cells and its 5-HT(1a) receptor in patients with major depression disorder. *J Affect Disord*, 124, 68-75.
- LIAO, K. P., ALFREDSSON, L. & KARLSON, E. W. 2009. Environmental influences on risk for rheumatoid arthritis. *Curr Opin Rheumatol*, 21, 279-83.
- LIE, B. A., VIKEN, M. K., ODEGARD, S., VAN DER HEIJDE, D., LANDEWE, R., UHLIG, T. & KVIEN, T. K. 2007. Associations between the PTPN22 1858C>T polymorphism and radiographic joint destruction in patients with rheumatoid arthritis: results from a 10-year longitudinal study. *Ann Rheum Dis*, 66, 1604-9.
- LIEBRICH, M., GUO, L. H., SCHLUESENER, H. J., SCHWAB, J. M., DIETZ, K., WILL, B. E. & MEYERMANN, R. 2007. Expression of interleukin-16 by tumor-associated macrophages/activated microglia in high-grade astrocytic brain tumors. *Arch Immunol Ther Exp (Warsz)*, 55, 41-7.
- LIMATOLA, C., CIOTTI, M. T., MERCANTI, D., SANTONI, A. & EUSEBI, F. 2002. Signaling pathways activated by chemokine receptor CXCR2 and AMPA-type glutamate receptors and involvement in granule cells survival. *J Neuroimmunol*, 123, 9-17.
- LIMATOLA, C., CIOTTI, M. T., MERCANTI, D., VACCA, F., RAGOZZINO, D., GIOVANNELLI, A., SANTONI, A., EUSEBI, F. & MILEDI, R. 2000. The chemokine growth-related gene product beta protects rat cerebellar granule cells from apoptotic cell death through alpha-amino-3-hydroxy-5-methyl-4-isoxazolepropionate receptors. *Proc Natl Acad Sci U S A*, 97, 6197-201.
- LIN, G. & LI, J. 2010. Elevation of serum IgG subclass concentration in patients with rheumatoid arthritis. *Rheumatol Int*, 30, 837-40.
- LINDQVIST, D., JANELIDZE, S., HAGELL, P., ERHARDT, S., SAMUELSSON, M., MINTHON, L., HANSSON, O., BJORKQVIST, M., TRASKMAN-BENDZ, L. & BRUNDIN, L. 2009. Interleukin-6 is elevated in the cerebrospinal fluid of suicide attempters and related to symptom severity. *Biol Psychiatry*, 66, 287-92.
- LISIGNOLI, G., TONEGUZZI, S., POZZI, C., PIACENTINI, A., RICCIO, M., FERRUZZI, A., GUALTIERI, G. & FACCHINI, A. 1999. Proinflammatory cytokines and chemokine production and expression by human osteoblasts isolated from patients with rheumatoid arthritis and osteoarthritis. *J Rheumatol*, 26, 791-9.
- LIST, J., MOSER, R. P., STEUER, M., LOUDON, W. G., BLACKLOCK, J. B. & GRIMM, E. A. 1992. Cytokine responses to intraventricular injection of interleukin 2 into patients with leptomeningeal carcinomatosis: rapid induction of tumor necrosis factor alpha, interleukin 1 beta, interleukin 6, gamma-interferon, and soluble interleukin 2 receptor (Mr 55,000 protein). *Cancer Res*, 52, 1123-8.
- LITTELJOHN, D., CUMMINGS, A., BRENNAN, A., GILL, A., CHUNDURI, S., ANISMAN, H. & HAYLEY, S. 2010. Interferon-gamma deficiency modifies the effects of a chronic stressor in mice: Implications for psychological pathology. *Brain Behav Immun*, 24, 462-73.

- LIU, K. K. & DOROVINI-ZIS, K. 2009. Regulation of CXCL12 and CXCR4 expression by human brain endothelial cells and their role in CD4⁺ and CD8⁺ T cell adhesion and transendothelial migration. *J Neuroimmunol*, 215, 49-64.
- LLEDO, P. M., ALONSO, M. & GRUBB, M. S. 2006. Adult neurogenesis and functional plasticity in neuronal circuits. *Nat Rev Neurosci*, 7, 179-93.
- LO FERMO, S., BARONE, R., PATTI, F., LAISA, P., CAVALLARO, T. L., NICOLETTI, A. & ZAPPIA, M. 2010. Outcome of psychiatric symptoms presenting at onset of multiple sclerosis: a retrospective study. *Mult Scler*, 16, 742-8.
- LORRE, K., VAN DAMME, J. & CEUPPENS, J. L. 1990. A bidirectional regulatory network involving IL 2 and IL 4 in the alternative CD2 pathway of T cell activation. *Eur J Immunol*, 20, 1569-75.
- LOSSINSKY, A. S. & SHIVERS, R. R. 2004. Structural pathways for macromolecular and cellular transport across the blood-brain barrier during inflammatory conditions. Review. *Histol Histopathol*, 19, 535-64.
- LU, L. D., STUMP, K. L. & SEAVEY, M. M. 2010. Novel Method of Monitoring Trace Cytokines and Activated STAT Molecules in the Paws of Arthritic Mice using Multiplex Bead Technology. *BMC Immunol*, 11, 55.
- LU, M., GROVE, E. A. & MILLER, R. J. 2002. Abnormal development of the hippocampal dentate gyrus in mice lacking the CXCR4 chemokine receptor. *Proc Natl Acad Sci U S A*, 99, 7090-5.
- LU, Y., CHRISTIAN, K. & LU, B. 2008. BDNF: a key regulator for protein synthesis-dependent LTP and long-term memory? *Neurobiol Learn Mem*, 89, 312-23.
- LUCASSEN, P. J., STUMPEL, M. W., WANG, Q. & ARONICA, E. 2010. Decreased numbers of progenitor cells but no response to antidepressant drugs in the hippocampus of elderly depressed patients. *Neuropharmacology*, 58, 940-9.
- LUHESHI, N. M., MCCOLL, B. W. & BROUGH, D. 2009. Nuclear retention of IL-1 alpha by necrotic cells: a mechanism to dampen sterile inflammation. *Eur J Immunol*, 39, 2973-80.
- LUROSS, J. A. & WILLIAMS, N. A. 2001. The genetic and immunopathological processes underlying collagen-induced arthritis. *Immunology*, 103, 407-16.
- LUSITANI, D., MALAWISTA, S. E. & MONTGOMERY, R. R. 2003. Calprotectin, an abundant cytosolic protein from human polymorphonuclear leukocytes, inhibits the growth of *Borrelia burgdorferi*. *Infect Immun*, 71, 4711-6.
- LUTTICHAU, H. R. 2010. The cytomegalovirus UL146 gene product vCXCL1 targets both CXCR1 and CXCR2 as an agonist. *J Biol Chem*, 285, 9137-46.
- LYDEN, D., HATTORI, K., DIAS, S., COSTA, C., BLAIKIE, P., BUTROS, L., CHADBURN, A., HEISSIG, B., MARKS, W., WITTE, L., WU, Y., HICKLIN, D., ZHU, Z., HACKETT, N. R., CRYSTAL, R. G., MOORE, M. A., HAJJAR, K. A., MANOVA, K., BENEZRA, R. & RAFII, S. 2001. Impaired recruitment of bone-marrow-derived endothelial and hematopoietic precursor cells blocks tumor angiogenesis and growth. *Nat Med*, 7, 1194-201.
- LYNCH, J. L. & BANKS, W. A. 2008. Opiate modulation of IL-1alpha, IL-2, and TNF-alpha transport across the blood-brain barrier. *Brain Behav Immun*, 22, 1096-102.
- MACGREGOR, A. J., SNIEDER, H., RIGBY, A. S., KOSKENVUO, M., KAPRIO, J., AHO, K. & SILMAN, A. J. 2000. Characterizing the quantitative genetic contribution to rheumatoid arthritis using data from twins. *Arthritis Rheum*, 43, 30-7.
- MAES, M. 2010. Depression is an inflammatory disease, but cell-mediated immune activation is the key component of depression. *Prog Neuropsychopharmacol Biol Psychiatry*.

- MAGEED, R. A., ADAMS, G., WOODROW, D., PODHAJECER, O. L. & CHERNAJOVSKY, Y. 1998. Prevention of collagen-induced arthritis by gene delivery of soluble p75 tumour necrosis factor receptor. *Gene Ther*, 5, 1584-92.
- MAIER, S. F. 2003. Bi-directional immune-brain communication: Implications for understanding stress, pain, and cognition. *Brain Behav Immun*, 17, 69-85.
- MAJER, M., WELBERG, L. A., CAPURON, L., PAGNONI, G., RAISON, C. L. & MILLER, A. H. 2008. IFN-alpha-induced motor slowing is associated with increased depression and fatigue in patients with chronic hepatitis C. *Brain Behav Immun*, 22, 870-80.
- MALBERG, J. E., EISCH, A. J., NESTLER, E. J. & DUMAN, R. S. 2000. Chronic antidepressant treatment increases neurogenesis in adult rat hippocampus. *J Neurosci*, 20, 9104-10.
- MALEMUD, C. J. 2007. Growth hormone, VEGF and FGF: involvement in rheumatoid arthritis. *Clin Chim Acta*, 375, 10-9.
- MALETIC-SAVATIC, M., VINGARA, L. K., MANGANAS, L. N., LI, Y., ZHANG, S., SIERRA, A., HAZEL, R., SMITH, D., WAGSHUL, M. E., HENN, F., KRUPP, L., ENIKOLOPOV, G., BENVENISTE, H., DJURIC, P. M. & PELCZER, I. 2008. Metabolomics of neural progenitor cells: a novel approach to biomarker discovery. *Cold Spring Harb Symp Quant Biol*, 73, 389-401.
- MALFAIT, A. M., BUTLER, D. M., PRESKY, D. H., MAINI, R. N., BRENNAN, F. M. & FELDMANN, M. 1998. Blockade of IL-12 during the induction of collagen-induced arthritis (CIA) markedly attenuates the severity of the arthritis. *Clin Exp Immunol*, 111, 377-83.
- MANABE, N., ODA, H., NAKAMURA, K., KUGA, Y., UCHIDA, S. & KAWAGUCHI, H. 1999. Involvement of fibroblast growth factor-2 in joint destruction of rheumatoid arthritis patients. *Rheumatology (Oxford)*, 38, 714-20.
- MANES, T. D. & POBER, J. S. 2008. Antigen presentation by human microvascular endothelial cells triggers ICAM-1-dependent transendothelial protrusion by, and fractalkine-dependent transendothelial migration of, effector memory CD4+ T cells. *J Immunol*, 180, 8386-92.
- MANESS, L. M., KASTIN, A. J. & BANKS, W. A. 1998. Relative contributions of a CVO and the microvascular bed to delivery of blood-borne IL-1alpha to the brain. *Am J Physiol*, 275, E207-12.
- MANFE, V., KOCHOYAN, A., BOCK, E. & BEREZIN, V. 2010. Peptides derived from specific interaction sites of the fibroblast growth factor 2-FGF receptor complexes induce receptor activation and signaling. *J Neurochem*, 114, 74-86.
- MANI, N., KHAIBULLINA, A., KRUM, J. M. & ROSENSTEIN, J. M. 2005. Astrocyte growth effects of vascular endothelial growth factor (VEGF) application to perinatal neocortical explants: receptor mediation and signal transduction pathways. *Exp Neurol*, 192, 394-406.
- MANTOVANI, A., BONECCHI, R. & LOCATI, M. 2006. Tuning inflammation and immunity by chemokine sequestration: decoys and more. *Nat Rev Immunol*, 6, 907-18.
- MARCHETTI, L., KLEIN, M., SCHLETT, K., PFIZENMAIER, K. & EISEL, U. L. 2004. Tumor necrosis factor (TNF)-mediated neuroprotection against glutamate-induced excitotoxicity is enhanced by N-methyl-D-aspartate receptor activation. Essential role of a TNF receptor 2-mediated phosphatidylinositol 3-kinase-dependent NF-kappa B pathway. *J Biol Chem*, 279, 32869-81.
- MARINOVA-MUTAFCHIEVA, L., WILLIAMS, R. O., MAURI, C., MASON, L. J., WALMSLEY, M. J., TAYLOR, P. C., FELDMANN, M. & MAINI, R. N. 2000. A

- comparative study into the mechanisms of action of anti-tumor necrosis factor alpha, anti-CD4, and combined anti-tumor necrosis factor alpha/anti-CD4 treatment in early collagen-induced arthritis. *Arthritis Rheum*, 43, 638-44.
- MARSHALL, G. D., JR. 1992. Cytokines: clinical potentials for the allergic patient. *Allergy Proc*, 13, 311-5.
- MARTEL-PELLETIER, J., WELSCH, D. J. & PELLETIER, J. P. 2001. Metalloproteases and inhibitors in arthritic diseases. *Best Pract Res Clin Rheumatol*, 15, 805-29.
- MARTINON, F. & TSCHOPP, J. 2005. NLRs join TLRs as innate sensors of pathogens. *Trends Immunol*, 26, 447-54.
- MARTINOWICH, K., MANJI, H. & LU, B. 2007. New insights into BDNF function in depression and anxiety. *Nat Neurosci*, 10, 1089-93.
- MARUMO, T., SCHINI-KERTH, V. B. & BUSSE, R. 1999. Vascular endothelial growth factor activates nuclear factor-kappaB and induces monocyte chemoattractant protein-1 in bovine retinal endothelial cells. *Diabetes*, 48, 1131-7.
- MASSA, P. T. 1993. Specific suppression of major histocompatibility complex class I and class II genes in astrocytes by brain-enriched gangliosides. *J Exp Med*, 178, 1357-63.
- MATRISCIANO, F., BONACCORSO, S., RICCIARDI, A., SCACCIANOCE, S., PANACCIONE, I., WANG, L., RUBERTO, A., TATARELLI, R., NICOLETTI, F., GIRARDI, P. & SHELTON, R. C. 2009. Changes in BDNF serum levels in patients with major depression disorder (MDD) after 6 months treatment with sertraline, escitalopram, or venlafaxine. *J Psychiatr Res*, 43, 247-54.
- MATSUKI, T., NAKAE, S., SUDO, K., HORAI, R. & IWAKURA, Y. 2006. Abnormal T cell activation caused by the imbalance of the IL-1/IL-1R antagonist system is responsible for the development of experimental autoimmune encephalomyelitis. *Int Immunol*, 18, 399-407.
- MAURI, C., WILLIAMS, R. O., WALMSLEY, M. & FELDMANN, M. 1996. Relationship between Th1/Th2 cytokine patterns and the arthritogenic response in collagen-induced arthritis. *Eur J Immunol*, 26, 1511-8.
- MCCARRON, R. M., WANG, L., COWAN, E. P. & SPATZ, M. 1991. Class II MHC antigen expression by cultured human cerebral vascular endothelial cells. *Brain Res*, 566, 325-8.
- MCCOLL, B. W., ROTHWELL, N. J. & ALLAN, S. M. 2007. Systemic inflammatory stimulus potentiates the acute phase and CXC chemokine responses to experimental stroke and exacerbates brain damage via interleukin-1- and neutrophil-dependent mechanisms. *J Neurosci*, 27, 4403-12.
- MCCOLL, B. W., ROTHWELL, N. J. & ALLAN, S. M. 2008. Systemic inflammation alters the kinetics of cerebrovascular tight junction disruption after experimental stroke in mice. *J Neurosci*, 28, 9451-62.
- MCEWEN, B. S. 2005. Glucocorticoids, depression, and mood disorders: structural remodeling in the brain. *Metabolism*, 54, 20-3.
- MCGONAGLE, D. 2010. The history of erosions in rheumatoid arthritis: are erosions history? *Arthritis Rheum*, 62, 312-5.
- MCINNES, I. B. & SCHETT, G. 2007. Cytokines in the pathogenesis of rheumatoid arthritis. *Nat Rev Immunol*, 7, 429-42.
- MCKIMMIE, C. S., JOHNSON, N., FOOKS, A. R. & FAZAKERLEY, J. K. 2005. Viruses selectively upregulate Toll-like receptors in the central nervous system. *Biochem Biophys Res Commun*, 336, 925-33.
- MCKINLEY, M. J., MCALLEN, R. M., DAVERN, P., GILES, M. E., PENSCHOW, J., SUNN, N., USCHAKOV, A. & OLDFIELD, B. J. 2003. The sensory

- circumventricular organs of the mammalian brain. *Adv Anat Embryol Cell Biol*, 172, III-XII, 1-122, back cover.
- MCCMAHAN, C. J., SLACK, J. L., MOSLEY, B., COSMAN, D., LUPTON, S. D., BRUNTON, L. L., GRUBIN, C. E., WIGNALL, J. M., JENKINS, N. A., BRANNAN, C. I. & ET AL. 1991. A novel IL-1 receptor, cloned from B cells by mammalian expression, is expressed in many cell types. *EMBO J*, 10, 2821-32.
- MCCMAHON, E. J., BAILEY, S. L., CASTENADA, C. V., WALDNER, H. & MILLER, S. D. 2005. Epitope spreading initiates in the CNS in two mouse models of multiple sclerosis. *Nat Med*, 11, 335-9.
- MCCMANUS, C. M., BROSNAN, C. F. & BERMAN, J. W. 1998. Cytokine induction of MIP-1 alpha and MIP-1 beta in human fetal microglia. *J Immunol*, 160, 1449-55.
- MCCMENAMIN, P. G., WEALTHALL, R. J., DEVERALL, M., COOPER, S. J. & GRIFFIN, B. 2003. Macrophages and dendritic cells in the rat meninges and choroid plexus: three-dimensional localisation by environmental scanning electron microscopy and confocal microscopy. *Cell Tissue Res*, 313, 259-69.
- MEDAWAR, P. B. 1948. Immunity to homologous grafted skin; the fate of skin homografts transplanted to the brain, to subcutaneous tissue, and to the anterior chamber of the eye. *Br J Exp Pathol*, 29, 58-69.
- MEDZHITOV, R. 2007. TLR-mediated innate immune recognition. *Seminars in Immunology*, 19, 1-2.
- MEDZHITOV, R. & JANEWAY, C., JR. 2000. Innate immunity. *N Engl J Med*, 343, 338-44.
- MEHRA, A., LEE, K. H. & HATZIMANIKATIS, V. 2003. Insights into the relation between mRNA and protein expression patterns: I. Theoretical considerations. *Biotechnol Bioeng*, 84, 822-33.
- MENTINK-KANE, M. M. & WYNN, T. A. 2004. Opposing roles for IL-13 and IL-13 receptor alpha 2 in health and disease. *Immunol Rev*, 202, 191-202.
- MILJKOVIC, D., MOMCILOVIC, M., STOJANOVIC, I., STOSIC-GRUJICIC, S., RAMIC, Z. & MOSTARICA-STOJKOVIC, M. 2007. Astrocytes stimulate interleukin-17 and interferon-gamma production in vitro. *J Neurosci Res*, 85, 3598-606.
- MILLER, A. H., SPENCER, R. L., HASSETT, J., KIM, C., RHEE, R., CIUREA, D., DHABHAR, F., MCEWEN, B. & STEIN, M. 1994. Effects of selective type I and II adrenal steroid agonists on immune cell distribution. *Endocrinology*, 135, 1934-44.
- MILLIGAN, E. D., NGUYEN, K. T., DEAK, T., HINDE, J. L., FLESHNER, M., WATKINS, L. R. & MAIER, S. F. 1998. The long term acute phase-like responses that follow acute stressor exposure are blocked by alpha-melanocyte stimulating hormone. *Brain Res*, 810, 48-58.
- MILLWARD, J. M., CARUSO, M., CAMPBELL, I. L., GAULDIE, J. & OWENS, T. 2007. IFN-gamma-induced chemokines synergize with pertussis toxin to promote T cell entry to the central nervous system. *J Immunol*, 178, 8175-82.
- MINDHAM, R. H., BAGSHAW, A., JAMES, S. A. & SWANNELL, A. J. 1981. Factors associated with the appearance of psychiatric symptoms in rheumatoid arthritis. *J Psychosom Res*, 25, 429-35.
- MING, G. L. & SONG, H. 2005. Adult neurogenesis in the mammalian central nervous system. *Annu Rev Neurosci*, 28, 223-50.
- MOHANKUMAR, S. M., MOHANKUMAR, P. S. & QUADRI, S. K. 1999. Lipopolysaccharide-induced changes in monoamines in specific areas of the brain: blockade by interleukin-1 receptor antagonist. *Brain Res*, 824, 232-7.

- MOHLER, K. M., TORRANCE, D. S., SMITH, C. A., GOODWIN, R. G., STREMLER, K. E., FUNG, V. P., MADANI, H. & WIDMER, M. B. 1993. Soluble tumor necrosis factor (TNF) receptors are effective therapeutic agents in lethal endotoxemia and function simultaneously as both TNF carriers and TNF antagonists. *J Immunol*, 151, 1548-61.
- MONJE ML, TODA H & PALMER TD 2003. Inflammatory blockade restores adult hippocampal neurogenesis. *Science*, 302, 1760-5.
- MONJE, M. L., TODA, H. & PALMER, T. D. 2003. Inflammatory blockade restores adult hippocampal neurogenesis. *Science*, 302, 1760-5.
- MOORE, K. W., DE WAAL MALEFYT, R., COFFMAN, R. L. & O'GARRA, A. 2001. Interleukin-10 and the interleukin-10 receptor. *Annu Rev Immunol*, 19, 683-765.
- MOR, F., QUINTANA, F. J. & COHEN, I. R. 2004. Angiogenesis-inflammation cross-talk: vascular endothelial growth factor is secreted by activated T cells and induces Th1 polarization. *J Immunol*, 172, 4618-23.
- MORITA, Y., YAMAMURA, M., NISHIDA, K., HARADA, S., OKAMOTO, H., INOUE, H., OHMOTO, Y., MODLIN, R. L. & MAKINO, H. 1998. Expression of interleukin-12 in synovial tissue from patients with rheumatoid arthritis. *Arthritis Rheum*, 41, 306-14.
- MOSMANN, T. R. & SAD, S. 1996. The expanding universe of T-cell subsets: Th1, Th2 and more. *Immunol Today*, 17, 138-46.
- MUKHERJEE, P., WU, B., MAYTON, L., KIM, S. H., ROBBINS, P. D. & WOOLEY, P. H. 2003. TNF receptor gene therapy results in suppression of IgG2a anticollagen antibody in collagen induced arthritis. *Ann Rheum Dis*, 62, 707-14.
- MULLAZEHI, M., MATHSSON, L., LAMPA, J. & RONNELID, J. 2007. High anti-collagen type-II antibody levels and induction of proinflammatory cytokines by anti-collagen antibody-containing immune complexes in vitro characterise a distinct rheumatoid arthritis phenotype associated with acute inflammation at the time of disease onset. *Ann Rheum Dis*, 66, 537-41.
- MUNN, D. H. & MELLOR, A. L. 2007. Indoleamine 2,3-dioxygenase and tumor-induced tolerance. *J Clin Invest*, 117, 1147-54.
- MURPHY, C. A., LANGRISH, C. L., CHEN, Y., BLUMENSCHEN, W., MCCLANAHAN, T., KASTELEIN, R. A., SEDGWICK, J. D. & CUA, D. J. 2003. Divergent pro- and antiinflammatory roles for IL-23 and IL-12 in joint autoimmune inflammation. *J Exp Med*, 198, 1951-7.
- MURRAY, F., SMITH, D. W. & HUTSON, P. H. 2008. Chronic low dose corticosterone exposure decreased hippocampal cell proliferation, volume and induced anxiety and depression like behaviours in mice. *Eur J Pharmacol*, 583, 115-27.
- MUSSENER, A., LITTON, M. J., LINDROOS, E. & KLARESKOG, L. 1997. Cytokine production in synovial tissue of mice with collagen-induced arthritis (CIA). *Clin Exp Immunol*, 107, 485-93.
- MUZIO, L., CAVASINNI, F., MARINARO, C., BERGAMASCHI, A., BERGAMI, A., PORCHERI, C., CERRI, F., DINA, G., QUATTRINI, A., COMI, G., FURLAN, R. & MARTINO, G. 2010. Cxcl10 enhances blood cells migration in the sub-ventricular zone of mice affected by experimental autoimmune encephalomyelitis. *Mol Cell Neurosci*, 43, 268-80.
- MYERS, L. K., MIYAHARA, H., TERATO, K., SEYER, J. M., STUART, J. M. & KANG, A. H. 1995. Collagen-induced arthritis in B10.RIII mice (H-2r): identification of an arthritogenic T-cell determinant. *Immunology*, 84, 509-13.

- MYINT, A. M., LEONARD, B. E., STEINBUSCH, H. W. & KIM, Y. K. 2005. Th1, Th2, and Th3 cytokine alterations in major depression. *J Affect Disord*, 88, 167-73.
- NAGASHIMA, M., YOSHINO, S., ISHIWATA, T. & ASANO, G. 1995. Role of vascular endothelial growth factor in angiogenesis of rheumatoid arthritis. *J Rheumatol*, 22, 1624-30.
- NAIR, A., FREDERICK, T. J. & MILLER, S. D. 2008. Astrocytes in multiple sclerosis: a product of their environment. *Cell Mol Life Sci*, 65, 2702-20.
- NANCE, D. M. & SANDERS, V. M. 2007. Autonomic innervation and regulation of the immune system (1987-2007). *Brain Behav Immun*, 21, 736-45.
- NANDAKUMAR, K. S., SVENSSON, L. & HOLMDAHL, R. 2003. Collagen type II-specific monoclonal antibody-induced arthritis in mice: description of the disease and the influence of age, sex, and genes. *Am J Pathol*, 163, 1827-37.
- NATAH, S. S., MOUIHATE, A., PITTMAN, Q. J. & SHARKEY, K. A. 2005. Disruption of the blood-brain barrier during TNBS colitis. *Neurogastroenterol Motil*, 17, 433-46.
- NATHAN, C. F., MURRAY, H. W., WIEBE, M. E. & RUBIN, B. Y. 1983. Identification of interferon-gamma as the lymphokine that activates human macrophage oxidative metabolism and antimicrobial activity. *J Exp Med*, 158, 670-89.
- NELL, V. P., MACHOLD, K. P., STAMM, T. A., EBERL, G., HEINZL, H., UFFMANN, M., SMOLEN, J. S. & STEINER, G. 2005. Autoantibody profiling as early diagnostic and prognostic tool for rheumatoid arthritis. *Ann Rheum Dis*, 64, 1731-6.
- NELMS, K., KEEGAN, A. D., ZAMORANO, J., RYAN, J. J. & PAUL, W. E. 1999. The IL-4 receptor: signaling mechanisms and biologic functions. *Annu Rev Immunol*, 17, 701-38.
- NGUYEN, M. D., JULIEN, J. P. & RIVEST, S. 2002. Innate immunity: the missing link in neuroprotection and neurodegeneration? *Nat Rev Neurosci*, 3, 216-27.
- NIE, Z., JACOBY, D. B. & FRYER, A. D. 2009. Etanercept prevents airway hyperresponsiveness by protecting neuronal M2 muscarinic receptors in antigen-challenged guinea pigs. *Br J Pharmacol*, 156, 201-10.
- NIKCEVICH, K. M., GORDON, K. B., TAN, L., HURST, S. D., KROEPFL, J. F., GARDINIER, M., BARRETT, T. A. & MILLER, S. D. 1997. IFN-gamma-activated primary murine astrocytes express B7 costimulatory molecules and prime naive antigen-specific T cells. *J Immunol*, 158, 614-21.
- NIKI, Y., YAMADA, H., KIKUCHI, T., TOYAMA, Y., MATSUMOTO, H., FUJIKAWA, K. & TADA, N. 2004. Membrane-associated IL-1 contributes to chronic synovitis and cartilage destruction in human IL-1 alpha transgenic mice. *J Immunol*, 172, 577-84.
- NISHIOKU, T., MATSUMOTO, J., DOHGU, S., SUMI, N., MIYAO, K., TAKATA, F., SHUTO, H., YAMAUCHI, A. & KATAOKA, Y. 2010a. Tumor necrosis factor-alpha mediates the blood-brain barrier dysfunction induced by activated microglia in mouse brain microvascular endothelial cells. *J Pharmacol Sci*, 112, 251-4.
- NISHIOKU, T., YAMAUCHI, A., TAKATA, F., WATANABE, T., FURUSHO, K., SHUTO, H., DOHGU, S. & KATAOKA, Y. 2010b. Disruption of the blood-brain barrier in collagen-induced arthritic mice. *Neurosci Lett*, 482, 208-11.
- NOLAN, T., HANDS, R. E. & BUSTIN, S. A. 2006. Quantification of mRNA using real-time RT-PCR. *Nat Protoc*, 1, 1559-82.

- NYFFELER, M., YEE, B. K., FELDON, J. & KNUESEL, I. 2010. Abnormal differentiation of newborn granule cells in age-related working memory impairments. *Neurobiol Aging*, 31, 1956-74.
- O'CONNOR, J. C., LAWSON, M. A., ANDRE, C., MOREAU, M., LESTAGE, J., CASTANON, N., KELLEY, K. W. & DANTZER, R. 2009. Lipopolysaccharide-induced depressive-like behavior is mediated by indoleamine 2,3-dioxygenase activation in mice. *Mol Psychiatry*, 14, 511-22.
- O'GARRA, A. & ARAI, N. 2000. The molecular basis of T helper 1 and T helper 2 cell differentiation. *Trends Cell Biol*, 10, 542-50.
- O'KEEFE, G. M., NGUYEN, V. T. & BENVENISTE, E. N. 1999. Class II transactivator and class II MHC gene expression in microglia: modulation by the cytokines TGF-beta, IL-4, IL-13 and IL-10. *Eur J Immunol*, 29, 1275-85.
- O'KEEFE, G. M., NGUYEN, V. T. & BENVENISTE, E. N. 2002. Regulation and function of class II major histocompatibility complex, CD40, and B7 expression in macrophages and microglia: Implications in neurological diseases. *J Neurovirol*, 8, 496-512.
- O'NEILL, M. J. & CLEMENS, J. A. 2001. Rodent models of global cerebral ischemia. *Curr Protoc Neurosci*, Chapter 9, Unit9 5.
- O'SHEA, J. J., MA, A. & LIPSKY, P. 2002. Cytokines and autoimmunity. *Nat Rev Immunol*, 2, 37-45.
- O'SULLIVAN, J. B., RYAN, K. M., HARKIN, A. & CONNOR, T. J. 2010. Noradrenaline reuptake inhibitors inhibit expression of chemokines IP-10 and RANTES and cell adhesion molecules VCAM-1 and ICAM-1 in the CNS following a systemic inflammatory challenge. *J Neuroimmunol*, 220, 34-42.
- OGATA, N., KOURO, T., YAMADA, A., KOIKE, M., HANAI, N., ISHIKAWA, T. & TAKATSU, K. 1998. JAK2 and JAK1 constitutively associate with an interleukin-5 (IL-5) receptor alpha and beta subunit, respectively, and are activated upon IL-5 stimulation. *Blood*, 91, 2264-71.
- OHMACHI, Y., FUJIMURA, H., OTSUKA, E., MIYAZAKI, T., TORIUMI, W., KITAMURA, K. & DOI, K. 2002. Recovery process of arthritis induced by 6-sulfanilamidoindazole (6SAI) in rats. *Histol Histopathol*, 17, 437-44.
- OHNISHI, Y., TSUTSUMI, A., SAKAMAKI, T. & SUMIDA, T. 2003. T cell epitopes of type II collagen in HLA-DRB1*0101 or DRB1*0405-positive Japanese patients with rheumatoid arthritis. *Int J Mol Med*, 11, 331-5.
- OKAMOTO, Y., GOTOH, Y., TOKUI, H., MIZUNO, A., KOBAYASHI, Y. & NISHIDA, M. 2000. Characterization of the cytokine network at a single cell level in mice with collagen-induced arthritis using a dual color ELISPOT assay. *J Interferon Cytokine Res*, 20, 55-61.
- OLSON, J. K. & MILLER, S. D. 2004. Microglia initiate central nervous system innate and adaptive immune responses through multiple TLRs. *J Immunol*, 173, 3916-24.
- OLSZEWSKI, W. L., PAZDUR, J., KUBASIEWICZ, E., ZALESKA, M., COOKE, C. J. & MILLER, N. E. 2001. Lymph draining from foot joints in rheumatoid arthritis provides insight into local cytokine and chemokine production and transport to lymph nodes. *Arthritis Rheum*, 44, 541-9.
- OMARI, K. M. & DOROVINI-ZIS, K. 2003. CD40 expressed by human brain endothelial cells regulates CD4+ T cell adhesion to endothelium. *J Neuroimmunol*, 134, 166-78.
- OPAL, S. M. & DEPALO, V. A. 2000. Anti-inflammatory cytokines. *Chest*, 117, 1162-72.
- OZTAS, B., AKGUL, S. & ARSLAN, F. B. 2004. Influence of surgical pain stress on the blood-brain barrier permeability in rats. *Life Sci*, 74, 1973-9.

- PACE, T. W., HU, F. & MILLER, A. H. 2007. Cytokine-effects on glucocorticoid receptor function: relevance to glucocorticoid resistance and the pathophysiology and treatment of major depression. *Brain Behav Immun*, 21, 9-19.
- PALEOLOG, E. M. 2002. Angiogenesis in rheumatoid arthritis. *Arthritis Res*, 4 Suppl 3, S81-90.
- PALEOLOG, E. M., YOUNG, S., STARK, A. C., MCCLOSKEY, R. V., FELDMANN, M. & MAINI, R. N. 1998. Modulation of angiogenic vascular endothelial growth factor by tumor necrosis factor alpha and interleukin-1 in rheumatoid arthritis. *Arthritis Rheum*, 41, 1258-65.
- PALHAGEN, S., QI, H., MARTENSSON, B., WALINDER, J., GRANERUS, A. K. & SVENNINGSSON, P. 2010. Monoamines, BDNF, IL-6 and corticosterone in CSF in patients with Parkinson's disease and major depression. *J Neurol*, 257, 524-32.
- PALMBLAD, K., ERLANDSSON-HARRIS, H., TRACEY, K. J. & ANDERSSON, U. 2001. Dynamics of early synovial cytokine expression in rodent collagen-induced arthritis : a therapeutic study using a macrophage-deactivating compound. *Am J Pathol*, 158, 491-500.
- PAN, M., KANG, I., CRAFT, J. & YIN, Z. 2004. Resistance to development of collagen-induced arthritis in C57BL/6 mice is due to a defect in secondary, but not in primary, immune response. *J Clin Immunol*, 24, 481-91.
- PAN, W., CSERNUS, B. & KASTIN, A. J. 2003. Upregulation of p55 and p75 receptors mediating TNF-alpha transport across the injured blood-spinal cord barrier. *J Mol Neurosci*, 21, 173-84.
- PAN, W. & KASTIN, A. J. 2002. TNFalpha transport across the blood-brain barrier is abolished in receptor knockout mice. *Exp Neurol*, 174, 193-200.
- PAN, W., KASTIN, A. J., DANIEL, J., YU, C., BARYSHNIKOVA, L. M. & VON BARTHELD, C. S. 2007. TNFalpha trafficking in cerebral vascular endothelial cells. *J Neuroimmunol*, 185, 47-56.
- PAN, Z. K., FISHER, C., LI, J. D., JIANG, Y., HUANG, S. & CHEN, L. Y. 2011. Bacterial LPS up-regulated TLR3 expression is critical for antiviral response in human monocytes: evidence for negative regulation by CYLD. *Int Immunol*.
- PARKIN, J. & COHEN, B. 2001. An overview of the immune system. *Lancet*, 357, 1777-89.
- PARRISH, W. R., ROSAS-BALLINA, M., GALLOWITSCH-PUERTA, M., OCHANI, M., OCHANI, K., YANG, L. H., HUDSON, L., LIN, X., PATEL, N., JOHNSON, S. M., CHAVAN, S., GOLDSTEIN, R. S., CZURA, C. J., MILLER, E. J., AL-ABED, Y., TRACEY, K. J. & PAVLOV, V. A. 2008. Modulation of TNF release by choline requires alpha7 subunit nicotinic acetylcholine receptor-mediated signaling. *Mol Med*, 14, 567-74.
- PASHENKOV, M., HUANG, Y. M., KOSTULAS, V., HAGLUND, M., SODERSTROM, M. & LINK, H. 2001. Two subsets of dendritic cells are present in human cerebrospinal fluid. *Brain*, 124, 480-92.
- PASQUINI, M., SPECA, A., MASTROENI, S., DELLE CHIAIE, R., STERNBERG, C. N. & BIONDI, M. 2008. Differences in depressive thoughts between major depressive disorder, IFN-alpha-induced depression, and depressive disorders among cancer patients. *J Psychosom Res*, 65, 153-6.
- PASTOR-SOLER, N. M., FISHER, J. S., SHARPE, R., HILL, E., VAN HOEK, A., BROWN, D. & BRETON, S. 2010. Aquaporin 9 expression in the developing rat epididymis is modulated by steroid hormones. *Reproduction*, 139, 613-21.

- PAXINOS, G. & WATSON, C. 1998. *The rat brain in stereotaxic coordinates*, San Diego, Academic Press.
- PENDER, M. P., CSURHES, P. A., GREER, J. M., MOWAT, P. D., HENDERSON, R. D., CAMERON, K. D., PURDIE, D. M., MCCOMBE, P. A. & GOOD, M. F. 2000. Surges of increased T cell reactivity to an encephalitogenic region of myelin proteolipid protein occur more often in patients with multiple sclerosis than in healthy subjects. *J Immunol*, 165, 5322-31.
- PERERA, T. D., COPLAN, J. D., LISANBY, S. H., LIPIRA, C. M., ARIF, M., CARPIO, C., SPITZER, G., SANTARELLI, L., SCHARF, B., HEN, R., ROSOKLIJA, G., SACKEIM, H. A. & DWORK, A. J. 2007. Antidepressant-induced neurogenesis in the hippocampus of adult nonhuman primates. *J Neurosci*, 27, 4894-901.
- PERERA, T. D., PARK, S. & NEMIROVSKAYA, Y. 2008. Cognitive role of neurogenesis in depression and antidepressant treatment. *Neuroscientist*, 14, 326-38.
- PHARES, T. W., KEAN, R. B., MIKHEEVA, T. & HOOPER, D. C. 2006. Regional differences in blood-brain barrier permeability changes and inflammation in the apathogenic clearance of virus from the central nervous system. *J Immunol*, 176, 7666-75.
- PITT, B. & DELDIN, P. J. 2010. Depression and cardiovascular disease: have a happy day--just smile! *Eur Heart J*, 31, 1036-7.
- PLOTKIN, S. R., BANKS, W. A. & KASTIN, A. J. 1996. Comparison of saturable transport and extracellular pathways in the passage of interleukin-1 alpha across the blood-brain barrier. *J Neuroimmunol*, 67, 41-7.
- PLUMPE, T., EHNINGER, D., STEINER, B., KLEMPIN, F., JESSBERGER, S., BRANDT, M., ROMER, B., RODRIGUEZ, G. R., KRONENBERG, G. & KEMPERMANN, G. 2006. Variability of doublecortin-associated dendrite maturation in adult hippocampal neurogenesis is independent of the regulation of precursor cell proliferation. *BMC Neurosci*, 7, 77.
- POLAZZI, E. & CONTESTABILE, A. 2002. Reciprocal interactions between microglia and neurons: from survival to neuropathology. *Rev Neurosci*, 13, 221-42.
- PONCHEL, F., TOOMES, C., BRANSFIELD, K., LEONG, F. T., DOUGLAS, S. H., FIELD, S. L., BELL, S. M., COMBARET, V., PUISIEUX, A., MIGHELL, A. J., ROBINSON, P. A., INGLEHEARN, C. F., ISAACS, J. D. & MARKHAM, A. F. 2003. Real-time PCR based on SYBR-Green I fluorescence: an alternative to the TaqMan assay for a relative quantification of gene rearrangements, gene amplifications and micro gene deletions. *BMC Biotechnol*, 3, 18.
- POPE, S. M., BRANDT, E. B., MISHRA, A., HOGAN, S. P., ZIMMERMANN, N., MATTHAEI, K. I., FOSTER, P. S. & ROTHENBERG, M. E. 2001. IL-13 induces eosinophil recruitment into the lung by an IL-5- and eotaxin-dependent mechanism. *J Allergy Clin Immunol*, 108, 594-601.
- PRESKY, D. H., YANG, H., MINETTI, L. J., CHUA, A. O., NABAVI, N., WU, C. Y., GATELY, M. K. & GUBLER, U. 1996. A functional interleukin 12 receptor complex is composed of two beta-type cytokine receptor subunits. *Proc Natl Acad Sci U S A*, 93, 14002-7.
- PRICE, C. J., HOYDA, T. D. & FERGUSON, A. V. 2008. The area postrema: a brain monitor and integrator of systemic autonomic state. *Neuroscientist*, 14, 182-94.
- PUJOL, F., KITABGI, P. & BOUDIN, H. 2005. The chemokine SDF-1 differentially regulates axonal elongation and branching in hippocampal neurons. *J Cell Sci*, 118, 1071-80.

- PUNNONEN, J., AVERSA, G., COCKS, B. G., MCKENZIE, A. N., MENON, S., ZURAWSKI, G., DE WAAL MALEFYT, R. & DE VRIES, J. E. 1993. Interleukin 13 induces interleukin 4-independent IgG4 and IgE synthesis and CD23 expression by human B cells. *Proc Natl Acad Sci U S A*, 90, 3730-4.
- QIAN, L., WEI, S. J., ZHANG, D., HU, X., XU, Z., WILSON, B., EL-BENNA, J., HONG, J. S. & FLOOD, P. M. 2008. Potent anti-inflammatory and neuroprotective effects of TGF-beta1 are mediated through the inhibition of ERK and p47phox-Ser345 phosphorylation and translocation in microglia. *J Immunol*, 181, 660-8.
- QU, Z., HUANG, X. N., AHMADI, P., ANDRESEVIC, J., PLANCK, S. R., HART, C. E. & ROSENBAUM, J. T. 1995. Expression of basic fibroblast growth factor in synovial tissue from patients with rheumatoid arthritis and degenerative joint disease. *Lab Invest*, 73, 339-46.
- QUAN, N., SUNDAR, S. K. & WEISS, J. M. 1994. Induction of interleukin-1 in various brain regions after peripheral and central injections of lipopolysaccharide. *J Neuroimmunol*, 49, 125-34.
- QUAN, N., WHITESIDE, M. & HERKENHAM, M. 1998. Time course and localization patterns of interleukin-1beta messenger RNA expression in brain and pituitary after peripheral administration of lipopolysaccharide. *Neuroscience*, 83, 281-93.
- QUARANTINI, L. C., BRESSAN, R. A., GALVAO, A., BATISTA-NEVES, S., PARANA, R. & MIRANDA-SCIPPA, A. 2007. Incidence of psychiatric side effects during pegylated interferon- alpha retreatment in nonresponder hepatitis C virus-infected patients. *Liver Int*, 27, 1098-102.
- QUINONES, M. P., KALKONDE, Y., ESTRADA, C. A., JIMENEZ, F., RAMIREZ, R., MAHIMAINATHAN, L., MUMMIDI, S., CHOUDHURY, G. G., MARTINEZ, H., ADAMS, L., MACK, M., REDDICK, R. L., MAFFI, S., HARALAMBOUS, S., PROBERT, L., AHUJA, S. K. & AHUJA, S. S. 2008. Role of astrocytes and chemokine systems in acute TNFalpha induced demyelinating syndrome: CCR2-dependent signals promote astrocyte activation and survival via NF-kappaB and Akt. *Mol Cell Neurosci*, 37, 96-109.
- RAGHAVENDRA, V., TANGA, F. Y. & DELEO, J. A. 2004. Complete Freund's adjuvant-induced peripheral inflammation evokes glial activation and proinflammatory cytokine expression in the CNS. *Eur J Neurosci*, 20, 467-73.
- RAISON, C. L., CAPURON, L. & MILLER, A. H. 2006. Cytokines sing the blues: inflammation and the pathogenesis of depression. *Trends Immunol*, 27, 24-31.
- RAISON, C. L., DANTZER, R., KELLEY, K. W., LAWSON, M. A., WOOLWINE, B. J., VOGT, G., SPIVEY, J. R., SAITO, K. & MILLER, A. H. 2010. CSF concentrations of brain tryptophan and kynurenines during immune stimulation with IFN-alpha: relationship to CNS immune responses and depression. *Mol Psychiatry*, 15, 393-403.
- RAISON, C. L., WOOLWINE, B. J., DEMETRASHVILI, M. F., BORISOV, A. S., WEINREIB, R., STAAB, J. P., ZAJECKA, J. M., BRUNO, C. J., HENDERSON, M. A., REINUS, J. F., EVANS, D. L., ASNIS, G. M. & MILLER, A. H. 2007. Paroxetine for prevention of depressive symptoms induced by interferon-alpha and ribavirin for hepatitis C. *Aliment Pharmacol Ther*, 25, 1163-74.
- RANKINE, E. L., HUGHES, P. M., BOTHAM, M. S., PERRY, V. H. & FELTON, L. M. 2006. Brain cytokine synthesis induced by an intraparenchymal injection of LPS is reduced in MCP-1-deficient mice prior to leucocyte recruitment. *Eur J Neurosci*, 24, 77-86.

- RAO, M. S. & SHETTY, A. K. 2004. Efficacy of doublecortin as a marker to analyse the absolute number and dendritic growth of newly generated neurons in the adult dentate gyrus. *Eur J Neurosci*, 19, 234-46.
- REFAELI, Y., VAN PARIJS, L., LONDON, C. A., TSCHOPP, J. & ABBAS, A. K. 1998. Biochemical mechanisms of IL-2-regulated Fas-mediated T cell apoptosis. *Immunity*, 8, 615-23.
- REIJERKERK, A., KOOIJ, G., VAN DER POL, S. M., KHAZEN, S., DIJKSTRA, C. D. & DE VRIES, H. E. 2006. Diapedesis of monocytes is associated with MMP-mediated occludin disappearance in brain endothelial cells. *FASEB J*, 20, 2550-2.
- REVEST, J. M., DUPRET, D., KOEHL, M., FUNK-REITER, C., GROSJEAN, N., PIAZZA, P. V. & ABROUS, D. N. 2009. Adult hippocampal neurogenesis is involved in anxiety-related behaviors. *Mol Psychiatry*, 14, 959-67.
- REYES, T. M., WALKER, J. R., DECINO, C., HOGENESCH, J. B. & SAWCHENKO, P. E. 2003. Categorically distinct acute stressors elicit dissimilar transcriptional profiles in the paraventricular nucleus of the hypothalamus. *J Neurosci*, 23, 5607-16.
- RIAZI, K., GALIC, M. A., KUZMISKI, J. B., HO, W., SHARKEY, K. A. & PITTMAN, Q. J. 2008. Microglial activation and TNF α production mediate altered CNS excitability following peripheral inflammation. *Proc Natl Acad Sci U S A*, 105, 17151-6.
- RIOJA, I., BUSH, K. A., BUCKTON, J. B., DICKSON, M. C. & LIFE, P. F. 2004. Joint cytokine quantification in two rodent arthritis models: kinetics of expression, correlation of mRNA and protein levels and response to prednisolone treatment. *Clin Exp Immunol*, 137, 65-73.
- RIZZO, L. V., XU, H., CHAN, C. C., WIGGERT, B. & CASPI, R. R. 1998. IL-10 has a protective role in experimental autoimmune uveoretinitis. *Int Immunol*, 10, 807-14.
- ROBAEYS, G., DE BIE, J., WICHERS, M. C., BRUCKERS, L., NEVENS, F., MICHELSEN, P., VAN RANST, M. & BUNTINX, F. 2007. Early prediction of major depression in chronic hepatitis C patients during peg-interferon alpha-2b treatment by assessment of vegetative-depressive symptoms after four weeks. *World J Gastroenterol*, 13, 5736-40.
- ROCCARO, A. M., RUSSO, F., CIRULLI, T., DI PIETRO, G., VACCA, A. & DAMMACCO, F. 2005. Antiangiogenesis for rheumatoid arthritis. *Curr Drug Targets Inflamm Allergy*, 4, 27-30.
- ROHLEDER, N., WOLF, J. M. & WOLF, O. T. 2010. Glucocorticoid sensitivity of cognitive and inflammatory processes in depression and posttraumatic stress disorder. *Neurosci Biobehav Rev*, 35, 104-114.
- ROLLS, A., SHECHTER, R., LONDON, A., ZIV, Y., RONEN, A., LEVY, R. & SCHWARTZ, M. 2007. Toll-like receptors modulate adult hippocampal neurogenesis. *Nat Cell Biol*, 9, 1081-8.
- ROMAGNANI, S. 1994. Lymphokine production by human T cells in disease states. *Annu Rev Immunol*, 12, 227-57.
- ROSENSTEIN, J. M., MANI, N., KHAIBULLINA, A. & KRUM, J. M. 2003. Neurotrophic effects of vascular endothelial growth factor on organotypic cortical explants and primary cortical neurons. *J Neurosci*, 23, 11036-44.
- ROSLONIEC, E. F., CREMER, M., KANG, A. H., MYERS, L. K. & BRAND, D. D. 2010. Collagen-induced arthritis. *Curr Protoc Immunol*, Chapter 15, Unit 15 5 1-25.
- ROTTMAN, J. B. 1999a. Key role of chemokines and chemokine receptors in inflammation, immunity, neoplasia, and infectious disease. *Vet Pathol*, 36, 357-67.

- ROTTMAN, J. B. 1999b. Key role of chemokines and chemokine receptors in inflammation, immunity, neoplasia, and infectious disease. *Veterinary Pathology*, 36, 357-367.
- ROWAN, A. D., HUI, W., CAWSTON, T. E. & RICHARDS, C. D. 2003. Adenoviral gene transfer of interleukin-1 in combination with oncostatin M induces significant joint damage in a murine model. *Am J Pathol*, 162, 1975-84.
- RUBIO, N. & SANZ-RODRIGUEZ, F. 2007. Induction of the CXCL1 (KC) chemokine in mouse astrocytes by infection with the murine encephalomyelitis virus of Theiler. *Virology*, 358, 98-108.
- SAARELAINEN, T., HENDOLIN, P., LUCAS, G., KOPONEN, E., SAIRANEN, M., MACDONALD, E., AGERMAN, K., HAAPASALO, A., NAWA, H., ALOYZ, R., ERNFORS, P. & CASTREN, E. 2003. Activation of the TrkB neurotrophin receptor is induced by antidepressant drugs and is required for antidepressant-induced behavioral effects. *J Neurosci*, 23, 349-57.
- SAHAY, A., DREW, M. R. & HEN, R. 2007. Dentate gyrus neurogenesis and depression. *Prog Brain Res*, 163, 697-722.
- SAHAY, A. & HEN, R. 2007. Adult hippocampal neurogenesis in depression. *Nat Neurosci*, 10, 1110-5.
- SAKATA, K., JIN, L. & JHA, S. 2010. Lack of promoter IV-driven BDNF transcription results in depression-like behavior. *Genes Brain Behav*, 9, 712-21.
- SAKATA, Y., MORIMOTO, A., LONG, N. C. & MURAKAMI, N. 1991. Fever and acute-phase response induced in rabbits by intravenous and intracerebroventricular injection of interleukin-6. *Cytokine*, 3, 199-203.
- SANTARELLI, L., SAXE, M., GROSS, C., SURGET, A., BATTAGLIA, F., DULAWA, S., WEISSTAUB, N., LEE, J., DUMAN, R., ARANCIO, O., BELZUNG, C. & HEN, R. 2003. Requirement of hippocampal neurogenesis for the behavioral effects of antidepressants. *Science*, 301, 805-9.
- SASAKI, M., LANKFORD, K. L., BROWN, R. J., RUDDLE, N. H. & KOCSIS, J. D. 2010. Focal experimental autoimmune encephalomyelitis in the Lewis rat induced by immunization with myelin oligodendrocyte glycoprotein and intraspinal injection of vascular endothelial growth factor. *Glia*, 58, 1523-31.
- SATO, S., REINER, S. L., JENSEN, M. A. & ROOS, R. P. 1997. Central nervous system cytokine mRNA expression following Theiler's murine encephalomyelitis virus infection. *J Neuroimmunol*, 76, 213-23.
- SAWADA, M., KONDO, N., SUZUMURA, A. & MARUNOUCHI, T. 1989. Production of tumor necrosis factor-alpha by microglia and astrocytes in culture. *Brain Res*, 491, 394-7.
- SAWADA, M., SUZUMURA, A., ITOH, Y. & MARUNOUCHI, T. 1993. Production of interleukin-5 by mouse astrocytes and microglia in culture. *Neurosci Lett*, 155, 175-8.
- SAWADA, M., SUZUMURA, A. & MARUNOUCHI, T. 1992. TNF alpha induces IL-6 production by astrocytes but not by microglia. *Brain Res*, 583, 296-9.
- SAXE, M. D., BATTAGLIA, F., WANG, J. W., MALLERET, G., DAVID, D. J., MONCKTON, J. E., GARCIA, A. D., SOFRONIEW, M. V., KANDEL, E. R., SANTARELLI, L., HEN, R. & DREW, M. R. 2006. Ablation of hippocampal neurogenesis impairs contextual fear conditioning and synaptic plasticity in the dentate gyrus. *Proc Natl Acad Sci U S A*, 103, 17501-6.
- SCHAEFER, C. J., LAWRENCE, W. D. & WOOLEY, P. H. 1999. Influence of long term silicone implantation on type II collagen induced arthritis in mice. *Ann Rheum Dis*, 58, 503-9.

- SCHIAVON, A. P., MILANI, H., ROMANINI, C. V., FORESTI, M. L., CASTRO, O. W., GARCIA-CAIRASCO, N. & DE OLIVEIRA, R. M. 2010. Imipramine enhances cell proliferation and decreases neurodegeneration in the hippocampus after transient global cerebral ischemia in rats. *Neurosci Lett*, 470, 43-8.
- SCHIEPERS, O. J., WICHERS, M. C. & MAES, M. 2005. Cytokines and major depression. *Prog Neuropsychopharmacol Biol Psychiatry*, 29, 201-17.
- SCHMID-GRENDELMEIER, P., ALTZNAUER, F., FISCHER, B., BIZER, C., STRAUMANN, A., MENZ, G., BLASER, K., WUTHRICH, B. & SIMON, H. U. 2002. Eosinophils express functional IL-13 in eosinophilic inflammatory diseases. *J Immunol*, 169, 1021-7.
- SCHNYDRIG, S., KORNER, L., LANDWEER, S., ERNST, B., WALKER, G., OTTEN, U. & KUNZ, D. 2007. Peripheral lipopolysaccharide administration transiently affects expression of brain-derived neurotrophic factor, corticotropin and proopiomelanocortin in mouse brain. *Neurosci Lett*, 429, 69-73.
- SCHROETER, M. & JANDER, S. 2005. T-cell cytokines in injury-induced neural damage and repair. *Neuromolecular Med*, 7, 183-95.
- SCHUERWEGH, A. J., VAN OFFEL, J. F., STEVENS, W. J., BRIDTS, C. H. & DE CLERCK, L. S. 2003. Influence of therapy with chimeric monoclonal tumour necrosis factor-alpha antibodies on intracellular cytokine profiles of T lymphocytes and monocytes in rheumatoid arthritis patients. *Rheumatology (Oxford)*, 42, 541-8.
- SCHULZ, M. & ENGELHARDT, B. 2005. The circumventricular organs participate in the immunopathogenesis of experimental autoimmune encephalomyelitis. *Cerebrospinal Fluid Res*, 2, 8.
- SCHULZE-KOOPS, H. & KALDEN, J. R. 2001. The balance of Th1/Th2 cytokines in rheumatoid arthritis. *Best Pract Res Clin Rheumatol*, 15, 677-91.
- SEDGWICK, J. D., MOSSNER, R., SCHWENDER, S. & TER MEULEN, V. 1991. Major histocompatibility complex-expressing nonhematopoietic astroglial cells prime only CD8+ T lymphocytes: astroglial cells as perpetuators but not initiators of CD4+ T cell responses in the central nervous system. *J Exp Med*, 173, 1235-46.
- SEGHEZZI, G., PATEL, S., REN, C. J., GUALANDRIS, A., PINTUCCI, G., ROBBINS, E. S., SHAPIRO, R. L., GALLOWAY, A. C., RIFKIN, D. B. & MIGNATTI, P. 1998. Fibroblast growth factor-2 (FGF-2) induces vascular endothelial growth factor (VEGF) expression in the endothelial cells of forming capillaries: an autocrine mechanism contributing to angiogenesis. *J Cell Biol*, 141, 1659-73.
- SEGUIN, J. A., BRENNAN, J., MANGANO, E. & HAYLEY, S. 2009. Proinflammatory cytokines differentially influence adult hippocampal cell proliferation depending upon the route and chronicity of administration. *Neuropsychiatr Dis Treat*, 5, 5-14.
- SEINO, K., AZUMA, M., BASHUDA, H., FUKAO, K., YAGITA, H. & OKUMURA, K. 1995. CD86 (B70/B7-2) on endothelial cells co-stimulates allogeneic CD4+ T cells. *Int Immunol*, 7, 1331-7.
- SELVARAJ, S. K., GIRI, R. K., PERELMAN, N., JOHNSON, C., MALIK, P. & KALRA, V. K. 2003. Mechanism of monocyte activation and expression of proinflammatory cytochemokines by placenta growth factor. *Blood*, 102, 1515-24.
- SEYMOUR, H. E., WORSLEY, A., SMITH, J. M. & THOMAS, S. H. 2001. Anti-TNF agents for rheumatoid arthritis. *Br J Clin Pharmacol*, 51, 201-8.
- SHAFTEL, S. S., CARLSON, T. J., OLSCHOWKA, J. A., KYRKANIDES, S., MATOUSEK, S. B. & O'BANION, M. K. 2007. Chronic interleukin-1beta expression in mouse brain leads to leukocyte infiltration and neutrophil-independent

- blood brain barrier permeability without overt neurodegeneration. *J Neurosci*, 27, 9301-9.
- SHARSHAR, T., HOPKINSON, N. S., ORLIKOWSKI, D. & ANNANE, D. 2005. Science review: The brain in sepsis-culprit and victim. *Crit Care*, 9, 37-44.
- SHEA-DONOHUE, T., THOMAS, K., CODY, M. J., AIPING, Z., DETOLLA, L. J., KOPYDLOWSKI, K. M., FUKATA, M., LIRA, S. A. & VOGEL, S. N. 2008. Mice deficient in the CXCR2 ligand, CXCL1 (KC/GRO-alpha), exhibit increased susceptibility to dextran sodium sulfate (DSS)-induced colitis. *Innate Immunol*, 14, 117-24.
- SHEARER, W. T., REUBEN, J. M., MULLINGTON, J. M., PRICE, N. J., LEE, B. N., SMITH, E. O., SZUBA, M. P., VAN DONGEN, H. P. & DINGES, D. F. 2001. Soluble TNF-alpha receptor 1 and IL-6 plasma levels in humans subjected to the sleep deprivation model of spaceflight. *J Allergy Clin Immunol*, 107, 165-70.
- SHEN, C. H., TSAI, R. Y., SHIH, M. S., LIN, S. L., TAI, Y. H., CHIEN, C. C. & WONG, C. S. 2011. Etanercept restores the antinociceptive effect of morphine and suppresses spinal neuroinflammation in morphine-tolerant rats. *Anesth Analg*, 112, 454-9.
- SHENG, W. S., HU, S., HEGG, C. C., THAYER, S. A. & PETERSON, P. K. 2000. Activation of human microglial cells by HIV-1 gp41 and Tat proteins. *Clin Immunol*, 96, 243-51.
- SHENG, W. S., HU, S., KRAVITZ, F. H., PETERSON, P. K. & CHAO, C. C. 1995. Tumor necrosis factor alpha upregulates human microglial cell production of interleukin-10 in vitro. *Clin Diagn Lab Immunol*, 2, 604-8.
- SHI, S. S., SHAO, S. H., YUAN, B. P., PAN, F. & LI, Z. L. 2010. Acute stress and chronic stress change brain-derived neurotrophic factor (BDNF) and tyrosine kinase-coupled receptor (TrkB) expression in both young and aged rat hippocampus. *Yonsei Med J*, 51, 661-71.
- SHIBUYA, K., ROBINSON, D., ZONIN, F., HARTLEY, S. B., MACATONIA, S. E., SOMOZA, C., HUNTER, C. A., MURPHY, K. M. & O'GARRA, A. 1998. IL-1 alpha and TNF-alpha are required for IL-12-induced development of Th1 cells producing high levels of IFN-gamma in BALB/c but not C57BL/6 mice. *J Immunol*, 160, 1708-16.
- SHIMAMURA, N., MATCHETT, G., SOLAROGLU, I., TSUBOKAWA, T., OHKUMA, H. & ZHANG, J. 2006. Inhibition of integrin alphavbeta3 reduces blood-brain barrier breakdown in focal ischemia in rats. *J Neurosci Res*, 84, 1837-47.
- SHIN, W. H., LEE, D. Y., PARK, K. W., KIM, S. U., YANG, M. S., JOE, E. H. & JIN, B. K. 2004. Microglia expressing interleukin-13 undergo cell death and contribute to neuronal survival in vivo. *Glia*, 46, 142-52.
- SIMON, N. M., MCNAMARA, K., CHOW, C. W., MASER, R. S., PAPAKOSTAS, G. I., POLLACK, M. H., NIERENBERG, A. A., FAVA, M. & WONG, K. K. 2008. A detailed examination of cytokine abnormalities in Major Depressive Disorder. *Eur Neuropsychopharmacol*, 18, 230-3.
- SIMS, J. E., MARCH, C. J., COSMAN, D., WIDMER, M. B., MACDONALD, H. R., MCMAHAN, C. J., GRUBIN, C. E., WIGNALL, J. M., JACKSON, J. L., CALL, S. M. & ET AL. 1988. cDNA expression cloning of the IL-1 receptor, a member of the immunoglobulin superfamily. *Science*, 241, 585-9.
- SINGH, M. M. 1970. A unifying hypothesis on the biochemical basis of affective disorder. *Psychiatr Q*, 44, 706-24.
- SKINNER, R. A., GIBSON, R. M., ROTHWELL, N. J., PINTEAUX, E. & PENNY, J. I. 2009. Transport of interleukin-1 across cerebromicrovascular endothelial cells. *Br J Pharmacol*, 156, 1115-23.

- SLETTENAAR, V. I. & WILSON, J. L. 2006. The chemokine network: a target in cancer biology? *Adv Drug Deliv Rev*, 58, 962-74.
- SMITH, M. A., MAKINO, S., KVETNANSKY, R. & POST, R. M. 1995. Stress and glucocorticoids affect the expression of brain-derived neurotrophic factor and neurotrophin-3 mRNAs in the hippocampus. *J Neurosci*, 15, 1768-77.
- SNYDER, J. S., HONG, N. S., MCDONALD, R. J. & WOJTOWICZ, J. M. 2005. A role for adult neurogenesis in spatial long-term memory. *Neuroscience*, 130, 843-52.
- SOFRONIEW, M. V. 2009. Molecular dissection of reactive astrogliosis and glial scar formation. *Trends Neurosci*, 32, 638-47.
- SOFRONIEW, M. V. & VINTERS, H. V. 2010. Astrocytes: biology and pathology. *Acta Neuropathol*, 119, 7-35.
- SONG, C., LIN, A., BONACCORSO, S., HEIDE, C., VERKERK, R., KENIS, G., BOSMANS, E., SCHARPE, S., WHELAN, A., COSYNS, P., DE JONGH, R. & MAES, M. 1998. The inflammatory response system and the availability of plasma tryptophan in patients with primary sleep disorders and major depression. *J Affect Disord*, 49, 211-9.
- SONOBE, Y., LIANG, J., JIN, S., ZHANG, G., TAKEUCHI, H., MIZUNO, T. & SUZUMURA, A. 2008. Microglia express a functional receptor for interleukin-23. *Biochem Biophys Res Commun*, 370, 129-33.
- SPIES, C. M., BARTHOLOME, B., BERKI, T., BURMESTER, G. R., RADBRUCH, A., SCHEFFOLD, A. & BUTTGEREIT, F. 2007. Membrane glucocorticoid receptors (mGCR) on monocytes are up-regulated after vaccination. *Rheumatology (Oxford)*, 46, 364-5.
- SREDNI-KENIGSBUCH, D. 2002. TH1/TH2 cytokines in the central nervous system. *Int J Neurosci*, 112, 665-703.
- SRIRAM, S. & STEINER, I. 2005. Experimental allergic encephalomyelitis: a misleading model of multiple sclerosis. *Ann Neurol*, 58, 939-45.
- STALDER, A. K., PAGENSTECHE, A., YU, N. C., KINCAID, C., CHIANG, C. S., HOBBS, M. V., BLOOM, F. E. & CAMPBELL, I. L. 1997. Lipopolysaccharide-induced IL-12 expression in the central nervous system and cultured astrocytes and microglia. *J Immunol*, 159, 1344-51.
- STASIUK, L. M., ABEHSIRA-AMAR, O. & FOURNIER, C. 1996. Collagen-induced arthritis in DBA/1 mice: cytokine gene activation following immunization with type II collagen. *Cell Immunol*, 173, 269-75.
- STEMME, V., RYMO, L., RISBERG, B. & STEMME, S. 2001. Quantitative analysis of specific mRNA species in minute cell samples by RT-PCR and flow cytometry. *J Immunol Methods*, 249, 223-33.
- STERNBERG, E. M. 2006. Neural regulation of innate immunity: a coordinated nonspecific host response to pathogens. *Nat Rev Immunol*, 6, 318-28.
- STOLINA, M., BOLON, B., MIDDLETON, S., DWYER, D., BROWN, H., DURYEA, D., ZHU, L., ROHNER, A., PRETORIUS, J., KOSTENUIK, P., FEIGE, U. & ZACK, D. 2009. The evolving systemic and local biomarker milieu at different stages of disease progression in rat adjuvant-induced arthritis. *J Clin Immunol*, 29, 158-74.
- STOLL, M., CAPPER, D., DIETZ, K., WARTH, A., SCHLEICH, A., SCHLASZUS, H., MEYERMANN, R. & MITTELBRONN, M. 2006. Differential microglial regulation in the human spinal cord under normal and pathological conditions. *Neuropathol Appl Neurobiol*, 32, 650-61.
- STOLP, H. B., DZIEGIELEWSKA, K. M., EK, C. J., HABGOOD, M. D., LANE, M. A., POTTER, A. M. & SAUNDERS, N. R. 2005a. Breakdown of the blood-brain barrier to proteins in white matter of the developing brain following systemic inflammation. *Cell Tissue Res*, 320, 369-78.

- STOLP, H. B., DZIEGIELEWSKA, K. M., EK, C. J., POTTER, A. M. & SAUNDERS, N. R. 2005b. Long-term changes in blood-brain barrier permeability and white matter following prolonged systemic inflammation in early development in the rat. *Eur J Neurosci*, 22, 2805-16.
- STOLP, H. B., EK, C. J., JOHANSSON, P. A., DZIEGIELEWSKA, K. M., BETHGE, N., WHEATON, B. J., POTTER, A. M. & SAUNDERS, N. R. 2009. Factors involved in inflammation-induced developmental white matter damage. *Neurosci Lett*, 451, 232-6.
- STOLP, H. B., EK, C. J., JOHANSSON, P. A., DZIEGIELEWSKA, K. M., POTTER, A. M., HABGOOD, M. D. & SAUNDERS, N. R. 2007. Effect of minocycline on inflammation-induced damage to the blood-brain barrier and white matter during development. *Eur J Neurosci*, 26, 3465-74.
- STRAUB, R. H., PONGRATZ, G., SCHOLMERICH, J., KEES, F., SCHAIBLE, T. F., ANTONI, C., KALDEN, J. R. & LORENZ, H. M. 2003. Long-term anti-tumor necrosis factor antibody therapy in rheumatoid arthritis patients sensitizes the pituitary gland and favors adrenal androgen secretion. *Arthritis Rheum*, 48, 1504-12.
- STROMNES, I. M., CERRETTI, L. M., LIGGITT, D., HARRIS, R. A. & GOVERMAN, J. M. 2008. Differential regulation of central nervous system autoimmunity by T(H)1 and T(H)17 cells. *Nat Med*, 14, 337-42.
- SUH, H. S., ZHAO, M. L., RIVIECCIO, M., CHOI, S., CONNOLLY, E., ZHAO, Y., TAKIKAWA, O., BROSNAN, C. F. & LEE, S. C. 2007. Astrocyte indoleamine 2,3-dioxygenase is induced by the TLR3 ligand poly(I:C): mechanism of induction and role in antiviral response. *J Virol*, 81, 9838-50.
- SUVANNAVEJH, G. C., LEE, H. O., PADILLA, J., DAL CANTO, M. C., BARRETT, T. A. & MILLER, S. D. 2000. Divergent roles for p55 and p75 tumor necrosis factor receptors in the pathogenesis of MOG(35-55)-induced experimental autoimmune encephalomyelitis. *Cell Immunol*, 205, 24-33.
- SUZUKI, T., HIGGINS, P. J. & CRAWFORD, D. R. 2000. Control selection for RNA quantitation. *Biotechniques*, 29, 332-7.
- SWIFT, M. E., KLEINMAN, H. K. & DIPIETRO, L. A. 1999. Impaired wound repair and delayed angiogenesis in aged mice. *Lab Invest*, 79, 1479-87.
- SZEKANECZ, Z., BESENYEI, T., PARAGH, G. & KOCH, A. E. 2009. Angiogenesis in rheumatoid arthritis. *Autoimmunity*, 42, 563-73.
- SZEKANECZ, Z., KIM, J. & KOCH, A. E. 2003. Chemokines and chemokine receptors in rheumatoid arthritis. *Semin Immunol*, 15, 15-21.
- TAJIMA, Y., KISHIMOTO, R., SUDOH, K. & MATSUMOTO, A. 2004. Multiple central nervous system lesions associated with rheumatoid arthritis. *Arch Neurol*, 61, 1794-5.
- TAKAHASHI, T., IKEDA, K., ISHIKAWA, M., KITAMURA, N., TSUKASAKI, T., NAKAMA, D. & KAMEDA, T. 2005. Anxiety, reactivity, and social stress-induced cortisol elevation in humans. *Neuro Endocrinol Lett*, 26, 351-4.
- TAKEUCHI, H., JIN, S., WANG, J., ZHANG, G., KAWANOKUCHI, J., KUNO, R., SONOBE, Y., MIZUNO, T. & SUZUMURA, A. 2006. Tumor necrosis factor-alpha induces neurotoxicity via glutamate release from hemichannels of activated microglia in an autocrine manner. *J Biol Chem*, 281, 21362-8.
- TAKEUCHI, O., HOSHINO, K., KAWAI, T., SANJO, H., TAKADA, H., OGAWA, T., TAKEDA, K. & AKIRA, S. 1999. Differential roles of TLR2 and TLR4 in recognition of gram-negative and gram-positive bacterial cell wall components. *Immunity*, 11, 443-51.
- TALIAZ, D., STALL, N., DAR, D. E. & ZANGEN, A. 2010. Knockdown of brain-derived neurotrophic factor in specific brain sites precipitates behaviors

- associated with depression and reduces neurogenesis. *Mol Psychiatry*, 15, 80-92.
- TAN, L., GORDON, K. B., MUELLER, J. P., MATIS, L. A. & MILLER, S. D. 1998. Presentation of proteolipid protein epitopes and B7-1-dependent activation of encephalitogenic T cells by IFN-gamma-activated SJL/J astrocytes. *J Immunol*, 160, 4271-9.
- TAYAL, V. & KALRA, B. S. 2008. Cytokines and anti-cytokines as therapeutics--an update. *Eur J Pharmacol*, 579, 1-12.
- TAYLOR, P. C., PETERS, A. M., PALEOLOG, E., CHAPMAN, P. T., ELLIOTT, M. J., MCCLOSKEY, R., FELDMANN, M. & MAINI, R. N. 2000. Reduction of chemokine levels and leukocyte traffic to joints by tumor necrosis factor alpha blockade in patients with rheumatoid arthritis. *Arthritis Rheum*, 43, 38-47.
- TE VELDE, A. A., HUIJBENS, R. J., HEIJE, K., DE VRIES, J. E. & FIGDOR, C. G. 1990. Interleukin-4 (IL-4) inhibits secretion of IL-1 beta, tumor necrosis factor alpha, and IL-6 by human monocytes. *Blood*, 76, 1392-7.
- TENNAKOON, D. K., SMITH, R., STEWART, M. D., SPENCER, T. E., NAYAK, M. & WELSH, C. J. 2001. Ovine IFN-tau modulates the expression of MHC antigens on murine cerebrovascular endothelial cells and inhibits replication of Theiler's virus. *J Interferon Cytokine Res*, 21, 785-92.
- TERRANDO, N., MONACO, C., MA, D., FOXWELL, B. M., FELDMANN, M. & MAZE, M. 2010. Tumor necrosis factor-alpha triggers a cytokine cascade yielding postoperative cognitive decline. *Proc Natl Acad Sci U S A*, 107, 20518-22.
- THAYER, J. F. & STERNBERG, E. M. 2009. Neural concomitants of immunity--focus on the vagus nerve. *Neuroimage*, 47, 908-10.
- THOMAS, J. W., THIEU, T. H., BYRD, V. M. & MILLER, G. G. 2000. Acidic fibroblast growth factor in synovial cells. *Arthritis Rheum*, 43, 2152-9.
- THOMAS, S. R., SALAHIFAR, H., MASHIMA, R., HUNT, N. H., RICHARDSON, D. R. & STOCKER, R. 2001. Antioxidants inhibit indoleamine 2,3-dioxygenase in IFN-gamma-activated human macrophages: posttranslational regulation by pyrrolidine dithiocarbamate. *J Immunol*, 166, 6332-40.
- THORNTON, S., BOIVIN, G. P., KIM, K. N., FINKELMAN, F. D. & HIRSCH, R. 2000. Heterogeneous effects of IL-2 on collagen-induced arthritis. *J Immunol*, 165, 1557-63.
- THORNTON, S., DUWEL, L. E., BOIVIN, G. P., MA, Y. & HIRSCH, R. 1999. Association of the course of collagen-induced arthritis with distinct patterns of cytokine and chemokine messenger RNA expression. *Arthritis Rheum*, 42, 1109-18.
- TIMONEN, M., VILO, K., HAKKO, H., SARKIOJA, T., YLIKULJU, M., MEYER-ROCHOW, V. B., VAISANEN, E. & RASANEN, P. 2003. Suicides in persons suffering from rheumatoid arthritis. *Rheumatology (Oxford)*, 42, 287-91.
- TJURMINA, O. A., GOLDSTEIN, D. S., PALKOVITS, M. & KOPIN, I. J. 1999. Alpha2-adrenoceptor-mediated restraint of norepinephrine synthesis, release, and turnover during immobilization in rats. *Brain Res*, 826, 243-52.
- TOBINICK, E. L. & GROSS, H. 2008. Rapid cognitive improvement in Alzheimer's disease following perispinal etanercept administration. *J Neuroinflammation*, 5, 2.
- TOBON, G. J., YOUINOU, P. & SARAUX, A. 2010. The environment, geo-epidemiology, and autoimmune disease: Rheumatoid arthritis. *J Autoimmun*.
- TOUSSIROT, E. & ROUDIER, J. 2008. Epstein-Barr virus in autoimmune diseases. *Best Pract Res Clin Rheumatol*, 22, 883-96.

- TOWN, T., NIKOLIC, V. & TAN, J. 2005. The microglial "activation" continuum: from innate to adaptive responses. *J Neuroinflammation*, 2, 24.
- TRACEY, K. J. 2002. The inflammatory reflex. *Nature*, 420, 853-9.
- TREHARNE, G. J., LYONS, A. C. & KITAS, G. D. 2000. Suicidal ideation in patients with rheumatoid arthritis. Research may help identify patients at high risk. *BMJ*, 321, 1290.
- TRENTHAM, D. E., TOWNES, A. S. & KANG, A. H. 1977. Autoimmunity to type II collagen an experimental model of arthritis. *J Exp Med*, 146, 857-68.
- TSAI, P. L., YEH, J. H., CHEN, W. H. & LEE, C. C. 2008. Rheumatoid arthritis with neurological involvement manifested as hemispheric masses. *Eur Neurol*, 59, 190-1.
- TSAO, N., HSU, H. P., WU, C. M., LIU, C. C. & LEI, H. Y. 2001. Tumour necrosis factor-alpha causes an increase in blood-brain barrier permeability during sepsis. *J Med Microbiol*, 50, 812-21.
- TSUDA, M., MASUDA, T., KITANO, J., SHIMOYAMA, H., TOZAKI-SAITOH, H. & INOUE, K. 2009. IFN-gamma receptor signaling mediates spinal microglia activation driving neuropathic pain. *Proc Natl Acad Sci U S A*, 106, 8032-7.
- TSUJI, F., YOSHIMI, M., KATSUTA, O., TAKAI, M., ISHIHARA, K. & AONO, H. 2009. Point mutation of tyrosine 759 of the IL-6 family cytokine receptor, gp130, augments collagen-induced arthritis in DBA/1J mice. *BMC Musculoskelet Disord*, 10, 23.
- TURESSON, C. & MATTESON, E. L. 2004. Management of extra-articular disease manifestations in rheumatoid arthritis. *Curr Opin Rheumatol*, 16, 206-11.
- TYRING, S., GOTTLIEB, A., PAPP, K., GORDON, K., LEONARDI, C., WANG, A., LALLA, D., WOOLLEY, M., JAHREIS, A., ZITNIK, R., CELLA, D. & KRISHNAN, R. 2006. Etanercept and clinical outcomes, fatigue, and depression in psoriasis: double-blind placebo-controlled randomised phase III trial. *Lancet*, 367, 29-35.
- UGUZ, F., AKMAN, C., KUCUKSARAC, S. & TUFEKCI, O. 2009. Anti-tumor necrosis factor-alpha therapy is associated with less frequent mood and anxiety disorders in patients with rheumatoid arthritis. *Psychiatry Clin Neurosci*, 63, 50-5.
- URIBE-SAN MARTIN, R., HERRERA-MOLINA, R., OLAVARRIA, L., RAMIREZ, G. & VON BERNHARDI, R. 2009. Reduction of beta-amyloid-induced neurotoxicity on hippocampal cell cultures by moderate acidosis is mediated by transforming growth factor beta. *Neuroscience*, 158, 1338-47.
- VALLIERES, L., CAMPBELL, I. L., GAGE, F. H. & SAWCHENKO, P. E. 2002. Reduced hippocampal neurogenesis in adult transgenic mice with chronic astrocytic production of interleukin-6. *J Neurosci*, 22, 486-92.
- VAN SNICK, J. 1990. Interleukin-6: an overview. *Annu Rev Immunol*, 8, 253-78.
- VAN ZWAM, M., HUIZINGA, R., MELIEF, M. J., WIERENGA-WOLF, A. F., VAN MEURS, M., VOERMAN, J. S., BIBER, K. P., BODDEKE, H. W., HOPKEN, U. E., MEISEL, C., MEISEL, A., BECHMANN, I., HINTZEN, R. Q., T HART, B. A., AMOR, S., LAMAN, J. D. & BOVEN, L. A. 2009. Brain antigens in functionally distinct antigen-presenting cell populations in cervical lymph nodes in MS and EAE. *J Mol Med*, 87, 273-86.
- VARGHESE, F. P. & BROWN, E. S. 2001. The Hypothalamic-Pituitary-Adrenal Axis in Major Depressive Disorder: A Brief Primer for Primary Care Physicians. *Prim Care Companion J Clin Psychiatry*, 3, 151-155.
- VIVIANI, B., GARDONI, F., BARTESAGHI, S., CORSINI, E., FACCHI, A., GALLI, C. L., DI LUCA, M. & MARINOVICH, M. 2006. Interleukin-1 beta released by gp120

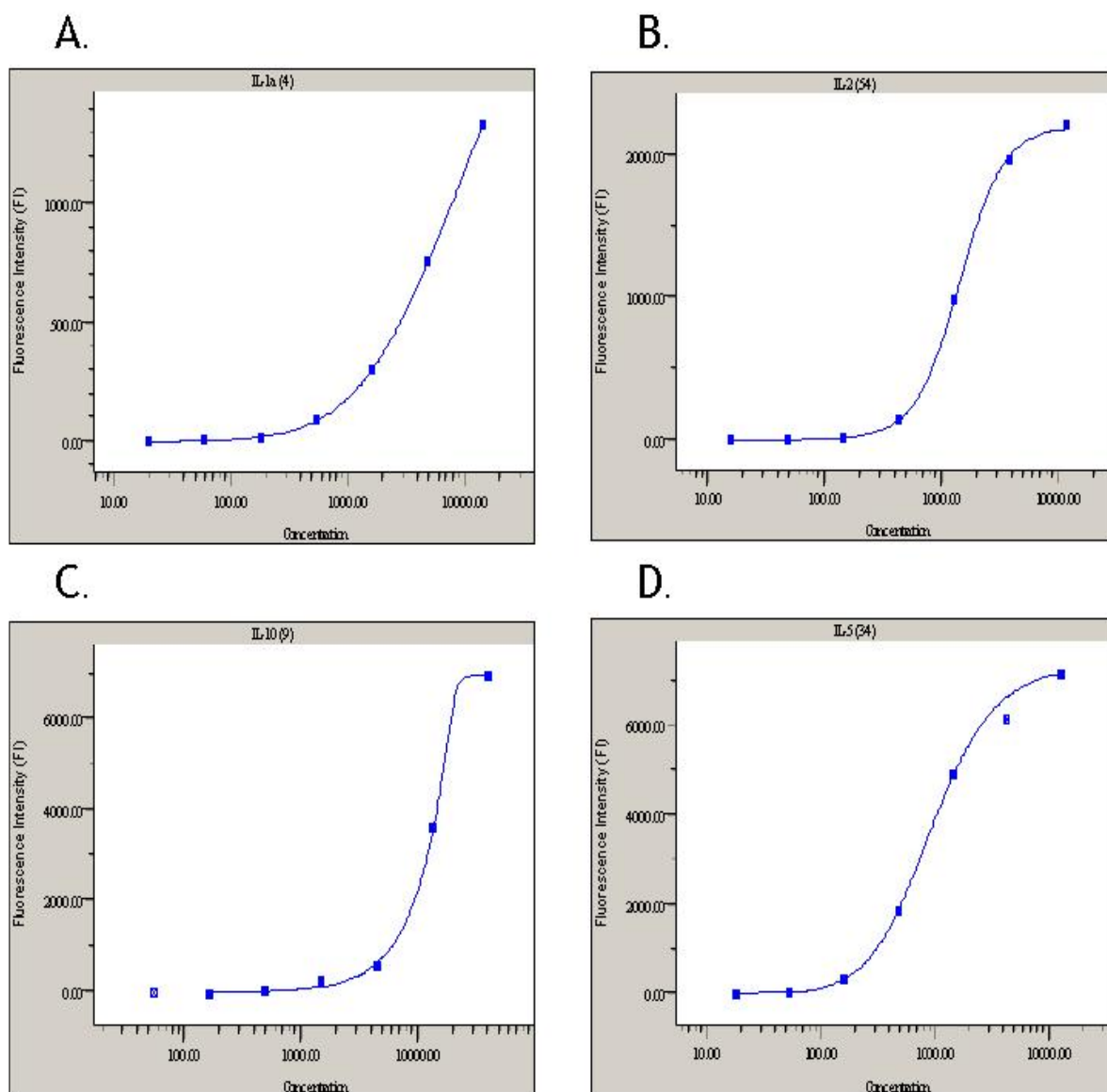
- drives neural death through tyrosine phosphorylation and trafficking of NMDA receptors. *J Biol Chem*, 281, 30212-22.
- VLKOLINSKY, R., SIGGINS, G. R., CAMPBELL, I. L. & KRUCKER, T. 2004. Acute exposure to CXC chemokine ligand 10, but not its chronic astroglial production, alters synaptic plasticity in mouse hippocampal slices. *J Neuroimmunol*, 150, 37-47.
- VON GUNTEN, A. & RON, M. A. 2004. Hippocampal volume and subjective memory impairment in depressed patients. *Eur Psychiatry*, 19, 438-40.
- VON WEDEL-PARLOW, M., WOLTE, P. & GALLA, H. J. 2009. Regulation of major efflux transporters under inflammatory conditions at the blood-brain barrier in vitro. *J Neurochem*, 111, 111-8.
- WAAGE, A., KAUFMANN, C., ESPEVIK, T. & HUSBY, G. 1989. Interleukin-6 in synovial fluid from patients with arthritis. *Clin Immunol Immunopathol*, 50, 394-8.
- WALTER, B. A., VALERA, V. A., TAKAHASHI, S., MATSUNO, K. & USHIKI, T. 2006. Evidence of antibody production in the rat cervical lymph nodes after antigen administration into the cerebrospinal fluid. *Arch Histol Cytol*, 69, 37-47.
- WANG, D. D. & BORDEY, A. 2008. The astrocyte odyssey. *Prog Neurobiol*, 86, 342-67.
- WANG, H. Y., LI, W., BENEDETTI, N. J. & LEE, D. H. 2003. Alpha 7 nicotinic acetylcholine receptors mediate beta-amyloid peptide-induced tau protein phosphorylation. *J Biol Chem*, 278, 31547-53.
- WANG, J. W., DAVID, D. J., MONCKTON, J. E., BATTAGLIA, F. & HEN, R. 2008. Chronic fluoxetine stimulates maturation and synaptic plasticity of adult-born hippocampal granule cells. *J Neurosci*, 28, 1374-84.
- WANG, T., LEE, M. H., JOHNSON, T., ALLIE, R., HU, L., CALABRESI, P. A. & NATH, A. 2010. Activated T-cells inhibit neurogenesis by releasing granzyme B: rescue by Kv1.3 blockers. *J Neurosci*, 30, 5020-7.
- WANG, T., TOWN, T., ALEXOPOULOU, L., ANDERSON, J. F., FIKRIG, E. & FLAVELL, R. A. 2004. Toll-like receptor 3 mediates West Nile virus entry into the brain causing lethal encephalitis. *Nat Med*, 10, 1366-73.
- WANG, X. Q., PENG, Y. P., LU, J. H., CAO, B. B. & QIU, Y. H. 2009a. Neuroprotection of interleukin-6 against NMDA attack and its signal transduction by JAK and MAPK. *Neurosci Lett*, 450, 122-6.
- WANG, Y., JIN, K., MAO, X. O., XIE, L., BANWAIT, S., MARTI, H. H. & GREENBERG, D. A. 2007. VEGF-overexpressing transgenic mice show enhanced post-ischemic neurogenesis and neuromigration. *J Neurosci Res*, 85, 740-7.
- WANG, Z., ZHAO, C., YU, L., ZHOU, W. & LI, K. 2009b. Regional metabolic changes in the hippocampus and posterior cingulate area detected with 3-Tesla magnetic resonance spectroscopy in patients with mild cognitive impairment and Alzheimer disease. *Acta Radiol*, 50, 312-9.
- WATKINS, L. R. & MAIER, S. F. 1999. Implications of immune-to-brain communication for sickness and pain. *Proc Natl Acad Sci U S A*, 96, 7710-3.
- WATSON, K. & FAN, G. H. 2005. Macrophage inflammatory protein 2 inhibits beta-amyloid peptide (1-42)-mediated hippocampal neuronal apoptosis through activation of mitogen-activated protein kinase and phosphatidylinositol 3-kinase signaling pathways. *Mol Pharmacol*, 67, 757-65.

- WEINER, H. L. 2008. A shift from adaptive to innate immunity: a potential mechanism of disease progression in multiple sclerosis. *J Neurol*, 255 Suppl 1, 3-11.
- WEINER, H. L. & FRENKEL, D. 2006. Immunology and immunotherapy of Alzheimer's disease. *Nat Rev Immunol*, 6, 404-16.
- WESTMORELAND, S. V., ALVAREZ, X., DEBAKKER, C., AYE, P., WILSON, M. L., WILLIAMS, K. C. & LACKNER, A. A. 2002. Developmental expression patterns of CCR5 and CXCR4 in the rhesus macaque brain. *J Neuroimmunol*, 122, 146-58.
- WHITNEY, N. P., EIDEM, T. M., PENG, H., HUANG, Y. & ZHENG, J. C. 2009. Inflammation mediates varying effects in neurogenesis: relevance to the pathogenesis of brain injury and neurodegenerative disorders. *J Neurochem*, 108, 1343-59.
- WILLIAMS, J. W., JR., MULROW, C. D., CHIQUETTE, E., NOEL, P. H., AGUILAR, C. & CORNELL, J. 2000a. A systematic review of newer pharmacotherapies for depression in adults: evidence report summary. *Ann Intern Med*, 132, 743-56.
- WILLIAMS, R. O. 2006. Pathogenesis and therapy of rheumatoid arthritis. *Ernst Schering Found Symp Proc*, 107-30.
- WILLIAMS, R. O., MARINOVA-MUTAFCHIEVA, L., FELDMANN, M. & MAINI, R. N. 2000b. Evaluation of TNF-alpha and IL-1 blockade in collagen-induced arthritis and comparison with combined anti-TNF-alpha/anti-CD4 therapy. *J Immunol*, 165, 7240-5.
- WILSON, C. M., GABER, M. W., SABEK, O. M., ZAWASKI, J. A. & MERCHANT, T. E. 2009. Radiation-induced astrogliosis and blood-brain barrier damage can be abrogated using anti-TNF treatment. *Int J Radiat Oncol Biol Phys*, 74, 934-41.
- WINOCUR, G., WOJTOWICZ, J. M., SEKERES, M., SNYDER, J. S. & WANG, S. 2006. Inhibition of neurogenesis interferes with hippocampus-dependent memory function. *Hippocampus*, 16, 296-304.
- WOLF, S. A., STEINER, B., AKPINARLI, A., KAMMERTOENS, T., NASSENSTEIN, C., BRAUN, A., BLANKENSTEIN, T. & KEMPERMANN, G. 2009a. CD4-positive T lymphocytes provide a neuroimmunological link in the control of adult hippocampal neurogenesis. *J Immunol*, 182, 3979-84.
- WOLF, S. A., STEINER, B., WENGNER, A., LIPP, M., KAMMERTOENS, T. & KEMPERMANN, G. 2009b. Adaptive peripheral immune response increases proliferation of neural precursor cells in the adult hippocampus. *FASEB J*, 23, 3121-8.
- WOLFE, F. & MICHAUD, K. 2009. Predicting depression in rheumatoid arthritis: the signal importance of pain extent and fatigue, and comorbidity. *Arthritis Rheum*, 61, 667-73.
- WONG, G. H., BARTLETT, P. F., CLARK-LEWIS, I., BATTYE, F. & SCHRADER, J. W. 1984. Inducible expression of H-2 and Ia antigens on brain cells. *Nature*, 310, 688-91.
- WOOD, D. D., IHRIE, E. J., DINARELLO, C. A. & COHEN, P. L. 1983. Isolation of an interleukin-1-like factor from human joint effusions. *Arthritis Rheum*, 26, 975-83.
- WU, Y., PENG, H., CUI, M., WHITNEY, N. P., HUANG, Y. & ZHENG, J. C. 2009. CXCL12 increases human neural progenitor cell proliferation through Akt-1/FOXO3a signaling pathway. *J Neurochem*, 109, 1157-67.
- XU, D., JIANG, H. R., KEWIN, P., LI, Y., MU, R., FRASER, A. R., PITMAN, N., KUROWSKA-STOLARSKA, M., MCKENZIE, A. N., MCINNES, I. B. & LIEW, F. Y.

2008. IL-33 exacerbates antigen-induced arthritis by activating mast cells. *Proc Natl Acad Sci U S A*, 105, 10913-8.
- XU, H., DAWSON, R., CRANE, I. J. & LIVERSIDGE, J. 2005. Leukocyte diapedesis in vivo induces transient loss of tight junction protein at the blood-retina barrier. *Invest Ophthalmol Vis Sci*, 46, 2487-94.
- XU, J. & DREW, P. D. 2007. Peroxisome proliferator-activated receptor-gamma agonists suppress the production of IL-12 family cytokines by activated glia. *J Immunol*, 178, 1904-13.
- YADAV, M. C., BURUDI, E. M., ALIREZAEI, M., FLYNN, C. C., WATRY, D. D., LANIGAN, C. M. & FOX, H. S. 2007. IFN-gamma-induced IDO and WRS expression in microglia is differentially regulated by IL-4. *Glia*, 55, 1385-96.
- YAMASHITA, A., YONEMITSU, Y., OKANO, S., NAKAGAWA, K., NAKASHIMA, Y., IRISA, T., IWAMOTO, Y., NAGAI, Y., HASEGAWA, M. & SUEISHI, K. 2002. Fibroblast growth factor-2 determines severity of joint disease in adjuvant-induced arthritis in rats. *J Immunol*, 168, 450-7.
- YANG, I., HAN, S. J., KAUR, G., CRANE, C. & PARSA, A. T. 2010. The role of microglia in central nervous system immunity and glioma immunology. *J Clin Neurosci*, 17, 6-10.
- YANG, I., KREMEN, T. J., GIOVANNONE, A. J., PAIK, E., ODESA, S. K., PRINS, R. M. & LIAU, L. M. 2004. Modulation of major histocompatibility complex Class I molecules and major histocompatibility complex-bound immunogenic peptides induced by interferon-alpha and interferon-gamma treatment of human glioblastoma multiforme. *J Neurosurg*, 100, 310-9.
- YANG, M. H., WU, F. X., XIE, C. M., QING, Y. F., WANG, G. R., GUO, X. L., TANG, Z., ZHOU, J. G. & YUAN, G. H. 2009. Expression of CC chemokine ligand 5 in patients with rheumatoid arthritis and its correlation with disease activity and medication. *Chin Med Sci J*, 24, 50-4.
- YOO, S. A., BAE, D. G., RYOO, J. W., KIM, H. R., PARK, G. S., CHO, C. S., CHAE, C. B. & KIM, W. U. 2005. Arginine-rich anti-vascular endothelial growth factor (anti-VEGF) hexapeptide inhibits collagen-induced arthritis and VEGF-stimulated productions of TNF-alpha and IL-6 by human monocytes. *J Immunol*, 174, 5846-55.
- YOUNG, A. & KODURI, G. 2007. Extra-articular manifestations and complications of rheumatoid arthritis. *Best Pract Res Clin Rheumatol*, 21, 907-27.
- YOUNG, S. H., ANTONINI, J. M., ROBERTS, J. R., ERDELY, A. D. & ZEIDLER-ERDELY, P. C. 2008. Performance evaluation of cytometric bead assays for the measurement of lung cytokines in two rodent models. *J Immunol Methods*, 331, 59-68.
- YU, C., KASTIN, A. J., TU, H., WATERS, S. & PAN, W. 2007. TNF activates P-glycoprotein in cerebral microvascular endothelial cells. *Cell Physiol Biochem*, 20, 853-8.
- ZAHEER, A., ZAHEER, S., THANGAVEL, R., WU, Y., SAHU, S. K. & YANG, B. 2008. Glia maturation factor modulates beta-amyloid-induced glial activation, inflammatory cytokine/chemokine production and neuronal damage. *Brain Res*, 1208, 192-203.
- ZHANG, H., PODOJIL, J. R., LUO, X. & MILLER, S. D. 2008. Intrinsic and induced regulation of the age-associated onset of spontaneous experimental autoimmune encephalomyelitis. *J Immunol*, 181, 4638-47.
- ZHANG, K., GHARAEI-KERMANI, M., MCGARRY, B., REMICK, D. & PHAN, S. H. 1997. TNF-alpha-mediated lung cytokine networking and eosinophil recruitment in pulmonary fibrosis. *J Immunol*, 158, 954-9.

- ZHAO, C., TENG, E. M., SUMMERS, R. G., JR., MING, G. L. & GAGE, F. H. 2006. Distinct morphological stages of dentate granule neuron maturation in the adult mouse hippocampus. *J Neurosci*, 26, 3-11.
- ZHU, C. B., BLAKELY, R. D. & HEWLETT, W. A. 2006. The proinflammatory cytokines interleukin-1beta and tumor necrosis factor-alpha activate serotonin transporters. *Neuropsychopharmacology*, 31, 2121-31.
- ZHU, Y., YANG, G. Y., AHLEMEYER, B., PANG, L., CHE, X. M., CULMSEE, C., KLUMPP, S. & KRIEGLSTEIN, J. 2002a. Transforming growth factor-beta 1 increases bad phosphorylation and protects neurons against damage. *J Neurosci*, 22, 3898-909.
- ZHU, Y., YU, T., ZHANG, X. C., NAGASAWA, T., WU, J. Y. & RAO, Y. 2002b. Role of the chemokine SDF-1 as the meningeal attractant for embryonic cerebellar neurons. *Nat Neurosci*, 5, 719-20.
- ZITTERMANN, S. I. & ISSEKUTZ, A. C. 2006. Basic fibroblast growth factor (bFGF, FGF-2) potentiates leukocyte recruitment to inflammation by enhancing endothelial adhesion molecule expression. *Am J Pathol*, 168, 835-46.
- ZIV, Y., RON, N., BUTOVSKY, O., LANDA, G., SUDAI, E., GREENBERG, N., COHEN, H., KIPNIS, J. & SCHWARTZ, M. 2006. Immune cells contribute to the maintenance of neurogenesis and spatial learning abilities in adulthood. *Nat Neurosci*, 9, 268-75.
- ZLOKOVIC, B. V. 2008. The blood-brain barrier in health and chronic neurodegenerative disorders. *Neuron*, 57, 178-201.
- ZOZULYA, A. L., CLARKSON, B. D., ORTLER, S., FABRY, Z. & WIENDL, H. 2010. The role of dendritic cells in CNS autoimmunity. *J Mol Med*, 88, 535-44.
- ZOZULYA, A. L., ORTLER, S., LEE, J., WEIDENFELLER, C., SANDOR, M., WIENDL, H. & FABRY, Z. 2009. Intracerebral dendritic cells critically modulate encephalitogenic versus regulatory immune responses in the CNS. *J Neurosci*, 29, 140-52.
- ZOZULYA, A. L. & WIENDL, H. 2008. The role of regulatory T cells in multiple sclerosis. *Nat Clin Pract Neurol*, 4, 384-98.
- ZUVICH, R. L., MCCAULEY, J. L., PERICAK-VANCE, M. A. & HAINES, J. L. 2009. Genetics and pathogenesis of multiple sclerosis. *Semin Immunol*, 21, 328-33.
- ZWERINA, J., REDLICH, K., POLZER, K., JOOSTEN, L., KRONKE, G., DISTLER, J., HESS, A., PUNDT, N., PAP, T., HOFFMANN, O., GASSER, J., SCHEINECKER, C., SMOLEN, J. S., VAN DEN BERG, W. & SCHETT, G. 2007. TNF-induced structural joint damage is mediated by IL-1. *Proc Natl Acad Sci U S A*, 104, 11742-7.

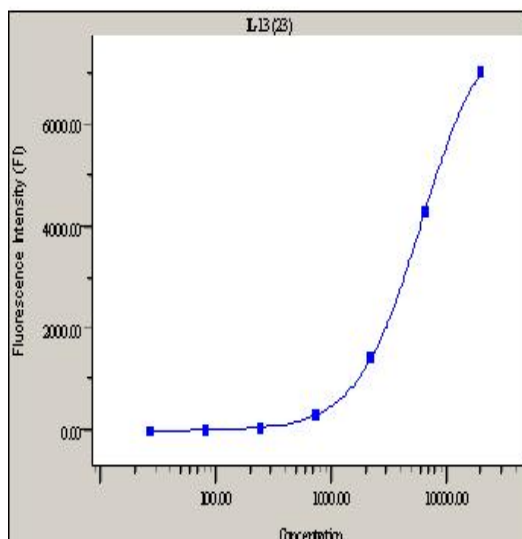
9 Appendices



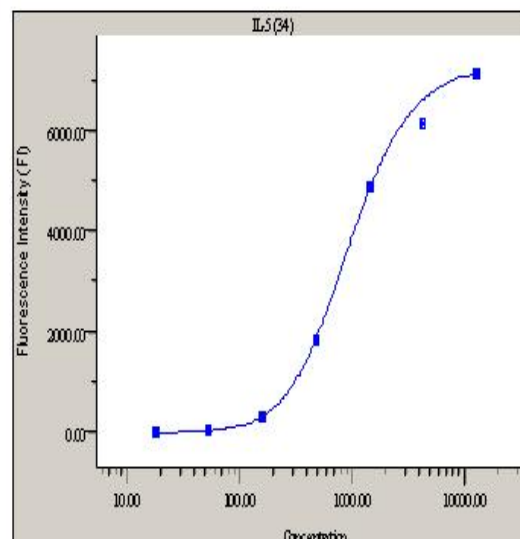
Appendix 1A; Standard curves of the Luminex assay

Validations of assay performance as assessed by Standard curves of IL-1 α (A), IL-2 (B), IL-10 (C) and IL-5 (D), IL-13 proteins obtained from Luminex cytokine 20-Plex assay. Standards were prepared according to manufacturer's instructions, and all standards were run in triplicate. Readings were obtained using BioPlex 200 hardware running BioPlex Manager software.

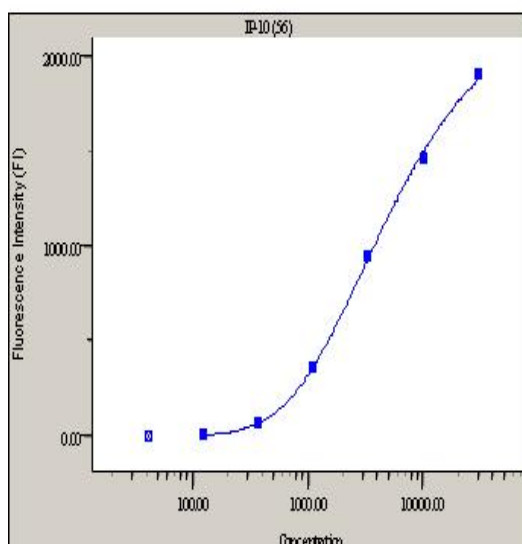
E.



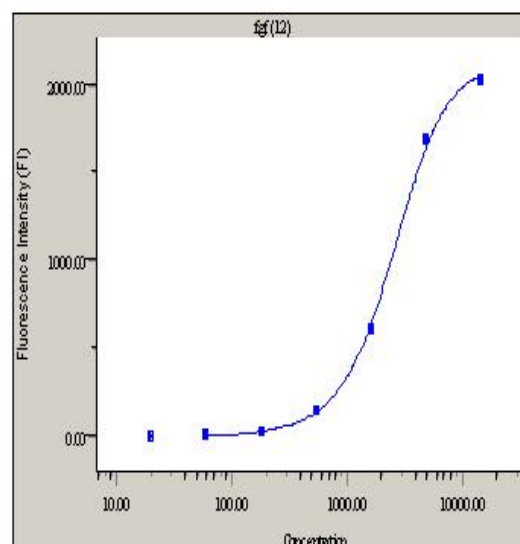
F.



G.



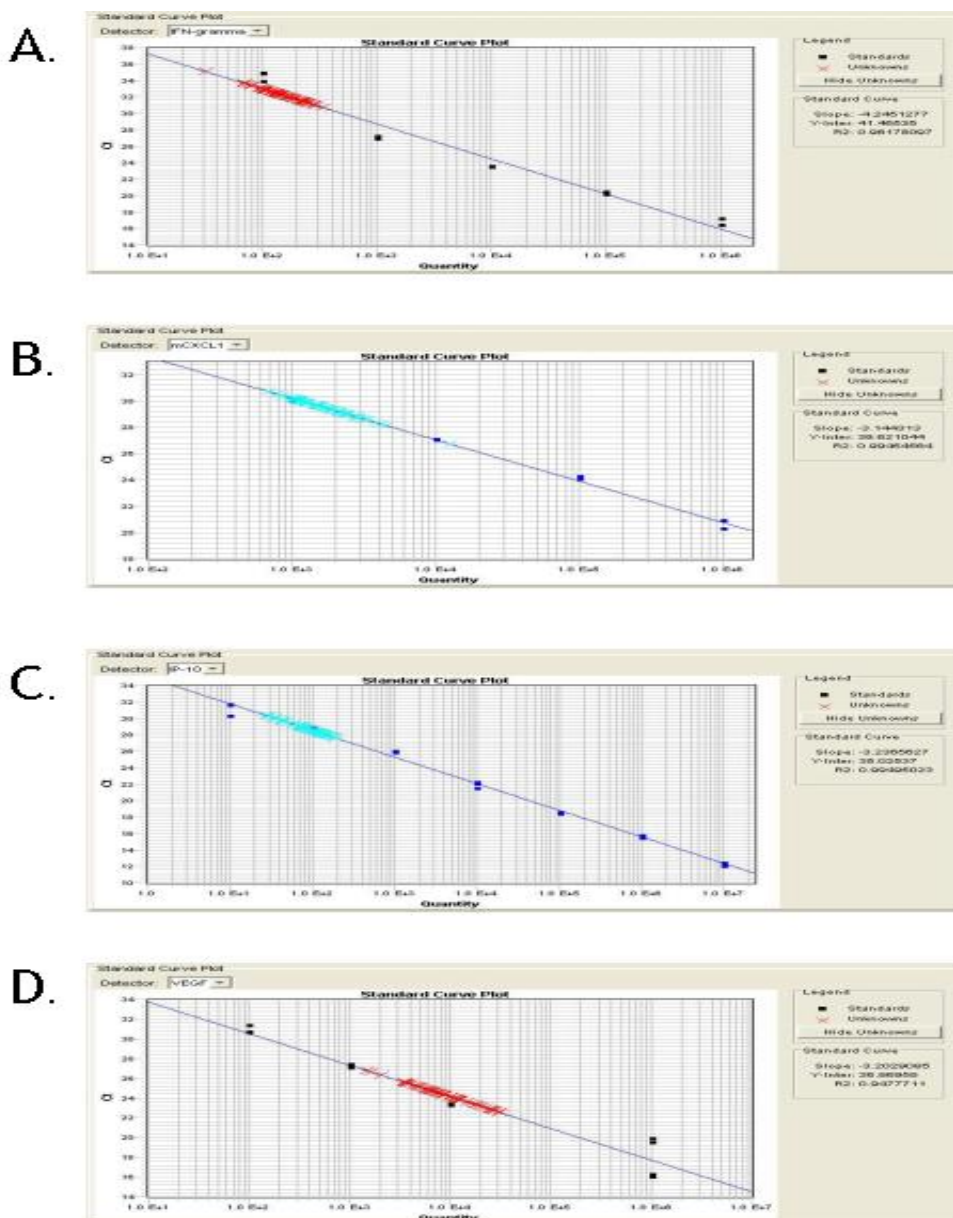
H.



Appendix 1B; Standard curves of the Luminex assay

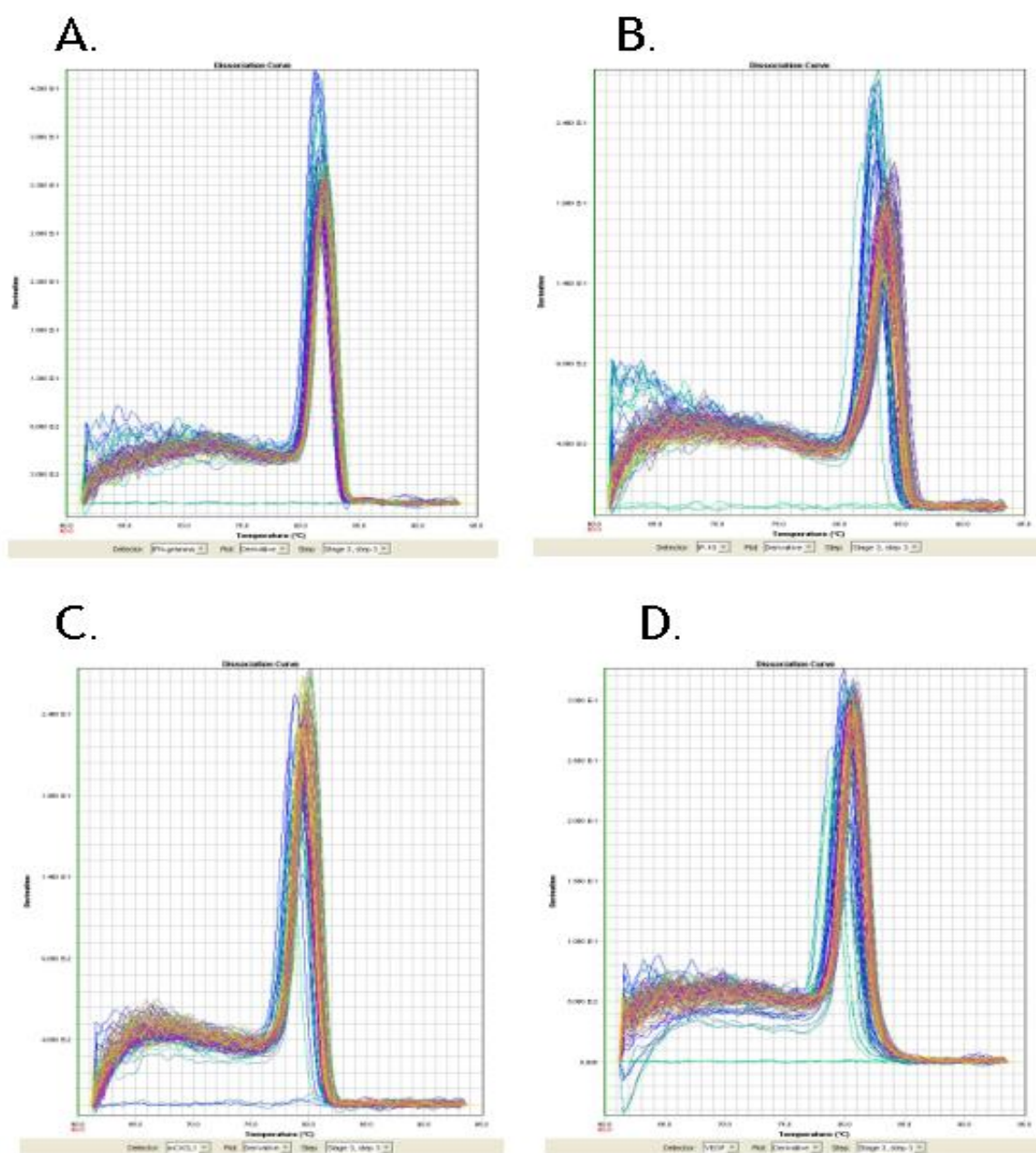
Validations of assay performance as assessed by Standard curves of IL-13 (E), CXCL-1 (F), CXCL10 (G) and FGF2 (H) proteins obtained from Luminex cytokine 20-Plex assay.

Standards were prepared according to manufacturer's instructions, and all standards were run in triplicate. Readings were obtained using BioPlex 200 hardware running BioPlex Manager software.



Appendix 2; Real-time PCR standard curve of inflammatory mediators

Real-time PCR standard curves of IFN- γ (A), CXCL1 (B), CXCL10 (C), VEGF (D) were generated by amplifications of serial dilutions of known quantities of plasmids containing the target sequences. Plasmid containing IFN- γ , CXCL1, CXCL10, and VEGF genes was 10 fold serially diluted to obtain dilutions ranging from 106 to 102 copies amplified by real-time PCR. These standard curves plotting each Ct value against the log quantity of each standard mRNA copy number were used to extrapolate absolute mRNA copy numbers of inflammatory mediator gene expressions in brain samples. Each dot plot on the standard curve linear dynamic range represents gene expression value (copy number) of each standard, while each point in the graph represents gene expression value (copy number) of each sample.



Appendix 3 Melting curves of IFN- γ (A), CXCL1 (B), CXCL10 (C), VEGF (D) confirm specificity of PCR amplification

